Immunopeptidomics – Development of therapeutic vaccines for the treatment of leukemia

Immunpeptidomik – Entwicklung therapeutischer Vakzinen zur Behandlung von Leukämien

Dissertation

der Mathematisch-Naturwissenschaftlichen Fakultät
der Eberhard Karls Universität Tübingen
zur Erlangung des Grades eines
Doktors der Naturwissenschaften
(Dr. rer. nat.)

vorgelegt von
M. Sc. Annika Stephanie Nelde
aus Tübingen

Tübingen
2019

Gedruckt mit Genehmigung der Mathematisch-Naturwissenschaftlichen Fakultät der Eberhard Karls Universität Tübingen.

Tag der mündlichen Prüfung:	07.02.2020
Dekan:	Prof. Dr. Wolfgang Rosenstiel
1. Berichterstatter:	Prof. Dr. Stefan Stevanović
2. Berichterstatter:	Prof. Dr. Hans-Georg Rammensee
3. Berichterstatter:	Prof. Dr. med. Markus Manz

für all diejenigen, die mir ein

Lächeln ins Gesicht zaubern

CONTENT

1. PREFACE

This thesis gives an overview over the projects I had the pleasure to work on during the years of my PhD thesis. Furthermore, I aim to provide an insight into the rapidly developing field of mass spectrometry-based immunopeptidomics and T-cell-based immunotherapy approaches focusing on leukemia patients. Obviously, this thesis can only summarize and present the main projects and outcomes of my work at the Department of Immunology. Beside the projects within the Department of Immunology at the University of Tübingen and the Department of Hematology and Oncology at the University Hospital Tübingen I also had the opportunity to work together with several other outstanding researches in numerous cooperation projects.

2. PUBLICATIONS

The marked (*) publications or manuscripts in preparation are presented in this thesis in more detail. Author contributions are described at the beginning of the corresponding chapter, respectively.

Research articles:

*****Nelde A, Schuster H, Kowalewski DJ, Salih HR, Volkmer JP, Chen JY, Rücker-Braun E, Paczulla AM, Marcu A, Roerden M, Bichmann L, Bilich T, Bauer J, Heitmann JS, Kohlbacher O, Neidert MC, Schetelig J, Schmitz M, Majeti R, Weisman IL, Lengerke C, Rammensee H-G, Stevanović S, and Walz JS. Development of a therapeutic peptide vaccine for the treatment of acute myeloid leukemia based on naturally presented HLA ligands of AML progenitor cells. *Manuscript in preparation.*

Bilich T, Nelde A, Bauer J, Walz S, Roerden M, Salih HR, Weisel K, Besemer B, Marcu A, Lübke M, Schuhmacher J, Neidert MC, Rammensee H-G, Stevanović S, and Walz JS. Mass spectrometry-based identification of a BCMA-derived T-cell epitope for antigen-specific immunotherapy in multiple myeloma. *Blood Cancer Journal. Under revision.*

Lübke M, Spalt S, Kowalewski DJ, Zimmermann C, Bauersfeld L, Nelde A, Bichmann L, Marcu A, Peper JK, Kohlbacher O, Walz JS, Khanh Le-Trilling VT, Hengel H, Rammensee H-G, Stevanović S, and Halenius A. HCMV deletion models enable the identification of physiologically relevant T-cell epitopes. *Journal of Experimental Medicine. Under revision.*

PUBLICATIONS

Ghosh M, Gauger M, Marcu A, Nelde A, Denk M, Rammensee H-G, and Stevanović S. Guidance document: validation of a high-performance liquid chromatography-tandem mass spectrometry immunopeptidomics assay for the identification of HLA ligands suitable for pharmaceutical therapies. *Molecular & Cellular Proteomics. Under revision.*

Bichmann L, Nelde A, Ghosh M, Mohr C, Peltzer A, Kuchenbecker L, Heumos L, Sachsenberg T, Walz JS, Stevanović S, Rammensee H-G, and Kohlbacher O. MHCquant: Automated and reproducible data analysis for immunopeptidomics. *Journal of Proteome Research. In press.*

Belnoue E, Mayol JF, Carboni S, Di Bernardino Besson W, Dupuychaffray E, Nelde A, Stevanović S, Santiago-Raber ML, Walker PR, and Derouazi M. Targeting self and neo-epitopes with a modular self-adjuvanting cancer vaccine. *JCI Insight* 4 (11): e127305 (2019).

*Bilich T[#], Nelde A[#], Bichmann L, Roerden M, Salih HR, Kowalewski DJ, Schuster H, Tsou CC, Marcu A, Neidert MC, Lübke M, Rieth J, Schemionek M, Brümmendorf TH, Vucinic V, Niederwieser D, Bauer J, Märklin M, Peper JK, Klein R, Kohlbacher O, Kanz L, Rammensee H-G, Stevanović S, and Walz JS. The HLA ligandome landscape of chronic myeloid leukemia delineates novel T-cell epitopes for immunotherapy. *Blood* 133 (6): 550-565 (2019).
[#]Authors contributed equally to this work.

Walz JS, Kowalewski DJ, Backert L, Nelde A, Kohlbacher O, Weide B, Kanz L, Salih HR, Rammensee H-G, and Stevanović S. Favorable immune signature in CLL patients, defined by antigen-specific T-cell responses, might prevent second skin cancers. *Leukemia and Lymphoma:* 1-10 (2018).

*Nelde A, Kowalewski DJ, Backert L, Schuster H, Werner JO, Klein R, Kohlbacher O, Kanz L, Salih HR, Rammensee H-G, Stevanović S, and Walz JS. HLA ligandome analysis of primary chronic lymphocytic leukemia (CLL) cells under lenalidomide treatment confirms the suitability of lenalidomide for combination with T-cell-based immunotherapy. *Oncoimmunology* 7(4): e1316438 (2017).

Heidenreich F, Rücker-Braun E, Walz JS, Eugster A, Kuhn D, Dietz S, Nelde A, Tunger A, Wehner R, Link CS, Middeke JM, Stolzel F, Tonn T, Stevanović S, Rammensee H-G, Bonifacio E, Bachmann M, Zeis M, Ehninger G, Bornhauser M, Schetelig J, and Schmitz M. Mass spectrometry-based identification of a naturally presented receptor tyrosine kinase-like orphan receptor 1-derived epitope recognized by CD8(+) cytotoxic T cells. *Haematologica* 102: e460-e4 (2017).

Nelde A, Walz JS, Kowalewski DJ, Schuster H, Wolz OO, Peper JK, Cardona Gloria Y, Langerak AW, Muggen AF, Claus R, Bonzheim I, Fend F, Salih HR, Kanz L, Rammensee H-G, Stevanović S, and Weber AN. HLA class I-restricted MYD88 L265P-derived peptides as specific targets for lymphoma immunotherapy. *Oncoimmunology* 6: e1219825 (2017).

Walz S, Stickel JS, Kowalewski DJ, Schuster H, Weisel K, Backert L, Kahn S, Nelde A, Stroh T, Handel M, Kohlbacher O, Kanz L, Salih HR, Rammensee H-G, and Stevanović S. The antigenic landscape of multiple myeloma: mass spectrometry (re)defines targets for T-cell-based immunotherapy. *Blood* 126:1203-1213 (2015).

Review articles:

Roerden M, Nelde A, Walz JS. Neoantigens in hematological malignancies – ultimate targets for immunotherapy? *Submitted to Frontiers in Immunology.*

Nelde A, Kowalewski DJ, and Stevanović S. Purification and Identification of Naturally Presented MHC Class I and II Ligands. *Antigen Processing: 123-136 (2019).*

Bauer J, Nelde A, Bilich T, and Walz JS. Antigen targets for the development of immunotherapies in leukemia. *International Journal of Molecular Sciences 20 (6):1397 (2019).*

3. SUMMARY

With the development and clinical success of immune checkpoint inhibitors, T-cell-based immunotherapy has been revolutionized. Therefore, in recent years special emphasis was placed on the identification of the target structures of the anti-tumor T-cell responses. These target structures are represented by tumor-associated or tumor-specific antigens presented on the surface of tumor cells *via* human leukocyte antigen (HLA) molecules. Further, the tremendous evolving field of mass spectrometry enables nowadays the direct identification of naturally presented HLA ligands from primary human samples in undreamt depth. This thesis aims to provide an insight into the rapidly developing field of mass spectrometry-based immunopeptidomics and the development of T-cell-based immunotherapeutic approaches for leukemia patients.

For chronic lymphocytic leukemia (CLL) our group characterized tumor-associated antigens, which are associated with improved survival. This antigen panel is currently investigated in a first-in-man multicentric clinical phase II study (iVAC-CLL01, NCT02802943) of patient-individualized peptide vaccination in CLL patients. However, CLL is associated with a profound immune defect, which could hamper the clinical success of T-cell-based immunotherapy. Therefore, the combination of antigen-specific T-cell-based immunotherapy with immunomodulatory drugs such as lenalidomide represents a promising approach to overcome this immune defect. In the first part of this thesis we therefore performed a longitudinal study on the influence and effect of lenalidomide on the immunopeptidome of primary CLL cells. Mass spectrometry-based profiling identified only minor effects on HLA-restricted peptide presentation and confirmed stable presentation of the previously described CLL-associated antigens under lenalidomide treatment. Therefore, lenalidomide was validated as suitable combination partner for tailored T-cell-based immunotherapeutic approaches in CLL patients.

In the second and third part of this thesis, we applied a mass spectrometry-based approach to identify naturally presented, HLA-restricted chronic myeloid leukemia (CML)- and acute myeloid leukemia (AML)-associated peptides, respectively. Therefore, we utilized a comparative profiling approach using a comprehensive dataset of different benign tissues. For AML, we furthermore mapped the immunopeptidome of enriched leukemic progenitor cells (LPCs) and defined additional LPC-associated antigens. Notably, we were also able to identify mutation-derived neoepitopes in primary AML samples. Functional characterization revealed spontaneous T-cell responses against the novel identified CML- and AML-associated peptides in patient samples and their ability to induce multifunctional and cytotoxic antigen-specific T cells. These antigens are thus prime candidates for T-cell-based immunotherapeutic approaches for CML and AML patients.

4. ZUSAMMENFASSUNG

Mit der Entwicklung und dem klinischen Erfolg der Immuncheckpoint-Inhibitoren hat die T-Zell-basierte Immuntherapie eine Revolution erlebt. In den letzten Jahren rückte deshalb die Identifizierung der Zielstrukturen der Anti-Tumor-T-Zellantworten immer weiter in den Fokus. Diese Zielstrukturen sind Tumor-assoziierte oder Tumor-spezifische Antigene, die auf der Oberfläche von Tumorzellen über humane Leukozytenantigene (HLA) präsentiert werden. Zudem ermöglicht das sich enorm entwickelnde Feld der Massenspektrometrie heute die direkte Identifizierung von natürlich präsentierten HLA-Liganden aus humanen Primärproben in ungeahnter Tiefe. Diese Arbeit soll einen Einblick in das Gebiet der Massenspektrometrie-basierten Immunpeptidomik und in die Entwicklung T-Zell-basierter immuntherapeutischer Ansätzen für Leukämiepatienten geben.

Für die chronisch lymphatische Leukämie (CLL) identifizierte unsere Gruppe Tumor-assoziierte Antigene, die mit verbessertem Überleben assoziiert sind. Diese Antigene werden derzeit in einer ersten multizentrischen klinischen Phase-II-Studie (iVAC-CLL01, NCT02802943) als patienten-individuelle Peptidimpfung bei CLL-Patienten untersucht. Die CLL ist jedoch durch einen umfassenden Immundefekt gekennzeichnet, der den klinischen Erfolg der T-Zell-basierten Immuntherapie beeinträchtigen könnte. Die Kombination der Antigen-spezifischen T-Zell-basierten Immuntherapie mit immunmodulatorischen Medikamenten wie Lenalidomid stellt daher einen vielversprechenden Ansatz zur Überwindung dieses Immundefektes dar. In einer longitudinalen Verlaufsstudie untersuchten wir deshalb den Einfluss von Lenalidomid auf das Immunpeptidom von primären CLL-Zellen. Die Massenspektrometrie-basierte Untersuchung zeigte nur geringe Auswirkungen auf die HLA-restringierte Peptidpräsentation und bestätigte die stabile Präsentation der beschriebenen CLL-assoziierten Antigene unter Lenalidomidbehandlung. So konnte Lenalidomid als geeigneter Kombinationspartner für die T-Zell-basierte Immuntherapie bei CLL-Patienten validiert werden.

Für die chronisch myeloische Leukämie (CML) und die akute myeloische Leukämie (AML) identifizierten wir mittels Massenspektrometrie-basierter Analyse und dem Vergleich mit einem umfassenden Datensatz gesunder Gewebe natürlich präsentierte, HLA-restringierte CML- und AML-assoziierte Peptide. Für die AML analysierten wir außerdem das Immunpeptidom von angereicherten leukämischen Vorläuferzellen, um Vorläuferzell-assoziierte Antigene zu definieren. Des Weiteren konnten wir zusätzlich Mutations-abgeleitete Neoepitope in primären AML-Proben identifizieren. Mittels funktioneller Charakterisierung dieser neu definierten Antigene konnten spontane T-Zell-Antworten in Patientenproben sowie die Induktion multifunktionaler und zytotoxischer Antigen-spezifischer T-Zellen nachgewiesen werden. Diese Antigene stellen somit vielversprechende Kandidaten für T-Zell-basierte immuntherapeutische Ansätze in CML- und AML-Patienten dar.

5. INTRODUCTION

5.1. HEMATOLOGIC MALIGNANCIES

Hematologic malignancies comprise all types of neoplastic diseases of hematopoietic and lymphatic tissues including leukemia and lymphoma. The term *leukemia* is derived from the Greek words *leukos* and *heima* referring to the massive accumulation of leukocytes in the blood of leukemia patients. Leukemia was first described as a malignant disease in the middle of the 19th century, as physicians became aware that leukocytosis can occur in the absence of infection.[1, 2] Due to Paul Ehrlich's development of a cell staining method that allows distinction of blood cells,[3] the different types of leukemia were first classified and distinguishable. Today, leukemia is classified into four major types – acute lymphoblastic leukemia (ALL), acute myeloid leukemia (AML), chronic lymphocytic leukemia (CLL), and chronic myeloid leukemia (CML), as well as a number of less common types. The main clinical and pathological differences between these four types are their progression rates (chronic versus acute), as well as the cell types from which they originate and develop (myeloid versus lymphoid). Chronic leukemias are characterized by the accumulation of relatively mature but still abnormal leukocytes over a long period of time. In contrast, immature precursor cells proliferate and accumulate rapidly in acute leukemias.[4, 5] Since Paul Ehrlich's discovery, and especially in recent decades, our understanding of the pathogenesis and biology of hematologic malignancies, and particularly leukemia, has changed dramatically. This advanced knowledge has led to significant and impressive advances in diagnosis and treatment options, as well as clinical outcomes of patients suffering from these malignancies.

5.1.1. CHRONIC LYMPHOCYTIC LEUKEMIA

The B-cell malignancy CLL is characterized by the accumulation of small, mature, monoclonal CD5^{+} B lymphocytes in the blood, bone marrow, and secondary lymphoid tissues.[6] CLL is the most common leukemia in adults[7, 8] and is diagnosed especially in elderly patients with a median age at diagnosis of 70 years.[8] The 5-year survival rate of 85%[8] is relatively high compared to acute leukemias. Depending on the mutational status of the immunoglobulin heavy-chain variable region gene (*IGHV*), two main subtypes of CLL can be classified and distinguished. The *IGHV* mutational status reflects the stage of B-cell differentiation from which the malignant clone originates. CLL cells with mutated *IGHV* have already undergone differentiation with somatic hypermutation of their immunoglobulin in the germinal centers. Typically, patients with unmutated *IGHV* typically suffer from a more aggressive disease then patients with mutated *IGHV*.[9, 10] Besides *IGHV*, which does not contribute to the malignant transformation, the mutational landscape of CLL comprises relatively few chromosomal alterations or somatic mutations. The most common chromosomal alterations include deletions in

the chromosomes 11, 13, and 17 as well as trisomy 12.[11] Furthermore, several somatic mutations in genes such as *TP53*, *MYD88*, and *NOTCH1* were identified within the last years; however, distinct mutations are mainly not very common.[12, 13]

For clinical classification two different systems – the Rai and the Binet classification – are normally applied. In the United States, the Rai staging system is more commonly used, while in Europe physicians utilized mainly the Binet classification. Both systems define low, intermediate, and high risk groups.[14, 15]

CLL disease progresses very slowly and most often patients are asymptomatic at the time of diagnosis. Therefore, therapy is solely recommended at disease progression or after the development of first symptoms.[16] In the last years, the treatment landscape for CLL patients underwent remarkable progress and became more and more CLL-specific. Now standard of care for most patients includes chemotherapy in combination with anti-CD20 antibodies (*e.g.* rituximab or obinutuzumab) or the bruton tyrosine kinase inhibitor ibrutinib as single agent.[17] Nevertheless, these treatment options are still not curative, show significant relapse rates, and are not always well tolerated by the patients. Therefore, basic scientific research and preclinical and clinical trials are ongoing, especially focusing on combination therapies,[18] with the aim to further improve the overall outcome and ultimately achieve a permanent cure for these patients.

5.1.2. CHRONIC MYELOID LEUKEMIA

CML is a myeloproliferative disorder characterized by the balanced genetic translocation between chromosomes 9 and 22, the so-called Philadelphia chromosome, resulting in the fusion of the Abelson murine leukemia viral oncogene homolog 1 (*ABL1*) gene with the breakpoint cluster region (*BCR*) gene.[19] As a result of this translocation the constitutively active fusion oncoprotein BCR-ABL, a tyrosine kinase, is expressed. Several different breakpoints have been identified generating different transcripts, termed for example b3a2, b2a2, e1a2, or e19a2. Depending on the junction site the resulting fusion proteins are named p210, which is the most common form, p190, or p230.[20] The expression of this oncoprotein was identified as the primary cause of the disease.[21, 22] BCR-ABL promotes growth and replication of the malignant cells through activation of downstream MAP kinase pathways signaling through Ras, Raf, Myc, and STAT. This enables a cytokine-independent cell cycle and proliferation of the CML cells.[23-26]

In less than a decade, the prognosis of CML has shifted from a life-threatening disease to a disorder that is compatible with a normal lifespan by a simple lifelong oral medication. This advance was accomplished by the discovery of tyrosine kinase inhibitors (TKIs), which target and inhibit the BCR-ABL fusion protein. This development has led to the achievement of durable cytogenetic, deep

molecular remissions and an impressive improvement in the prognosis of CML patients.[27] Since the introduction of the first TKI imatinib in 2000, the annual mortality of CML patients has decreased dramatically from 10 – 20% to only 1 – 2%.[28] Therefore, TKIs are now the first-line treatment for CML patients with five available approved TKIs.[29-33] Since this therapy can have significant side effects and prolonged therapy further increases the risk of developing drug resistance or tolerance,[34, 35] several clinical trials are investigating discontinuation of TKI therapy in patients with stable deep molecular response.[36, 37] However, since only a few patients are able to permanently stop TKI therapy without suffering from molecular relapse[36, 37] lifelong TKI therapy remains the standard of care for most CML patients. Therefore, further research and development of clinically effective therapeutic approaches with minor side effects are needed to allow more patients to permanently stop TKI treatment without suffering from relapse and to achieve high cure rates in CML.

5.1.3. ACUTE MYELOID LEUKEMIA

AML is a heterogeneous disease of myeloid precursors, characterized by the rapid and uncontrolled proliferation and accumulation of clonal, undifferentiated myeloid blasts in the bone marrow and blood of patients.[38, 39] AML is the most common acute leukemia in adults with a median age of 68 years at diagnosis, and one-third of patients being older than 75 years.[40] With a 5-year survival rate of 28%, the prognosis and long-term survival of AML patients still remains exceptionally poor with high relapse rates.[41]

The classification of AML in several subgroups was originally performed by the French-American-British (FAB) system, which divides AML into eight subtypes, M0 through M7, based on the cell type the leukemia arises from and its degree of maturation.[42, 43] This descriptive classification without any clinical relevance was replaced by the classification of the World Health Organization (WHO) in 2008 (Table 1), which influences clinical management, prognosis, and therapy.[7] Furthermore, the European LeukemiaNet (ELN) also classified different AML subgroups.[44, 45] According to the WHO definition, AML is diagnosed by the presence of ≥ 20% blasts in the bone marrow or peripheral blood. Further, independent of the blast count, the identification of distinct recurrent cytogenetic abnormalities such as translocations or mutations determines the diagnosis of AML.[46, 47] Since the first WHO classification in 2008, several advances and developments in the identification of novel biomarkers were made, largely due to increased availability of gene expression analyses and next-generation sequencing approaches calling for the continuous revision of this classification.[48]

Table 1: WHO classification of AML and related precursor neoplasm

AML with recurrent genetic abnormalities			
AML with translocations between chromosome 8 and 21		*t(8;21)(q22;q22)*	*RUNX1/RUNX1T1*
AML with inversions or internal translocations in chromosome 16		*inv(16)(p13.1q22) or t(16;16)(p13.1;q22)*	*CBFB/MYH11*
APL with translocations between chromosome 15 and 17		*t(15;17)(q22;q21)*	*PML/RARA*
AML with translocations between chromosome 9 and 11		*t(9;11)(p22;q23)*	*MLLT3/MLL*
AML with translocations between chromosome 6 and 9		*t(6;9)(p23;q34)*	*DEK/NUP214*
AML with inversions or internal translocations in chromosome 3		*inv(3)(q21q26.2) t(3;3)(q21;q26.2)*	*RPN1/EVI1*
Megakaryoblastic AML with translocations between chromosome 1 and 22		*t(1;22)(p13;q13)*	*RBM15/MKL1*
AML with mutated NPM1			*NPM1*
AML with biallelic mutations of the CEBPA gene			*CEBPA*
AML with mutated RUNX1			*RUNX1*
AML with myelodysplasia-related changes			
Therapy-related myeloid neoplasms			
AML not otherwise specified			
AML with minimal differentiation	*Acute monoblastic and monocytic leukemia*		
AML without maturation	*Acute erythroid leukemia*		
AML with maturation	*Acute basophilic leukemia*		
Acute myelomonocytic leukemia	*Acute panmyelosis with myelofibrosis*		
Myeloid sarcoma			
Myeloid proliferations related to Down syndrome			

Abbreviations: AML, acute myeloid leukemia; APL, acute promyelocytic leukemia; t, translocation; inv, inversion. Adapted from Swerdlow *et al.*[7]

5.1.3.1. Recurrent mutations in AML

The analysis of the cytogenetic and molecular genetic landscape of AML, as reflected in the WHO classification of AML subtypes[7], represents an important factor in the prognosis and selection of the most effective therapy for each individual patient. The spectrum of chromosomal abnormalities is heterogeneous, including recurrent chromosomal translocations such as t(8;21), t(15;17), and inv(16), but also hundreds of infrequent or even patient-individual aberrations. Besides balanced genomic rearrangements or fusion genes, AML patients can also harbor chromosomal aneuploidies, including -5/5q, -7/7q, -17/17q, or -12/12q.[49]

The translocation t(8;21)(q22;q22) is one of the most frequent rearrangements in AML, observed in approximately 12% of AML patients.[50] As a consequence of this genetic translocation, the transcription factor fusion protein RUNX1-RUNX1T1 is expressed, which leads to transcriptional dysregulation in AML blasts.[51] Interestingly, point mutations in RUNX1 are also frequently identified in cytogenetically normal AML.[52]

The fusion protein of the transcription factor core-binding factor subunit beta (CBFB) and the smooth muscle myosin heavy chain (MYH11), generated by the translocation t(16;16)(p13;q22) or the inversion inv(16)(p13q22), can be identified in about 10% of AML cases.[53] The CBFB-MYH11 protein inhibits the differentiation of myeloid leukemic cells[54] and acts as a transcriptional repressor.[55]

Besides structural chromosomal abnormalities, AML can harbor recurrent somatic mutations in several genes such as nucleophosmin (*NPM1)*, FMS-like tyrosine kinase 3 (*FLT3)*, *CEBPA*, *TP53*, or *ASXL1*. However, it should be mentioned that AML is one of the malignancies with the lowest mutational burden among all human cancers, with only approximately ten coding mutations per patient.[56-59]

The most common genetic alterations in AML are mutations in the *NPM1* gene. About 35% of all AML patients carry NPM1 mutations[60] correlated with a beneficial outcome with increased complete remission and improved overall survival rates.[61] NPM1 is a nucleolar phosphoprotein with multiple cellular functions, including regulation of ribosome biogenesis and transport,[62] maintenance of genomic stability, and DNA repair.[63] The majority of NPM1 mutations are frameshift insertions restricted to exon 12 (Figure 1) that generate a new nuclear export signal motif, which causes aberrant cytoplasmic accumulation of mutated NPM1 protein.[60, 64]

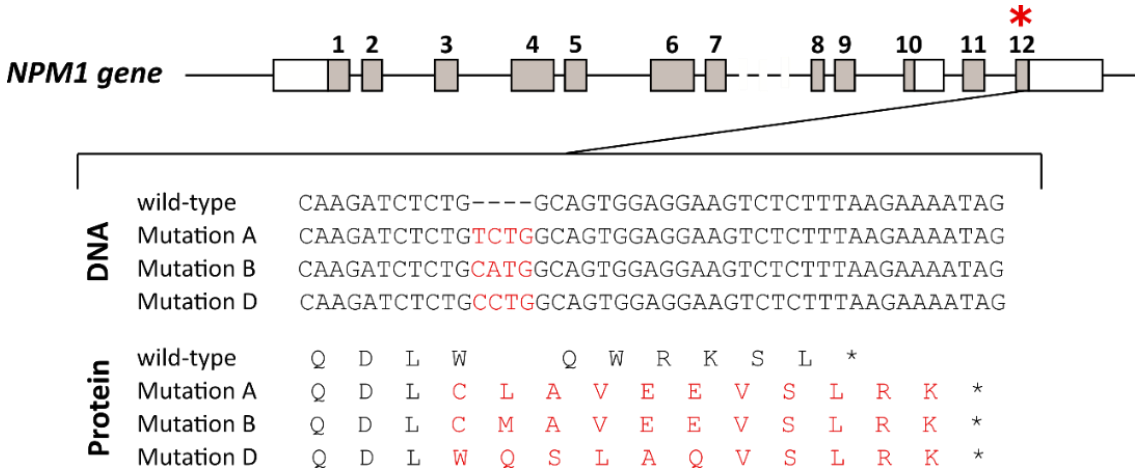

Figure 1: *NPM1* gene structure with the most common mutations identified in AML. The mutational hotspot within the *NPM1* gene is located in exon 12. The frameshift mutations lead to an altered C-terminus of the protein. Mutation A is the most prominent mutation with a frequency of 75 – 80%. Exon 10 is only part of isoform 3. Adapted from Falini *et al.*[65] and Thiede *et al.*[64]

Besides the described mutations in the *NPM1* gene, mutations in the membrane-bound receptor tyrosine kinase FLT3 are very common. FLT3 is mutated in about 30 – 35% of all AML cases,[66] either by in-frame internal tandem duplications (ITD)[67] or by point mutations within the activation loop of the tyrosine kinase domain (TKD).[68] FLT3 possesses a crucial role in early stages of hematopoiesis.[69] Both types of mutations lead to a constitutive activation of the FLT3 receptor in a ligand-independent manner.[70] Further recurrent mutations in AML are found in isocitrate dehydrogenases (IDHs) in about 20% of all AML patients.[71] The most common mutations are IDH1-R132, IDH2-R172, and IDH2-R140 leading to aberrant DNA methylation and blockade of the cellular differentiation.[72] Understanding the function of recurrent mutations can help to develop novel targeted therapies that could supplement the standard therapy of AML patients.

5.1.3.2. Standard therapy of AML

Treatment of AML patients remained largely unchanged for four decades. The standard of care for patients eligible to intensive treatment is still represented by a chemotherapeutic induction therapy, combining anthracyclines for three days with cytarabine for seven days, known as "3+7" regimen.[73] But it has become apparent that AML is a complex and heterogenic disease with several diverse subgroups, which require specific adaptation of therapeutic approaches. Genomic and cytogenetic analyses and the discovery of the importance of recurrent somatic mutations promote the development of several novel agents, which will allow a higher degree of personalization in the treatment of AML. Increased knowledge of the prognostic significance of recurrent genomic alterations now found its way into the clinic, as molecular mutations are part of routine testing and thereby influence treatment decisions.

In 2017 and 2018, the US Food and Drug Administration (FDA) and the European Medicines Agency (EMA) granted the first drug approvals for the treatment of AML since more than 40 years. Midostaurin (Rydapt®), a multikinase inhibitor, was approved in combination with standard cytarabine and daunorubicin induction and cytarabine consolidation for the treatment of adult patients with newly diagnosed FLT3-mutated AML based on a phase III study demonstrating prolonged overall survival.[74] Furthermore, gemtuzumab ozogamicin (Mylotarg®), an anti-CD33 antibody-drug conjugate with the cytotoxic substance calicheamicin,[75] was re-approved by both regulatory authorities in combination with chemotherapy for newly diagnosed CD33-positive AML.

Additionally, in August 2017 and July 2018 the FDA granted regular approval to the IDH2 and IDH1 inhibitors enasidenib (Idhifa®)[76, 77] and ivosidenib (Tibsovo®)[78] for the treatment of IDH-mutated AML, respectively. In the end of 2018, the FDA also granted an accelerated approval of the BCL-2 inhibitor venetoclax (Venclexta®)[79, 80] in combination with azacytidine, decitabine, or low-dose cytarabine for newly-diagnosed elderly AML patients. Commonly expressed in hematological neoplasms[81] with an essential role for the survival of AML cells,[82] the anti-apoptotic protein B-cell leukemia/lymphoma-2 (BCL-2) represents a suitable target for AML therapy. For the last-mentioned agents, the approvals of the EMA are still pending.

5.1.3.3. Development of novel therapies for AML

Besides the already approved novel drugs, several other targeted therapies are under development and are currently investigated in preclinical studies and clinical trials.

Several different surface antigens are qualified as potential targets for different kinds of antibody-based therapeutic approaches. These include the myeloid surface antigens CD33 and CD123 as well as leukemia stem cell markers such as CD25, CD44, CD96, FLT3 and TIM-3. The application of antibodies targeting these markers is hampered by their lack of tumor-specificity, as the majority of

them is also expressed on benign myeloid cells, which increase on-target/off-tumor side effects of such therapies.

CD33 (Siglec-3) is a member of the sialic acid-binding immunoglobulin (Ig)-like lectins, a subset of the Ig superfamily[83] and was confirmed to be expressed by both AML blasts and leukemic stem cells.[84] Besides the approved drug gemtuzumab ozogamicin (Mylotarg®), other formats targeting CD33 are under development, such as the CD33/CD3 bispecific T-cell engager (BiTE) AMG 330, which already exhibits promising first results in clinical studies.[85, 86]

The interleukin-3 receptor, CD123, promotes the survival and proliferation of myeloid cells through the binding of interleukin-3 and represents a very promising therapeutic target as its expression on normal hematopoietic stem cells is lower compared to CD33.[87] CD123 can be targeted in two different ways. On the one hand, antibody-based approaches using different formats are under investigation.[88, 89] On the other hand, due to the fact that CD123 represents a receptor, several studies focus on agents based on the natural ligand IL-3. In one example, a truncated form of the diphtheria toxin was fused to IL-3 resulting in potent blast cell killing.[90] The final results of a phase I/II study[91] utilizing this approach are expected to be published soon.

Another reasonable target on the surface of AML cells is FLT3 (CD135), as an increased expression of this receptor can be measured on leukemic blasts in comparison to normal cells. The chimeric Fc-optimized monoclonal antibody FLYSYN binds specifically to FLT3, independent of its mutational status, and triggers antibody-dependent cell-mediated cytotoxicity (ADCC)[92]. FLYSYN is currently evaluated in a clinical study.[93] Moreover, the FLYSYN antibody was further used in the framework of a bispecific antibody targeting FLT3 and CD3, which revealed enhanced cellular cytotoxicity against FLT3-expressing AML cells in comparison to the monoclonal antibody alone.[94] In addition, FLT3 can not only be targeted by antibody-based approaches but also by direct inhibition of its kinase activity *via* competitive inhibition. Besides the first approved FLT3 inhibitor midostaurin,[95] several other inhibitors have been developed and are currently under preclinical and clinical investigation. First-generation FLT3 inhibitors such as tandutinib,[96] sunitinib,[97] sorafenib,[98, 99] midostaurin,[74] and lestaurtinib[100] are relatively unspecific for the FLT3 kinase resulting in off-target inhibition and therefore increased toxicity. Second-generation inhibitors, including quizartinib,[101] crenolanib,[102] ponatinib,[103] and gilteritinib,[104] are more specific and potent with lower side effects.

With the development and clinical success of immune checkpoint inhibitors, the field of immune-oncology, especially for solid tumors,[105, 106] was revolutionized in recent years. For the rational selection of suitable immune checkpoint inhibitors for the treatment of AML, the identification of targetable immune checkpoints in AML is crucial. Programmed cell death receptor-1 (PD-1) and OX40 were identified as potential important checkpoint receptors in AML patients.[107] Further studies

confirmed that PD-L1 (programmed cell death ligand-1) expression is associated with a more aggressive disease and early relapse.[108, 109] Moreover, a gradual increase in PD-1 and PD-L1 expression was detected on T cells and AML blasts, respectively, with progression from MDS to AML and during AML relapse.[110] Cytotoxic T lymphocyte-associated molecule-4 (CTLA-4) also harbors an import role in the immune escape of AML and blockade of CTLA-4 could enhance T-cell-mediated killing of residual leukemic cells.[111] As a result, various immune checkpoint inhibitors are now evaluated in several clinical trials for the treatment of AML patients. First results highlight the effective and well-tolerated therapy with immune checkpoint inhibitors especially for relapsed AML after allogenic stem cell transplantation and provide a rationale for further clinical investigation.[112-114]

5.1.3.4. Leukemic progenitor cells – targeting the invincible?

Despite considerable advances in the treatment of AML and initially high remission rates, the majority of patients suffer from relapse during the course of disease, which in turn leads to the high mortality rate of AML. The main reason for occurrence of relapse is the presence of the so-called minimal residual disease (MRD), characterized by the persistence of residual chemoresistant leukemic stem and progenitor cells (LPCs) in the bone marrow of patients.[115-118] These LPCs represent a low frequent subpopulation with stem cell properties, including self-renewal capacity, distinct from the bulk of leukemic blasts. The phenotype of LPCs displays a complex heterogeneity, but several studies consider that the $CD34^+CD38^-$ population is the most relevant, as this fraction is able to induce leukemia in immunodeficient NOD/SCID mice even after transfer of very low cell numbers and thereby reproduce the complete leukemia disease.[118, 119] The fact that LPCs exist outside the $CD34^+CD38^-$ fraction was first proposed in the late 1990s, when researches could verify that $CD34^-$ cells were also capable to initiate leukemia in immune-deficient mice.[120] Nevertheless, several studies clearly have proven that the $CD34^+CD38^-$ fraction contains the most important leukemia-initiating cells[116, 121] and demonstrated that the $CD34^+CD38^-$ frequency correlates with therapy outcome and relapse-free survival.[116, 122] Therefore, targeting LPCs and inducing their complete elimination to prevent relapses and thereby improve the outcome of AML patients is one of the most critical steps for further development of novel therapeutic options.

For LPC-directed therapy the selection of suitable targets and the optimal time point are fundamental. The targets should be highly expressed by LPCs, but not by other cells especially normal hematopoietic progenitor cells (HPCs), and preferentially presented in the majority of patients to enable broadly applicable therapies. So far, novel therapeutic options for the elimination of LPCs focus on LPC-specific surface markers, LPC-related molecular pathways, or the LPC microenvironment. These therapeutic approaches aim primarily at the specific elimination of LPCs, but also at the combined targeting of both LPCs and AML blasts. Several cell surface markers have

been proposed as potential LPC-associated targets, such as CD33,[123] TIM3,[124] or CD44,[125] and various approaches targeting these markers are currently investigated in clinical trials. Furthermore, small-molecule inhibitors interfering LPC-specific signaling pathways, such as perifosine, an AKT inhibitor,[126] or carfilzomib, a proteasome inhibitor,[127] as well as immune-sensitizing agents, such as PARP1 inhibitors[128], are currently evaluated for the treatment of AML patients.

The more profound understanding and knowledge of LPC function and appearance might significantly improve the prognosis, therapy, and survival of AML patients and will hopefully reduce the high relapse rate of this malignancy in the future.

5.2. CANCER IMMUNOTHERAPY

Already in ancient Egypt 2,600 years before Christ, the high official Imhotep treated tumors by specifically provoking infections on the tumor site[129]. The idea of activating and harnessing the power of the immune system to fight cancer cells was then again pursued in the late 19th century by William B. Coley, who recognized spontaneous remissions of cancer patients after developing acute bacterial skin infections (erysipelas). After this observation, Coley injected streptococcus bacteria in patients with soft tissue sarcomas to stimulate an immune attack. These were the first experimental efforts to activate the immune system of cancer patients and initiate an anti-cancer immune response.[130-132] However, it lasted about 100 years until allogeneic hematopoietic stem cell transplantation (HSCT), the first effective immunotherapy, found its way into clinical routine.[133] This immunotherapy remains still an important pillar in the standard treatment of cancer especially for leukemias. Its effectiveness is explained by the induction of a graft-versus-leukemia effect by the adoptively transferred donor T cells.[134] This effect represents a proof of concept for the application and breakthrough of immunotherapy in the treatment of cancer. The field of immunotherapy has undergone incredible changes and tremendous progress over the past decades and has reached a milestone with the clinical advance of immune checkpoint inhibitors especially in solid tumors.[105, 106, 135] The understanding of the complex mechanisms of the immune system and how cancer cells evade the immune system is indispensable for the development of novel, clinically effective immunotherapeutic approaches.

5.2.1. THE IMMUNE SYSTEM – BASIS FOR EFFECTIVE IMMUNOTHERAPY

For effective cancer immunotherapy both the innate as well as the adaptive part of the immune system are relevant. The innate immune system is composed of cellular components, including dendritic cells (DCs), macrophages, granulocytes, mast cells, and natural killer cells, and non-cellular (humoral) components such as the complement system.[136] Especially DCs link the innate to the adaptive immune system by their function as professional antigen-presenting cells (APCs) presenting

protein fragments derived from incorporated pathogens and destroyed cells on their cell surface on major histocompatibility complex (MHC) molecules to cells of the adaptive immune system.[137] The cells of the adaptive immunity are lymphocytes, which are divided into B and T cells. T cells can be further subdivided into $CD8^+$ cytotoxic T lymphocytes (CTLs), $CD4^+$ T helper cells (T_h cells), as well as regulatory T cells (T_{reg} cells). The activation of naïve T cells is accomplished by the presentation of their cognate antigen through MHC molecules of APCs and requires three signals – T-cell receptor (TCR) recognition of MHC-presented peptides, costimulatory signals, and cytokines – to induce their activation, differentiation, and proliferation.[138, 139] Primarily, the role of the immune system is the distinction between self and non-self to protect the body from viruses, bacteria, or other pathogens. But the immune system is also capable to recognize and eliminate transformed malignant cells through T cells representing the main pillar of anti-cancer immunity.

5.2.1.1. Antigen presentation

For the recognition of transformed malignant cells by T cells, the presentation of tumor-specific or tumor-associated protein fragments by MHC molecules is of paramount importance. In humans, MHC is referred to as the human leukocyte antigen (HLA) complex. HLA molecules are distinguished into HLA class I and class II molecules. These two classes show apart from a cell type-dependent expression, differences in their molecular structure as well as distinct antigen processing pathways of the peptides they present. Both gene classes are highly polymorphic, encoded by a huge variety of different alleles. Furthermore, every individual carries a set of different genes for both classes, *e.g.* HLA-A, -B, and -C for class I.

HLA class I molecules are expressed by all nucleated cells and present small protein fragments, peptides of 8 – 12 amino acid lengths, of cytosolic and nuclear source proteins to $CD8^+$ T cells. The peptides are generated through the degradation of proteins mainly by proteasomes and then transported into the endoplasmic reticulum (ER) mainly *via* the transporter associated with antigen processing (TAP) (Figure 2). In the ER, the peptides are loaded onto heterodimeric HLA class I molecules, which are assembled of a polymorphic heavy chain and the light chain β_2-microglobulin (β_2m). The

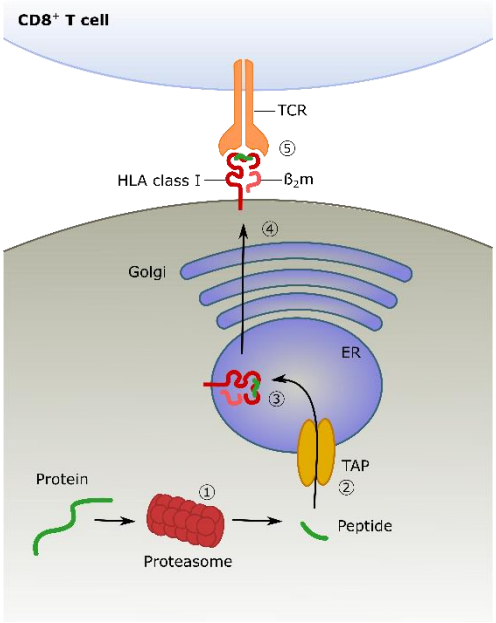

Figure 2: Simplified schema of HLA class I antigen processing. Intracellular proteins are degraded by the proteasome (1), originating peptides are transported *via* the transporter associated with antigen presentation (TAP) into the endoplasmic reticulum (2) and loaded onto HLA class I molecules (3). Peptide-HLA complexes are transported *via* the Golgi apparatus to the plasma membrane (4) for antigen presentation to the T-cell receptor (TCR) of $CD8^+$ T cells (5). Adapted from Neefjes *et al.*[140]

peptide-HLA class I complexes are then transported *via* the Golgi apparatus to the plasma membrane for antigen presentation to $CD8^+$ T cells.[140, 141]

A special feature of HLA molecules is their huge polymorphism, which results in a variety of peptide-binding grooves of the different allotypes encoded by distinct alleles. Thereby, every allotype binds peptides with a specific binding motif. The binding motif typically comprises two so-called anchor positions representing those amino acids which are the main determinants for peptide binding.[142, 143]

Likewise to HLA class I molecules, HLA class II molecules are encoded by three polymorphic genes (HLA-DR, -DQ, -DP) that harbor specific peptide binding properties. In contrast to HLA class I, HLA class II molecules bind 8 – 25 amino acid long peptides (Figure 3) and are more promiscuous concerning peptide binding.[144] HLA class II molecules are primarily expressed by professional APCs, including DCs, macrophages, and B cells, but it was also demonstrated that malignant cells express these antigens.[145, 146] The HLA class II antigen presentation pathway starts with the assembly of the α- and β-chains in the ER, which are stabilized by the invariant chain. This complex is then transported into late endosomal compartments, where the invariant chain is digested to a residual class II-associated invariant chain peptide (CLIP). Peptides derived from extracellular proteins, which are degraded in the endosomal pathway, are then exchanged with the CLIP. The peptide-HLA class II complexes are transported to the plasma membrane and present their bound peptide to $CD4^+$ T cells.[140] Furthermore, HLA class I and II antigen processing are linked over so-called cross-presentation enabling the presentation of exogenous antigens on HLA class I molecules especially in DCs.[147] These mechanisms of antigen presentation of self- and non-self peptides to immune cells are the main pillar of anti-cancer immunity.

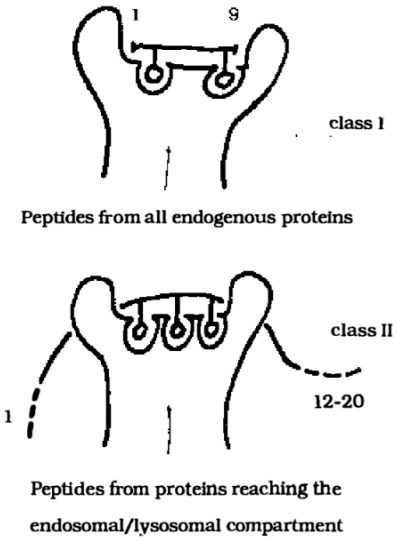

Figure 3: The principle differences between HLA class I and class II-restricted peptide binding in a simplistic view.[142]

5.2.1.2. The interaction between immune system and malignant cells

The theory of a reciprocal interaction between the immune system and malignant cells was first proposed more than 50 years ago as cancer immunosurveillance hypothesis[148-150] and was adapted to the cancer immunoediting hypothesis over the last decades as new insights were constantly gained.[151] Nowadays, the model of cancer immunoediting encompasses the three phases elimination, equilibrium, and escape and is widely accepted. Several studies have supported our understanding of the complex relationship between immune cells and cancer cells and identified

crucial points for therapeutic interventions.

Tumor cell development and the transformation of normal cells into malignant cells is a gradual process, which requires critical genetic alterations and mutations for example in tumor suppressor genes, oncogenes, and DNA damage repair genes. Consequently, the transformed cells start unregulated proliferation and acquire further mutations. As a result of these cellular changes, the malignant cells present tumor antigens on their HLA molecules, which can be classified into differentiation antigens, mutation-derived antigens, overexpressed antigens, cancer/testis antigens (CTAs), or viral antigens. The presentation of these tumor-associated (TAAs) or tumor-specific antigens (TSAs) to cells of the immune system drives the destruction of the transformed cells by the immune system. This first phase of cancer immunoediting is therefore described as elimination, which represents the classical concept of cancer immunosurveillance.

When tumors escape this immunosurveillance, for example by the outgrowth of poorly immunogenic tumor cell clones, which lack such rejection antigens, a period of latency, the so-called equilibrium phase, begins. With clinically detectable malignant disease the escape phase of the tumor is reached. Tumor escape occurs through several mechanisms and is characterized by the selection of tumor clones, which will then continue to progress. These escape mechanisms could comprise the loss of immunogenicity by downregulation or even loss of HLA expression, the resistance to inhibitory factors secreted by immune cells within the tumor microenvironment, or the secretion of inhibitory molecules by the tumor itself hampering the function of tumor-specific immune cells.[152] Interestingly, our group could not verify that downregulation or loss of HLA expression is such an important mechanism of tumor escape as we could demonstrate high HLA surface expression on several different tumor entities.[153]

The profound understanding of the complex interplay between the immune system and cancer cells is fundamental for the rational design of novel anti-cancer immunotherapies.

5.2.2. CANCER IMMUNOTHERAPY APPROACHES IN LEUKEMIA

As already mentioned in the beginning of this chapter, immunotherapy has fundamentally changed the landscape of cancer treatment especially for solid tumors in recent years. In the following sections, different immunotherapeutic approaches and concepts will be discussed more precisely with a special focus on anti-leukemia treatments.

Beside the manipulation of immune checkpoints or pathways, the field of immunotherapy dramatically extends beyond immune checkpoint inhibitor therapy by direct targeting of malignant cells through TAAs or TSAs. This field of antigen-specific immunotherapy is developing at a rapid pace – novel approaches are constantly being established and additional target structures are

discovered. In general, several distinct concepts can be roughly distinguished: antibody-based concepts, adoptive cell transfer (ACT), and vaccination strategies.

5.2.2.1. Antibody-based immunotherapy

One of the most clinically effective antibody-based immunotherapeutic strategies is the modulation and inhibition of immune checkpoints, particularly CTLA-4, PD-1, or PD-L1. The 2018 Nobel Prize in Physiology or Medicine has been awarded to James P. Allison and Tasuku Honjo, whose groundbreaking work enabled the development of immune checkpoint inhibitors that have revolutionized the treatment of several solid tumors in recent years, especially melanoma.[105, 106, 135] However, the success and effectiveness of immune checkpoint inhibitor therapy depends on various factors. In particular, the mutational burden of the tumor,[154, 155] HLA class I genotype,[156] preexisting anti-tumor immunity,[157] and (over-)expression of checkpoint inhibitor ligands by the tumor[158] further determine the effectiveness of immune checkpoint inhibitor therapy. Despite the low mutational burden,[56-59] first clinical studies have already demonstrated initial promising results of immune checkpoint inhibitor therapy also in leukemias[112-114].

Beyond the modulation of immune checkpoints, direct targeting of TAAs and TSAs by different antibody-based approaches dramatically changed the treatment landscape of leukemias in recent years.

Tumor-directed monoclonal antibodies, including bispecific antibodies such as BiTEs or antibody drug conjugates, are currently under development and some of them have already been approved. Monoclonal antibodies bind specific tumor antigens and thereby activate antibody-dependent cytotoxicity, affect downstream signals, directly block receptors, or recruit immune cells. Antibody drug conjugates combine antigen-specific antibodies with an additional cytotoxic agent such as microtubule inhibitors or DNA-damaging chemotherapeutic drugs.[159] One remarkably effective antibody-based immunotherapy approach, particularly for the treatment of B-cell leukemias, involves the application of chimeric antigen receptor (CAR) T cells as a form of ACT. CARs combine antigen-binding domains – in most cases a single-chain variable fragment (scFv) derived from the variable domains of antibodies specific for the antigen of choice – through a linker and transmembrane domain with a signaling module derived from intracellular signaling domains of different costimulatory molecules such as CD3ζ, CD28, OX40, or CD137 (4-1BB). In comparison to other ACT approaches using TCR-engineered T cells or autologous tumor-infiltrating lymphocytes (TILs), CAR T cells act independent of HLA expression on the tumor and further costimulation.[160, 161]

Several surface molecules that can be targeted by the above described antibody-based immunotherapeutic approaches were identified in the last decades and a number of preclinical and clinical studies investigated the potential of these approaches and targets for leukemia patients.

The targeted therapy against the lineage-specific marker CD19 commonly expressed on B cells has led to the greatest and most notable clinical success in the treatment of B-cell leukemias since the introduction of stem cell transplantation. CD19 CAR T cells have revealed remarkable anti-tumor activity in patients with refractory B-cell malignancies and were therefore approved in 2017 and 2018 by the FDA for the treatment of ALL and different subtypes of lymphoma.[162, 163] Additionally, the CD19-directed CD3 BiTE blinatumomab represents an outstanding example for the successful development of a bispecific antibody targeting the CD19 antigen. Blinatumomab, also known as AMG103, is FDA-approved for the treatment of ALL and significantly prolonged overall survival of these patients.[164] Furthermore, targeting another lineage-specific molecule demonstrated great benefits in B-cell malignancies. The anti-CD20 monoclonal antibody rituximab is already part of the standard therapy for CLL and other B-cell lymphomas.[165] Nevertheless, targeting only one single antigen can lead to the general problem of epitope loss. Therefore, other B-cell lineage-specific surface markers such as CD22 or especially combinatorial targeting of more than one marker are under investigation and will improve the treatment of B-cell malignancies in the future.

For myeloid leukemias especially the myeloid lineage-specific antigens CD33 and CD123 are interesting antigens to target. As described in more detail above Gemtuzumab ozogamicin (Mylotarg®), a CD33-directed antibody drug conjugate, is already FDA-approved for the treatment of AML. Especially for AML, targeting of the overexpressed surface receptor FLT3 by monoclonal antibodies such as FLYSYN[166] or bispecific antibody compounds[92] already exhibited first promising results.

Most of these antibody-based agents are yet under development, but harbor the potential to supplement the current treatment options in the future to control and even eliminate hematological malignancies especially for those diseases expressing a common dominant antigen.

5.2.2.2. Adoptive cell transfer

The above described CAR T cells can be classified on the one hand as antibody-based immunotherapies but on the other hand also as a form of ACT. In general, ACT administers specific anti-tumor immune cells including T lymphocytes, natural killer cells, or DCs to induce a robust anti-tumor response in the patient.[167, 168] Adoptively transferred T cells are either naturally occurring tumor-specific TILs derived from the tumor or genetically modified T cells derived from blood-circulating T lymphocytes. For this purpose, the T cells are isolated from the blood or tumor mass, manipulated and expanded *ex vivo,* and then reinfused into the lymphodepleted patient. For genetic modification either cloned TCR or CAR constructs targeting tumor-specific antigens are transferred into the T cells. For gene transfer different methods such as transient mRNA transfection,[169] retroviral vectors,[170] lentiviral vectors,[171] transposons,[172] or homologous

recombination after gene editing[173] are utilized. TCR-engineered T cells and TILs act in an HLA-dependent way whereas CAR T cells recognize their antigen HLA-independently. Many ACT-based therapies reached late-phase clinical trials[174, 175] or were already approved for the treatment of different B-cell malignancies. Regarding hematological malignancies, the development of further ACT strategies represents an advancement of standard of care approaches applying autologous and allogenic HSCT.

5.2.2.3. Vaccine-based immunotherapeutic approaches

The current success of T-cell-based immunotherapies, in particular of CAR T cells[176-178] and immune checkpoint inhibitors,[179-181] as well as the immunogenicity of leukemias observed by the graft-versus-leukemia effect after HSCT[134], provide evidence that the induction of a specific immune response also through vaccine-based immunotherapy is feasible and could contribute to the elimination of hematological malignancies. Therapeutic cancer vaccines are designed to generate new antigen-specific T-cell responses or amplify preexisting responses against malignant cells. Furthermore, such T-cell-based immunotherapies are expected to provide an anti-tumor memory and therefore permanently protect the patient against the specific cancer at least as long as the cancer cells present the target antigens.

The four key components of an optimal cancer vaccine are: 1) suitable tumor antigens, 2) vaccine composition, 3) strong immune adjuvants, and 4) delivery vehicles.[182] In the following section these key components will be discussed in more detail.

Tumor antigens – the more specific, the more effective?

Tumor antigens can be roughly divided into the two classes of TAAs and TSAs. TAAs include overexpressed antigens, tissue differentiation antigens, or aberrantly expressed or processed antigens as well as CTAs, whereas TSAs are mutation-derived neoantigens or antigens generated from oncogenic viral proteins.[182] The identification and selection of the optimal target antigen for effective vaccination has long been the major priority in the area of immunotherapy.

Tissue-specific antigens, so-called differentiation antigens, are cell lineage-specific expressed antigens from which a tumor and its corresponding normal tissue arise from. Tissue differentiation antigens, which are widely used for vaccination approaches include for example prostate-specific membrane antigen (PSMA),[183] melanoma antigen recognized by T cells 1 (MART1, Melan-A),[184] or gp100.[185] These antigens are limited to few cancer entities and are also well established and popular targets for antibody-based approaches.[182]

Aberrantly expressed or processed antigens include all types of classical or cryptic peptides that are specifically presented on tumor cells due to differential tumor-specific antigen processing or other

cellular processes, which are altered in tumor cells and thereby influencing the presentation of antigens. Cryptic peptides for example emerge from tumor-specific proteasomal splicing, non-canonical translation events, or non-coding sequences such as introns or antisense transcripts.[186-189] Furthermore, distinct peptides from normal cellular proteins could be presented in a tumor-associated fashion in comparison to other peptides derived from the same source protein. So far, the complex process of HLA ligand formation, frequently altered in tumor cells leading to the expression of tumor-associated HLA ligands, is not perfectly understood.[190-192]

CTAs are tumor-associated germline antigens and are therefore more tumor-specific than differentiation antigens.[193] Several CTAs like the melanoma-associated antigen (MAGE) family, NY-ESO1, or MUC1 have been investigated in different vaccination approaches in the last years.[194, 195]

The last group of TAAs includes overexpressed self-proteins or peptides. The identification of overexpressed antigens can be utilized by two different ways, which will be discussed in a later section in more detail. On the one hand, overexpressed proteins can be determined by gene expression analyses and HLA-restricted peptides of those proteins can be predicted through *in silico* methods.[196-198] With the special focus on leukemias, several leukemia-associated antigens (LAAs), including WT1,[197] PR1,[199] and RHAMM,[198] have been identified with this approach and found their way into clinical phase I/II vaccination trials. On the other hand, direct identification approaches using a mass spectrometry-based strategy have been applied more and more in recent years enabling the comprehensive identification of HLA ligands of leukemic cells.[153, 200-203]

A major disadvantage of all these TAAs is that they are also presented on normal tissues and therefore lack full tumor specificity causing an existing central tolerance of antigen-specific T cells, which must be overcome by the vaccine. In comparison, TSAs are clearly tumor-specific with no expression on normal tissues and cells, thereby on-target/off-tumor effects can be completely avoided. TSAs can be divided into two groups: mutation-derived neoantigens or oncogenic viral proteins.

Antigens derived from oncogenic viruses have been identified in virus-induced cancers such as human papillomavirus (HPV)-associated cervical cancer and others. Vaccination approaches with viral antigens have already shown efficacy in both, preventive[204] and therapeutic[205] settings.

Antigens derived from cancer-specific mutations, so-called neoantigens, are ideal targets for antigen-specific immunotherapy due to their specificity and high immunogenic potential. For several years, only indirect evidence of neoepitope presentation by detection of neoepitope-specific T cells was possible.[206] Recently, direct evidence of HLA-presented neoantigens was accomplished by mass spectrometry.[207-209] The encouraging potential of neoantigen-based vaccination approaches was already investigated in phase I clinical trials assessing personalized neoantigen-based vaccines in

melanoma patients.[210, 211] However, it is extremely important to keep in mind that most mutations are individual for single patients and are therefore not suitable for broadly applicable therapies. Only a small set of mutations are recurrent in single cancer entities. Furthermore, several studies demonstrated that only a very small fraction of mutations at the DNA sequence level results in peptides naturally presented on HLA molecules.[209, 210, 212] Nevertheless, neoantigen-based immunotherapy approaches have proven their potential in early clinical trials. Through the improved high-throughput analysis of tumor exome and RNA sequencing data together with enhanced mass spectrometry analysis, these approaches will provide and discover additional novel epitopes and undergo broad clinical investigation for several cancer entities in the near future.

Vaccine composition – cells, peptides, or nucleic acids?

Besides the selection of suitable tumor rejection antigens, the vaccine composition is also of great importance. During the last years several different approaches of diverse compositions and formulations have been investigated. Cancer vaccines can be applied as cells containing or presenting the antigen of choice or as peptides, proteins, or nucleic acids (DNA/RNA), which directly represent or encode for the target antigen.

Cell-based vaccine approaches either use whole tumor cells, tumor cell lysates,[213, 214] or DCs that are genetically modified or antigen-loaded.[215] DC vaccination was first explored in a clinical trial already 25 years ago.[216] Since then, a variety of DC subsets, different culture protocols, and treatment regimens have been developed and tested. As a result, the first therapeutic vaccine was approved by the FDA in 2010 and by the EMA in 2013.[217] However, the approval was withdrawn by the EMA in 2015.[218] The major disadvantage of cell-based vaccines is the tremendous effort for the production of patient-individualized clinical vaccines manufactured under GMP conditions. However, these vaccines can score with encouraging clinical results also in patients with advanced cancers.[219, 220]

Nucleic acid-based approaches applying DNA or RNA vaccines are being intensively studied in recent years. The huge advantage of such vaccines are the built-in immune adjuvants as specific forms of DNA and RNA can stimulate the innate immune system *via* toll-like receptors (TLRs).[221, 222]

Peptide-based vaccines offer a range of advantages compared to other approaches. Peptides are easier and less expensive to synthesize even in GMP quality. Induced immune responses can be monitored in an antigen-specific manner due to the exact knowledge of the vaccinated epitope. Furthermore, they can be produced in a modular premanufactured “warehouse” system, so multiple peptides can be easily combined to multipeptide vaccines for individual patients. One major drawback of the approach is the HLA restriction of unique peptides calling for complete patient-individualized peptide vaccine cocktails or the limitation to broadly applicable peptides matching the most prevalent HLA allotypes and thereby excluding single patients. Peptide-based cancer vaccines

are proven to be safe and well-tolerated, but so far have low therapeutic effects and limited immunogenicity.[223, 224] To overcome this obstacle the combination with suitable adjuvants and/or delivery systems or combinatorial therapies remains an important pillar for clinical effective peptide-based vaccination approaches.

Multipeptide vaccination approaches for example the phase II clinical trial with the vaccine IMA901 already demonstrated clinically effectiveness and an association of peptide-specific T-cell responses with overall survival of the patients.[225] However, these positive results could not be confirmed in a phase III clinical trial,[226] possibly due to the combination of the peptide vaccine with the TKI Sunitinib, for which a negative impact on cytotoxic T-cell response was previously described.[227] Another phase I multipeptide vaccination trial in glioblastoma patients combining unmutated with mutated antigens showed favorable safety and a strong immunogenicity. Unmutated antigens predominantly elicited $CD8^+$ T cell responses, whereas neoantigens induced mainly $CD4^+$ T-cell responses.[228]

Adjuvants – nothing without activation?

The efficacy of cancer vaccines additionally depends on strong adjuvants and immunomodulators, which provide a general immune stimulus, thereby inducing a stronger anti-tumor immune response. Adjuvants represent a diverse range of molecules and materials and with the increasing understanding of immune cell function and their interaction with growing tumors novel adjuvants are available and are investigated in diverse vaccination settings.[229]

One popular adjuvant is GM-CSF, which recruits and activates APCs at the side of injection. Nevertheless, the overall adjuvant effect of GM-CSF is weak[225, 230] and strongly depends on the administered doses as high concentrations might even inhibit T-cell function.[231]

A huge repertoire of several TLR-based immune adjuvants are already available or under development and high expectations have been placed on these adjuvants. TLR agonist such as poly-ICLC, monophosphoryl lipid A (MPL), or CpG oligodeoxynucleotide activate the innate immune system through their binding to TLRs. The TLR7/8 agonist imiquimod (Aldara®), a single-stranded RNA, is one of the most common TLR agonist used in recent clinical vaccination trials.[232] Another very promising TLR-based adjuvant is a derivate of the TLR2-targeting synthetic analogue of the bacterial lipopeptide Pam_3Cys-Ser-Ser. Recently, the induction of a strong anti-vaccine T-cell response after peptide vaccination together with this Pam_3Cys derivative was described.[229, 233, 234]

Since the efficacy of therapeutic cancer vaccines are so far limited, further development and clinical investigation of strong adjuvants is relevant for the clinical success of T-cell-based immunotherapies especially in the context of peptide-based vaccination approaches.

Delivery vehicles – last but not least

Delivery vehicles are an essential component of cancer vaccines especially for peptide-/protein- and nucleic acid-based vaccines as these vaccines must be protected from fast degradation. Furthermore, some of these agents are at the same time delivery vehicles and exhibit adjuvant effects. Delivery vehicles can be composed for example of emulsions, liposomes, or virosomes. Emulsions such as Montanide ISA 51 (incomplete Freund's adjuvant analogue) are the most common vehicles used in clinical trials.[235] Montanide, a water-in-oil emulsion, has a depot effect and slowly releases the antigen at the injection site.[236] Several other delivery vehicles are currently in development and are investigated in preclinical and clinical trials. The selection of the best suitable adjuvant and delivery vehicles has a strong impact on the effectiveness and immunogenicity of cancer vaccines.

Despite the large number of different antigens, adjuvants, delivery strategies, and formulations that have been tested to date, comparative data of all these approaches are currently almost non-existent. Therefore, key questions on the most effective antigens, type of adjuvant, administration approach, dose, route, and schedule remain still to be answered. Furthermore, for clinical effective application of cancer vaccines optimal combination therapies still need to be identified.

5.2.2.4. Clinical effective cancer vaccination – novel therapy combinations

Even though cancer vaccines may be effective in cases of early cancer diagnosis or in the setting of MRD, therapeutic cancer vaccines most likely require the combination with other treatments to overcome tumor-mediated immunosuppression and to be clinically effective in established cancers. The range of possible combinations is endless. Combinatorial approaches of cancer vaccines with immune checkpoint inhibitors, neutralizing antibodies to inhibitory cytokines, small molecule inhibition of T_{regs}, or immunomodulatory drugs are already investigated in several studies.[237-240]

Especially immunomodulatory drugs such as lenalidomide (Revlimid®) and pomalidomide (Actimid®) are potent modulators of cellular immune and cytokine responses. The effects of these agents include enhanced T-cell responses,[241] reduction of T_{regs},[242] and the reconstitution of the defective T-cell immune synapse especially in malignancies with profound immune defects.[243, 244] These preclinical investigations clearly indicate that the combination of T-cell-based immunotherapies with immunomodulatory agents harbor a considerable potential for further treatment developments.

The future of cancer treatment will include combinations of different anti-tumor immune therapies, which will likely stimulate more robust T-cell responses and improve clinical responses and outcome in cancer and leukemia patients.

5.3. IMMUNOPEPTIDOMICS

The knowledge about and the identification of the entirety of HLA-presented peptides, which is referred to as the HLA ligandome or the immunopeptidome, its regulation, changes, and adaptations during malignant transformation or under specific therapies is indispensable for gaining insight into the fundamental rules of immune recognition and for the development of innovative and novel immunotherapeutic approaches. The field of immunopeptidomics, which deals with the mass spectrometry-based identification of the HLA ligandome, has grown rapidly in recent years as a result of numerous technical and bioinformatic advances and has become an important component in the development and application of novel anti-cancer immunotherapies. Immunopeptidomics does not only enable the identification of promising naturally presented TAAs with potential for clinical applications,[153, 200-203] but also increases our understanding of disease and disease progression and supports the development of novel biomarkers.[245, 246]

For several years the identification of tumor-associated overexpressed antigens or mutation-derived neoantigens was solely based on genome and transcriptome sequencing followed by *in silico* prediction of HLA-presented peptides using algorithms such as SYFPEITHI[247] and NetMHCpan.[248] The large number of predicted candidates had then to be screened for immunogenicity by extensive *in vitro* assays. Furthermore, a huge drawback of prediction-based approaches lies in the distorted correlation of gene expression with HLA-restricted antigen presentation and in the immunopeptidome being an independent complex layer molded by the antigen presentation machinery and therefore not necessarily mirrored the transcriptome nor the proteome.[209, 249-251]

With the tremendous development and progress in liquid chromatography, mass spectrometry, and bioinformatics the large-scale and in-depth direct identification of up to ten thousands of HLA-presented peptides from one single primary patient sample became feasible.[153, 200-203] Especially the development of orbitrap mass analyzers extremely improved speed, accuracy, resolution, and dynamic range. Furthermore, advances in bioinformatics enable remarkably fast spectra interpretation and peptide annotation in a high-throughput fashion. In contrast to epitope prediction algorithms, the mass spectrometry-based mapping of the immunopeptidome is the only unbiased approach for the comprehensive identification of tumor rejection antigen candidates validating the natural processing and presentation of these antigens.[252] The translation of immunopeptidomics into the clinic is already investigated in different clinical trials,[253, 254] but the low-throughput sample capacity due to many sample handling steps is a major issue. Recently, a high-throughput platform for sequential immunoaffinity purifications of several samples simultaneously has been described, which could accelerate sample analysis.[255]

In the next years, mass spectrometry-based immunopeptidomics will guide the development and advances of further vaccination-based immunotherapies and will therefore contribute to the improvement of clinically effective and patient-individualized T-cell-based immunotherapeutic approaches such as peptide vaccination for cancer patients.

5.4. AIM OF THIS STUDY

The ongoing development and advancement of novel and innovative therapeutic options for the treatment of hematological neoplasms in recent years will evermore enable a more specific, clinically effective, and patient-individualized treatment of leukemia patients. In most hematological neoplasms the established therapies are able to achieve remissions, but the persistence of residual malignant cells often leads to relapses and therefore a permanent cure for the majority of patients still remains impossible. Therefore, the development of novel, clinically effective therapeutic approaches especially for the prevention of relapses is still indispensable. Thus, the aims of all projects presented in this thesis are the development and the improvement of broadly applicable peptide-based immunotherapies for leukemia patients. On the one hand, the identification and characterization of novel tumor-associated antigens for CML and AML will allow the definition of target candidates for peptide-based immunotherapy approaches. On the other hand, the combination of peptide-based immunotherapy with immunomodulatory agents call for the thorough characterization of the effect of the combinatorial drugs on the immunopeptidome of the tumor cells, as investigated here for CLL and lenalidomide. With these projects we would like to contribute to the development of novel therapeutic options for leukemia patients in the rapidly developing field of T-cell-based immunotherapy.

5.5. REFERENCES

1. Kampen KR. The discovery and early understanding of leukemia. *Leuk Res* 36(1): 6-13 (2012).
2. Piller G. Leukaemia - a brief historical review from ancient times to 1950. *Br J Haematol* 112(2): 282-292 (2001).
3. Ehrlich P. Methodologische Beiträge zur Physiologie und Pathologie der verschiedenen Formen der Leukocyten. *Zeitschrift für klinische Medizin* Band 1 (1880).
4. Olsen M. Overview of Hematologic Malignancies. In *Hematologic Malignancies in Adults*, Olsen M and Zitella LJ. (2013) Oncology Nursing Society: Pittsburgh.
5. Vardiman JW. The World Health Organization (WHO) classification of tumors of the hematopoietic and lymphoid tissues: an overview with emphasis on the myeloid neoplasms. *Chem Biol Interact* 184(1-2): 16-20 (2010).
6. Kipps TJ, Stevenson FK, Wu CJ, Croce CM, Packham G, Wierda WG, O'Brien S, Gribben J, and Rai K. Chronic lymphocytic leukaemia. *Nat Rev Dis Primers* 3: 17008 (2017).
7. Swerdlow S, Campo E, Harris N, Jaffe E, Pileri S, Stein H, and Thiele J. WHO Classification of Tumours of Haematopoietic and Lymphoid Tissues. *World Health Organization* 4th ed (2008).
8. Cancer Stat Facts: Leukemia - Chronic Lymphocytic Leukemia (CLL). 2019; Available from: https://seer.cancer.gov/statfacts/html/clyl.html.
9. Hamblin TJ, Davis Z, Gardiner A, Oscier DG, and Stevenson FK. Unmutated Ig V(H) genes are associated with a more aggressive form of chronic lymphocytic leukemia. *Blood* 94(6): 1848-1854 (1999).
10. Damle RN, Wasil T, Fais F, Ghiotto F, Valetto A, Allen SL, Buchbinder A, Budman D, Dittmar K, Kolitz J, Lichtman SM, Schulman P, Vinciguerra VP, Rai KR, Ferrarini M, and Chiorazzi N. Ig V gene mutation status and CD38 expression as novel prognostic indicators in chronic lymphocytic leukemia. *Blood* 94(6): 1840-1847 (1999).
11. Döhner H, Stilgenbauer S, Benner A, Leupolt E, Kröber A, Bullinger L, Döhner K, Bentz M, and Lichter P. Genomic aberrations and survival in chronic lymphocytic leukemia. *N Engl J Med* 343(26): 1910-1916 (2000).
12. Landau DA, Tausch E, Taylor-Weiner AN, Stewart C, Reiter JG, Bahlo J, Kluth S, Bozic I, Lawrence M, Böttcher S, Carter SL, Cibulskis K, Mertens D, Sougnez CL, Rosenberg M, Hess JM, Edelmann J, Kless S, Kneba M, Ritgen M, Fink A, Fischer K, Gabriel S, Lander ES, Nowak MA, Dohner H, Hallek M, Neuberg D, Getz G, Stilgenbauer S, and Wu CJ. Mutations driving CLL and their evolution in progression and relapse. *Nature* 526(7574): 525-530 (2015).
13. Puente XS, Beà S, Valdés-Mas R, Villamor N, Gutiérrez-Abril J, Martín-Subero JI, Munar M, Rubio-Pérez C, Jares P, Aymerich M, Baumann T, Beekman R, Belver L, Carrio A, Castellano G, Clot G, Colado E, Colomer D, Costa D, Delgado J, Enjuanes A, Estivill X, Ferrando AA, Gelpí JL, González B, González S, González M, Gut M, Hernández-Rivas JM, López-Guerra M, Martín-García D, Navarro A, Nicolás P, Orozco M, Payer ÁR, Pinyol M, Pisano DG, Puente DA, Queirós AC, Quesada V, Romeo-Casabona CM, Royo C, Royo R, Rozman M, Russiñol N, Salaverría I, Stamatopoulos K, Stunnenberg HG, Tamborero D, Terol MJ, Valencia A, López-Bigas N, Torrents D, Gut I, López-Guillermo A, López-Otín C, and Campo E. Non-coding recurrent mutations in chronic lymphocytic leukaemia. *Nature* 526(7574): 519-524 (2015).
14. Rai KR, Sawitsky A, Cronkite EP, Chanana AD, Levy RN, and Pasternack BS. Clinical staging of chronic lymphocytic leukemia. *Blood* 46(2): 219-234 (1975).
15. Binet JL, Leporrier M, Dighiero G, Charron D, D'Athis P, Vaugier G, Beral HM, Natali JC, Raphael M, Nizet B, and Follezou JY. A clinical staging system for chronic lymphocytic leukemia: prognostic significance. *Cancer* 40(2): 855-864 (1977).
16. Hallek M, Cheson BD, Catovsky D, Caligaris-Cappio F, Dighiero G, Döhner H, Hillmen P, Keating M, Montserrat E, Chiorazzi N, Stilgenbauer S, Rai KR, Byrd JC, Eichhorst B, O'Brien S, Robak T, Seymour JF, and Kipps TJ. iwCLL guidelines for diagnosis, indications for treatment, response assessment, and supportive management of CLL. *Blood* 131(25): 2745-2760 (2018).
17. Eichhorst B, Robak T, Montserrat E, Ghia P, Hillmen P, Hallek M, Buske C, and Esmo Guidelines Committee. Chronic lymphocytic leukaemia: ESMO Clinical Practice Guidelines for diagnosis, treatment and follow-up. *Ann Oncol* 26 Suppl 5: v78-84 (2015).
18. Khan M and Siddiqi T. Targeted Therapies in CLL: Monotherapy Versus Combination Approaches. *Curr Hematol Malig Rep* 13(6): 525-533 (2018).
19. Nowell P and Hungerford D. A minute chromosome in human chronic granulocytic leukemia. *Science* 132: 1497 (1960).
20. Melo JV. The diversity of BCR-ABL fusion proteins and their relationship to leukemia phenotype. *Blood* 88(7): 2375-2384 (1996).
21. Guo JQ, Wang JY, and Arlinghaus RB. Detection of BCR-ABL proteins in blood cells of benign phase chronic myelogenous leukemia patients. *Cancer Res* 51(11): 3048-3051 (1991).
22. Konopka JB, Watanabe SM, and Witte ON. An alteration of the human c-abl protein in K562 leukemia cells unmasks associated tyrosine kinase activity. *Cell* 37(3): 1035-1042 (1984).
23. Mandanas RA, Leibowitz DS, Gharehbaghi K, Tauchi T, Burgess GS, Miyazawa K, Jayaram HN, and Boswell HS. Role of p21 RAS in p210 bcr-abl transformation of murine myeloid cells. *Blood* 82(6): 1838-1847 (1993).
24. Okuda K, Matulonis U, Salgia R, Kanakura Y, Druker B, and Griffin JD. Factor independence of human myeloid leukemia cell lines is associated with increased phosphorylation of the proto-oncogene Raf-1. *Exp Hematol* 22(11): 1111-1117 (1994).
25. Sawyers CL, Callahan W, and Witte ON. Dominant negative MYC blocks transformation by ABL oncogenes. *Cell* 70(6): 901-910 (1992).

26. Shuai K, Halpern J, ten Hoeve J, Rao X, and Sawyers CL. Constitutive activation of STAT5 by the BCR-ABL oncogene in chronic myelogenous leukemia. *Oncogene* 13(2): 247-254 (1996).
27. Hehlmann R, Müller MC, Lauseker M, Hanfstein B, Fabarius A, Schreiber A, Proetel U, Pletsch N, Pfirrmann M, Haferlach C, Schnittger S, Einsele H, Dengler J, Falge C, Kanz L, Neubauer A, Kneba M, Stegelmann F, Pfreundschuh M, Waller CF, Spiekermann K, Baerlocher GM, Ehninger G, Heim D, Heimpel H, Nerl C, Krause SW, Hossfeld DK, Kolb HJ, Hasford J, Saussele S, and Hochhaus A. Deep molecular response is reached by the majority of patients treated with imatinib, predicts survival, and is achieved more quickly by optimized high-dose imatinib: results from the randomized CML-study IV. *J Clin Oncol* 32(5): 415-423 (2014).
28. Jabbour E and Kantarjian H. Chronic myeloid leukemia: 2016 update on diagnosis, therapy, and monitoring. *Am J Hematol* 91(2): 252-265 (2016).
29. O'Brien SG, Guilhot F, Larson RA, Gathmann I, Baccarani M, Cervantes F, Cornelissen JJ, Fischer T, Hochhaus A, Hughes T, Lechner K, Nielsen JL, Rousselot P, Reiffers J, Saglio G, Shepherd J, Simonsson B, Gratwohl A, Goldman JM, Kantarjian H, Taylor K, Verhoef G, Bolton AE, Capdeville R, Druker BJ, and IRIS Investigators. Imatinib compared with interferon and low-dose cytarabine for newly diagnosed chronic-phase chronic myeloid leukemia. *N Engl J Med* 348(11): 994-1004 (2003).
30. Cortes JE, Kim DW, Kantarjian HM, Brümmendorf TH, Dyagil I, Griskevicius L, Malhotra H, Powell C, Gogat K, Countouriotis AM, and Gambacorti-Passerini C. Bosutinib versus imatinib in newly diagnosed chronic-phase chronic myeloid leukemia: results from the BELA trial. *J Clin Oncol* 30(28): 3486-3492 (2012).
31. Kantarjian H, Shah NP, Hochhaus A, Cortes J, Shah S, Ayala M, Moiraghi B, Shen Z, Mayer J, Pasquini R, Nakamae H, Huguet F, Boqué C, Chuah C, Bleickardt E, Bradley-Garelik MB, Zhu C, Szatrowski T, Shapiro D, and Baccarani M. Dasatinib versus imatinib in newly diagnosed chronic-phase chronic myeloid leukemia. *N Engl J Med* 362(24): 2260-2270 (2010).
32. Saglio G, Kim DW, Issaragrisil S, le Coutre P, Etienne G, Lobo C, Pasquini R, Clark RE, Hochhaus A, Hughes TP, Gallagher N, Hoenekopp A, Dong M, Haque A, Larson RA, Kantarjian HM, and ENESTnd Investigators. Nilotinib versus imatinib for newly diagnosed chronic myeloid leukemia. *N Engl J Med* 362(24): 2251-2259 (2010).
33. Kantarjian HM, Kim D-W, Pinilla-Ibarz J, Coutre PDL, Paquette R, Chuah C, Nicolini FE, Apperley J, Khoury HJ, Talpaz M, DiPersio JF, Baccarani M, Lustgarten S, Haluska FG, Guilhot F, Deininger MWN, Hochhaus A, Hughes TP, Shah NP, and Cortes JE. Ponatinib (PON) in patients (pts) with Philadelphia chromosome-positive (Ph+) leukemias resistant or intolerant to dasatinib or nilotinib, or with the T315I mutation: Longer-term follow up of the PACE trial. *J Clin Oncol* 32(15_suppl): 7081-7081 (2014).
34. Machova Polakova K, Kulvait V, Benesova A, Linhartova J, Klamova H, Jaruskova M, de Benedittis C, Haferlach T, Baccarani M, Martinelli G, Stopka T, Ernst T, Hochhaus A, Kohlmann A, and Soverini S. Next-generation deep sequencing improves detection of BCR-ABL1 kinase domain mutations emerging under tyrosine kinase inhibitor treatment of chronic myeloid leukemia patients in chronic phase. *J Cancer Res Clin Oncol* 141(5): 887-899 (2015).
35. Schmidt M, Rinke J, Schäfer V, Schnittger S, Kohlmann A, Obstfelder E, Kunert C, Ziermann J, Winkelmann N, Eigendorff E, Haferlach T, Haferlach C, Hochhaus A, and Ernst T. Molecular-defined clonal evolution in patients with chronic myeloid leukemia independent of the BCR-ABL status. *Leukemia* 28(12): 2292-2299 (2014).
36. Mahon FX, Réa D, Guilhot J, Guilhot F, Huguet F, Nicolini F, Legros L, Charbonnier A, Guerci A, Varet B, Etienne G, Reiffers J, Rousselot P, and Intergroupe Français des Leucémies Myéloides Chronïques. Discontinuation of imatinib in patients with chronic myeloid leukaemia who have maintained complete molecular remission for at least 2 years: the prospective, multicentre Stop Imatinib (STIM) trial. *Lancet Oncol* 11(11): 1029-1035 (2010).
37. Saussele S, Richter J, Guilhot J, Gruber FX, Hjorth-Hansen H, Almeida A, Janssen J, Mayer J, Koskenvesa P, Panayiotidis P, Olsson-Strömberg U, Martinez-Lopez J, Rousselot P, Vestergaard H, Ehrencrona H, Kairisto V, Machová Poláková K, Müller MC, Mustjoki S, Berger MG, Fabarius A, Hofmann WK, Hochhaus A, Pfirrmann M, Mahon FX, and EURO-SKI investigators. Discontinuation of tyrosine kinase inhibitor therapy in chronic myeloid leukaemia (EURO-SKI): a prespecified interim analysis of a prospective, multicentre, non-randomised, trial. *Lancet Oncol* 19(6): 747-757 (2018).
38. Ding L, Ley TJ, Larson DE, Miller CA, Koboldt DC, Welch JS, Ritchey JK, Young MA, Lamprecht T, McLellan MD, McMichael JF, Wallis JW, Lu C, Shen D, Harris CC, Dooling DJ, Fulton RS, Fulton LL, Chen K, Schmidt H, Kalicki-Veizer J, Magrini VJ, Cook L, McGrath SD, Vickery TL, Wendl MC, Heath S, Watson MA, Link DC, Tomasson MH, Shannon WD, Payton JE, Kulkarni S, Westervelt P, Walter MJ, Graubert TA, Mardis ER, Wilson RK, and DiPersio JF. Clonal evolution in relapsed acute myeloid leukaemia revealed by whole-genome sequencing. *Nature* 481(7382): 506-510 (2012).
39. Papaemmanuil E, Gerstung M, Bullinger L, Gaidzik VI, Paschka P, Roberts ND, Potter NE, Heuser M, Thol F, Bolli N, Gundem G, Van Loo P, Martincorena I, Ganly P, Mudie L, McLaren S, O'Meara S, Raine K, Jones DR, Teague JW, Butler AP, Greaves MF, Ganser A, Döhner K, Schlenk RF, Döhner H, and Campbell PJ. Genomic Classification and Prognosis in Acute Myeloid Leukemia. *N Engl J Med* 374(23): 2209-2221 (2016).
40. Howlader N, Noone A, Krapcho M, Miller D, Bishop K, Kosary C, Yu M, Ruhl J, Tatalovich Z, Mariotto A, Lewis D, Chen H, Feuer E, and Cronin K. SEER Cancer Statistics Review, 1975-2014, National Cancer Institute. Bethesda, MD, https://seer.cancer.gov/csr/1975_2014/, based on November 2016 SEER data submission, posted to the SEER web site, April 2017.
41. Cancer Stat Facts: Leukemia - Acute Myeloid Leukemia (AML). 2019; Available from: https://seer.cancer.gov/statfacts/html/amyl.html.
42. Bennett JM, Catovsky D, Daniel MT, Flandrin G, Galton DA, Gralnick HR, and Sultan C. Proposed revised criteria for the classification of acute myeloid leukemia. A report of the French-American-British Cooperative Group. *Ann Intern Med* 103(4): 620-625 (1985).

43. Hassan K, Qureshi M, Shafi S, Ikram N, and Akhtar MJ. Acute myeloid leukemia-FAB classification and its correlation with clinico-haematological features. *J Pak Med Assoc* 43(10): 200-203 (1993).
44. Döhner H, Estey EH, Amadori S, Appelbaum FR, Büchner T, Burnett AK, Dombret H, Fenaux P, Grimwade D, Larson RA, Lo-Coco F, Naoe T, Niederwieser D, Ossenkoppele GJ, Sanz MA, Sierra J, Tallman MS, Löwenberg B, and Bloomfield CD. Diagnosis and management of acute myeloid leukemia in adults: recommendations from an international expert panel, on behalf of the European LeukemiaNet. *Blood* 115(3): 453-474 (2010).
45. Döhner H, Estey E, Grimwade D, Amadori S, Appelbaum FR, Büchner T, Dombret H, Ebert BL, Fenaux P, Larson RA, Levine RL, Lo-Coco F, Naoe T, Niederwieser D, Ossenkoppele GJ, Sanz M, Sierra J, Tallman MS, Tien HF, Wei AH, Löwenberg B, and Bloomfield CD. Diagnosis and management of AML in adults: 2017 ELN recommendations from an international expert panel. *Blood* 129(4): 424-447 (2017).
46. Falini B, Tiacci E, Martelli MP, Ascani S, and Pileri SA. New classification of acute myeloid leukemia and precursor-related neoplasms: changes and unsolved issues. *Discov Med* 10(53): 281-292 (2010).
47. Taylor J, Xiao W, and Abdel-Wahab O. Diagnosis and classification of hematologic malignancies on the basis of genetics. *Blood* 130(4): 410-423 (2017).
48. Arber DA, Orazi A, Hasserjian R, Thiele J, Borowitz MJ, Le Beau MM, Bloomfield CD, Cazzola M, and Vardiman JW. The 2016 revision to the World Health Organization classification of myeloid neoplasms and acute leukemia. *Blood* 127(20): 2391-2405 (2016).
49. Yang JJ, Park TS, and Wan TS. Recurrent Cytogenetic Abnormalities in Acute Myeloid Leukemia. *Methods Mol Biol* 1541: 223-245 (2017).
50. Peterson LF and Zhang DE. The 8;21 translocation in leukemogenesis. *Oncogene* 23(24): 4255-4262 (2004).
51. Tonks A, Pearn L, Musson M, Gilkes A, Mills KI, Burnett AK, and Darley RL. Transcriptional dysregulation mediated by RUNX1-RUNX1T1 in normal human progenitor cells and in acute myeloid leukaemia. *Leukemia* 21(12): 2495-2505 (2007).
52. Greif PA, Konstandin NP, Metzeler KH, Herold T, Pasalic Z, Ksienzyk B, Dufour A, Schneider F, Schneider S, Kakadia PM, Braess J, Sauerland MC, Berdel WE, Büchner T, Woermann BJ, Hiddemann W, Spiekermann K, and Bohlander SK. RUNX1 mutations in cytogenetically normal acute myeloid leukemia are associated with a poor prognosis and up-regulation of lymphoid genes. *Haematologica* 97(12): 1909-1915 (2012).
53. Van der Reijden BA, de Wit L, van der Poel S, Luiten EB, Lafage-Pochitaloff M, Dastugue N, Gabert J, Löwenberg B, and Jansen JH. Identification of a novel CBFB-MYH11 transcript: implications for RT-PCR diagnosis. *Hematol J* 2(3): 206-209 (2001).
54. Kundu M and Liu PP. Function of the inv(16) fusion gene CBFB-MYH11. *Curr Opin Hematol* 8(4): 201-205 (2001).
55. Hiebert SW, Lutterbach B, and Amann J. Role of co-repressors in transcriptional repression mediated by the t(8;21), t(16;21), t(12;21), and inv(16) fusion proteins. *Curr Opin Hematol* 8(4): 197-200 (2001).
56. Alexandrov LB, Nik-Zainal S, Wedge DC, Aparicio SA, Behjati S, Biankin AV, Bignell GR, Bolli N, Borg A, Børresen-Dale AL, Boyault S, Burkhardt B, Butler AP, Caldas C, Davies HR, Desmedt C, Eils R, Eyfjörd JE, Foekens JA, Greaves M, Hosoda F, Hutter B, Ilicic T, Imbeaud S, Imielinski M, Jäger N, Jones DT, Jones D, Knappskog S, Kool M, Lakhani SR, López-Otín C, Martin S, Munshi NC, Nakamura H, Northcott PA, Pajic M, Papaemmanuil E, Paradiso A, Pearson JV, Puente XS, Raine K, Ramakrishna M, Richardson AL, Richter J, Rosenstiel P, Schlesner M, Schumacher TN, Span PN, Teague JW, Totoki Y, Tutt AN, Valdés-Mas R, van Buuren MM, van 't Veer L, Vincent-Salomon A, Waddell N, Yates LR, Australian Pancreatic Cancer Genome Initiative, ICGC Breast Cancer Consortium, ICGC MMML-Seq Consortium, ICGC PedBrain, Zucman-Rossi J, Futreal PA, McDermott U, Lichter P, Meyerson M, Grimmond SM, Siebert R, Campo E, Shibata T, Pfister SM, Campbell PJ, and Stratton MR. Signatures of mutational processes in human cancer. *Nature* 500(7463): 415-421 (2013).
57. Yan XJ, Xu J, Gu ZH, Pan CM, Lu G, Shen Y, Shi JY, Zhu YM, Tang L, Zhang XW, Liang WX, Mi JQ, Song HD, Li KQ, Chen Z, and Chen SJ. Exome sequencing identifies somatic mutations of DNA methyltransferase gene DNMT3A in acute monocytic leukemia. *Nat Genet* 43(4): 309-315 (2011).
58. Vogelstein B, Papadopoulos N, Velculescu VE, Zhou S, Diaz LA, Jr., and Kinzler KW. Cancer genome landscapes. *Science* 339(6127): 1546-1558 (2013).
59. Cancer Genome Atlas Research Network, Ley TJ, Miller C, Ding L, Raphael BJ, Mungall AJ, Robertson A, Hoadley K, Triche TJ, Laird PW, Baty JD, Fulton LL, Fulton R, Heath SE, Kalicki-Veizer J, Kandoth C, Klco JM, Koboldt DC, Kanchi KL, Kulkarni S, Lamprecht TL, Larson DE, Lin L, Lu C, McLellan MD, McMichael JF, Payton J, Schmidt H, Spencer DH, Tomasson MH, Wallis JW, Wartman LD, Watson MA, Welch J, Wendl MC, Ally A, Balasundaram M, Birol I, Butterfield Y, Chiu R, Chu A, Chuah E, Chun HJ, Corbett R, Dhalla N, Guin R, He A, Hirst C, Hirst M, Holt RA, Jones S, Karsan A, Lee D, Li HI, Marra MA, Mayo M, Moore RA, Mungall K, Parker J, Pleasance E, Plettner P, Schein J, Stoll D, Swanson L, Tam A, Thiessen N, Varhol R, Wye N, Zhao Y, Gabriel S, Getz G, Sougnez C, Zou L, Leiserson MD, Vandin F, Wu HT, Applebaum F, Baylin SB, Akbani R, Broom BM, Chen K, Motter TC, Nguyen K, Weinstein JN, Zhang N, Ferguson ML, Adams C, Black A, Bowen J, Gastier-Foster J, Grossman T, Lichtenberg T, Wise L, Davidsen T, Demchok JA, Shaw KR, Sheth M, Sofia HJ, Yang L, Downing JR and Eley G. Genomic and epigenomic landscapes of adult de novo acute myeloid leukemia. *N Engl J Med* 368(22): 2059-2074 (2013).
60. Falini B, Mecucci C, Tiacci E, Alcalay M, Rosati R, Pasqualucci L, La Starza R, Diverio D, Colombo E, Santucci A, Bigerna B, Pacini R, Pucciarini A, Liso A, Vignetti M, Fazi P, Meani N, Pettirossi V, Saglio G, Mandelli F, Lo-Coco F, Pelicci PG, and Martelli MF. Cytoplasmic nucleophosmin in acute myelogenous leukemia with a normal karyotype. *N Engl J Med* 352(3): 254-266 (2005).

61. Jain P, Kantarjian H, Patel K, Faderl S, Garcia-Manero G, Benjamini O, Borthakur G, Pemmaraju N, Kadia T, Daver N, Nazha A, Luthra R, Pierce S, Cortes J, and Ravandi F. Mutated NPM1 in patients with acute myeloid leukemia in remission and relapse. *Leuk Lymphoma* 55(6): 1337-1344 (2014).
62. Yu Y, Maggi LB, Jr., Brady SN, Apicelli AJ, Dai MS, Lu H, and Weber JD. Nucleophosmin is essential for ribosomal protein L5 nuclear export. *Mol Cell Biol* 26(10): 3798-3809 (2006).
63. Okuda M. The role of nucleophosmin in centrosome duplication. *Oncogene* 21(40): 6170-6174 (2002).
64. Thiede C, Koch S, Creutzig E, Steudel C, Illmer T, Schaich M, and Ehninger G. Prevalence and prognostic impact of NPM1 mutations in 1485 adult patients with acute myeloid leukemia (AML). *Blood* 107(10): 4011-4020 (2006).
65. Falini B, Martelli MP, Pileri SA, and Mecucci C. Molecular and alternative methods for diagnosis of acute myeloid leukemia with mutated NPM1: flexibility may help. *Haematologica* 95(4): 529-534 (2010).
66. Levis M and Small D. FLT3: ITDoes matter in leukemia. *Leukemia* 17(9): 1738-1752 (2003).
67. Nakao M, Yokota S, Iwai T, Kaneko H, Horiike S, Kashima K, Sonoda Y, Fujimoto T, and Misawa S. Internal tandem duplication of the flt3 gene found in acute myeloid leukemia. *Leukemia* 10(12): 1911-1928 (1996).
68. Yamamoto Y, Kiyoi H, Nakano Y, Suzuki R, Kodera Y, Miyawaki S, Asou N, Kuriyama K, Yagasaki F, Shimazaki C, Akiyama H, Saito K, Nishimura M, Motoji T, Shinagawa K, Takeshita A, Saito H, Ueda R, Ohno R, and Naoe T. Activating mutation of D835 within the activation loop of FLT3 in human hematologic malignancies. *Blood* 97(8): 2434-2439 (2001).
69. Dolence JJ, Gwin KA, Shapiro MB, and Medina KL. Flt3 signaling regulates the proliferation, survival, and maintenance of multipotent hematopoietic progenitors that generate B cell precursors. *Exp Hematol* 42(5): 380-393 e3 (2014).
70. Bruserud Ø, Hovland R, Wergeland L, Huang TS, and Gjertsen BT. Flt3-mediated signaling in human acute myelogenous leukemia (AML) blasts: a functional characterization of Flt3-ligand effects in AML cell populations with and without genetic Flt3 abnormalities. *Haematologica* 88(4): 416-428 (2003).
71. Im AP, Sehgal AR, Carroll MP, Smith BD, Tefferi A, Johnson DE, and Boyiadzis M. DNMT3A and IDH mutations in acute myeloid leukemia and other myeloid malignancies: associations with prognosis and potential treatment strategies. *Leukemia* 28(9): 1774-1783 (2014).
72. Reitman ZJ and Yan H. Isocitrate dehydrogenase 1 and 2 mutations in cancer: alterations at a crossroads of cellular metabolism. *J Natl Cancer Inst* 102(13): 932-941 (2010).
73. Murphy T and Yee KWL. Cytarabine and daunorubicin for the treatment of acute myeloid leukemia. *Expert Opin Pharmacother* 18(16): 1765-1780 (2017).
74. Stone R, Mandrekar S, Sanford B, Geyer S, Bloomfield C, Dohner K, Thiede C, Marcucci G, Lo-Coco F, Klisovic R, Wei A, Sierra J, Sanz M, Brandwein J, de Witte T, Niederwieser D, Appelbaum F, Medeiros B, Tallman M, Krauter J, Schlenk R, Ganser A, Serve H, Ehninger G, Amadori S, Larson R, and Dohner H. The multi-kinase inhibitor midostaurin (M) prolongs survival compared with placebo (P) in combination with daunorubicin (D)/cytarabine (C) induction (ind), high-dose C consolidation (consol), and as maintenance (maint) therapy in newly diagnosed acute myeloid leukemia (AML) patients (pts) age 18-60 with FLT3 mutations (muts): an international prospective randomized (rand) P-controlled double-blind trial (CALGB10603/RATIFY [Alliance]). *Blood* 126(6) (2015).
75. Castaigne S, Pautas C, Terré C, Renneville A, Gardin C, Suarez F, Caillot D, Berthon C, Rousselot P, Preudhomme C, Morisset L, Lebras KC, Chevret S, and Dombret H. Final Analysis of the ALFA 0701 Study. *Blood* 124(21): 376-376 (2014).
76. Kim ES. Enasidenib: First Global Approval. *Drugs* 77(15): 1705-1711 (2017).
77. Stein EM, DiNardo CD, Pollyea DA, Fathi AT, Roboz GJ, Altman JK, Stone RM, DeAngelo DJ, Levine RL, Flinn IW, Kantarjian HM, Collins R, Patel MR, Frankel AE, Stein A, Sekeres MA, Swords RT, Medeiros BC, Willekens C, Vyas P, Tosolini A, Xu Q, Knight RD, Yen KE, Agresta S, de Botton S, and Tallman MS. Enasidenib in mutant IDH2 relapsed or refractory acute myeloid leukemia. *Blood* 130(6): 722-731 (2017).
78. DiNardo CD, Stein EM, de Botton S, Roboz GJ, Altman JK, Mims AS, Swords R, Collins RH, Mannis GN, Pollyea DA, Donnellan W, Fathi AT, Pigneux A, Erba HP, Prince GT, Stein AS, Uy GL, Foran JM, Traer E, Stuart RK, Arellano ML, Slack JL, Sekeres MA, Willekens C, Choe S, Wang H, Zhang V, Yen KE, Kapsalis SM, Yang H, Dai D, Fan B, Goldwasser M, Liu H, Agresta S, Wu B, Attar EC, Tallman MS, Stone RM, and Kantarjian HM. Durable Remissions with Ivosidenib in IDH1-Mutated Relapsed or Refractory AML. *N Engl J Med* 378(25): 2386-2398 (2018).
79. DiNardo CD, Pratz K, Pullarkat V, Jonas BA, Arellano M, Becker PS, Frankfurt O, Konopleva M, Wei AH, Kantarjian HM, Xu T, Hong WJ, Chyla B, Potluri J, Pollyea DA, and Letai A. Venetoclax combined with decitabine or azacitidine in treatment-naive, elderly patients with acute myeloid leukemia. *Blood* 133(1): 7-17 (2019).
80. Goldberg AD, Horvat TZ, Hsu M, Devlin SM, Cuello BM, Daley RJ, King AC, Buie LW, Glass JL, Mauro MJ, Stein EM, Berman E, Klimek VM, and Tallman MS. Venetoclax Combined with Either a Hypomethylating Agent or Low-Dose Cytarabine Shows Activity in Relapsed and Refractory Myeloid Malignancies. *Blood* 130(Suppl 1): 1353-1353 (2017).
81. Campos L, Rouault JP, Sabido O, Oriol P, Roubi N, Vasselon C, Archimbaud E, Magaud JP, and Guyotat D. High expression of bcl-2 protein in acute myeloid leukemia cells is associated with poor response to chemotherapy. *Blood* 81(11): 3091-3096 (1993).
82. Vaux DL, Cory S, and Adams JM. Bcl-2 gene promotes haemopoietic cell survival and cooperates with c-myc to immortalize pre-B cells. *Nature* 335(6189): 440-442 (1988).
83. Freeman SD, Kelm S, Barber EK, and Crocker PR. Characterization of CD33 as a new member of the sialoadhesin family of cellular interaction molecules. *Blood* 85(8): 2005-2012 (1995).
84. Ehninger A, Kramer M, Röllig C, Thiede C, Bornhäuser M, von Bonin M, Wermke M, Feldmann A, Bachmann M, Ehninger G, and Oelschlägel U. Distribution and levels of cell surface expression of CD33 and CD123 in acute myeloid leukemia. *Blood Cancer J* 4: e218 (2014).

85. Laszlo GS, Gudgeon CJ, Harrington KH, Dell'Aringa J, Newhall KJ, Means GD, Sinclair AM, Kischel R, Frankel SR, and Walter RB. Cellular determinants for preclinical activity of a novel CD33/CD3 bispecific T-cell engager (BiTE) antibody, AMG 330, against human AML. *Blood* 123(4): 554-561 (2014).
86. Ravandi F, Stein AS, Kantarjian HM, Walter RB, Paschka P, Jongen-Lavrencic M, Ossenkoppele GJ, Yang Z, Mehta B, and Subklewe M. A Phase 1 First-in-Human Study of AMG 330, an Anti-CD33 Bispecific T-Cell Engager (BiTE®) Antibody Construct, in Relapsed/Refractory Acute Myeloid Leukemia (R/R AML). *Blood* 132(Suppl 1): 25-25 (2018).
87. Testa U, Pelosi E, and Frankel A. CD 123 is a membrane biomarker and a therapeutic target in hematologic malignancies. *Biomark Res* 2(1): 4 (2014).
88. Li F, Sutherland MK, Yu C, Walter RB, Westendorf L, Valliere-Douglass J, Pan L, Cronkite A, Sussman D, Klussman K, Ulrich M, Anderson ME, Stone IJ, Zeng W, Jonas M, Lewis TS, Goswami M, Wang SA, Senter PD, Law CL, Feldman EJ, and Benjamin DR. Characterization of SGN-CD123A, A Potent CD123-Directed Antibody-Drug Conjugate for Acute Myeloid Leukemia. *Mol Cancer Ther* 17(2): 554-564 (2018).
89. Xie LH, Biondo M, Busfield SJ, Arruda A, Yang X, Vairo G, and Minden MD. CD123 target validation and preclinical evaluation of ADCC activity of anti-CD123 antibody CSL362 in combination with NKs from AML patients in remission. *Blood Cancer J* 7(6): e567 (2017).
90. Frankel AE, McCubrey JA, Miller MS, Delatte S, Ramage J, Kiser M, Kucera GL, Alexander RL, Beran M, Tagge EP, Kreitman RJ, and Hogge DE. Diphtheria toxin fused to human interleukin-3 is toxic to blasts from patients with myeloid leukemias. *Leukemia* 14(4): 576-585 (2000).
91. ClinicalTrials.gov [Internet]. Bethesda (MD) National Library of Medicine (US). Identifier: NCT00397579. DT388IL3 Fusion Protein in Treating Patients With Acute Myeloid Leukemia or Myelodysplastic Syndromes. 2006 Nov 9 [cited 2019 Apr 03]; Available from: https://clinicaltrials.gov/ct2/show/NCT00397579.
92. Hofmann M, Grosse-Hovest L, Nübling T, Pyż E, Bamberg ML, Aulwurm S, Bühring HJ, Schwartz K, Haen SP, Schilbach K, Rammensee H-G, Salih HR, and Jung G. Generation, selection and preclinical characterization of an Fc-optimized FLT3 antibody for the treatment of myeloid leukemia. *Leukemia* 26(6): 1228-1237 (2012).
93. ClinicalTrials.gov [Internet]. Bethesda (MD) National Library of Medicine (US). Identifier: NCT02789254. FLYSYN in MRD Positive AML (FLYSYN-101). (2016 June 2).
94. Durben M, Schmiedel D, Hofmann M, Vogt F, Nübling T, Pyz E, Bühring HJ, Rammensee H-G, Salih HR, Grosse-Hovest L, and Jung G. Characterization of a bispecific FLT3 X CD3 antibody in an improved, recombinant format for the treatment of leukemia. *Mol Ther* 23(4): 648-655 (2015).
95. Rasko JEJ and Hughes TP. First Approved Kinase Inhibitor for AML. *Cell* 171(5): 981 (2017).
96. DeAngelo DJ, Stone RM, Heaney ML, Nimer SD, Paquette RL, Klisovic RB, Caligiuri MA, Cooper MR, Lecerf JM, Karol MD, Sheng S, Holford N, Curtin PT, Druker BJ, and Heinrich MC. Phase 1 clinical results with tandutinib (MLN518), a novel FLT3 antagonist, in patients with acute myelogenous leukemia or high-risk myelodysplastic syndrome: safety, pharmacokinetics, and pharmacodynamics. *Blood* 108(12): 3674-3681 (2006).
97. Fiedler W, Kayser S, Kebenko M, Janning M, Krauter J, Schittenhelm M, Götze K, Weber D, Göhring G, Teleanu V, Thol F, Heuser M, Döhner K, Ganser A, Döhner H, and Schlenk RF. A phase I/II study of sunitinib and intensive chemotherapy in patients over 60 years of age with acute myeloid leukaemia and activating FLT3 mutations. *Br J Haematol* 169(5): 694-700 (2015).
98. Ravandi F, Arana Yi C, Cortes JE, Levis M, Faderl S, Garcia-Manero G, Jabbour E, Konopleva M, O'Brien S, Estrov Z, Borthakur G, Thomas D, Pierce S, Brandt M, Pratz K, Luthra R, Andreeff M, and Kantarjian H. Final report of phase II study of sorafenib, cytarabine and idarubicin for initial therapy in younger patients with acute myeloid leukemia. *Leukemia* 28(7): 1543-1545 (2014).
99. Serve H, Krug U, Wagner R, Sauerland MC, Heinecke A, Brunnberg U, Schaich M, Ottmann O, Duyster J, Wandt H, Fischer T, Giagounidis A, Neubauer A, Reichle A, Aulitzky W, Noppeney R, Blau I, Kunzmann V, Stuhlmann R, Kramer A, Kreuzer KA, Brandts C, Steffen B, Thiede C, Müller-Tidow C, Ehninger G, and Berdel WE. Sorafenib in combination with intensive chemotherapy in elderly patients with acute myeloid leukemia: results from a randomized, placebo-controlled trial. *J Clin Oncol* 31(25): 3110-3118 (2013).
100. Knapper S, Russell N, Gilkes A, Hills RK, Gale RE, Cavenagh JD, Jones G, Kjeldsen L, Grunwald MR, Thomas I, Konig H, Levis MJ, and Burnett AK. A randomized assessment of adding the kinase inhibitor lestaurtinib to first-line chemotherapy for FLT3-mutated AML. *Blood* 129(9): 1143-1154 (2017).
101. Schiller GJ, Tallman MS, Goldberg SL, Perl AE, Marie J-P, Martinelli G, Larson RA, Russell N, Trone D, Gammon G, Levis MJ, and Cortes JE. Final results of a randomized phase 2 study showing the clinical benefit of quizartinib (AC220) in patients with FLT3-ITD positive relapsed or refractory acute myeloid leukemia. *J Clin Oncol* 32(15_suppl): 7100-7100 (2014).
102. Wang ES, Stone RM, Tallman MS, Walter RB, Eckardt JR, and Collins R. Crenolanib, a Type I FLT3 TKI, Can be Safely Combined with Cytarabine and Anthracycline Induction Chemotherapy and Results in High Response Rates in Patients with Newly Diagnosed FLT3 Mutant Acute Myeloid Leukemia (AML). *Blood* 128(22): 1071-1071 (2016).
103. Shah NP, Talpaz M, Deininger MW, Mauro MJ, Flinn IW, Bixby D, Lustgarten S, Gozgit JM, Clackson T, Turner CD, Haluska FG, Kantarjian H, and Cortes JE. Ponatinib in patients with refractory acute myeloid leukaemia: findings from a phase 1 study. *Br J Haematol* 162(4): 548-552 (2013).
104. Perl AE, Altman JK, Cortes J, Smith C, Litzow M, Baer MR, Claxton D, Erba HP, Gill S, Goldberg S, Jurcic JG, Larson RA, Liu C, Ritchie E, Schiller G, Spira AI, Strickland SA, Tibes R, Ustun C, Wang ES, Stuart R, Röllig C, Neubauer A, Martinelli G, Bahceci E, and Levis M. Selective inhibition of FLT3 by gilteritinib in relapsed or refractory acute myeloid leukaemia: a multicentre, first-in-human, open-label, phase 1-2 study. *Lancet Oncol* 18(8): 1061-1075 (2017).

105. Wolchok JD, Kluger H, Callahan MK, Postow MA, Rizvi NA, Lesokhin AM, Segal NH, Ariyan CE, Gordon RA, Reed K, Burke MM, Caldwell A, Kronenberg SA, Agunwamba BU, Zhang X, Lowy I, Inzunza HD, Feely W, Horak CE, Hong Q, Korman AJ, Wigginton JM, Gupta A, and Sznol M. Nivolumab plus ipilimumab in advanced melanoma. *N Engl J Med* 369(2): 122-133 (2013).
106. Topalian SL, Hodi FS, Brahmer JR, Gettinger SN, Smith DC, McDermott DF, Powderly JD, Carvajal RD, Sosman JA, Atkins MB, Leming PD, Spigel DR, Antonia SJ, Horn L, Drake CG, Pardoll DM, Chen L, Sharfman WH, Anders RA, Taube JM, McMiller TL, Xu H, Korman AJ, Jure-Kunkel M, Agrawal S, McDonald D, Kollia GD, Gupta A, Wigginton JM, and Sznol M. Safety, activity, and immune correlates of anti-PD-1 antibody in cancer. *N Engl J Med* 366(26): 2443-2454 (2012).
107. Daver N, Basu S, Garcia-Manero G, Cortes JE, Ravandi F, Ning J, Xiao LC, Juliana L, Kornblau SM, Konopleva M, Andreeff M, Flores W, Bueso-Ramos CE, Somani N, Blando J, Allison J, Kantarjian HM, and Sharma P. Defining the Immune Checkpoint Landscape in Patients (pts) with Acute Myeloid Leukemia (AML). *Blood* 128(22): 2900-2900 (2016).
108. Graf M, Reif S, Hecht K, Pelka-Fleischer R, Kroell T, Pfister K, and Schmetzer H. High expression of costimulatory molecules correlates with low relapse-free survival probability in acute myeloid leukemia (AML). *Ann Hematol* 84(5): 287-297 (2005).
109. Chen X, Liu S, Wang L, Zhang W, Ji Y, and Ma X. Clinical significance of B7-H1 (PD-L1) expression in human acute leukemia. *Cancer Biol Ther* 7(5): 622-627 (2008).
110. Schnorfeil FM, Lichtenegger FS, Emmerig K, Schlueter M, Neitz JS, Draenert R, Hiddemann W, and Subklewe M. T cells are functionally not impaired in AML: increased PD-1 expression is only seen at time of relapse and correlates with a shift towards the memory T cell compartment. *J Hematol Oncol* 8: 93 (2015).
111. Saudemont A and Quesnel B. In a model of tumor dormancy, long-term persistent leukemic cells have increased B7-H1 and B7.1 expression and resist CTL-mediated lysis. *Blood* 104(7): 2124-2133 (2004).
112. Daver N, Garcia-Manero G, Basu S, Boddu PC, Alfayez M, Cortes JE, Konopleva M, Ravandi-Kashani F, Jabbour E, Kadia T, Nogueras-Gonzalez GM, Ning J, Pemmaraju N, DiNardo CD, Andreeff M, Pierce SA, Gordon T, Kornblau SM, Flores W, Alhamal Z, Bueso-Ramos C, Jorgensen JL, Patel KP, Blando J, Allison JP, Sharma P, and Kantarjian H. Efficacy, Safety, and Biomarkers of Response to Azacitidine and Nivolumab in Relapsed/Refractory Acute Myeloid Leukemia: A Nonrandomized, Open-Label, Phase II Study. *Cancer Discov* 9(3): 370-383 (2019).
113. Kadia TM, Cortes JE, Ghorab A, Ravandi F, Jabbour E, Daver NG, Alvarado Y, Ohanian M, Konopleva M, and Kantarjian HM. Nivolumab (Nivo) maintenance (maint) in high-risk (HR) acute myeloid leukemia (AML) patients. *J Clin Oncol* 36(15_suppl) (2018).
114. Albring JC, Inselmann S, Sauer T, Schliemann C, Altvater B, Kailayangiri S, Rössig C, Hartmann W, Knorrenschild JR, Sohlbach K, Groth C, Lohoff M, Neubauer A, Berdel WE, Burchert A, and Stelljes M. PD-1 checkpoint blockade in patients with relapsed AML after allogeneic stem cell transplantation. *Bone Marrow Transplant* 52(2): 317-320 (2017).
115. Hope KJ, Jin L, and Dick JE. Acute myeloid leukemia originates from a hierarchy of leukemic stem cell classes that differ in self-renewal capacity. *Nat Immunol* 5(7): 738-743 (2004).
116. van Rhenen A, Feller N, Kelder A, Westra AH, Rombouts E, Zweegman S, van der Pol MA, Waisfisz Q, Ossenkoppele GJ, and Schuurhuis GJ. High stem cell frequency in acute myeloid leukemia at diagnosis predicts high minimal residual disease and poor survival. *Clin Cancer Res* 11(18): 6520-6527 (2005).
117. Ishikawa F, Yoshida S, Saito Y, Hijikata A, Kitamura H, Tanaka S, Nakamura R, Tanaka T, Tomiyama H, Saito N, Fukata M, Miyamoto T, Lyons B, Ohshima K, Uchida N, Taniguchi S, Ohara O, Akashi K, Harada M, and Shultz LD. Chemotherapy-resistant human AML stem cells home to and engraft within the bone-marrow endosteal region. *Nat Biotechnol* 25(11): 1315-1321 (2007).
118. Bonnet D and Dick JE. Human acute myeloid leukemia is organized as a hierarchy that originates from a primitive hematopoietic cell. *Nat Med* 3(7): 730 (1997).
119. Lapidot T, Sirard C, Vormoor J, Murdoch B, Hoang T, Caceres-Cortes J, Minden M, Paterson B, Caligiuri MA, and Dick JE. A Cell Initiating Human Acute Myeloid Leukaemia after Transplantation into SCID Mice. *Nature* 367(6464): 645-648 (1994).
120. Terpstra W, Prins A, Ploemacher RE, Wognum BW, Wagemaker G, Löwenberg B, and Wielenga JJ. Long-term leukemia-initiating capacity of a CD34-subpopulation of acute myeloid leukemia. *Blood* 87(6): 2187-2194 (1996).
121. Ng SW, Mitchell A, Kennedy JA, Chen WC, McLeod J, Ibrahimova N, Arruda A, Popescu A, Gupta V, Schimmer AD, Schuh AC, Yee KW, Bullinger L, Herold T, Görlich D, Büchner T, Hiddemann W, Berdel WE, Wörmann B, Cheok M, Preudhomme C, Dombret H, Metzeler K, Buske C, Löwenberg B, Valk PJ, Zandstra PW, Minden MD, Dick JE, and Wang JC. A 17-gene stemness score for rapid determination of risk in acute leukaemia. *Nature* 540(7633): 433-437 (2016).
122. Terwijn M, Zeijlemaker W, Kelder A, Rutten AP, Snel AN, Scholten WJ, Pabst T, Verhoef G, Löwenberg B, Zweegman S, Ossenkoppele GJ, and Schuurhuis GJ. Leukemic stem cell frequency: a strong biomarker for clinical outcome in acute myeloid leukemia. *PLoS One* 9(9): e107587 (2014).
123. Jawad M, Seedhouse C, Mony U, Grundy M, Russell NH, and Pallis M. Analysis of factors that affect in vitro chemosensitivity of leukaemic stem and progenitor cells to gemtuzumab ozogamicin (Mylotarg) in acute myeloid leukaemia. *Leukemia* 24(1): 74-80 (2010).
124. Kikushige Y, Shima T, Takayanagi S, Urata S, Miyamoto T, Iwasaki H, Takenaka K, Teshima T, Tanaka T, Inagaki Y, and Akashi K. TIM-3 Is a Promising Target to Selectively Kill Acute Myeloid Leukemia Stem Cells. *Cell Stem Cell* 7(6): 708-717 (2010).
125. Gadhoum SZ, Madhoun NY, Abuelela AF, and Merzaban JS. Anti-CD44 antibodies inhibit both mTORC1 and mTORC2: a new rationale supporting CD44-induced AML differentiation therapy. *Leukemia* 30(12): 2397-2401 (2016).

126. Papa V, Tazzari PL, Chiarini F, Cappellini A, Ricci F, Billi AM, Evangelisti C, Ottaviani E, Martinelli G, Testoni N, McCubrey JA, and Martelli AM. Proapoptotic activity and chemosensitizing effect of the novel Akt inhibitor perifosine in acute myelogenous leukemia cells. *Leukemia* 22(1): 147-160 (2008).
127. van der Helm LH, Bosman MC, Schuringa JJ, and Vellenga E. Effective targeting of primitive AML CD 34+ cells by the second-generation proteasome inhibitor carfilzomib. *Br J Haematol* 171(4): 652-655 (2015).
128. Paczulla AM, Rothfelder K, Raffel S, Konantz M, Steinbacher J, Wang H, Tandler C, Mbarga M, Schaefer T, Falcone M, Nievergall E, Dörfel D, Hanns P, Passweg JR, Lutz C, Schwaller J, Zeiser R, Blazar BR, Caligiuri MA, Dirnhofer S, Lundberg P, Kanz L, Quintanilla-Martinez L, Steinle A, Trumpp A, Salih HR, and Lengerke C. Absence of NKG2D ligands defines leukaemia stem cells and mediates their immune evasion. *Nature* 572(7768): 254-259 (2019).
129. Kucerova P and Cervinkova M. Spontaneous regression of tumour and the role of microbial infection--possibilities for cancer treatment. *Anti-Cancer Drugs* 27(4): 269-277 (2016).
130. Hoption Cann SA, van Netten JP, and van Netten C. Dr William Coley and tumour regression: a place in history or in the future. *Postgrad Med J* 79(938): 672-680 (2003).
131. McCarthy EF. The toxins of William B. Coley and the treatment of bone and soft-tissue sarcomas. *Iowa Orthop J* 26: 154-158 (2006).
132. Coley WB. The Treatment of Inoperable Sarcoma by Bacterial Toxins (the Mixed Toxins of the Streptococcus erysipelas and the Bacillus prodigiosus). *Proc R Soc Med* 3(Surg Sect): 1-48 (1910).
133. Thomas ED, Buckner CD, Banaji M, Clift RA, Fefer A, Flournoy N, Goodell BW, Hickman RO, Lerner KG, Neiman PE, Sale GE, Sanders JE, Singer J, Stevens M, Storb R, and Weiden PL. One hundred patients with acute leukemia treated by chemotherapy, total body irradiation, and allogeneic marrow transplantation. *Blood* 49(4): 511-533 (1977).
134. Kolb H-J. Graft-versus-leukemia effects of transplantation and donor lymphocytes. *Blood* 112(12): 4371-4383 (2008).
135. Hodi FS, O'Day SJ, McDermott DF, Weber RW, Sosman JA, Haanen JB, Gonzalez R, Robert C, Schadendorf D, Hassel JC, Akerley W, van den Eertwegh AJ, Lutzky J, Lorigan P, Vaubel JM, Linette GP, Hogg D, Ottensmeier CH, Lebbé C, Peschel C, Quirt I, Clark JI, Wolchok JD, Weber JS, Tian J, Yellin MJ, Nichol GM, Hoos A, and Urba WJ. Improved survival with ipilimumab in patients with metastatic melanoma. *N Engl J Med* 363(8): 711-723 (2010).
136. Medzhitov R and Janeway C. Innate immune recognition: mechanisms and pathways. *Immunol Rev* 173: 89-97 (2000).
137. Medzhitov R and Janeway C. Innate immunity: impact on the adaptive immune response. *Curr Opin Immunol* 9(1): 4-9 (1997).
138. Delves PJ and Roitt IM. The immune system. First of two parts. *N Engl J Med* 343(1): 37-49 (2000).
139. Delves PJ and Roitt IM. The immune system. Second of two parts. *N Engl J Med* 343(2): 108-117 (2000).
140. Neefjes J, Jongsma ML, Paul P, and Bakke O. Towards a systems understanding of MHC class I and MHC class II antigen presentation. *Nat Rev Immunol* 11(12): 823-836 (2011).
141. Vyas JM, Van der Veen AG, and Ploegh HL. The known unknowns of antigen processing and presentation. *Nat Rev Immunol* 8(8): 607-618 (2008).
142. Rammensee H-G, Falk K, and Rötzschke O. Peptides naturally presented by MHC class I molecules. *Annu Rev Immunol* 11: 213-244 (1993).
143. Falk K, Rötzschke O, Stevanović S, Jung G, and Rammensee H-G. Allele-specific motifs revealed by sequencing of self-peptides eluted from MHC molecules. *Nature* 351(6324): 290-296 (1991).
144. Sinigaglia F and Hammer J. Defining rules for the peptide-MHC class II interaction. *Curr Opin Immunol* 6(1): 52-56 (1994).
145. He Y, Rozeboom L, Rivard CJ, Ellison K, Dziadziuszko R, Yu H, Zhou C, and Hirsch FR. MHC class II expression in lung cancer. *Lung Cancer* 112: 75-80 (2017).
146. Park IA, Hwang SH, Song IH, Heo SH, Kim YA, Bang WS, Park HS, Lee M, Gong G, and Lee HJ. Expression of the MHC class II in triple-negative breast cancer is associated with tumor-infiltrating lymphocytes and interferon signaling. *PLoS One* 12(8): e0182786 (2017).
147. Kurts C, Robinson BW, and Knolle PA. Cross-priming in health and disease. *Nat Rev Immunol* 10(6): 403-414 (2010).
148. Burnet M. Immunological Factors in the Process of Carcinogenesis. *Br Med Bull* 20(2): 154-158 (1964).
149. Burnet FM. Immunological surveillance in neoplasia. *Transplant Rev* 7(1): 3-25 (1971).
150. Burnet FM. The concept of immunological surveillance. *Prog Exp Tumor Res* 13: 1-27 (1970).
151. Dunn GP, Old LJ, and Schreiber RD. The three Es of cancer immunoediting. *Annu Rev Immunol* 22: 329-360 (2004).
152. Ribatti D. The concept of immune surveillance against tumors. The first theories. *Oncotarget* 8(4): 7175-7180 (2017).
153. Berlin C, Kowalewski DJ, Schuster H, Mirza N, Walz S, Handel M, Schmid-Horch B, Salih HR, Kanz L, Rammensee H-G, Stevanović S, and Stickel JS. Mapping the HLA ligandome landscape of acute myeloid leukemia: a targeted approach toward peptide-based immunotherapy. *Leukemia* 29(3): 647-659 (2015).
154. Snyder A, Makarov V, Merghoub T, Yuan J, Zaretsky JM, Desrichard A, Walsh LA, Postow MA, Wong P, Ho TS, Hollmann TJ, Bruggeman C, Kannan K, Li Y, Elipenahli C, Liu C, Harbison CT, Wang L, Ribas A, Wolchok JD, and Chan TA. Genetic basis for clinical response to CTLA-4 blockade in melanoma. *N Engl J Med* 371(23): 2189-2199 (2014).
155. Rizvi NA, Hellmann MD, Snyder A, Kvistborg P, Makarov V, Havel JJ, Lee W, Yuan J, Wong P, Ho TS, Miller ML, Rekhtman N, Moreira AL, Ibrahim F, Bruggeman C, Gasmi B, Zappasodi R, Maeda Y, Sander C, Garon EB, Merghoub T, Wolchok JD, Schumacher TN, and Chan TA. Cancer immunology. Mutational landscape determines sensitivity to PD-1 blockade in non-small cell lung cancer. *Science* 348(6230): 124-128 (2015).
156. Chowell D, Morris LGT, Grigg CM, Weber JK, Samstein RM, Makarov V, Kuo F, Kendall SM, Requena D, Riaz N, Greenbaum B, Carroll J, Garon E, Hyman DM, Zehir A, Solit D, Berger M, Zhou R, Rizvi NA, and Chan TA. Patient HLA class I genotype influences cancer response to checkpoint blockade immunotherapy. *Science* 359(6375): 582-587 (2018).

157. Tumeh PC, Harview CL, Yearley JH, Shintaku IP, Taylor EJ, Robert L, Chmielowski B, Spasic M, Henry G, Ciobanu V, West AN, Carmona M, Kivork C, Seja E, Cherry G, Gutierrez AJ, Grogan TR, Mateus C, Tomasic G, Glaspy JA, Emerson RO, Robins H, Pierce RH, Elashoff DA, Robert C, and Ribas A. PD-1 blockade induces responses by inhibiting adaptive immune resistance. *Nature* 515(7528): 568-571 (2014).
158. Reck M, Rodríguez-Abreu D, Robinson AG, Hui R, Csőszi T, Fülöp A, Gottfried M, Peled N, Tafreshi A, Cuffe S, O'Brien M, Rao S, Hotta K, Leiby MA, Lubiniecki GM, Shentu Y, Rangwala R, Brahmer JR, and Keynote-024 Investigators. Pembrolizumab versus Chemotherapy for PD-L1-Positive Non-Small-Cell Lung Cancer. *N Engl J Med* 375(19): 1823-1833 (2016).
159. Marin-Acevedo JA, Soyano AE, Dholaria B, Knutson KL, and Lou Y. Cancer immunotherapy beyond immune checkpoint inhibitors. *J Hematol Oncol* 11(1): 8 (2018).
160. Pettitt D, Arshad Z, Smith J, Stanic T, Holländer G, and Brindley D. CAR-T Cells: A Systematic Review and Mixed Methods Analysis of the Clinical Trial Landscape. *Mol Ther* 26(2): 342-353 (2018).
161. June CH, O'Connor RS, Kawalekar OU, Ghassemi S, and Milone MC. CAR T cell immunotherapy for human cancer. *Science* 359(6382): 1361-1365 (2018).
162. Neelapu SS, Locke FL, Bartlett NL, Lekakis LJ, Miklos DB, Jacobson CA, Braunschweig I, Oluwole OO, Siddiqi T, Lin Y, Timmerman JM, Stiff PJ, Friedberg JW, Flinn IW, Goy A, Hill BT, Smith MR, Deol A, Farooq U, McSweeney P, Munoz J, Avivi I, Castro JE, Westin JR, Chavez JC, Ghobadi A, Komanduri KV, Levy R, Jacobsen ED, Witzig TE, Reagan P, Bot A, Rossi J, Navale L, Jiang Y, Aycock J, Elias M, Chang D, Wiezorek J, and Go WY. Axicabtagene Ciloleucel CAR T-Cell Therapy in Refractory Large B-Cell Lymphoma. *N Engl J Med* 377(26): 2531-2544 (2017).
163. Maude SL, Laetsch TW, Buechner J, Rives S, Boyer M, Bittencourt H, Bader P, Verneris MR, Stefanski HE, Myers GD, Qayed M, De Moerloose B, Hiramatsu H, Schlis K, Davis KL, Martin PL, Nemecek ER, Yanik GA, Peters C, Baruchel A, Boissel N, Mechinaud F, Balduzzi A, Krueger J, June CH, Levine BL, Wood P, Taran T, Leung M, Mueller KT, Zhang Y, Sen K, Lebwohl D, Pulsipher MA, and Grupp SA. Tisagenlecleucel in Children and Young Adults with B-Cell Lymphoblastic Leukemia. *N Engl J Med* 378(5): 439-448 (2018).
164. Kantarjian H, Stein A, Gökbuget N, Fielding AK, Schuh AC, Ribera JM, Wei A, Dombret H, Foà R, Bassan R, Arslan Ö, Sanz MA, Bergeron J, Demirkan F, Lech-Maranda E, Rambaldi A, Thomas X, Horst HA, Brüggemann M, Klapper W, Wood BL, Fleishman A, Nagorsen D, Holland C, Zimmerman Z, and Topp MS. Blinatumomab versus Chemotherapy for Advanced Acute Lymphoblastic Leukemia. *N Engl J Med* 376(9): 836-847 (2017).
165. Salles G, Barrett M, Foà R, Maurer J, O'Brien S, Valente N, Wenger M, and Maloney DG. Rituximab in B-Cell Hematologic Malignancies: A Review of 20 Years of Clinical Experience. *Adv Ther* 34(10): 2232-2273 (2017).
166. Misra D, Frankel A, Hall P, Liu TF, Black J, Moore JO, de Castro C, Gockerman JP, Gasparetto C, Horwitz M, Davis PH, Chao NJ, and Rizzieri DA. The use of DT388-IL3 fusion protein in patients with refractory acute myeloid leukemia (AML). *Blood* 104(11): 212b-212b (2004).
167. Houot R, Schultz LM, Marabelle A, and Kohrt H. T-cell-based Immunotherapy: Adoptive Cell Transfer and Checkpoint Inhibition. *Cancer Immunol Res* 3(10): 1115-1122 (2015).
168. Met Ö, Jensen KM, Chamberlain CA, Donia M, and Svane IM. Principles of adoptive T cell therapy in cancer. *Semin Immunopathol* 41(1): 49-58 (2019).
169. Zhao Y, Zheng Z, Cohen CJ, Gattinoni L, Palmer DC, Restifo NP, Rosenberg SA, and Morgan RA. High-efficiency transfection of primary human and mouse T lymphocytes using RNA electroporation. *Mol Ther* 13(1): 151-159 (2006).
170. Clay TM, Custer MC, Sachs J, Hwu P, Rosenberg SA, and Nishimura MI. Efficient transfer of a tumor antigen-reactive TCR to human peripheral blood lymphocytes confers anti-tumor reactivity. *J Immunol* 163(1): 507-513 (1999).
171. Tsuji T, Yasukawa M, Matsuzaki J, Ohkuri T, Chamoto K, Wakita D, Azuma T, Niiya H, Miyoshi H, Kuzushima K, Oka Y, Sugiyama H, Ikeda H, and Nishimura T. Generation of tumor-specific, HLA class I-restricted human Th1 and Tc1 cells by cell engineering with tumor peptide-specific T-cell receptor genes. *Blood* 106(2): 470-476 (2005).
172. Peng PD, Cohen CJ, Yang S, Hsu C, Jones S, Zhao Y, Zheng Z, Rosenberg SA, and Morgan RA. Efficient nonviral Sleeping Beauty transposon-based TCR gene transfer to peripheral blood lymphocytes confers antigen-specific antitumor reactivity. *Gene Ther* 16(8): 1042-1049 (2009).
173. Eyquem J, Mansilla-Soto J, Giavridis T, van der Stegen SJ, Hamieh M, Cunanan KM, Odak A, Gönen M, and Sadelain M. Targeting a CAR to the TRAC locus with CRISPR/Cas9 enhances tumour rejection. *Nature* 543(7643): 113-117 (2017).
174. Nguyen LT, Saibil SD, Sotov V, Le MX, Khoja L, Ghazarian D, Bonilla L, Majeed H, Hogg D, Joshua AM, Crump M, Franke N, Spreafico A, Hansen A, Al-Habeeb A, Leong W, Easson A, Reedijk M, Goldstein DP, McCready D, Yasufuku K, Waddell T, Cypel M, Pierre A, Zhang B, Boross-Harmer S, Cipollone J, Nelles M, Scheid E, Fyrsta M, Lo CS, Nie J, Yam JY, Yen PH, Gray D, Motta V, Elford AR, DeLuca S, Wang L, Effendi S, Ellenchery R, Hirano N, Ohashi PS, and Butler MO. Phase II clinical trial of adoptive cell therapy for patients with metastatic melanoma with autologous tumor-infiltrating lymphocytes and low-dose interleukin-2. *Cancer Immunol Immunother* 68(5): 773-785 (2019).
175. Fesnak AD, June CH, and Levine BL. Engineered T cells: the promise and challenges of cancer immunotherapy. *Nat Rev Cancer* 16(9): 566-581 (2016).
176. Porter DL, Hwang WT, Frey NV, Lacey SF, Shaw PA, Loren AW, Bagg A, Marcucci KT, Shen A, Gonzalez V, Ambrose D, Grupp SA, Chew A, Zheng Z, Milone MC, Levine BL, Melenhorst JJ, and June CH. Chimeric antigen receptor T cells persist and induce sustained remissions in relapsed refractory chronic lymphocytic leukemia. *Sci Transl Med* 7(303): 303ra139 (2015).
177. Garfall AL, Maus MV, Hwang WT, Lacey SF, Mahnke YD, Melenhorst JJ, Zheng Z, Vogl DT, Cohen AD, Weiss BM, Dengel K, Kerr ND, Bagg A, Levine BL, June CH, and Stadtmauer EA. Chimeric Antigen Receptor T Cells against CD19 for Multiple Myeloma. *N Engl J Med* 373(11): 1040-1047 (2015).

178. Maude SL, Frey N, Shaw PA, Aplenc R, Barrett DM, Bunin NJ, Chew A, Gonzalez VE, Zheng Z, Lacey SF, Mahnke YD, Melenhorst JJ, Rheingold SR, Shen A, Teachey DT, Levine BL, June CH, Porter DL, and Grupp SA. Chimeric antigen receptor T cells for sustained remissions in leukemia. *N Engl J Med* 371(16): 1507-1517 (2014).
179. Armand P, Shipp MA, Ribrag V, Michot JM, Zinzani PL, Kuruvilla J, Snyder ES, Ricart AD, Balakumaran A, Rose S, and Moskowitz CH. Programmed Death-1 Blockade With Pembrolizumab in Patients With Classical Hodgkin Lymphoma After Brentuximab Vedotin Failure. *J Clin Oncol* 34(31): 3733-3739 (2016).
180. Ansell SM, Lesokhin AM, Borrello I, Halwani A, Scott EC, Gutierrez M, Schuster SJ, Millenson MM, Cattry D, Freeman GJ, Rodig SJ, Chapuy B, Ligon AH, Zhu L, Grosso JF, Kim SY, Timmerman JM, Shipp MA, and Armand P. PD-1 blockade with nivolumab in relapsed or refractory Hodgkin's lymphoma. *N Engl J Med* 372(4): 311-319 (2015).
181. ClinicalTrials.gov [Internet]. Bethesda (MD) National Library of Medicine (US). Identifier: NCT02011945 A Phase 1B Study to Investigate the Safety and Preliminary Efficacy for the Combination of Dasatinib Plus Nivolumab in Patients With Chronic Myeloid Leukemia. 2013 Dec 16 [cited 2018 May 05]; Available from: https://clinicaltrials.gov/ct2/show/NCT02011945.
182. Hu Z, Ott PA, and Wu CJ. Towards personalized, tumour-specific, therapeutic vaccines for cancer. *Nat Rev Immunol* 18(3): 168-182 (2018).
183. Kübler H, Scheel B, Gnad-Vogt U, Miller K, Schultze-Seemann W, Vom Dorp F, Parmiani G, Hampel C, Wedel S, Trojan L, Jocham D, Maurer T, Rippin G, Fotin-Mleczek M, von der Mülbe F, Probst J, Hoerr I, Kallen KJ, Lander T, and Stenzl A. Self-adjuvanted mRNA vaccination in advanced prostate cancer patients: a first-in-man phase I/IIa study. *J Immunother Cancer* 3(1): 26 (2015).
184. Pavlick AC, Blazquez A, Meseck M, Donovan MJ, Castillo-Martin M, Thin TH, Sabado R, Mandeli JP, Gnjatic S, Friedlander PA, and Bhardwaj N. A phase II open labeled, randomized study of poly-ICLC matured dendritic cells for NY-ESO-1 and Mean-A peptide vaccination compared to Montanide, in melanoma patients in complete clinical remission. *J Clin Oncol* 37(15_suppl): 9538-9538 (2019).
185. Schwartzentruber DJ, Lawson DH, Richards JM, Conry RM, Miller DM, Treisman J, Gailani F, Riley L, Conlon K, Pockaj B, Kendra KL, White RL, Gonzalez R, Kuzel TM, Curti B, Leming PD, Whitman ED, Balkissoon J, Reintgen DS, Kaufman H, Marincola FM, Merino MJ, Rosenberg SA, Choyke P, Vena D, and Hwu P. gp100 peptide vaccine and interleukin-2 in patients with advanced melanoma. *N Engl J Med* 364(22): 2119-2127 (2011).
186. Liepe J, Marino F, Sidney J, Jeko A, Bunting DE, Sette A, Kloetzel PM, Stumpf MP, Heck AJ, and Mishto M. A large fraction of HLA class I ligands are proteasome-generated spliced peptides. *Science* 354(6310): 354-358 (2016).
187. Mishto M and Liepe J. Post-Translational Peptide Splicing and T Cell Responses. *Trends Immunol* 38(12): 904-915 (2017).
188. Laumont CM, Daouda T, Laverdure JP, Bonneil É, Caron-Lizotte O, Hardy MP, Granados DP, Durette C, Lemieux S, Thibault P, and Perreault C. Global proteogenomic analysis of human MHC class I-associated peptides derived from non-canonical reading frames. *Nat Commun* 7: 10238 (2016).
189. Erhard F, Halenius A, Zimmermann C, L'Hernault A, Kowalewski DJ, Weekes MP, Stevanović S, Zimmer R, and Dölken L. Improved Ribo-seq enables identification of cryptic translation events. *Nat Methods* 15(5): 363-366 (2018).
190. Reeves E and James E. Antigen processing and immune regulation in the response to tumours. *Immunology* 150(1): 16-24 (2017).
191. Leone P, Shin EC, Perosa F, Vacca A, Dammacco F, and Racanelli V. MHC class I antigen processing and presenting machinery: organization, function, and defects in tumor cells. *J Natl Cancer Inst* 105(16): 1172-1187 (2013).
192. Seliger B, Maeurer MJ, and Ferrone S. Antigen-processing machinery breakdown and tumor growth. *Immunol Today* 21(9): 455-464 (2000).
193. da Silva VL, Fonseca AF, Fonseca M, da Silva TE, Coelho AC, Kroll JE, de Souza JES, Stransky B, de Souza GA, and de Souza SJ. Genome-wide identification of cancer/testis genes and their association with prognosis in a pan-cancer analysis. *Oncotarget* 8(54): 92966-92977 (2017).
194. Sonpavde G, Wang M, Peterson LE, Wang HY, Joe T, Mims MP, Kadmon D, Ittmann MM, Wheeler TM, Gee AP, Wang RF, and Hayes TG. HLA-restricted NY-ESO-1 peptide immunotherapy for metastatic castration resistant prostate cancer. *Invest New Drugs* 32(2): 235-242 (2014).
195. Krishnadas DK, Shusterman S, Bai F, Diller L, Sullivan JE, Cheerva AC, George RE, and Lucas KG. A phase I trial combining decitabine/dendritic cell vaccine targeting MAGE-A1, MAGE-A3 and NY-ESO-1 for children with relapsed or therapy-refractory neuroblastoma and sarcoma. *Cancer Immunol Immunother* 64(10): 1251-1260 (2015).
196. Schneider V, Egenrieder S, Götz M, Herbst C, Greiner J, and Hofmann S. Specific immune responses against epitopes derived from Aurora kinase A and B in acute myeloid leukemia. *Leuk Lymphoma* 54(7): 1500-1504 (2013).
197. Oka Y, Tsuboi A, Nakata J, Nishida S, Hosen N, Kumanogoh A, Oji Y, and Sugiyama H. Wilms' Tumor Gene 1 (WT1) Peptide Vaccine Therapy for Hematological Malignancies: From CTL Epitope Identification to Recent Progress in Clinical Studies Including a Cure-Oriented Strategy. *Oncol Res Treat* 40(11): 682-690 (2017).
198. Greiner J, Schmitt A, Giannopoulos K, Rojewski MT, Götz M, Funk I, Ringhoffer M, Bunjes D, Hofmann S, Ritter G, Döhner H, and Schmitt M. High-dose RHAMM-R3 peptide vaccination for patients with acute myeloid leukemia, myelodysplastic syndrome and multiple myeloma. *Haematologica* 95(7): 1191-1197 (2010).
199. Qazilbash MH, Wieder E, Thall PF, Wang X, Rios R, Lu S, Kanodia S, Ruisaard KE, Giralt SA, Estey EH, Cortes J, Komanduri KV, Clise-Dwyer K, Alatrash G, Ma Q, Champlin RE, and Molldrem JJ. PR1 peptide vaccine induces specific immunity with clinical responses in myeloid malignancies. *Leukemia* 31(3): 697-704 (2017).
200. Walz S, Stickel JS, Kowalewski DJ, Schuster H, Weisel K, Backert L, Kahn S, Nelde A, Stroh T, Handel M, Kohlbacher O, Kanz L, Salih HR, Rammensee H-G, and Stevanović S. The antigenic landscape of multiple myeloma: mass spectrometry (re)defines targets for T-cell-based immunotherapy. *Blood* 126(10): 1203-1213 (2015).

201. Peper JK, Bösmüller HC, Schuster H, Gückel B, Hörzer H, Roehle K, Schäfer R, Wagner P, Rammensee H-G, Stevanović S, Fend F, and Staebler A. HLA ligandomics identifies histone deacetylase 1 as target for ovarian cancer immunotherapy. *Oncoimmunology* 5(5): e1065369 (2016).
202. Schuster H, Peper JK, Bösmüller HC, Röhle K, Backert L, Bilich T, Ney B, Löffler MW, Kowalewski DJ, Trautwein N, Rabsteyn A, Engler T, Braun S, Haen SP, Walz JS, Schmid-Horch B, Brucker SY, Wallwiener D, Kohlbacher O, Fend F, Rammensee H-G, Stevanović S, Staebler A, and Wagner P. The immunopeptidomic landscape of ovarian carcinomas. *Proc Natl Acad Sci U S A* 114(46): E9942-E9951 (2017).
203. Kowalewski DJ, Schuster H, Backert L, Berlin C, Kahn S, Kanz L, Salih HR, Rammensee H-G, Stevanović S, and Stickel JS. HLA ligandome analysis identifies the underlying specificities of spontaneous antileukemia immune responses in chronic lymphocytic leukemia (CLL). *Proc Natl Acad Sci U S A* 112(2): E166-E175 (2015).
204. Harper DM, Franco EL, Wheeler C, Ferris DG, Jenkins D, Schuind A, Zahaf T, Innis B, Naud P, De Carvalho NS, Roteli-Martins CM, Teixeira J, Blatter MM, Korn AP, Quint W, Dubin G, and GlaxoSmithKline HPV Vaccine Study Group. Efficacy of a bivalent L1 virus-like particle vaccine in prevention of infection with human papillomavirus types 16 and 18 in young women: a randomised controlled trial. *Lancet* 364(9447): 1757-1765 (2004).
205. Kenter GG, Welters MJ, Valentijn AR, Lowik MJ, Berends-van der Meer DM, Vloon AP, Essahsah F, Fathers LM, Offringa R, Drijfhout JW, Wafelman AR, Oostendorp J, Fleuren GJ, van der Burg SH, and Melief CJ. Vaccination against HPV-16 oncoproteins for vulvar intraepithelial neoplasia. *N Engl J Med* 361(19): 1838-1847 (2009).
206. Lu YC, Yao X, Li YF, El-Gamil M, Dudley ME, Yang JC, Almeida JR, Douek DC, Samuels Y, Rosenberg SA, and Robbins PF. Mutated PPP1R3B Is Recognized by T Cells Used To Treat a Melanoma Patient Who Experienced a Durable Complete Tumor Regression. *J Immunol* 190(12): 6034-6042 (2013).
207. Yadav M, Jhunjhunwala S, Phung QT, Lupardus P, Tanguay J, Bumbaca S, Franci C, Cheung TK, Fritsche J, Weinschenk T, Modrusan Z, Mellman I, Lill JR, and Delamarre L. Predicting immunogenic tumour mutations by combining mass spectrometry and exome sequencing. *Nature* 515(7528): 572-576 (2014).
208. Kalaora S, Barnea E, Merhavi-Shoham E, Qutob N, Teer JK, Shimony N, Schachter J, Rosenberg SA, Besser MJ, Admon A, and Samuels Y. Use of HLA peptidomics and whole exome sequencing to identify human immunogenic neo-antigens. *Oncotarget* 7(5): 5110-5117 (2016).
209. Bassani-Sternberg M, Bräunlein E, Klar R, Engleitner T, Sinitcyn P, Audehm S, Straub M, Weber J, Slotta-Huspenina J, Specht K, Martignoni ME, Werner A, Hein R, H. BD, Peschel C, Rad R, Cox J, Mann M, and Krackhardt AM. Direct identification of clinically relevant neoepitopes presented on native human melanoma tissue by mass spectrometry. *Nat Commun* 7: 13404 (2016).
210. Ott PA, Hu Z, Keskin DB, Shukla SA, Sun J, Bozym DJ, Zhang W, Luoma A, Giobbie-Hurder A, Peter L, Chen C, Olive O, Carter TA, Li S, Lieb DJ, Eisenhaure T, Gjini E, Stevens J, Lane WJ, Javeri I, Nellaiappan K, Salazar AM, Daley H, Seaman M, Buchbinder EI, Yoon CH, Harden M, Lennon N, Gabriel S, Rodig SJ, Barouch DH, Aster JC, Getz G, Wucherpfennig K, Neuberg D, Ritz J, Lander ES, Fritsch EF, Hacohen N, and Wu CJ. An immunogenic personal neoantigen vaccine for patients with melanoma. *Nature* 547(7662): 217-221 (2017).
211. Sahin U, Derhovanessian E, Miller M, Kloke BP, Simon P, Löwer M, Bukur V, Tadmor AD, Luxemburger U, Schrörs B, Omokoko T, Vormehr M, Albrecht C, Paruzynski A, Kuhn AN, Buck J, Heesch S, Schreeb KH, Müller F, Ortseifer I, Vogler I, Godehardt E, Attig S, Rae R, Breitkreuz A, Tolliver C, Suchan M, Martic G, Hohberger A, Sorn P, Diekmann J, Ciesla J, Waksmann O, Brück AK, Witt M, Zillgen M, Rothermel A, Kasemann B, Langer D, Bolte S, Diken M, Kreiter S, Nemecek R, Gebhardt C, Grabbe S, Höller C, Utikal J, Huber C, Loquai C, and Türeci Ö. Personalized RNA mutanome vaccines mobilize poly-specific therapeutic immunity against cancer. *Nature* 547(7662): 222-226 (2017).
212. Finn OJ and Rammensee H-G. Is It Possible to Develop Cancer Vaccines to Neoantigens, What Are the Major Challenges, and How Can These Be Overcome? Neoantigens: Nothing New in Spite of the Name. *Cold Spring Harb Perspect Biol* 10(11) (2018).
213. Le DT, Wang-Gillam A, Picozzi V, Greten TF, Crocenzi T, Springett G, Morse M, Zeh H, Cohen D, Fine RL, Onners B, Uram JN, Laheru DA, Lutz ER, Solt S, Murphy AL, Skoble J, Lemmens E, Grous J, Dubensky T, Jr., Brockstedt DG, and Jaffee EM. Safety and survival with GVAX pancreas prime and Listeria Monocytogenes-expressing mesothelin (CRS-207) boost vaccines for metastatic pancreatic cancer. *J Clin Oncol* 33(12): 1325-1333 (2015).
214. Burkhardt UE, Hainz U, Stevenson K, Goldstein NR, Pasek M, Naito M, Wu D, Ho VT, Alonso A, Hammond NN, Wong J, Sievers QL, Brusic A, McDonough SM, Zeng W, Perrin A, Brown JR, Canning CM, Koreth J, Cutler C, Armand P, Neuberg D, Lee JS, Antin JH, Mulligan RC, Sasada T, Ritz J, Soiffer RJ, Dranoff G, Alyea EP, and Wu CJ. Autologous CLL cell vaccination early after transplant induces leukemia-specific T cells. *J Clin Invest* 123(9): 3756-3765 (2013).
215. Pyzer AR, Avigan DE, and Rosenblatt J. Clinical trials of dendritic cell-based cancer vaccines in hematologic malignancies. *Hum Vaccin Immunother* 10(11): 3125-3131 (2014).
216. Mukherji B, Chakraborty NG, Yamasaki S, Okino T, Yamase H, Sporn JR, Kurtzman SK, Ergin MT, Ozols J, and Meehan J. Induction of antigen-specific cytolytic T cells in situ in human melanoma by immunization with synthetic peptide-pulsed autologous antigen presenting cells. *Proc Natl Acad Sci U S A* 92(17): 8078-8082 (1995).
217. Cheever MA and Higano CS. PROVENGE (Sipuleucel-T) in prostate cancer: the first FDA-approved therapeutic cancer vaccine. *Clin Cancer Res* 17(11): 3520-3526 (2011).
218. Abou-El-Enein M, Elsanhoury A, and Reinke P. Overcoming Challenges Facing Advanced Therapies in the EU Market. *Cell Stem Cell* 19(3): 293-297 (2016).
219. Palucka K and Banchereau J. Dendritic-cell-based therapeutic cancer vaccines. *Immunity* 39(1): 38-48 (2013).
220. Sabado RL and Bhardwaj N. Cancer immunotherapy: dendritic-cell vaccines on the move. *Nature* 519(7543): 300-301 (2015).

221. Yang B, Jeang J, Yang A, Wu TC, and Hung CF. DNA vaccine for cancer immunotherapy. *Hum Vaccin Immunother* 10(11): 3153-3164 (2014).
222. Sahin U and Türeci Ö. Personalized vaccines for cancer immunotherapy. *Science* 359(6382): 1355-1360 (2018).
223. Tardón MC, Allard M, Dutoit V, Dietrich P-Y, and Walker PR. Peptides as cancer vaccines. *Curr Opin Pharmacol* 47: 20-26 (2019).
224. Bezu L, Kepp O, Cerrato G, Pol J, Fucikova J, Spisek R, Zitvogel L, Kroemer G, and Galluzzi L. Trial watch: Peptide-based vaccines in anticancer therapy. *Oncoimmunology* 7(12): e1511506 (2018).
225. Walter S, Weinschenk T, Stenzl A, Zdrojowy R, Pluzanska A, Szczylik C, Staehler M, Brugger W, Dietrich PY, Mendrzyk R, Hilf N, Schoor O, Fritsche J, Mahr A, Maurer D, Vass V, Trautwein C, Lewandrowski P, Flohr C, Pohla H, Stanczak JJ, Bronte V, Mandruzzato S, Biedermann T, Pawelec G, Derhovanessian E, Yamagishi H, Miki T, Hongo F, Takaha N, Hirakawa K, Tanaka H, Stevanović S, Frisch J, Mayer-Mokler A, Kirner A, Rammensee H-G, Reinhardt C, and Singh-Jasuja H. Multipeptide immune response to cancer vaccine IMA901 after single-dose cyclophosphamide associates with longer patient survival. *Nat Med* 18(8): 1254-1261 (2012).
226. Rini BI, Stenzl A, Zdrojowy R, Kogan M, Shkolnik M, Oudard S, Weikert S, Bracarda S, Crabb SJ, Bedke J, Ludwig J, Maurer D, Mendrzyk R, Wagner C, Mahr A, Fritsche J, Weinschenk T, Walter S, Kirner A, Singh-Jasuja H, Reinhardt C, and Eisen T. IMA901, a multipeptide cancer vaccine, plus sunitinib versus sunitinib alone, as first-line therapy for advanced or metastatic renal cell carcinoma (IMPRINT): a multicentre, open-label, randomised, controlled, phase 3 trial. *Lancet Oncol* 17(11): 1599-1611 (2016).
227. Gu Y, Zhao W, Meng F, Qu B, Zhu X, Sun Y, Shu Y, and Xu Q. Sunitinib impairs the proliferation and function of human peripheral T cell and prevents T-cell-mediated immune response in mice. *Clin Immunol* 135(1): 55-62 (2010).
228. Hilf N, Kuttruff-Coqui S, Frenzel K, Bukur V, Stevanović S, Gouttefangeas C, Platten M, Tabatabai G, Dutoit V, van der Burg SH, Thor Straten P, Martinez-Ricarte F, Ponsati B, Okada H, Lassen U, Admon A, Ottensmeier CH, Ulges A, Kreiter S, von Deimling A, Skardelly M, Migliorini D, Kroep JR, Idorn M, Rodon J, Piró J, Poulsen HS, Shraibman B, McCann K, Mendrzyk R, Löwer M, Stieglbauer M, Britten CM, Capper D, Welters MJP, Sahuquillo J, Kiesel K, Derhovanessian E, Rusch E, Bunse L, Song C, Heesch S, Wagner C, Kemmer-Brück A, Ludwig J, Castle JC, Schoor O, Tadmor AD, Green E, Fritsche J, Meyer M, Pawlowski N, Dorner S, Hoffgaard F, Rössler B, Maurer D, Weinschenk T, Reinhardt C, Huber C, Rammensee H-G, Singh-Jasuja H, Sahin U, Dietrich PY, and Wick W. Actively personalized vaccination trial for newly diagnosed glioblastoma. *Nature* 565(7738): 240-245 (2019).
229. Gouttefangeas C and Rammensee H-G. Personalized cancer vaccines: adjuvants are important, too. *Cancer Immunol Immunother* 67(12): 1911-1918 (2018).
230. Hoeller C, Michielin O, Ascierto PA, Szabo Z, and Blank CU. Systematic review of the use of granulocyte-macrophage colony-stimulating factor in patients with advanced melanoma. *Cancer Immunol Immunother* 65(9): 1015-1034 (2016).
231. Parmiani G, Castelli C, Pilla L, Santinami M, Colombo MP, and Rivoltini L. Opposite immune functions of GM-CSF administered as vaccine adjuvant in cancer patients. *Ann Oncol* 18(2): 226-232 (2007).
232. Steinhagen F, Kinjo T, Bode C, and Klinman DM. TLR-based immune adjuvants. *Vaccine* 29(17): 3341-3355 (2011).
233. Deres K, Schild H, Wiesmüller KH, Jung G, and Rammensee H-G. In vivo priming of virus-specific cytotoxic T lymphocytes with synthetic lipopeptide vaccine. *Nature* 342(6249): 561-564 (1989).
234. Rammensee H-G, Chandran A, Zelba H, Gouttefangeas C, Kowalewski D, Di Marco M, Haen S, Löffler M, Klein R, Laske K, Artzner K, Backert L, Schuster H, Schwenck J, la Fougére C, Pichler B, Kneilling M, Metzler G, Bauer J, Weide B, Schippert W, Stevanović S, and Wiesmüller KH. A new synthetic lipopeptide is a superior adjuvant for peptide vaccination. *14th Annual Meeting of the Association for Cancer Immunotherapy CIMT* (2016).
235. He X, Abrams SI, and Lovell JF. Peptide Delivery Systems for Cancer Vaccines. *Advanced Therapeutics* 1(5): 1800060 (2018).
236. Aucouturier J, Dupuis L, Deville S, Ascarateil S, and Ganne V. Montanide ISA 720 and 51: a new generation of water in oil emulsions as adjuvants for human vaccines. *Expert Rev Vaccines* 1(1): 111-118 (2002).
237. Khleif S. Strategies and designs for combination immune therapy. *J Transl Med* 13(Suppl 1): K7 (2015).
238. MacKay A, Weir G, Koblish H, Leahey AV, Kaliaperumal V, Tram C, Scherle P, and Stanford M. Combination of a T cell activating immunotherapy with immune modulators alters the tumor microenvironment and promotes more effective tumor control in preclinical models. *Cancer Res* 78(13 Supplement): 1761-1761 (2018).
239. Sharabi AB, Nirschl CJ, Kochel CM, Nirschl TR, Francica BJ, Velarde E, Deweese TL, and Drake CG. Stereotactic radiation therapy augments antigen-specific PD-1–mediated antitumor immune responses via cross-presentation of tumor antigen. *Cancer Immunol Res* 3(4): 345-355 (2015).
240. Ali OA, Lewin SA, Dranoff G, and Mooney DJ. Vaccines Combined with Immune Checkpoint Antibodies Promote Cytotoxic T-cell Activity and Tumor Eradication. *Cancer Immunol Res* 4(2): 95-100 (2016).
241. Krämer I, Engelhardt M, Fichtner S, Neuber B, Medenhoff S, Bertsch U, Hillengass J, Raab MS, Hose D, Ho AD, Goldschmidt H, and Hundemer M. Lenalidomide enhances myeloma-specific T-cell responses in vivo and in vitro. *Oncoimmunology* 5(5): e1139662 (2016).
242. Galustian C, Meyer B, Labarthe MC, Dredge K, Klaschka D, Henry J, Todryk S, Chen R, Muller G, Stirling D, Schafer P, Bartlett JB, and Dalgleish AG. The anti-cancer agents lenalidomide and pomalidomide inhibit the proliferation and function of T regulatory cells. *Cancer Immunol Immunother* 58(7): 1033-1045 (2009).
243. Ramsay AG, Johnson AJ, Lee AM, Gorgün G, Le Dieu R, Blum W, Byrd JC, and Gribben JG. Chronic lymphocytic leukemia T cells show impaired immunological synapse formation that can be reversed with an immunomodulating drug. *J Clin Invest* 118(7): 2427-2437 (2008).

244. Shanafelt TD, Ramsay AG, Zent CS, Leis JF, Tun HW, Call TG, LaPlant B, Bowen D, Pettinger A, Jelinek DF, Hanson CA, and Kay NE. Long-term repair of T-cell synapse activity in a phase II trial of chemoimmunotherapy followed by lenalidomide consolidation in previously untreated chronic lymphocytic leukemia (CLL). *Blood* 121(20): 4137-4141 (2013).
245. Bassani-Sternberg M, Barnea E, Beer I, Avivi I, Katz T, and Admon A. Soluble plasma HLA peptidome as a potential source for cancer biomarkers. *Proc Natl Acad Sci U S A* 107(44): 18769-18776 (2010).
246. Ritz D, Gloger A, Neri D, and Fugmann T. Purification of soluble HLA class I complexes from human serum or plasma deliver high quality immuno peptidomes required for biomarker discovery. *Proteomics* 17(1-2) (2017).
247. Rammensee H-G, Bachmann J, Emmerich NP, Bachor OA, and Stevanovic S. SYFPEITHI: database for MHC ligands and peptide motifs. *Immunogenetics* 50(3-4): 213-9 (1999).
248. Hoof I, Peters B, Sidney J, Pedersen LE, Sette A, Lund O, Buus S, and Nielsen M. NetMHCpan, a method for MHC class I binding prediction beyond humans. *Immunogenetics* 61(1): 1-13 (2009).
249. Weinzierl AO, Lemmel C, Schoor O, Müller M, Kruger T, Wernet D, Hennenlotter J, Stenzl A, Klingel K, Rammensee H-G, and Stevanović S. Distorted relation between mRNA copy number and corresponding major histocompatibility complex ligand density on the cell surface. *Mol Cell Proteomics* 6(1): 102-113 (2007).
250. Fortier MH, Caron E, Hardy MP, Voisin G, Lemieux S, Perreault C, and Thibault P. The MHC class I peptide repertoire is molded by the transcriptome. *J Exp Med* 205(3): 595-610 (2008).
251. Bassani-Sternberg M, Pletscher-Frankild S, Jensen LJ, and Mann M. Mass spectrometry of human leukocyte antigen class I peptidomes reveals strong effects of protein abundance and turnover on antigen presentation. *Mol Cell Proteomics* 14(3): 658-673 (2015).
252. Freudenmann LK, Marcu A, and Stevanović S. Mapping the tumour human leukocyte antigen (HLA) ligandome by mass spectrometry. *Immunology* 154(3): 331-345 (2018).
253. Wick W, Dietrich PY, Kuttruff S, Hilf N, Frenzel K, Admon A, van der Burg SH, von Deimling A, Gouttefangeas C, Kroep JR, Martinez-Ricarte F, Okada H, Ottensmeier C, Ponsati B, Poulsen HS, Stevanović S, Tabatabai G, Rammensee H-G, Sahin U, and Singh H. GAPVAC-101: First-in-human trial of a highly personalized peptide vaccination approach for patients with newly diagnosed glioblastoma. *J Clin Oncol* 36(15): 2000-2000 (2018).
254. Bilich T, Nelde A, Kowalewski DJ, Kanz L, Rammensee H-G, Stevanović S, Salih HR, and Walz JS. Definition and Characterization of a Peptide Warehouse for the Patient-Individualized Peptide Vaccination Study (iVAC-L-CLL01) after First Line Therapy of CLL. *Blood* 130(Suppl 1): 5346-5346 (2017).
255. Chong C, Marino F, Pak H, Racle J, Daniel RT, Müller M, Gfeller D, Coukos G, and Bassani-Sternberg M. High-throughput and Sensitive Immunopeptidomics Platform Reveals Profound Interferongamma-Mediated Remodeling of the Human Leukocyte Antigen (HLA) Ligandome. *Mol Cell Proteomics* 17(3): 533-548 (2018).

6. RESULTS

The results section of this thesis is divided into three separate parts. Part I and II are published manuscripts where the author of this thesis is the first or shared first author, respectively. Part III is in preparation for submission.

Part I **"HLA ligandome analysis of primary chronic lymphocytic leukemia (CLL) cells under lenalidomide treatment confirms the suitability of lenalidomide for combination with T-cell-based immunotherapy"** investigates the influence of the immunomodulatory drug lenalidomide on the HLA ligandome of primary CLL cells and especially on the presentation of the previously described CLL-associated antigens identified in the publication "HLA ligandome analysis identifies the underlying specificities of spontaneous antileukemia immune responses in chronic lymphocytic leukemia (CLL)" by Daniel Kowalewski and colleagues published in *Proceedings of the National Academy of Sciences* in 2015.

Part II **"The HLA ligandome landscape of chronic myeloid leukemia delineates novel T-cell epitopes for immunotherapy"** and Part III **"Development of a therapeutic peptide vaccine for the treatment of acute myeloid leukemia based on naturally presented HLA ligands of AML progenitor cells"** both describe state of the art immunopeptidomics characterizing the immunopeptidomic landscape of CML and AML in comparison to benign human cells and tissues and the consequent identification of leukemia-associated antigens suitable for tailored T-cell-based immunotherapy approaches for CML and AML patients, respectively. Furthermore, the focus of Part III lies on the characterization of the immunopeptidome not only of normal AML blasts cells, but especially of LPCs, which are the main reason for the high relapse rates in AML, and thereby the definition of LPC-associated antigens is of great importance for the specific targeting of these cells.

6.1. PART I:

HLA LIGANDOME ANALYSIS OF PRIMARY CHRONIC LYMPHOCYTIC LEUKEMIA (CLL) CELLS UNDER LENALIDOMIDE TREATMENT CONFIRMS THE SUITABILITY OF LENALIDOMIDE FOR COMBINATION WITH T-CELL-BASED IMMUNOTHERAPY

Annika Nelde[1], Daniel J. Kowalewski[1,2], Linus Backert[1,3], Heiko Schuster[1,2], Jan-Ole Werner[4], Reinhild Klein[4], Oliver Kohlbacher[3,5,6], Lothar Kanz[4], Helmut R. Salih[4,7], Hans-Georg Rammensee[1,8], Stefan Stevanović[1,8], Juliane S. Walz[4]

[1] Institute for Cell Biology, Department of Immunology, University of Tübingen, Germany
[2] Immatics Biotechnologies GmbH, Tübingen, Germany
[3] Applied Bioinformatics, Center for Bioinformatics and Department of Computer Science, University of Tübingen, Germany
[4] Department of Hematology and Oncology, University of Tübingen, Germany
[5] Quantitative Biology Center, University of Tübingen, Germany
[6] Biomolecular Interactions, Max Planck Institute for Developmental Biology, Tübingen, Germany
[7] Clinical Cooperation Unit Translational Immunology, German Cancer Consortium (DKTK), DKFZ partner site Tübingen
[8] German Cancer Consortium (DKTK), DKFZ partner site Tübingen

A.N. planned, performed and analyzed most experiments including the treatment of cells, quantification of HLA surface molecules, HLA immunoprecipitation experiments, and mass spectrometry analysis. A.N. contributed all figures and tables and was strongly involved in writing the manuscript.

Oncoimmunology (2017) 7(4): e1316438

6.1.1. ABSTRACT

Recent studies suggest that CLL is an immunogenic disease, which might be effectively targeted by antigen-specific T-cell-based immunotherapy. However, CLL is associated with a profound immune defect, which might represent a critical limitation for mounting clinically effective anti-tumor immune responses. As several studies have demonstrated that lenalidomide can reinforce effector T-cell responses in CLL, the combination of T-cell-based immunotherapy with the immunomodulatory drug lenalidomide represents a promising approach to overcome the immunosuppressive state in CLL. Antigen-specific immunotherapy also requires the robust presentation of tumor-associated HLA-presented antigens on target cells. We thus performed a longitudinal study of the effect of lenalidomide on the HLA ligandome of primary CLL cells *in vitro*. We showed that lenalidomide exposure does not affect absolute HLA class I and II surface expression levels on primary CLL cells. Importantly, semi-quantitative mass spectrometric analyses of the HLA peptidome of three CLL patient samples found only minor qualitative and quantitative effects of lenalidomide on HLA class I- and II-restricted peptide presentation. Furthermore, we confirmed stable presentation of previously described CLL-associated antigens under lenalidomide treatment. Strikingly, among the few HLA ligands showing significant modulation under lenalidomide treatment, we identified upregulated IKZF-derived peptides, which may represent a direct reflection of the cereblon-mediated effect of lenalidomide on CLL cells. Since we could not observe any relevant influence of lenalidomide on the established CLL-associated antigen targets of anti-cancer T-cell responses, this study validates the suitability of lenalidomide for the combination with antigen-specific T-cell-based immunotherapies.

6.1.2. INTRODUCTION

In recent years T-cell-based immunotherapy has become a main pillar of anti-cancer therapy.[1-9] However, profound immune defects in some cancer entities and immune escape mechanisms represent major limitations of these immunotherapeutic approaches.[10, 11] In order to overcome this obstacle and thereby to increase overall response rates in cancer patients, the combination of T-cell-based therapies with immunomodulatory drugs seems indispensable.

CLL represents a B-cell malignancy that shows characteristics of immunogenicity and immunosuppression: The immunogenicity, which is documented by graft-versus-leukemia effects after HSCT[12, 13] and by cases of spontaneous remissions after viral infections,[14] as well as favorable immune effector-to-target cell ratios in the MRD setting, suggest that CLL might be effectively targeted by T-cell-based immunotherapy.[15] On the other hand, CLL is associated with profound immune defects, characterized by defective $CD8^+$ and $CD4^+$ T-cell function,[16] increased frequencies of regulatory T cells[17] and defective immunological synapse formation,[18] which result in increased susceptibility to recurrent infections as well as failure to mount effective anti-tumor immune

responses. Lenalidomide, an immunomodulatory compound targeting both cancer cells and their microenvironment, has shown substantial activity in several hematological malignancies.[19] It has been approved for the treatment of multiple myeloma, myelodysplastic syndrome and mantle cell lymphoma and is currently investigated for the treatment of CLL.[20, 21] Several preclinical and clinical studies have proven the positive immunomodulatory effect of lenalidomide treatment on T-cell responses in CLL, demonstrating enhanced antigen uptake and improved priming of $CD8^+$ T cells by APCs,[22] reduction of regulatory T cells,[23] increased frequency of functional $CD8^+$ and $CD4^+$ T cells,[24] upregulation of costimulatory molecules on CLL cells[25] as well as the reconstitution of the defective T-cell immune synapse.[18, 26] Therefore, lenalidomide can be considered well suited for combination with antigen-specific T-cell-based immunotherapeutic approaches in CLL.

We recently conducted a study characterizing the antigenic landscape of CLL by mass spectrometric analysis of naturally presented HLA ligands and identified a panel of CLL-specific $CD8^+$ and $CD4^+$ T-cell epitope targets suitable for T-cell-based immunotherapy approaches in CLL patients.[27] Anti-cancer drugs can have marked effects on the HLA ligandome of tumor cells,[28, 29] including changes in HLA surface expression,[30, 31] the HLA allotype distribution,[32] as well as the induction of novel treatment-associated ligands.[33] For the combination of T-cell-based immunotherapy with other anti-cancer drugs it is thus of great importance to characterize the effects of these drugs not only on the effector cells but also on the antigenic landscape of the target cells. For lenalidomide it was recently shown that its clinical activity in CLL is not only mediated *via* the microenvironment but also by direct inhibition of CLL cell proliferation *via* cereblon.[34] This leads to the upregulation of the cyclin-dependent kinase inhibitor p21WAF1/Cip1 and to the increased degradation of the transcription factors IKZF1 and IKZF3.[34] These direct effects of lenalidomide might influence HLA ligand presentation of CLL cells. In the present study, we therefore comprehensively and semi-quantitatively mapped the impact of lenalidomide on HLA-restricted antigen presentation in primary CLL samples.

6.1.3. METHODS

Patients and blood samples

Peripheral blood mononuclear cells (PBMCs) from CLL patients (≥ 88% CLL cells) prior to therapy were isolated by density gradient centrifugation (Biocoll, L 6113). Informed written consent was obtained in accordance with the Declaration of Helsinki protocol. The study was performed according to the guidelines of the local ethics committee (373/2011BO2). Patient characteristics are provided in Table S1.

In vitro lenalidomide treatment of primary CLL samples

Primary CLL samples were cultured in RPMI1640 medium (life technologies, 52400-025) supplemented with 10% fetal bovine serum (life technologies, 10270-106), 1% penicillin/ streptomycin (Sigma, P4333), 1% non-essential amino acids (Biochrom, K 0293) and 1% sodium pyruvate (Biochrom, L 0473) and incubated with lenalidomide (0.5 µM, Selleckchem, S1029) for 24 or 48 hours (t_{24h} and t_{48h}). Controls were incubated with 0.005% DMSO as vehicle control for 24 or 48 hours. Cell viability analysis was performed using trypan blue exclusion staining. Experiments were conducted in three biological replicates where indicated. Therefor isolated PBMCs of the same blood sample were split into three portions for each condition and treated in parallel. Please note that one HLA class I data set (UPN1 untreated #3 t_{24h}) did not pass the quality control threshold of 500 ligands for being included in label-free quantitation (LFQ) analysis and had to be replaced by UPN1 untreated #2 t_{24h}. All analyses based on LFQ data therefore implement UPN1 untreated #2 compared with lenalidomide #3 as the data set #3 for lenalidomide-induced modulation at t_{24h}. For the HLA class I dataset of UPN2 the mass spectrometry analysis could only be performed at t_{24h} because of technical problems during the measurement of the lenalidomide t_{48h} dataset. Due to a low number of HLA class II ligands identified for UPN2 (mean: 149 HLA class II ligands per condition) this data set was excluded from the analyses. Sample characteristics including cell count, cell viability and HLA class I and II ligand IDs are provided in Table S2.

Quantification of HLA surface expression

HLA surface expression on $CD19^+CD5^+$ CLL cells and $CD19^+CD5^-$ autologous B cells of CLL patients was analyzed using the QIFIKIT bead-based quantitative flow cytometric assay (Dako, K0078) according to manufacturer's instructions as described before.[35] In brief, samples were stained with the pan-HLA class I specific monoclonal antibody (mAb) W6/32 (produced in-house), the HLA-DR-specific mAB L243 (produced in-house) or IgG isotype control (BioLegend, 400202), respectively. Surface marker staining was carried out with directly labeled APC anti-human CD19 (BioLegend, 302212), PE anti-human CD5 (BioLegend, 300608) and APC-H7 anti-human CD3 (BD, 641406) antibodies. Aqua fluorescent reactive dye (life technologies, L34957) was used as viability marker. Flow cytometric analysis was performed on a FACSCanto II Analyzer (BD).

Isolation of HLA ligands from primary CLL samples

HLA class I and class II molecules were isolated using standard immunoaffinity purification as described before,[36] using the pan-HLA class I-specific mAb W6/32, the pan-HLA class II-specific mAb Tü-39, and the HLA-DR-specific mAB L243 (all produced in-house) to extract HLA ligands. All samples of each patient were adjusted to identical cell counts prior to HLA ligand isolation.

Analysis of HLA ligands by liquid chromatography-tandem mass spectrometry (LC-MS/MS)

HLA ligand extracts were analyzed in five technical replicates as described previously.[27] In brief, peptide samples were separated by nanoflow high-performance LC (RSLCnano, Thermo Fisher Scientific) using a 50 µm x 25 cm PepMap rapid separation liquid chromatography column (Thermo Fisher Scientific) and a gradient ranging from 2.4% to 32.0% acetonitrile over the course of 90 min. Eluting peptides were analyzed in an online-coupled LTQ Orbitrap Fusion Lumos mass spectrometer (Thermo Fisher Scientific) using a top speed collision-induced dissociation (CID) fragmentation method for samples of UPN1 and UPN3. Samples of UPN2 were analyzed in an online-coupled LTQ Orbitrap XL mass spectrometer (Thermo Fisher Scientific) using a top 5 CID fragmentation method.

Database search and HLA annotation

Data processing was performed as described previously.[27] In brief, for UPN1 and UPN3 (orbitrap fragment spectra) the SEQUEST HT search engine (University of Washington)[37] and for UPN2 (ion trap fragment spectra) the Mascot search engine (Mascot 2.2.04; Matrix Science) were used to search the human proteome as comprised in the Swiss-Prot database (20,279 reviewed protein sequences, September 27th 2013) without enzymatic restriction. Precursor mass tolerance was set to 5 ppm, and fragment mass tolerance to 0.5 Da for ion trap spectra analyzed by Mascot and 0.02 Da for orbitrap spectra analyzed by SEQUEST HT, respectively. Oxidized methionine was allowed as a dynamic modification. The false discovery rate (FDR) was estimated using the Percolator algorithm[38] and limited to 5% for HLA class I and 1% for HLA class II. Peptide lengths were limited to 8 – 12 amino acids for HLA class I and to 8 – 25 amino acids for HLA class II. Protein inference was disabled, allowing for multiple protein annotations of peptides. HLA class I and class II annotation was performed using NetMHCpan 3.0[39, 40] and NetMHCIIpan 3.1[41] annotating peptides with IC_{50} scores or percentile rank below 500 nM or 2%, respectively. In cases of multiple possible annotations, the HLA allotype yielding the lowest rank/score was selected.

Label-free quantitation of HLA ligand presentation

For LFQ of the relative abundances of HLA ligands over the course of lenalidomide treatment, the total cell numbers of all samples per patient were normalized by adjusting the implemented volume of cell lysate prior to HLA ligand isolation. LC-MS/MS analysis was performed in five technical replicates for each sample. 500 HLA ligands per sample in five merged technical replicates were set as threshold for the inclusion of the sample in LFQ analysis. Relative quantification of HLA ligands was performed based on the area of the corresponding precursor extracted ion chromatograms using ProteomeDiscoverer 1.4.1.14. Peptide identifications and their measured intensities are provided in supplemental data 1-6 (Access *via* www.bloodjournal.org/content/128/22/3234). Reproducibility of quantitation across biological replicates in the LFQ strategy using matching between runs is shown in

a correlation analysis of the MS-measured intensities of identified HLA ligands (Figure S2). In order to cope with the common problem of missing values in DDA MS and label-free quantitative proteomics[42-44] we utilized a LFQ strategy using matching between runs to reduce missing values in quantitation by lowering FDR cutoffs. High quality peptide spectrum matches filtered for 5% FDR and subsequently screened for predicted HLA binding (NetMHCpan 3.0 rank < 2% or affinity < 500 nM) were used to generate seed lists for semi-quantitative volcano plot analysis. The sequences from these seed lists were then queried across all runs without applying any filtering for spectral quality criteria (XCorr, FDR) to extract areas for IDs not passing these thresholds. For Volcano plot analysis "one hit wonders" (peptides only found in one technical replicate) were discarded and the sample-specific limit of detection (LOD) was calculated as the median of the five lowest areas and inserted for missing areas to allow for fold-change calculation of HLA ligands detected in only one of both conditions. Technical replicates as well as experiments/conditions were normalized based on the summed intensities of all identified precursors in each MS run. Subsequently, the ratios of the mean areas of the individual peptides in the five LFQ-MS runs of each sample were calculated and unpaired, heteroskedastic two-tailed *t*-tests implementing Benjamini-Hochberg correction were performed using an in-house R script (v3.2.3).

Software and statistical analysis

Flow cytometric data analysis was performed using FlowJo 10.0.7 (Treestar). An in-house Python script was used for permutation analysis for the calculation of FDRs of treatment-associated peptides at different presentation frequencies, as described previously.[27] Briefly, the numbers of original treatment-associated peptides identified based on the analysis of the treated and untreated samples were compared to random simulated treatment-associated peptides. Simulated treated and untreated samples were generated *in silico* based on random weighted sampling from the entirety of peptide identifications in both original conditions. These randomized virtual ligandomes were used to define virtual treatment-associated peptides based on simulated cohorts of treated versus untreated samples. The process of peptide randomization, cohort assembly and identification of treatment-associated peptides was repeated 1,000 times and the mean values of resultant decoy identifications as well as the corresponding FDRs for any chosen frequency of treatment-exclusive peptide presentation were calculated. Of note, due to the limited number of biological replicates in UPN2 and UPN3 permutation analysis could only be performed for UPN1. In-house R scripts were utilized for volcano plots and longitudinal analysis of relative HLA ligand abundances. The longitudinal analysis of relative HLA ligand abundances utilizes the mean of three biological replicates. Overlap analysis were performed using BioVenn.[45] GraphPad Prism 6.0 (GraphPad Software) was used for statistical analysis. Comparative analysis of HLA surface expression was based on unpaired *t*-tests.

6.1.4. RESULTS

***In vitro* lenalidomide has no significant impact on HLA surface expression of primary CLL cells**

In order to assess the impact of lenalidomide on HLA surface expression, we performed longitudinal quantification of HLA class I and II surface molecule counts on primary CLL cells as well as autologous B cells of four patients upon *in vitro* incubation with lenalidomide. First, we analyzed the cytotoxicity of treatment with low dose (0.5 µM) lenalidomide on primary CLL samples. Viability analyses showed no significant difference between lenalidomide-treated cells and untreated controls, with mean cell viability of 71% and 74% at t_{48h}, respectively. With regard to HLA class I expression on $CD19^{+}CD5^{+}$ CLL cells, no significant impact of lenalidomide compared to untreated controls was observed (fold-change 0.92 – 1.02, t_{48h}), with expression levels ranging from 60,000 – 125,000 molecules/cell (Figure 1A and B). For HLA class II a slight increase of HLA surface molecules after lenalidomide treatment was detectable (fold-change 1.25 – 1.43, t_{48h}) with expression levels ranging from 29,000 – 201,000 molecules/cell (Figure 1C and D). In line, HLA class I and II quantification of autologous $CD19^{+}CD5^{-}$ B cells showed no significant impact of *in vitro* lenalidomide exposure compared to untreated controls (Figure S1).

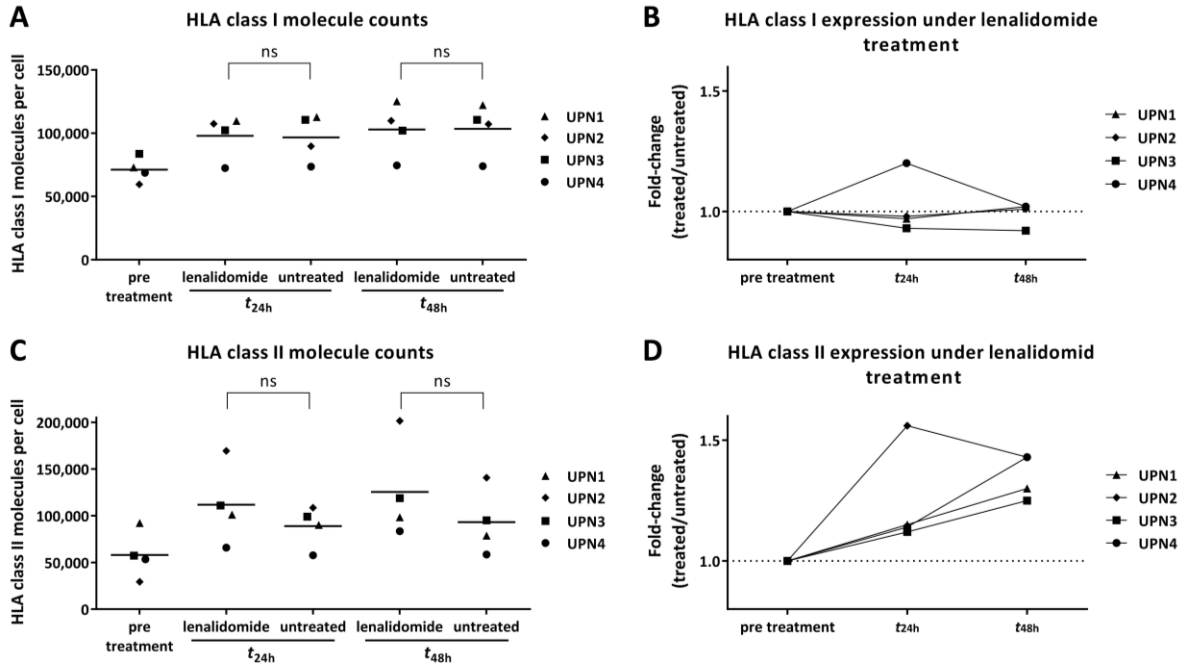

Figure 1: Effect of *in vitro* lenalidomide treatment on HLA class I and II surface expression on primary CLL cells. Quantification of HLA surface expression was performed using a bead-based flow cytometric assay using the pan-HLA class I-specific monoclonal antibody W6/32 and the HLA-DR-specific monoclonal antibody L243. Absolute counts of HLA class I (A) and HLA class II (C) surface molecules on primary $CD19^{+}CD5^{+}$ CLL cells (n = 4) treated *in vitro* with lenalidomide. Longitudinal analysis of relative changes (normalized to untreated controls) in HLA class I (B) and HLA class II (D) surface expression on primary CLL cells under *in vitro* lenalidomide treatment. Abbreviations: ns, not significant ($P \geq 0.05$, unpaired *t*-tests); UPN, uniform patient number.

Relative quantitation of HLA class I peptide presentation on primary CLL cells under *in vitro* lenalidomide treatment

To assess changes in HLA class I ligandome composition, direct mass spectrometric analysis of HLA class I ligand extracts was performed for three primary CLL samples prior to treatment and at t_{24h} and t_{48h}, as well as for the corresponding untreated controls. Based on available PBMC counts (Figure 2A) we performed *in vitro* lenalidomide treatment for UPN1 in three biological replicates and for UPN2 and UPN3 in single experiments. In total 6,991 unique naturally presented HLA class I ligands representing 3,983 source proteins were identified on these primary CLL cells (n = 3, Figure 2A, Supplemental Data 1-3, access *via* www.bloodjournal.org/content/128/22/3234). Within this dataset we were able to detect 35 different HLA-matched CLL-associated ligands (UPN1, 27; UPN2, 5; UPN3, 4) described in a previous study by our group (Figure 2A and B).[27] Using the summed peptide intensities of all FDR-filtered HLA ligand identifications as an indirect measure of total peptide abundance, we did not detect any major decrease of total HLA class I peptide presentation on lenalidomide-treated cells (t_{24h} and t_{48h} combined) compared to levels prior to treatment or untreated controls (UPN1, +35.1%; UPN2, -11.4%; UPN3, +3.1%; Figure 2C, Figure S4A and D).

A

UPN	PBMC count	class I ligand IDs	protein IDs	identified CLL-associated ligands
1	4.2×10^9	4,603	2,921	27
2	1.4×10^9	1,073	1,131	5
3	2.0×10^9	1,710	1,524	4
total		**6,991**	**3,983**	**35**

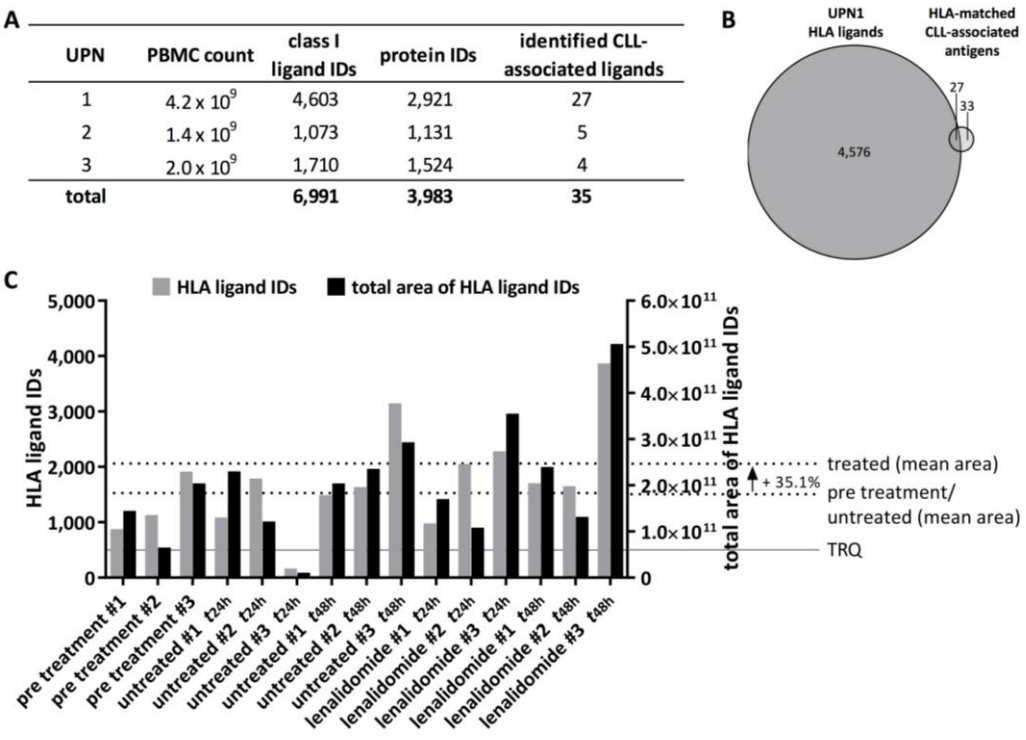

Figure 2: Mass spectrometric analysis of the HLA class I-presented peptidome of primary CLL cells under *in vitro* lenalidomide treatment. (A) Overview of PBMC count, unique HLA class I ligand IDs, representing source protein IDs and the number of identified HLA-matched CLL-associated antigens identified by mass spectrometry of analyzed primary CLL samples (n = 3). (B) Overlap analysis of HLA class I ligands identified on UPN1 with HLA-matched CLL-associated class I antigens identified in an earlier study. (C) HLA class I ligand extracts of UPN1 before *in vitro* treatment and at t_{24h} and t_{48h} after incubation with 0.5 µM lenalidomide or 0.005% DMSO (vehicle control) were analyzed in biological triplicates. The number of HLA ligand identifications and the summed area of their extracted ion chromatograms are indicated in grey and black bars, respectively. The threshold for relative quantitation (TRQ) was set to 500 HLA ligand IDs. Abbreviations: UPN, uniform patient number; TRQ, threshold for relative quantitation.

Lenalidomide has no substantial influence on the relative abundance of HLA-presented peptides and does not induce cryptic, treatment-associated HLA ligands

A first basic qualitative comparison of the HLA peptidomes of untreated versus lenalidomide-treated primary CLL cells using overlap analyses of HLA ligand identifications based on high quality peptide spectrum matches filtered for 5% FDR and HLA binding affinity suggests considerable differences in HLA ligandome composition. Comparison of the untreated samples (UPN1, 2 and 3 cells prior to treatment, and at t_{24h} and t_{48h} without lenalidomide exposure) with the treated samples revealed 8.3% (382/4,603 HLA ligands), 43.7% (469/1,073 HLA ligands), and 30.9% (529/1,710 HLA ligands) of the HLA ligandomes of UPN1, 2 and 3 to be exclusively presented on untreated cells, respectively. Whereas 22.3% (1,026/4,603 HLA ligands, UPN1), 4.8% (51/1,073 HLA ligands, UPN2), and 12.3% (210/1,710 HLA ligands, UPN3) of the HLA ligandomes were only detectable after treatment with lenalidomide (Figure 3A, Figure S4B and E). Out of the 1,287 treatment-exclusive HLA ligands 284 (22%) were never identified on any benign or malignant tissue comprised in our in-house database containing 260 HLA ligandomes of various normal tissues and organ specimens as well as 262 ligandomes of different malignant entities. In order to asses if any of these treatment-exclusive HLA ligands are significantly associated with lenalidomide treatment, we plotted the frequencies of peptide detection in the two different conditions (lenalidomide-treated n = 6, untreated n = 8, UPN1) and calculated the significance thresholds for treatment-associated presentation of HLA ligands based on permutation analysis as described previously (Figure 3B and S8A).[27] Notably, none of the 1,026 UPN1 HLA ligands exclusively detected on treated cells was found to reach the thresholds for significant association with lenalidomide treatment ($P < 0.05$).

Due to the fact that the missing value problem[42-44] is a major concern in data-dependent acquisition mass spectrometry (DDA MS) and label-free quantitative proteomics, we further used the strategy of matching between runs which reduces missing values in quantitation by lowering FDR cutoffs and thus results in more robust quantitation of peptides across conditions even in runs with lower numbers of FDR-filtered peptide identifications. The identified HLA ligand sequences – based on high quality peptide spectrum matches and 5% FDR – were queried among all runs without applying any filtering for spectral quality criteria (XCorr, FDR) to extract areas for IDs not passing these thresholds. Using this LFQ strategy we semi-quantitatively assessed HLA class I ligand presentation during *in vitro* lenalidomide treatment. We observed no relevant plasticity of the HLA class I ligandome of UPN1 after treatment with lenalidomide (0.03% up-modulation, 0.00% down-modulation, mean of three biological replicates) at t_{24h} compared to untreated controls (Figure 3C, single biological replicate analysis Figure S3A). At t_{48h} similar proportions of modulation were observed (0.00% up-modulation, 0.03% down-modulation, Figure 3D, single biological replicate analysis Figure S3B). The only HLA ligands that showed significant alteration in their abundance under lenalidomide treatment are the

IKZF1-derived peptide APHARNGLSL$_{419-428}$ (up-modulation at t_{24h}) and the IL1B-derived peptide SVDPKNYPK$_{200-208}$ (down-modulation at t_{48h}). Strikingly, plotting HLA ligand presentation of untreated UPN1 controls at t_{24h} and t_{48h} compared to levels of cells prior to lenalidomide treatment yielded even higher proportions of modulated HLA class I ligands, with 3.04% (2.96% up-modulation, 0.08% down-modulation) and 6.30% (4.15% up-modulation, 2.15% down-modulation) of HLA ligands significantly altered in their abundance at t_{24h} at t_{48h}, respectively (Figure 3E and F, single biological replicate analysis Figure S3C and D).

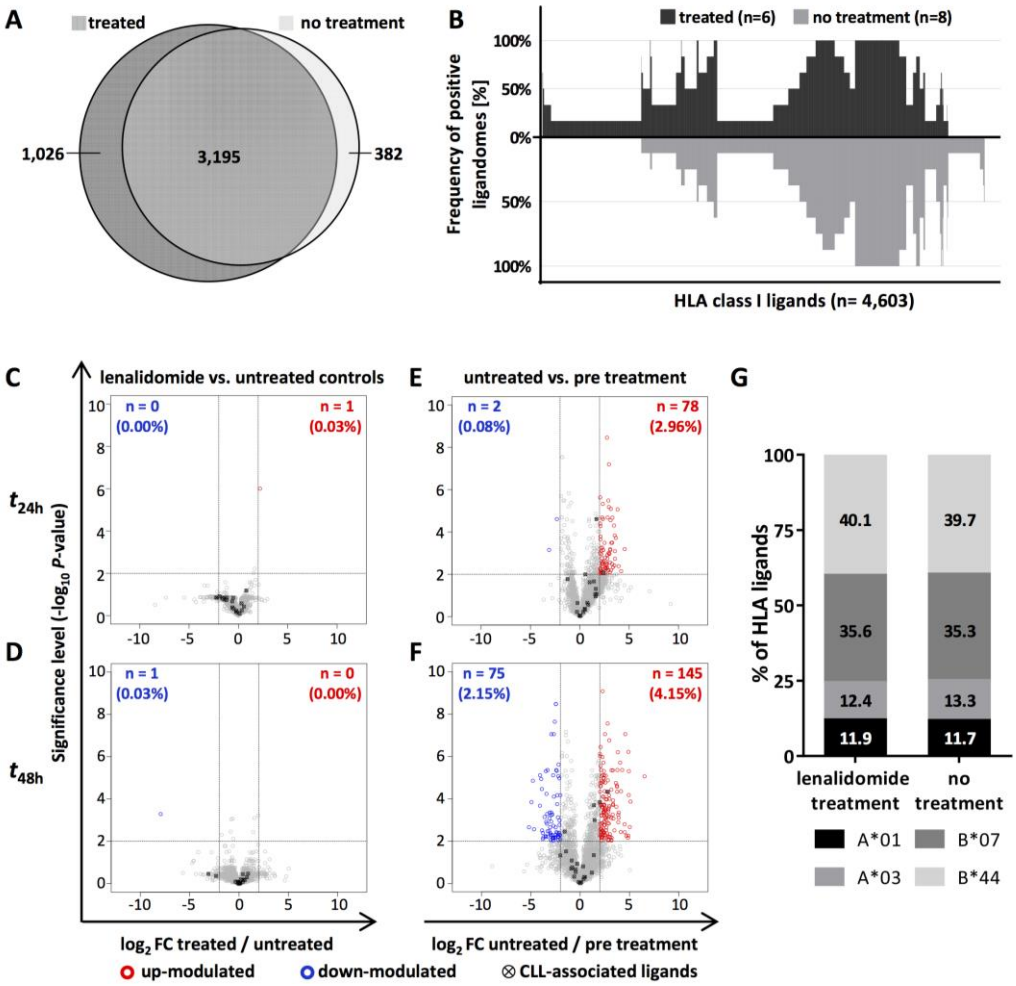

Figure 3: Quantitative and qualitative influence of *in vitro* lenalidomide treatment on the HLA class I peptidome of UPN1. (A) Overlap analysis of HLA class I ligands identified on lenalidomide- versus untreated (vehicle controls and pre treatment) cells. (B) Frequency-based analysis of peptide presentation on treated versus untreated (vehicle controls and pre treatment) UPN1 cells. HLA class I ligands are indicated on the x-axis, the frequency of positive ligandomes on the y-axis. (C-F) Volcano plots of the relative abundances of HLA ligands on UPN1 cells comparing the conditions indicated combining three biological replicates. Each dot represents a specific HLA ligand. Log_2 fold-changes of peptide abundance are indicated on the x-axis, the corresponding significance levels after multitesting correction ($-log_{10}$ *P*-value) on the y-axis. HLA ligands showing significant up- or down-modulation (≥ log_2 2-fold-change in abundance with $P < 0.01$) are highlighted in red and blue, respectively. The absolute numbers and percentages of significantly modulated ligands are specified in the corresponding quadrants. (C, D) Volcano plots comparing HLA ligand abundances on lenalidomide- versus untreated cells at t_{24h} and t_{48h}, respectively. (E, F) Control volcano plots comparing HLA ligand abundances on untreated cells at t_{24h} and t_{48h} to baseline levels prior to treatment. (G) Distribution of HLA restrictions among peptides identified on lenalidomide-treated (n = 4,221 peptides) versus untreated (vehicle controls and pre treatment) primary CLL cells (n = 3,577 peptides). Abbreviations: rep, replicate; vs., versus; FC, fold-change.

Gene ontology enrichment analysis (PANTHER version 11.1)[46, 47] comparing the source proteins of all identified HLA ligands on UPN1 with the up- and down-modulated source proteins identified in the volcano plot analysis using single biological replicates showed no significant protein enrichment of distinct biological processes. Lenalidomide treatment of UPN2 and UPN3 resulted in similarly low HLA ligandome plasticity (Figure S4C and F), which confirms that lenalidomide has no relevant influence on the HLA-presented peptidome of primary CLL cells. Furthermore, no differences in the HLA allotype distribution of the HLA ligands identified on lenalidomide-treated and untreated samples were detected (Figure 3G).

In vitro lenalidomide mediates no substantial quantitative or qualitative influence on the HLA class II ligandome of primary CLL cells

Because of the important role of $CD4^+$ T cells in anti-cancer immune responses[48-50] optimal target selection for T-cell-based immunotherapy may benefit from the inclusion of HLA class II epitopes. For the selection of such epitopes it is thus also necessary to map the effects of lenalidomide on the HLA class II ligandome. We identified a total of 6,767 unique HLA class II ligands representing 1,642 source proteins on primary CLL cells (n = 3, Figure 4A, Supplemental Data 4-6, access *via* www.bloodjournal.org/content/128/22/3234). Within this dataset we were able to detect 92 unique CLL-associated HLA class II epitopes described in a previous study (Figure 4A).[27] A first basic overlap analysis suggested considerable qualitative differences in the composition of HLA class II ligandomes on untreated versus lenalidomide-treated primary CLL cells. However, none of the 417/3,631 (11.5%) and 524/3,755 (14.0%) HLA class II ligands of UPN1 and 3 that showed exclusive presentation on lenalidomide-treated cells (Figure 4B and S6A) was found to reach the significance thresholds calculated based on permutation analysis (Figure 4C and S8B). Implementing LFQ using matching between runs we further semi-quantitatively assessed HLA class II ligand presentation during *in vitro* lenalidomide treatment. We observed no relevant plasticity of the HLA class II ligandome of UPN1 after treatment with lenalidomide with 0.11% and 0.06% of UPN1 ligands (mean of three biological replicates) showing significant modulation at t_{24h} and t_{48h} compared to untreated controls, respectively (Figure 4D and E, single biological replicate analysis Figure S5A and B). HLA ligand presentation of untreated UPN1 cells compared to the levels of cells prior to lenalidomide treatment yielded even higher proportions of modulated HLA class II ligands, with 3.05% and 6.54% of HLA ligands significantly altered in their abundance at t_{24h} and t_{48h}, respectively (Figure 4F and G, single biological replicate analysis Figure S5C and D). *In vitro* lenalidomide treatment of UPN3 resulted in similar HLA ligandome plasticity (Figure S6B and S7), which confirms that lenalidomide has no relevant influence on the relative abundances of HLA class II-presented peptides of primary CLL cells.

A

UPN	cell count	class II ligand IDs	protein IDs	identified CLL-associated ligands
1	4.2×10^9	3,631	867	37
2	1.4×10^9	461	347	13
3	2.0×10^9	3,755	1,183	68
total		**6,767**	**1,642**	**92**

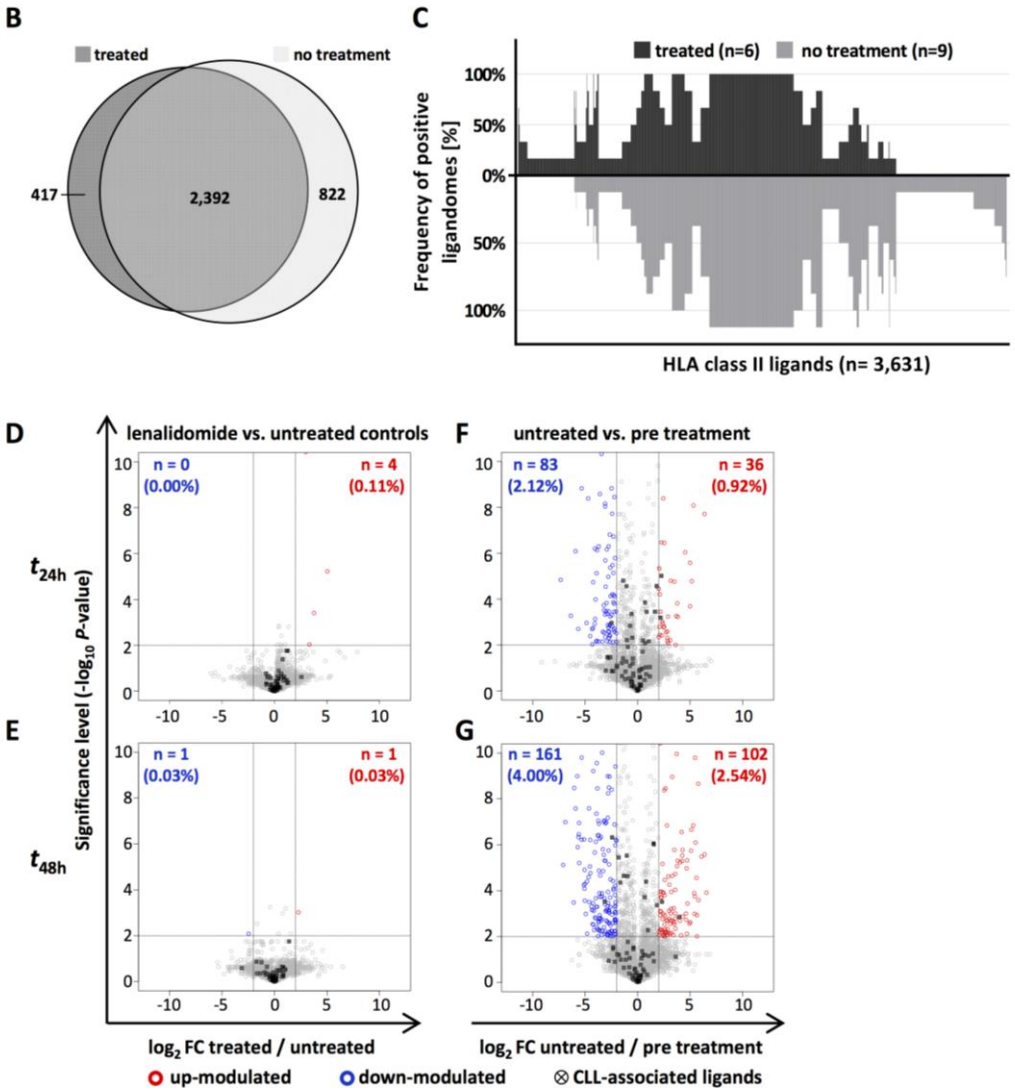

Figure 4: Quantitative and qualitative influence of *in vitro* lenalidomide treatment on the HLA class II peptidome of primary CLL cells. (A) Overview of PBMC count, unique HLA class II ligand IDs, corresponding source proteins and the number of unique CLL-associated antigens identified by mass spectrometry of analyzed primary CLL samples (n = 3). (B) Overlap analysis of HLA class II ligands identified on lenalidomide-treated versus untreated (vehicle controls and pre treatment) cells (UPN1). (C) Frequency-based analysis of peptide presentation on treated versus untreated (vehicle controls and pre treatment) UPN1 cells. HLA class II ligands are indicated on the x-axis, the frequency of positive ligandomes on the y-axis. (D-G) Volcano plots of modulation in the relative abundances of HLA class II ligands on UPN1 cells comparing the conditions indicated. Each dot represents a specific HLA ligand. Log_2 fold-changes of peptide abundance are indicated on the x-axis, the corresponding significance levels after multitesting correction ($-log_{10}$ *P*-value) on the y-axis. HLA ligands showing significant up- or down-modulation (≥ log_2 2-fold-change in abundance with $P < 0.01$) are highlighted in red and blue, respectively. The absolute numbers and percentages of significantly modulated ligands are specified in the corresponding quadrants. (D, E) Volcano plots comparing HLA ligand abundances on lenalidomide- versus untreated cells at t_{24h} and t_{48h}, respectively. (F, G) Control volcano plots comparing HLA ligand abundances on untreated cells at t_{24h} and t_{48h} to baseline levels prior to treatment. Abbreviations: UPN, uniform patient number; rep, replicate; vs., versus; FC, fold-change.

CLL-associated HLA ligands show robust presentation under lenalidomide treatment

As stable presentation of CLL-associated antigens is indispensable for the rational combination of lenalidomide with T-cell-based immunotherapy approaches, we next longitudinally analyzed the presentation kinetics of established CLL-associated HLA class I and class II ligands upon lenalidomide treatment. For UPN1 18/27 HLA class I and 29/37 HLA class II ligands could be longitudinally analyzed, as for these peptides MS2 identifications and quantifiable precursor extracted ion chromatograms were available for at least one replicate at each time point. CLL-associated HLA class I ligands showed only slight modulation due to lenalidomide treatment with median $\log_2$ fold-change (treated/untreated, mean of three replicates) of 0.28 (range -0.24 to 1.11) and 0.41 (range 0.21 to 1.00) at t_{24h} and t_{48h}, respectively (Figure 5A, Table S3). Tracking of these specific peptides in single replicate volcano plot analyses confirmed for 17/18 (94.4%) of these CLL-associated HLA ligands that the observed modulation did not reach statistical significance (Figure S3A and B). Similar results were obtained for CLL-associated HLA class II ligands with median $\log_2$ fold-change of -0.01 (range -0.81 to 1.23) and -0.22 (range -1.05 to 0.41) at t_{24h} and t_{48h}, respectively (Figure 5B, Table S4). 26/29 (89.7%) of these HLA class II ligands showed non-significant modulation in the single replicate volcano plot analysis (Figure S5A and B), confirming the robust presentation of the CLL-associated antigens under lenalidomide exposure.

IKZF1- and IKZF3-derived HLA ligands are selectively and significantly up-modulated under lenalidomide treatment of primary CLL cells

As the IKZF1-derived HLA class I ligand APHARNGLSL$_{419-428}$ showed significant up-modulation under lenalidomide treatment (UPN1, Figure 3C) we aimed to analyze whether the direct inhibition of CLL cell proliferation *via* cereblon caused by lenalidomide is reflected in the HLA ligandome of treated primary CLL cells. We screened the HLA ligandome of UPN1 for the presence of IKZF1- and IKZF3-derived ligands, as these two transcription factors undergo increased proteasomal degradation under lenalidomide treatment.[34, 51] We identified two length variants of an IKZF1-derived HLA class I ligand (APHARNGLSL$_{419-428}$, B*07:02; APHARNGL$_{419-426}$, B*07:02) and one IKZF3-derived HLA class I ligand (AEMGSERAL$_{246-254}$, B*44:02). Strikingly, the IKZF3-derived ligand was detected exclusively on CLL cells after lenalidomide treatment and the IKZF1-derived ligands showed substantial up-modulation under lenalidomide treatment with median $\log_2$ fold-changes (treated/untreated, mean of three replicates) of 1.25 and 1.72 at t_{24h} and t_{48h}, respectively (Figure 5C). In the single replicate volcano plot analysis comparing the HLA ligandomes of lenalidomide-treated cells with cells prior to treatment, the IKZF1-derived ligand APHARNGLSL reached significance thresholds ($\log_2$ fold-change ≥ 2, $P \leq 0.01$ after multitesting correction) for up-modulation in 2/3 biological replicates at both, t_{24h} and t_{48h} (Figure 5D and E).

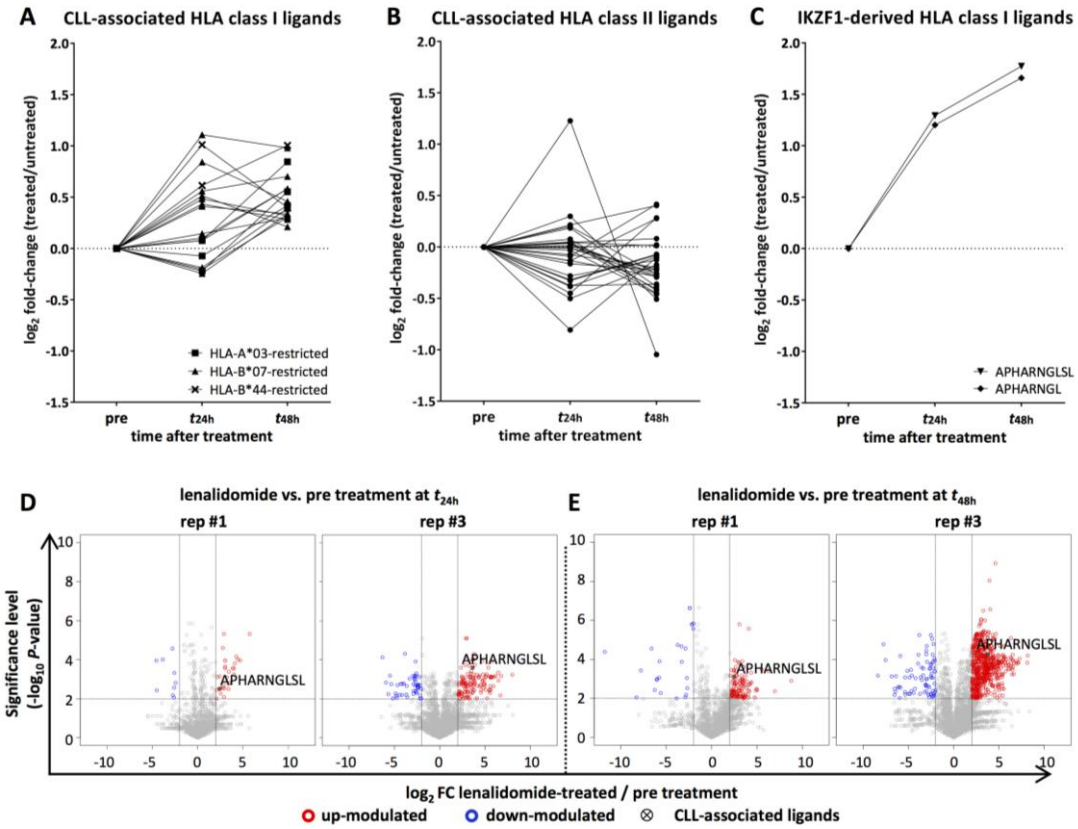

Figure 5: Kinetics of CLL-associated and IKZF1-derived HLA ligand presentation on primary CLL cells (UPN1) after treatment with lenalidomide. (A-C) Longitudinal analysis of the presentation of CLL-associated HLA class I (A) and class II (B) ligands as wells as IKZF1-derived HLA class I ligands (C) after *in vitro* treatment with lenalidomide. Modulation in peptide abundance is indicated on the y-axis as $\log_2$ fold-change compared to untreated controls. (D, E) Volcano plots of the modulation in the relative abundances of HLA ligands on UPN1 cells comparing lenalidomide-treated cell with cells prior to treatment at t_{24h} (D) and t_{48h} (E). Each dot represents a specific HLA ligand. Log_2 fold-changes of peptide abundance are indicated on the x-axis, the corresponding significance levels after multitesting correction ($-\log_{10}$ *P*-value) on the y-axis. HLA ligands showing significant up- or down-modulation ($\geq \log_2$ 2-fold-change in abundance with $P < 0.01$) are highlighted in red and blue, respectively. The significantly modulated IKZF1-derived HLA class I ligand ($\text{APHARNGLSL}_{419\text{-}428}$ B*07:02) is labeled in black. Abbreviations: vs., versus; rep, replicate; FC, fold-change.

6.1.5. DISCUSSION

The positive effects of the immunomodulatory drug lenalidomide on antibody-dependent natural killer cell-mediated cytotoxicity,[52] antigen presentation by DCs[22] as well as T-cell function and activation[23, 24] suggest that lenalidomide is a promising compound for combination with T-cell-based immunotherapeutic approaches.[53] As precise and effective antigen-specific cancer immunotherapy requires the exact knowledge of presentation patterns and kinetics of tumor-associated HLA-presented epitopes that can act as rejection antigens, a potential impact of lenalidomide on antigen presentation of target cells would be of paramount interest. To our knowledge, this is the first study that evaluates the influence of lenalidomide on the HLA-presented immunopeptidome of primary cancer cells. Our previous studies indicated that a mass spectrometry-based approach is highly efficient in longitudinally mapping the effect of anti-cancer drugs on the HLA ligandome[32] as well as for identification of physiological targets of anti-cancer T-cell responses in patients with hematological malignancies.[27, 54, 55] In CLL, this strategy enabled us to establish a panel of highly

specific, immunogenic and pathophysiologically relevant CLL-associated antigens, which may be implemented for antigen-specific immunotherapy.[27] However, profound immune defects in CLL patients might constitute a major limitation for such T-cell-based approaches.[16-18] Combination of specific T-cell-based approaches with the immunomodulatory agent lenalidomide may represent a suitable option to overcome the immunosuppressive state in CLL.[26] The present study was designed to analyze the impact of lenalidomide on the HLA-presented antigenic landscape of primary CLL cells, thereby allowing the informed selection of robustly presented targets for antigen-specific immunotherapy. We utilized the dose of 0.5 µM of lenalidomide for *in vitro* treatment of primary CLL cells, which was previously shown to be adequate to induce the reported positive effects on the microenvironment of CLL, especially on T cells.[18] To take into account the kinetics of HLA peptide processing and presentation[56] we implemented two time points of longitudinal HLA ligandome analysis at t_{24h} and $t_{48h.}$ We found that lenalidomide does not cause a significant alteration of HLA class I and II surface expression on CLL and autologous B cells in contrast to several other anti-cancer drugs.[30, 31, 57, 58] The quantitative and qualitative changes in the HLA class I and II ligandome following lenalidomide treatment were very moderate compared to the previously reported effects of carfilzomib and bortezomib on HLA ligand presentation.[32, 59] Furthermore, no relevant alterations in the HLA allotype distribution or in the presentation of previously defined CLL-associated HLA ligands were detected, which enables a straightforward target selection in CLL patients irrespective of lenalidomide treatment. Recent data demonstrated the induction of novel, cryptic, treatment-associated HLA ligands for anti-cancer drugs like decitabine[33] and carfilzomib.[32] In this study we demonstrate that lenalidomide does not significantly induce cryptic, treatment-associated antigens. However, we detected a significant up-modulation of IKZF1-derived HLA-presented peptides under lenalidomide exposure, which might be due to the direct effect of lenalidomide on CLL cells *via* cereblon-driven proteasomal degradation of this transcription factor. Further studies will be needed to evaluate the impact of IKZF1- and IKZF3-induced peptides under lenalidomide treatment, especially concerning their eligibility as novel T-cell epitopes.

Together, our study shows that *in vitro* lenalidomide has no relevant influence on the HLA-presented immunopeptidome of primary CLL cells and therefore adds novel important aspects toward characterizing lenalidomide as a suitable agent for the combination with T-cell-based immunotherapy. Based on these results we implemented a phase II peptide vaccination study combining our CLL-associated HLA ligands[27] with lenalidomide treatment following first-line therapy of CLL patients (NCT02802943).[60]

6.1.6. REFERENCES

1. Couzin-Frankel J. Breakthrough of the year 2013. Cancer immunotherapy. *Science* 342(6165): 1432-1433 (2013).
2. McDermott DF, Drake CG, Sznol M, Choueiri TK, Powderly JD, Smith DC, Brahmer JR, Carvajal RD, Hammers HJ, Puzanov I, Hodi FS, Kluger HM, Topalian SL, Pardoll DM, Wigginton JM, Kollia GD, Gupta A, McDonald D, Sankar V, Sosman JA, and Atkins MB. Survival, Durable Response, and Long-Term Safety in Patients With Previously Treated Advanced Renal Cell Carcinoma Receiving Nivolumab. *J Clin Oncol* 33(18): 2013-2020 (2015).
3. Brahmer J, Reckamp KL, Baas P, Crinò L, Eberhardt WE, Poddubskaya E, Antonia S, Pluzanski A, Vokes EE, Holgado E, Waterhouse D, Ready N, Gainor J, Arén Frontera O, Havel L, Steins M, Garassino MC, Aerts JG, Domine M, Paz-Ares L, Reck M, Baudelet C, Harbison CT, Lestini B, and Spigel DR. Nivolumab versus Docetaxel in Advanced Squamous-Cell Non-Small-Cell Lung Cancer. *N Engl J Med* 373(2): 123-135 (2015).
4. Gettinger SN, Horn L, Gandhi L, Spigel DR, Antonia SJ, Rizvi NA, Powderly JD, Heist RS, Carvajal RD, Jackman DM, Sequist LV, Smith DC, Leming P, Carbone DP, Pinder-Schenck MC, Topalian SL, Hodi FS, Sosman JA, Sznol M, McDermott DF, Pardoll DM, Sankar V, Ahlers CM, Salvati M, Wigginton JM, Hellmann MD, Kollia GD, Gupta AK, and Brahmer JR. Overall Survival and Long-Term Safety of Nivolumab (Anti-Programmed Death 1 Antibody, BMS-936558, ONO-4538) in Patients With Previously Treated Advanced Non-Small-Cell Lung Cancer. *J Clin Oncol* 33(18): 2004-2012 (2015).
5. Riley JL. Combination checkpoint blockade--taking melanoma immunotherapy to the next level. *N Engl J Med* 369(2): 187-189 (2013).
6. Robbins PF, Kassim SH, Tran TL, Crystal JS, Morgan RA, Feldman SA, Yang JC, Dudley ME, Wunderlich JR, Sherry RM, Kammula US, Hughes MS, Restifo NP, Raffeld M, Lee CC, Li YF, El-Gamil M, and Rosenberg SA. A pilot trial using lymphocytes genetically engineered with an NY-ESO-1-reactive T-cell receptor: long-term follow-up and correlates with response. *Clin Cancer Res* 21(5): 1019-1027 (2015).
7. Kochenderfer JN, Dudley ME, Kassim SH, Somerville RP, Carpenter RO, Stetler-Stevenson M, Yang JC, Phan GQ, Hughes MS, Sherry RM, Raffeld M, Feldman S, Lu L, Li YF, Ngo LT, Goy A, Feldman T, Spaner DE, Wang ML, Chen CC, Kranick SM, Nath A, Nathan DA, Morton KE, Toomey MA, and Rosenberg SA. Chemotherapy-refractory diffuse large B-cell lymphoma and indolent B-cell malignancies can be effectively treated with autologous T cells expressing an anti-CD19 chimeric antigen receptor. *J Clin Oncol* 33(6): 540-549 (2015).
8. Porter DL, Levine BL, Kalos M, Bagg A, and June CH. Chimeric antigen receptor-modified T cells in chronic lymphoid leukemia. *N Engl J Med* 365(8): 725-733 (2011).
9. Walter S, Weinschenk T, Stenzl A, Zdrojowy R, Pluzanska A, Szczylik C, Staehler M, Brugger W, Dietrich PY, Mendrzyk R, Hilf N, Schoor O, Fritsche J, Mahr A, Maurer D, Vass V, Trautwein C, Lewandrowski P, Flohr C, Pohla H, Stanczak JJ, Bronte V, Mandruzzato S, Biedermann T, Pawelec G, Derhovanessian E, Yamagishi H, Miki T, Hongo F, Takaha N, Hirakawa K, Tanaka H, Stevanović S, Frisch J, Mayer-Mokler A, Kirner A, Rammensee H-G, Reinhardt C, and Singh-Jasuja H. Multipeptide immune response to cancer vaccine IMA901 after single-dose cyclophosphamide associates with longer patient survival. *Nat Med* 18(8): 1254-1261 (2012).
10. Ahmad M, Rees RC, and Ali SA. Escape from immunotherapy: possible mechanisms that influence tumor regression/progression. *Cancer Immunol Immunother* 53(10): 844-854 (2004).
11. Gao J, Shi LZ, Zhao H, Chen J, Xiong L, He Q, Chen T, Roszik J, Bernatchez C, Woodman SE, Chen PL, Hwu P, Allison JP, Futreal A, Wargo JA, and Sharma P. Loss of IFN-gamma Pathway Genes in Tumor Cells as a Mechanism of Resistance to Anti-CTLA-4 Therapy. *Cell* 167(2): 397-404 e9 (2016).
12. Russell NH, Byrne JL, Faulkner RD, Gilyead M, Das-Gupta EP, and Haynes AP. Donor lymphocyte infusions can result in sustained remissions in patients with residual or relapsed lymphoid malignancy following allogeneic haemopoietic stem cell transplantation. *Bone Marrow Transplant* 36(5): 437-441 (2005).
13. Gribben JG, Zahrieh D, Stephans K, Bartlett-Pandite L, Alyea EP, Fisher DC, Freedman AS, Mauch P, Schlossman R, Sequist LV, Soiffer RJ, Marshall B, Neuberg D, Ritz J, and Nadler LM. Autologous and allogeneic stem cell transplantations for poor-risk chronic lymphocytic leukemia. *Blood* 106(13): 4389-4396 (2005).
14. Ribera JM, Viñolas N, Urbano-Ispizua A, Gallart T, Montserrat E, and Rozman C. "Spontaneous" complete remissions in chronic lymphocytic leukemia: report of three cases and review of the literature. *Blood Cells* 12(2): 471-483 (1987).
15. Ritgen M, Stilgenbauer S, von Neuhoff N, Humpe A, Brüggemann M, Pott C, Raff T, Kröber A, Bunjes D, Schlenk R, Schmitz N, Döhner H, Kneba M, and Dreger P. Graft-versus-leukemia activity may overcome therapeutic resistance of chronic lymphocytic leukemia with unmutated immunoglobulin variable heavy-chain gene status: implications of minimal residual disease measurement with quantitative PCR. *Blood* 104(8): 2600-2602 (2004).
16. Riches JC, Davies JK, McClanahan F, Fatah R, Iqbal S, Agrawal S, Ramsay AG, and Gribben JG. T cells from CLL patients exhibit features of T-cell exhaustion but retain capacity for cytokine production. *Blood* 121(9): 1612-1621 (2013).
17. Jak M, Mous R, Remmerswaal EB, Spijker R, Jaspers A, Yagüe A, Eldering E, Van Lier RA, and Van Oers MH. Enhanced formation and survival of CD4+ CD25hi Foxp3+ T-cells in chronic lymphocytic leukemia. *Leuk Lymphoma* 50(5): 788-801 (2009).
18. Ramsay AG, Johnson AJ, Lee AM, Gorgün G, Le Dieu R, Blum W, Byrd JC, and Gribben JG. Chronic lymphocytic leukemia T cells show impaired immunological synapse formation that can be reversed with an immunomodulating drug. *J Clin Invest* 118(7): 2427-2437 (2008).
19. Zeldis JB, Knight R, Hussein M, Chopra R, and Muller G. A review of the history, properties, and use of the immunomodulatory compound lenalidomide. *Ann N Y Acad Sci* 1222: 76-82 (2011).

20. Bühler A, Wendtner CM, Kipps TJ, Rassenti L, Fraser GA, Michallet AS, Hillmen P, Dürig J, Gregory SA, Kalaycio M, Aurran-Schleinitz T, Trentin L, Gribben JG, Chanan-Khan A, Purse B, Zhang J, De Bedout S, Mei J, Hallek M, and Stilgenbauer S. Lenalidomide treatment and prognostic markers in relapsed or refractory chronic lymphocytic leukemia: data from the prospective, multicenter phase-II CLL-009 trial. *Blood Cancer J* 6: e404 (2016).
21. Liang L, Zhao M, Zhu YC, Hu X, Yang LP, and Liu H. Efficacy of lenalidomide in relapsed/refractory chronic lymphocytic leukemia patient: a systematic review and meta-analysis. *Ann Hematol* 95(9): 1473-1482 (2016).
22. Henry JY, Labarthe MC, Meyer B, Dasgupta P, Dalgleish AG, and Galustian C. Enhanced cross-priming of naive CD8+ T cells by dendritic cells treated by the IMiDs(R) immunomodulatory compounds lenalidomide and pomalidomide. *Immunology* 139(3): 377-385 (2013).
23. Galustian C, Meyer B, Labarthe MC, Dredge K, Klaschka D, Henry J, Todryk S, Chen R, Muller G, Stirling D, Schafer P, Bartlett JB, and Dalgleish AG. The anti-cancer agents lenalidomide and pomalidomide inhibit the proliferation and function of T regulatory cells. *Cancer Immunol Immunother* 58(7): 1033-1045 (2009).
24. Lee BN, Gao H, Cohen EN, Badoux X, Wierda WG, Estrov Z, Faderl SH, Keating MJ, Ferrajoli A, and Reuben JM. Treatment with lenalidomide modulates T-cell immunophenotype and cytokine production in patients with chronic lymphocytic leukemia. *Cancer* 117(17): 3999-4008 (2011).
25. Aue G, Njuguna N, Tian X, Soto S, Hughes T, Vire B, Keyvanfar K, Gibellini F, Valdez J, Boss C, Samsel L, McCoy JP, Wilson WH, Pittaluga S, and Wiestner A. Lenalidomide-induced upregulation of CD80 on tumor cells correlates with T-cell activation, the rapid onset of a cytokine release syndrome and leukemic cell clearance in chronic lymphocytic leukemia. *Haematologica* 94(9): 1266-1273 (2009).
26. Shanafelt TD, Ramsay AG, Zent CS, Leis JF, Tun HW, Call TG, LaPlant B, Bowen D, Pettinger A, Jelinek DF, Hanson CA, and Kay NE. Long-term repair of T-cell synapse activity in a phase II trial of chemoimmunotherapy followed by lenalidomide consolidation in previously untreated chronic lymphocytic leukemia (CLL). *Blood* 121(20): 4137-4141 (2013).
27. Kowalewski DJ, Schuster H, Backert L, Berlin C, Kahn S, Kanz L, Salih HR, Rammensee H-G, Stevanović S, and Stickel JS. HLA ligandome analysis identifies the underlying specificities of spontaneous antileukemia immune responses in chronic lymphocytic leukemia (CLL). *Proc Natl Acad Sci U S A* 112(2): E166-E175 (2015).
28. Pang B, Qiao X, Janssen L, Velds A, Groothuis T, Kerkhoven R, Nieuwland M, Ovaa H, Rottenberg S, van Tellingen O, Janssen J, Huijgens P, Zwart W, and Neefjes J. Drug-induced histone eviction from open chromatin contributes to the chemotherapeutic effects of doxorubicin. *Nat Commun* 4: 1908 (2013).
29. Reits EA, Hodge JW, Herberts CA, Groothuis TA, Chakraborty M, Wansley EK, Camphausen K, Luiten RM, de Ru AH, Neijssen J, Griekspoor A, Mesman E, Verreck FA, Spits H, Schlom J, van Veelen P, and Neefjes JJ. Radiation modulates the peptide repertoire, enhances MHC class I expression, and induces successful antitumor immunotherapy. *J Exp Med* 203(5): 1259-1271 (2006).
30. Shi J, Tricot GJ, Garg TK, Malaviarachchi PA, Szmania SM, Kellum RE, Storrie B, Mulder A, Shaughnessy JD, Jr., Barlogie B, and van Rhee F. Bortezomib down-regulates the cell-surface expression of HLA class I and enhances natural killer cell-mediated lysis of myeloma. *Blood* 111(3): 1309-1317 (2008).
31. Yang G, Gao M, Zhang Y, Kong Y, Gao L, Tao Y, Han Y, Wu H, Meng X, Xu H, Zhan F, Wu X, and Shi J. Carfilzomib enhances natural killer cell-mediated lysis of myeloma linked with decreasing expression of HLA class I. *Oncotarget* 6(29): 26982-26994 (2015).
32. Kowalewski DJ, Walz S, Backert L, Schuster H, Kohlbacher O, Weisel K, Rittig SM, Kanz L, Salih HR, Rammensee H-G, Stevanović S, and Stickel JS. Carfilzomib alters the HLA-presented peptidome of myeloma cells and impairs presentation of peptides with aromatic C-termini. *Blood Cancer J* 6: e411 (2016).
33. Shraibman B, Melamed Kadosh D, Barnea E, and Admon A. HLA peptides derived from tumor antigens induced by inhibition of DNA methylation for development of drug-facilitated immunotherapy. *Mol Cell Proteomics* 15(9): 3058-3070 (2016).
34. Fecteau JF, Corral LG, Ghia EM, Gaidarova S, Futalan D, Bharati IS, Cathers B, Schwaederlé M, Cui B, Lopez-Girona A, Messmer D, and Kipps TJ. Lenalidomide inhibits the proliferation of CLL cells via a cereblon/p21(WAF1/Cip1)-dependent mechanism independent of functional p53. *Blood* 124(10): 1637-1644 (2014).
35. Berlin C, Kowalewski DJ, Schuster H, Mirza N, Walz S, Handel M, Schmid-Horch B, Salih HR, Kanz L, Rammensee H-G, Stevanović S, and Stickel JS. Mapping the HLA ligandome landscape of acute myeloid leukemia: a targeted approach toward peptide-based immunotherapy. *Leukemia* 29(3): 647-659 (2015).
36. Kowalewski DJ and Stevanović S. Biochemical large-scale identification of MHC class I ligands. *Methods Mol Biol* 960: 145-157 (2013).
37. Eng JK, McCormack AL, and Yates JR. An approach to correlate tandem mass spectral data of peptides with amino acid sequences in a protein database. *J Am Soc Mass Spectrom* 5(11): 976-989 (1994).
38. Käll L, Canterbury JD, Weston J, Noble WS, and MacCoss MJ. Semi-supervised learning for peptide identification from shotgun proteomics datasets. *Nat Methods* 4(11): 923-925 (2007).
39. Nielsen M and Andreatta M. NetMHCpan-3.0; improved prediction of binding to MHC class I molecules integrating information from multiple receptor and peptide length datasets. *Genome Med* 8(1): 33 (2016).
40. Hoof I, Peters B, Sidney J, Pedersen LE, Sette A, Lund O, Buus S, and Nielsen M. NetMHCpan, a method for MHC class I binding prediction beyond humans. *Immunogenetics* 61(1): 1-13 (2009).
41. Andreatta M, Karosiene E, Rasmussen M, Stryhn A, Buus S, and Nielsen M. Accurate pan-specific prediction of peptide-MHC class II binding affinity with improved binding core identification. *Immunogenetics* 67(11-12): 641-650 (2015).

42. Lazar C, Gatto L, Ferro M, Bruley C, and Burger T. Accounting for the Multiple Natures of Missing Values in Label-Free Quantitative Proteomics Data Sets to Compare Imputation Strategies. *J Proteome Res* 15(4): 1116-1125 (2016).
43. Liu H, Sadygov RG, and Yates JR. A model for random sampling and estimation of relative protein abundance in shotgun proteomics. *Anal Chem* 76(14): 4193-4201 (2004).
44. Stead DA, Paton NW, Missier P, Embury SM, Hedeler C, Jin B, Brown AJ, and Preece A. Information quality in proteomics. *Brief Bioinform* 9(2): 174-188 (2008).
45. Hulsen T, de Vlieg J, and Alkema W. BioVenn - a web application for the comparison and visualization of biological lists using area-proportional Venn diagrams. *BMC Genomics* 9: 488 (2008).
46. Mi H, Huang X, Muruganujan A, Tang H, Mills C, Kang D, and Thomas PD. PANTHER version 11: expanded annotation data from Gene Ontology and Reactome pathways, and data analysis tool enhancements. *Nucleic Acids Res* 45(D1): D183-D189 (2017).
47. Mi H, Muruganujan A, Casagrande JT, and Thomas PD. Large-scale gene function analysis with the PANTHER classification system. *Nat Protoc* 8(8): 1551-1566 (2013).
48. Tran E, Turcotte S, Gros A, Robbins PF, Lu YC, Dudley ME, Wunderlich JR, Somerville RP, Hogan K, Hinrichs CS, Parkhurst MR, Yang JC, and Rosenberg SA. Cancer immunotherapy based on mutation-specific CD4+ T cells in a patient with epithelial cancer. *Science* 344(6184): 641-645 (2014).
49. Sun JC, Williams MA, and Bevan MJ. CD4+ T cells are required for the maintenance, not programming, of memory CD8+ T cells after acute infection. *Nat Immunol* 5(9): 927-933 (2004).
50. Schoenberger SP, Toes RE, van der Voort EI, Offringa R, and Melief CJ. T-cell help for cytotoxic T lymphocytes is mediated by CD40-CD40L interactions. *Nature* 393(6684): 480-483 (1998).
51. Krönke J, Udeshi ND, Narla A, Grauman P, Hurst SN, McConkey M, Svinkina T, Heckl D, Comer E, Li X, Ciarlo C, Hartman E, Munshi N, Schenone M, Schreiber SL, Carr SA, and Ebert BL. Lenalidomide causes selective degradation of IKZF1 and IKZF3 in multiple myeloma cells. *Science* 343(6168): 301-305 (2014).
52. Wu L, Adams M, Carter T, Chen R, Muller G, Stirling D, Schafer P, and Bartlett JB. Lenalidomide enhances natural killer cell and monocyte-mediated antibody-dependent cellular cytotoxicity of rituximab-treated CD20+ tumor cells. *Clin Cancer Res* 14(14): 4650-4657 (2008).
53. Nooka AK, Wang M, Yee AJ, Thomas SK, O'Donnell EK, Shah JJ, Kaufman JL, Lonial S, Richardson PG, and Noopur Raje NS. Updated Results of a Phase 1/2a, Dose Escalation Study of PVX-410 Multi-Peptide Cancer Vaccine in Patients with Smoldering Multiple Myeloma (SMM). *Blood* 126:4246 (2015).
54. Kowalewski DJ, Stevanović S, Rammensee H-G, and Stickel JS. Antileukemia T-cell responses in CLL - We don't need no aberration. *Oncoimmunology* 4(7): e1011527 (2015).
55. Walz S, Stickel JS, Kowalewski DJ, Schuster H, Weisel K, Backert L, Kahn S, Nelde A, Stroh T, Handel M, Kohlbacher O, Kanz L, Salih HR, Rammensee H-G, and Stevanović S. The antigenic landscape of multiple myeloma: mass spectrometry (re)defines targets for T-cell-based immunotherapy. *Blood* 126(10): 1203-1213 (2015).
56. Milner E, Barnea E, Beer I, and Admon A. The turnover kinetics of major histocompatibility complex peptides of human cancer cells. *Mol Cell Proteomics* 5(2): 357-365 (2006).
57. Sato H, Suzuki Y, Ide M, Katoh T, Noda SE, Ando K, Oike T, Yoshimoto Y, Okonogi N, Mimura K, Asao T, Kuwano H, and Nakano T. HLA class I expression and its alteration by preoperative hyperthermo-chemoradiotherapy in patients with rectal cancer. *PLoS One* 9(9): e108122 (2014).
58. Matsuoka H, Eura M, Chikamatsu K, Nakano K, Kanzaki Y, Masuyama K, and Ishikawa T. Low doses of anticancer drugs increase susceptibility of tumor cells to lysis by autologous killer cells. *Anticancer Res* 15(1): 87-92 (1995).
59. Milner E, Gutter-Kapon L, Bassani-Strenberg M, Barnea E, Beer I, and Admon A. The effect of proteasome inhibition on the generation of the human leukocyte antigen (HLA) peptidome. *Mol Cell Proteomics* 12(7): 1853-1864 (2013).
60. ClinicalTrials.gov [Internet]. Bethesda (MD) National Library of Medicine (US). Identifier: NCT02802943. Patient individualized peptide vaccination in combination with lenalidomide after first line therapy of CLL. 2016 June 16 [cited 2016 Sep 06]; Available from: https://clinicaltrials.gov/ct2/show/NCT02802943?term=NCT02802943&rank=1.

6.2. PART II:

THE HLA LIGANDOME LANDSCAPE OF CHRONIC MYELOID LEUKEMIA DELINEATES NOVEL T-CELL EPITOPES FOR IMMUNOTHERAPY

Tatjana Bilich[1,2,*], Annika Nelde[1,2,*], Leon Bichmann[1,3], Malte Roerden[2], Helmut R. Salih[2,4], Daniel J. Kowalewski[1,5], Heiko Schuster[1,5], Chih-Chiang Tsou[6], Ana Marcu[1], Marian C. Neidert[7], Maren Lübke[1], Jonas Rieth[1], Mirle Schemionek[8], Tim H. Brümmendorf[8], Vladan Vucinic[9], Dietger Niederwieser[9], Jens Bauer[1,2], Melanie Märklin[4], Janet K. Peper[1], Reinhild Klein[2], Oliver Kohlbacher[3,10,11,12], Lothar Kanz[2], Hans-Georg Rammensee[1,13], Stefan Stevanović[1,13], Juliane S. Walz[2,#]

[1] Institute for Cell Biology, Department of Immunology, University of Tübingen, Germany
[2] Department of Hematology and Oncology, University Hospital Tübingen, Germany
[3] Applied Bioinformatics, Center for Bioinformatics and Department of Computer Science, University of Tübingen, Germany
[4] Clinical Cooperation Unit Translational Immunology, German Cancer Consortium (DKTK), DKFZ partner site Tübingen, Germany
[5] Immatics Biotechnologies GmbH, Tübingen, Germany
[6] Immatics US, Houston, Texas
[7] Department of Neurosurgery, Clinical Neuroscience Center, University Hospital Zurich and University of Zurich, Switzerland
[8] Department of Hematology, Oncology, Hemostaseology, and SCT, University Hospital RWTH Aachen, Germany
[9] Department of Hematology and Oncology, University Hospital Leipzig, Germany
[10] Quantitative Biology Center, University of Tübingen, Germany
[11] Biomolecular Interactions, Max-Planck-Institute for Developmental Biology, Tübingen, Germany
[12] Institute for Translational Bioinformatics, University Hospital Tübingen, Germany
[13] German Cancer Consortium (DKTK), DKFZ partner site Tübingen, Germany
* These authors contributed equally to this work.

A.N. and T.B. contributed equally to this work. A.N. planned, performed and analyzed all HLA ligandome experiments including quantification of HLA surface molecules, HLA immunoprecipitation experiments, and mass spectrometry analysis. A.N. contributed figures 1 – 4, supplemental tables S1 – S2, S4 – S10 as well as supplemental figures S1 – S9. A.N. was strongly involved in writing the manuscript.

Blood (2019) 133.6: 550-565

6.2.1. ABSTRACT

Anti-leukemia immunity plays an important role in disease control and maintenance of TKI-free remission in CML. Thus, antigen-specific immunotherapy holds promise to strengthen immune control in CML, but requires the identification of CML-associated targets. In this study, we used a mass spectrometry-based approach to identify naturally presented, HLA class I- and class II-restricted peptides in primary CML samples. Comparative HLA ligandome profiling using a comprehensive dataset of different hematological benign specimen and samples of CML patients in deep molecular remission delineated a panel of novel, frequently presented, CML-exclusive peptides. These non-mutated target antigens are of particular relevance since our extensive data mining approach suggests absence of naturally presented, BCR-ABL- and ABL-BCR-derived, HLA-restricted peptides and lack of frequent, tumor-exclusive presentation of known CTAs and LAAs. Functional characterization revealed spontaneous T-cell responses against the newly identified CML-associated peptides in CML patient samples and their ability to induce multifunctional and cytotoxic antigen-specific T cells *de novo* in samples of healthy volunteers and CML patients. These antigens are thus prime candidates for T-cell-based immunotherapeutic approaches that may prolong TKI-free survival and even mediate cure of CML patients.

6.2.2. INTRODUCTION

CML is characterized by the translocation t(9;22), which leads to the formation of the BCR-ABL fusion transcript.[1, 2] To inhibit the resulting fusion protein, which mediates constitutive tyrosine kinase activity, five approved TKIs are available, which have led to an impressive improvement in the prognosis of CML patients.[3-7] Currently, the main treatment goal in CML is the achievement of a so-called deep molecular remission (MR), in which discontinuation of TKI therapy can be considered. However, only few patients are able to permanently stop TKI therapy without suffering from molecular relapse.[8, 9] Thus, lifelong TKI therapy is the standard of care for most CML patients, but can associate with significant side effects and the risk of developing resistance to TKIs.[10, 11] Several studies provided evidence that immunological control may contribute to and even represent a marker for the achievement of deep MR in CML patients under TKI treatment (CML_{TKI}) and treatment-free remission (TFR). The restoration of immune responses is characterized by increased natural killer (NK) and T-cell responses,[12] reduced PD-1 expression on T cells,[12] and the correlation of CD62L expression on T cells[13] in patients with MR as well as by the association of increased natural killer cell count[14] and $CD86^+$ plasmacytoid dendritic cell count and function[15] with TFR.

In turn, reinforcing CML-specific immune responses by T-cell-based immunotherapy may serve to enlarge the fraction of patients achieving long-term TFR or even cure. It has been shown that "non-specific" immunotherapy approaches, such as allogeneic stem cell transplantation or interferon-α therapy, enable long-lasting remissions in CML patients after discontinuation of TKI therapy.[16-20] Immune checkpoint inhibitors, which have revolutionized the treatment of many solid tumors in recent years,[21-23] are currently being evaluated in CML therapy.[24] More advanced strategies to treat CML patients comprise agents inducing an immune response specifically directed against the leukemic cells, such as vaccines,[25-27] TCR mimic antibodies,[28-30] or engineered T cells.[31, 32] The prerequisite for such T-cell-based immunotherapeutic approaches is the identification of targets for CML-specific T-cell responses, which in general are represented by tumor-associated HLA-presented peptides on malignant cells.[33, 34] Several studies have suggested neoepitopes arising from tumor-specific mutations as central specificities of checkpoint inhibitor induced T-cell responses in solid tumors with high mutational burden.[33, 35] However, the role of neoantigens for T-cell responses in cancer entities with low mutational burden, including CML, remains unclear. Besides neoantigens, we and others identified non-mutated, tumor-associated HLA peptides that are able to induce peptide-specific T-cell responses and can serve as targets for T-cell-based immunotherapy approaches.[36-39] In recent years, we implemented the characterization of such tumor-associated antigens in hematological malignancies based on the direct isolation of naturally presented HLA ligands from leukemia cells and their subsequent identification by mass spectrometry (MS). For AML, CLL, and multiple myeloma we so far identified more than 100 tumor-exclusive, highly frequent antigens, which were validated as immunogenic targets for T-cell-based immunotherapy approaches.[38, 40, 41] An extensive meta-analysis of our HM immunopeptidome data revealed only a small set of entity-spanning antigens, which were predominantly characterized by low presentation frequencies within the different patient cohorts,[42] indicating that T-cell-based immunotherapies for hematological malignancies should be designed in an entity-specific manner. For CML, only very few non-mutated tumor-associated antigens[43-46] or peptides derived from the BCR-ABL fusion region[47-49] have been described so far and validated as immunogenic targets of anti-cancer T-cell responses.[50-52] Here, we comprehensively mapped the landscape of naturally presented HLA class I and II peptides in primary CML samples to identify novel CML-associated antigens covering a broad range of HLA allotypes. These antigens were further validated for their potential to induce T-cell responses particularly in the context of immunomodulatory effects induced by TKI treatment in CML patients.[53-56]

6.2.3. METHODS

Detailed method descriptions can be found in the supplement.

Patients and blood samples

PBMCs from CML patients were collected at the Departments of Hematology and Oncology in Tübingen, Leipzig, and Aachen, Germany. Patient characteristics are provided in Table S1.

HLA surface molecule quantification

HLA surface expression was determined using the QIFIKIT quantification flow cytometric assay (Dako).[40, 57] Cells were stained with the pan-HLA class I-specific W6/32, the HLA-DR-specific L243 mAbs, or isotype control. Surface marker staining was performed with fluorescence-conjugated antibodies against CD33, CD13, CD117, and CD34.

Isolation of HLA ligands

HLA molecules were isolated by standard immunoaffinity purification[40, 58] using the mAbs W6/32, Tü-39, and L243.

Analysis of HLA ligands by LC-MS/MS

HLA ligand extracts were analyzed as described previously.[38] Peptides were separated by nanoflow high-performance LC. Eluted peptides were analyzed in an online-coupled LTQ Orbitrap XL mass spectrometer. Furthermore, parallel reaction monitoring (PRM) targeting BCR-ABL- and ABL-BCR-derived peptides (Table S2) was performed on an Orbitrap Fusion Lumos mass spectrometer.

Data processing

Data processing was performed as described previously.[38, 57] The Proteome Discoverer (v1.3, Thermo Fisher) was used to integrate the search results of the Mascot search engine (v2.2.04, Matrix Science) against the human proteome (Swiss-Prot database). For the search of BCR-ABL- and ABL-BCR-derived neoantigens the human proteome was extended by BCR-ABL sequences from the TrEMBL database and by published ABL-BCR sequences.[59, 60]

The FDR (estimated by the Percolator algorithm 2.04[61]) was limited to 5% for HLA class I and 1% for HLA class II. HLA class I annotation was performed using SYFPEITHI 1.0[62] and NetMHCpan 3.0.[63, 64] The lists of HLA class I and II peptides identified on CML, CML_{MR}, and hematological benign tissue samples are provided in supplemental data 1 (Access *via* www.bloodjournal.org/content/133/6/550).

Peptide synthesis

Peptides were produced by the peptide synthesizer Liberty Blue (CEM) using the 9-fluorenylmethyl-oxycarbonyl/tert-butyl strategy.[65]

Amplification of peptide-specific T cells and IFNγ ELISPOT assay

PBMCs from CML patients and healthy volunteers (HVs) were pulsed with 1 µg/mL (class I) or 5 µg/mL (class II) per peptide and cultured for 12 days.[38, 40] Peptide-stimulated PBMCs were analyzed by enzyme-linked immunospot (ELISPOT) assay.[41, 66]

aAPC priming of naïve $CD8^+$ T cells

Priming of peptide-specific CTLs was conducted using artificial antigen-presenting cells (aAPCs).[37, 67] Magnetic-activated cell-sorted $CD8^+$ T cells were cultured with IL-2 and IL-7. Weekly stimulation with peptide-loaded aAPCs and IL-12 was performed four times.

Cytokine and tetramer staining

The functionality of peptide-specific $CD8^+$ T cells was analyzed by intracellular cytokine staining (ICS).[66, 68] Cells were pulsed with peptide, Brefeldin A, and GolgiStop. Staining was performed using mAbs against CD8, TNF, IFNγ, and CD107a. Frequency of peptide-specific $CD8^+$ T cells was determined by anti-CD8 and tetramer staining.[69]

Cytotoxicity assay

Cytolytic capacity of peptide-specific $CD8^+$ T cells was analyzed using the flow cytometry-based VITAL assay.[70, 71] Autologous target cells were either loaded with test peptides or irrelevant control peptides and labeled with CFSE or FarRed, respectively. Effector cells were added in the indicated effector to target ratios. Specific lysis of peptide-loaded target cells was calculated relative to control targets.

Data availability

The mass spectrometry data have been deposited to the ProteomeXchange Consortium (http://proteomecentral.proteomexchange.org) *via* the PRIDE[72] partner repository with the dataset identifier PXD010450.

6.2.4. RESULTS

Myeloid and precursor cells of primary CML samples express high levels of HLA molecules

T-cell-based immunotherapy requires sufficient HLA expression on target cells, which in case of CML constitute myeloid cells and myeloid precursor cells. Thus, as a first step we quantified HLA surface expression on $CD33^+$ and $CD13^+$ myeloid cells as well as on $CD117^+CD34^+$ precursor cells using PBMCs of CML patients (n = 7, Table S1). HLA class I surface levels showed substantial heterogeneity with molecule counts/cell of 78,600 – 202,100 (mean 153,600) for $CD33^+$ cells and 69,500 – 322,000 (mean 184,600) for $CD13^+$ cells (Figure 1A). HLA class II expression ranged from 37,700 – 230,000 (mean 101,200) molecules/cell for DR^+CD33^+ cells and 39,000 – 286,300 (mean 158,900) molecules/cell for DR^+CD13^+ cells (Figure 1B). Notably, highest HLA surface levels were detected on precursor cells with 112,000 – 316,500 (mean 221,100) and 99,700 – 487,200 (mean 228,300) molecules/cell for HLA class I and II, respectively (Figure 1A,B).

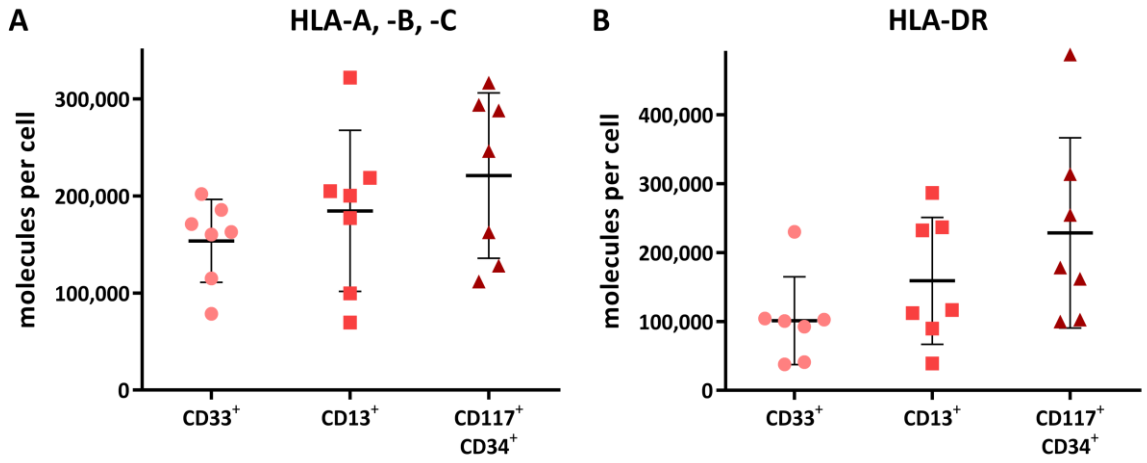

Figure 1: HLA surface expression of primary CML cells. (A) HLA class I and (B) HLA-DR expression was determined by flow cytometry for $CD33^+$ and $CD13^+$ myeloid cells as well as $CD117^+CD34^+$ precursor cells from peripheral blood of CML patients (n = 7) at the time of diagnosis. Data points represent individual samples. Horizontal lines indicate mean values ± SD.

MS identifies naturally presented, CML-associated HLA class I ligands in CML patient samples

MS analysis of 21 primary CML samples revealed a total of 11,945 unique HLA class I ligands (range 535 – 2,107, mean 1,080 per sample) from 5,478 source proteins (Figure S3A, supplemental data 1, access *via* www.bloodjournal.org/content/133/6/550), obtaining 82% of the estimated maximum attainable coverage in HLA ligand source proteins (Figure 2A). For the identification of CML-associated antigens we established a comparative cohort of hematological benign tissues (n = 108) including PBMCs (n = 63), granulocytes (n = 14), $CD19^+$ B cells (n = 5), bone marrow (n = 18), and $CD34^+$ HPCs (n = 8). A total of 51,232 different naturally presented HLA class I ligands (range 101 – 7,587, mean 1,404 per sample) from 11,437 source proteins (supplemental data 1, access *via* www.bloodjournal.org/content/133/6/550), obtaining 95% of maximum attainable coverage

(Figure S4A), were identified. Furthermore, we created an additional comparative benign ligandome dataset of PBMCs from CML patients in deep MR (CML_{MR}, n = 15) comprising a total of 5,907 unique HLA class I ligands (range 311 – 1,145, mean 655 per sample, supplemental data 1, access *via* www.bloodjournal.org/content/133/6/550).

The CML cohort included a total of 31 different HLA class I allotypes, the most frequent being HLA-C*07 (n = 11), -A*02 (n = 10), -A*03 (n = 8), -B*07 (n = 7), and -B*35 (n = 6, Figure S5A). Among the world population[73, 74] 99.3% of the individuals carry at least one HLA class I allotype that is represented within this cohort (Figure S6A). The comparative hematological benign cohort showed an HLA allotype population coverage of 99.9% (Figure S6B) and matched 89% of HLA-A, 100% of HLA-B, and 88% of HLA-C allotypes within the CML cohort (Figure S5B).

To identify CML-associated antigens, we performed comparative HLA class I ligandome profiling of the CML cohort with the hematological benign and CML_{MR} cohorts. Overlap analysis revealed 2,600 HLA class I ligands to be presented exclusively on CML samples (Figure 2B) and never detected on hematological benign or CML_{MR} samples. For the identification of broadly applicable, CML-associated antigens, we aimed for the selection of target antigens that not only fulfill the criterium of CML-exclusivity, but also exhibit high prevalence within the CML cohort. At a target-definition FDR of < 5% (< 1%) a total of 23 (5) HLA class I ligands with a representation frequency ≥ 19% (≥ 24%) were identified (Figure 2C and S7A, Table S4). The most common HLA allotype restrictions of these HLA ligands included HLA-A*02, -A*03, -A*11, and -B*07. To identify CML-associated targets with even higher representation frequencies, we subsequently performed HLA allotype-specific immunopeptidome profiling. Setting target FDR to < 5% (< 1%) we identified 4 (1) HLA-A*02, 35 (15) HLA-A*03, 3 (0) HLA-A*11, and 8 (2) HLA-B*07-restricted ligands with representation frequencies of ≥ 40% (≥ 50%), ≥ 38% (≥ 50%), ≥ 80% (≥ 80%), ≥ 43% (≥ 57%), respectively (Figure 2D-G and S7B-E, Table S4). To further validate these CML-associated targets we compared them with an additional benign dataset comprising 28 different non-hematological tissue entities (n = 166, including for example liver, lung, brain, skin) with a total of 128,590 unique HLA class I peptides from 16,405 source proteins. Thus, we selected a panel of eight CML-exclusive target antigens including two HLA-A*02-, three HLA-A*03-, one HLA-A*11-, and two HLA-B*07-restricted ligands for further immunological characterization.

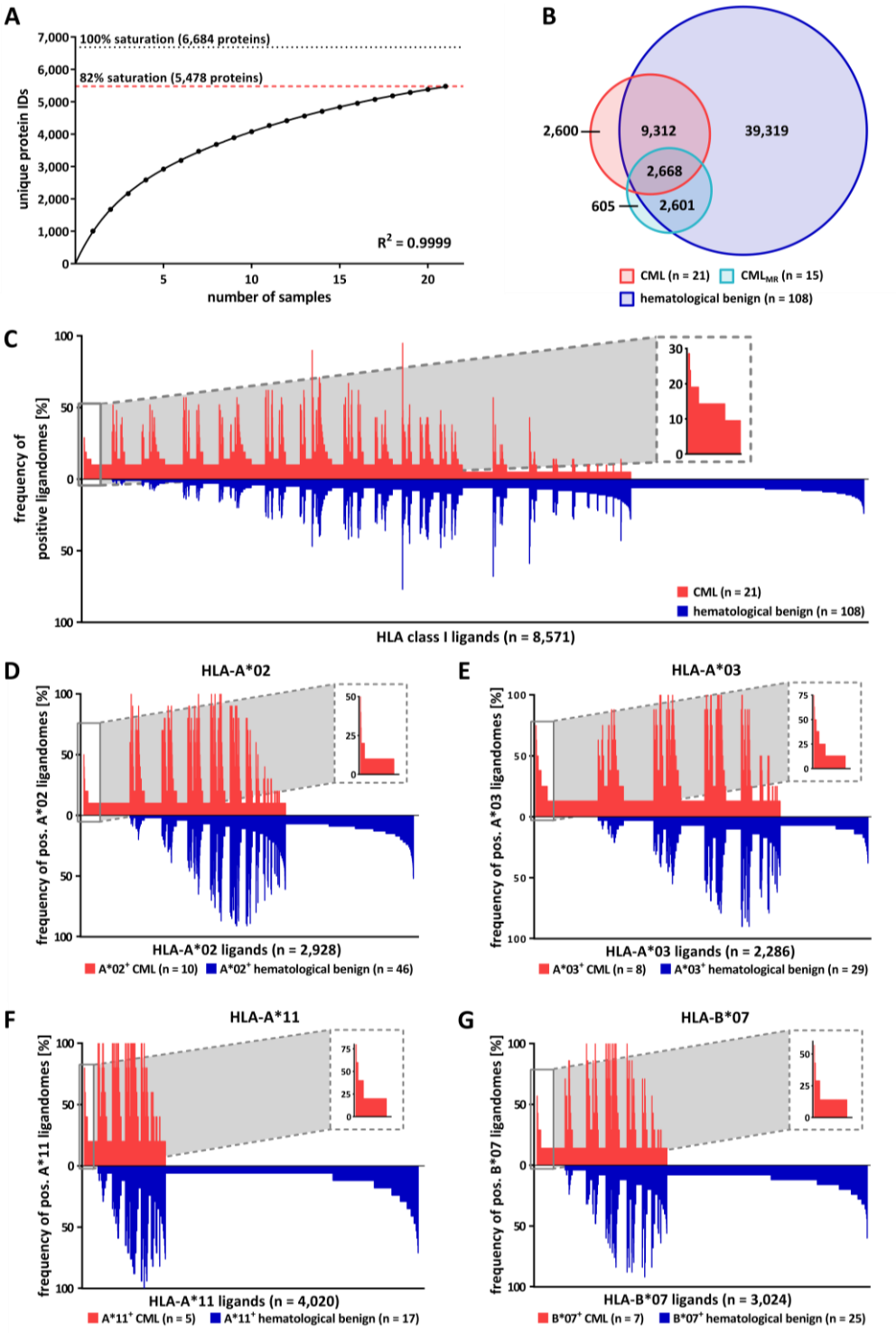

Figure 2: Comparative HLA class I ligandome profiling and identification of CML-associated antigens. (A) Saturation analysis of HLA class I ligand source proteins of the CML patient cohort. Number of unique HLA ligand source protein identifications shown as a function of cumulative HLA ligandome analysis of CML samples (n = 21). Exponential regression allowed for the robust calculation (R^2 = 0.9999) of the maximum attainable number of different source protein identifications (dotted line). The dashed red line depicts the source proteome coverage achieved in our CML patient cohort. (B) Overlap analysis of HLA class I ligand identifications of primary CML samples (n = 21), CML_{MR} samples from patients in deep MR (n = 15), and hematological benign samples (n = 108) including PBMCs (n = 63), granulocytes (n = 14), $CD19^+$ B cells (n = 5), bone marrow (n = 18), and $CD34^+$ HPCs (n = 8). (C) Comparative profiling of HLA class I ligands based on the frequency of HLA-restricted presentation in CML and hematological benign ligandomes. Frequencies of positive immunopeptidomes for the respective HLA ligands (x-axis) are indicated on the y-axis. To allow for better readability, HLA ligands identified on < 5% of the samples within the respective cohort were not depicted in this plot. The box on the left and its magnification highlight the subset of CML-associated antigens showing CML-exclusive, highly frequent presentation. (D-G) Allotype-specific comparative profiling of (D) HLA-A*02, (E) -A*03, (F) -A*11, as well as (G) -B*07 positive samples as described above. Abbreviations: IDs, identifications; pos., positive.

HLA class II ligandome profiling delineates three novel groups of CML-associated antigens

Mapping the HLA class II ligandomes of 20 primary CML samples, we identified 5,991 different HLA class II-restricted peptides (range 172 – 1,162, mean 641 per sample) derived from 1,302 source proteins (Figure S3B, supplemental data 1, access *via* www.bloodjournal.org/content/133/6/550), achieving 72% of maximum attainable coverage (Figure 3A). Our HLA class II hematological benign tissue cohort (n = 88, PBMCs (n = 38), granulocytes (n = 18), $CD19^+$ B cells (n = 9), bone marrow (n = 15), $CD34^+$ HPCs (n = 8)) comprised 42,753 unique peptides (range 111 – 6,267, mean 1,197 per sample) from 4,877 source proteins (supplemental data 1, access *via* www.bloodjournal.org/content/133/6/550), obtaining 84% of maximum attainable coverage (Figure S4B). The benign CML_{MR} ligandome dataset (n = 15) included a total of 1,529 HLA class II peptides (range 74 – 281, mean 164 per sample, supplemental data 1, access *via* www.bloodjournal.org/content/133/6/550).

For the identification of HLA class II-restricted, CML-associated antigens, we established an innovative HLA class II ligandome profiling platform, which delineated three groups of antigens: peptide targets, protein targets, and hotspot targets. First, we performed comparative ligandome profiling on peptide level. Overlap analysis revealed 1,949 peptides to be exclusively presented on CML (Figure 3B) and never detected on hematological benign or CML_{MR} samples. Of these, 36 peptides were identified with a representation frequency ≥ 20% based on an FDR < 1%. However, 30/36 peptide targets showed length variants (> 50% overlap) presented on benign hematological samples and were therefore excluded (peptide targets, Figure 3C and S8A, Table S5). Further ligandome profiling was performed on HLA class II source protein level. Based on an FDR < 5% (< 1%), a total of 4 (2) source proteins were identified with a frequency ≥ 20% (≥ 25%) representing 10 (4) unique HLA class II peptides (protein targets, Figure 3D and S8B, Table S5). As a third group of CML-associated antigens we analyzed CML-exclusive hotspots by peptide clustering, which validated the previously described targets and identified one additional CML-associated hotspot with a representation frequency of 20% comprising three unique HLA class II peptides (hotspot targets, Figure 3E, Table S5). Subsequent validation of these targets using our non-hematological benign tissue dataset (n = 166, 28 tissues, 143,652 HLA class II peptides, 13,410 source proteins) delineated a panel of six strongly CML-associated target antigens for immunological characterization.

Notably, most of the identified targets showed unusual short peptide lengths for HLA class II-restricted peptides (mean 12 amino acids), which is reflected by a general length distribution shift in myeloid cell-containing samples representing shorter HLA class II-restricted peptides (Figure 3F, S9).

Figure 3: (A) Saturation analysis of HLA class II peptide source proteins of the CML patient cohort. Number of unique HLA peptide source protein identifications as a function of cumulative HLA ligandome analysis of CML samples (n = 20). Exponential regression allowed for the robust calculation (R^2 = 0.9997) of the maximum attainable number of different source protein identifications (dotted line). The dashed red line depicts the source proteome coverage achieved in our CML patient cohort. (B) Overlap analysis of HLA class II peptides of primary CML samples (n = 20), CML_{MR} samples from patients in deep MR (n = 15), and hematological benign samples (n = 88) including PBMCs (n = 38), granulocytes (n = 18), $CD19^+$ B cells (n = 9), bone marrow (n = 15), and $CD34^+$ HPCs (n = 8).

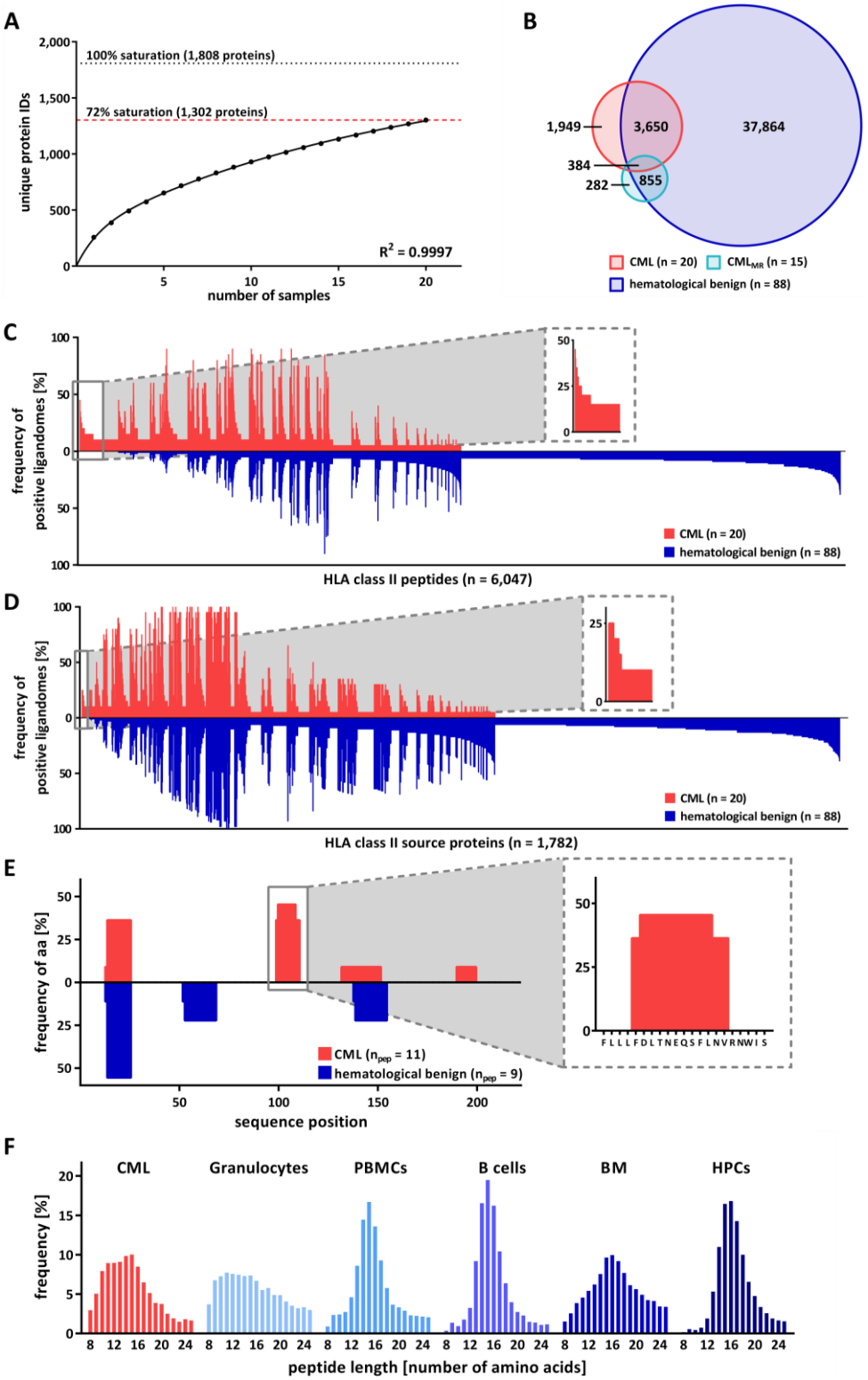

Figure 3 continued: (C-D) Comparative profiling of (C) HLA class II peptides and (D) HLA class II source proteins based on the frequency of HLA-restricted presentation in CML and hematological benign ligandomes. Frequencies of positive immunopeptidomes for the respective HLA peptides or source proteins (x-axis) are indicated on the y-axis. To allow for better readability, HLA peptides or source proteins identified on < 5% of the samples within the respective cohort are not depicted. The boxes on the left and their magnifications highlight the subset of CML-associated antigens showing CML-exclusive, highly frequent presentation in CML samples. (E) Hotspot analysis of the protein RB27A by peptide clustering. Identified peptides were mapped to their amino acid positions within the source protein. Representation frequencies of amino acid counts within each cohort for the respective amino acid position (x-axis) were calculated and are indicated on the y-axis. The box and its magnification highlight the identified hotspot with the respective amino acids on the x-axis. (F) Tissue-specific HLA class II peptide length distribution (number of amino acids) of all identified peptides on primary CML samples (n = 20), granulocytes (n = 18), PBMCs (n = 38), $CD19^+$ B cells (n = 9), bone marrow (n = 15), and $CD34^+$ HPCs (n = 8). Abbreviations: IDs, identifications; aa, amino acid; n_{pep}, number of peptides.

The role of cancer/testis and leukemia-associated antigens as well as BCR-ABL-derived neoantigens in the immunopeptidome of CML

Beside the definition of novel CML-associated antigens, we focused on the identification and ranking of established CTAs[75, 76] and LAAs[43, 77] in our dataset of naturally presented HLA peptides. We identified 170 different HLA class I and 382 class II peptides from 39 and 18 CTAs, respectively, as well as 1,429 class I and 3,428 class II peptides from 131 and 77 LAAs, respectively (Table S6 – 9). Notably, these antigens were not only represented in CML immunopeptidomes but also on hematological benign samples (Figure 4). Hence, this analysis delineated only a small panel of seven (4% of total) CML-exclusive but infrequent CTAs and LAAs, which represent suitable candidates for T-cell-based immunotherapy in selected CML patients. As the characteristic BCR-ABL translocation may result in the presentation of BCR-ABL or ABL-BCR neoepitopes, we further screened our CML cohort for naturally presented, BCR-ABL- and ABL-BCR-derived peptides by DDA of all CML samples as well as targeted PRM of four CML samples (Table S2). Despite the fact that the BCR-ABL and ABL-BCR fusion sites potentially provide HLA binding motifs for several HLA allotypes, no naturally presented HLA peptides were identified.

HLA class I-restricted CML-associated antigens induce functional peptide-specific T cells in samples of HVs and CML patients

To confirm immunogenicity and detect preexisting memory T-cell responses against the identified CML-associated antigens (Figure 5A) we performed IFNγ ELISPOT and tetramer staining assays using HLA-matched PBMCs from CML_{TKI} patients and HVs. We observed IFNγ secretion for 1/8 CML-associated ligands in 2/17 (12%) analyzed CML_{TKI} patients (Figure 5B), but also for two peptides in one HV (Figure S10), respectively. Cross-reacting microorganism- or virus-specific T cells as reason for the observed T-cell responses in single HVs appears unlikely, as no sequence similarity of the CML-associated antigens with proteins from microorganisms and virus was determined. In addition, low frequent peptide-specific $CD8^+$ T cells were detected by tetramer staining for 4/8 peptides in 3/18 CML_{TKI} patient samples after 12-d stimulation without any detectable preexisting peptide-specific T cells *ex vivo* prior to stimulation (Figure S11). To assess the immunogenicity of the remaining HLA class I-restricted ligands we performed *in vitro* aAPC-based priming experiments using $CD8^+$ T cells of both, HVs and CML patients. Effective priming and expansion of antigen-specific T cells was observed for all eight CML-associated peptides in ≥ 70% of analyzed HVs with frequencies of peptide-specific T cells ranging from 0.1 – 33.9% (mean 2.2%) within the $CD8^+$ T-cell population (Figure 5A,C and S12).

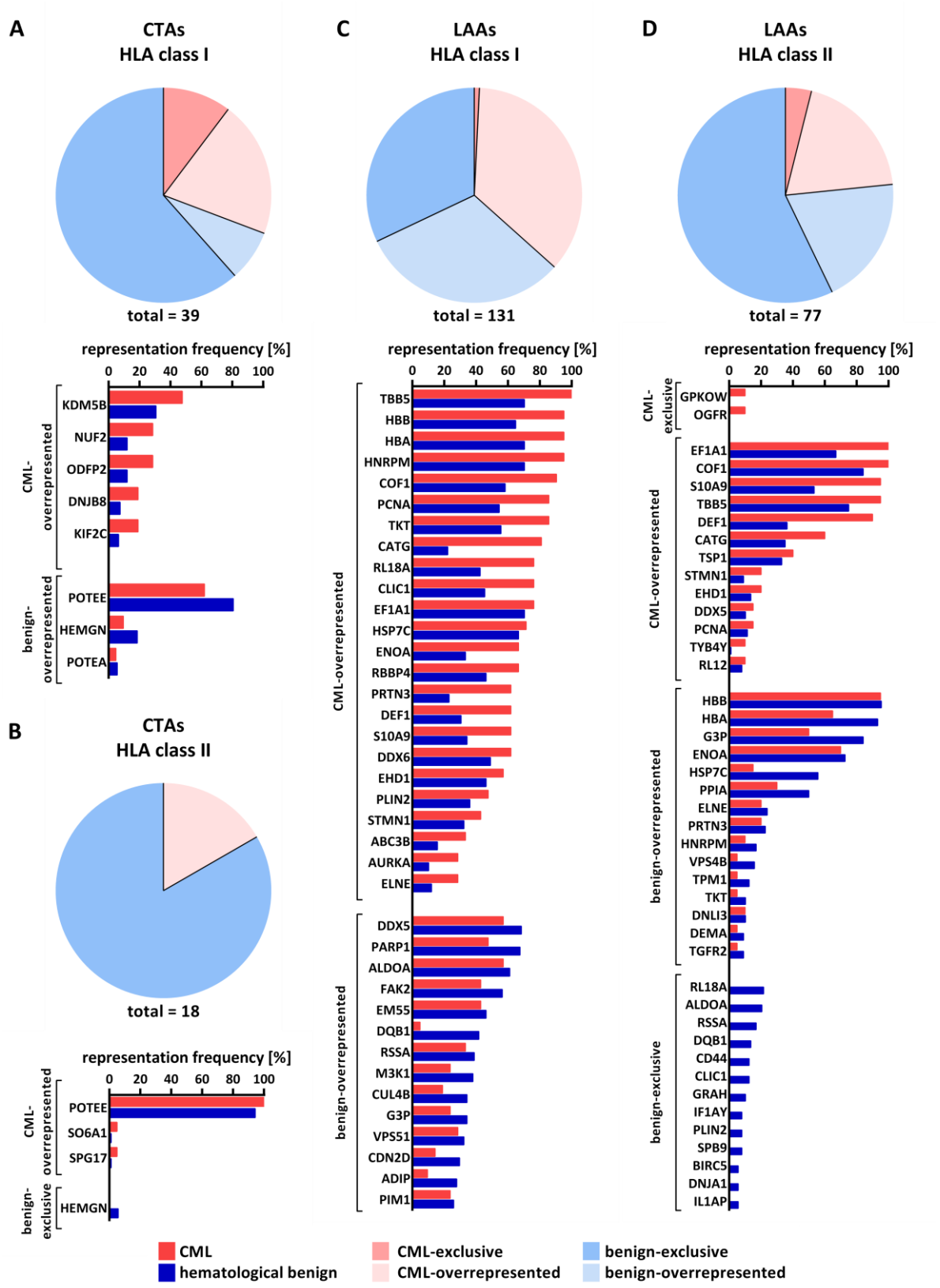

Figure 4: Representation of published CTAs and LAAs in CML and hematological benign HLA ligandomes. Representation frequencies of published CTAs in HLA (A) class I and (B) class II ligandomes as well as published LAAs in HLA (C) class I and (D) class II ligandomes in CML patient and hematological benign samples. Pie charts indicate total amount of identified CTAs and LAAs assigned to their degree of CML-association (CML-exclusive, CML-overrepresented, benign-overrepresented, benign-exclusive). Bar diagrams depict relative representation [%] of respective antigens on CML and hematological benign samples allocated to their CML-association. Only antigens with representation frequencies (A, B, D) > 5% or (C) > 25% in the respective cohort are shown. Abbreviations: CTAs, cancer/testis antigens; LAAs, leukemia-associated antigens.

A

Peptide ID	Peptide sequence	Source protein	CD8⁺ T-cell response in CML	CD8⁺ T-cell response in HVs	*in vitro* CD8⁺ T-cell priming in HVs	*in vitro* CD8⁺ T-cell priming in CML
$P1_{A*02}$	ALHPLVILNI	CSN6	2/17 (12%)	0/12 (0%)	5/6 (83%)	1/3 (33%)
$P2_{A*02}$	KQGFEPPSFV	GELS	0/17 (0%)	0/12 (0%)	6/7 (86%)	1/5 (20%)
$P3_{A*03}$	RTAGHPLTR	PTN7	0/10 (0%)	0/25 (0%)	9/10 (90%)	1/4 (25%)
$P4_{A*03}$	HLLEQVAPK	PLSL	0/7 (0%)	1/24 (4%)	7/10 (70%)	2/2 (100%)
$P5_{A*03}$	KIFWIPLSH	DHRS9	0/7 (0%)	0/12 (0%)	5/5 (100%)	n.t.
$P6_{A*11}$	AVNPGVVVR	BPI	0/3 (0%)	0/15 (0%)	3/3 (100%)	n.t.
$P7_{B*07}$	RAMVARLGL	CD24	0/5 (0%)	0/12 (0%)	6/6 (100%)	1/1 (100%)
$P8_{B*07}$	APGQPLRVL	CEBPE	0/5 (0%)	1/12 (8%)	6/6 (100%)	n.t.

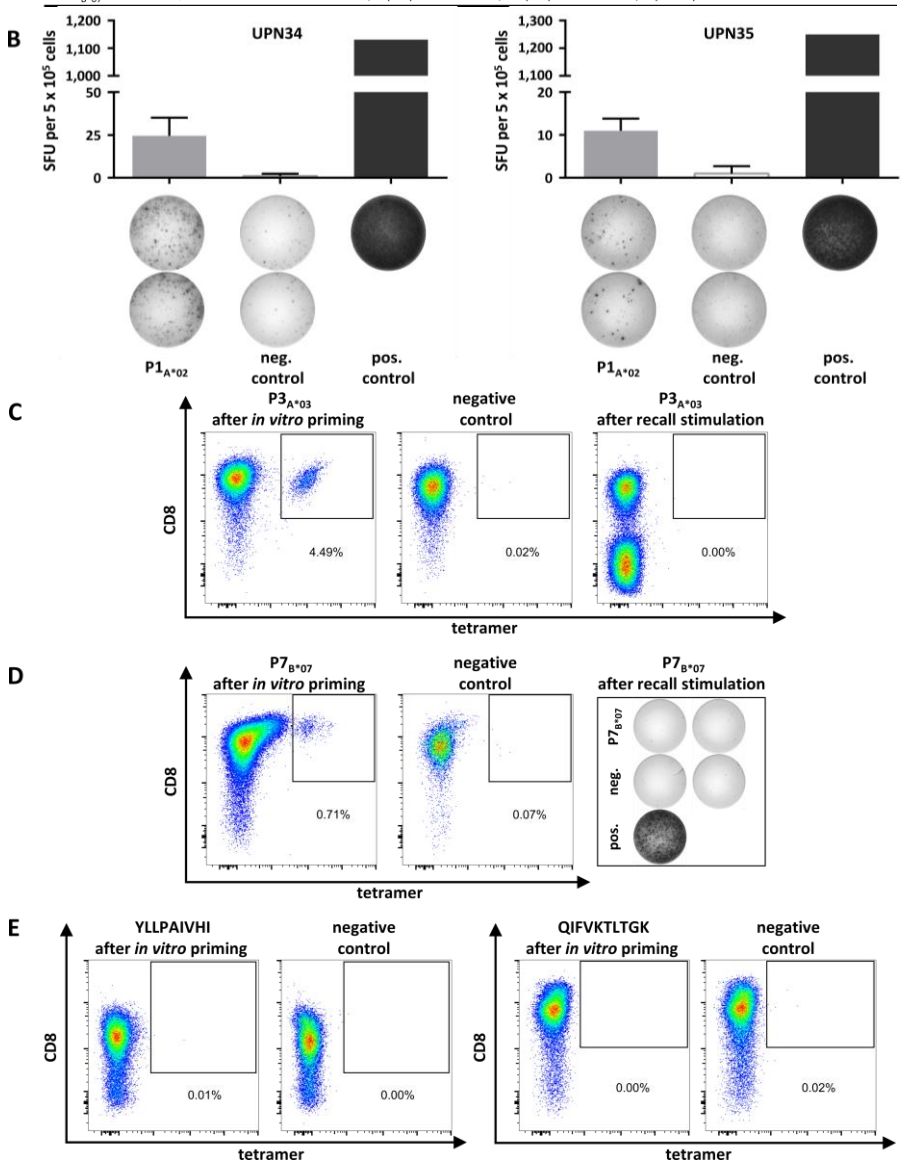

Figure 5: Immunogenicity of HLA class I-restricted, CML-associated antigens. (A) Immunogenicity analysis results of the eight HLA class I-restricted, CML-associated peptides with their respective frequencies of preexisting immune recognition by PBMCs of CML patients or HVs in IFNγ ELISPOT assays ($CD8^+$ T-cell response in CML/HVs) as well as frequencies of peptide-specific $CD8^+$ T cells detected after *in vitro* aAPC-based priming experiments with naïve $CD8^+$ T cells of HVs and CML patients. (B) Examples of CML-associated ligands evaluated in IFNγ ELISPOT assays after 12-d stimulation using PBMCs of CML patients. Results are shown for immunoreactive peptides only. PHA was used as positive control. HLA-A*02-restricted DDX5_HUMAN$_{148-156}$ peptide YLLPAIVHI served as negative control. Data are expressed as mean ± SD of two independent replicates. (C, D) Naïve $CD8^+$ T cells from (C) HVs as well as from (D) CML patients were primed *in vitro* using aAPCs. Graphs show single, viable cells stained for CD8 and PE-conjugated multimers of indicated specificity. Tetramer staining was performed after four stimulation cycles with peptide-loaded aAPCs. The left panels show $P3_{A*03}$- or $P7_{B*07}$-tetramer staining, respectively. The middle panels (negative control) depict $P3_{A*03}$- or $P7_{B*07}$-tetramer staining of respective T cells primed with an irrelevant peptide. The right panels show T cells from the same donor that were tested for the absence of preexisting memory T cells after 12-d recall stimulation by either (C) tetramer staining or (D) IFNγ ELISPOT assay. (E) Tetramer staining after four stimulation cycles with negative control peptide-loaded aAPCs (HLA-A*02, YLLPAIVHI, DDX5_HUMAN$_{148-156}$ and HLA-A*03, QIFVKTLTGK, UBC_HUMAN$_{2-11}$). Abbreviations: ID, identification; HVs, healthy volunteers; n.t., not tested; UPN, uniform patient number; SFU, spot forming unit; neg., negative; pos., positive.

Furthermore, all analyzed CML-associated peptides induced peptide-specific T cells using CML patient samples with frequencies of 0.1 – 2.2% (mean 0.4%) within the $CD8^+$ T-cell population (Figure 5A,D). Notably, peptide-specific immune responses were even induced in CML_{TKI} patient samples that had not shown preexisting immune responses. Priming experiments with control peptides frequently presented by HLA-A*02 and -A*03 on both, tumor and benign tissues (peptide presentation > 90% in HLA-matched sources), confirmed CML-specificity of the induced T-cell responses (Figure 5E). Furthermore, multifunctionality of peptide-specific T cells was shown for 6/8 CML-associated peptides by IFNγ and TNF production and upregulation of the degranulation marker CD107a (Figure 6A,B). Finally, cytotoxicity assays with polyclonal peptide-specific effector T cells revealed the capacity to induce antigen-specific lysis for 3/4 analyzed peptides (Figure 6A,C-E and S13).

Reduced functionality of $CD8^+$ T cells in CML_{TKI} patients

Subsequently, we reasoned that weak preexisting immune responses against the CML-associated, HLA class I-restricted peptides in our IFNγ ELISPOT assays could have been caused by an impairment of $CD8^+$ T-cell functionality that reportedly occurs upon TKI treatment.[53-56] Therefore, we compared T-cell responses against viral epitopes of CML_{TKI} patients, HVs, and CLL patients[38] in IFNγ ELISPOT assays. While $CD8^+$ T-cell counts themselves were not reduced in CML_{TKI} patients (Figure 7A), we observed significantly reduced IFNγ release of T cells compared to HVs and CLL patients ($p < 0.001$, Figure 7B). In contrast, no significantly reduced IFNγ production upon stimulation with HLA class II-restricted viral epitopes was observed (Figure 7C). These results were confirmed by the functional characterization of six HLA class II-restricted, CML-associated peptides in IFNγ ELISPOT assays (Figure 7D,E). Frequencies of $CD4^+$ T-cell responses reached up to 24% (4/17) of analyzed CML patient samples, however, with some peptides only analyzed in pooled read-outs due to low cell numbers.

Taken together, we characterized a panel of novel, CML-associated, HLA class I and II antigens, which even in the context of the immunosuppressive effects induced by TKI treatment were able to induce multifunctional T-cell responses and therefore could serve as prime targets for the development of antigen-specific immunotherapies in CML.

A

Peptide ID	Peptide sequence	Source protein	ICS of peptide-specific CD8⁺ T cells	VITAL assay
$P1_{A*02}$	ALHPLVILNI	CSN6	negative	positive
$P2_{A*02}$	KQGFEPPSFV	GELS	TNF⁺ / IFNγ⁺	n.t.
$P3_{A*03}$	RTAGHPLTR	PTN7	TNF⁺ / IFNγ⁺ / CD107a⁺	n.t.
$P4_{A*03}$	HLLEQVAPK	PLSL	TNF⁺ / IFNγ⁺ / CD107a⁺	negative
$P5_{A*03}$	KIFWIPLSH	DHRS9	TNF⁺ / IFNγ⁺ / CD107a⁺	positive
$P6_{A*11}$	AVNPGVVVR	BPI	TNF⁺ / IFNγ⁺ / CD107a⁺	n.t.
$P7_{B*07}$	RAMVARLGL	CD24	TNF⁺ / IFNγ⁺ / CD107a⁺	positive
$P8_{B*07}$	APGQPLRVL	CEBPE	negative	n.t.

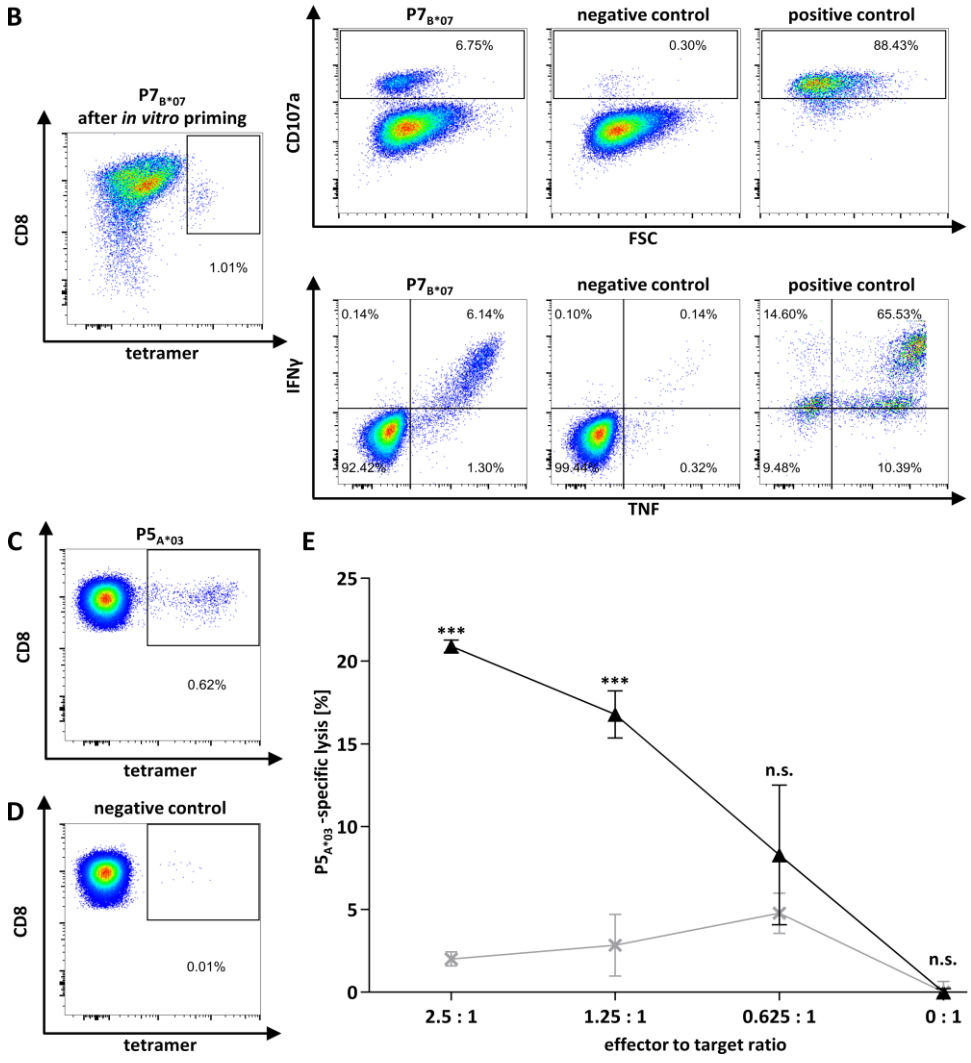

Figure 6: Functional characterization of CML-associated antigen-specific CD8⁺ T cells. (A) Functional characterization of CML-associated antigen-specific CD8⁺ T cells including their CD107a and cytokine expression profile detected by ICS following aAPC-based priming experiments and their cytotoxic capability (VITAL assay). (B) Representative example of increased IFNγ and TNF production as well as CD107a expression after stimulation with the respective $P7_{B*07}$-peptide used for the stimulation with aAPCs compared to the corresponding negative control peptide (HLA-B*07, TPGPGVRYPL, $NEF\_HV1BR_{128-137}$). PMA and ionomycin served as positive control. The $P7_{B*07}$-specific CD8⁺ T-cell population showed a frequency of 1.01% as detected by tetramer staining (leftmost panel). (C-E) Selective cytotoxicity of $P5_{A*03}$-specific effector T cells analyzed in a VITAL cytotoxicity assay with *in vitro* primed CD8⁺ T cells of an HV. (C,D) Tetramer staining of polyclonal effector cells before performance of the VITAL assay determined the amount of $P5_{A*03}$-specific effector cells in the (C) population of successfully $P5_{A*03}$-primed CD8⁺ T cells and in the (D) population of control cells from the same donor primed with an HLA-matched irrelevant peptide. (E) At an effector to target ratio of 2.5:1, $P5_{A*03}$-specific effectors (black) exerted 20.9% (±0.4%) $P5_{A*03}$-specific and significant higher lysis of $P5_{A*03}$-loaded autologous target cells in comparison to control peptide-loaded target cells (HLA-A*03, RLRPGGKKK, GAG_HV1BR_{20-28}). $P5_{A*03}$-unspecific effectors (grey) only showed 2.0% (±0.4%) unspecific lysis of the same targets. Results are shown as mean ± SEM for three independent replicates. Abbreviations: ID, identification; n.t., not tested; ICS, intracellular cytokine staining; FSC, forward scatter; n.s., not significant; *** $p < 0.001$.

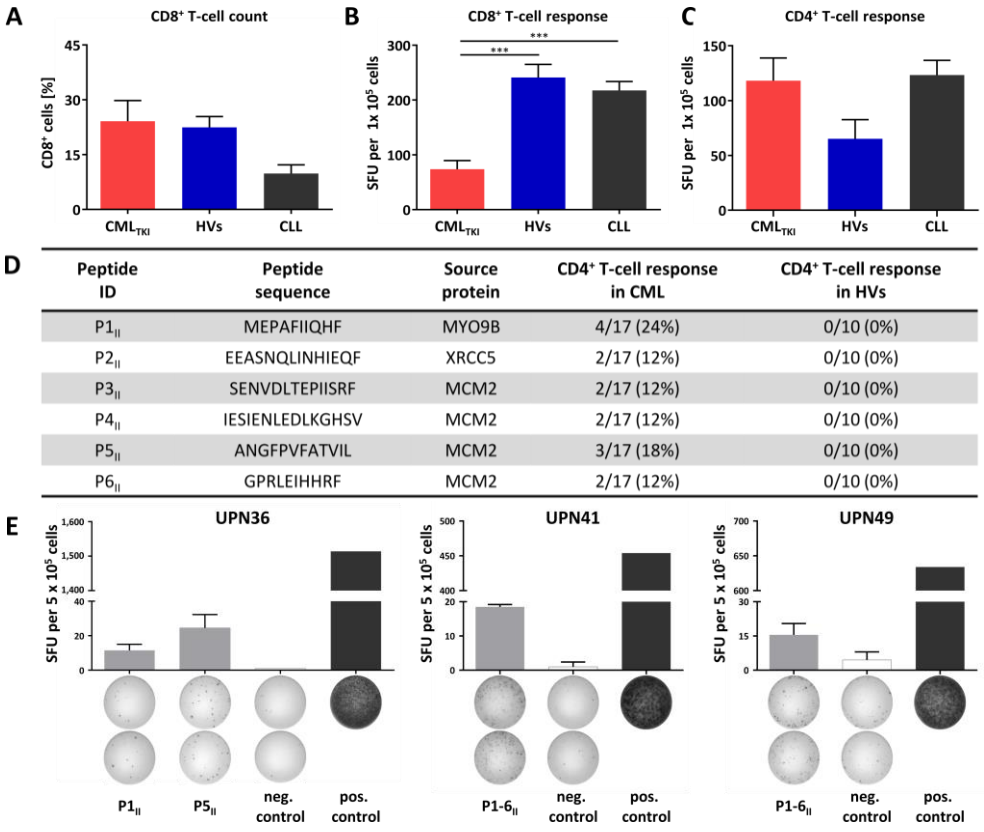

Peptide ID	Peptide sequence	Source protein	CD4⁺ T-cell response in CML	CD4⁺ T-cell response in HVs
$P1_{II}$	MEPAFIIQHF	MYO9B	4/17 (24%)	0/10 (0%)
$P2_{II}$	EEASNQLINHIEQF	XRCC5	2/17 (12%)	0/10 (0%)
$P3_{II}$	SENVDLTEPIISRF	MCM2	2/17 (12%)	0/10 (0%)
$P4_{II}$	IESIENLEDLKGHSV	MCM2	2/17 (12%)	0/10 (0%)
$P5_{II}$	ANGFPVFATVIL	MCM2	3/17 (18%)	0/10 (0%)
$P6_{II}$	GPRLEIHHRF	MCM2	2/17 (12%)	0/10 (0%)

Figure 7: General functionality of T cells in CML_{TKI} patients and immunogenicity of HLA class II-restricted, CML-associated antigens. (A) $CD8^+$ T-cell counts of CML patients under TKI treatment (CML_{TKI}, n = 7) compared to HVs (n = 10) and CLL patients (n = 10). (B,C) Retrospective analysis of preexisting immune responses directed against (B) HLA class I- and (C) HLA class II-restricted viral T-cell epitopes (Table S3) analyzed in IFNγ ELISPOT assays after 12-d recall stimulation of PBMCs from CML_{TKI} patients (HLA class I n = 10, HLA class II n = 12), HVs (HLA class I n = 14, HLA class II n = 6), and CLL patients (HLA class I n = 31, HLA class II n = 24). (D) HLA class II-restricted, CML-associated peptides with their corresponding source proteins and frequencies of preexisting immune recognition by $CD4^+$ T cells of CML patients or HVs in IFNγ ELISPOT assays after 12-d stimulation. (E) Examples of CML-associated, HLA class II-restricted peptides evaluated in IFNγ ELISPOT assays using PBMCs of CML patients. Results are shown for immunoreactive peptides only. PHA was used as positive control. HLA class II-restricted $FLNA\_HUMAN_{1669\text{-}1683}$ peptide ETVITVDTKAAGKGK served as negative control. Results for UPN41 and UPN49 are shown as pool read-outs of all six HLA class II-restricted, CML-associated peptides due to low cell numbers. Data are expressed as mean ± SD of two independent replicates. Abbreviations: HVs, healthy volunteers; SFU, spot forming unit; ID, identification; UPN, uniform patient number; neg., negative; pos., positive; *** $p < 0.001$.

6.2.5. DISCUSSION

Several studies have shown that immunological control plays a major role in the course of disease and for treatment success in CML.[12, 14, 16] Therefore, various immunotherapeutic approaches are currently being evaluated[17-20, 24, 29] with the main goal to achieve deep remissions that enable long-term TKI-free survival or even cure of CML patients. An attractive approach is the further development of tailored peptide-based immunotherapy, which enables specific and minor side effect targeting of CML cells. Therefore, the identification of novel, naturally presented, highly frequent, CML-associated target antigens is required. In this study, we present a large-scale immunopeptidomics-based approach to identify and functionally characterize such CML-associated HLA class I- and II-restricted peptides.

We confirmed strong HLA surface expression on myeloid cells as well as on hematopoietic precursor cells of CML patients in a range comparable to different healthy hematological cell types[40, 41] as well

as other hematological malignancies[38, 40, 41] and solid tumors,[37] which constitutes a major prerequisite for immunotherapeutic approaches. The comprehensive comparison of HLA ligandomes of CML samples with benign tissues and PBMC samples of CML_{MR} patients revealed a total of 50 CML-associated HLA class I ligands for four of the most common HLA allotypes.[78] Allele-specific prevalence of these CML-associated targets reached up to 80%. This enables both, the personalized composition of for example multipeptide vaccine cocktails, and the broadly applicable off-the-shelf development of single peptide-based immunotherapeutic approaches, such as adoptive T-cell transfer or TCR therapies.

Beside cytotoxic $CD8^+$ T cells, $CD4^+$ T cells play important direct and indirect roles in anti-cancer immunity.[79-85] Thus, we expanded our profiling approach to the HLA class II peptidome identifying 19 additional CML-associated peptides. Interestingly, length distribution of HLA class II-restricted peptides could be correlated to specific cell types and lineages, as myeloid cell-derived peptides are in general represented by shorter peptide sequences. This is in line with the previous observation that the immunopeptidome directly mirrors cell type biology and specificity, which is not only reflected by the general peptide composition[42] but also by the length distribution of HLA-presented peptides as demonstrated by our data.

As spontaneous, pathophysiologically relevant T-cell responses against non-mutated, leukemia-associated antigens were described for other hematological malignancies,[38, 86, 87] we analyzed our CML patient cohort for preexisting T-cell responses against our newly defined targets. Of note, while preexisting T-cell responses against HLA class II peptides were identified with comparable frequencies as previously described for CLL,[38] AML,[40] and MM,[41] functional T cells targeting HLA class I antigens were only low frequent in CML_{TKI} patient samples. In line with previous studies reporting a negative[53-56] or dysregulating[88] impact of TKI treatment on immune responses, $CD8^+$ T-cell functionality in our CML_{TKI} patient cohort was impaired, potentially explaining the reduced frequencies of preexisting memory T-cell responses to CML-associated HLA class I ligands. Of note, as no CML patients without TKI treatment were included in this study, the reduced T-cell functionality could not be directly correlated to TKI treatment and might also be linked to a general immunosuppressive state in CML disease caused by for example HLA-G,[89] elevated myeloid-derived suppressor,[12] and regulatory T cells,[12, 90] as well as increased PD-1 expression on immune cells.[12] However, the immunogenicity of all our CML-associated HLA class I antigens was proven by *in vitro* induction of multifunctional and cytotoxic T cells of HVs. Strikingly, CML-specific T cells could also be induced *de novo* using PBMCs of CML_{TKI} patients, which qualifies the identified targets as promising candidates for peptide-based immunotherapy approaches not only in CML patients after termination of TKI therapy, but even for tailored combinations with TKI treatment. Furthermore, several studies could show a pathophysiological relevance of preexisting peptide-specific T-cell responses

concerning clinical outcomes in cancer patients[38, 86, 87] suggesting that such T-cell response, induced or boosted by peptide-based immunotherapies, might achieve clinical effectiveness.

Mutated neoantigens have been described as the main specificities of anti-cancer T-cell responses induced by immune checkpoint inhibitors in solid tumors with high mutational burden.[91] However, only a very small fraction of mutations at the DNA sequence level results in peptides naturally presented in the HLA ligandome.[92-94] This raises the question of the relevance of mutated neoepitopes for T-cell-based immunotherapy, in particular for malignancies with low mutational burden, including CML. Despite an extensive search for naturally presented, BCR-ABL- and ABL-BCR-derived peptides, none could be validated in our CML cohort by MS. However, we have to emphasize that absence of evidence means not evidence of absence as the sensitivity of shotgun mass spectrometric discovery approaches, even in the context of immense technical improvements in the last decades,[95] is for sure limited since the HLA immunopeptidome is a highly dynamic, rich, and complex assembly of peptides. Therefore, we cannot exclude low level presentation of mutation-derived peptides in our CML patient cohort. Nevertheless, mass spectrometry-based immunopeptidomics is currently the only unbiased methodology to identify the entirety of naturally processed and presented HLA peptides in primary tissue samples,[96] which enables us to identify and characterize target antigens in low mutational burden cancer entities that are i) non-mutated, ii) naturally presented, iii) highly frequent, and iv) tumor-specific.

This is further emphasized as the extensive screen in our CML and hematological benign cohorts for HLA-presented peptides derived from previously described CTAs[75, 76] and LAAs[43, 77] revealed no highly frequent, tumor-exclusive presentation. Together with previous findings showing a distorted correlation of gene expression and HLA-restricted antigen presentation with the immunopeptidome neither mirroring the transcriptome nor the proteome,[40, 93, 97-100] this precludes, in our view, these antigens as optimal candidates for T-cell-based immunotherapy. Nevertheless, tumor exclusivity can either be determined on the level of HLA ligands or on the level of entire antigens. In the study at hand, the CTA and LAA analysis was performed on the level of entire antigens and does not consider presentation of CTA- and LAA-derived single HLA ligands as they could potentially be tumor-exclusive due to differential antigen processing in cancer cells.

In conclusion, the cell biology-specific character of the immunopeptidome[42] calls for entity-centered identification of tumor-associated targets. Therefore, our study provides profound insights into the naturally presented immunopeptidome of CML, delineating a panel of novel, immunogenic, non-mutated, CML-associated T-cell epitopes. These antigens aid the development of different antigen-specific therapeutic approaches, which may provide options to enable achievement of deep remission, long-term TKI-free survival, or even cure for CML patients.

6.2.6. REFERENCES

1. Brehme M, Hantschel O, Colinge J, Kaupe I, Planyavsky M, Köcher T, Mechtler K, Bennett KL, and Superti-Furga G. Charting the molecular network of the drug target Bcr-Abl. *Proc Natl Acad Sci U S A* 106(18): 7414-7419 (2009).
2. Nowell PC and Hungerford DA. Chromosome studies on normal and leukemic human leukocytes. *J Natl Cancer Inst* 25: 85-109 (1960).
3. O'Brien SG, Guilhot F, Larson RA, Gathmann I, Baccarani M, Cervantes F, Cornelissen JJ, Fischer T, Hochhaus A, Hughes T, Lechner K, Nielsen JL, Rousselot P, Reiffers J, Saglio G, Shepherd J, Simonsson B, Gratwohl A, Goldman JM, Kantarjian H, Taylor K, Verhoef G, Bolton AE, Capdeville R, Druker BJ, and IRIS Investigators. Imatinib compared with interferon and low-dose cytarabine for newly diagnosed chronic-phase chronic myeloid leukemia. *N Engl J Med* 348(11): 994-1004 (2003).
4. Cortes JE, Kim DW, Kantarjian HM, Brümmendorf TH, Dyagil I, Griskevicius L, Malhotra H, Powell C, Gogat K, Countouriotis AM, and Gambacorti-Passerini C. Bosutinib versus imatinib in newly diagnosed chronic-phase chronic myeloid leukemia: results from the BELA trial. *J Clin Oncol* 30(28): 3486-3492 (2012).
5. Kantarjian H, Shah NP, Hochhaus A, Cortes J, Shah S, Ayala M, Moiraghi B, Shen Z, Mayer J, Pasquini R, Nakamae H, Huguet F, Boqué C, Chuah C, Bleickardt E, Bradley-Garelik MB, Zhu C, Szatrowski T, Shapiro D, and Baccarani M. Dasatinib versus imatinib in newly diagnosed chronic-phase chronic myeloid leukemia. *N Engl J Med* 362(24): 2260-2270 (2010).
6. Saglio G, Kim DW, Issaragrisil S, le Coutre P, Etienne G, Lobo C, Pasquini R, Clark RE, Hochhaus A, Hughes TP, Gallagher N, Hoenekopp A, Dong M, Haque A, Larson RA, Kantarjian HM, and ENESTnd Investigators. Nilotinib versus imatinib for newly diagnosed chronic myeloid leukemia. *N Engl J Med* 362(24): 2251-2259 (2010).
7. Kantarjian HM, Kim D-W, Pinilla-Ibarz J, Coutre PDL, Paquette R, Chuah C, Nicolini FE, Apperley J, Khoury HJ, Talpaz M, DiPersio JF, Baccarani M, Lustgarten S, Haluska FG, Guilhot F, Deininger MWN, Hochhaus A, Hughes TP, Shah NP, and Cortes JE. Ponatinib (PON) in patients (pts) with Philadelphia chromosome-positive (Ph+) leukemias resistant or intolerant to dasatinib or nilotinib, or with the T315I mutation: Longer-term follow up of the PACE trial. *J Clin Oncol* 32(15_suppl): 7081-7081 (2014).
8. Mahon FX, Réa D, Guilhot J, Guilhot F, Huguet F, Nicolini F, Legros L, Charbonnier A, Guerci A, Varet B, Etienne G, Reiffers J, Rousselot P, and Intergroupe Français des Leucémies Myéloides Chroniques. Discontinuation of imatinib in patients with chronic myeloid leukaemia who have maintained complete molecular remission for at least 2 years: the prospective, multicentre Stop Imatinib (STIM) trial. *Lancet Oncol* 11(11): 1029-1035 (2010).
9. Saussele S, Richter J, Guilhot J, Gruber FX, Hjorth-Hansen H, Almeida A, Janssen J, Mayer J, Koskenvesa P, Panayiotidis P, Olsson-Strömberg U, Martinez-Lopez J, Rousselot P, Vestergaard H, Ehrencrona H, Kairisto V, Machová Poláková K, Müller MC, Mustjoki S, Berger MG, Fabarius A, Hofmann WK, Hochhaus A, Pfirrmann M, Mahon FX, and EURO-SKI investigators. Discontinuation of tyrosine kinase inhibitor therapy in chronic myeloid leukaemia (EURO-SKI): a prespecified interim analysis of a prospective, multicentre, non-randomised, trial. *Lancet Oncol* 19(6): 747-757 (2018).
10. Machova Polakova K, Kulvait V, Benesova A, Linhartova J, Klamova H, Jaruskova M, de Benedittis C, Haferlach T, Baccarani M, Martinelli G, Stopka T, Ernst T, Hochhaus A, Kohlmann A, and Soverini S. Next-generation deep sequencing improves detection of BCR-ABL1 kinase domain mutations emerging under tyrosine kinase inhibitor treatment of chronic myeloid leukemia patients in chronic phase. *J Cancer Res Clin Oncol* 141(5): 887-899 (2015).
11. Schmidt M, Rinke J, Schäfer V, Schnittger S, Kohlmann A, Obstfelder E, Kunert C, Ziermann J, Winkelmann N, Eigendorff E, Haferlach T, Haferlach C, Hochhaus A, and Ernst T. Molecular-defined clonal evolution in patients with chronic myeloid leukemia independent of the BCR-ABL status. *Leukemia* 28(12): 2292-2299 (2014).
12. Hughes A, Clarson J, Tang C, Vidovic L, White DL, Hughes TP, and Yong AS. CML patients with deep molecular responses to TKI have restored immune effectors and decreased PD-1 and immune suppressors. *Blood* 129(9): 1166-1176 (2017).
13. Sopper S, Mustjoki S, White D, Hughes T, Valent P, Burchert A, Gjertsen BT, Gastl G, Baldauf M, Trajanoski Z, Giles F, Hochhaus A, Ernst T, Schenk T, Janssen JJ, Ossenkoppele GJ, Porkka K, and Wolf D. Reduced CD62L expression on T cells and increased soluble CD62L levels predict molecular response to tyrosine kinase inhibitor therapy in early chronic-phase chronic myelogenous leukemia. *J Clin Oncol* 35(2): 175-184 (2017).
14. Rea D, Henry G, Khaznadar Z, Etienne G, Guilhot F, Nicolini F, Guilhot J, Rousselot P, Huguet F, Legros L, Gardembas M, Dubruille V, Guerci-Bresler A, Charbonnier A, Maloisel F, Ianotto JC, Villemagne B, Mahon FX, Moins-Teisserenc H, Dulphy N, and Toubert A. Natural killer-cell counts are associated with molecular relapse-free survival after imatinib discontinuation in chronic myeloid leukemia: the IMMUNOSTIM study. *Haematologica* 102(8): 1368-1377 (2017).
15. Schütz C, Inselmann S, Saussele S, Dietz CT, Müller MC, Eigendorff E, Brendel CA, Metzelder SK, Brümmendorf TH, Waller C, Dengler J, Goebeler ME, Herbst R, Freunek G, Hanzel S, Illmer T, Wang Y, Lange T, Finkernagel F, Hehlmann R, Huber M, Neubauer A, Hochhaus A, Guilhot J, Mahon FX, Pfirrmann M, and Burchert A. Expression of the CTLA-4 ligand CD86 on plasmacytoid dendritic cells (pDC) predicts risk of disease recurrence after treatment discontinuation in CML. *Leukemia* 32(4): 1054 (2018).
16. Burchert A, Saussele S, Eigendorff E, Müller MC, Sohlbach K, Inselmann S, Schütz C, Metzelder SK, Ziermann J, Kostrewa P, Hoffmann J, Hehlmann R, Neubauer A, and Hochhaus A. Interferon alpha 2 maintenance therapy may enable high rates of treatment discontinuation in chronic myeloid leukemia. *Leukemia* 29(6): 1331-1335 (2015).
17. Simonsson B, Gedde-Dahl T, Markevärn B, Remes K, Stentoft J, Almqvist A, Björeman M, Flogegård M, Koskenvesa P, Lindblom A, Malm C, Mustjoki S, Myhr-Eriksson K, Ohm L, Räsänen A, Sinisalo M, Själander A, Strömberg U, Bjerrum OW, Ehrencrona H, Gruber F, Kairisto V, Olsson K, Sandin F, Nagler A, Nielsen JL, Hjorth-Hansen H, Porkka K, and

Nordic CML Study Group. Combination of pegylated IFN-α2b with imatinib increases molecular response rates in patients with low- or intermediate-risk chronic myeloid leukemia. *Blood* 118(12): 3228-3235 (2011).
18. Hjorth-Hansen H, Stentoft J, Richter J, Koskenvesa P, Höglund M, Dreimane A, Porkka K, Gedde-Dahl T, Gjertsen BT, Gruber FX, Stenke L, Eriksson KM, Markevärn B, Lübking A, Vestergaard H, Udby L, Bjerrum OW, Persson I, Mustjoki S, and Olsson-Strömberg U. Safety and efficacy of the combination of pegylated interferon-alpha2b and dasatinib in newly diagnosed chronic-phase chronic myeloid leukemia patients. *Leukemia* 30(9): 1853-1860 (2016).
19. Gratwohl A, Brand R, Apperley J, Crawley C, Ruutu T, Corradini P, Carreras E, Devergie A, Guglielmi C, Kolb HJ, and Niederwieser D. Allogeneic hematopoietic stem cell transplantation for chronic myeloid leukemia in Europe 2006: transplant activity, long-term data and current results. An analysis by the Chronic Leukemia Working Party of the European Group for Blood and Marrow Transplantation (EBMT). *Haematologica* 91(4): 513-521 (2006).
20. Kebriaei P, Detry MA, Giralt S, Carrasco-Yalan A, Anagnostopoulos A, Couriel D, Khouri IF, Anderlini P, Hosing C, Alousi A, Champlin RE, and de Lima M. Long-term follow-up of allogeneic hematopoietic stem-cell transplantation with reduced-intensity conditioning for patients with chronic myeloid leukemia. *Blood* 110(9): 3456-3462 (2007).
21. Wolchok JD, Kluger H, Callahan MK, Postow MA, Rizvi NA, Lesokhin AM, Segal NH, Ariyan CE, Gordon RA, Reed K, Burke MM, Caldwell A, Kronenberg SA, Agunwamba BU, Zhang X, Lowy I, Inzunza HD, Feely W, Horak CE, Hong Q, Korman AJ, Wigginton JM, Gupta A, and Sznol M. Nivolumab plus ipilimumab in advanced melanoma. *N Engl J Med* 369(2): 122-133 (2013).
22. Topalian SL, Hodi FS, Brahmer JR, Gettinger SN, Smith DC, McDermott DF, Powderly JD, Carvajal RD, Sosman JA, Atkins MB, Leming PD, Spigel DR, Antonia SJ, Horn L, Drake CG, Pardoll DM, Chen L, Sharfman WH, Anders RA, Taube JM, McMiller TL, Xu H, Korman AJ, Jure-Kunkel M, Agrawal S, McDonald D, Kollia GD, Gupta A, Wigginton JM, and Sznol M. Safety, activity, and immune correlates of anti-PD-1 antibody in cancer. *N Engl J Med* 366(26): 2443-2454 (2012).
23. Hodi FS, O'Day SJ, McDermott DF, Weber RW, Sosman JA, Haanen JB, Gonzalez R, Robert C, Schadendorf D, Hassel JC, Akerley W, van den Eertwegh AJ, Lutzky J, Lorigan P, Vaubel JM, Linette GP, Hogg D, Ottensmeier CH, Lebbé C, Peschel C, Quirt I, Clark JI, Wolchok JD, Weber JS, Tian J, Yellin MJ, Nichol GM, Hoos A, and Urba WJ. Improved survival with ipilimumab in patients with metastatic melanoma. *N Engl J Med* 363(8): 711-723 (2010).
24. ClinicalTrials.gov [Internet]. Bethesda (MD) National Library of Medicine (US). Identifier: NCT02011945 A Phase 1B Study to Investigate the Safety and Preliminary Efficacy for the Combination of Dasatinib Plus Nivolumab in Patients With Chronic Myeloid Leukemia. 2013 Dec 16 [cited 2018 May 05]; Available from: https://clinicaltrials.gov/ct2/show/NCT02011945.
25. Qazilbash MH, Wieder E, Thall PF, Wang X, Rios R, Lu S, Kanodia S, Ruisaard KE, Giralt SA, Estey EH, Cortes J, Komanduri KV, Clise-Dwyer K, Alatrash G, Ma Q, Champlin RE, and Molldrem JJ. PR1 peptide vaccine induces specific immunity with clinical responses in myeloid malignancies. *Leukemia* 31(3): 697-704 (2017).
26. Maslak PG, Dao T, Krug LM, Chanel S, Korontsvit T, Zakhaleva V, Zhang R, Wolchok JD, Yuan J, Pinilla-Ibarz J, Berman E, Weiss M, Jurcic J, Frattini MG, and Scheinberg DA. Vaccination with synthetic analog peptides derived from WT1 oncoprotein induces T-cell responses in patients with complete remission from acute myeloid leukemia. *Blood* 116(2): 171-179 (2010).
27. Oka Y, Tsuboi A, Oji Y, Kawase I, and Sugiyama H. WT1 peptide vaccine for the treatment of cancer. *Curr Opin Immunol* 20(2): 211-220 (2008).
28. Dao T, Pankov D, Scott A, Korontsvit T, Zakhaleva V, Xu Y, Xiang J, Yan S, de Morais Guerreiro MD, Veomett N, Dubrovsky L, Curcio M, Doubrovina E, Ponomarev V, Liu C, O'Reilly RJ, and Scheinberg DA. Therapeutic bispecific T-cell engager antibody targeting the intracellular oncoprotein WT1. *Nat Biotechnol* 33(10): 1079-1086 (2015).
29. Dubrovsky L, Pankov D, Brea EJ, Dao T, Scott A, Yan S, O'Reilly RJ, Liu C, and Scheinberg DA. A TCR-mimic antibody to WT1 bypasses tyrosine kinase inhibitor resistance in human BCR-ABL+ leukemias. *Blood* 123(21): 3296-3304 (2014).
30. Chang AY, Dao T, Gejman RS, Jarvis CA, Scott A, Dubrovsky L, Mathias MD, Korontsvit T, Zakhaleva V, Curcio M, Hendrickson RC, Liu C, and Scheinberg DA. A therapeutic T cell receptor mimic antibody targets tumor-associated PRAME peptide/HLA-I antigens. *J Clin Invest* 127(7): 2705-2718 (2017).
31. O'Reilly RJ, Dao T, Koehne G, Scheinberg D, and Doubrovina E. Adoptive transfer of unselected or leukemia-reactive T-cells in the treatment of relapse following allogeneic hematopoietic cell transplantation. *Semin Immunol* 22(3): 162-172 (2010).
32. Rafiq S, Purdon TJ, Daniyan AF, Koneru M, Dao T, Liu C, Scheinberg DA, and Brentjens RJ. Optimized T-cell receptor-mimic chimeric antigen receptor T cells directed toward the intracellular Wilms Tumor 1 antigen. *Leukemia* 31(8): 1788-1797 (2017).
33. Snyder A, Makarov V, Merghoub T, Yuan J, Zaretsky JM, Desrichard A, Walsh LA, Postow MA, Wong P, Ho TS, Hollmann TJ, Bruggeman C, Kannan K, Li Y, Elipenahli C, Liu C, Harbison CT, Wang L, Ribas A, Wolchok JD, and Chan TA. Genetic basis for clinical response to CTLA-4 blockade in melanoma. *N Engl J Med* 371(23): 2189-2199 (2014).
34. Falk K, Rötzschke O, Stevanović S, Jung G, and Rammensee H-G. Allele-specific motifs revealed by sequencing of self-peptides eluted from MHC molecules. *Nature* 351(6324): 290-296 (1991).
35. van Rooij N, van Buuren MM, Philips D, Velds A, Toebes M, Heemskerk B, van Dijk LJ, Behjati S, Hilkmann H, El Atmioui D, Nieuwland M, Stratton MR, Kerkhoven RM, Kesmir C, Haanen JB, Kvistborg P, and Schumacher TN. Tumor exome analysis reveals neoantigen-specific T-cell reactivity in an ipilimumab-responsive melanoma. *J Clin Oncol* 31(32): e439-e442 (2013).
36. Godet Y, Fabre E, Dosset M, Lamuraglia M, Levionnois E, Ravel P, Benhamouda N, Cazes A, Le Pimpec-Barthes F, Gaugler B, Langlade-Demoyen P, Pivot X, Saas P, Maillère B, Tartour E, Borg C, and Adotévi O. Analysis of spontaneous tumor-specific CD4 T-cell immunity in lung cancer using promiscuous HLA-DR telomerase-derived epitopes: potential synergistic effect with chemotherapy response. *Clin Cancer Res* 18(10): 2943-2953 (2012).

37. Schuster H, Peper JK, Bösmüller HC, Röhle K, Backert L, Bilich T, Ney B, Löffler MW, Kowalewski DJ, Trautwein N, Rabsteyn A, Engler T, Braun S, Haen SP, Walz JS, Schmid-Horch B, Brucker SY, Wallwiener D, Kohlbacher O, Fend F, Rammensee H-G, Stevanović S, Staebler A, and Wagner P. The immunopeptidomic landscape of ovarian carcinomas. *Proc Natl Acad Sci U S A* 114(46): E9942-E9951 (2017).
38. Kowalewski DJ, Schuster H, Backert L, Berlin C, Kahn S, Kanz L, Salih HR, Rammensee HG, Stevanovic S, and Stickel JS. HLA ligandome analysis identifies the underlying specificities of spontaneous antileukemia immune responses in chronic lymphocytic leukemia (CLL). *Proc Natl Acad Sci U S A* 112(2): E166-E175 (2015).
39. Kowalewski DJ, Stevanović S, Rammensee H-G, and Stickel JS. Antileukemia T-cell responses in CLL - We don't need no aberration. *Oncoimmunology* 4(7): e1011527 (2015).
40. Berlin C, Kowalewski DJ, Schuster H, Mirza N, Walz S, Handel M, Schmid-Horch B, Salih HR, Kanz L, Rammensee H-G, Stevanović S, and Stickel JS. Mapping the HLA ligandome landscape of acute myeloid leukemia: a targeted approach toward peptide-based immunotherapy. *Leukemia* 29(3): 647-659 (2015).
41. Walz S, Stickel JS, Kowalewski DJ, Schuster H, Weisel K, Backert L, Kahn S, Nelde A, Stroh T, Handel M, Kohlbacher O, Kanz L, Salih HR, Rammensee H-G, and Stevanović S. The antigenic landscape of multiple myeloma: mass spectrometry (re)defines targets for T-cell-based immunotherapy. *Blood* 126(10): 1203-1213 (2015).
42. Backert L, Kowalewski DJ, Walz S, Schuster H, Berlin C, Neidert MC, Schemionek M, Brümmendorf TH, Vucinic V, Niederwieser D, Kanz L, Salih HR, Kohlbacher O, Weisel K, Rammensee H-G, Stevanović S, and Walz JS. A meta-analysis of HLA peptidome composition in different hematological entities: Entity-specific dividing lines and "pan-leukemia" antigens. *Oncotarget* 8(27): 43915-43924 (2017).
43. Greiner J and Schmitt M. Leukemia-associated antigens as target structures for a specific immunotherapy in chronic myeloid leukemia. *Eur J Haematol* 80(6): 461-468 (2008).
44. Molldrem JJ, Lee PP, Wang C, Champlin RE, and Davis MM. A PR1-human leukocyte antigen-A2 tetramer can be used to isolate low-frequency cytotoxic T lymphocytes from healthy donors that selectively lyse chronic myelogenous leukemia. *Cancer Res* 59(11): 2675-2681 (1999).
45. Molldrem JJ, Lee PP, Kant S, Wieder E, Jiang W, Lu S, Wang C, and Davis MM. Chronic myelogenous leukemia shapes host immunity by selective deletion of high-avidity leukemia-specific T cells. *J Clin Invest* 111(5): 639-647 (2003).
46. Rezvani K, Brenchley JM, Price DA, Kilical Y, Gostick E, Sewell AK, Li J, Mielke S, Douek DC, and Barrett AJ. T-cell responses directed against multiple HLA-A*0201-restricted epitopes derived from Wilms' tumor 1 protein in patients with leukemia and healthy donors: identification, quantification, and characterization. *Clin Cancer Res* 11(24): 8799-8807 (2005).
47. Greco G, Fruci D, Accapezzato D, Barnaba V, Nisini R, Alimena G, Montefusco E, Vigneti E, Butler R, Tanigaki N, and Tosi R. Two brc-abl junction peptides bind HLA-A3 molecules and allow specific induction of human cytotoxic T lymphocytes. *Leukemia* 10(4): 693-699 (1996).
48. Nieda M, Nicol A, Kikuchi A, Kashiwase K, Taylor K, Suzuki K, Tadokoro K, and Juji T. Dendritic cells stimulate the expansion of bcr-abl specific CD8+ T cells with cytotoxic activity against leukemic cells from patients with chronic myeloid leukemia. *Blood* 91(3): 977-983 (1998).
49. Kessler JH, Bres-Vloemans SA, van Veelen PA, de Ru A, Huijbers IJ, Camps M, Mulder A, Offringa R, Drijfhout JW, Leeksma OC, Ossendorp F, and Melief CJ. BCR-ABL fusion regions as a source of multiple leukemia-specific CD8+ T-cell epitopes. *Leukemia* 20(10): 1738-1750 (2006).
50. Pinilla-Ibarz J, Cathcart K, Korontsvit T, Soignet S, Bocchia M, Caggiano J, Lai L, Jimenez J, Kolitz J, and Scheinberg DA. Vaccination of patients with chronic myelogenous leukemia with bcr-abl oncogene breakpoint fusion peptides generates specific immune responses. *Blood* 95(5): 1781-1787 (2000).
51. Cathcart K, Pinilla-Ibarz J, Korontsvit T, Schwartz J, Zakhaleva V, Papadopoulos EB, and Scheinberg DA. A multivalent bcr-abl fusion peptide vaccination trial in patients with chronic myeloid leukemia. *Blood* 103(3): 1037-1042 (2004).
52. Bocchia M, Gentili S, Abruzzese E, Fanelli A, Iuliano F, Tabilio A, Amabile M, Forconi F, Gozzetti A, Raspadori D, Amadori S, and Lauria F. Effect of a p210 multipeptide vaccine associated with imatinib or interferon in patients with chronic myeloid leukaemia and persistent residual disease: a multicentre observational trial. *Lancet* 365(9460): 657-662 (2005).
53. Fei F, Yu Y, Schmitt A, Rojewski MT, Chen B, Greiner J, Götz M, Guillaume P, Döhner H, Bunjes D, and Schmitt M. Dasatinib exerts an immunosuppressive effect on CD8+ T cells specific for viral and leukemia antigens. *Exp Hematol* 36(10): 1297-1308 (2008).
54. Chen J, Schmitt A, Chen B, Rojewski M, Rübeler V, Fei F, Yu Y, Yu X, Ringhoffer M, von Harsdorf S, Greiner J, Götzz M, Guillaume P, Döhner H, Bunjes D, and Schmitt M. Nilotinib hampers the proliferation and function of CD8+ T lymphocytes through inhibition of T cell receptor signalling. *J Cell Mol Med* 12(5B): 2107-2118 (2008).
55. Seggewiss R, Loré K, Greiner E, Magnusson MK, Price DA, Douek DC, Dunbar CE, and Wiestner A. Imatinib inhibits T-cell receptor-mediated T-cell proliferation and activation in a dose-dependent manner. *Blood* 105(6): 2473-2479 (2005).
56. Rohon P, Porkka K, and Mustjoki S. Immunoprofiling of patients with chronic myeloid leukemia at diagnosis and during tyrosine kinase inhibitor therapy. *Eur J Haematol* 85(5): 387-398 (2010).
57. Nelde A, Kowalewski DJ, Backert L, Schuster H, Werner JO, Klein R, Kohlbacher O, Kanz L, Salih HR, Rammensee HG, Stevanovic S, and Walz JS. HLA ligandome analysis of primary chronic lymphocytic leukemia (CLL) cells under lenalidomide treatment confirms the suitability of lenalidomide for combination with T-cell-based immunotherapy. *Oncoimmunology* 128(22): 3234 (2018).
58. Kowalewski DJ and Stevanović S. Biochemical large-scale identification of MHC class I ligands. *Methods Mol Biol* 960: 145-157 (2013).

59. Melo JV, Gordon DE, Cross NC, and Goldman JM. The ABL-BCR fusion gene is expressed in chronic myeloid leukemia. *Blood* 81(1): 158-165 (1993).
60. Berke Z, Andersen MH, Pedersen M, Fugger L, Zeuthen J, and Haurum JS. Peptides spanning the junctional region of both the abl/bcr and the bcr/abl fusion proteins bind common HLA class I molecules. *Leukemia* 14(3): 419-426 (2000).
61. Käll L, Canterbury JD, Weston J, Noble WS, and MacCoss MJ. Semi-supervised learning for peptide identification from shotgun proteomics datasets. *Nat Methods* 4(11): 923-925 (2007).
62. Schuler MM, Nastke MD, and Stevanović S. SYFPEITHI: database for searching and T-cell epitope prediction. *Methods Mol Biol* 409: 75-93 (2007).
63. Nielsen M and Andreatta M. NetMHCpan-3.0; improved prediction of binding to MHC class I molecules integrating information from multiple receptor and peptide length datasets. *Genome Med* 8(1): 33 (2016).
64. Hoof I, Peters B, Sidney J, Pedersen LE, Sette A, Lund O, Buus S, and Nielsen M. NetMHCpan, a method for MHC class I binding prediction beyond humans. *Immunogenetics* 61(1): 1-13 (2009).
65. Sturm T, Leinders-Zufall T, Maček B, Walzer M, Jung S, Pömmerl B, Stevanović S, Zufall F, Overath P, and Rammensee H-G. Mouse urinary peptides provide a molecular basis for genotype discrimination by nasal sensory neurons. *Nat Commun* 4: 1616 (2013).
66. Widenmeyer M, Griesemann H, Stevanović S, Feyerabend S, Klein R, Attig S, Hennenlotter J, Wernet D, Kuprash DV, Sazykin AY, Pascolo S, Stenzl A, Gouttefangeas C, and Rammensee H-G. Promiscuous survivin peptide induces robust CD4+ T-cell responses in the majority of vaccinated cancer patients. *Int J Cancer* 131(1): 140-149 (2012).
67. Walter S, Herrgen L, Schoor O, Jung G, Wernet D, Bühring HJ, Rammensee H-G, and Stevanović S. Cutting edge: predetermined avidity of human CD8 T cells expanded on calibrated MHC/anti-CD28-coated microspheres. *J Immunol* 171(10): 4974-4978 (2003).
68. Neumann A, Hörzer H, Hillen N, Klingel K, Schmid-Horch B, Bühring HJ, Rammensee H-G, Aebert H, and Stevanović S. Identification of HLA ligands and T-cell epitopes for immunotherapy of lung cancer. *Cancer Immunol Immunother* 62(9): 1485-1497 (2013).
69. Rudolf D, Silberzahn T, Walter S, Maurer D, Engelhard J, Wernet D, Bühring HJ, Jung G, Kwon BS, Rammensee H-G, and Stevanović S. Potent costimulation of human CD8 T cells by anti-4-1BB and anti-CD28 on synthetic artificial antigen presenting cells. *Cancer Immunol Immunother* 57(2): 175-183 (2008).
70. Nelde A, Walz JS, Kowalewski DJ, Schuster H, Wolz OO, Peper JK, Cardona Gloria Y, Langerak AW, Muggen AF, Claus R, Bonzheim I, Fend F, Salih HR, Kanz L, Rammensee HG, Stevanovic S, and Weber AN. HLA class I-restricted MYD88 L265P-derived peptides as specific targets for lymphoma immunotherapy. *Oncoimmunology* 126(23): 2750 (2017).
71. Hermans IF, Silk JD, Yang J, Palmowski MJ, Gileadi U, McCarthy C, Salio M, Ronchese F, and Cerundolo V. The VITAL assay: a versatile fluorometric technique for assessing CTL- and NKT-mediated cytotoxicity against multiple targets in vitro and in vivo. *J Immunol Methods* 285(1): 25-40 (2004).
72. Vizcaíno JA, Deutsch EW, Wang R, Csordas A, Reisinger F, Ríos D, Dianes JA, Sun Z, Farrah T, Bandeira N, Binz PA, Xenarios I, Eisenacher M, Mayer G, Gatto L, Campos A, Chalkley RJ, Kraus HJ, Albar JP, Martinez-Bartolomé S, Apweiler R, Omenn GS, Martens L, Jones AR, and Hermjakob H. ProteomeXchange provides globally coordinated proteomics data submission and dissemination. *Nat Biotechnol* 32(3): 223-226 (2014).
73. Bui HH, Sidney J, Dinh K, Southwood S, Newman MJ, and Sette A. Predicting population coverage of T-cell epitope-based diagnostics and vaccines. *BMC Bioinform* 7: 153 (2006).
74. Vita R, Overton JA, Greenbaum JA, Ponomarenko J, Clark JD, Cantrell JR, Wheeler DK, Gabbard JL, Hix D, Sette A, and Peters B. The immune epitope database (IEDB) 3.0. *Nucleic Acids Res* 43(Database issue): D405-D412 (2015).
75. Almeida LG, Sakabe NJ, deOliveira AR, Silva MC, Mundstein AS, Cohen T, Chen YT, Chua R, Gurung S, Gnjatic S, Jungbluth AA, Caballero OL, Bairoch A, Kiesler E, White SL, Simpson AJ, Old LJ, Camargo AA, and Vasconcelos AT. CTdatabase: a knowledge-base of high-throughput and curated data on cancer-testis antigens. *Nucleic Acids Res* 37(Database issue): D816-D819 (2009).
76. GTEx Consortium. The Genotype-Tissue Expression (GTEx) project. *Nat Genet* 45(6): 580-585 (2013).
77. Smahel M. Antigens in chronic myeloid leukemia: implications for vaccine development. *Cancer Immunol Immunother* 60(12): 1655-1668 (2011).
78. González-Galarza FF, Takeshita LY, Santos EJ, Kempson F, Maia MH, da Silva AL, Teles e Silva AL, Ghattaoraya GS, Alfirevic A, Jones AR, and Middleton D. Allele frequency net 2015 update: new features for HLA epitopes, KIR and disease and HLA adverse drug reaction associations. *Nucleic Acids Res* 43(Database issue): D784-D788 (2015).
79. Schoenberger SP, Toes RE, van der Voort EI, Offringa R, and Melief CJ. T-cell help for cytotoxic T lymphocytes is mediated by CD40-CD40L interactions. *Nature* 393(6684): 480-483 (1998).
80. Janssen EM, Lemmens EE, Wolfe T, Christen U, von Herrath MG, and Schoenberger SP. CD4+ T cells are required for secondary expansion and memory in CD8+ T lymphocytes. *Nature* 421(6925): 852-856 (2003).
81. Mumberg D, Monach PA, Wanderling S, Philip M, Toledano AY, Schreiber RD, and Schreiber H. $CD4^+$ T cells eliminate MHC class II-negative cancer cells in vivo by indirect effects of IFN-γ. *Proc Natl Acad Sci U S A* 96(15): 8633-8638 (1999).
82. Greiner J, Ono Y, Hofmann S, Schmitt A, Mehring E, Götz M, Guillaume P, Döhner K, Mytilineos J, Döhner H, and Schmitt M. Mutated regions of nucleophosmin 1 elicit both CD4(+) and CD8(+) T-cell responses in patients with acute myeloid leukemia. *Blood* 120(6): 1282-1289 (2012).
83. Perez-Diez A, Joncker NT, Choi K, Chan WF, Anderson CC, Lantz O, and Matzinger P. CD4 cells can be more efficient at tumor rejection than CD8 cells. *Blood* 109(12): 5346-5354 (2007).
84. Sun JC, Williams MA, and Bevan MJ. CD4+ T cells are required for the maintenance, not programming, of memory CD8+ T cells after acute infection. *Nat Immunol* 5(9): 927-933 (2004).

85. Tran E, Turcotte S, Gros A, Robbins PF, Lu YC, Dudley ME, Wunderlich JR, Somerville RP, Hogan K, Hinrichs CS, Parkhurst MR, Yang JC, and Rosenberg SA. Cancer immunotherapy based on mutation-specific CD4+ T cells in a patient with epithelial cancer. *Science* 344(6184): 641-645 (2014).
86. Casalegno-Garduño R, Schmitt A, Spitschak A, Greiner J, Wang L, Hilgendorf I, Hirt C, Ho AD, Freund M, and Schmitt M. Immune responses to WT1 in patients with AML or MDS after chemotherapy and allogeneic stem cell transplantation. *Int J Cancer* 138(7): 1792-1801 (2015).
87. Hojjat-Farsangi M, Jeddi-Tehrani M, Daneshmanesh AH, Mozaffari F, Moshfegh A, Hansson L, Razavi SM, Sharifian RA, Rabbani H, Österborg A, Mellstedt H, and Shokri F. Spontaneous immunity against the receptor tyrosine kinase ROR1 in patients with chronic lymphocytic leukemia. *PLoS One* 10(11): e0142310 (2015).
88. Kreutzman A, Porkka K, and Mustjoki S. Immunomodulatory effects of tyrosine kinase inhibitors. *Int Trends Immun* 1(3): 17-28 (2013).
89. Caocci G, Greco M, Arras M, Cusano R, Orrù S, Martino B, Abruzzese E, Galimberti S, Mulas O, Trucas M, Littera R, Lai S, Carcassi C, and La Nasa G. HLA-G molecules and clinical outcome in Chronic Myeloid Leukemia. *Leuk Res* 61: 1-5 (2017).
90. Rojas JM, Wang L, Owen S, Knight K, Watmough SJ, and Clark RE. Naturally occurring CD4+ CD25+ FOXP3+ T-regulatory cells are increased in chronic myeloid leukemia patients not in complete cytogenetic remission and can be immunosuppressive. *Exp Hematol* 38(12): 1209-1218 (2010).
91. Alexandrov LB, Nik-Zainal S, Wedge DC, Aparicio SA, Behjati S, Biankin AV, Bignell GR, Bolli N, Borg A, Børresen-Dale AL, Boyault S, Burkhardt B, Butler AP, Caldas C, Davies HR, Desmedt C, Eils R, Eyfjörd JE, Foekens JA, Greaves M, Hosoda F, Hutter B, Ilicic T, Imbeaud S, Imielinski M, Jäger N, Jones DT, Jones D, Knappskog S, Kool M, Lakhani SR, López-Otín C, Martin S, Munshi NC, Nakamura H, Northcott PA, Pajic M, Papaemmanuil E, Paradiso A, Pearson JV, Puente XS, Raine K, Ramakrishna M, Richardson AL, Richter J, Rosenstiel P, Schlesner M, Schumacher TN, Span PN, Teague JW, Totoki Y, Tutt AN, Valdés-Mas R, van Buuren MM, van 't Veer L, Vincent-Salomon A, Waddell N, Yates LR, Australian Pancreatic Cancer Genome Initiative, ICGC Breast Cancer Consortium, ICGC MMML-Seq Consortium, ICGC PedBrain, Zucman-Rossi J, Futreal PA, McDermott U, Lichter P, Meyerson M, Grimmond SM, Siebert R, Campo E, Shibata T, Pfister SM, Campbell PJ, and Stratton MR. Signatures of mutational processes in human cancer. *Nature* 500(7463): 415-421 (2013).
92. Finn OJ and Rammensee H-G. Is It Possible to Develop Cancer Vaccines to Neoantigens, What Are the Major Challenges, and How Can These Be Overcome? Neoantigens: Nothing New in Spite of the Name. *Cold Spring Harb Perspect Biol* 10(11) (2018).
93. Bassani-Sternberg M, Bräunlein E, Klar R, Engleitner T, Sinitcyn P, Audehm S, Straub M, Weber J, Slotta-Huspenina J, Specht K, Martignoni ME, Werner A, Hein R, H. BD, Peschel C, Rad R, Cox J, Mann M, and Krackhardt AM. Direct identification of clinically relevant neoepitopes presented on native human melanoma tissue by mass spectrometry. *Nat Commun* 7: 13404 (2016).
94. Ott PA, Hu Z, Keskin DB, Shukla SA, Sun J, Bozym DJ, Zhang W, Luoma A, Giobbie-Hurder A, Peter L, Chen C, Olive O, Carter TA, Li S, Lieb DJ, Eisenhaure T, Gjini E, Stevens J, Lane WJ, Javeri I, Nellaiappan K, Salazar AM, Daley H, Seaman M, Buchbinder EI, Yoon CH, Harden M, Lennon N, Gabriel S, Rodig SJ, Barouch DH, Aster JC, Getz G, Wucherpfennig K, Neuberg D, Ritz J, Lander ES, Fritsch EF, Hacohen N, and Wu CJ. An immunogenic personal neoantigen vaccine for patients with melanoma. *Nature* 547(7662): 217-221 (2017).
95. Freudenmann LK, Marcu A, and Stevanović S. Mapping the tumour human leukocyte antigen (HLA) ligandome by mass spectrometry. *Immunology* 154(3): 331-345 (2018).
96. Bassani-Sternberg M and Coukos G. Mass spectrometry-based antigen discovery for cancer immunotherapy. *Curr Opin Immunol* 41: 9-17 (2016).
97. Weinzierl AO, Lemmel C, Schoor O, Müller M, Kruger T, Wernet D, Hennenlotter J, Stenzl A, Klingel K, Rammensee H-G, and Stevanović S. Distorted relation between mRNA copy number and corresponding major histocompatibility complex ligand density on the cell surface. *Mol Cell Proteomics* 6(1): 102-113 (2007).
98. Fortier MH, Caron E, Hardy MP, Voisin G, Lemieux S, Perreault C, and Thibault P. The MHC class I peptide repertoire is molded by the transcriptome. *J Exp Med* 205(3): 595-610 (2008).
99. Bassani-Sternberg M, Pletscher-Frankild S, Jensen LJ, and Mann M. Mass spectrometry of human leukocyte antigen class I peptidomes reveals strong effects of protein abundance and turnover on antigen presentation. *Mol Cell Proteomics* 14(3): 658-673 (2015).
100. Neidert MC, Kowalewski DJ, Silginer M, Kapolou K, Backert L, Freudenmann LK, Peper JK, Marcu A, Wang SS, Walz JS, Wolpert F, Rammensee H-G, Henschler R, Lamszus K, Westphal M, Roth P, Regli L, Stevanović S, Weller M, and Eisele G. The natural HLA ligandome of glioblastoma stem-like cells: antigen discovery for T cell-based immunotherapy. *Acta Neuropathol* 135(6): 923-938 (2018).

6.3. PART III:

DEVELOPMENT OF A THERAPEUTIC PEPTIDE VACCINE FOR THE TREATMENT OF ACUTE MYELOID LEUKEMIA BASED ON NATURALLY PRESENTED HLA LIGANDS OF AML PROGENITOR CELLS

Annika Nelde[1,2], Heiko Schuster[2,3], Daniel J. Kowalewski[2,3], Helmut R. Salih[1,4], Jens-Peter Volkmer[5], James Y. Chen[5], Elke Rücker-Braun[6,7], Anna M. Paczulla[3,8], Ana Marcu[2], Malte Roerden[9], Leon Bichmann[2,10], Tatjana Bilich[1,2], Jens Bauer[1,2], Jonas S. Heitmann[1,9], Oliver Kohlbacher[4,10-13], Marian C. Neidert[14], Johannes Schetelig[6,15], Marc Schmitz[7,16-19], Ravi Majeti[5,20], Irving L. Weissmann[5], Claudia Lengerke[8,21,22], Hans-Georg Rammensee[2,4,22], Stefan Stevanović[2,4,22], Juliane S. Walz[1,4,9]

[1] Clinical Collaboration Unit Translational Immunology, German Cancer Consortium (DKTK), University Hospital Tübingen, Germany
[2] Institute for Cell Biology, Department of Immunology, University of Tübingen, Germany
[3] Immatics Biotechnologies GmbH, Tübingen, Germany
[4] Cluster of Excellence iFIT (EXC 2180) "Image-Guided and Functionally Instructed Tumor Therapies", University of Tübingen, Germany
[5] Institute for Stem Cell Biology and Regenerative Medicine and the Ludwig Cancer Center, Stanford University School of Medicine, Stanford, California, United States of America
[6] Department of Medicine I, University Hospital of Dresden, Germany
[7] Center for Regenerative Therapies Dresden, TU Dresden, Germany
[8] University of Basel and University Hospital Basel, Department of Biomedicine, Switzerland
[9] Department of Hematology and Oncology, University Hospital Tübingen, Germany
[10] Applied Bioinformatics, Center for Bioinformatics and Department of Computer Science, University of Tübingen, Germany
[11] Quantitative Biology Center, University of Tübingen, Germany
[12] Biomolecular Interactions, Max-Planck-Institute for Developmental Biology, Tübingen, Germany
[13] Institute for Translational Bioinformatics, University Hospital Tübingen, Germany
[14] Department of Neurosurgery, Clinical Neuroscience Center, University Hospital Zurich and University of Zurich, Switzerland
[15] DKMS German Bone Marrow Donor Center, Clinical Trials Unit, Dresden, Germany
[16] Institute of Immunology, Medical Faculty Carl Gustav Carus, TU Dresden, Germany
[17] National Center for Tumor Diseases, University Hospital Carl Gustav Carus, TU Dresden, Germany
[18] German Cancer Research Center (DKFZ), Heidelberg, Germany
[19] German Cancer Consortium (DKTK), Dresden, Germany
[20] Department of Medicine, Division of Hematology, Stanford University School of Medicine, Stanford, California, United States of America
[21] University of Basel and University Hospital Basel, Clinic for Hematology, Switzerland
[22] German Cancer Consortium (DKTK), DKFZ partner site Tübingen, Germany

A.N. planned and performed most experiments of this study including enrichment of leukemic progenitor cells, enrichment of healthy hematopoietic progenitor cells, quantification of HLA surface molecules, HLA immunoprecipitation experiments of AML and hematological benign samples, mass spectrometry analysis, immunogenicity testing of candidate epitopes, data analysis and interpretation, unless mentioned otherwise. A.N. designed and created all figures and tables. A.N. wrote the manuscript.

Unpublished, manuscript in preparation.

6.3.1. ABSTRACT

Despite the efforts in the development of novel therapeutic opportunities for hematological malignancies in recent years, AML is still characterized by high relapse rates and a poor overall survival. This is mainly caused by the persistence of residual chemoresistant LPCs after standard chemotherapy, the so-called minimal residual disease. To maintain long-lasting remissions, novel strategies such as T-cell-based immunotherapy approaches are required to eliminate these cells. The basis for clinically successful T-cell-based immunotherapy is the availability of suitable target antigens for example HLA-presented tumor-associated peptides. Therefore, the knowledge of suitable HLA-restricted targets presented exclusively on AML is indispensable. Furthermore, specific targeting of LPCs requires not only AML-associated antigens, but the selection of targets presented on these low frequent progenitor cells. In this study, we therefore enriched $CD34^{+}CD38^{-}$ LPCs of primary AML samples and utilized a mass spectrometric approach to identify novel AML- and especially LPC-associated unmutated antigens presented on HLA class I and class II molecules. Remarkably, we were also able to detect naturally presented neoantigens derived from mutated NPM1 and IDH2 in this low mutational burden malignancy. Functional characterization of our novel defined unmutated and mutated targets revealed spontaneous T-cell responses in AML patient samples and healthy volunteers and confirmed the ability of these antigens to induce multifunctional and cytolytic active T cells. Thus, these newly defined AML- and LPC-associated HLA-restricted peptides represent suitable target antigens for T-cell-based immunotherapeutic approaches such as peptide vaccination for AML patients with the potential to eliminate even the so far barely targetable LPCs.

6.3.2. INTRODUCTION

AML is characterized by high relapse rates[1] after standard chemotherapy caused by the persistence of residual chemoresistant leukemic stem and progenitor cells, the so-called MRD.[2-4] The clinical significance of these LPCs is highlighted by the strong prognostic value of MRD presence after therapy indicating an increased risk of relapse and correlating with a shorter survival of AML patients.[5-7] The persistence of these self-renewable LPCs after conventional therapy explains the still high relapse rates, poor overall survival, and high mortality rate of AML patients. Thus, novel strategies are needed to eliminate MRD and eradicate quiescent LPCs to maintain long-lasting remissions and improve the long-term outcome of AML patients. Targeting LPCs more specifically therefore represents a key therapeutic strategy for the future. In recent years, several therapeutic strategies for the specific targeting of LPCs were investigated such as antibody-based targeting of LPC-associated surface markers[8-10] or small molecule inhibitors interfering with LPC-specific signaling pathways.[11, 12] Nevertheless, so far none of these LPC-targeting approaches found its way into the clinic and novel approaches are still required. The immunogenicity of AML and other hematological

neoplasms is demonstrated by the graft-versus-leukemia effect after allogenic stem cell transplantation[13, 14] as well as by the current success of antigen-specific T-cell-based immunotherapies including CAR T cells[15-17] and bispecific antibodies[18-20]. This raises the hope that antigen-specific immunotherapies could also target LPCs. Therefore, the knowledge and availability of suitable targets on the tumor cells and LPCs is indispensable. However, suitable tumor-associated surface targets on LPCs are extremely limited. On the other hand, HLA-based approaches targeting tumor-associated peptides presented on HLA molecules on the surface of tumor cells offering a wider range of potential target antigens due to the presentation of intracellular proteins.

In a previous publication, we already mapped and characterized the immunopeptidome of primary AML samples by mass spectrometry-based analysis and identified AML-associated $CD4^+$ and $CD8^+$ T-cell epitopes.[21] To further directly identify LPC-specific or LPC-associated HLA-restricted antigens the isolation or enrichment of these cells, which were first described by Bonnet and Dick more than 20 years ago,[22] is crucial. The phenotype of LPCs displays a complex heterogeneity, but several studies consider that the $CD34^+CD38^-$ population is the most relevant, as this fraction is functionally defined by their ability to reproduce the leukemic disease in immunodeficient mice.[22, 23]

Until a few years ago, suitable target antigens for T-cell-based immunotherapies are defined either by tumor-associated transcriptional overexpression or from tumor-specific mutations instead of target selection based on mass spectrometry-based immunopeptidomics. For several years, the identification of mutation-derived neoantigens was based on *in silico* predictions and T-cell-based assays.[24] The development of advanced mass spectrometers enables the direct identification of HLA-restricted mutation-derived peptides and recently the natural presentation of neoantigens in different tumor entities was demonstrated.[25-27] Nevertheless, AML represents a low mutational burden leukemia,[28-30] which might hamper the direct identification of neoepitopes by mass spectrometry. Yet, the mutational landscape of AML covers several recurrent and clonal driver mutations in genes like *NPM1*,[31] *FLT3*,[32, 33] *DNMT3A*,[34, 35] and *IDH1*[36] increasing their attractiveness as broadly applicable tumor rejection antigens.

In this study, we comprehensively mapped the immunopeptidome of naturally presented HLA class I and class II peptides of primary AML progenitor cells and AML blasts and identified a novel panel of broadly applicable unmutated AML- and LPC-associated antigens. Furthermore, we extensively screened the immunopeptidomes of primary AML and LPC samples for the occurrence of naturally presented neoantigens and identified HLA class I- and class II-restricted neoepitopes derived from mutated NPM1 and IDH2. These novel unmutated and mutated antigens were further analyzed for their potential to induce antigen-specific T-cell responses and were thereby validated as target antigens for T-cell-based immunotherapeutic approaches in AML patients.

6.3.3. METHODS

Further method descriptions can be found in the supplement.

Patients and blood samples

For HLA ligandome analysis, PBMCs or bone marrow mononuclear cells (BMNCs) from AML patients at the time of diagnosis, at relapse, or in MR were collected at the Departments of Hematology and Oncology in Tübingen and Dresden, Germany as well as at the Department of Medicine, Divisions of Hematology and Medical Oncology at the San Francisco University of California, CA, United States. For T-cell-based assays, PBMCs from HVs and AML patients after allogenic stem cell transplantation or in complete remission at different time points were collected. Cells were isolated by density gradient centrifugation and stored at -80°C until further use for subsequent LPC enrichment, HLA immunoprecipitation, or T-cell-based assays. Informed consent was obtained in accordance with the Declaration of Helsinki protocol. The study was performed according to the guidelines of the local ethics committees (373/2011B02, 454/2016B02). HLA typing was carried out by the Department of Hematology and Oncology, Tübingen, Germany. Patient and sample characteristics are provided in Tables S1-S5.

HLA surface molecule quantification and hematopoietic progenitor subtype phenotyping

HLA surface expression was determined using the QIFIKIT bead-based quantification flow cytometric assay (Dako) according to the manufacturer´s instructions as described before.[21, 37] In brief, cells were stained either with the pan-HLA class I-specific W6/32 mAb, the HLA-DR-specific L243 mAb (produced in-house), or IgG isotype control (BioLegend), respectively. Polyclonal goat FITC anti-mouse antibody (Dako) was used as secondary antibody. After washing with normal mouse serum (affymetrix eBioscience) surface marker staining was performed. LPCs were stained with PE/Cy7 anti-human CD38, APC anti-human CD34, and Pacific Blue anti-human CD45 antibodies (all BD). HV-derived HPCs and their cell subtype populations[38, 39] were stained with PE/Cy7 anti-human CD38 (BD), APC anti-human CD34 (BD), APC/Cy7 anti-human CD90 (BioLegend), PE anti-human CD117 (BioLegend), as well as Pacific Blue anti-human lineage cocktail (CD3, CD14, CD16, CD19, CD20, CD56) (BioLegend) antibodies. Aqua fluorescent reactive dye (Invitrogen) was used as viability marker. Analyses were performed on a FACS Canto II cytometer (BD). For HLA quantification ≥ 100 cells are required in the respective cell population.

Flow cytometry analysis of LPC frequencies

PBMC samples of AML patients collected at the Department of Hematology and Oncology in Tübingen were analyzed for the frequency of $CD34^+CD38^-$ LPCs to identify suitable patient samples for further LPC enrichment. Therefore, cells were stained with PE/Cy7 anti-human CD38 (BioLegend), APC anti-human CD34 (BD), and V450 anti-human CD45 (BD) antibodies. Aqua fluorescent reactive dye (Invitrogen) was used as viability marker. Analysis was performed on a FACS Canto II cytometer (BD).

LPC enrichment of AML patient samples

Enrichment of LPCs of seven AML samples (UPN3-8, UPN11) was performed by Dr. Heiko Schuster during his internship in the working group of Professor Irving Weissmann at the Institute for Stem Cell Biology and Regenerative Medicine, Stanford, CA, United States. PBMCs were stained with PE/Cy7 anti-human CD38, APC anti-human CD34, and PerCP/Cy5.5 anti-human CD3, CD19, CD20, and CD56 mAbs. The cells were sorted on three to six different cell sorters (Beckton Dickinson FACSAria II and FACSAria III) simultaneously. Due to the extremely long sorting times of 28 – 55 h per sample using fluorescence-based sorting, we establish a magnetic-activated cell sorting (MACS) protocol for LPC enrichment at the Department of Immunology, Tübingen, Germany.

MACS of LPCs was performed using the human CD34 MultiSort and CD38 MicroBead Kits (both Miltenyi) enabling the subsequent sorting of cells by the two markers resulting in the three cell populations $CD34^-$, $CD34^+CD38^+$, and $CD34^+CD38^-$. After sorting, cells were stained with PE/Cy7 anti-human CD38 (BioLegend), APC anti-human CD34 (BD), and V450 anti-human CD45 (BD) mAb to determine the purity. Aqua fluorescent reactive dye (Invitrogen) was used as viability marker. Analyses were performed on a FACS Canto II cytometer (BD). The immunopeptidomes of sorted cell populations were analyzed separately. For comparative profiling of LPCs and blasts, the immunopeptidomes of $CD34^-$ and $CD34^+CD38^+$ cell populations of MACS-sorted patient samples were combined and analyzed as blast samples.

Enrichment of $CD34^+$ HPCs of HVs

$CD34^+$ HPCs were magnetically enriched (CD34 MicroBead Kit, human, Miltenyi) from hematopoietic stem cell aphereses from G-CSF mobilized blood donations of HVs and patients with non-hematological malignancies (*e.g.* germ cell tumors).

Mice and xenotransplantation assays

Xenotransplantation assays were performed by Anna M. Paczulla at the Department of Biomedicine, University of Basel and University Hospital Basel, Switzerland. NOD.Cg-*Prkdc*^{scid} *IL2rg*^{tmWjl}/Sz mice (NSG, Jackson Laboratory, Bar Harbor, ME, USA) were maintained under pathogen-free conditions

according to the Swiss federal and state regulations. All animal experiments were approved by the Veterinäramt Basel-Stadt (24981). Xenotransplantation assays were performed as previously described.[40] In brief, 6 x 10^5 primary human presorted $CD34^+CD38^-$, $CD34^+CD38^+$ and $CD34^-$ AML cells were transplanted *via* intrafemoral injection into eight weeks old female NSG mice (n = 4 – 5 per group). Engraftment was monitored as previously described[40] *via* routine bone marrow punctures or assessment of peripheral blood. Engraftment was defined as ≥ 1% human leukemic cells in murine PB or BM as analyzed by multicolor flow cytometry using antibodies against human leukemic antigens. The panel includes fluorescent antibodies against human CD33, CD34, CD133, CD117, CD45 (BD Biosciences), CD14, CD13 (eBiosciences), CD3, and CD19 (BioLegend). All mice underwent final BM, PB and organ assessment by multicolor flow cytometry.

Isolation of HLA ligands

HLA class I and II molecules were isolated by standard immunoaffinity purification as described before,[41] using the pan-HLA class I-specific W6/32 mAb, the pan-HLA class II-specific Tü-39 mAb, and the HLA-DR-specific L243 mAb (all produced in-house) to extract HLA ligands.

Analysis of HLA ligands by LC-MS/MS

HLA ligand extracts were analyzed as described previously.[42] Peptides were separated by nanoflow high-performance liquid chromatography (RSLCnano, Thermo Fisher Scientific) using a 50 µm x 25 cm PepMap rapid separation liquid chromatography column (Thermo Fisher Scientific) and a gradient ranging from 2.4% to 32.0% acetonitrile over the course of 90 min. Eluting peptides were analyzed in an online-coupled LTQ Orbitrap XL or LTQ Orbitrap Fusion Lumos mass spectrometer (Thermo Fisher Scientific) equipped with a nanoelectron spray ion source using a data dependent acquisition mode employing a top five or a top speed CID fragmentation method (normalized collision energy 35%), respectively. Mass range for HLA class I peptide analysis was set to 400 – 650 m/z with charge states 2+ and 3+ selected for fragmentation. For HLA class II peptide analysis mass range was limited to 300 – 1,500 m/z for the LTQ Orbitrap XL and to 400 – 1,000 m/z for the LTQ Orbitrap Fusion Lumos with charge states 2+ to 5+ selected for fragmentation. The AML *discovery dataset* was measured on a LTQ Orbitrap Fusion Lumos, the *validation dataset*[21] was analyzed on a LTQ Orbitrap XL.

Data processing and HLA annotation

Data processing was performed as described previously.[42] In brief, the SEQUEST HT search engine (University of Washington)[43] was used to search the human proteome as comprised in the Swiss-Prot database (20,279 reviewed protein sequences, September 27th 2013) without enzymatic restriction. Precursor mass tolerance was set to 5 ppm, and fragment mass tolerance to 0.5 Da for ion trap spectra and 0.02 Da for orbitrap spectra, respectively. Oxidized methionine was allowed as a dynamic

modification. The FDR was estimated using the Percolator algorithm[44] and limited to 5% for HLA class I and 1% for HLA class II. Peptide lengths were limited to 8 – 12 amino acids for HLA class I and to 8 – 25 amino acids for HLA class II. Protein inference was disabled, allowing for multiple protein annotations of peptides. HLA class I annotation was performed using NetMHCpan 4.0[45, 46] and SYFPEITHI[47] annotating peptides with percentile rank below 2% and ≥ 60% of the maximal score, respectively. For comparative profiling peptides only presented on one sample with a PSM count ≤ 3 ("one hit wonders") were removed. HLA ligand isolation and mass spectrometry experiments of the comparative non-hematological benign database were performed by Ana Marcu.

Screening for neoepitopes

Due to the fact that no mutation data was available accept for the mutations routinely tested in the clinic (FLT3-ITD, FLT-TKD, NPM1, inv(16), t(8;21), t(15;17)) we used a non-patient-individual $_{mut}$FASTA, which includes the TOP100 recurrent AML-associated missense mutations specified in the COSMIC database (www.cancer.sanger.ac.uk)[48] supplemented with the most common NPM1 frame shift mutations (type A, B, C, D, and E)[31] as well as FLT3-ITD[49] and FLT3-TKD[50-54] mutations (Table S6). Data processing of AML immunopeptidomics data with the $_{mut}$FASTA were performed as described above. To minimize false positive identifications, we applied more stringent filter criteria with 5% FDR for HLA class I and 1% for HLA class II, XCorr ≥ 1, and ΔScore ≥ 0.2, which is a measure of the difference between the XCorr for the two best peptide sequences annotated to a distinct spectrum. After manual spectrum validation, candidate neoepitopes were produced as isotope-labeled synthetic peptides and used for spectral comparison and validation.

Amplification of peptide-specific T cells and IFNγ ELISPOT assay

PBMCs from AML patients and HVs were pulsed with 1 µg/mL (class I) or 5 µg/mL (class II) per peptide and cultured for 12 days adding 20 U/mL IL-2 (Novartis) on days 3, 5, and 7.[21, 42] Peptide-stimulated PBMCs were analyzed by ELISPOT assay on day 12.[55, 56] Spots were counted using an ImmunoSpot S5 analyzer (CTL) and T-cell responses were considered positive when > 10 spots/500,000 cells were counted and the mean spot count was at least three-fold higher than the mean spot count of the negative control according to the cancer immunoguiding program guidelines.[57]

aAPC priming of naïve CD8$^+$ T cells

Priming of peptide-specific CTLs was conducted using aAPCs as described before.[58, 59] MACS-sorted CD8$^+$ T cells were cultured with IL-2 and IL-7. Weekly stimulation with peptide-loaded aAPCs and IL-12 was performed four times.

Cytokine and tetramer staining

The frequency and functionality of peptide-specific $CD8^+$ T cells was analyzed by tetramer and ICS as described previously[56, 60]. For ICS, cells were pulsed with 10 µg/mL of individual peptide and incubated with 10 µg/mL Brefeldin A (Sigma-Aldrich) and 10 µg/mL GolgiStop (BD) for 12 – 16 h. Staining was performed using Cytofix/Cytoperm (BD), PerCP anti-human CD8, Pacific Blue anti-human TNF, FITC anti-human CD107a (BioLegend), and PE anti-human IFNγ mABs (BD). PMA and ionomycin (Sigma-Aldrich) served as positive control. Negative control peptides are listed in Table S7. The frequency of peptide-specific $CD8^+$ T cells after aAPC-based priming was determined by PE/Cy7 anti-human CD8 mAb (Biolegend) and HLA:peptide tetramer-PE staining. Tetramers of the same HLA allotype containing irrelevant control peptides were used as negative control. The priming was considered successful if the frequency of peptide-specific $CD8^+$ T cells was > 0.1% of $CD8^+$ T cells within the viable single cell population and at least three-fold higher than the frequency of peptide-specific $CD8^+$ T cells in the negative control. The same evaluation criteria were applied for ICS results. Samples were analyzed on a FACS Canto II cytometer (BD).

Cytotoxicity assay

Cytolytic capacity of peptide-specific $CD8^+$ T cells was analyzed using the flow cytometry-based VITAL assay as described before.[61, 62] Autologous $CD8^-$ PBMCs were loaded with test peptide or HLA-matched control peptide and labeled with CFSE or FarRed, respectively. Effector cells were added in the indicated effector to target ratios. Specific lysis of peptide-loaded target cells was calculated relative to control targets.

Software and statistical analysis

An in-house Python script was used for the calculation of FDRs of AML-associated peptides at different presentation frequencies.[42] Hotspot analysis (hotspot length ≥ 8 amino acids) of HLA class II ligandomes was performed using an in-house R script that maps identified peptides according to their sequence onto its source protein and calculates representation frequencies of single amino acid positions within the respective cohorts. A comparative ligandome representation matrix (“heatmap”) was constructed by grouping peptide identifications according to their corresponding source proteins or HLA ligands of the same allotype restriction and assigning binary labels for being present in a given sample or not. Columns (source proteins/HLA ligands) and rows (samples) of the binary matrix were hierarchically clustered applying “complete linkage” as clustering method and Pearson correlation as distance measure using the pheatmap R package v.1.0.10. Overlap analysis was performed using BioVenn.[63] The population coverage of HLA allotypes was calculated by the IEDB population coverage tool (www.iedb.org).[64, 65] Flow cytometric data was analyzed using FlowJo 10.0.8 (Treestar). All figures and statistical analyses were generated using GraphPad Prism 6.0 (GraphPad Software).

6.3.4. RESULTS

Leukemic progenitor cells of primary AML samples express high levels of HLA surface molecules

T-cell-based immunotherapy requires sufficient HLA surface expression on target cells, which in case of AML constitute not only AML blasts but also LPCs. Thus, as a first step we quantified HLA surface expression on $CD34^+CD38^+$ AML blasts as well as on $CD34^+CD38^-$ precursor cells using primary $CD34^+$ AML samples (n = 15, Table S8) at the time of diagnosis. HLA class I surface levels showed substantial heterogeneity with molecule counts per cell of 35,200 – 327,200 (n = 15, mean 115,300) for $CD34^+CD38^+$ blasts and 31,100 – 310,100 (n = 12, mean 99,100) for $CD34^+CD38^-$ LPCs (Figure 1A, Table S8) demonstrating that LPCs express equal amounts of HLA class I molecules compared to $CD34^+CD38^+$ blasts. HLA class II expression was slightly but not significantly lower on LPCs compared to autologous $CD34^+CD38^+$ blasts. The HLA-DR expression ranged from 4,000 – 63,500 (n = 14, mean 24,000) molecules per cell for blasts and from 1,200 – 48,500 (n = 11, mean 18,500) molecules per cell for LPCs (Figure 1B, Table S8).

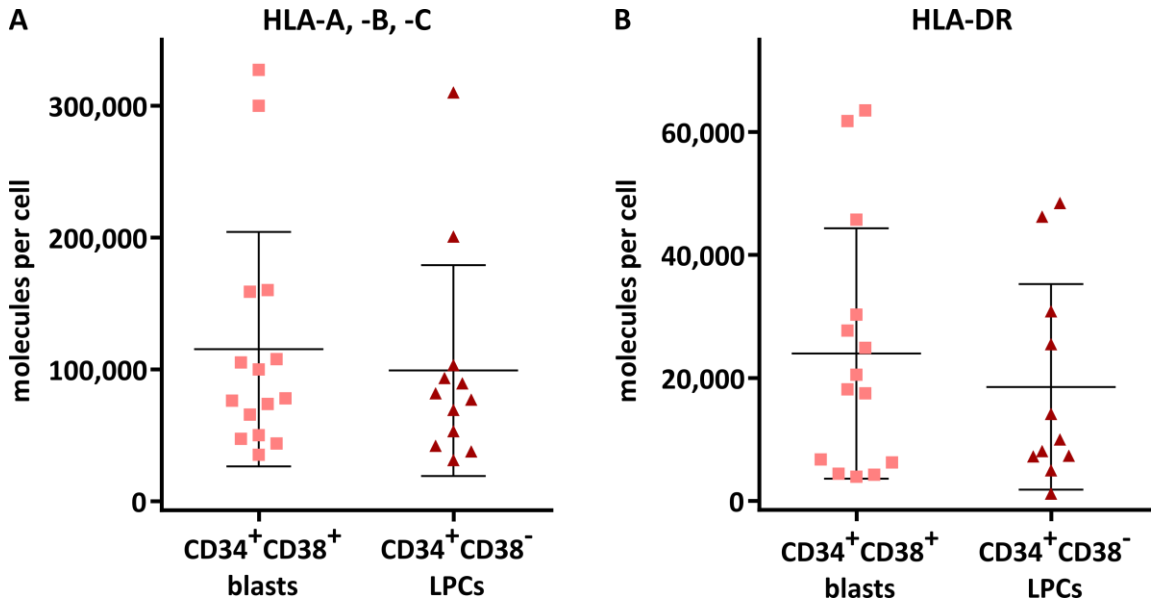

Figure 1: HLA class I and class II surface expression on primary AML blasts and autologous LPCs. (A) HLA class I and (B) HLA-DR expression was determined by flow cytometry for $CD34^+CD38^+$ AML blasts and $CD34^+CD38^-$ LPCs in $CD34^+$ AML patient samples (n = 15) at the time of diagnosis. Data points represent individual samples. Horizontal lines indicate mean values ± SD. Abbreviation: LPCs, leukemic progenitor cells.

Enrichment of $CD34^+CD38^-$ leukemic progenitor cells from primary AML samples for HLA ligandome analysis

Specific targeting of residual chemoresistant LPCs in the MRD setting by antigen-based immunotherapy approaches might allow in the future the prevention of AML disease relapses. For the identification of suitable target antigens that are presented not only on AML blasts but also on LPCs the enrichment of these cells is indispensable. Therefore, we quantified $CD34^+CD38^-$ LPC frequencies in PBMC samples of AML patients at the time of diagnosis (n = 26, mean 3.89%, range

0.00 – 40.60%, Figure 2A, Table S9) and selected suitable samples (n = 11) with a clinically determined $CD34^+$ phenotype, white blood cell counts (WBCs) ≥ 70,000/µl, and blood blast counts ≥ 50% for subsequent LPC enrichment (Figure 2B, S1-S2, Table S9). Thereby, LPC frequencies could be significantly enriched from 8.53% (range 0.02 – 40.60%) within the original PBMC fractions to 84.43% (range 40.00% – 99.70%) in the LPC_{enr} fractions (Figure 2C).

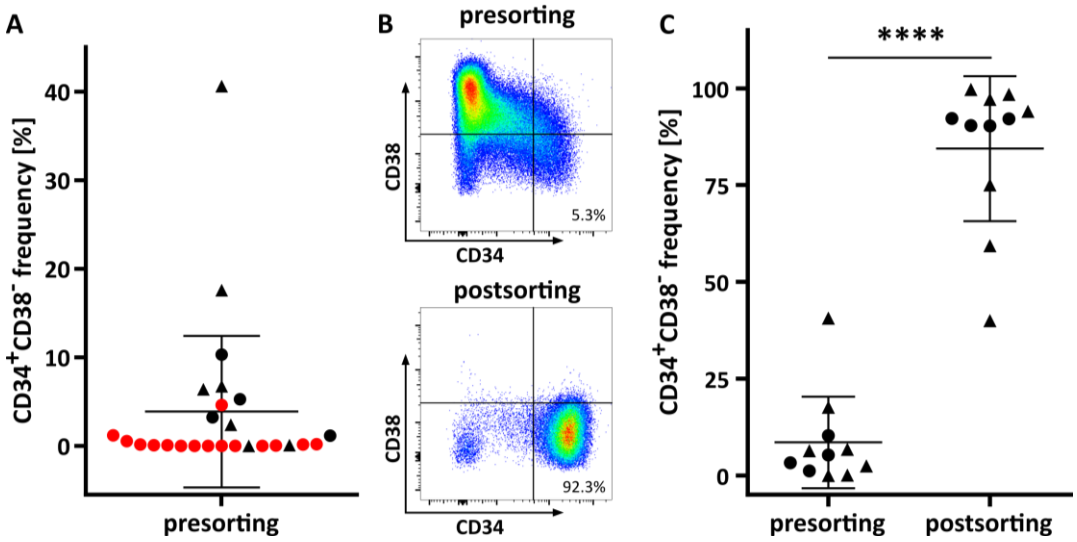

Figure 2: Enrichment of $CD34^+CD38^-$ LPCs from PBMC samples of AML patients. (A) Frequencies of $CD34^+CD38^-$ LPCs in all analyzed PBMC samples of AML patients. Samples marked in red were excluded from subsequent LPC enrichment due to insufficient LPC frequencies and PBMC counts. (B) Representative flow cytometry analysis of pre- and postenriched LPC frequencies of UPN10. (C) Frequencies of $CD34^+CD38^-$ LPCs pre- and postenrichment. Samples marked with a triangle were FACS-enriched, samples indicated by circles were MACS-enriched. Data points represent individual samples. Horizontal lines indicate mean values ± SD. Abbreviation: ****, $P < 0.0001$.

In vivo engraftment of leukemic cells in NOD/SCID/IL2Rγ^{null} mice

To prove the clonogenic potential of the enriched LPC populations, Anna M. Paczulla performed exemplary transplantation experiments of $CD34^+CD38^+$ AML blasts and enriched $CD34^+CD38^-$ LPCs of UPN01 in NOD/SCID/IL2Rγ^{null} (NSG) mice (n = 4 for $CD34^+CD38^-$ LPCs, n = 5 for $CD34^+CD38^+$ blasts) at the Lengerke Lab at the Department of Biomedicine, University of Basel and University Hospital Basel, Switzerland. Therefore, 6 x 10^5 cells of each cell population were transplanted intrafemorally into NSG mice, respectively. Infiltration of $CD33^+$ cells in the bone marrow could be detected in both groups 31 weeks after transplantation. We analyzed the leukemic burden by determination of human $CD33^+$ and $CD33^+CD117^+$ cell frequencies in the bone marrow, peripheral blood, spleen, and liver (Figure 3A,B). However, no significant differences between mice transplanted with $CD34^+CD38^+$ AML blasts or with enriched $CD34^+CD38^-$ LPCs could be detected. Furthermore, we examined the distribution of $CD34^+CD38^+$, $CD34^+CD38^-$, $CD34^-CD38^+$, and $CD34^-CD38^-$ cell populations within the $CD33^+$ cells in different murine organs (Figure 3C-F). The frequencies of the different cell populations revealed no differences between both groups.

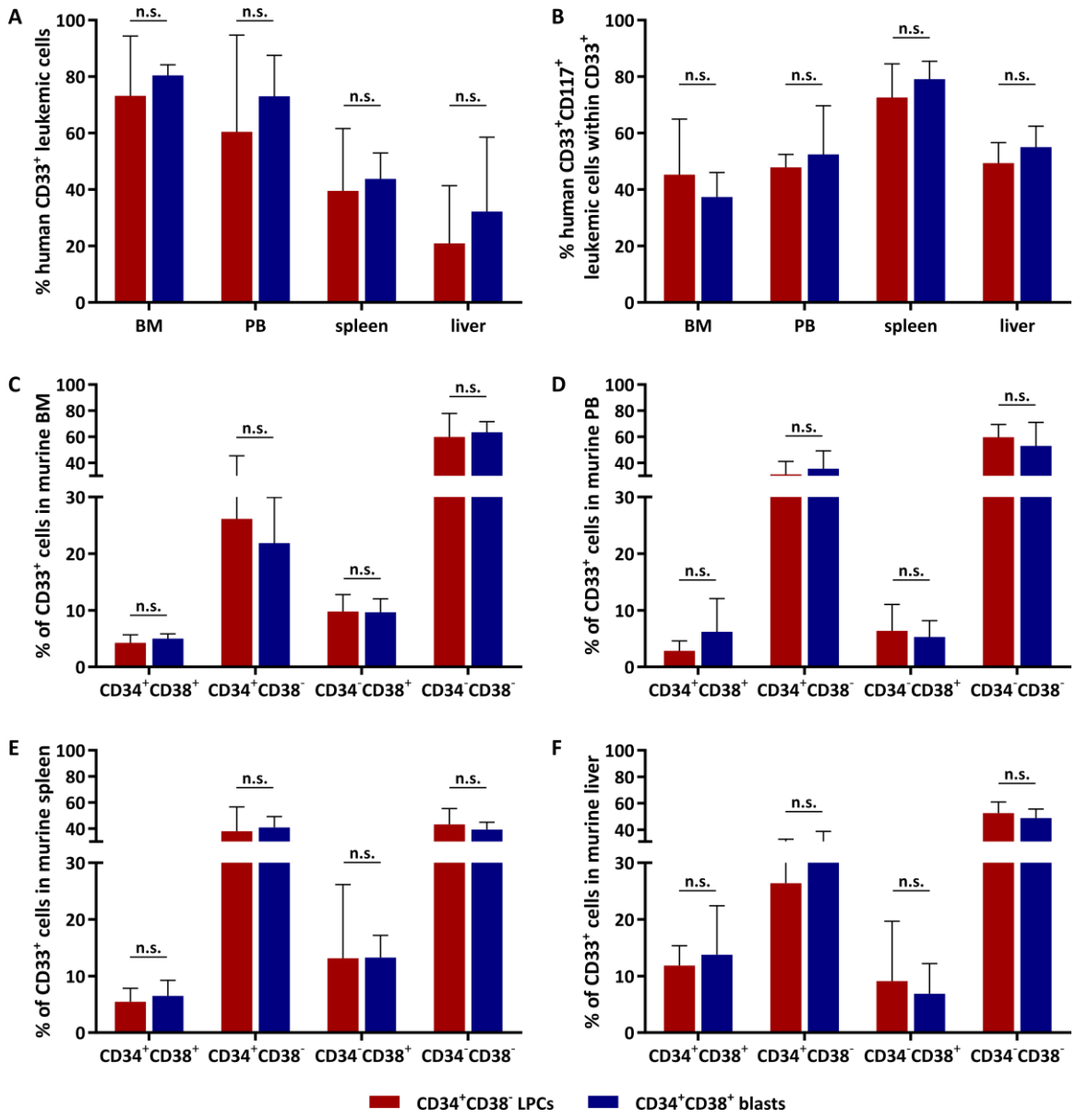

Figure 3: *In vivo* leukemic engraftment of CD34$^+$CD38$^+$ blasts and CD34$^+$CD38$^-$ LPCs in NOD/SCID/IL2Rγ^{null} mice. (A,B) Frequency of human (A) CD33$^+$ and (B) CD117$^+$ (within the CD33$^+$) leukemic cells in the bone marrow, peripheral blood, spleen, and liver of mice 31 weeks after intrafemoral transplantation of 6 x 10^5 human CD34$^+$CD38$^-$ LPCs and CD34$^+$CD38$^+$ blasts in NOD/SCID/IL2Rγ^{null} mice (n = 4 for LPCs, n = 5 for blasts), respectively. (C-F) Distribution of CD34$^+$CD38$^+$, CD34$^+$CD38$^-$, CD34$^-$CD38$^+$, and CD34$^-$CD38$^-$ cell populations within the CD33$^+$ cells in murine (C) bone marrow, (D) peripheral blood, (E) spleen, and (F) liver. Abbreviations: BM, bone marrow; PB, peripheral blood; n.s., not significant.

Establishment of a comparative dataset of HPCs from healthy individuals

For the precise identification and definition of suitable tumor-associated non-mutated antigens for T-cell-based immunotherapies, the thorough comparison of HLA ligands identified on malignant cells with the immunopeptidome of healthy cells is indispensable. Our in-house immunopeptidome database of various benign tissues contained a set of samples reflecting several different tissues and cell types (e.g. spleen, liver, brain, lymph node, PBMCs). Especially for the identification of LPC-associated antigens, the comparative profiling with HLA ligands presented on HPCs is of paramount importance. The frequency of Lin$^-$CD34$^+$ HPCs in normal PBMC samples of HVs is extremely low with a mean frequency of 0.18% (n = 10, range 0.04% – 0.28%, Figure S3) suggesting that the HLA

ligandome of these cells will be extremely underestimated in the immunopeptidome of total PBMC samples. Therefore, we enriched CD34$^+$ HPCs including all different subtypes of hematopoietic progenitors from hematopoietic stem cell aphereses of G-CSF mobilized blood of HVs or patients with non-hematological malignancies (*e.g.* germ cell tumors) for subsequent HLA ligandome analysis (n = 8, Figure 4A,B). Thereby, the frequency of CD34$^+$ HPCs could be enriched from 22.94% (range 0.88% – 50.17%) to 88.43% (range 41.70% – 99.73%). Notably, the enrichment increases all different subtypes of hematopoietic progenitors (Figure 4C) including CD34$^+$CD38$^-$CD90$^+$ hematopoietic stem cells (HSCs), CD34$^+$CD38$^-$CD90$^-$ multipotent progenitors (MPPs), CD34$^+$CD38$^+$CD117$^+$ common myeloid progenitors (CMPs), and CD34$^+$CD38$^+$CD117^{low} common lymphoid progenitors (CLPs). The major subtype within the enriched CD34$^+$ HPC fractions is represented by CMPs with a medium frequency of 79.35% (range 65.47% – 92.02%).

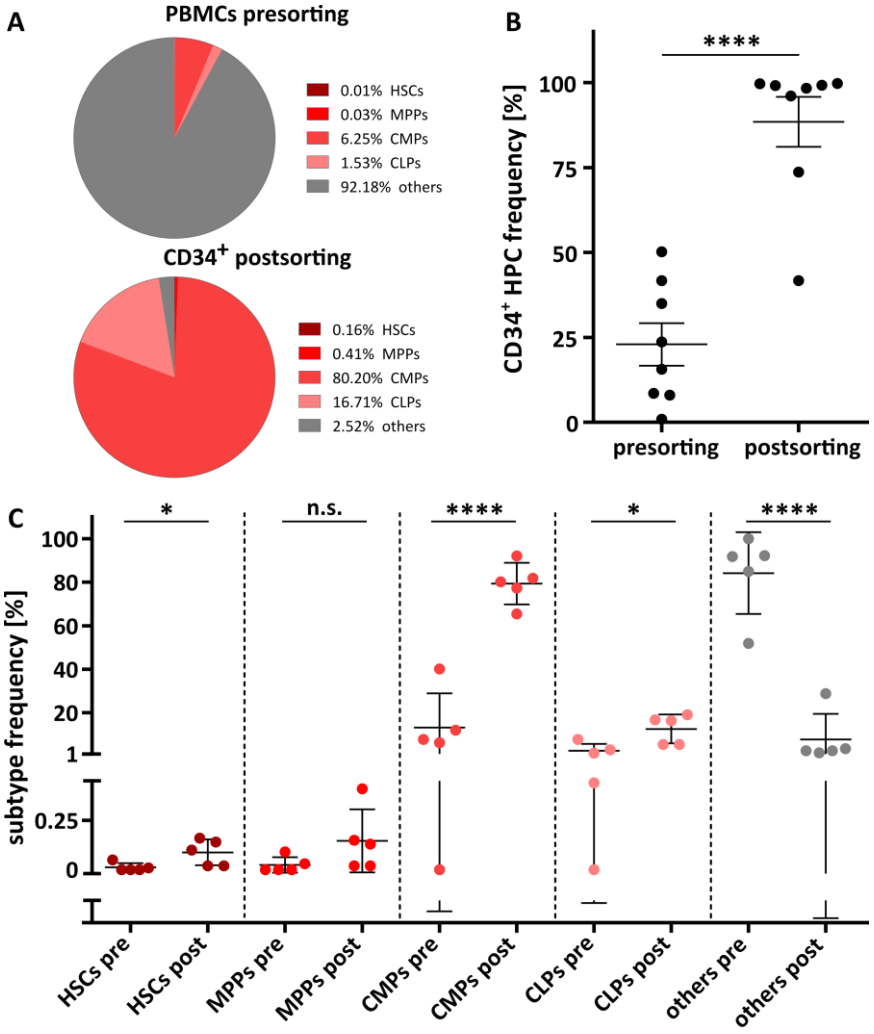

Figure 4: Enrichment of CD34$^+$ HPCs from HVs. (A) Representative pie chart depicting the frequencies of different subtypes of CD34$^+$ hematopoietic progenitors pre- and postenrichment of CD34$^+$ cells. (B) Frequencies of CD34$^+$ HPCs pre- and postenrichment (n = 8). (C) HPC subtype frequencies pre- and postenrichment. Data points represent individual samples. Horizontal lines indicate mean values ± SD. Abbreviations: PBMCs, peripheral blood mononuclear cells; HSCs, CD34$^+$CD38$^-$CD90$^+$ hematopoietic stem cells; MPPs, CD34$^+$CD38$^-$CD90$^-$ multipotent progenitors; CMPs, CD34$^+$CD38$^+$CD117$^+$ common myeloid progenitors; CLPs, CD34$^+$CD38$^+$CD117^{low} common lymphoid progenitors; others, other cell types not included in the four subtypes of hematopoietic progenitors; HPC, CD34$^+$ hematopoietic progenitor; pre, preenrichment; post, postenrichment; n.s., not significant; *, $P < 0.01$; ****, $P < 0.0001$.

Furthermore, we quantified the HLA surface expression of total CD34$^+$ HPCs as well as of the four different progenitor subtypes. HLA class I surface level staining of CD34$^+$ HPCs revealed considerable heterogeneity between different samples with molecule counts per cell of 92,300 – 295,600 (mean 184,800). For CD34$^+$CD38$^-$CD90$^+$ HSCs and CD34$^+$CD38$^-$CD90$^-$ MPPs HLA surface quantification could not be performed due to low cell numbers. The other two hematopoietic progenitor subtypes showed similar high HLA class I surface expression with mean molecule counts per cell of 243,500 for CMPs and 185,400 for CLPs (Figure 5A). In comparison, all HPC subtypes exhibited considerably lower HLA class II expression. HLA-DR expression ranged from 6,700 to 97,500 (mean 43,000) for the entirety of CD34$^+$ HPCs. The HLA-DR surface expression on CMPs and CLPs was determined to 53,100 and 37,800 mean molecule counts per cell, respectively (Figure 5B).

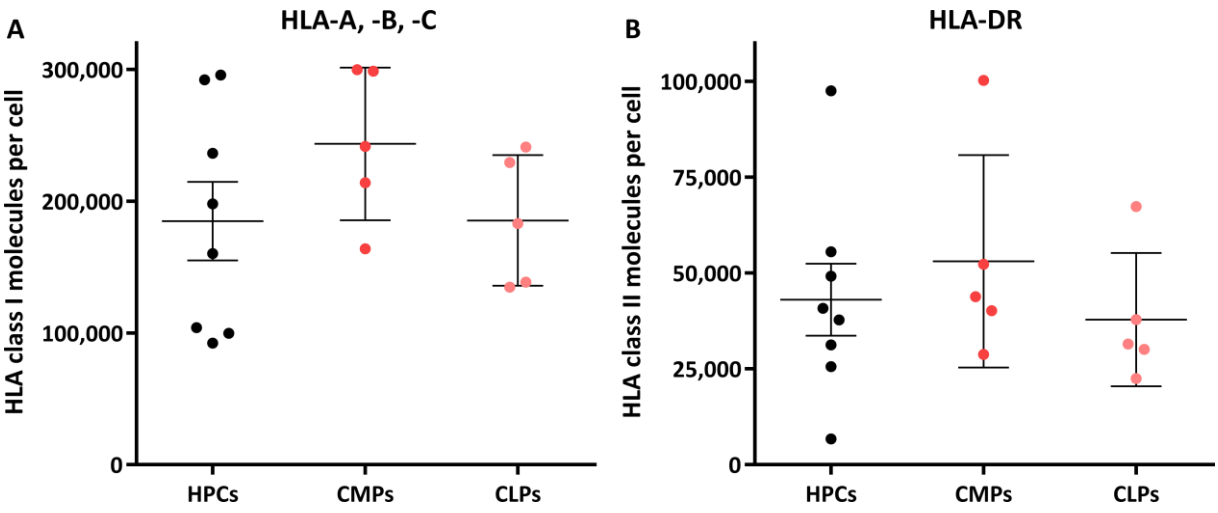

Figure 5: HLA surface expression of CD34$^+$ HPCs and HPC subtypes of HVs. (A) HLA class I and (B) HLA-DR expression was determined by flow cytometry for CD34$^+$ HPCs (n = 8), CD34$^+$CD38$^+$CD117$^+$ CMPs (n = 5), and CD34$^+$CD38$^+$CD117^{low} CLPs (n = 5). For CD34$^+$CD38$^-$CD90$^+$ HSCs and CD34$^+$CD38$^-$CD90$^-$ MPPs no informative HLA surface quantification could be performed due to too low cell numbers. Data points represent individual samples. Horizontal lines indicate mean values ± SD. Abbreviations: HPCs, CD34$^+$ hematopoietic progenitor cells; HSCs, CD34$^+$CD38$^-$CD90$^+$ hematopoietic stem cells; MPPs, CD34$^+$CD38$^-$CD90$^-$ multipotent progenitors; CMPs, CD34$^+$CD38$^+$CD117$^+$ common myeloid progenitors; CLPs, CD34$^+$CD38$^+$CD117^{low} common lymphoid progenitors.

Setup of a comparative dataset of healthy PBMCs of AML patients in molecular remission

Besides the immunopeptidome database of different cell types and tissues from healthy donors, we additionally set up a further comparative dataset comprising PBMC samples of AML patients that received MRD-negative MR without allogenic stem cell transplantation (AML_{MR}, n = 8, Table S3). For all patients in this cohort the identification of MRD was molecularly determined using different MRD markers such as CBFB/MYH11, NPM1, or RUNX1/RUNX1T1 mutations. Analyses of the HLA class I ligandomes of these samples resulted in a total of 7,465 unique HLA class I ligands representing 4,318 different source proteins. The number of identified HLA ligands per donor ranged from 472 to 2,270 (mean 1,229, Figure 6).

Furthermore, we mapped the HLA class II ligandomes and were able to identify a total of 6,553 unique HLA class II peptides from 1,364 different source proteins with peptide identifications ranging

from 858 to 1,770 (mean 1,302) per sample (Figure 6). We used this dataset as an additional comparative benign cohort to validate our AML-associated class I and class II targets.

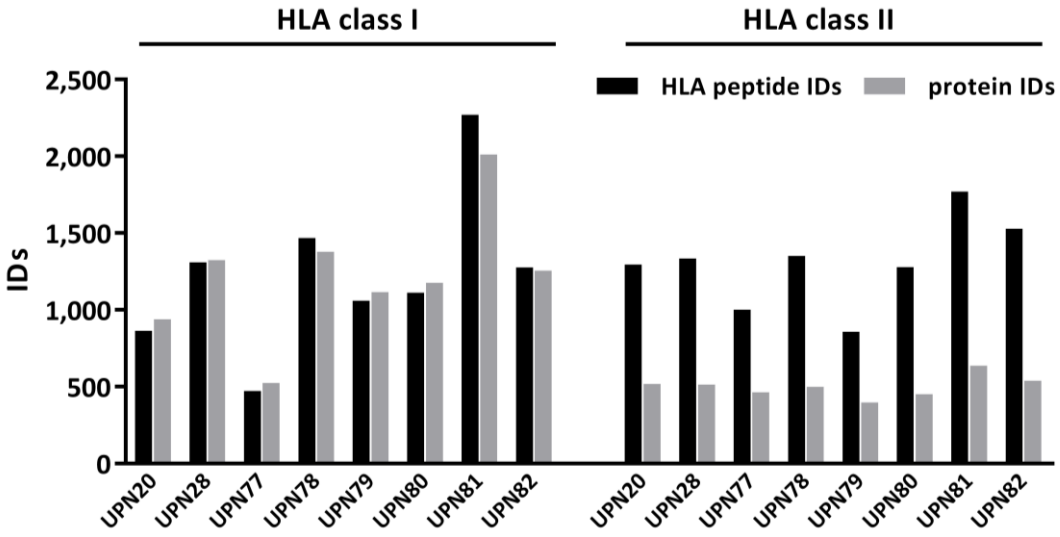

Figure 6: HLA class I and II peptide and source protein yields of PBMC samples from AML_{MR} patients. HLA class I ligand or class II peptide and respective source protein yields of PBMC samples from AML_{MR} patients (n = 8) as identified by mass spectrometry are indicated in black and grey bars, respectively. Abbreviations: IDs, identifications; UPN, uniform patient number.

Establishment of a novel extended AML patient cohort for in depth immunopeptidome analysis

The tremendous technical progress and various improvements in the area of mass spectrometry in the last decades, especially with the development of orbitrap mass analyzers as well as hybrid and tribrid instruments combining the advantage and strengths of different mass analyzers, have revolutionized the field of mass spectrometry.[66-68] Thus, we are now able to analyze the immunopeptidome of primary patient samples in more depth than still a few years ago. In previous work of our group,[21] we analyzed the immunopeptidomic landscape of 15 primary AML patient samples using an LTQ Orbitrap XL mass spectrometer and identified a panel of AML-associated $CD4^+$ and $CD8^+$ T-cell epitopes by comparative profiling with 30 PBMC and 5 BMNC samples from healthy donors. In recent years we established a novel and considerably bigger AML patient cohort (n = 52), in the following referred to as the *discovery dataset* (Table 1 and S1), for which we analyzed the immunopeptidome on an Orbitrap Fusion Lumos Tribrid mass spectrometer allowing a deeper insight into the entirety of presented HLA ligands compared to the LTQ Orbitrap XL dataset (n = 15 published samples, n = 9 additional samples), in the following termed *validation dataset* (Table 1 and S2). For an equivalent comparison of the two datasets the *validation dataset* was reprocessed using the search engine SEQUEST HT as utilized for the *discovery dataset*. Furthermore, in the last years our in-house comparative benign immunopeptidomics dataset was extremely increased by means of sample quantity and coverage of different cell types and tissues.

Table 1: Patient characteristics overview

Characteristics	*Discovery cohort*	*Validation cohort*	Total
Patients	52	24	76
# of HLA class I ligandomes	47	18	65
# of HLA class II ligandomes	47	20	67
Age [yr]			
Median	60	64	63
Range	21 - 89	22 - 87	21 - 89
Sex [no. (%)]			
Male	21 (40.4)	12 (50.0)	33 (43.4)
Female	24 (46.2)	12 (50.0)	36 (47.4)
n.a.	7 (13.5)	0 (0.0)	7 (9.2)
WHO classification [no. (%)]			
AML, NOS	9 (17.3)	2 (8.3)	11 (14.5)
Recurrent genetic abnormalities	27 (51.9)	14 (58.3)	41 (53.9)
Therapy-related	1 (1.9)	0 (0.0)	1 (1.3)
Myelodysplasia-related changes	7 (13.5)	6 (25.0)	13 (17.1)
n.a.	8 (15.4)	2 (8.3)	10 (13.2)
FAB classification [no. (%)]			
M0	1 (1.9)	1 (4.2)	2 (2.6)
M1	7 (13.5)	4 (16.7)	11 (14.5)
M1/M2	1 (1.9)	0 (0.0)	1 (1.3)
M2	5 (9.6)	8 (33.3)	13 (17.1)
M3	0 (0.0)	0 (0.0)	0 (0.0)
M4	6 (11.5)	4 (16.7)	10 (13.2)
M4/5	2 (3.8)	1 (4.2)	3 (3.9)
M5	10 (19.2)	5 (20.8)	15 (19.7)
M6	0 (0.0)	0 (0.0)	0 (0.0)
M7	0 (0.0)	0 (0.0)	0 (0.0)
n.a.	20 (38.5)	1 (4.2)	21 (27.6)

Characteristics	*Discovery cohort*	*Validation cohort*	Total
WBC [10^3/µl]			
Median	83	70	79
Range	3 - 500	11 - 96	3 - 500
Blasts [%]			
Median	83	84	83
Range	31 - 100	27 - 96	27 - 100
Previous therapy [no. (%)]			
Cytarabine	4 (7.7)	0 (0.0)	4 (5.3)
Anthracycline-based CT	1 (1.9)	0 (0.0)	1 (1.3)
Demethylating agents	3 (5.8)	2 (8.3)	5 (6.6)
Hydroxyurea	3 (5.8)	0 (0.0)	3 (3.9)
Combinations	1 (1.9)	0 (0.0)	1 (1.3)
No therapy	28 (53.8)	22 (91.7)	50 (65.8)
n.a.	12 (23.1)	0 (0.0)	12 (15.8)
NPM1 mutation [no. (%)]			
NPM1 mutated	19 (36.5)	9 (37.5)	28 (36.8)
type A	17 (32.7)	8 (33.3)	25 (32.9)
type B	0 (0.0)	1 (4.2)	1 (1.3)
type D	1 (1.9)	0 (0.0)	1 (1.3)
type n.a.	1 (1.9)	0 (0.0)	1 (1.3)
NPM1 unmutated	26 (50.0)	13 (54.2)	39 (51.3)
n.a.	7 (13.5)	2 (8.3)	9 (11.8)
FLT3 mutation [no. (%)]			
FLT3 mutated	14 (26.9)	14 (58.3)	28 (36.8)
FLT3-TKD	1 (1.9)	1 (4.2)	2 (2.6)
FLT3-ITD	13 (25.0)	13 (54.2)	26 (34.2)
FLT3 unmutated	28 (53.8)	8 (33.3)	36 (47.4)
n.a.	10 (19.2)	2 (8.3)	12 (15.8)

Abbreviations: yr, years; no., numbers; n.a., not available; WHO, World Health Organization; NOS, not otherwise specified; FAB, French-American-British; WBC, white blood cell count; CT, chemotherapy; TKD, tyrosine kinase domain; ITD, internal tandem duplication.

Mapping the HLA class I ligandomes of the novel AML patient samples (*discovery dataset*, n = 47) we were able to identify a total of 72,042 unique HLA class I ligands representing 10,906 different source proteins, obtaining 97% of the estimated maximal attainable coverage in HLA ligand source proteins (Figure S4A). The number of identified HLA ligands per patient ranged from 542 to 11,240 (mean 3,592, Figure 7A). In comparison, the reprocessing of the published *validation dataset* (n = 18) revealed only a total of 13,366 different HLA class I ligands from 6,008 unique source proteins, achieving solely 81% of maximum attainable coverage (Figure S4B). Thereby, HLA class I ligand numbers ranged from 764 to 2,578 (mean 1,189) per patient (Figure 7B). Overlap analysis of the two datasets revealed that the novel *discovery dataset* enables the identification of 61,226 novel HLA class I ligands and of 5,210 novel source proteins. Solely, 15% (10,816/72,042) of the HLA ligands within the AML *discovery dataset* were already identified before with the *validation dataset* (Figure 7C). 19% (2,550/13,366) of HLA class I ligands identified within the *validation dataset* are not

represented within the *discovery dataset*. However, nearly all of these ligands are either identified on benign samples or were identified only on one single AML sample.

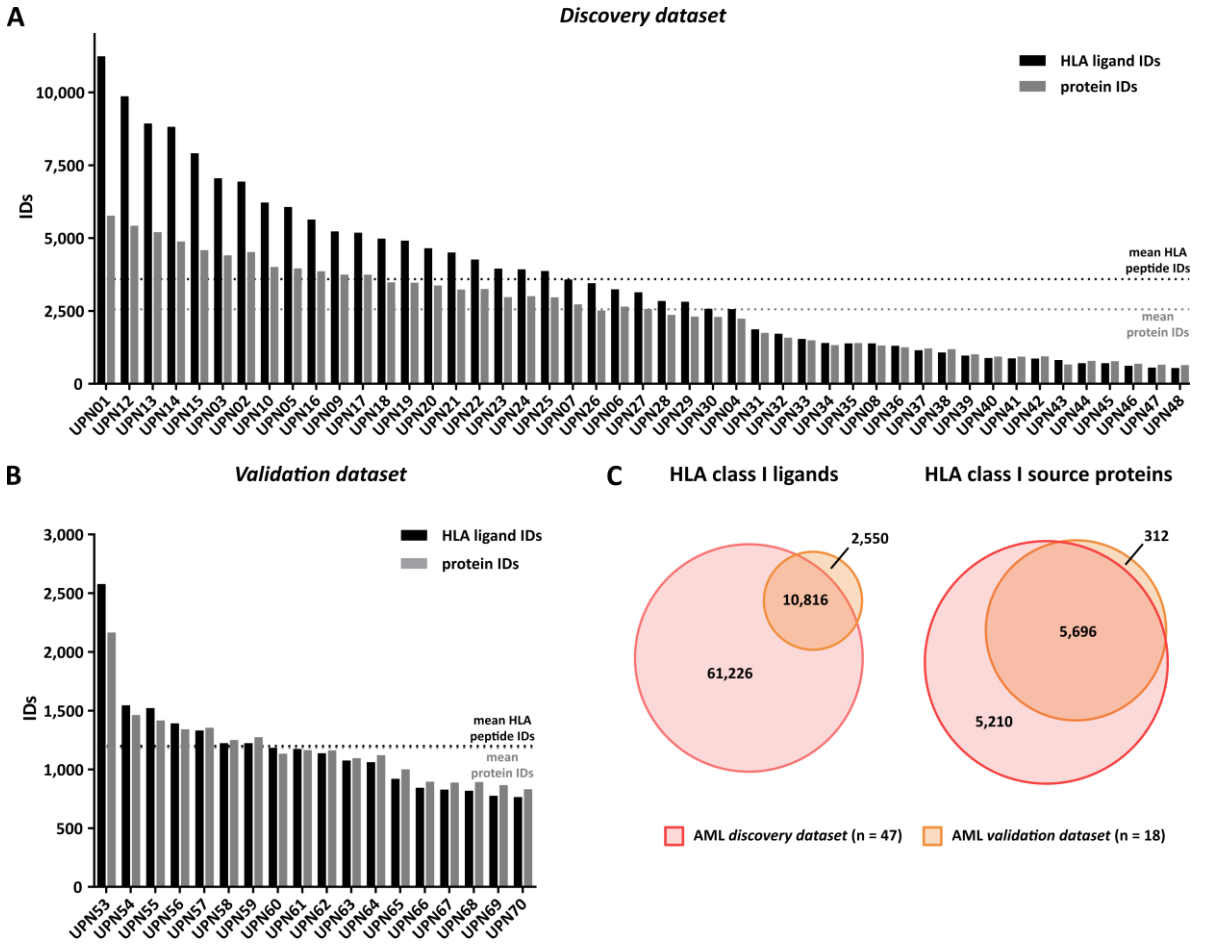

Figure 7: HLA class I ligand and source protein yields of AML *discovery* and *validation datasets*. (A,B) HLA class I ligand and respective source protein yields isolated from primary AML samples within the (A) *discovery dataset* (n = 47) analyzed on an Orbitrap Fusion Lumos Tribrid mass spectrometer and the (B) *validation dataset* (n = 18) investigated on a LTQ Orbitrap XL mass spectrometer. (C) Overlap analyses of HLA class I ligand (left) and source protein (right) identifications of AML *discovery* and AML *validation* samples. Abbreviations: IDs, identifications; UPN, uniform patient number.

The *discovery dataset* included a total of 47 different HLA class I allotypes, the most frequent being HLA-C*07 (n = 26), -A*02 (n = 23), -A*01 (n = 14), -C*03 (n = 14), -B*44 (n = 13), -B*07 (n = 12), -B*08 (n = 11), and -A*24 (n = 10). The *validation dataset* covered 34 different HLA class I allotypes (Figure S5A). Hence, 96.5% and 86.0% of the individuals of the world population[65, 66] carry at least three HLA class I allotypes represented in the *discovery* and the *validation dataset*, respectively (Figure S6A,B).

The analysis of HLA class II ligandomes revealed for the AML *discovery dataset* (n = 47) a total of 61,205 unique HLA class II peptides representing 5,922 different source proteins, obtaining 85% of the estimated maximal attainable coverage in HLA peptide source proteins (Figure S4C). The number of identified HLA peptides per sample ranged from 590 to 10,733 (mean 2,835, Figure 8A). In contrast, in the reprocessing analysis of the already published *validation dataset* (n = 20) we only identified a total of 6,004 unique HLA class II peptides from 1,652 source proteins, achieving 74% of

maximal attainable coverage (Figure S4D). The number of peptides per patient was considerably lower with 150 to 875 identifications per sample (mean 477, Figure 8B). Overlap analysis of the two datasets exhibited that the novel *discovery dataset* allows the identification of 57,099 novel HLA class II peptides and of 4,486 novel source proteins. Solely, 7% (4,106/61,205) of the HLA class II peptides within the AML *discovery dataset* were already identified before with the *validation dataset* (Figure 8C).

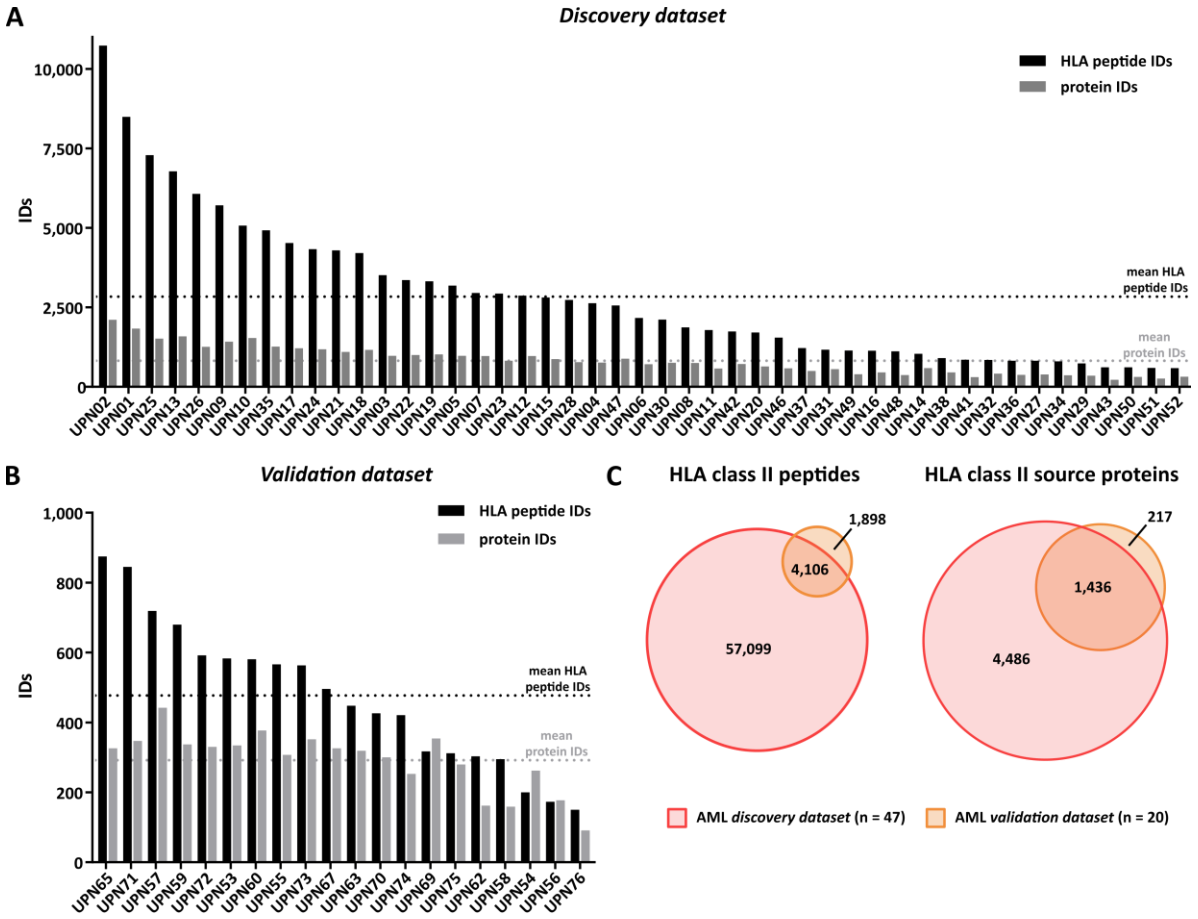

Figure 8: HLA class II peptide and source protein yields of AML *discovery* and *validation datasets*. (A, B) HLA class II peptide and respective source protein yields of AML samples of the (A) *discovery dataset* (n = 47) analyzed on the Orbitrap Fusion Lumos Tribrid mass spectrometer and the (B) *validation dataset* (n = 20) investigated on the LTQ Orbitrap XL Hybrid mass spectrometer. (C) Overlap analyses of HLA class II peptides (left) and source protein (right) identifications of AML *discovery* and AML *validation* samples. Abbreviations: IDs, identifications; UPN, uniform patient number.

These comparative analyses clearly demonstrated the substantial differences between the AML *discovery* and *validation dataset* not only in terms of cohort size but especially pinpoint on the impact of state-of-the-art mass spectrometers for immunopeptidomics analysis of primary patient samples. This clearly highlights the requirement of continuous expansion of tumor-derived immunopeptidomics databases for the definition of suitable targets for T-cell-based immunotherapy approaches.

HLA class I ligandome profiling identified novel naturally presented, AML- and LPC-associated HLA ligands in primary AML patient samples

For the definition of AML-associated HLA class I-presented antigens we performed comparative HLA ligandome profiling of the AML *discovery dataset* (n = 47) with a huge benign tissue immunopeptidomics database (n = 332) comprising different hematological benign cell types and tissues (n = 130), including PBMCs, granulocytes, $CD19^+$ B cells, bone marrow, and $CD34^+$ HPCs, as well as several non-hematological benign tissues (n = 202) such as spleen, liver, heart, skin, and others. For comparative profiling we excluded peptides that were only presented on one sample with a PSM count ≤ 3 ("one hit wonders"). The benign tissue database included 72,129 unique HLA class I ligands representing 13,179 different source proteins. 52 different HLA class I allotypes were covered by the benign cohort and matched 93% of HLA-A, 100% of HLA-B, and 92% of HLA-C allotypes within the AML *discovery cohort* (Figure S5B). Overlap analysis revealed 13,019 HLA class I ligands and 498 source proteins to be presented exclusively on AML samples (Figure 9A) and never be identified on any hematological or non-hematological benign tissue. For the selection of broadly applicable, AML-associated antigens, we not only focused on AML-exclusivity but also on antigens that exhibit high representation frequencies within the AML cohort (at least 20%). Without regard to the different HLA allotypes of the samples, we identified one HLA class I ligand (RFPPTPPLF, $BC11A_{258-266}$) with a representation frequency ≥ 20% (Figure 9B) fulfilling the target-definition FDR of < 1% (Figure S7A). This peptide could be identified with such a high representation frequency over the total cohort due to its presentation on different HLA allotypes (HLA-A*23, -A*24, -A*32, -C*04, -C*07, -C*08, -C*14). For the identification of AML-associated targets with allotype-specific higher frequencies, we performed in a next step HLA allotype-specific immunopeptidome profiling. With a target-FDR of < 5% (< 1%) we were able to identify 48 (12) HLA-A*01, 28 (3) HLA-A*02, 187 (27) HLA-B*07, 161 (161) HLA-B*08, and 11 (0) HLA-C*07-restricted ligands with representation frequencies of ≥ 29% (≥ 36%), ≥ 22% (≥ 31%), ≥ 25% (≥ 42%), ≥ 27% (≥ 27%), and ≥ 23% (≥ 23%) that were not presented on any HLA-matched or HLA-unmatched benign samples (Figure 9C, S7B-F, S8 and Table S10). To further validate these AML-associated targets we compared them with the additional established AML_{MR} dataset (n = 8) leading to the rejection of 2/436 (0.46%) targets. Furthermore, seven HLA ligands were identified as targets presented on several different HLA allotypes. Thus, 427 unique HLA class I-restricted ligands were identified as high frequent AML-exclusive targets. Of these 427 targets 46 could also be identified in the *validation dataset*.

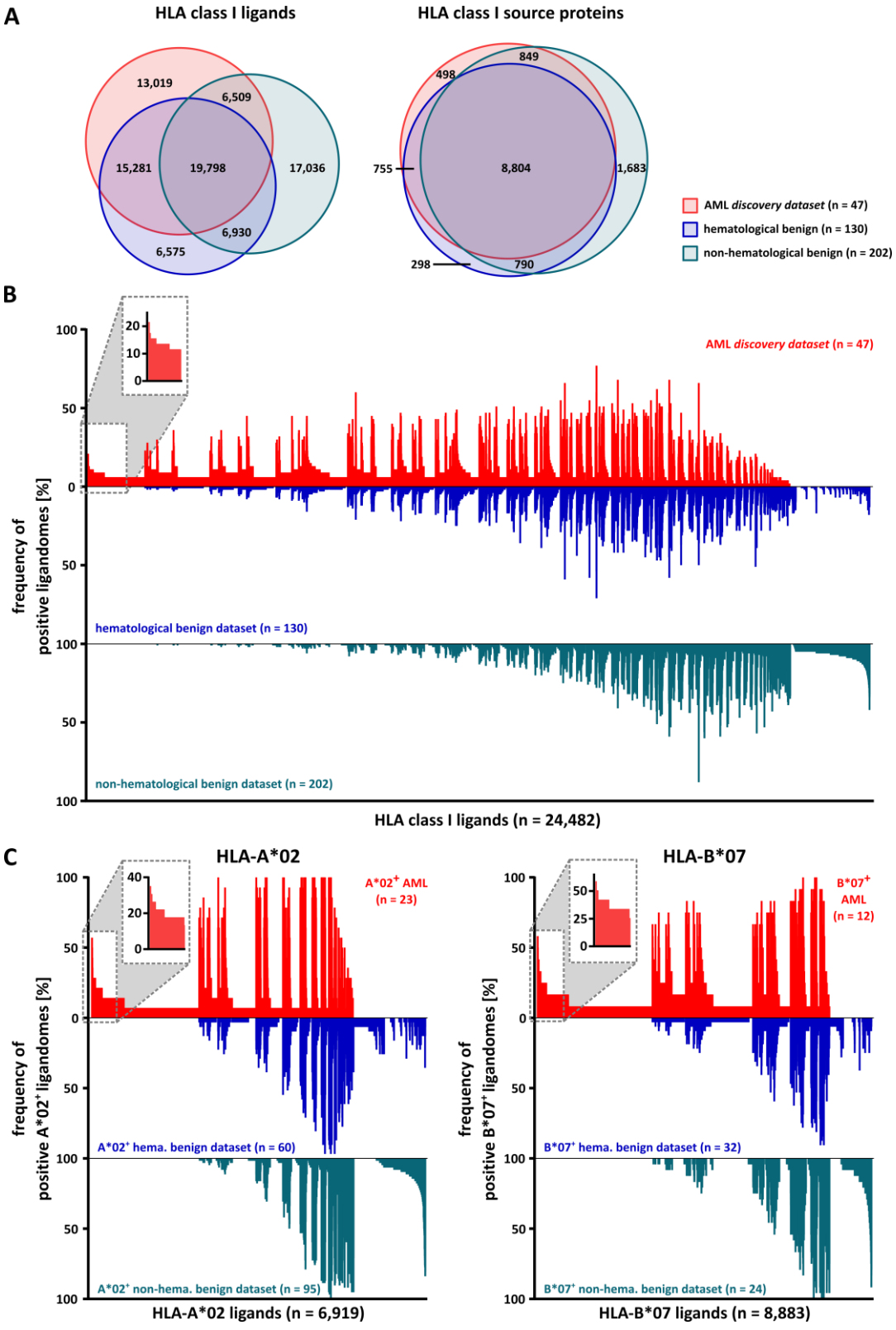

Figure 9: Comparative HLA class I ligandome profiling and identification of AML-associated antigens. (A) Overlap analysis of HLA class I ligand and source protein identifications of primary AML samples (*discovery dataset*, n = 47) and hematological (n = 130) and non-hematological benign samples (n = 202). (B) Comparative profiling of HLA class I ligands based on the frequency of HLA-restricted presentation in AML and benign ligandomes. Frequencies of positive immunopeptidomes for the respective HLA ligands (x-axis) are indicated on the y-axis. To allow for better readability, HLA ligands identified on <5% of the samples within the respective cohort were not depicted in this plot. The box on the left and its magnification highlight the subset of AML-associated antigens showing AML-exclusive, highly frequent presentation. (C) Representative examples of allotype-specific comparative profiling of HLA-A*02 and HLA-B*07 positive samples as described above. Abbreviation: hema., hematological.

For the identification of suitable antigens to target not only AML blasts but especially LPCs, we performed mass spectrometry-based class I immunopeptidome characterization of our cohort of LPC_{enr} and LPC-depleted patient samples (n = 10). Thereby, we were able to identify a total of 35,356 unique HLA class I ligands from 8,751 different source proteins with 16,342 different HLA ligands identified on LPC_{enr} samples and 32,961 on LPC-depleted blasts samples. The number of identified HLA ligands per sample ranged from 127 to 7,603 (mean 2,077) for LPC_{enr} samples and from 1,151 to 10,489 (mean 4,964) for autologous blast samples (Figure 10, Table S11). The cohort of LPC_{enr} samples (n = 10) included a total of 28 different HLA class I allotypes, the most frequent being HLA-B*44 (n = 6), -C*07 (n = 6), -A*01 (n = 4), -B*08 (n = 4), -A*02 (n = 3), and -A*23 (n = 3).

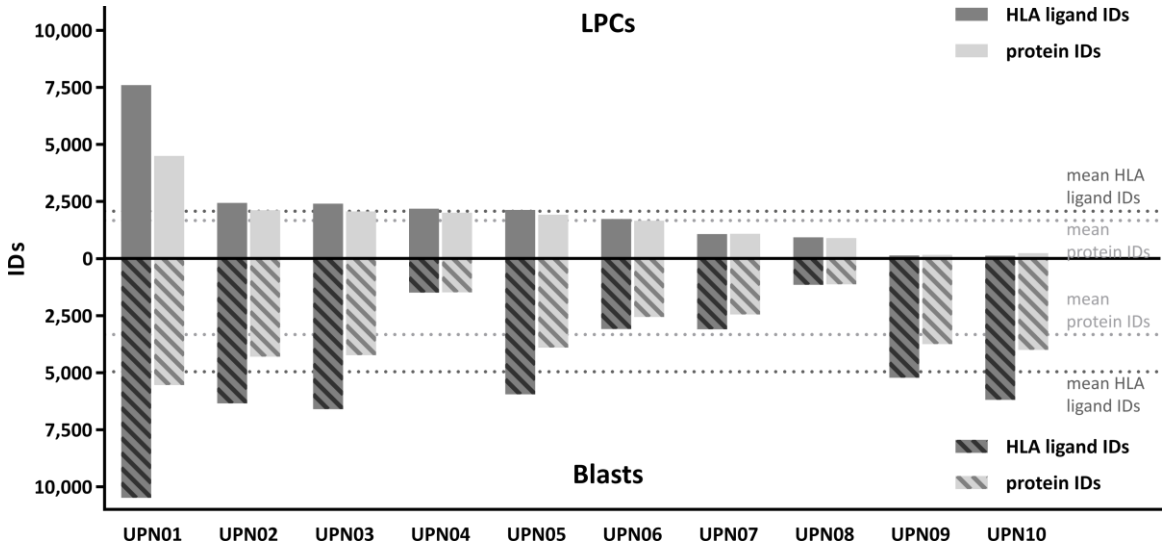

Figure 10: HLA class I ligand and source protein identifications of LPC_{enr} patient samples. HLA class I ligand and source protein identifications of LPC_{enr} and autologous LPC-depleted blast samples. Abbreviations: IDs, identifications; LPCs, leukemic progenitor cells; UPN, uniform patient number.

To identify AML-associated antigens that are LPC-exclusive or presented on both AML blasts and precursors we performed comparative profiling of immunopeptidomes of LPCs with the AML *discovery dataset* comprising the LPC-depleted blast samples and non-sorted AML samples and our benign database. First, overlap analysis revealed 115 HLA class I ligands to be exclusively presented on LPCs (Figure 11A). Due to the small cohort size of LPC_{enr} samples and the distinct HLA allotypes of the samples, these 115 LPC-exclusive peptides did not contain any high frequent represented peptides. Solely, 2/115 HLA ligands were presented on at least two samples, respectively (Figure 11B). These peptides are the HLA-A*01-restricted ligand DIWPNPLQY and the HLA-B*14- and C*07-restricted ligand SRVFIGNL. Nevertheless, the most interesting antigens are those which are presented on both, AML blasts and progenitors. Overlap analysis revealed 2,322 different HLA ligands to be such LPC-associated AML antigens (Figure 11A). Notably, only 89/2,322 could be identified on at least two samples (2/10, 20%). All the others were identified only on one LPC_{enr} sample (Figure 11B) even though the LPC_{enr} cohort included several samples that share distinct HLA allotypes.

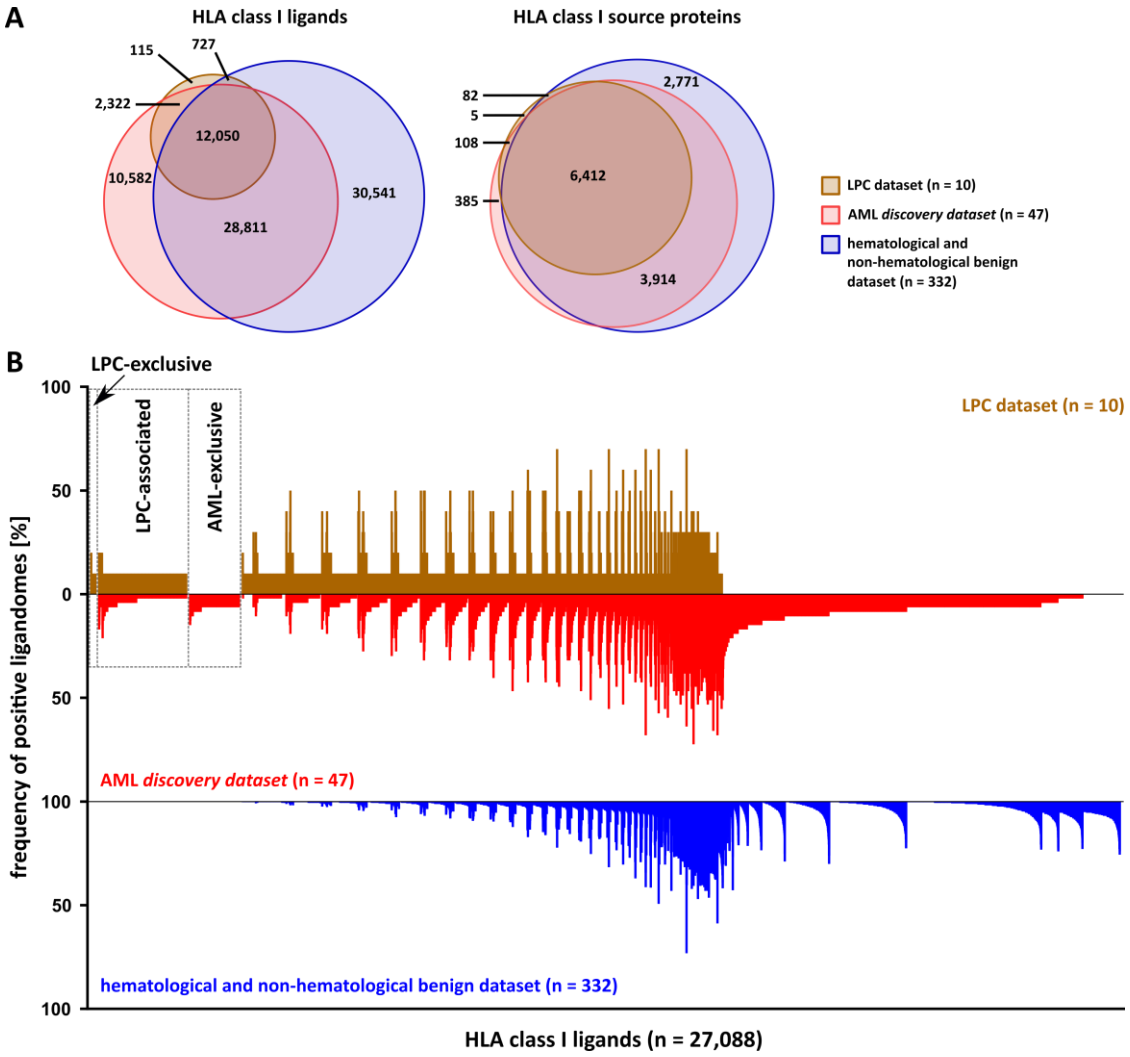

Figure 11: Comparative profiling of HLA class I ligandomes of LPC_{enr} patient samples. Comparative profiling of LPC_{enr} samples with the AML *discovery dataset* comprising the LPC-depleted blast samples as well as unsorted AML samples and the hematological and non-hematological benign dataset. (A) Overlap analysis of HLA class I ligand and source protein identifications of primary LPC_{enr} samples (n = 10), AML samples (*discovery dataset*, n = 47) and hematological (n = 130) and non-hematological benign samples (n = 202). (B) Comparative profiling of HLA class I ligands based on the frequency of HLA-restricted presentation in LPC_{enr}, AML and benign ligandomes. Frequencies of positive immunopeptidomes for the respective HLA ligands (x-axis) are indicated on the y-axis. To allow for better readability, HLA ligands identified on <5% of the samples within the respective cohort were not depicted in this plot. The boxes on the left highlight the subset of LPC-exclusive antigens, LPC-associated antigens showing presentation on both LPCs and AML blasts, and AML-exclusive antigens. Abbreviation: LPCs, leukemic progenitor cells.

For immunological characterization, we screened the novel defined AML-associated targets (Table S10) for presentation on LPCs to define rejection antigens that induce AML- and LPC-specific T-cell responses. Thus, we selected a panel of 15 LPC-associated AML target antigens, including three HLA-A*01, -A*02, -B*07, -B*08, -C*07-restricted ligands, respectively. Prior to immunological experiments those HLA peptide identifications were validated with isotope-labeled synthetic peptides (Figure S9).

HLA class II ligandome analysis delineated novel AML- and LPC-associated antigens

For clinical effective T-cell-based immunotherapy approaches the additional activation of $CD4^+$ T cells is indispensable.[69-72] Therefore, we aim to identify additional AML- and LPC-associated HLA class II-presented antigens by comparative profiling of the AML *discovery dataset* (n = 47) with our huge benign ligandome database (n = 312) comprising different hematological benign cell types and tissues (n = 89), including PBMCs, granulocytes, $CD19^+$ B cells, bone marrow, and $CD34^+$ HPCs, as well as non-hematological benign tissue samples (n = 223). This benign tissue database contained 110,255 unique HLA class II peptides from 7,624 different source proteins. Comparative profiling of HLA class II immunopeptidomics data was performed using our established previously published HLA class II ligandome profiling platform to identify peptide targets, protein targets, and hotspot targets.[73] First, overlap analysis revealed 10,931 HLA class II peptides and 311 source proteins to be presented exclusively on AML samples (Figure 12A). Of those, five (45) peptides were identified with a representation frequency ≥ 20% (≥ 15%) based on a target-FDR < 1%. However, 4/5 (40/45) peptide targets showed length variants (> 50% overlap) presented on benign samples and were therefore disqualified as suitable target antigens yielding finally five HLA class II AML-associated peptide targets with a representation frequency ≥ 15% (Figure 12B and S10A, Table S12). Additional ligandome profiling was conducted on HLA class II source protein level to define AML-associated protein targets. Based on a target-FDR < 1%, we identified two source proteins with a frequency ≥ 15% representing nine unique HLA class II peptides (Figure 12C and S10B, Table S12). As a third group of highly interesting HLA class II-presented antigens, we identified hotspot targets by peptide clustering. Thereby, we were able to validate the previously identified peptide targets and delineate an additional panel of five hotspots with representation frequencies ≥ 15% in five different source proteins representing 20 unique HLA class II peptides (Figure 13 and S11, Table S12). In total, we were able to define a set of 34 unique AML-associated HLA class II peptides derived from 11 different source proteins with our innovative HLA class II ligandome profiling platform (Table S12).

For the selection of effective rejection antigens directing the anti-leukemia T-cell response not only against AML blasts but especially against AML progenitor cells, we performed mass spectrometry-based immunopeptidomics on our LPC-enriched samples (n = 11). We identified a total of 30,907 HLA class II peptides (16,638 on LPCs, 25,128 on autologous blasts). The number of identified HLA peptides per sample ranged from 450 to 6,218 (mean 2,018) for LPC_{enr} samples and from 468 to 10,217 (mean 3,790) for blast samples (Figure 14, Table S11). For the identification of LPC-exclusive and LPC-associated antigens we performed comparative profiling (excluding “one hit wonders”) of immunopeptidomes of LPC_{enr} samples with the AML *discovery dataset* comprising the LPC-depleted blast samples and non-sorted AML samples and our benign database.

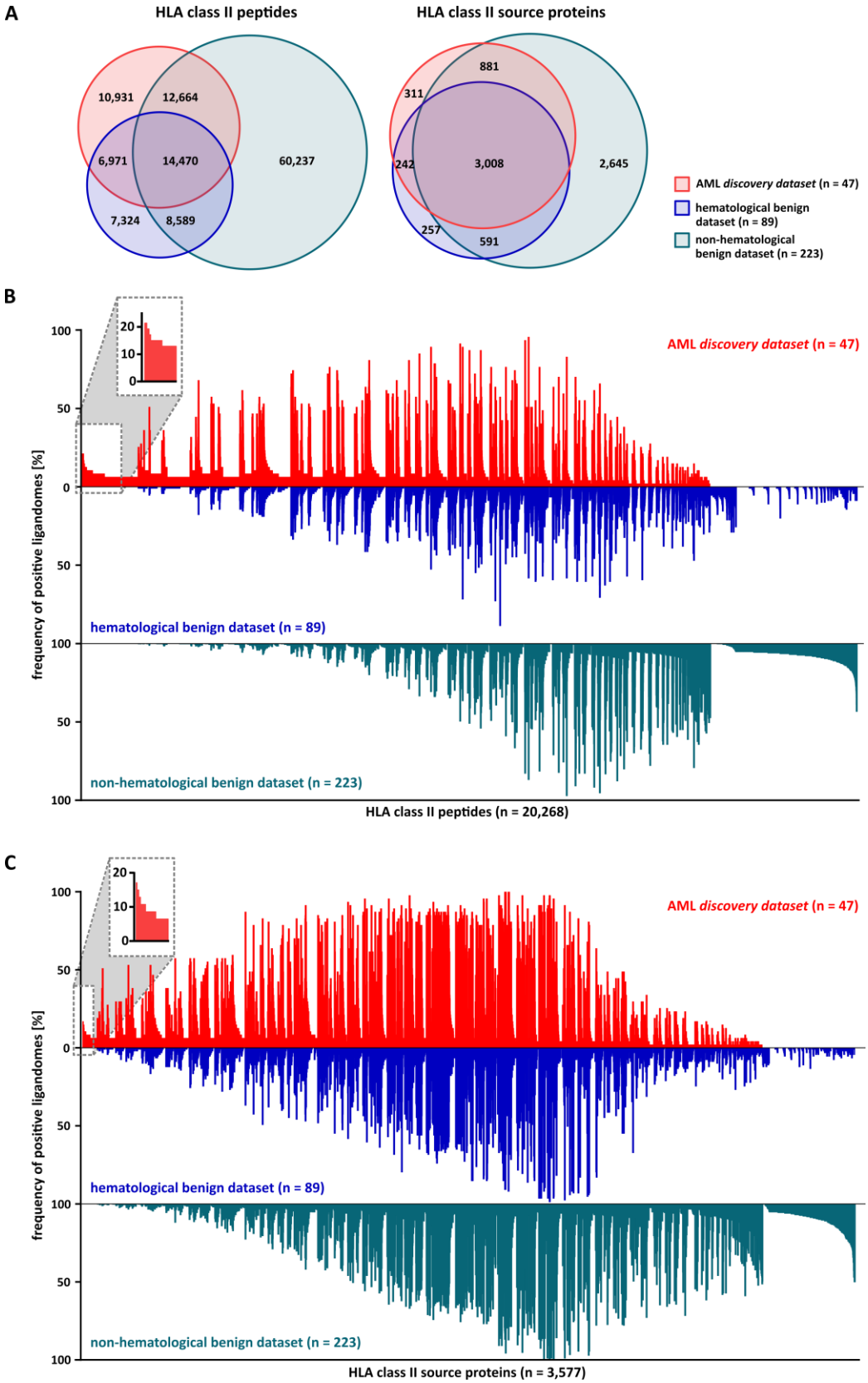

Figure 12: Comparative HLA class II ligandome profiling and identification of AML-associated peptide and protein targets. (A) Overlap analysis of HLA class II peptide and source protein identifications of primary AML samples (*discovery dataset*, n = 47) and hematological (n = 89) and non-hematological benign samples (n = 223). (B, C) Comparative profiling of (B) HLA class II peptides and (C) HLA source proteins based on the frequency of HLA-restricted presentation in AML and benign ligandomes define peptide and protein targets. Frequencies of positive immunopeptidomes for the respective identifications (x-axis) are indicated on the y-axis. To allow for better readability, HLA peptides or source proteins identified on < 5% of the samples within the respective cohort were not depicted in this plot. The boxes on the left and their magnifications highlight the subset of AML-associated antigens showing AML-exclusive, highly frequent presentation.

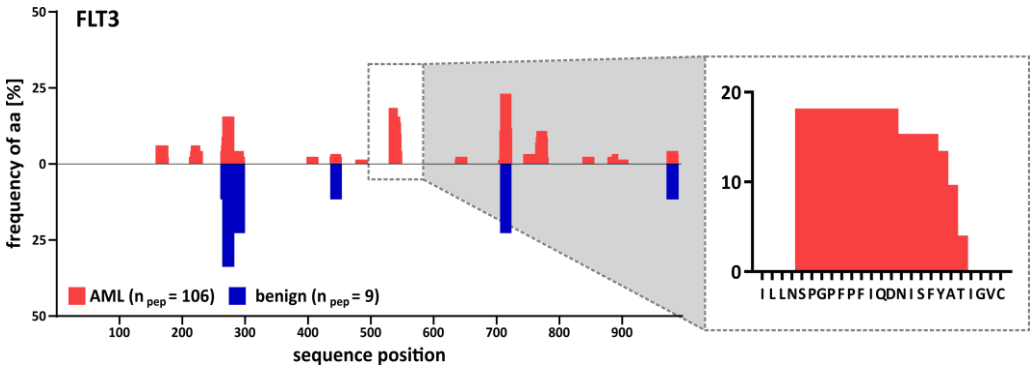

Figure 13: Identification of AML-associated hotspot targets. Hotspot analysis of the protein FLT3 by peptide clustering. Representation frequencies of amino acid counts within each cohort for the respective amino acid position (x-axis) are indicated on the y-axis. The box and its magnification highlight the identified hotspot with the respective amino acids on the x-axis. Abbreviations: aa, amino acid; n_{pep}, number of peptides.

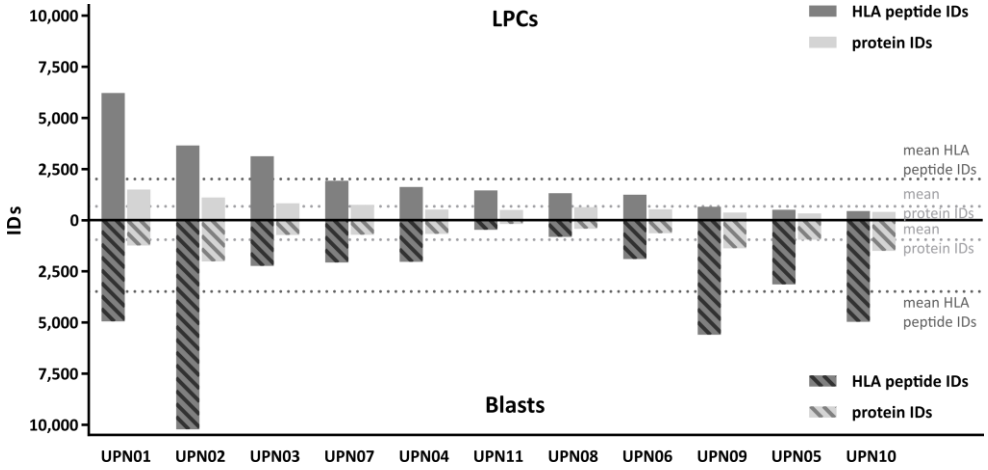

Figure 14: HLA class II peptide and source protein identifications of LPC_{enr} patient samples. HLA class II peptide and source protein identifications of LPC_{enr} and autologous LPC-depleted blast samples. Abbreviations: IDs, identifications; LPCs, leukemic progenitor cells; UPN, uniform patient number.

Overlap analysis revealed 996 HLA class II peptides and 15 source proteins to be exclusively presented on LPC_{enr} samples and 2,288 peptides and 60 proteins to be found on both, AML blast and LPC_{enr} samples (Figure 15A). Focusing on LPC-exclusive antigens, the dataset revealed only one high frequent (≥ 20%) peptide target (PHRKKKPFIEKKKAVSFHLVHR), but no high frequent protein or hotspot targets. Therefore, we concentrated on LPC-associated targets identified on both, AML blasts and LPCs. Of 2,288 AML- and LPC-shared peptides, 31 are identified with a representation frequency ≥ 20%. Of these, four did not exhibited length variants (> 50% overlap) presented on benign samples and were therefore qualified as suitable peptide targets (Figure 15B, Table S13). For protein targets, the dataset included three source proteins with representation frequencies ≥ 20% representing eight different HLA class II peptides (Figure 15C, Table S13).

For immunological characterization we aimed to select such AML-associated targets (Table S12) that are not only presented by AML blasts but additionally were identified on LPCs together with LPC-exclusive and LPC-associated targets (Table S13). Thus, we selected a panel of 14 HLA class II target antigens for immunological characterization. Prior to immunological experiments those HLA peptide identifications were validated with isotope-labeled synthetic peptides (Figure S12).

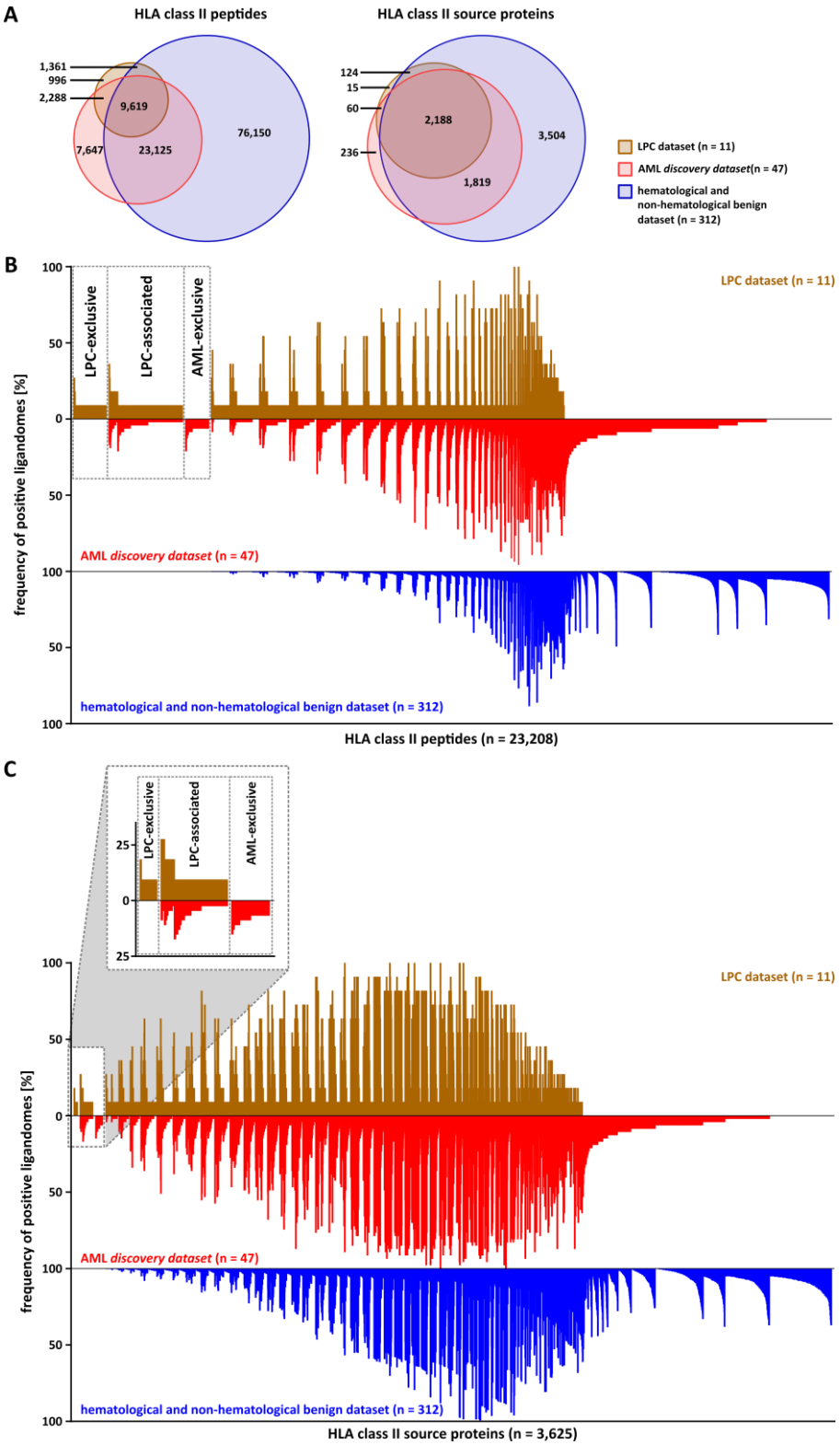

Figure 15: Comparative profiling of HLA class II ligandomes of LPC_{enr} patient samples. Comparative profiling of LPC_{enr} samples with the AML *discovery dataset* comprising the LPC-depleted blast samples as well as unsorted AML samples and the hematological and non-hematological benign samples. (A) Overlap analysis of HLA class II peptide and source protein identifications of primary LPC_{enr} samples (n = 11), AML samples (*discovery dataset*, n = 47) and hematological (n = 89) and non-hematological benign samples (n = 223). (B,D) Comparative profiling of HLA class II (B) peptides and (C) source proteins based on the frequency of HLA-restricted presentation in LPC_{enr}, AML and benign ligandomes. Frequencies of positive immunopeptidomes for the respective HLA peptide or source protein (x-axis) are indicated on the y-axis. To allow for better readability, HLA peptides or source proteins identified on < 5% of the samples within the respective cohort were not depicted in this plot. The boxes on the left highlight the subset of LPC-exclusive antigens, LPC-associated antigens showing presentation on both LPCs and AML blasts, and AML-exclusive antigens. Abbreviations: LPCs, leukemic progenitor cells.

Comparative analysis of novel AML-associated antigens with previously defined targets

In a previous work of our group, we identified 132 AML-associated antigens representing 325 unique HLA class I ligands (341 peptide – HLA allotype combinations, 325 unique peptides) and 36 antigens providing a panel of 152 different HLA class II peptides by comparing the HLA ligandomes of 15 primary AML patient samples with 35 healthy controls.[21] The selection of suitable antigens was performed solely on protein level. In the study at hand, we identified a novel panel of AML-associated HLA class I and class II-presented antigens and reanalyzed the previously defined targets (Table 2).

In a first step, we analyzed the AML-exclusivity of the previously defined HLA class I targets. 130/132 (98.5%) source proteins and 202/325 (62.2%) HLA ligands defined in the previous work as AML-exclusive are now identified in our expanded benign sample database and are therefore excluded as suitable targets. Some antigens and HLA ligands are classified in the present analysis as one hit wonders, are not identified by the other search engine, or are absent in the *discovery dataset*. Therefore, only 38/325 (11.7%) of the previously defined HLA class I-restricted peptide targets remain AML-exclusive in the novel dataset. Most of these peptides exhibited only low representation frequencies in the *discovery dataset*. Solely 1/325 (0.3%) previously defined HLA class I targets was again identified as AML-associated target (FPRFVNVTV, B*07 target).

Table 2: Comparison of previously defined AML-associated antigens[21] with the extended benign database and the novel AML *discovery dataset*

	HLA class I		HLA class II	
	HLA source protein level	HLA ligand level	HLA source protein level	HLA peptide level
# of previously defined antigen targets	132	325	36	152
# of IDs identified on expanded benign sample database	130/132 (98.5%)	202/325 (62.2%)	35/36 (97.2%)	119/152 (78.3%)
# of IDs not identified in the *discovery dataset*	1/132 (0.8%)	26/325 (8.0%)	0/36 (0.0%)	5/152 (3.3%)
# of IDs not identified by SEQUEST HT or solely identified as one hit wonders	1/132 (0.8%)	59/325 (18.2%)	1/36 (2.8%)	14/152 (9.2%)
# of previously defined antigen targets remaining AML-exclusive	0/132 (0.0%)	38/325 (11.7%)	0/36 (0.0%)	14/152 (9.2%)
# of previously defined antigen targets defined also as targets in this study	0/132 (0.0%)	1/325 (0.3%)	0/36 (0.0%)	1/152 (0.7%)

For HLA class II, 35/36 (97.2%) source proteins and 119/152 (78.3%) HLA peptides previously defined as AML-associated targets did not exhibited AML-exclusivity after comparison with the latest benign database. After exclusion of one hit wonders, 14/152 (9.2%) HLA class II peptides remain AML-exclusive with 1/152 (0.7%) peptides being an AML-associated target also in the novel definition (GNQLFRINEANQLMQ, AML-associated peptide target). These results clearly demonstrate on the one hand the importance of a continual extension of the benign tissue database but on the other hand indicate also the strength of our selection processes as we identified also identical targets in both analyses.

The role of neoantigens in the immunopeptidome of AML

To analyze the role of neoantigens in the immunopeptidome of primary AML samples, we screened our AML cohorts (*discovery* and *validation dataset*, HLA class I n = 65, HLA class II n = 67) for naturally presented HLA class I and class II-presented neoantigens derived from recurrent AML-specific missense mutations as well as recurrent mutations in NPM1 and FLT3 (Table S6). For HLA class I, we were able to identify and validate two different neoepitopes both derived from the frameshift mutation NPM1 type A: the HLA-A*11-restricted peptide AVEEVSLRK and the HLA-A*03-restricted peptide LAVEEVSLR (Figure 16 and S9, Table 3). A total of 22/65 (33.9%) patients within our HLA class I immunopeptidome dataset carry a NPM1 mutation. NPM1 type A and type D mutations result in the same protein alterations and are identified in 21 AML patients. Of these 21 patients five and three patients harbor the HLA allotypes A*03 and A*11, respectively. The HLA-A*03-restricted peptide LAVEEVSLR was detected on 1/5 (20.0%) HLA-A*03^{+} NPM1-mutated patients, whereas the HLA-A*11-restricted peptide AVEEVSLRK was even identified on 3/3 (100.0%) HLA-A*11^{+} NPM1-mutated AML patients. Unmutated NPM1-derived ($NPM1_{WT}$) peptides are commonly presented on benign and malignant samples and no differences in the abundance in the presentation of $NPM1_{WT}$ peptides between NPM1-mutated and -unmutated samples could be detected. In our HLA class I dataset we were able to identify 29 different $NPM1_{WT}$-derived HLA ligands.

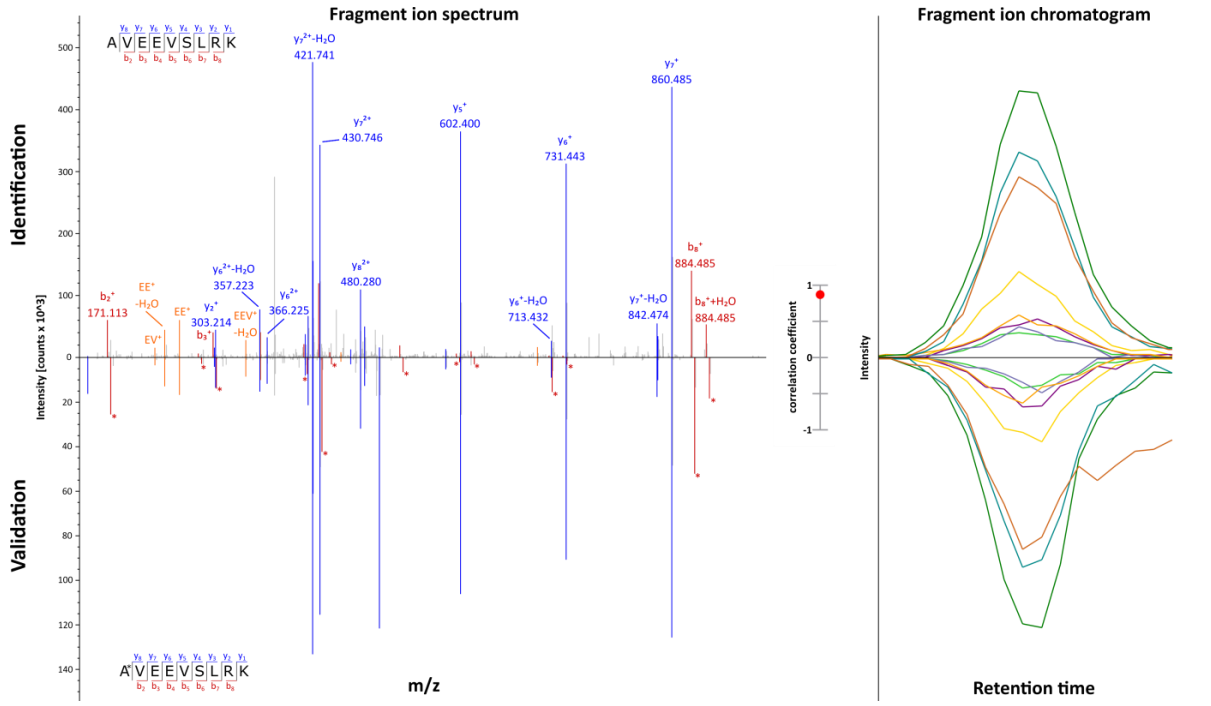

Figure 16: $NPM1_{mut}$-derived HLA-A*11-restricted neoantigen AVEEVSLRK. Representative example of mass spectrometry-based neoantigen validation using the corresponding synthetic peptide. The experimentally eluted peptide $P16_{A*11\_mut}$ (*identification,* above the x-axis) was validated with the isotope-labeled synthetic peptide (validation, mirrored on the x-axis). Identified b- and y-ions are marked in the fragment ion spectrum (left site) in red and blue, respectively. Internal fragments are labeled in orange. Ions containing the isotopic labeled amino acid alanine are marked with an asterisk. The calculated spectral correlation coefficient is depicted in the middle. Coelution of the isotope-labeled synthetic peptide with the experimentally peptide validated equal retention times (fragment ion chromatogram, right panel).

In the HLA class II ligandomes we could demonstrate the presentation of the IDH2 R140Q-derived neoepitope KLKKMWKSPNGTIQNILGGTVF (Figure S12, Table 3) in one patient sample. Interestingly, we were able to detect the corresponding wildtype peptide (KLKKMWKSPNGTIRNILGGTVF) on benign and AML samples including UPN27 validating the processing and presentation of this protein domain on HLA class II molecules. Other unmutated IDH2-derived ($IDH2_{WT}$) peptides are frequently found in the immunopeptidomes of benign and malignant samples. In total, we identified 140 different $IDH2_{WT}$-derived peptides. All identified class I and class II neoepitopes were validated by isotope-labeled synthetic peptides.

Table 3: Identified neoantigens in primary AML samples.

Peptide ID	Sequence	Mutation	Mutation type	HLA restriction	Patient
$P16_{A*11\_mut}$	AVEEVSLRK	NPM1 type A	frameshift mutation	A*11	UPN15, UPN36, UPN64
$P17_{A*03\_mut}$	LAVEEVSLR	NPM1 type A	frameshift mutation	A*03	UPN16
$P15_{II\_mut}$	KLKKMWKSPNGTI**Q**NILGGTVF	IDH2 R140Q	missense mutation	class II	UPN27

Abbreviations: ID, identifications; mut, mutation-derived; UPN, uniform patient number. Position of the missense mutation in the peptide sequence is marked in bold.

Comparative profiling of $FLT3_{WT}$- and $FLT3_{mut}$-derived immunopeptidomes revealed no specific HLA ligandome patterns for distinct AML subtypes

For the definition of broadly applicable tumor vaccines it is of tremendous importance to focus on the selection of such targets that are presented on AML independent of different clinical subtypes such as FLT3-mutated ($FLT3_{mut}$) or FLT3-unmutated ($FLT3_{WT}$) AML. Therefore, we screened our HLA class I target panel for presentation on $FLT3_{mut}$ (n = 14) and $FLT3_{WT}$ (n = 25) patient samples within the AML *discovery dataset* (Table 4). 362/427 (85%) HLA class I targets were identified in both patient cohorts and are therefore suitable for broad applicable T-cell-based immunotherapeutic approaches.

Table 4: Identification of HLA class I-restricted AML-associated targets in $FLT3_{mut}$ and $FLT3_{WT}$ patients.

HLA allotype	# of $FLT3_{mut}$ patients	# of $FLT3_{WT}$ patients	# of targets	# of targets identified on $FLT3_{mut}$ patients	# of targets identified on $FLT3_{WT}$ patients	# of targets identified on both cohorts
all	14	25	1	1/1 (100%)	1/1 (100%)	1/1 (100%)
A*01	5	5	48	48/48 (100%)	41/48 (85%)	41/48 (85%)
A*02	6	14	28	28/28 (100%)	28/28 (100%)	28/28 (100%)
B*07	5	6	185	149/185 (81%)	182/185 (98%)	146/185 (79%)
B*08	2	5	161	160/161 (99%)	143/161 (89%)	142/161 (88%)
C*07	8	14	11	11/11 (100%)	11/11 (100%)	11/11 (100%)
total	**14**	**25**	**427 (*)**	**390/427 (91%)**	**399/427 (93%)**	**362/427 (85%)**

* Not equal to the sum of all single HLA allotypes due to duplicates indicating peptides, which are identified on several allotypes.

In a next step, we examined the differences in the entirety of $FLT3_{mut}$ and $FLT3_{WT}$ immunopeptidomes by comparative profiling. Overlap analysis revealed 824/8,879 (9.3%) of $FLT3_{mut}$ source proteins to be exclusively presented on $FLT3_{mut}$ samples in comparison to $FLT3_{WT}$ cells (Figure 17A). However, these differences could be explained by slightly different HLA allotype distributions within both cohorts (Figure S13) as well as the different cohort sizes demonstrated by random cohort sampling using the

same number of samples per cohort, which resulted in similar overlap results (data not shown). Comparison of AML-derived ligandomes with our in-house benign database (n = 332) indicated 95/451 (21.1%) AML-exclusive source proteins to be $FLT3_{mut}$-associated. However, solely two of these 95 $FLT3_{mut}$-associated source proteins were identified with frequencies ≥ 15% (Figure 17B). In a next step, we performed cluster analysis using a comparative ligandome representation matrix of all source proteins identified in the AML *discovery dataset* (n = 47). Samples were hierarchically clustered due to the presentation of different source proteins. Thereby, no clear clustering concerning the parameters of interest (FAB and WHO classification, Sex, Age, NPM1 and FLT3 mutation status) could be identified (Figure 18A). Nevertheless, samples that share single HLA allotypes tend to cluster together. Thus, we performed the same analysis on HLA-A*02^{+} patient samples using only HLA-A*02-restricted peptides (Figure 18B). Again, no significant clustering concerning our parameters of interest could be observed indicating no specific immunopeptidome pattern of clinical subgroups and no substantial influence or effect of these parameters on the entirety of the immunopeptidome. Interestingly, in this analysis the two HLA-A*02:05^{+} samples cluster together clearly separated from the other HLA-A*02:01^{+} samples. Furthermore, panther pathway analysis of $FLT3_{mut}$- and $FLT3_{WT}$-derived source proteins delineates no enriched signaling pathway in one of the two cohorts (data not shown).

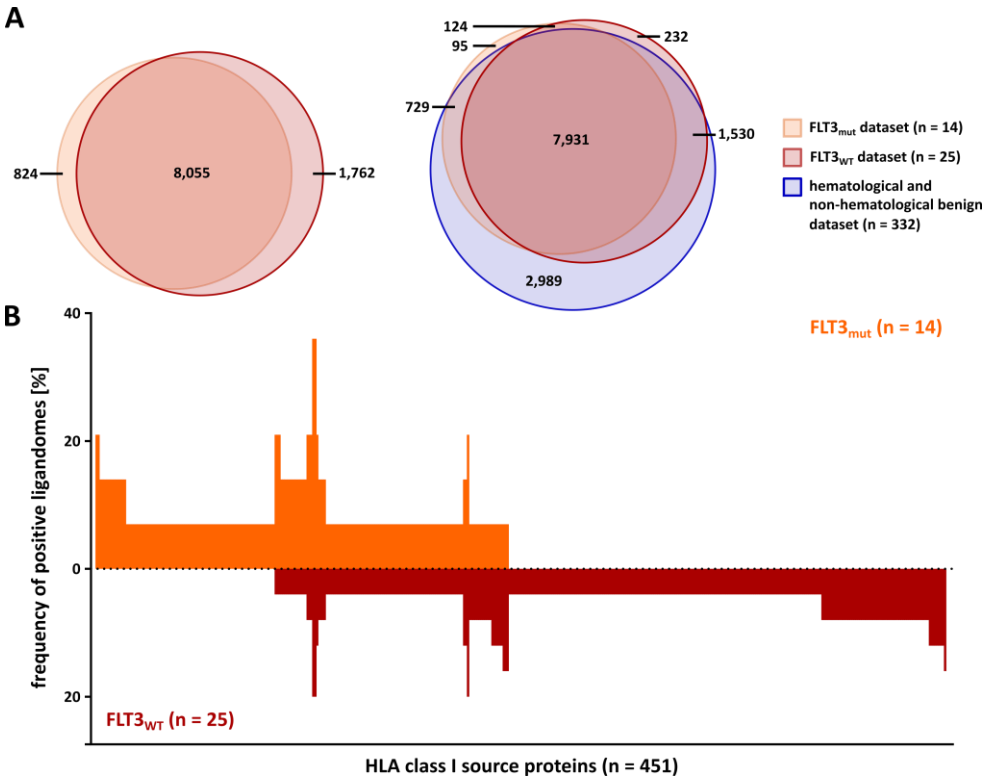

Figure 17: Comparative profiling of $FLT3_{WT}$- and $FLT3_{mut}$-derived immunopeptidomes. (A) Overlap analysis of HLA class I source protein identifications of $FLT3_{WT}$- (n = 25) and $FLT3_{mut}$- (n = 14) derived immunopeptidomes alone (left panel) and together with benign immunopeptidomes (n = 332, right panel). (B) Comparative profiling of AML-exclusive HLA class I source proteins based on the frequency of HLA-restricted presentation in $FLT3_{WT}$ (n = 25) and $FLT3_{mut}$ (n = 14) ligandomes. Frequencies of positive immunopeptidomes for the respective HLA source protein (x-axis) are indicated on the y-axis. Abbreviations: $FLT3_{mut}$, FLT3-mutated AML samples; $FLT3_{WT}$, FLT3-unmutated AML samples.

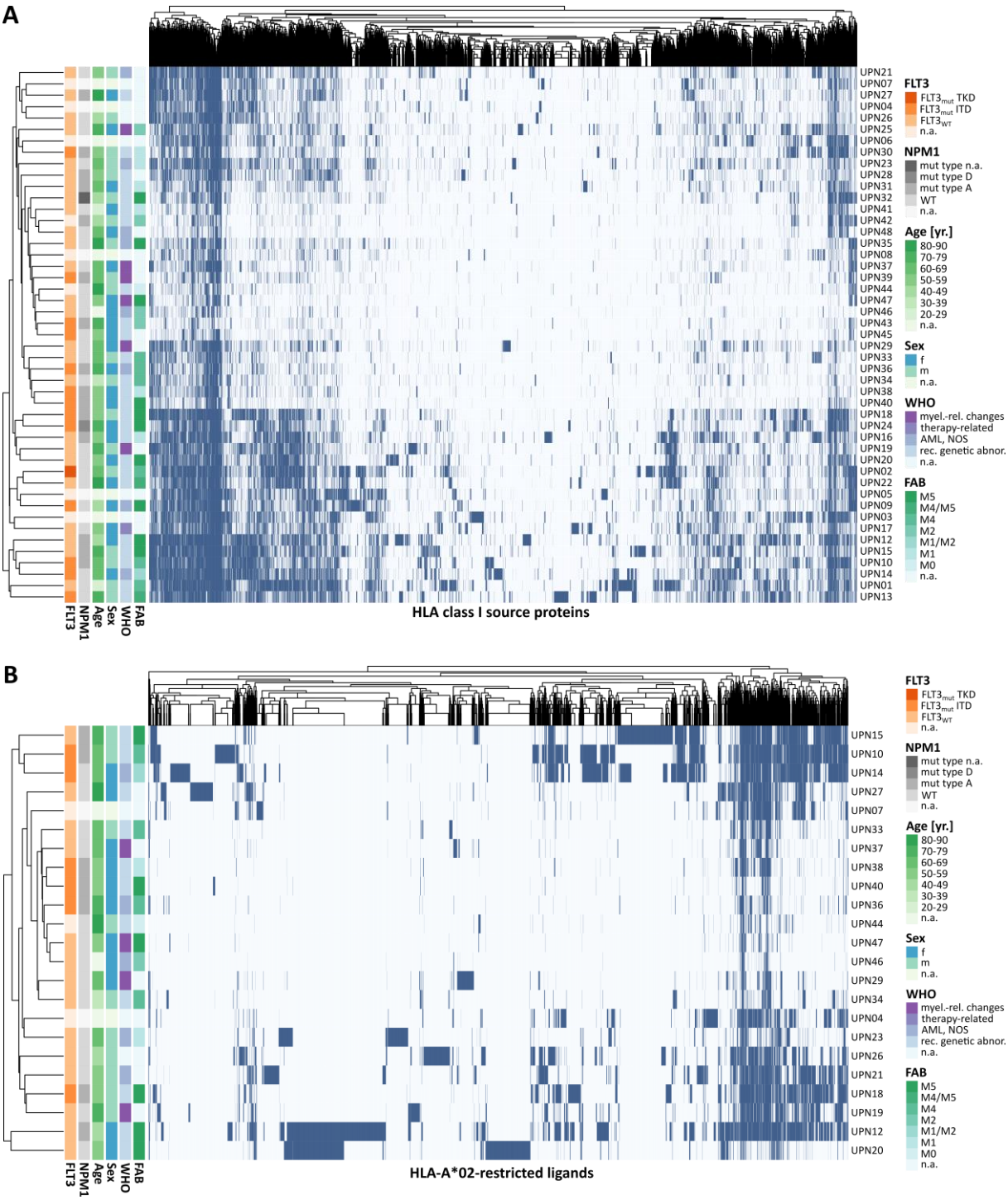

Figure 18: Cluster analysis. (A,B) Cluster analysis using a comparative ligandome representation matrix created with (A) HLA class I source protein and (B) HLA-A*02-restricted HLA ligand identifications on primary AML samples within the AML *discovery dataset*. Dark blue indicates the identification of at least on single HLA class I ligand of the respective source protein, light blue specifies source proteins not identified in the respective sample. Abbreviations: WHO, AML classification according to the World Health Organization; FAB, AML classification according to the French-American-British system; UPN, uniform patient number; $FLT3_{mut}$, FLT3-mutated AML samples; $FLT3_{WT}$, FLT3-unmutated AML samples; TKD, tyrosine kinase domain; ITD, internal tandem duplications; n.a., not available; yr., years; f, female; m, male; myel.-rel., myelodysplasia-related changes; NOS, not otherwise specified; rec., recurrent; abnor., abnormalities.

HLA class I-restricted AML-associated antigens induce functional peptide-specific T cells

For functional characterization of the novel defined AML-associated HLA class I targets (Table 5), we performed screenings for preexisting memory T-cell responses in PBMC samples of HVs and AML patients in remission by IFNγ ELISPOT assays and ICS. Preliminary results showed no memory T-cell responses against 16/17 targets in HV samples (Table 5, Figure 19A). Each target was tested in at least eight HLA-matched donors. For HLA-C-restricted peptides, screening was performed in HLA-B*07$^+$ HVs due to no available HLA-C typing and the known linkage disequilibrium of HLA-B*07 and -C*07[74, 75]. Notably, 1/17 HLA class I targets, the HLA-C*07-restricted peptide $P15_{C*07}$, exhibited spontaneous but weak T-cell responses in 2/8 (25%) HVs. HLA-C typing of these donors is ongoing to validate the HLA-C restriction. Interestingly, we could demonstrated by ICS that the $P15_{C*07}$-specific T-cell response is elicited by CD4$^+$ T cells instead of CD8$^+$ T cells. In AML patient samples, we could detect spontaneous T-cell responses against 5/14 tested peptides (Table 5, Figure 19B,C). Especially for the mutation-derived peptide $P17_{A*03\_mut}$, we could detect an extremely high response rate of 71% (5/7 AML patients). Interestingly, the $P16_{A*11\_mut}$-specific T-cell response detected in the PBMC sample of UPN23 was demonstrated *via* ICS to be elicited by CD4$^+$ T cells (Figure 19D). Furthermore, T-cell responses against peptides derived from mutated NPM1 could be detected not only in patients harboring the mutation, but also in patients without the specific mutation. In further experiments, we will screen more AML patients for preexisting T-cell responses against our target antigens using IFNγ ELISPOT and ICS assays.

Table 5: AML-associated HLA class I-restricted peptides for functional characterization.

Peptide ID	Peptide sequence	Source protein	HLA restriction	T-cell response in		*in vitro* CD8$^+$ T-cell priming in		ICS of peptide-specific induced CD8$^+$ T cells in		VITAL assay
				AML	HV	AML	HV	AML	HV	
$P1_{A*01}$	DIDTRSEFY	ARP2	A*01	0/3 (0%)	0/10 (0%)	n.t.	n.t.	-	-	-
$P2_{A*01}$	FSEYFGAIY	MYNN	A*01	0/2 (0%)	0/10 (0%)	n.t.	n.t.	-	-	-
$P3_{A*01}$	YLDGRLEPLY	CEBPA	A*01	0/2 (0%)	0/10 (0%)	n.t.	n.t.	-	-	-
$P4_{A*02}$	SLLEADPFL	CCNA1	A*02	0/11 (0%)	0/10 (0%)	1/1 (100%)	2/2 (100%)	neg.	TNF$^+$ / IFNγ$^+$	-
$P5_{A*02}$	IILDALPQL	DOCK8	A*02	0/11 (0%)	0/10 (0%)	n.t.	2/2 (100%)	-	TNF$^+$ / IFNγ$^+$ / CD107a$^+$	-
$P6_{A*02}$	ILNDVAMFL	RUS1	A*02	0/10 (0%)	0/10 (0%)	n.t.	1/1 (100%)	-	TNF$^+$ / IFNγ$^+$	-
$P7_{B*07}$	APESKHKSSL	STT3B	B*07	1/6 (17%)	0/10 (0%)	n.t.	n.t.	-	-	-
$P8_{B*07}$	APGLHLEL	IRF7	B*07	0/5 (0%)	0/10 (0%)	n.t.	n.t.	-	-	-
$P9_{B*07}$	APTIVGKSSL	OST48	B*07	0/5 (0%)	0/10 (0%)	n.t.	n.t.	-	-	-
$P10_{B*08}$	DLDTRVAL	APCF2	B*08	n.t.	0/10 (0%)	n.t.	n.t.	-	-	-
$P11_{B*08}$	APTPRIKAEL	TLE1	B*08/B*07	n.t.	0/10 (0%)	n.t.	n.t.	-	-	-
$P12_{B*08}$	EGYGRYLDL	SF3A3	B*08/B*14	n.t.	0/10 (0%)	n.t.	n.t.	-	-	-
$P13_{C*07}$	SRPPLLGF	UBE3B	C*07	1/5 (20%)	0/8 (0%)$^{\#}$	n.t.	n.t.	-	-	-
$P14_{C*07}$	AYHELAQVY	CSN3	C*07	0/5 (0%)	0/8 (0%)$^{\#}$	n.t.	n.t.	-	-	-
$P15_{C*07}$	IYSGYIFDY	RALY	C*07	1/5 (20%)	2/8 (25%)$^{\#}$*	n.t.	n.t.	-	-	-
$P16_{A*11\_mut}$	AVEEVSLRK	NPM type A mutation	A*11	1/12 (8%)*	0/9 (0%)	1/7 (14%)	3/3 (100%)	neg.	TNF$^+$ / IFNγ$^+$ / CD107a$^+$	pos.
$P17_{A*03\_mut}$	LAVEEVSLR	NPM type A mutation	A*03	5/7 (71%)	0/9 (0%)	n.t.	n.t.	-	-	-

Abbreviations: * ICS revealed CD4-mediated T-cell response; $^{\#}$ HLA-C*07-restricted peptides were screened for T-cell responses in HVs using HLA-B*07$^+$ HV samples. ID, identification; mut, mutation-derived; n.t., not tested; HVs, healthy volunteers; ICS, intracellular cytokine staining; neg., negative; pos., positive.

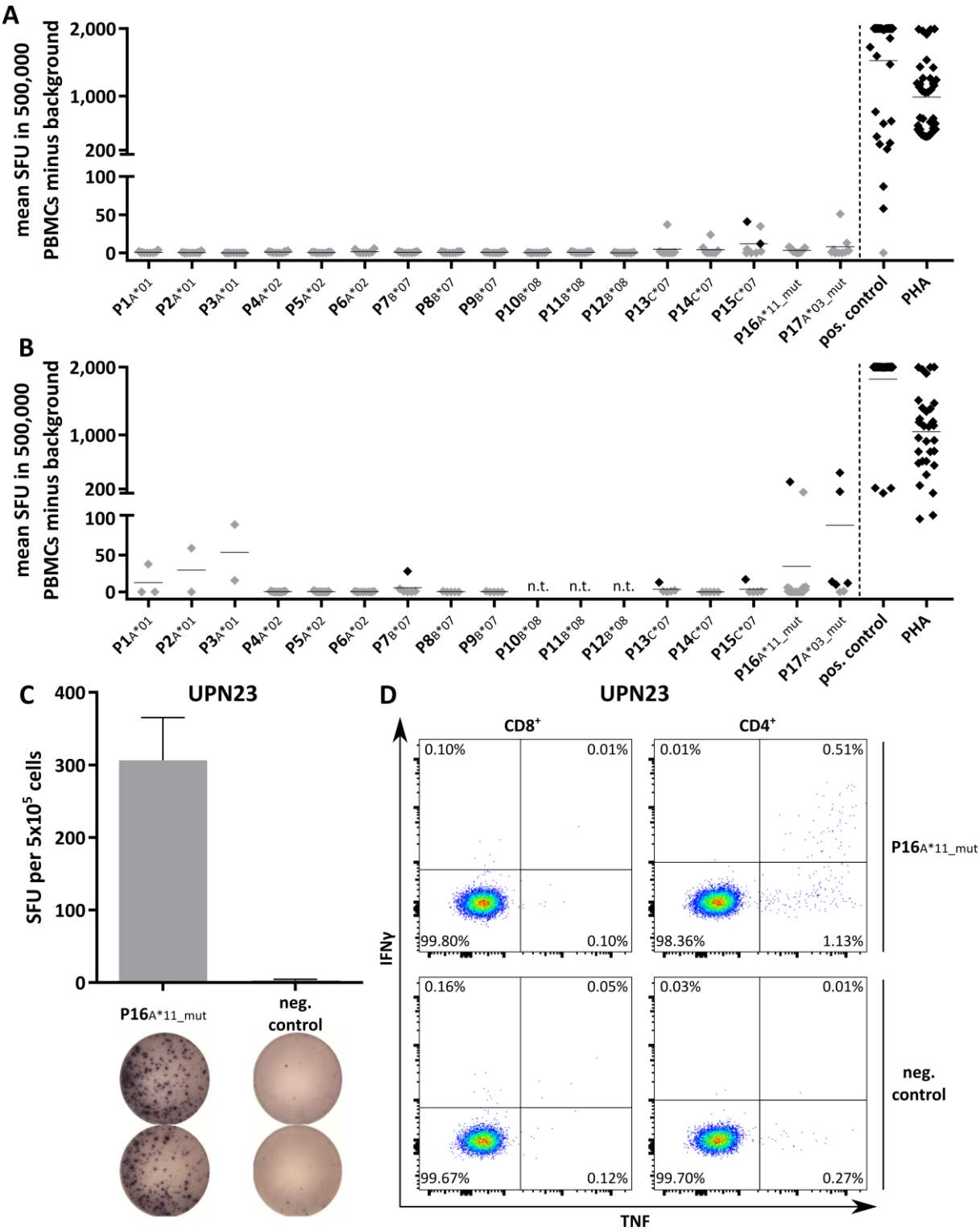

Figure 19: Memory T-cell responses against HLA class I-restricted AML-associated antigens. AML-associated HLA class I ligands were evaluated for their immunogenic potential by screening for memory T-cell responses in HV and AML patient samples using IFNγ ELISPOT and ICS assays. (A,B) Preliminary IFNγ ELISPOT results of AML-associated antigens in (A) HV and (B) AML patient samples. Shown are mean numbers of spot forming units (SFU) in 500,000 PBMCs per duplicate for each tested donor or patient minus the mean spot numbers of the negative control (background) of the respective donor or patient. Each point represents a single donor or patient. Spot counts of > 2,000 were set to 2,000 because of inaccurate spot counts due to technical limitations. Positively evaluated spot counts are depicted in black, negatively evaluated spot counts in grey. Lines indicate the mean number of SFU per peptide. (C,D) Representative example of IFNγ ELISPOT and ICS results detected in AML patient samples. T-cell responses in UPN23 against $P16_{A*11\_mut}$ detected by (C) IFNγ ELISPOT and (D) ICS. Abbreviations: SFU, spot forming unit; PBMCs, peripheral blood mononuclear cells; PHA, phytohemagglutinin; neg., negative.

Furthermore, we performed aAPC-based *in vitro* priming of naïve $CD8^+$ T cells of AML patients and HVs. So far, we tested the NPM1 mutation-derived peptide $P16_{A*11\_mut}$ for *de novo* induction of peptide-specific T cells as well as the three HLA-A*02-restricted targets. All three HLA-A*02-restricted targets could induce peptide-specific cytokine-producing $CD8^+$ T cells in HVs (Table 5). The peptide $P16_{A*11\_mut}$ was already screened using AML patient samples as well as PBMCs of HVs. For AML patient samples, we were able to induce peptide-specific T cells in 1/7 (14%) patients with frequencies of peptide-specific $CD8^+$ T cells up to 0.14% (Figure 20A). In HV samples peptide-specific T cells were induced in 3/3 (100%) samples with frequencies of peptide-specific $CD8^+$ T cells up to 4.00% (Figure 20B). These differences between AML patient samples and HV samples might be explained by the number of accessible $CD8^+$ T cells as the available number of $CD8^+$ T cells was considerably higher for HVs (range 50×10^6 - 110×10^6, mean 83×10^6) compared to AML patients (range 3×10^6 - 65×10^6, mean 18×10^6). *De novo* peptide-specific T-cell induction was proven by tetramer staining (Figure 20A,B) and IFNγ ELISPOT (data not shown) after 12-d recall stimulation, which elicited no preexisting peptide-specific memory T cells. The $P16_{A*11\_mut}$-specific $CD8^+$ T cells were multifunctional as revealed by ICS and cytotoxicity assay (Figure 20C-E). Peptide-specific $CD8^+$ T cells produced IFNγ and TNF and expressed the degranulation marker CD107a after stimulation with the peptide $P16_{A*11\_mut}$ (Figure 20C). Furthermore, $P16_{A*11\_mut}$-specific $CD8^+$ T cells exhibited 81.8% peptide-specific cell lysis of peptide-loaded autologous target cells at an effector to target ratio of 1:1 compared to autologous target cells loaded with an HLA-matched control peptide (Figure 20D,E). IFNγ ELISPOT assays, *in vitro* priming experiments, and ICS assays are ongoing and will provide more insights into the immunogenicity of our novel AML-and LPC-associated HLA class I targets.

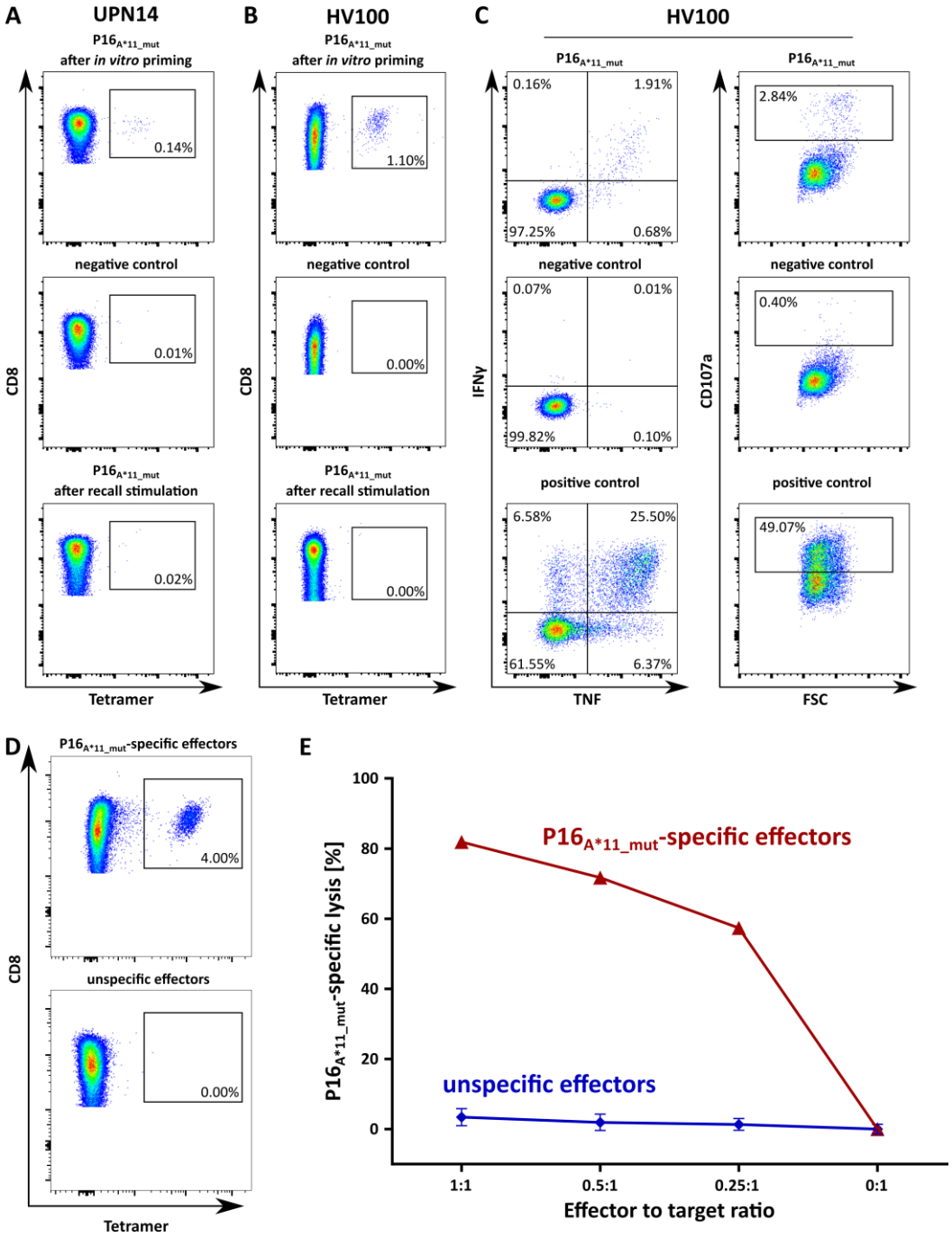

Figure 20: Immunogenicity of HLA class I-restricted AML-associated antigens. AML-associated HLA class I ligands were evaluated for their immunogenic potential by *in vitro* CD8$^+$ T-cell priming and cytotoxicity assays. (A,B) Representative example of *in vitro* priming of naïve CD8$^+$ T cells derived from an (A) AML patient and an (B) HV using aAPCs. Graphs show single, viable cells stained for CD8 and PE-conjugated multimers of indicated specificity. The upper panels show $P16_{A*11\_mut}$-specific tetramer staining. The middle panels (negative control) depict $P16_{A*11\_mut}$-specific tetramer staining of T cells from the same patient or donor primed with an irrelevant HLA-matched peptide. The lower panels exhibit T cells from the same patient or donor that were screened for the absence of preexisting memory T cells after 12-d recall stimulation by tetramer staining. (C) IFNγ and TNF production as well as CD107a expression of peptide-specific *in vitro* primed CD8$^+$ T cells after stimulation by the peptide used for *in vitro* priming or by an HLA-matched control peptide. PMA and ionomycin served as positive control. (D,E) Cytotoxicity of $P16_{A*11mut}$-specific effector T cells was analyzed in the VITAL cytotoxicity assay with *in vitro* primed CD8$^+$ T cells of an HV. (D) Tetramer staining of polyclonal effector cells before performance of the VITAL assay determined the amount of $P16_{A*11\_mut}$-specific effector cells in the population of successfully $P16_{A*11\_mut}$-primed CD8$^+$ T cells (upper panel) and in the population of control cells from the same donor primed with an HLA-matched control peptide (lower panel). (E) Effector to target-dependent $P16_{A*11\_mut}$-specific lysis (red) of $P16_{A*11\_mut}$ peptide-loaded autologous target cells in comparison to HLA-matched control peptide-loaded target cells. Unspecific effectors (blue) did not exhibit $P16_{A*11\_mut}$-specific lysis of the same targets. Unspecific effectors were evaluated in three independent replicates and results are shown as mean ± SEM for the tree replicates. Abbreviations: UPN, uniform patient number; HV, healthy volunteer; FSC, forward scatter.

Memory T cells against the novel HLA class II-presented AML- and LPC-associated antigens are identified in AML patients and HVs

For functional characterization and immunogenicity analysis of our novel defined AML- and LPC-associated HLA class II-restricted targets, we performed IFNγ ELISPOT assays and ICS with PBMC samples of AML patients in remission and HVs upon 12-d recall stimulation with our targets (Table 6, Figure 21).

Table 6: AML-associated HLA class II-restricted peptides for functional characterization.

Peptide ID	Target class	Peptide sequence	Source protein	T-cell response in AML	T-cell response in HVs	ICS of $CD4^+$ T cells in AML	ICS of $CD4^+$ T cells in HVs
$P1_{II}$	peptide target	GNQLFRINEANQLMQ	GALNT7	3/9 (33%)	3/15 (20%)	TNF^+	TNF^+ / $IFN\gamma^+$
$P2_{II}$	peptide target	DRQQMEALTRYLRAAL	CLC11	0/9 (0%)	1/15 (7%)	-	n.t.
$P3_{II}$	peptide target	LGQEVALNANTKNQKIR	APOB	0/9 (0%)	1/15 (7%)	-	TNF^+ / $IFN\gamma^+$
$P4_{II}$	peptide target	NGRTFHLTRTLTVK	IL1AP	1/6 (17%)	5/15 (33%)	TNF^+ / $IFN\gamma^+$	TNF^+ / $IFN\gamma^+$
$P5_{II}$	protein target	SKPGVIFLTKKGRRF	CCL23	0/6 (0%)	4/15 (27%)	-	TNF^+ / $IFN\gamma^+$
$P6_{II}$	hotspot target	SPGPFPFIQDNISFYA	FLT3	1/6 (17%)	1/14 (7%)	neg.	neg.
$P7_{II}$	hotspot target	LDTMRQIQVFEDEPAR	IL1AP	0/5 (0%)	0/14 (0%)	-	-
$P8_{II}$	hotspot target	VVGYALDYNEYFRDL	HPRT	1/3 (33%)	1/14 (7%)	neg.	n.t.
$P9_{II}$	hotspot target	IGSYIERDVTPAIM	KIT	0/3 (0%)	0/14 (0%)	-	-
$P10_{II}$	LPC-exclusive peptide target	PHRKKKPFIEKKKAVSFHLVHR	LTV1	0/2 (0%)	2/14 (14%)	-	TNF^+ / $IFN\gamma^+$
$P11_{II}$	LPC-associated peptide target	KHLHYWFVESQKDPEN	PPGB	0/1 (0%)	0/14 (0%)	-	-
$P12_{II}$	LPC-associated peptide target	ETLHKFASKPASEFVK	ITAL	0/1 (0%)	0/14 (0%)	-	-
$P13_{II}$	LPC-associated protein target	DRVKLGTDYRLHLSPV	TACT (CD96)	0/1 (0%)	2/14 (14%)	-	n.t.
$P14_{II}$	LPC-associated protein target	ERPEWIHVDSRPF	G6PC3	0/1 (0%)	0/14 (0%)	-	-
$P15_{II\_mut}$	neoepitope	KLKKMWKSPNGTIQNILGGTVF	IDHP R140Q	1/9 (11%)	5/15 (33%)	n.t.	TNF^+ / $IFN\gamma^+$
$P5_{II\_HHV8P}$	corresponding viral peptide of $P5_{II}$	SKPGVIFLTKRGRQV	VMI2_HHV8P	0/3 (0%)	0/5 (0%)	-	-

ICS could only be performed after detection of peptide-specific T cells in ELISPOT assays. Abbreviations: ID, identification; LPC, leukemic progenitor cells. HHV8P, human herpesvirus 8 type P; HVs, healthy volunteers; ICS, intracellular cytokine staining; n.t., not tested; neg. negative.

So far, we observed spontaneous preexisting T-cell responses against 10/15 (67%) peptides in HVs (Figure 21A,B) and against 5/15 (33%) targets in AML patient samples (Figure 21C,D) validating these peptides as valid T-cell epitopes. For AML patient screening the number of tested patients is still small and will be increased in future experiments. The overall response rate reached up to 33% per peptide (Figure 22). So far, 8/10 peptides, which exhibited T-cell responses in ELISPOT assays, were also analyzed in ICS, whereas all T-cell responses could be validated to be $CD4^+$ T-cell-mediated responses with detectable TNF and IFNγ production upon peptide stimulation for 6/8 peptides (Table 6, Figure 21B,D). For HVs, we calculated the correlation between detected T-cell responses against our HLA class II targets and the age of the donors. Notably, we could not detect any correlation concerning donor-individual peptide recognition rate or total T-cell responses with the age of the donors (data not shown).

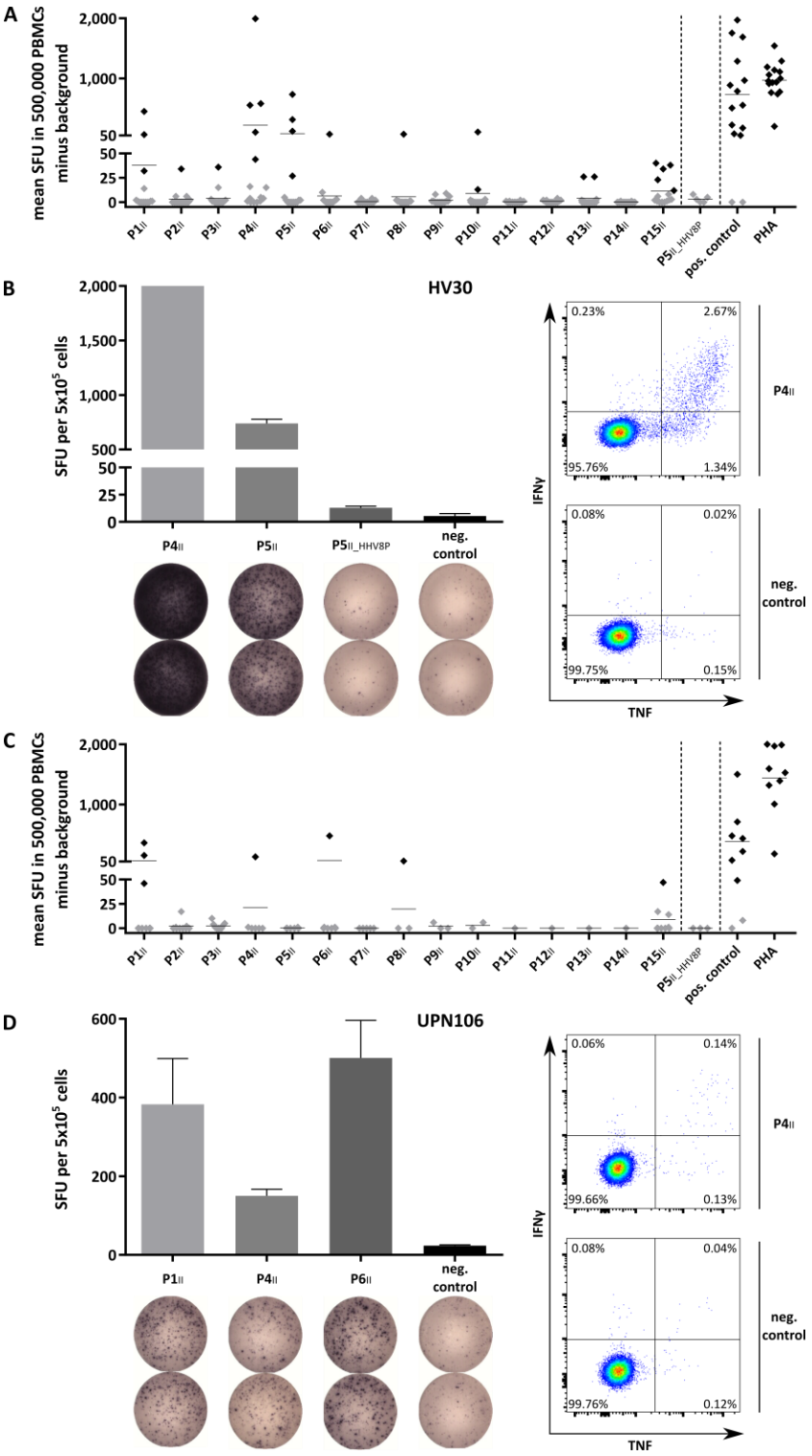

Figure 21: Immunogenicity of HLA class II-restricted AML- and LPC-associated antigens. AML- and LPC-associated peptides were screened for memory T-cell responses in PBMC samples of HVs and AML patients by IFNγ ELISPOT and ICS assays after 12-d recall stimulation. PHA and a peptide mix of viral positive peptides were used as positive controls. The Filamin-A-derived peptide ETVITVDTKAAGKGK served as negative control. (A, C) IFNγ ELISPOT results of AML- and LPC-associated antigens in (A) HVs and (C) AML patient samples. Shown are mean numbers of spot forming units (SFU) in 500,000 PBMCs per duplicate for each tested donor or patient minus the mean spot numbers of the negative control (background) of the respective donor or patient. Each point represents a single donor or patient. Spot counts of > 2,000 were set to 2,000 because of inaccurate spot count due to technical limitations. Positively evaluated spot counts are depicted in black, negatively evaluated spot counts in grey. Lines indicate the mean number of SFU per peptide. (B, D) Representative examples of single IFNγ ELISPOT (left site) and intracellular cytokine staining (ICS, right site) results of PBMC samples of (B) an HV and (D) an AML patient. Data are expressed as mean ± SD of two independent replicates. Abbreviations: SFU, spot forming unit; PBMCs, peripheral blood mononuclear cells; PHA, phytohemagglutinin; HV, healthy volunteer; neg. negative; UPN, uniform patient number.

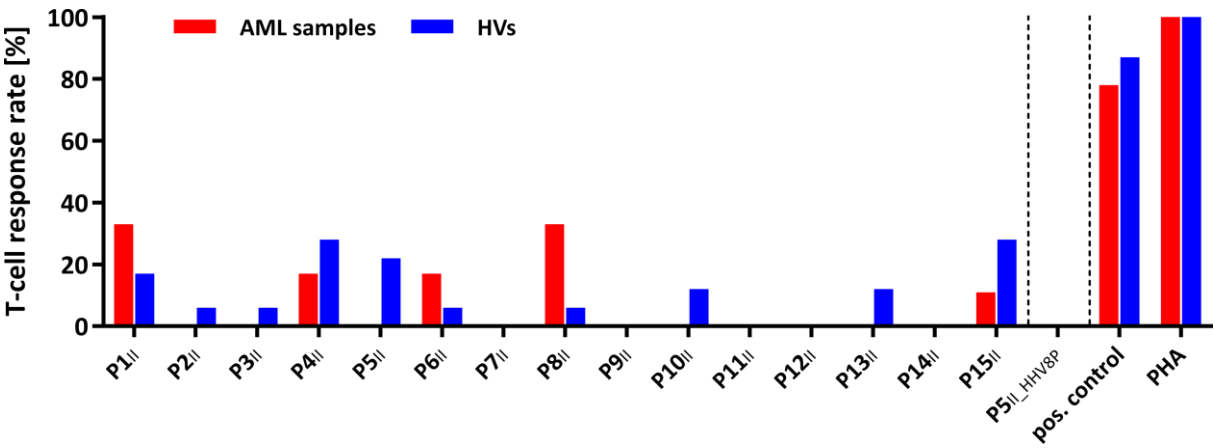

Figure 22: T-cell response rates against AML- and LPC-associated antigens. Total T-cell response rates against AML- and LPC-associated antigens (Table 6) in AML patient and HV PBMC samples as determined by IFNγ ELISPOT assays. Abbreviations: PHA, phytohemagglutinin; HVs, healthy volunteers; pos. positive.

To exclude detection of T-cell responses against SNPs, we screened our AML-associated targets for published SNPs in the dbSNP (www.ncbi.nlm.nih.gov/SNP/),[76] which might be a reason for the high response rates in HVs. We identified 6 – 23 SNPs per peptide (mean 11) with frequencies ≤ 0.05% for 14/15 peptides. For peptide $P5_{II}$ SNPs with frequencies up to 1.46% (rs80219613, R14L or R14H corresponding to position within peptide) are reported. Thus, cross-reactivity against these low frequent SNPs could be excluded as a reason for our higher frequent detectable T-cell responses.

To avoid cross-reactivity to pathogen-derived peptides, we analyzed the similarity of all our targets to pathogen-derived peptides and published SNPs. Thereby we identified one corresponding viral peptide to the CCL23-derived peptide SKPGVIFLTKKGRRF ($P5_{II}$). The viral counterpart peptide SKPGVIFLTKRGRQV ($P5_{II\_HHV8P}$) differs only in 3/15 amino acids in comparison to our target (Figure 23).

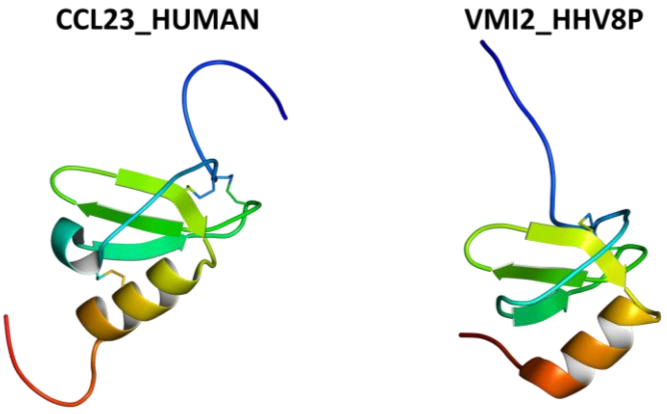


```
CCL23_HUMAN  1   MKVSVAALSCLMLVTALGSQARVTKDAETEFMMSKLPLENPVLLDRFHATSADCCISYTP
VMI2_HHV8P   1   MD-----TKGILLV---------------AVLTALLCLQSGDTLGASWHRPDKCCLGYQK
                 *.      . ::**                .: : * *:.   *.       .**:.*

CCL23_HUMAN 61   RSIPCSLLESYFETNSECSKPGVIFLTKKGRRFCANPSDKQVQVCVRMLKLDTRIKTRKN
VMI2_HHV8P  41   RPLPQVLLSSWYPTSQLCSKPGVIFLTKRGRQVCADKSKDWVKKLMQQLPVTAR------
                 * :*  **.*:: *.. ***********:**:.**: *.. *:  :: * : :*
```

Figure 23: Similarity of the AML-associated target $P5_{II}$ to a virus-derived peptide. Structural[77, 78] and sequence[79, 80] comparison of CCL23_HUMAN (PDB ID: 1G91)[81] and VMI2_HHV8P (PDB ID: 1HFN).[82] Sequence alignment with highlighted HLA-presented peptide $P5_{II}$ and its viral counterpart peptide. Similar amino acids are marked in green. The symbols underneath the alignment denoting the degree of conservation: An asterisk (*) indicates fully similar amino acids. A colon (:) and a period (.) indicates amino acids with strongly and weakly similar properties, respectively.

Furthermore, the different amino acids are very similar in their properties. $P5_{II\_HHV8P}$ is derived from the viral macrophage inflammatory protein 2 from the human herpesvirus 8 type P. Both source proteins are structurally extremely similar and bind chemokine receptors.[83, 84] To validate that the detected T-cell responses against $P5_{II}$ are $P5_{II}$-specific, we stimulated cells from the same donors that showed memory T-cell responses against $P5_{II}$ with the viral peptide $P5_{II\_HHV8P}$. Interestingly, $P5_{II\_HHV8P}$ could not be recognize by the $P5_{II}$-specific T cells as no T-cell responses could be detected by IFNγ ELISPOT assays after 12-d stimulation (Table 6, Figure 21A,C and 22) validating the detected immune response as specific for our AML-associated antigen target.

6.3.5. DISCUSSION

Despite the development and incredible progress in immunotherapeutic approaches for the treatment of cancer and leukemia patients in recent years, AML is still characterized by high relapse rates and a poor overall survival[1] mainly caused by the persistence of chemoresistant LPCs.[2-4] Therefore, targeting LPCs more specifically raises the hope to improve the long-term outcome of AML patients.

For clinical effective T-cell-based immunotherapeutic approaches such as peptide vaccination, one major prerequisite is the sufficient expression of HLA molecules on the target cells. We were able to quantify HLA surface expression on AML blasts and could confirm a high HLA expression comparable to previously described expression levels.[21] Notably, surface expression of HLA class I and class II molecules on LPCs are equivalent to AML blasts and therefore validate also LPCs as potential T-cell targets.

To target LPCs more specifically we aimed to analyze the immunopeptidome of enriched LPCs and especially select AML-associated antigen targets that are presented not only on AML blasts but also on LPCs. We therefore enriched $CD34^+CD38^-$ LPCs of 11 primary AML samples for subsequent isolation of HLA-presented peptides. Furthermore, we aimed to validate the clonogenic potential of these enriched LPCs by transplantation experiments in immunocompetent mice. These experiments revealed no difference in the clonogenic potential between AML blasts and enriched LPCs, but proved the *in vivo* engraftment of both cell populations. Notably, AML blasts showed the same clonogenic potential as LPC-enriched cells in terms of time to engraftment and leukemic burden in different tissue subsets, which might result from remaining progenitor cells in the AML blast population. Nevertheless, the *in vivo* engraftment in immunocompromised mice verified that the $CD34^+CD38^-$-enriched LPC population contains leukemic-initiating cells as already demonstrated in several previous studies.[22, 23] Further titration experiments might highlight the different LPC frequencies in AML blasts and LPC-enriched samples.

For the definition of suitable AML-associated target antigens, the comparative profiling with a large cohort of different benign tissues and cell types is indispensable to exclude HLA-presented peptides that could cause severe side effects, especially if these antigens should be used in highly active therapies, such as adoptive transfer of TCR-engineered T cells.[85] Therefore, we largely expanded our in-house benign database in the last years in terms of sample quantity as well as coverage of different cell types and tissues. Especially for the definition of LPC-associated antigens, we included enriched $CD34^+$ HPCs of healthy volunteers. Furthermore, we included additional PBMC samples of AML patients in molecular remission as benign samples in our comparative approach.

For the definition of broadly applicable AML- and LPC-associated target antigens, we not only focused on the establishment of an enriched LPC population but also on the formation of a novel increased AML immunopeptidomics database measured on a state-of-the-art tribrid mass spectrometer. Therefore, we could extremely increase the depth of AML immunopeptidomics compared to the previously published analysis of AML-associated targets.[21] With this new dataset we were able to define novel high frequent AML- and LPC-associated HLA class I- and class II-presented antigens for tailored T-cell-based approaches. Besides non-mutated self-antigens, we were indeed able to identify NPM1- and IDH2-derived neoantigens naturally presented on AML blasts on HLA class I and class II molecules, respectively. These results are in line with previously published studies, which demonstrated the presentation of NPM1-derived neoantigens on AML.[25, 27]

The still ongoing immunogenic characterization of these novel defined targets validated a panel of $CD8^+$ and $CD4^+$ T-cell epitopes. So far, we could detect only low frequent memory T-cell responses against single HLA class I-restricted targets in HVs and AML patients. Interestingly, these T-cell responses were elicited by $CD4^+$ T cells, which highlight the strong impact and central function of $CD4^+$ T cells as part of the anti-tumor immunity.[86] On the one hand, $CD4^+$ T cells are necessary for the optimal activation of cytotoxic $CD8^+$ T cells.[87, 88] But on the other hand, several groups already reported efficient anti-tumor immune responses mediated by $CD4^+$ T cells also in the absence of $CD8^+$ T cells.[72, 89-91] However, the exact mechanisms mediating tumor cell killing by $CD4^+$ T cells is not well understood so far. For tumor cells expressing HLA class II molecules on their surface direct cytotoxic effects via the Fas/Fas ligand[92] or the perforin/granzyme pathway[89] have been described. $CD4^+$ T-cell-mediated elimination of HLA class II-negative tumors takes place in an indirect manner via macrophages, natural killer cells, or angiostatic effects.[93-95] For HLA class II-restricted target peptides we discovered memory T-cell responses in up to 33% of AML patients and up to 28% of HVs indicating that anti-tumor $CD4^+$ T-cell responses are more frequently generated compared to $CD8^+$ T-cell responses. Notably, these T-cell responses seem to be very specific as no cross-reactivity against a viral peptide, with extreme similarity to one of our targets, could be detected.

Recently, the development of improved sequencing strategies enabled the identification of so-called benign clonal hematopoiesis of cells carrying mutations associated with AML and the discovery that clonal hematopoiesis is extremely common in 50 – 60 year old healthy individuals with frequencies up to 95%.[96] Our observed frequent memory $CD4^+$ T-cell responses might be a consequence of mutational events in healthy individuals resulting in epitope-spreading and T-cell responses also against unmutated AML-associated antigens. Nevertheless, we could not detect any correlation of detected T-cell responses in healthy individuals and the age of respective donors so far. Genes commonly affected by clonal hematopoiesis are especially genes of epigenetic modifiers such as DNMT3A and TET2.[96] Mutations in both genes were demonstrated to result in widespread DNA hyper- and hypomethylation,[97, 98] which might also influence the presentation of other unmutated AML-associated antigens.

In conclusion, our study demonstrated the feasibility of HLA ligand isolation of enriched LPCs and identified a panel of novel, immunogenic, non-mutated and mutated, AML- and LPC-associated $CD8^+$ and $CD4^+$ T-cell epitopes. These antigens could be utilized for the development of different antigen-specific immunotherapeutic approaches such as peptide-based vaccines, which may provide the opportunity to target LPCs and AML blasts more specifically especially in the context of MRD and thereby improve the long-term outcome of AML patients or even demonstrate curative potential.

6.3.6. REFERENCES

1. Cancer Stat Facts: Leukemia - Acute Myeloid Leukemia (AML). 2019; Available from: https://seer.cancer.gov/statfacts/html/amyl.html.
2. Hope KJ, Jin L, and Dick JE. Acute myeloid leukemia originates from a hierarchy of leukemic stem cell classes that differ in self-renewal capacity. *Nat Immunol* 5(7): 738-743 (2004).
3. van Rhenen A, Feller N, Kelder A, Westra AH, Rombouts E, Zweegman S, van der Pol MA, Waisfisz Q, Ossenkoppele GJ, and Schuurhuis GJ. High stem cell frequency in acute myeloid leukemia at diagnosis predicts high minimal residual disease and poor survival. *Clin Cancer Res* 11(18): 6520-6527 (2005).
4. Ishikawa F, Yoshida S, Saito Y, Hijikata A, Kitamura H, Tanaka S, Nakamura R, Tanaka T, Tomiyama H, Saito N, Fukata M, Miyamoto T, Lyons B, Ohshima K, Uchida N, Taniguchi S, Ohara O, Akashi K, Harada M, and Shultz LD. Chemotherapy-resistant human AML stem cells home to and engraft within the bone-marrow endosteal region. *Nat Biotechnol* 25(11): 1315-1321 (2007).
5. Buccisano F, Maurillo L, Del Principe MI, Del Poeta G, Sconocchia G, Lo-Coco F, Arcese W, Amadori S, and Venditti A. Prognostic and therapeutic implications of minimal residual disease detection in acute myeloid leukemia. *Blood* 119(2): 332-341 (2012).
6. Terwijn M, van Putten WL, Kelder A, van der Velden VH, Brooimans RA, Pabst T, Maertens J, Boeckx N, de Greef GE, Valk PJ, Preijers FW, Huijgens PC, Dräger AM, Schanz U, Jongen-Lavrecic M, Biemond BJ, Passweg JR, van Gelder M, Wijermans P, Graux C, Bargetzi M, Legdeur MC, Kuball J, de Weerdt O, Chalandon Y, Hess U, Verdonck LF, Gratama JW, Oussoren YJ, Scholten WJ, Slomp J, Snel AN, Vekemans MC, Löwenberg B, Ossenkoppele GJ, and Schuurhuis GJ. High prognostic impact of flow cytometric minimal residual disease detection in acute myeloid leukemia: data from the HOVON/SAKK AML 42A study. *J Clin Oncol* 31(31): 3889-3897 (2013).
7. Terwijn M, Zeijlemaker W, Kelder A, Rutten AP, Snel AN, Scholten WJ, Pabst T, Verhoef G, Löwenberg B, Zweegman S, Ossenkoppele GJ, and Schuurhuis GJ. Leukemic stem cell frequency: a strong biomarker for clinical outcome in acute myeloid leukemia. *PLoS One* 9(9): e107587 (2014).
8. Jawad M, Seedhouse C, Mony U, Grundy M, Russell NH, and Pallis M. Analysis of factors that affect in vitro chemosensitivity of leukaemic stem and progenitor cells to gemtuzumab ozogamicin (Mylotarg) in acute myeloid leukaemia. *Leukemia* 24(1): 74-80 (2010).
9. Kikushige Y, Shima T, Takayanagi S, Urata S, Miyamoto T, Iwasaki H, Takenaka K, Teshima T, Tanaka T, Inagaki Y, and Akashi K. TIM-3 Is a Promising Target to Selectively Kill Acute Myeloid Leukemia Stem Cells. *Cell Stem Cell* 7(6): 708-717 (2010).
10. Gadhoum SZ, Madhoun NY, Abuelela AF, and Merzaban JS. Anti-CD44 antibodies inhibit both mTORC1 and mTORC2: a new rationale supporting CD44-induced AML differentiation therapy. *Leukemia* 30(12): 2397-2401 (2016).
11. Papa V, Tazzari PL, Chiarini F, Cappellini A, Ricci F, Billi AM, Evangelisti C, Ottaviani E, Martinelli G, Testoni N, McCubrey JA, and Martelli AM. Proapoptotic activity and chemosensitizing effect of the novel Akt inhibitor perifosine in acute myelogenous leukemia cells. *Leukemia* 22(1): 147-160 (2008).
12. van der Helm LH, Bosman MC, Schuringa JJ, and Vellenga E. Effective targeting of primitive AML CD 34+ cells by the second-generation proteasome inhibitor carfilzomib. *Br J Haematol* 171(4): 652-655 (2015).
13. Horowitz MM, Gale RP, Sondel PM, Goldman J, Kersey J, Kolb H, Rimm A, Ringdén O, Rozman C, and Speck B. Graft-versus-leukemia reactions after bone marrow transplantation. *Blood* 75(3): 555-562 (1990).
14. Kolb H-J. Graft-versus-leukemia effects of transplantation and donor lymphocytes. *Blood* 112(12): 4371-4383 (2008).
15. Porter DL, Hwang WT, Frey NV, Lacey SF, Shaw PA, Loren AW, Bagg A, Marcucci KT, Shen A, Gonzalez V, Ambrose D, Grupp SA, Chew A, Zheng Z, Milone MC, Levine BL, Melenhorst JJ, and June CH. Chimeric antigen receptor T cells persist and induce sustained remissions in relapsed refractory chronic lymphocytic leukemia. *Sci Transl Med* 7(303): 303ra139 (2015).
16. Garfall AL, Maus MV, Hwang WT, Lacey SF, Mahnke YD, Melenhorst JJ, Zheng Z, Vogl DT, Cohen AD, Weiss BM, Dengel K, Kerr ND, Bagg A, Levine BL, June CH, and Stadtmauer EA. Chimeric Antigen Receptor T Cells against CD19 for Multiple Myeloma. *N Engl J Med* 373(11): 1040-1047 (2015).
17. Maude SL, Frey N, Shaw PA, Aplenc R, Barrett DM, Bunin NJ, Chew A, Gonzalez VE, Zheng Z, Lacey SF, Mahnke YD, Melenhorst JJ, Rheingold SR, Shen A, Teachey DT, Levine BL, June CH, Porter DL, and Grupp SA. Chimeric antigen receptor T cells for sustained remissions in leukemia. *N Engl J Med* 371(16): 1507-1517 (2014).
18. Kantarjian H, Stein A, Gökbuget N, Fielding AK, Schuh AC, Ribera JM, Wei A, Dombret H, Foà R, Bassan R, Arslan Ö, Sanz MA, Bergeron J, Demirkan F, Lech-Maranda E, Rambaldi A, Thomas X, Horst HA, Brüggemann M, Klapper W, Wood BL, Fleishman A, Nagorsen D, Holland C, Zimmerman Z, and Topp MS. Blinatumomab versus Chemotherapy for Advanced Acute Lymphoblastic Leukemia. *N Engl J Med* 376(9): 836-847 (2017).
19. Salles G, Barrett M, Foà R, Maurer J, O'Brien S, Valente N, Wenger M, and Maloney DG. Rituximab in B-Cell Hematologic Malignancies: A Review of 20 Years of Clinical Experience. *Adv Ther* 34(10): 2232-2273 (2017).
20. Hofmann M, Grosse-Hovest L, Nübling T, Pyż E, Bamberg ML, Aulwurm S, Bühring HJ, Schwartz K, Haen SP, Schilbach K, Rammensee H-G, Salih HR, and Jung G. Generation, selection and preclinical characterization of an Fc-optimized FLT3 antibody for the treatment of myeloid leukemia. *Leukemia* 26(6): 1228-1237 (2012).
21. Berlin C, Kowalewski DJ, Schuster H, Mirza N, Walz S, Handel M, Schmid-Horch B, Salih HR, Kanz L, Rammensee H-G, Stevanović S, and Stickel JS. Mapping the HLA ligandome landscape of acute myeloid leukemia: a targeted approach toward peptide-based immunotherapy. *Leukemia* 29(3): 647-659 (2015).

22. Bonnet D and Dick JE. Human acute myeloid leukemia is organized as a hierarchy that originates from a primitive hematopoietic cell. *Nat Med* 3(7): 730 (1997).
23. Lapidot T, Sirard C, Vormoor J, Murdoch B, Hoang T, Caceres-Cortes J, Minden M, Paterson B, Caligiuri MA, and Dick JE. A Cell Initiating Human Acute Myeloid Leukaemia after Transplantation into SCID Mice. *Nature* 367(6464): 645-648 (1994).
24. Greiner J, Ono Y, Hofmann S, Schmitt A, Mehring E, Götz M, Guillaume P, Döhner K, Mytilineos J, Döhner H, and Schmitt M. Mutated regions of nucleophosmin 1 elicit both CD4(+) and CD8(+) T-cell responses in patients with acute myeloid leukemia. *Blood* 120(6): 1282-1289 (2012).
25. van der Lee DI, Reijmers RM, Honders MW, Hagedoorn RS, de Jong RC, Kester MG, van der Steen DM, de Ru AH, Kweekel C, Bijen HM, Jedema I, Veelken H, van Veelen PA, Heemskerk MH, Falkenburg JHF, and Griffioen M. Mutated nucleophosmin 1 as immunotherapy target in acute myeloid leukemia. *J Clin Invest* 129(2): 774-785 (2019).
26. Bassani-Sternberg M, Bräunlein E, Klar R, Engleitner T, Sinitcyn P, Audehm S, Straub M, Weber J, Slotta-Huspenina J, Specht K, Martignoni ME, Werner A, Hein R, H. BD, Peschel C, Rad R, Cox J, Mann M, and Krackhardt AM. Direct identification of clinically relevant neoepitopes presented on native human melanoma tissue by mass spectrometry. *Nat Commun* 7: 13404 (2016).
27. Narayan R, Olsson N, Wagar LE, Medeiros BC, Meyer E, Czerwinski D, Khodadoust MS, Zhang L, Schultz L, Davis MM, Elias JE, and Levy R. Acute myeloid leukemia immunopeptidome reveals HLA presentation of mutated nucleophosmin. *PLoS One* 14(7): e0219547 (2019).
28. The Cancer Genome Atlas Research Network, Ley T, Miller C, Ding L, Raphael B, Mungall A, Robertson A, Hoadley K, Triche T, Laird P, Baty J, Fulton L, Fulton R, Heath S, Kalicki-Veizer J, Kandoth C, Klco J, Koboldt D, Kanchi K, Kulkarni S, Lamprecht T, Larson D, Lin L, Lu C, McLellan M, McMichael J, Payton J, Schmidt H, Spencer D, Tomasson M, Wallis J, Wartman L, Watson M, Welch J, Wendl M, Ally A, Balasundaram M, Birol I, Butterfield Y, Chiu R, Chu A, Chuah E, Chun H, Corbett R, Dhalla N, Guin R, He A, Hirst C, Hirst M, Holt R, Jones S, Karsan A, Lee D, Li H, Marra M, Mayo M, Moore R, Mungall K, Parker J, Pleasance E, Plettner P, Schein J, Stoll D, Swanson L, Tam A, Thiessen N, Varhol R, Wye N, Zhao Y, Gabriel S, Getz G, Sougnez C, Zou L, Leiserson M, Vandin F, Wu H, Applebaum F, Baylin S, Akbani R, Broom B, Chen K, Motter T, Nguyen K, Weinstein J, Zhang N, Ferguson M, Adams C, Black A, Bowen J, Gastier-Foster J, Grossman T, Lichtenberg T, Wise L, Davidsen T, Demchok J, Shaw K, Sheth M, Sofia H, Yang L, Downing J and Eley G. Genomic and Epigenomic Landscapes of Adult De Novo Acute Myeloid Leukemia. *N Engl J Med* 368(22): 2059-2074 (2013).
29. Kandoth C, McLellan MD, Vandin F, Ye K, Niu B, Lu C, Xie M, Zhang Q, McMichael JF, Wyczalkowski MA, Leiserson MDM, Miller CA, Welch JS, Walter MJ, Wendl MC, Ley TJ, Wilson RK, Raphael BJ, and Ding L. Mutational landscape and significance across 12 major cancer types. *Nature* 502(7471): 333-339 (2013).
30. Eisfeld AK, Mrózek K, Kohlschmidt J, Nicolet D, Orwick S, Walker CJ, Kroll KW, Blachly JS, Carroll AJ, Kolitz JE, Powell BL, Wang ES, Stone RM, de la Chapelle A, Byrd JC, and Bloomfield CD. The mutational oncoprint of recurrent cytogenetic abnormalities in adult patients with de novo acute myeloid leukemia. *Leukemia* 31(10): 2211-2218 (2017).
31. Falini B, Mecucci C, Tiacci E, Alcalay M, Rosati R, Pasqualucci L, La Starza R, Diverio D, Colombo E, Santucci A, Bigerna B, Pacini R, Pucciarini A, Liso A, Vignetti M, Fazi P, Meani N, Pettirossi V, Saglio G, Mandelli F, Lo-Coco F, Pelicci PG, and Martelli MF. Cytoplasmic nucleophosmin in acute myelogenous leukemia with a normal karyotype. *N Engl J Med* 352(3): 254-266 (2005).
32. Stirewalt DL and Radich JP. The role of FLT3 in haematopoietic malignancies. *Nat Rev Cancer* 3(9): 650-665 (2003).
33. Patel JP, Gönen M, Figueroa ME, Fernandez H, Sun Z, Racevskis J, Van Vlierberghe P, Dolgalev I, Thomas S, Aminova O, Huberman K, Cheng J, Viale A, Socci ND, Heguy A, Cherry A, Vance G, Higgins RR, Ketterling RP, Gallagher RE, Litzow M, van den Brink MR, Lazarus HM, Rowe JM, Luger S, Ferrando A, Paietta E, Tallman MS, Melnick A, Abdel-Wahab O, and Levine RL. Prognostic relevance of integrated genetic profiling in acute myeloid leukemia. *N Engl J Med* 366(12): 1079-1089 (2012).
34. Yamashita Y, Yuan J, Suetake I, Suzuki H, Ishikawa Y, Choi YL, Ueno T, Soda M, Hamada T, Haruta H, Takada S, Miyazaki Y, Kiyoi H, Ito E, Naoe T, Tomonaga M, Toyota M, Tajima S, Iwama A, and Mano H. Array-based genomic resequencing of human leukemia. *Oncogene* 29(25): 3723-3731 (2010).
35. Ley TJ, Ding L, Walter MJ, McLellan MD, Lamprecht T, Larson DE, Kandoth C, Payton JE, Baty J, Welch J, Harris CC, Lichti CF, Townsend RR, Fulton RS, Dooling DJ, Koboldt DC, Schmidt H, Zhang Q, Osborne JR, Lin L, O'Laughlin M, McMichael JF, Delehaunty KD, McGrath SD, Fulton LA, Magrini VJ, Vickery TL, Hundal J, Cook LL, Conyers JJ, Swift GW, Reed JP, Alldredge PA, Wylie T, Walker J, Kalicki J, Watson MA, Heath S, Shannon WD, Varghese N, Nagarajan R, Westervelt P, Tomasson MH, Link DC, Graubert TA, DiPersio JF, Mardis ER, and Wilson RK. DNMT3A mutations in acute myeloid leukemia. *N Engl J Med* 363(25): 2424-2433 (2010).
36. Mardis ER, Ding L, Dooling DJ, Larson DE, McLellan MD, Chen K, Koboldt DC, Fulton RS, Delehaunty KD, McGrath SD, Fulton LA, Locke DP, Magrini VJ, Abbott RM, Vickery TL, Reed JS, Robinson JS, Wylie T, Smith SM, Carmichael L, Eldred JM, Harris CC, Walker J, Peck JB, Du F, Dukes AF, Sanderson GE, Brummett AM, Clark E, McMichael JF, Meyer RJ, Schindler JK, Pohl CS, Wallis JW, Shi X, Lin L, Schmidt H, Tang Y, Haipek C, Wiechert ME, Ivy JV, Kalicki J, Elliott G, Ries RE, Payton JE, Westervelt P, Tomasson MH, Watson MA, Baty J, Heath S, Shannon WD, Nagarajan R, Link DC, Walter MJ, Graubert TA, DiPersio JF, Wilson RK, and Ley TJ. Recurring mutations found by sequencing an acute myeloid leukemia genome. *N Engl J Med* 361(11): 1058-1066 (2009).
37. Nelde A, Kowalewski DJ, Backert L, Schuster H, Werner JO, Klein R, Kohlbacher O, Kanz L, Salih HR, Rammensee HG, Stevanovic S, and Walz JS. HLA ligandome analysis of primary chronic lymphocytic leukemia (CLL) cells under lenalidomide treatment confirms the suitability of lenalidomide for combination with T-cell-based immunotherapy. *Oncoimmunology* 128(22): 3234 (2018).

38. Wang X, Shook J, Edinger M, Warner N, and Bush-Donovan C. Multiparametric immunophenotyping of human hematopoietic stem cells and progenitor cells by flowcytometry. *Sanjase CA: BD Biosciences* (2012).
39. Seita J and Weissman IL. Hematopoietic stem cell: self-renewal versus differentiation. *Wiley Interdiscip Rev Syst Biol Med* 2(6): 640-653 (2010).
40. Paczulla AM, Dirnhofer S, Konantz M, Medinger M, Salih HR, Rothfelder K, Tsakiris DA, Passweg JR, Lundberg P, and Lengerke C. Long-term observation reveals high-frequency engraftment of human acute myeloid leukemia in immunodeficient mice. *Haematologica* 102(5): 854-864 (2017).
41. Nelde A, Kowalewski DJ, and Stevanović S. Purification and Identification of Naturally Presented MHC Class I and II Ligands. In *Antigen Processing*. (2019) Springer. p. 123-136.
42. Kowalewski DJ, Schuster H, Backert L, Berlin C, Kahn S, Kanz L, Salih HR, Rammensee H-G, Stevanović S, and Stickel JS. HLA ligandome analysis identifies the underlying specificities of spontaneous antileukemia immune responses in chronic lymphocytic leukemia (CLL). *Proc Natl Acad Sci U S A* 112(2): E166-E175 (2015).
43. Eng JK, McCormack AL, and Yates JR. An approach to correlate tandem mass spectral data of peptides with amino acid sequences in a protein database. *J Am Soc Mass Spectrom* 5(11): 976-989 (1994).
44. Käll L, Canterbury JD, Weston J, Noble WS, and MacCoss MJ. Semi-supervised learning for peptide identification from shotgun proteomics datasets. *Nat Methods* 4(11): 923-925 (2007).
45. Nielsen M and Andreatta M. NetMHCpan-3.0; improved prediction of binding to MHC class I molecules integrating information from multiple receptor and peptide length datasets. *Genome Med* 8(1): 33 (2016).
46. Hoof I, Peters B, Sidney J, Pedersen LE, Sette A, Lund O, Buus S, and Nielsen M. NetMHCpan, a method for MHC class I binding prediction beyond humans. *Immunogenetics* 61(1): 1-13 (2009).
47. Rammensee H-G, Bachmann J, Emmerich NP, Bachor OA, and Stevanovic S. SYFPEITHI: database for MHC ligands and peptide motifs. *Immunogenetics* 50(3-4): 213-9 (1999).
48. Forbes SA, Beare D, Boutselakis H, Bamford S, Bindal N, Tate J, Cole CG, Ward S, Dawson E, Ponting L, Stefancsik R, Harsha B, Kok CY, Jia M, Jubb H, Sondka Z, Thompson S, De T, and Campbell PJ. COSMIC: somatic cancer genetics at high-resolution. *Nucleic Acids Res* 45(D1): D777-D783 (2017).
49. Smith CC, Wang Q, Chin CS, Salerno S, Damon LE, Levis MJ, Perl AE, Travers KJ, Wang S, Hunt JP, Zarrinkar PP, Schadt EE, Kasarskis A, Kuriyan J, and Shah NP. Validation of ITD mutations in FLT3 as a therapeutic target in human acute myeloid leukaemia. *Nature* 485(7397): 260-263 (2012).
50. Opatz S, Polzer H, Herold T, Konstandin NP, Ksienzyk B, Zellmeier E, Vosberg S, Graf A, Krebs S, Blum H, Hopfner KP, Kakadia PM, Schneider S, Dufour A, Braess J, Sauerland MC, Berdel WE, Büchner T, Woermann BJ, Hiddemann W, Spiekermann K, Bohlander SK, and Greif PA. Exome sequencing identifies recurring FLT3 N676K mutations in core-binding factor leukemia. *Blood* 122(10): 1761-1769 (2013).
51. Bacher U, Haferlach C, Kern W, Haferlach T, and Schnittger S. Prognostic relevance of FLT3-TKD mutations in AML: the combination matters--an analysis of 3082 patients. *Blood* 111(5): 2527-2537 (2008).
52. Thiede C, Steudel C, Mohr B, Schaich M, Schäkel U, Platzbecker U, Wermke M, Bornhäuser M, Ritter M, Neubauer A, Ehninger G, and Illmer T. Analysis of FLT3-activating mutations in 979 patients with acute myelogenous leukemia: association with FAB subtypes and identification of subgroups with poor prognosis. *Blood* 99(12): 4326-4335 (2002).
53. Vempati S, Reindl C, Kaza SK, Kern R, Malamoussi T, Dugas M, Mellert G, Schnittger S, Hiddemann W, and Spiekermann K. Arginine 595 is duplicated in patients with acute leukemias carrying internal tandem duplications of FLT3 and modulates its transforming potential. *Blood* 110(2): 686-694 (2007).
54. Yamamoto Y, Kiyoi H, Nakano Y, Suzuki R, Kodera Y, Miyawaki S, Asou N, Kuriyama K, Yagasaki F, Shimazaki C, Akiyama H, Saito K, Nishimura M, Motoji T, Shinagawa K, Takeshita A, Saito H, Ueda R, Ohno R, and Naoe T. Activating mutation of D835 within the activation loop of FLT3 in human hematologic malignancies. *Blood* 97(8): 2434-2439 (2001).
55. Walz S, Stickel JS, Kowalewski DJ, Schuster H, Weisel K, Backert L, Kahn S, Nelde A, Stroh T, Handel M, Kohlbacher O, Kanz L, Salih HR, Rammensee H-G, and Stevanović S. The antigenic landscape of multiple myeloma: mass spectrometry (re)defines targets for T-cell-based immunotherapy. *Blood* 126(10): 1203-1213 (2015).
56. Widenmeyer M, Griesemann H, Stevanović S, Feyerabend S, Klein R, Attig S, Hennenlotter J, Wernet D, Kuprash DV, Sazykin AY, Pascolo S, Stenzl A, Gouttefangeas C, and Rammensee H-G. Promiscuous survivin peptide induces robust CD4+ T-cell responses in the majority of vaccinated cancer patients. *Int J Cancer* 131(1): 140-149 (2012).
57. Britten CM, Gouttefangeas C, Welters MJ, Pawelec G, Koch S, Ottensmeier C, Mander A, Walter S, Paschen A, Müller-Berghaus J, Haas I, Mackensen A, Køllgaard T, thor Straten P, Schmitt M, Giannopoulos K, Maier R, Veelken H, Bertinetti C, Konur A, Huber C, Stevanović S, Wölfel T, and van der Burg SH. The CIMT-monitoring panel: a two-step approach to harmonize the enumeration of antigen-specific CD8+ T lymphocytes by structural and functional assays. *Cancer Immunol Immunother* 57(3): 289-302 (2008).
58. Schuster H, Peper JK, Bösmüller HC, Röhle K, Backert L, Bilich T, Ney B, Löffler MW, Kowalewski DJ, Trautwein N, Rabsteyn A, Engler T, Braun S, Haen SP, Walz JS, Schmid-Horch B, Brucker SY, Wallwiener D, Kohlbacher O, Fend F, Rammensee H-G, Stevanović S, Staebler A, and Wagner P. The immunopeptidomic landscape of ovarian carcinomas. *Proc Natl Acad Sci U S A* 114(46): E9942-E9951 (2017).
59. Walter S, Herrgen L, Schoor O, Jung G, Wernet D, Bühring HJ, Rammensee H-G, and Stevanović S. Cutting edge: predetermined avidity of human CD8 T cells expanded on calibrated MHC/anti-CD28-coated microspheres. *J Immunol* 171(10): 4974-4978 (2003).
60. Neumann A, Hörzer H, Hillen N, Klingel K, Schmid-Horch B, Bühring HJ, Rammensee H-G, Aebert H, and Stevanović S. Identification of HLA ligands and T-cell epitopes for immunotherapy of lung cancer. *Cancer Immunol Immunother* 62(9): 1485-1497 (2013).

61. Nelde A, Walz JS, Kowalewski DJ, Schuster H, Wolz OO, Peper JK, Cardona Gloria Y, Langerak AW, Muggen AF, Claus R, Bonzheim I, Fend F, Salih HR, Kanz L, Rammensee HG, Stevanovic S, and Weber AN. HLA class I-restricted MYD88 L265P-derived peptides as specific targets for lymphoma immunotherapy. *Oncoimmunology* 126(23): 2750 (2017).
62. Hermans IF, Silk JD, Yang J, Palmowski MJ, Gileadi U, McCarthy C, Salio M, Ronchese F, and Cerundolo V. The VITAL assay: a versatile fluorometric technique for assessing CTL- and NKT-mediated cytotoxicity against multiple targets in vitro and in vivo. *J Immunol Methods* 285(1): 25-40 (2004).
63. Hulsen T, de Vlieg J, and Alkema W. BioVenn - a web application for the comparison and visualization of biological lists using area-proportional Venn diagrams. *BMC Genomics* 9: 488 (2008).
64. Bui HH, Sidney J, Dinh K, Southwood S, Newman MJ, and Sette A. Predicting population coverage of T-cell epitope-based diagnostics and vaccines. *BMC Bioinform* 7: 153 (2006).
65. Vita R, Overton JA, Greenbaum JA, Ponomarenko J, Clark JD, Cantrell JR, Wheeler DK, Gabbard JL, Hix D, Sette A, and Peters B. The immune epitope database (IEDB) 3.0. *Nucleic Acids Res* 43(Database issue): D405-D412 (2015).
66. Hu Q, Noll RJ, Li H, Makarov A, Hardman M, and Cooks RG. The Orbitrap: a new mass spectrometer. *J Mass Spectrom* 40(4): 430-443 (2005).
67. Hardman M and Makarov AA. Interfacing the orbitrap mass analyzer to an electrospray ion source. *Anal Chem* 75(7): 1699-1705 (2003).
68. Freudenmann LK, Marcu A, and Stevanović S. Mapping the tumour human leukocyte antigen (HLA) ligandome by mass spectrometry. *Immunology* 154(3): 331-345 (2018).
69. Schoenberger SP, Toes RE, van der Voort EI, Offringa R, and Melief CJ. T-cell help for cytotoxic T lymphocytes is mediated by CD40-CD40L interactions. *Nature* 393(6684): 480-483 (1998).
70. Janssen EM, Lemmens EE, Wolfe T, Christen U, von Herrath MG, and Schoenberger SP. CD4+ T cells are required for secondary expansion and memory in CD8+ T lymphocytes. *Nature* 421(6925): 852-856 (2003).
71. Mumberg D, Monach PA, Wanderling S, Philip M, Toledano AY, Schreiber RD, and Schreiber H. $CD4^+$ T cells eliminate MHC class II-negative cancer cells in vivo by indirect effects of IFN-γ. *Proc Natl Acad Sci U S A* 96(15): 8633-8638 (1999).
72. Perez-Diez A, Joncker NT, Choi K, Chan WF, Anderson CC, Lantz O, and Matzinger P. CD4 cells can be more efficient at tumor rejection than CD8 cells. *Blood* 109(12): 5346-5354 (2007).
73. Bilich T, Nelde A, Bichmann L, Roerden M, Salih HR, Kowalewski DJ, Schuster H, Tsou CC, Marcu A, Neidert MC, Lübke M, Rieth J, Schemionek M, Brümmendorf TH, Vucinic V, Niederwieser D, Bauer J, Märklin M, Peper JK, Klein R, Kohlbacher O, Kanz L, Rammensee H-G, Stevanović S, and Walz JS. The HLA ligandome landscape of chronic myeloid leukemia delineates novel T-cell epitopes for immunotherapy. *Blood* 133(6): 550-565 (2019).
74. Schlott F, Steubl D, Ameres S, Moosmann A, Dreher S, Heemann U, Hösel V, Busch DH, and Neuenhahn M. Characterization and clinical enrichment of HLA-C* 07: 02-restricted Cytomegalovirus-specific CD8+ T cells. *PLoS One* 13(2): e0193554 (2018).
75. Schmidt AH, Baier D, Solloch UV, Stahr A, Cereb N, Wassmuth R, Ehninger G, and Rutt C. Estimation of high-resolution HLA-A,-B,-C,-DRB1 allele and haplotype frequencies based on 8862 German stem cell donors and implications for strategic donor registry planning. *Hum Immunol* 70(11): 895-902 (2009).
76. Sherry ST, Ward MH, Kholodov M, Baker J, Phan L, Smigielski EM, and Sirotkin K. dbSNP: the NCBI database of genetic variation. *Nucleic Acids Res* 29(1): 308-311 (2001).
77. Kinjo AR, Bekker GJ, Wako H, Endo S, Tsuchiya Y, Sato H, Nishi H, Kinoshita K, Suzuki H, Kawabata T, Yokochi M, Iwata T, Kobayashi N, Fujiwara T, Kurisu G, and Nakamura H. New tools and functions in data-out activities at Protein Data Bank Japan (PDBj). *Protein Sci* 27(1): 95-102 (2018).
78. Kinjo AR, Bekker GJ, Suzuki H, Tsuchiya Y, Kawabata T, Ikegawa Y, and Nakamura H. Protein Data Bank Japan (PDBj): updated user interfaces, resource description framework, analysis tools for large structures. *Nucleic Acids Res* 45(D1): D282-D288 (2017).
79. UniProt: a worldwide hub of protein knowledge. *Nucleic Acids Res* 47(D1): D506-D515 (2019).
80. Sievers F, Wilm A, Dineen D, Gibson TJ, Karplus K, Li W, Lopez R, McWilliam H, Remmert M, Söding J, Thompson JD, and Higgins DG. Fast, scalable generation of high-quality protein multiple sequence alignments using Clustal Omega. *Mol Syst Biol* 7: 539 (2011).
81. Rajarathnam K, Li Y, Rohrer T, and Gentz R. Solution structure and dynamics of myeloid progenitor inhibitory factor-1 (MPIF-1), a novel monomeric CC chemokine. *J Biol Chem* 276(7): 4909-4916 (2001).
82. Crump MP, Elisseeva E, Gong J, Clark-Lewis I, and Sykes BD. Structure/function of human herpesvirus-8 MIP-II (1-71) and the antagonist N-terminal segment (1-10). *FEBS Lett* 489(2-3): 171-175 (2001).
83. Berkhout TA, Gohil J, Gonzalez P, Nicols CL, Moores KE, Macphee CH, White JR, and Groot PH. Selective binding of the truncated form of the chemokine CKbeta8 (25-99) to CC chemokine receptor 1(CCR1). *Biochem Pharmacol* 59(5): 591-596 (2000).
84. Qin L, Kufareva I, Holden LG, Wang C, Zheng Y, Zhao C, Fenalti G, Wu H, Han GW, Cherezov V, Abagyan R, Stevens RC, and Handel TM. Structural biology. Crystal structure of the chemokine receptor CXCR4 in complex with a viral chemokine. *Science* 347(6226): 1117-1122 (2015).
85. Morgan RA, Chinnasamy N, Abate-Daga D, Gros A, Robbins PF, Zheng Z, Dudley ME, Feldman SA, Yang JC, Sherry RM, Phan GQ, Hughes MS, Kammula US, Miller AD, Hessman CJ, Stewart AA, Restifo NP, Quezado MM, Alimchandani M, Rosenberg AZ, Nath A, Wang T, Bielekova B, Wuest SC, Akula N, McMahon FJ, Wilde S, Mosetter B, Schendel DJ, Laurencot CM, and Rosenberg SA. Cancer regression and neurological toxicity following anti-MAGE-A3 TCR gene therapy. *J Immunother* 36(2): 133-151 (2013).

86. Ostrand-Rosenberg S. CD4+ T lymphocytes: a critical component of antitumor immunity. *Cancer Invest* 23(5): 413-419 (2005).
87. Ossendorp F, Mengedé E, Camps M, Filius R, and Melief CJ. Specific T helper cell requirement for optimal induction of cytotoxic T lymphocytes against major histocompatibility complex class II negative tumors. *J Exp Med* 187(5): 693-702 (1998).
88. Surman DR, Dudley ME, Overwijk WW, and Restifo NP. Cutting edge: CD4+ T cell control of CD8+ T cell reactivity to a model tumor antigen. *J Immunol* 164(2): 562-565 (2000).
89. Quezada SA, Simpson TR, Peggs KS, Merghoub T, Vider J, Fan X, Blasberg R, Yagita H, Muranski P, Antony PA, Restifo NP, and Allison JP. Tumor-reactive CD4(+) T cells develop cytotoxic activity and eradicate large established melanoma after transfer into lymphopenic hosts. *J Exp Med* 207(3): 637-650 (2010).
90. Muranski P, Boni A, Antony PA, Cassard L, Irvine KR, Kaiser A, Paulos CM, Palmer DC, Touloukian CE, Ptak K, Gattinoni L, Wrzesinski C, Hinrichs CS, Kerstann KW, Feigenbaum L, Chan CC, and Restifo NP. Tumor-specific Th17-polarized cells eradicate large established melanoma. *Blood* 112(2): 362-373 (2008).
91. Fujiwara H, Fukuzawa M, Yoshioka T, Nakajima H, and Hamaoka T. The role of tumor-specific Lyt-1+2- T cells in eradicating tumor cells in vivo. I. Lyt-1+2- T cells do not necessarily require recruitment of host's cytotoxic T cell precursors for implementation of in vivo immunity. *J Immunol* 133(3): 1671-1676 (1984).
92. Lundin KU, Screpanti V, Omholt H, Hofgaard PO, Yagita H, Grandien A, and Bogen B. CD4+ T cells kill Id+ B-lymphoma cells: FasLigand-Fas interaction is dominant in vitro but is redundant in vivo. *Cancer Immunol Immunother* 53(12): 1135-1145 (2004).
93. Corthay A, Lundin KU, Lorvik KB, Hofgaard PO, and Bogen B. Secretion of tumor-specific antigen by myeloma cells is required for cancer immunosurveillance by CD4+ T cells. *Cancer Res* 69(14): 5901-5907 (2009).
94. Haabeth OA, Lorvik KB, Hammarström C, Donaldson IM, Haraldsen G, Bogen B, and Corthay A. Inflammation driven by tumour-specific Th1 cells protects against B-cell cancer. *Nat Commun* 2: 240 (2011).
95. Bogen B, Fauskanger M, Haabeth OA, and Tveita A. $CD4^+$ T cells indirectly kill tumor cells via induction of cytotoxic macrophages in mouse models. *Cancer Immunol Immunother* (2019).
96. Young AL, Challen GA, Birmann BM, and Druley TE. Clonal haematopoiesis harbouring AML-associated mutations is ubiquitous in healthy adults. *Nat Commun* 7: 12484 (2016).
97. Rasmussen KD, Jia G, Johansen JV, Pedersen MT, Rapin N, Bagger FO, Porse BT, Bernard OA, Christensen J, and Helin K. Loss of TET2 in hematopoietic cells leads to DNA hypermethylation of active enhancers and induction of leukemogenesis. *Genes Dev* 29(9): 910-922 (2015).
98. Sandoval JE, Huang Y-H, Muise A, Goodell MA, and Reich NO. Mutations in the DNMT3A DNA methyltransferase in acute myeloid leukemia patients cause both loss and gain of function and differential regulation by protein partners. *J Biol Chem* 294(13): 4898-4910 (2019).

7. GENERAL DISCUSSION AND PERSPECTIVE

Cancer immunotherapy has undergone a breakthrough by the development and clinical success of immune checkpoint inhibitors.[1-3] In recent years, several antigen-specific T-cell-based immunotherapeutic studies[4-12] including peptide vaccination trials in solid tumors[4-6] and hematologic malignancies[8-10] have reported promising results in terms of *in vivo* immunogenicity of the vaccinated peptides and clinical responses. However, until now clinical effectiveness is limited to a minority of patients. To further improve T-cell-based immunotherapeutic approaches targeting HLA-presented peptides several factors such as optimal targets, time points of interventions, administration routes, adjuvants, or combination therapies need to be addressed, further developed, and improved. One main critical issue for effective antigen-based immunotherapy is based on the selection of suitable and broadly applicable antigen targets. These targets should be naturally presented with a high frequency and exclusively on tumor cells and should be further recognized by the T cells of the patients. Numerous studies have suggested mutation-derived neoepitopes as key antigens of anti-tumor T-cell responses after checkpoint inhibitor therapy in solid tumors.[13-15] However, the role of neoantigens and neoantigen-based T-cell responses in low mutational burden cancer entities such as leukemia still remains unclear. For CML, we therefore extensively screened our immunopeptidome dataset for BCR-ABL- and ABL-BCR-derived peptides without identifying any presented neoepitopes. Notably, for AML we were indeed able to identify and validate naturally presented HLA class I- and class II-restricted neoepitopes derived from recurrent mutations in NPM1 and IDH2 by mass spectrometry verifying the results of previously published studies.[16, 17] These results are encouraging and surprising since hematological malignancies in general show only a very low mutational burden,[18] as compared to other solid cancer entities. Several studies have emphasized that only a very small fraction of mutations at the DNA sequence level results in peptides naturally presented in the immunopeptidome of malignant cells.[4, 19-22] In detail, for various murine tumor cell lines several groups reported that the frequency of naturally presented neoantigens, calculated based on the total number of somatic non-synonymous mutations, solely ranged from 0.00% to 0.16%.[13, 21] Similar data is available for primary human tumor samples with frequencies ranging from 0.00% to 1.25% per sample.[20] Constant development of better and more sensitive mass spectrometers, improved acquisition methods, and novel bioinformatic data analysis such as *de novo* sequencing tools will allow the characterization of the immunopeptidome in even greater depth in the future.[23] Nevertheless, neoantigens in low mutational burden leukemia remain rare events and only have limited applicability for broad single peptide-based immunotherapy approaches. Furthermore, several studies have reported specific T-cell responses against *in silico* predicted peptides of CTAs or LAAs such as PRAME, PR1, and WT1.[24-27] For CML, we therefore extensively analyzed the role of such

published CTAs and LAAs in the immunopeptidome of primary CML samples, which were previously defined on the basis of transcriptional overexpression in malignant cells. Interestingly, we could demonstrate that these CTA- and LAA-derived peptides are mainly not exclusively presented on CML cells but are also presented on benign tissue samples and are therefore excluded as suitable targets in our analysis. These observations go hand in hand with previous studies, which have shown a very distorted correlation of gene expression and HLA-restricted antigen presentation and demonstrate that the immunopeptidome represents an independent level, formed by the cellular antigen presentation machinery, which is neither mirrored by the transcriptome nor the proteome.[20, 28-30] In our opinion this underlines the importance of the direct mass spectrometry-based analysis of the immunopeptidome of malignant cells and benign samples as comparative negative control for the identification and selection of suitable tumor-associated antigens. Due to the non-CML-exclusive presentation of the majority of published CTAs and LAAs in our dataset, we excluded them as suitable targets for T-cell-based immunotherapy as the lack of tumor-specificity can cause severe side effects, especially if these antigens should be used in highly active therapies, such as adoptive transfer of TCR-engineered T cells.[31] Nevertheless, one has to keep in mind that tumor-exclusivity can either be assessed on the level of HLA ligands or on the level of the entire antigen. The CTA and LAA analysis within this thesis and other studies[29, 32] was performed on the level of entire antigens and does not consider presentation of CTA- and LAA-derived single HLA ligands as these could potentially be tumor-exclusive due to differential antigen processing in malignant cells. One example for this is represented by the LAA PCNA, which shows only a CML-overrepresented characteristic on the entire antigen level. But still, the PCNA-derived HLA-A*03-restricted peptide RLVQGSILKK was identified in our analysis as CML-associated target antigen, due to the exclusive and highly frequent presentation of this single peptide in CML, and is thereby classified as a novel target for CML immunotherapy. For AML the overexpression of FLT3 in FLT3-mutated as well as unmutated blasts is well investigated.[33] Nevertheless, FLT3-derived HLA ligands are also presented on benign cells. But with the novel established method of hotspot clustering, we were able to identify HLA class II-restricted FLT3-derived peptides exclusively presented on AML blasts, which are therefore suitable for T-cell-based immunotherapy approaches in AML patients even without FLT3 mutation. These differences between HLA ligand and entire antigen level are furthermore emphasized by the comparison between the AML-associated antigens defined in a previous work of our group[29] and the ones identified within this study. Berlin *et al.* defined AML-associated antigens by comparative profiling of HLA class I source proteins of 15 primary AML patient samples with 30 PBMC and 5 BNMC samples of HVs, whereas here, we utilized an HLA allotype-specific HLA ligand-based definition of target antigens. The results provided in the study at hand clearly demonstrated the differences between those two approaches of target definition. Furthermore, those two studies differ also in other parts

and reflect the technical progress between the different mass spectrometers used for peptide identification as well as the size and depth of the benign immunopeptidome database used as comparative dataset. The impressive technical progress in mass spectrometry-based technologies over the last years provided the opportunity to nowadays identify several thousand peptides in a single mass spectrometry run and thereby analyze the immunopeptidome in greater depth.[23] Furthermore, since the publication in 2015[29], we were able to immensely increase our in-house benign tissue database not only in terms of sample numbers, but also by including a huge set of various different cell types (*e.g.* granulocytes, B cells, HPCs) and tissues (*e.g.* spleen, liver, bone marrow, kidney, brain).

Our group strongly focuses on an entity-specific approach since we could show in a previous extensive meta-analysis of different hematological malignancies that entity-spanning antigens are very rare and are predominantly characterized by low presentation frequencies.[34] This is emphasized by the results presented in this thesis for CML and AML. Solely, 2/427 (0.5%) AML-associated HLA class I antigens and 0/45 (0.0%) AML-associated HLA class II antigens were also identified as CML-associated antigens, although both leukemias are myeloid-derived neoplasms. This highlights again the need for the identification and formulation of entity-specific peptide vaccinations. For AML, we additionally performed subgroup analysis to identify alterations between immunopeptidomes of FLT3-mutated and unmutated samples. Interestingly, we identified only minor unspecific differences between the two cohorts, which could not clearly be explained by the mutation of FLT3. Oncogenic FLT3 including ITD as well as TKD mutations results in the constitutive activation of the FLT3 kinase and its downstream signaling pathways,[35] which might contribute to an altered immunopeptidome compared to FLT3-unmutated blasts. Nevertheless, increased FLT3 transcript levels[36] and FLT3 phosphorylation[37] are also observed in the majority of FLT3-unmutated AML, which may also contribute to the activation of FLT3 downstream pathways.[35] This aspect is supported by our subgroup analysis showing no obvious alterations in the immunopeptidome and the presentation of the majority of novel defined AML-associated targets on both clinical subgroups. Nevertheless, further subgroup analysis will investigate in more detail also the differences in the immunopeptidome between NPM1-mutated and -unmutated samples, pretreated versus untreated patient samples as well as between different ELN subgroups.

Besides the identification of novel suitable antigens, the further development of more potent adjuvants and combination therapies for T-cell-based immunotherapeutic approaches might help to improve the clinical effectiveness and success of such therapies. Especially for malignancies with profound immune defects such as described for CLL,[38-40] combinatorial therapies of T-cell-based immunotherapy approaches with systemic immunomodulatory agents such as lenalidomide or immune checkpoint inhibitors could overcome this immune impairment and might improve clinical

effectiveness of antigen-specific immunotherapies. For such combinations it is indispensable to thoroughly characterize and investigate the effect of the immunomodulatory agent on the immunopeptidome of the target cells to assure that the target structures for T-cell-based immunotherapy are robustly presented even under treatment with the combinatorial agent. It was already demonstrated that for example proteasome inhibitors remarkably impact antigen presentation, alter the immunopeptidome, and impair specific T-cell responses.[41-45] For low dose lenalidomide treatment we could confirm stable presentation of CLL-associated antigens and only minor qualitative and quantitative changes in the complete immunopeptidome of primary CLL cells were detected, qualifying lenalidomide as suitable combination partner for antigen-specific T-cell-based immunotherapeutic approaches. Based on these results we implemented a phase II peptide vaccination trial for CLL patients combining our CLL-associated HLA ligands[46] with lenalidomide treatment (NCT02802943).[47] Based on the recommendation of the data safety monitoring board, the treatment of MRD-positive patients with lenalidomide however has been discontinued as a precautionary step due to the fact that in the CLLM1 trial (NCT01556776) a few patients developed ALL after lenalidomide administration. Interestingly, in our *in vitro* experiments the treatment of lenalidomide induces the presentation of novel treatment-associated peptides derived from IKZF1 and IKZF3. These results highlight a further opportunity of combination therapies as those treatment-induced peptides might be suitable rejection antigens for antigen-specific immunotherapy-based treatment of patients undergoing such therapies. Furthermore, in recent years, several studies investigated the impact of different small molecule drugs such as decitabine[48] or chemical inhibitors such as ERAP1 inhibitors[49] for the targeted manipulation of the immunopeptidome of cancer cells. The inhibition of DNA methylation or the impairment of antigen processing resulted in novel antigenic peptides especially on cancer cells. For example ERAP1 inhibition could restore the presentation of tumor-associated antigenic peptides that are destroyed by cancer-specific up-regulation of ERAP1.[50-52] Such approaches could be utilized pharmacologically for the induction of antigenic shifts resulting in an enhanced drug-induced immunogenicity of cancer cells.

With the immunopeptidomics datasets acquired within this thesis several other interesting questions could be addressed in further studies. In recent years, researchers have begun to focus more and more on HLA-presented cryptic peptides and especially their role in anti-tumor immunity.[53-55] Cryptic peptides include proteasomal splice products, non-canonical translation products such as non-coding sequences (introns, 5´-UTRs, 3´-UTRs), or antisense transcripts.[55-59] In further work, we will analyze our here established leukemia immunopeptidomics datasets to screen for cryptic peptides either by *de novo* sequencing workflows[60, 61] or by utilizing dedicated protein databases (FASTAs) including cryptic peptide products as identified by ribosome profiling[55] to identify tumor-associated cryptic peptides as additional targets for T-cell-based immunotherapeutic approaches.

One additional interesting question to be further examined might be the contribution of our here defined tumor-associated HLA-presented targets to the soluble immunopeptidome identifiable in the plasma of cancer patients. Soluble HLA molecules (sHLA) could be identified in the plasma of patients suffering from different cancer entities.[62, 63] Peptides derived from sHLA may even predict response to therapy[63] or serve as biomarkers.[64-66]

The intended and already partially reached objective of our basic research on the immunopeptidome of hematological malignancies[29, 46, 67] is finally the translation into clinical application of personalized cancer immunotherapies especially of personalized peptide-based vaccinations. For CLL, we could initiate and are currently conducting a patient-individualized peptide vaccination multicentric clinical phase II study for CLL patients (iVAC-CLL01, NCT02802943) employing the CLL-associated HLA peptides identified with our mass spectrometry-based approach. With the results of the studies at hand such personalized peptide vaccination trials become now even feasible for AML and CML patients. I am convinced that peptide-based immunotherapies and especially peptide vaccination approaches will find their way into the clinic and with suitable combination therapies and optimal adjuvants will contribute to further improve the survival of leukemia patients in the future.

References

1. Wolchok JD, Kluger H, Callahan MK, Postow MA, Rizvi NA, Lesokhin AM, Segal NH, Ariyan CE, Gordon RA, Reed K, Burke MM, Caldwell A, Kronenberg SA, Agunwamba BU, Zhang X, Lowy I, Inzunza HD, Feely W, Horak CE, Hong Q, Korman AJ, Wigginton JM, Gupta A, and Sznol M. Nivolumab plus ipilimumab in advanced melanoma. *N Engl J Med* 369(2): 122-133 (2013).
2. Topalian SL, Hodi FS, Brahmer JR, Gettinger SN, Smith DC, McDermott DF, Powderly JD, Carvajal RD, Sosman JA, Atkins MB, Leming PD, Spigel DR, Antonia SJ, Horn L, Drake CG, Pardoll DM, Chen L, Sharfman WH, Anders RA, Taube JM, McMiller TL, Xu H, Korman AJ, Jure-Kunkel M, Agrawal S, McDonald D, Kollia GD, Gupta A, Wigginton JM, and Sznol M. Safety, activity, and immune correlates of anti-PD-1 antibody in cancer. *N Engl J Med* 366(26): 2443-2454 (2012).
3. Hodi FS, O'Day SJ, McDermott DF, Weber RW, Sosman JA, Haanen JB, Gonzalez R, Robert C, Schadendorf D, Hassel JC, Akerley W, van den Eertwegh AJ, Lutzky J, Lorigan P, Vaubel JM, Linette GP, Hogg D, Ottensmeier CH, Lebbé C, Peschel C, Quirt I, Clark JI, Wolchok JD, Weber JS, Tian J, Yellin MJ, Nichol GM, Hoos A, and Urba WJ. Improved survival with ipilimumab in patients with metastatic melanoma. *N Engl J Med* 363(8): 711-723 (2010).
4. Ott PA, Hu Z, Keskin DB, Shukla SA, Sun J, Bozym DJ, Zhang W, Luoma A, Giobbie-Hurder A, Peter L, Chen C, Olive O, Carter TA, Li S, Lieb DJ, Eisenhaure T, Gjini E, Stevens J, Lane WJ, Javeri I, Nellaiappan K, Salazar AM, Daley H, Seaman M, Buchbinder EI, Yoon CH, Harden M, Lennon N, Gabriel S, Rodig SJ, Barouch DH, Aster JC, Getz G, Wucherpfennig K, Neuberg D, Ritz J, Lander ES, Fritsch EF, Hacohen N, and Wu CJ. An immunogenic personal neoantigen vaccine for patients with melanoma. *Nature* 547(7662): 217-221 (2017).
5. Hilf N, Kuttruff-Coqui S, Frenzel K, Bukur V, Stevanović S, Gouttefangeas C, Platten M, Tabatabai G, Dutoit V, van der Burg SH, Thor Straten P, Martinez-Ricarte F, Ponsati B, Okada H, Lassen U, Admon A, Ottensmeier CH, Ulges A, Kreiter S, von Deimling A, Skardelly M, Migliorini D, Kroep JR, Idorn M, Rodon J, Piró J, Poulsen HS, Shraibman B, McCann K, Mendrzyk R, Löwer M, Stieglbauer M, Britten CM, Capper D, Welters MJP, Sahuquillo J, Kiesel K, Derhovanessian E, Rusch E, Bunse L, Song C, Heesch S, Wagner C, Kemmer-Brück A, Ludwig J, Castle JC, Schoor O, Tadmor AD, Green E, Fritsche J, Meyer M, Pawlowski N, Dorner S, Hoffgaard F, Rössler B, Maurer D, Weinschenk T, Reinhardt C, Huber C, Rammensee H-G, Singh-Jasuja H, Sahin U, Dietrich PY, and Wick W. Actively personalized vaccination trial for newly diagnosed glioblastoma. *Nature* 565(7738): 240-245 (2019).
6. Yoshitake Y, Fukuma D, Yuno A, Hirayama M, Nakayama H, Tanaka T, Nagata M, Takamune Y, Kawahara K, Nakagawa Y, Yoshida R, Hirosue A, Ogi H, Hiraki A, Jono H, Hamada A, Yoshida K, Nishimura Y, Nakamura Y, and Shinohara M. Phase II clinical trial of multiple peptide vaccination for advanced head and neck cancer patients revealed induction of immune responses and improved OS. *Clin Cancer Res* 21(2): 312-321 (2015).
7. Sahin U, Derhovanessian E, Miller M, Kloke BP, Simon P, Löwer M, Bukur V, Tadmor AD, Luxemburger U, Schrörs B, Omokoko T, Vormehr M, Albrecht C, Paruzynski A, Kuhn AN, Buck J, Heesch S, Schreeb KH, Müller F, Ortseifer I, Vogler

I, Godehardt E, Attig S, Rae R, Breitkreuz A, Tolliver C, Suchan M, Martic G, Hohberger A, Sorn P, Diekmann J, Ciesla J, Waksmann O, Brück AK, Witt M, Zillgen M, Rothermel A, Kasemann B, Langer D, Bolte S, Diken M, Kreiter S, Nemecek R, Gebhardt C, Grabbe S, Höller C, Utikal J, Huber C, Loquai C, and Türeci Ö. Personalized RNA mutanome vaccines mobilize poly-specific therapeutic immunity against cancer. *Nature* 547(7662): 222-226 (2017).

8. Qazilbash MH, Wieder E, Thall PF, Wang X, Rios R, Lu S, Kanodia S, Ruisaard KE, Giralt SA, Estey EH, Cortes J, Komanduri KV, Clise-Dwyer K, Alatrash G, Ma Q, Champlin RE, and Molldrem JJ. PR1 peptide vaccine induces specific immunity with clinical responses in myeloid malignancies. *Leukemia* 31(3): 697-704 (2017).
9. Maslak PG, Dao T, Krug LM, Chanel S, Korontsvit T, Zakhaleva V, Zhang R, Wolchok JD, Yuan J, Pinilla-Ibarz J, Berman E, Weiss M, Jurcic J, Frattini MG, and Scheinberg DA. Vaccination with synthetic analog peptides derived from WT1 oncoprotein induces T-cell responses in patients with complete remission from acute myeloid leukemia. *Blood* 116(2): 171-179 (2010).
10. Oka Y, Tsuboi A, Oji Y, Kawase I, and Sugiyama H. WT1 peptide vaccine for the treatment of cancer. *Curr Opin Immunol* 20(2): 211-220 (2008).
11. O'Reilly RJ, Dao T, Koehne G, Scheinberg D, and Doubrovina E. Adoptive transfer of unselected or leukemia-reactive T-cells in the treatment of relapse following allogeneic hematopoietic cell transplantation. *Semin Immunol* 22(3): 162-172 (2010).
12. Rafiq S, Purdon TJ, Daniyan AF, Koneru M, Dao T, Liu C, Scheinberg DA, and Brentjens RJ. Optimized T-cell receptor-mimic chimeric antigen receptor T cells directed toward the intracellular Wilms Tumor 1 antigen. *Leukemia* 31(8): 1788-1797 (2017).
13. Gubin MM, Zhang X, Schuster H, Caron E, Ward JP, Noguchi T, Ivanova Y, Hundal J, Arthur CD, Krebber WJ, Mulder GE, Toebes M, Vesely MD, Lam SS, Korman AJ, Allison JP, Freeman GJ, Sharpe AH, Pearce EL, Schumacher TN, Aebersold R, Rammensee H-G, Melief CJ, Mardis ER, Gillanders WE, Artyomov MN, and Schreiber RD. Checkpoint blockade cancer immunotherapy targets tumour-specific mutant antigens. *Nature* 515(7528): 577-581 (2014).
14. van Rooij N, van Buuren MM, Philips D, Velds A, Toebes M, Heemskerk B, van Dijk LJ, Behjati S, Hilkmann H, El Atmioui D, Nieuwland M, Stratton MR, Kerkhoven RM, Kesmir C, Haanen JB, Kvistborg P, and Schumacher TN. Tumor exome analysis reveals neoantigen-specific T-cell reactivity in an ipilimumab-responsive melanoma. *J Clin Oncol* 31(32): e439-e442 (2013).
15. Snyder A, Makarov V, Merghoub T, Yuan J, Zaretsky JM, Desrichard A, Walsh LA, Postow MA, Wong P, Ho TS, Hollmann TJ, Bruggeman C, Kannan K, Li Y, Elipenahli C, Liu C, Harbison CT, Wang L, Ribas A, Wolchok JD, and Chan TA. Genetic basis for clinical response to CTLA-4 blockade in melanoma. *N Engl J Med* 371(23): 2189-2199 (2014).
16. van der Lee DI, Reijmers RM, Honders MW, Hagedoorn RS, de Jong RC, Kester MG, van der Steen DM, de Ru AH, Kweekel C, Bijen HM, Jedema I, Veelken H, van Veelen PA, Heemskerk MH, Falkenburg JHF, and Griffioen M. Mutated nucleophosmin 1 as immunotherapy target in acute myeloid leukemia. *J Clin Invest* 129(2): 774-785 (2019).
17. Narayan R, Olsson N, Wagar LE, Medeiros BC, Meyer E, Czerwinski D, Khodadoust MS, Zhang L, Schultz L, Davis MM, Elias JE, and Levy R. Acute myeloid leukemia immunopeptidome reveals HLA presentation of mutated nucleophosmin. *PLoS One* 14(7): e0219547 (2019).
18. Alexandrov LB, Nik-Zainal S, Wedge DC, Aparicio SA, Behjati S, Biankin AV, Bignell GR, Bolli N, Borg A, Børresen-Dale AL, Boyault S, Burkhardt B, Butler AP, Caldas C, Davies HR, Desmedt C, Eils R, Eyfjörd JE, Foekens JA, Greaves M, Hosoda F, Hutter B, Ilicic T, Imbeaud S, Imielinski M, Jäger N, Jones DT, Jones D, Knappskog S, Kool M, Lakhani SR, López-Otín C, Martin S, Munshi NC, Nakamura H, Northcott PA, Pajic M, Papaemmanuil E, Paradiso A, Pearson JV, Puente XS, Raine K, Ramakrishna M, Richardson AL, Richter J, Rosenstiel P, Schlesner M, Schumacher TN, Span PN, Teague JW, Totoki Y, Tutt AN, Valdés-Mas R, van Buuren MM, van 't Veer L, Vincent-Salomon A, Waddell N, Yates LR, Australian Pancreatic Cancer Genome Initiative, ICGC Breast Cancer Consortium, ICGC MMML-Seq Consortium, ICGC PedBrain, Zucman-Rossi J, Futreal PA, McDermott U, Lichter P, Meyerson M, Grimmond SM, Siebert R, Campo E, Shibata T, Pfister SM, Campbell PJ, and Stratton MR. Signatures of mutational processes in human cancer. *Nature* 500(7463): 415-421 (2013).
19. Finn OJ and Rammensee H-G. Is It Possible to Develop Cancer Vaccines to Neoantigens, What Are the Major Challenges, and How Can These Be Overcome? Neoantigens: Nothing New in Spite of the Name. *Cold Spring Harb Perspect Biol* 10(11) (2018).
20. Bassani-Sternberg M, Bräunlein E, Klar R, Engleitner T, Sinitcyn P, Audehm S, Straub M, Weber J, Slotta-Huspenina J, Specht K, Martignoni ME, Werner A, Hein R, H. BD, Peschel C, Rad R, Cox J, Mann M, and Krackhardt AM. Direct identification of clinically relevant neoepitopes presented on native human melanoma tissue by mass spectrometry. *Nat Commun* 7: 13404 (2016).
21. Yadav M, Jhunjhunwala S, Phung QT, Lupardus P, Tanguay J, Bumbaca S, Franci C, Cheung TK, Fritsche J, Weinschenk T, Modrusan Z, Mellman I, Lill JR, and Delamarre L. Predicting immunogenic tumour mutations by combining mass spectrometry and exome sequencing. *Nature* 515(7528): 572-576 (2014).
22. Kalaora S, Barnea E, Merhavi-Shoham E, Qutob N, Teer JK, Shimony N, Schachter J, Rosenberg SA, Besser MJ, Admon A, and Samuels Y. Use of HLA peptidomics and whole exome sequencing to identify human immunogenic neo-antigens. *Oncotarget* 7(5): 5110-5117 (2016).
23. Freudenmann LK, Marcu A, and Stevanović S. Mapping the tumour human leukocyte antigen (HLA) ligandome by mass spectrometry. *Immunology* 154(3): 331-345 (2018).
24. Quintarelli C, Dotti G, De Angelis B, Hoyos V, Mims M, Luciano L, Heslop HE, Rooney CM, Pane F, and Savoldo B. Cytotoxic T lymphocytes directed to the preferentially expressed antigen of melanoma (PRAME) target chronic myeloid leukemia. *Blood* 112(5): 1876-1885 (2008).

25. Ochsenreither S, Fusi A, Geikowski A, Stather D, Busse A, Stroux A, Letsch A, and Keilholz U. Wilms' tumor protein 1 (WT1) peptide vaccination in AML patients: predominant TCR CDR3beta sequence associated with remission in one patient is detectable in other vaccinated patients. *Cancer Immunol Immunother* 61(3): 313-322 (2012).
26. Casalegno-Garduño R, Meier C, Schmitt A, Spitschak A, Hilgendorf I, Rohde S, Hirt C, Freund M, Pützer BM, and Schmitt M. Immune responses to RHAMM in patients with acute myeloid leukemia after chemotherapy and allogeneic stem cell transplantation. *Clin Dev Immunol* 2012: 146463 (2012).
27. Casalegno-Garduño R, Schmitt A, Spitschak A, Greiner J, Wang L, Hilgendorf I, Hirt C, Ho AD, Freund M, and Schmitt M. Immune responses to WT1 in patients with AML or MDS after chemotherapy and allogeneic stem cell transplantation. *Int J Cancer* 138(7): 1792-1801 (2016).
28. Weinzierl AO, Lemmel C, Schoor O, Müller M, Kruger T, Wernet D, Hennenlotter J, Stenzl A, Klingel K, Rammensee H-G, and Stevanović S. Distorted relation between mRNA copy number and corresponding major histocompatibility complex ligand density on the cell surface. *Mol Cell Proteomics* 6(1): 102-113 (2007).
29. Berlin C, Kowalewski DJ, Schuster H, Mirza N, Walz S, Handel M, Schmid-Horch B, Salih HR, Kanz L, Rammensee H-G, Stevanović S, and Stickel JS. Mapping the HLA ligandome landscape of acute myeloid leukemia: a targeted approach toward peptide-based immunotherapy. *Leukemia* 29(3): 647-659 (2015).
30. Bassani-Sternberg M, Pletscher-Frankild S, Jensen LJ, and Mann M. Mass spectrometry of human leukocyte antigen class I peptidomes reveals strong effects of protein abundance and turnover on antigen presentation. *Mol Cell Proteomics* 14(3): 658-673 (2015).
31. Morgan RA, Chinnasamy N, Abate-Daga D, Gros A, Robbins PF, Zheng Z, Dudley ME, Feldman SA, Yang JC, Sherry RM, Phan GQ, Hughes MS, Kammula US, Miller AD, Hessman CJ, Stewart AA, Restifo NP, Quezado MM, Alimchandani M, Rosenberg AZ, Nath A, Wang T, Bielekova B, Wuest SC, Akula N, McMahon FJ, Wilde S, Mosetter B, Schendel DJ, Laurencot CM, and Rosenberg SA. Cancer regression and neurological toxicity following anti-MAGE-A3 TCR gene therapy. *J Immunother* 36(2): 133-151 (2013).
32. Schuster H, Peper JK, Bösmüller HC, Rohle K, Backert L, Bilich T, Ney B, Loffler MW, Kowalewski DJ, Trautwein N, Rabsteyn A, Engler T, Braun S, Haen SP, Walz JS, Schmid-Horch B, Brucker SY, Wallwiener D, Kohlbacher O, Fend F, Rammensee HG, Stevanovic S, Staebler A, and Wagner P. The immunopeptidomic landscape of ovarian carcinomas. *Proc Natl Acad Sci U S A* 114(46): E9942-E9951 (2017).
33. Kuchenbauer F, Kern W, Schoch C, Kohlmann A, Hiddemann W, Haferlach T, and Schnittger S. Detailed analysis of FLT3 expression levels in acute myeloid leukemia. *Haematologica* 90(12): 1617-1625 (2005).
34. Backert L, Kowalewski DJ, Walz S, Schuster H, Berlin C, Neidert MC, Schemionek M, Brümmendorf TH, Vucinic V, Niederwieser D, Kanz L, Salih HR, Kohlbacher O, Weisel K, Rammensee H-G, Stevanović S, and Walz JS. A meta-analysis of HLA peptidome composition in different hematological entities: Entity-specific dividing lines and "pan-leukemia" antigens. *Oncotarget* 8(27): 43915-43924 (2017).
35. Takahashi S. Downstream molecular pathways of FLT3 in the pathogenesis of acute myeloid leukemia: biology and therapeutic implications. *J Hematol Oncol* 4(1): 13 (2011).
36. Ozeki K, Kiyoi H, Hirose Y, Iwai M, Ninomiya M, Kodera Y, Miyawaki S, Kuriyama K, Shimazaki C, and Akiyama H. Biologic and clinical significance of the FLT3 transcript level in acute myeloid leukemia. *Blood* 103(5): 1901-1908 (2004).
37. Zheng R, Levis M, Piloto O, Brown P, Baldwin BR, Gorin NC, Beran M, Zhu Z, Ludwig D, and Hicklin D. FLT3 ligand causes autocrine signaling in acute myeloid leukemia cells. *Blood* 103(1): 267-274 (2004).
38. Riches JC, Davies JK, McClanahan F, Fatah R, Iqbal S, Agrawal S, Ramsay AG, and Gribben JG. T cells from CLL patients exhibit features of T-cell exhaustion but retain capacity for cytokine production. *Blood* 121(9): 1612-1621 (2013).
39. Jak M, Mous R, Remmerswaal EB, Spijker R, Jaspers A, Yagüe A, Eldering E, Van Lier RA, and Van Oers MH. Enhanced formation and survival of CD4+ CD25hi Foxp3+ T-cells in chronic lymphocytic leukemia. *Leuk Lymphoma* 50(5): 788-801 (2009).
40. Ramsay AG, Johnson AJ, Lee AM, Gorgün G, Le Dieu R, Blum W, Byrd JC, and Gribben JG. Chronic lymphocytic leukemia T cells show impaired immunological synapse formation that can be reversed with an immunomodulating drug. *J Clin Invest* 118(7): 2427-2437 (2008).
41. Kowalewski DJ, Walz S, Backert L, Schuster H, Kohlbacher O, Weisel K, Rittig SM, Kanz L, Salih HR, Rammensee H-G, Stevanović S, and Stickel JS. Carfilzomib alters the HLA-presented peptidome of myeloma cells and impairs presentation of peptides with aromatic C-termini. *Blood Cancer J* 6: e411 (2016).
42. Harding CV, France J, Song R, Farah JM, Chatterjee S, Iqbal M, and Siman R. Novel dipeptide aldehydes are proteasome inhibitors and block the MHC-I antigen-processing pathway. *J Immunol* 155(4): 1767-1775 (1995).
43. Schwarz K, de Giuli R, Schmidtke G, Kostka S, van den Broek M, Kim KB, Crews CM, Kraft R, and Groettrup M. The selective proteasome inhibitors lactacystin and epoxomicin can be used to either up- or down-regulate antigen presentation at nontoxic doses. *J Immunol* 164(12): 6147-6157 (2000).
44. Rock KL, Gramm C, Rothstein L, Clark K, Stein R, Dick L, Hwang D, and Goldberg AL. Inhibitors of the proteasome block the degradation of most cell proteins and the generation of peptides presented on MHC class I molecules. *Cell* 78(5): 761-771 (1994).
45. Milner E, Gutter-Kapon L, Bassani-Strenberg M, Barnea E, Beer I, and Admon A. The effect of proteasome inhibition on the generation of the human leukocyte antigen (HLA) peptidome. *Mol Cell Proteomics* 12(7): 1853-1864 (2013).
46. Kowalewski DJ, Schuster H, Backert L, Berlin C, Kahn S, Kanz L, Salih HR, Rammensee H-G, Stevanović S, and Stickel JS. HLA ligandome analysis identifies the underlying specificities of spontaneous antileukemia immune responses in chronic lymphocytic leukemia (CLL). *Proc Natl Acad Sci U S A* 112(2): E166-E175 (2015).

47. ClinicalTrials.gov [Internet]. Bethesda (MD) National Library of Medicine (US). Identifier: NCT02802943. Patient individualized peptide vaccination in combination with lenalidomide after first line therapy of CLL. 2016 June 16 [cited 2016 Sep 06]; Available from: https://clinicaltrials.gov/ct2/show/NCT02802943?term=NCT02802943&rank=1.
48. Shraibman B, Melamed Kadosh D, Barnea E, and Admon A. HLA peptides derived from tumor antigens induced by inhibition of DNA methylation for development of drug-facilitated immunotherapy. *Mol Cell Proteomics* 15(9): 3058-3070 (2016).
49. Koumantou D, Barnea E, Martin-Esteban A, Maben Z, Papakyriakou A, Mpakali A, Kokkala P, Pratsinis H, Georgiadis D, Stern LJ, Admon A, and Stratikos E. Editing the immunopeptidome of melanoma cells using a potent inhibitor of endoplasmic reticulum aminopeptidase 1 (ERAP1). *Cancer Immunol Immunother* 68(8): 1245-1261 (2019).
50. James E, Bailey I, Sugiyarto G, and Elliott T. Induction of protective antitumor immunity through attenuation of ERAAP function. *J Immunol* 190(11): 5839-5846 (2013).
51. Hammer GE, Gonzalez F, James E, Nolla H, and Shastri N. In the absence of aminopeptidase ERAAP, MHC class I molecules present many unstable and highly immunogenic peptides. *Nat Immunol* 8(1): 101-108 (2007).
52. Keller M, Ebstein F, Bürger E, Textoris-Taube K, Gorny X, Urban S, Zhao F, Dannenberg T, Sucker A, Keller C, Saveanu L, Krüger E, Rothkötter HJ, Dahlmann B, Henklein P, Voigt A, Kuckelkorn U, Paschen A, Kloetzel PM, and Seifert U. The proteasome immunosubunits, PA28 and ER-aminopeptidase 1 protect melanoma cells from efficient MART-126-35 - specific T-cell recognition. *Eur J Immunol* 45(12): 3257-3268 (2015).
53. Liepe J, Sidney J, Lorenz FKM, Sette A, and Mishto M. Mapping the MHC Class I-Spliced Immunopeptidome of Cancer Cells. *Cancer Immunol Res* 7(1): 62-76 (2019).
54. Mishto M and Liepe J. Post-Translational Peptide Splicing and T Cell Responses. *Trends Immunol* 38(12): 904-915 (2017).
55. Erhard F, Halenius A, Zimmermann C, L'Hernault A, Kowalewski DJ, Weekes MP, Stevanović S, Zimmer R, and Dölken L. Improved Ribo-seq enables identification of cryptic translation events. *Nat Methods* 15(5): 363-366 (2018).
56. Liepe J, Marino F, Sidney J, Jeko A, Bunting DE, Sette A, Kloetzel PM, Stumpf MP, Heck AJ, and Mishto M. A large fraction of HLA class I ligands are proteasome-generated spliced peptides. *Science* 354(6310): 354-358 (2016).
57. Laumont CM, Daouda T, Laverdure JP, Bonneil É, Caron-Lizotte O, Hardy MP, Granados DP, Durette C, Lemieux S, Thibault P, and Perreault C. Global proteogenomic analysis of human MHC class I-associated peptides derived from non-canonical reading frames. *Nat Commun* 7: 10238 (2016).
58. Starck SR and Shastri N. Non-conventional sources of peptides presented by MHC class I. *Cell Mol Life Sci* 68(9): 1471-1479 (2011).
59. Goodenough E, Robinson TM, Zook MB, Flanigan KM, Atkins JF, Howard MT, and Eisenlohr LC. Cryptic MHC class I-binding peptides are revealed by aminoglycoside-induced stop codon read-through into the 3' UTR. *Proc Natl Acad Sci U S A* 111(15): 5670-5675 (2014).
60. Ma B, Zhang K, Hendrie C, Liang C, Li M, Doherty-Kirby A, and Lajoie G. PEAKS: powerful software for peptide de novo sequencing by tandem mass spectrometry. *Rapid Commun Mass Spectrom* 17(20): 2337-2342 (2003).
61. Medzihradszky KF and Chalkley RJ. Lessons in de novo peptide sequencing by tandem mass spectrometry. *Mass Spectrom Rev* 34(1): 43-63 (2015).
62. Shraibman B, Barnea E, Kadosh DM, Haimovich Y, Slobodin G, Rosner I, López-Larrea C, Hilf N, Kuttruff S, Song C, Britten C, Castle J, Kreiter S, Frenzel K, Tatagiba M, Tabatabai G, Dietrich PY, Dutoit V, Wick W, Platten M, Winkler F, von Deimling A, Kroep J, Sahuquillo J, Martinez-Ricarte F, Rodon J, Lassen U, Ottensmeier C, van der Burg SH, Thor Straten P, Poulsen HS, Ponsati B, Okada H, Rammensee H-G, Sahin U, Singh H, and Admon A. Identification of Tumor Antigens Among the HLA Peptidomes of Glioblastoma Tumors and Plasma. *Mol Cell Proteomics* 17(11): 2132-2145 (2018).
63. Hayun M, Itzkovich C, Barnea E, Admon A, Louria-Hayon I, and Ofran Y. Plasma Soluble HLA-Bound Peptides Derived from Acute Myeloid Leukemia Patients during Induction May Predict Individual Response to Therapy. *Blood* 132(Suppl 1): 2799-2799 (2018).
64. Bassani-Sternberg M, Barnea E, Beer I, Avivi I, Katz T, and Admon A. Soluble plasma HLA peptidome as a potential source for cancer biomarkers. *Proc Natl Acad Sci U S A* 107(44): 18769-18776 (2010).
65. Ritz D, Gloger A, Neri D, and Fugmann T. Purification of soluble HLA class I complexes from human serum or plasma deliver high quality immuno peptidomes required for biomarker discovery. *Proteomics* 17(1-2) (2017).
66. Santambrogio L and Rammensee H-G. Contribution of the plasma and lymph Degradome and Peptidome to the MHC Ligandome. *Immunogenetics* 71(3): 203-216 (2019).
67. Walz S, Stickel JS, Kowalewski DJ, Schuster H, Weisel K, Backert L, Kahn S, Nelde A, Stroh T, Handel M, Kohlbacher O, Kanz L, Salih HR, Rammensee H-G, and Stevanović S. The antigenic landscape of multiple myeloma: mass spectrometry (re)defines targets for T-cell-based immunotherapy. *Blood* 126(10): 1203-1213 (2015).

8. ABBREVIATIONS

aa	amino acid
aAPC	artificial antigen-presenting cell
ABL1	Abelson murine leukemia viral oncogene homolog 1
abnor.	abnormalities
ACT	adoptive cell transfer
ADCC	antibody-dependent cell-mediated cytotoxicity
ADE	human adenovirus
AGC	automatic gain control
ALL	acute lymphoblastic leukemia
AML	acute myeloid leukemia
AML_{MR}	AML patients in molecular remission
APC	antigen-presenting cell
APL	acute promyelocytic leukemia
β2m	β_2-microglobulin
BCL-2	B-cell leukemia/lymphoma-2
BCR	breakpoint cluster region
BiTE	bispecific T-cell engager
BM	bone marrow
BMNCs	bone marrow mononuclear cells
CAR	chimeric antigen receptor
CBFB	core-binding factor subunit beta
CD	cluster of differentiation
CID	collision-induced dissociation
CLIP	class II-associated invariant chain peptide
CLL	chronic lymphocytic leukemia
CLPs	common lymphoid progenitors
CML	chronic myeloid leukemia
CML_{MR}	CML patients in deep molecular remission
CML_{TKI}	CML patients under TKI treatment
CMPs	common myeloid progenitors
CT	chemotherapy
CTA	cancer/testis antigen
CTL	cytotoxic T lymphocyte
CTLA-4	cytotoxic T lymphocyte-associated molecule 4
DCs	dendritic cells
DDA	data-dependent acquisition
DKFZ	German Cancer Research Center
DKTK	German Cancer Consortium
DNA	deoxyribonucleic acid
E	IFNγ ELISPOT assay
EBV	Epstein-Barr virus
EBVB9	Epstein-Barr virus (strain B95-8)
ELISPOT	enzyme-linked immunospot
ELN	European LeukemiaNet
EMA	European Medicines Agency
ER	endoplasmic reticulum
f	female
FAB	French-American-British
FACS	fluorescence-activated cell sorting
FC	fold-change
FDA	US Food and Drug Administration
FDR	false discovery rate
FLT3	FMS-like tyrosine kinase 3
$FLT3_{mut}$	FLT3-mutated
$FLT3_{WT}$	FLT3-unmutated
FSC	forward scatter
HCMVA	human cytomegalovirus (strain AD169)
hema.	hematological
HHV8P	human herpesvirus 8 type P
HLA	human leukocyte antigen
HPCs	hematopoietic progenitor cells
HPV	human papillomavirus
HSCs	hematopoietic stem cells
HSCT	hematopoietic stem cell transplantation
HV1BR	human immunodeficiency virus type 1 group M
HVs	healthy volunteers
I34A1	Influenza A virus (strain A/Puerto Rico/8/1934 H1N1)
ICS	intracellular cytokine staining
IDH	isocitrate dehydrogenase
$IDH2_{WT}$	unmutated IDH2
IDs	identifications
IFN	interferon
Ig	immunoglobulin
IGHV	immunoglobulin heavy-chain variable region
Ii	invariant chain
IL	interleukin
inv	inversion
ITD	internal tandem duplication
L	HLA ligand isolation
LAA	leukemia-associated antigen
LC-MS/MS	liquid chromatography-tandem mass spectrometry
LFQ	label-free quantitation
L_{MR}	HLA ligandome analysis of patients in deep MR
LOD	limit of detection
LPCs	leukemic progenitor cells
LTQ	linear trap quadrupole
m	male
mAB	monoclonal antibody
MACS	magnetic activated cell sorting
MAGE	melanoma-associated antigen
MART1	melanoma antigen recognized by T cells 1
MHC	major histocompatibility complex
MPL	monophosphoryl lipid A
MPPs	multipotent progenitors
MR	molecular remission
MRD	minimal residual disease
MS	mass spectrometry
mut	mutation-derived
myel.-rel.	myelodysplasia-related changes
MYH11	myosin heavy chain 11
n.a.	not available, not applicable
n.d.	not detectable
neg.	negative
NM	no mutation
no.	number
NOS	not otherwise specified
n_{pep}	number of peptides
NPM1	nucleophosmin
n.s.	not significant, not specified
ns	not significant
NSG	NOD scid gamma
n.t.	not tested
P	*in vitro* aAPC-based priming
PB	peripheral blood

ABBREVIATIONS

PBMCs	peripheral blood mononuclear cells
PD-1	programmed cell death receptor-1
PD-L1	programmed cell death ligand-1
PE	R-phycoerythrin
PHA	phytohemagglutinin
pos.	positive
post	postenrichment
pre	preenrichment
PRM	parallel reaction monitoring
PSMA	prostate-specific membrane antigen
Q	HLA quantification
rec.	recurrent
rep	replicate
RNA	ribonucleic acid
RSLC	rapid separation liquid chromatography
scFv	single-chain variable fragment
SD	standard deviation
SEM	standard error of the mean
SFU	spot forming unit
sHLA	soluble HLA molecules
SSC	side scatter
t	translocation
T	tetramer staining
TAA	tumor-associated antigen
TAP	transporter associated with antigen processing
TCR	T-cell receptor
TFR	treatment-free remission
T_h cells	T helper cells
TILs	tumor-infiltrating lymphocytes
TKD	tyrosine kinase domain
TKI	tyrosine kinase inhibitor
TLR	Toll-like receptor
TNF	tumor-necrosis factor
T_{reg} cells	regulatory T cells
TRQ	threshold for relative quantitation
TSA	tumor-specific antigen
UPN	uniform patient number
UTR	untranslated region
vs.	versus
WBC	white blood cell count
WHO	World Health Organization
WT	wild type
y	years
yr	years

9. ACKNOWLEDGMENTS

Der Weg bis zu dieser Doktorarbeit war manchmal etwas steinig. Aber durch die Menschen an meiner Seite, Freunde, Kollegen und meine Familie wurden die letzten Jahre zu einer sehr schönen Zeit, an die ich mich gern zurück erinnern werde. Viele haben mich unterstützt und waren in jeder Situation, ob im Labor oder im Privatleben, für mich da. Dafür möchte ich mich bedanken. Danke für die vielen Gespräche, den Rückhalt und das gemeinsame Lachen!

Ein ganz besonderer Dank geht an meine Doktorväter Prof. Stefan Stevanović und Prof. Hans-Georg Rammensee. Zum einen für die Möglichkeit bei ihnen meine Promotion zu absolvieren, zum anderen aber auch für interessante Diskussionen und ihre Unterstützung bei allen Projekten und Ideen.

Nicht zu vergessen ist aber auch meine Chefin PD Dr. Juliane Walz. Vielen Dank, Juli für die letzten Jahre! Ich fühle mich in deiner kleinen, aber stetig wachsenden Juniorarbeitsgruppe sehr wohl. Danke für tolle Ideen, immer ein offenes Ohr, jegliche Unterstützung und viele tolle Momente.

Bedanken möchte ich mich auch für die finanzielle Unterstützung meiner Doktorarbeit durch das Promotionsstipendium der Landesgraduiertenförderung.

Meine Biologielehrerin Frau Jänicke hat mir mit ihrem ganz eigenen Enthusiasmus und ihrer Begeisterung die Liebe zur Biologie vermittelt – vielen Dank dafür!

Ein großes Dankeschön geht auch an alle Kollegen, die mich in den letzten Jahren im Laboralltag begleitet haben: Tati, Jens, Ulrike, Moni, Ana, Daniel, Leon, Linus, Lena F, Lena M, Marion, Michi, Nora und viele mehr.

Ganz besonders sind für mich Kollegen, die zu meinen besten Freunden wurden und mich durch jede schwere Situation begleitet haben. Vielen Dank, Maren und Heiko für eure Freundschaft, euren Halt und eure Unterstützung. Durch euch war das Labor mehr als nur Arbeit.

Natürlich lassen sich hier nicht alle aufzählen, das würde diese Seite sprengen. Deshalb an alle, die hier nicht namentlich stehen, aber denen ich auch so viel zu verdanken habe: Vielen Dank für alles!

Last but not least möchte ich ein ganz besonderes Dankeschön an alle meine Freunde außerhalb des Labors schicken! Egal, wie lange ihr schon Teil meines Lebens seid, ihr bringt mich zum Lachen, hört mir zu und seid einfach immer für mich da. Hier möchte ich vor allem Deborah, Julia, Tammy, Patrick Z, Timo, Dome, Patrick S, Jens L und Caro nennen.

Auch meine Familie war ein Rückhalt, der die letzten Jahre deutlich vereinfach hat. Vielen Dank, Mama, Stephan, Iris und Lukas!

Und ganz zum Schluss: Danke an alle, die mir immer wieder ein Lächeln ins Gesicht zaubern!

10. SUPPLEMENT OF PART I

Supplemental Table 1: Patient characteristics

UPN	Binet	Sex	Age	HLA typing	WBC [10^3/µl] [% CLL]	Analysis
1	A	f	79	A*01:01, A*03:01, B*07:02, B*44:02, DRB1*08:03, DRB1*13:01	171 [88]	Q, L
2	B	m	76	A*02:01, B*40:01, B*51:01, DRB1*08:01, DRB1*13:02	240 [95]	Q, L
3	A	f	62	A*02:01, A*11:01, B*39:06, B*50:01, DRB1*07:01, DRB1*08:01	108 [91]	Q, L
4	C	m	47	A*01:01, A*26:01, B*40:02, B*57:01, DRB1*03:01	223 [94]	Q

Abbreviations: UPN, uniform patient number; Binet, clinical stage of disease was assessed according to the Binet staging system (Binet *et al*. Cancer 1981); m, male; f, female; WBC, white blood cell count; Q, HLA quantification; L, HLA ligand isolation.

Supplemental Table 2: Sample characteristics

patient	sample	cell count before treatment	viability after treatment [%]	class I ligand IDs	class II ligand IDs
UPN1	pre treatment #1	2.80×10^8	100	839	1,926
	pre treatment #2	2.80×10^8	100	1,094	1,713
	pre treatment #3	2.80×10^8	100	1,879	1,845
	untreated #1 t_{24h}	2.80×10^8	76	1,047	2,028
	untreated #2 t_{24h}	2.80×10^8	73	1,754	1,545
	untreated #3 t_{24h}	2.80×10^8	90	129	1,459
	untreated #1 t_{48h}	2.80×10^8	75	1,452	1,504
	untreated #2 t_{48h}	2.80×10^8	64	1,597	1,811
	untreated #3 t_{48h}	2.80×10^8	64	3,112	1,583
	lenalidomide #1 t_{24h}	2.80×10^8	96	942	1,494
	lenalidomide #2 t_{24h}	2.80×10^8	83	2,013	1,546
	lenalidomide #3 t_{24h}	2.80×10^8	79	2,242	1,894
	lenalidomide #1 t_{48h}	2.80×10^8	66	1,669	2,140
	lenalidomide #2 t_{48h}	2.80×10^8	75	1,615	1,315
	lenalidomide #3 t_{48h}	2.80×10^8	70	3,833	1,576
UPN2	pre treatment	2.78×10^8	100	695	137
	untreated t_{24h}	2.78×10^8	97	737	213
	untreated t_{48h}	2.78×10^8	65	- *	295
	lenalidomide t_{24h}	2.78×10^8	88	616	54
	lenalidomide t_{48h}	2.78×10^8	62	- *	46
UPN3	pre treatment #1	2.00×10^8	100	693	1,893
	pre treatment #2	2.00×10^8	100	-**	1,614
	untreated #1 t_{24h}	2.00×10^8	85	909	1,804
	untreated #2 t_{24h}	2.00×10^8	72	-**	1,956
	untreated #1 t_{48h}	2.00×10^8	40	1,176	1,296
	untreated #2 t_{48h}	2.00×10^8	30	-**	1,753
	lenalidomide #1 t_{24h}	2.00×10^8	72	853	1,747
	lenalidomide #2 t_{24h}	2.00×10^8	62	-**	2,229
	lenalidomide #1 t_{48h}	2.00×10^8	25	1,009	1,356
	lenalidomide #2 t_{48h}	2.00×10^8	40	-**	1,830

* The HLA class I dataset for t_{48h} of UPN2 was excluded from the analysis because of technical problems during the measurement. ** Due to technical problems the HLA class I samples of the second biological replicate was lost. Abbreviation: UPN, uniform patient number.

Supplemental Table 3: Longitudinally mapping of CLL-associated HLA class I ligands identified on UPN1

sequence	source protein	HLA restriction	log2 fold-change (treated/untreated) at t_{24h}	log2 fold-change (treated/untreated) at t_{48h}
KITVPASQK	BLNK B-cell linker	A*03	-0.2207	0.5524
KIADFGLAR	CDK14 cyclin-dependent kinase 14	A*03	0.0768	0.8448
RTRDYASLPPK	DNMBP dynamin binding protein	A*03	-0.0734	0.4180
TPRTNNIEL	ASUN asunder spermatogenesis regulator	B*07	0.0770	0.5816
VPVPHTTAL	B4GALT1 UDP-Gal:betaGlcNAc beta 1,4-galactosyltransferase, polypeptide 1	B*07	0.8415	0.4579
SPTSSRTSSL	CELSR1 cadherin, EGF LAG seven-pass G-type receptor 1	B*07	-0.2051	0.3047
LPAYRAQLL	DMXL1 Dmx-like 1	B*07	1.1078	0.9805
KPRQSSPQL	DNMBP dynamin binding protein	B*07	0.4326	0.2831
APSEYRYTLL	ERP44 endoplasmic reticulum protein 44	B*07	0.4819	0.3183
SPRPPLGSSL	KDM2B lysine (K)-specific demethylase 2B	B*07	0.4107	0.3372
RPAGEPYNRKTL	PRR12 proline rich 12	B*07	0.5135	0.2106
APLQRSQSL	TBC1D22A TBC1 domain family, member 22A	B*07	-0.2444	0.3349
LPHSATVTL	TBC1D22A TBC1 domain family, member 22A	B*07	0.5584	0.7016
SPAPRTAL	TNFRSF13C tumor necrosis factor receptor superfamily, member 13C	B*07	0.0998	0.5796
TPSSRPASL	UBL7 ubiquitin-like 7	B*07	0.1437	0.2975
SPRASGSGL	ZNF296 zinc finger protein 296	B*07	-0.1879	0.3890
EEEEALQKKF	NELFE negative elongation factor complex member E	B*44	0.6136	1.0041
LENDQSLSF	TAGAP T-cell activation RhoGTPase activating protein	B*44	1.0109	0.3975

Supplemental Table 4: Longitudinally mapping of CLL-associated HLA class II ligands identified on UPN1

sequence	source protein	log2 fold-change (treated/untreated) at t_{24h}	log2 fold-change (treated/untreated) at t_{48h}
LAPLEGARFALVRE	A1BG alpha-1-B glycoprotein	0.0128	-0.2572
LAPLEGARFALVRED	A1BG alpha-1-B glycoprotein	-0.0111	-0.2205
VAIVQAVSAHRHR	CCR7 chemokine (C-C motif) receptor 7	-0.4500	0.2830
VAIVQAVSAHRHRA	CCR7 chemokine (C-C motif) receptor 7	-0.3847	-0.0960
LPSQAFEYILYNKG	CTSH cathepsin H	-0.1643	-0.2212
LPSQAFEYILYNKGI	CTSH cathepsin H	0.2004	-0.2632
LPSQAFEYILYNKGIm	CTSH cathepsin H	-0.0741	-0.2004
LPSQAFEYILYNKGImG	CTSH cathepsin H	0.0768	-0.4202
PSQAFEYILYNKG	CTSH cathepsin H	-0.0103	-0.2929
PSQAFEYILYNKGI	CTSH cathepsin H	-0.3196	-0.0706
PSQAFEYILYNKGIm	CTSH cathepsin H	0.2984	-0.5085
IKAEYKGRVTLKQYPR	FAIM3 Fas apoptotic inhibitory molecule 3	-0.2820	-0.1258
YPRKNLFLVEVTQLTESDS	FAIM3 Fas apoptotic inhibitory molecule 3	1.2282	-1.0464
YPRKNLFLVEVTQLTESDSG	FAIM3 Fas apoptotic inhibitory molecule 3	0.0372	-0.2812
SDGSFHASSSLTVK	FCGRT Fc fragment of IgG, receptor, transporter, alpha	-0.3753	-0.3612
VPSRMKYVYFQNNQIT	FMOD fibromodulin	-0.0021	0.0200
YNTYQVVQFNRLPL	LAMTOR3 late endosomal/lysosomal adaptor, MAPK and MTOR activator 3	0.0417	0.0119
YNTYQVVQFNRLPLVV	LAMTOR3 late endosomal/lysosomal adaptor, MAPK and MTOR activator 3	0.2144	0.4029
TPRENDTITIYSTINHSKESKPT	SLAMF6 SLAM family member 6	-0.1351	0.2769
ELERIQIQEAAKKKPG	SPOCK2 sparc/osteonectin, cwcv and kazal-like domains proteoglycan (testican) 2	-0.0902	0.4147

Supplemental Table 4 continued

sequence	source protein	log2 fold-change (treated/untreated) at t_{24h}	log2 fold-change (treated/untreated) at t_{48h}
ERIQIQEAAKKKPGI	SPOCK2 sparc/osteonectin, cwcv and kazal-like domains proteoglycan (testican) 2	-0.3276	-0.0780
LERIQIQEAAKKKPG	SPOCK2 sparc/osteonectin, cwcv and kazal-like domains proteoglycan (testican) 2	-0.8074	-0.1024
GEPLSYTRFSLARQ	TFRC transferrin receptor	-0.1331	-0.2869
GEPLSYTRFSLARQVD	TFRC transferrin receptor	0.1846	-0.3841
GEPLSYTRFSLARQVDG	TFRC transferrin receptor	0.0490	-0.4121
GGEPLSYTRFSLARQVD	TFRC transferrin receptor	-0.0315	-0.4599
GGEPLSYTRFSLARQVDG	TFRC transferrin receptor	0.0369	-0.4505

Supplemental Figure 1

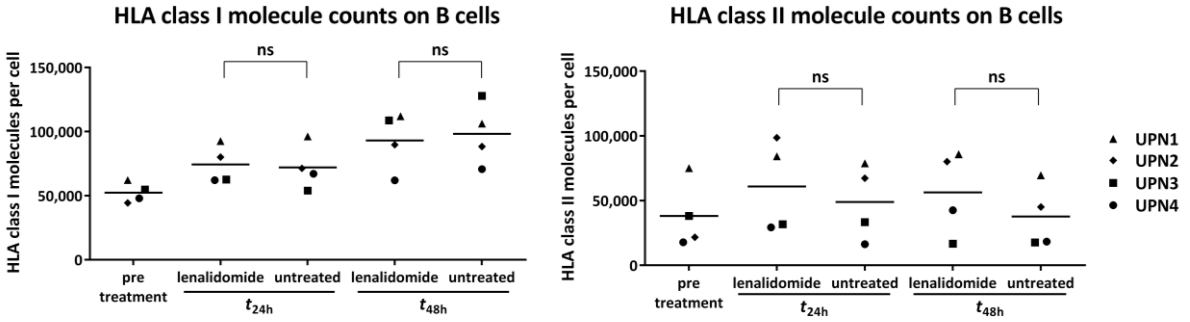

Figure S1: Effect of *in vitro* lenalidomide treatment on HLA class I and II surface expression on autologous B cells. Absolute counts of HLA class I (A) and HLA class II (B) surface molecules on autologous $CD19^{+}CD5^{-}$ B cells (n = 4) under *in vitro* lenalidomide treatment. Abbreviations: ns, not significant ($P \geq 0.05$); UPN, uniform patient number.

Supplemental Figure 2

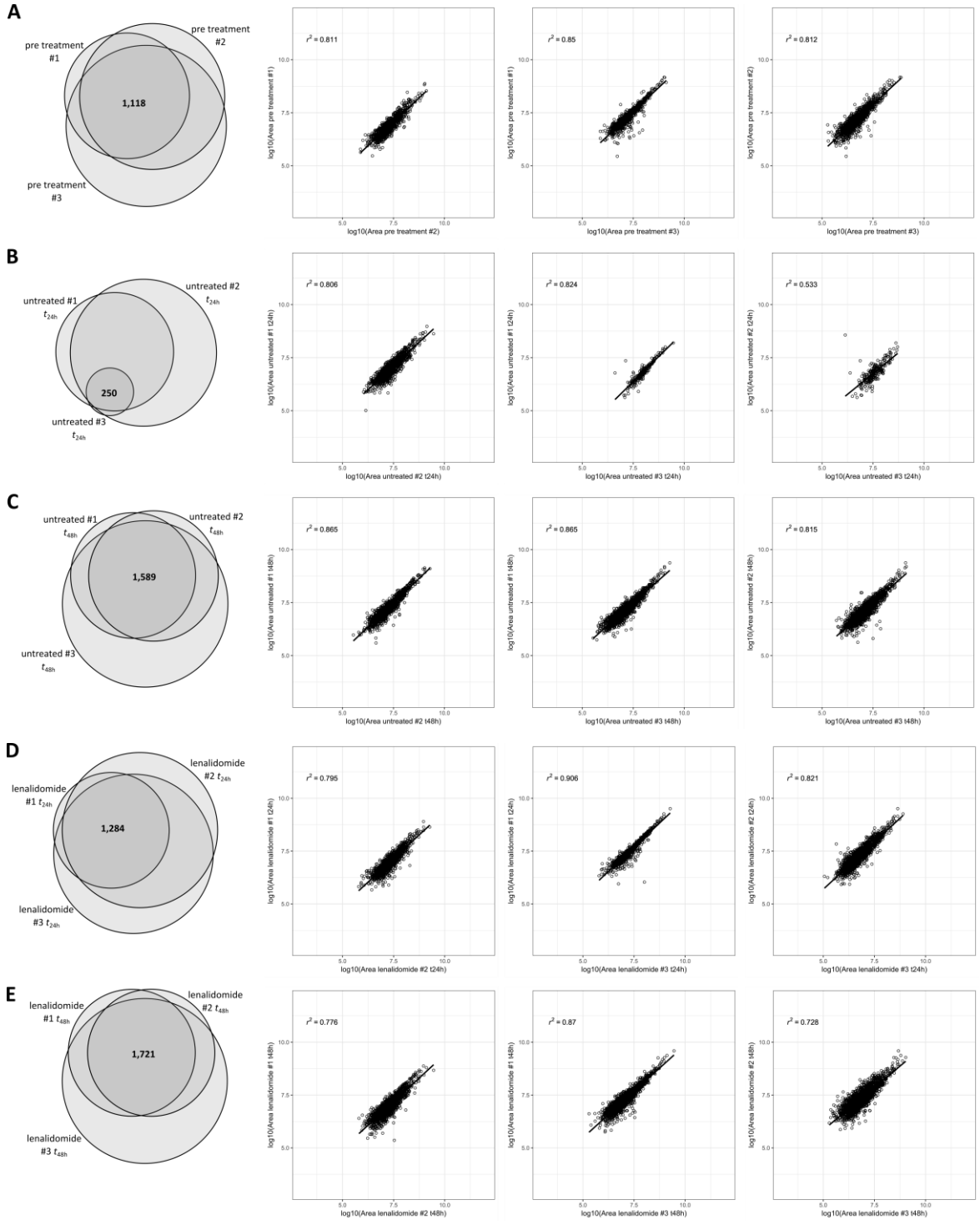

Figure S2: Comparison of mass spectrometric data of biological replicates of HLA class I-presented peptidomes of UPN1 cells. HLA class I ligand extracts of UPN1 before *in vitro* treatment (A) and at t_{24h} (B, D) and t_{48h} (C, E) after incubation with 0.5 µM lenalidomide or 0.005% DMSO (vehicle control) were analyzed in three biological replicates. Comparisons of biological replicates were performed using overlap analysis of HLA ligands as well as scatter plots depicting the $\log_{10}$ of the relative abundances (median area of extracted precursor ion chromatograms in FDR-unfiltered lists of five technical replicates) of HLA ligands on UPN1 cells comparing the conditions indicated. Each dot represents a specific HLA ligand. The regression line as well as the coefficient of determination r^2 are shown.

Supplemental Figure 3

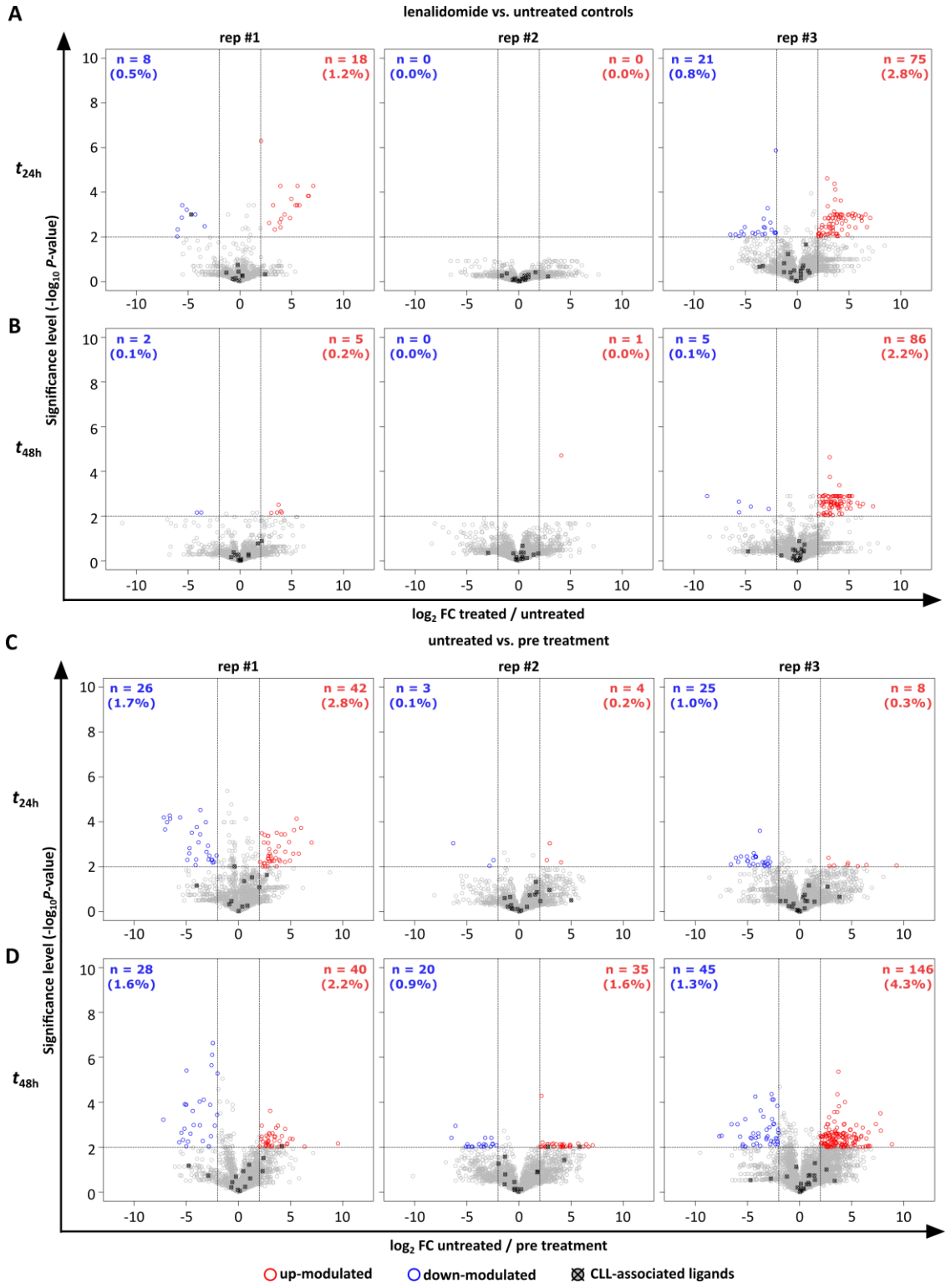

Figure S3: Mass spectrometric analysis of the HLA class I-presented peptidome of primary CLL cells (UPN1) under *in vitro* lenalidomide treatment in single biological replicate analysis. Volcano plots of the relative abundances of HLA ligands on UPN1 cells for each biological replicate separately comparing the conditions indicated at t_{24h} (A, C) and t_{48h} (B, D). Each dot represents a specific HLA ligand. Log_2 fold-changes of peptide abundance are indicated on the x-axis, the corresponding significance levels after Benjamini-Hochberg correction ($-log_{10}$ *P*-value) on the y-axis. HLA ligands showing significant up- or down-modulation (≥ log_2 2-fold-change in abundance with $P < 0.01$) are highlighted in red and blue, respectively. The absolute numbers and percentages of significantly modulated ligands are specified in the corresponding quadrants. Abbreviations: UPN, uniform patient number; vs., versus; FC, fold-change.

Supplemental Figure 4

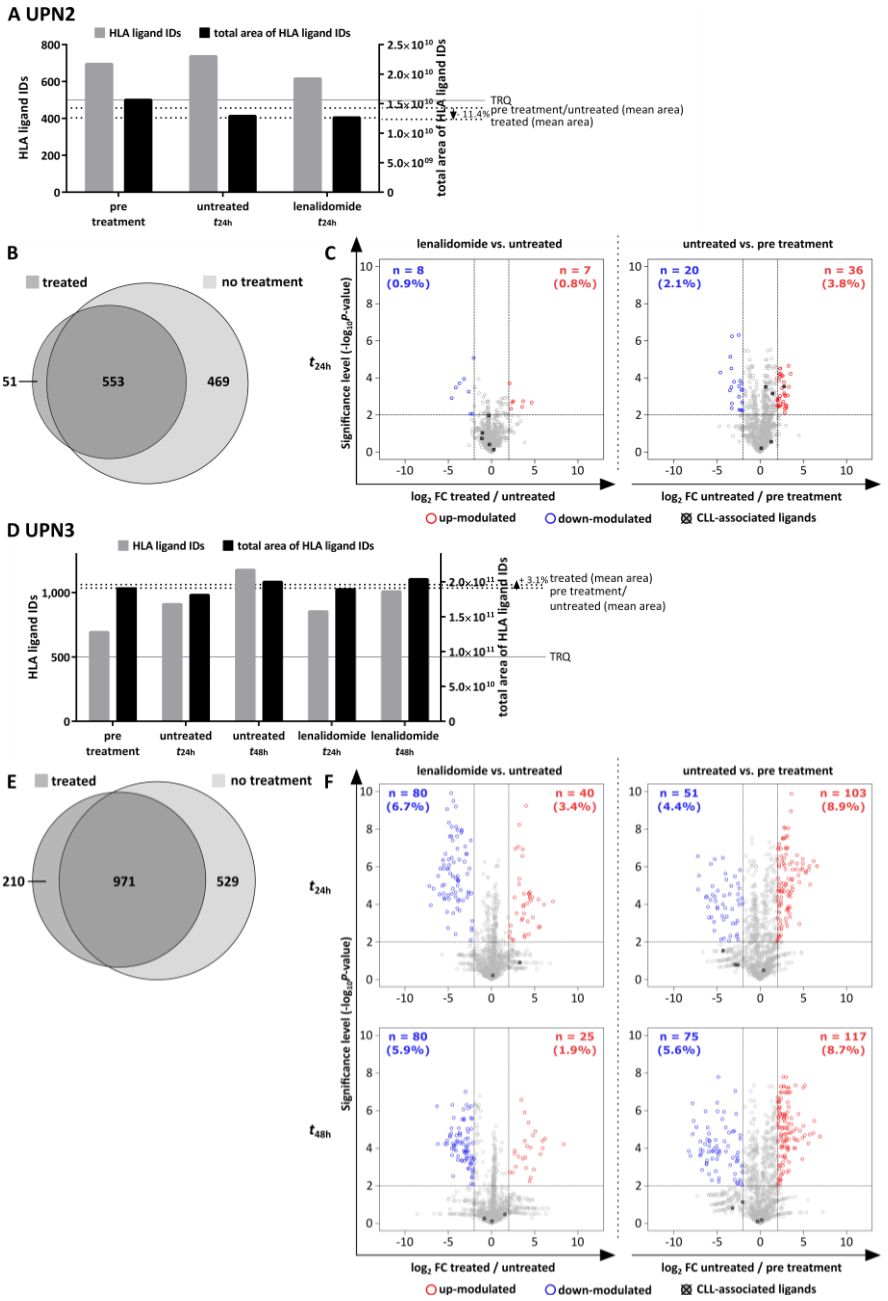

Figure S4: Mass spectrometric analysis of the HLA class I-presented peptidome of primary CLL cells (UPN2 and UPN3) under *in vitro* lenalidomide treatment. HLA class I ligand extracts of UPN2 (A) and UPN3 (D) before *in vitro* treatment and at t_{24h} and t_{48h} after incubation with 0.5 µM lenalidomide or 0.005% DMSO (vehicle control) were analyzed in single experiments. The number of HLA ligand identifications and the summed area of their extracted ion chromatograms are indicated in grey and black bars, respectively. The threshold for relative quantitation (TRQ) was set to 500 HLA ligand IDs. Overlap analysis of UPN2 (B) and UPN3 (E) HLA class I ligands identified on lenalidomide-treated versus untreated (vehicle controls and pre treatment) cells. Volcano plots of the relative abundances of HLA ligands on UPN2 (C) and UPN3 (F) cells comparing the conditions indicated. Each dot represents a specific HLA ligand. Log_2 fold-changes of their abundance are indicated on the x-axis, the corresponding significance levels after Benjamini-Hochberg correction ($-log_{10}$ *P*-value) on the y-axis. HLA ligands showing significant up- or down-modulation (≥ log_2 2-fold-change in abundance with $P < 0.01$) are highlighted in red and blue, respectively. The absolute numbers and percentages of significantly modulated ligands are specified in the corresponding quadrants. Volcano plots on the left comparing HLA ligand abundances on lenalidomide- versus untreated cells at t_{24h} and t_{48h}, respectively. On the right site control volcano plots comparing HLA ligand abundances on untreated cells at t_{24h} and t_{48h} to baseline levels prior to treatment. Abbreviations: UPN, uniform patient number; vs., versus; FC, fold-change; TRQ, threshold for relative quantitation.

Supplemental Figure 5

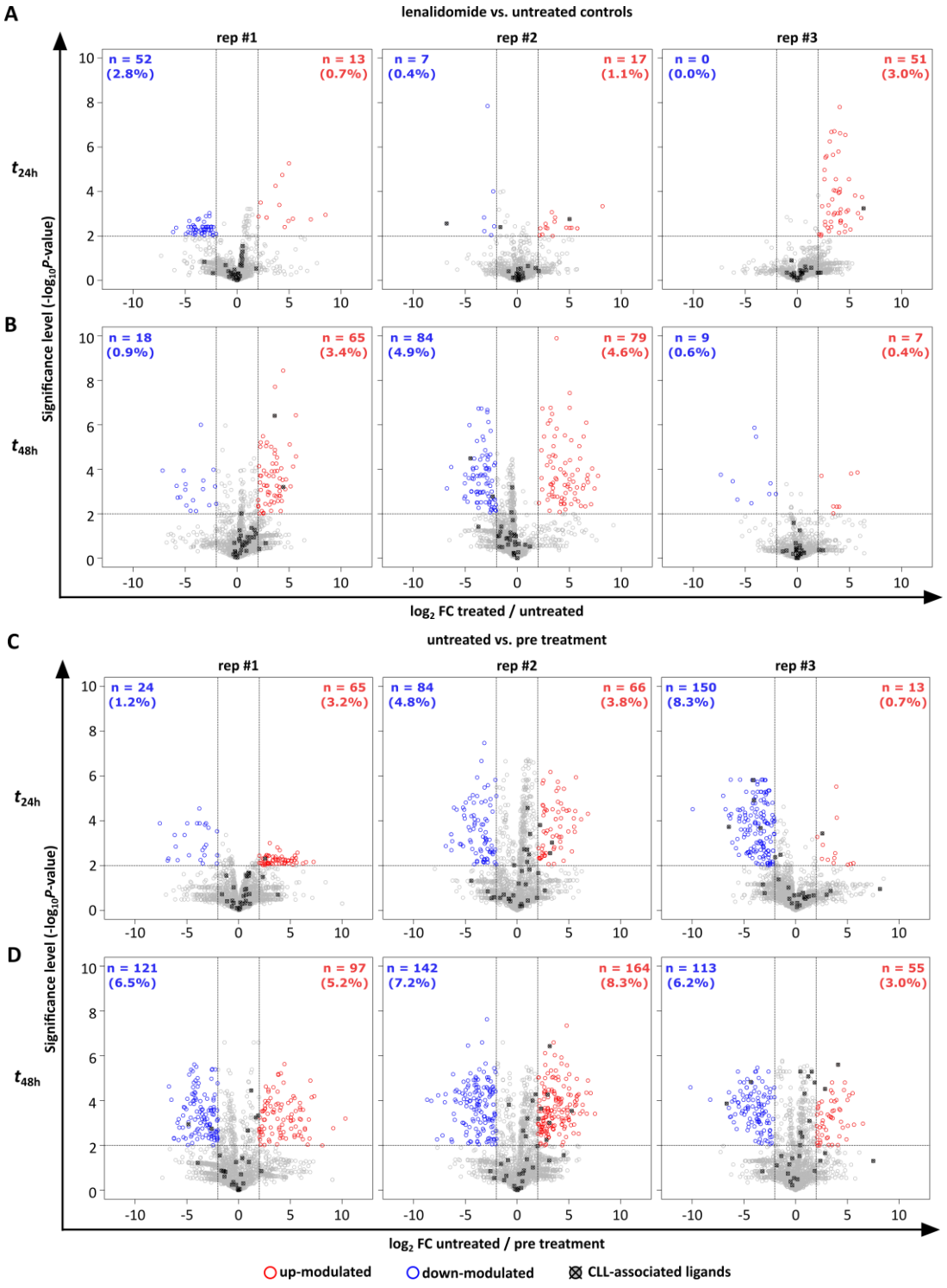

Figure S5: Mass spectrometric analysis of the HLA class II-presented peptidome of primary CLL cells (UPN1) under *in vitro* lenalidomide treatment in single biological replicate analysis. Volcano plots of the relative abundances of HLA class II ligands on UPN1 cells for each biological replicate separately comparing the conditions indicated at t_{24h} (A, C) and t_{48h} (B, D). Each dot represents a specific HLA ligand. Log_2 fold-changes of peptide abundance are indicated on the x-axis, the corresponding significance levels after Benjamini-Hochberg correction ($-log_{10}$ *P*-value) on the y-axis. HLA ligands showing significant up- or down-modulation (≥ log_2 2-fold-change in abundance with $P < 0.01$) are highlighted in red and blue, respectively. The absolute numbers and percentages of significantly modulated ligands are specified in the corresponding quadrants. Abbreviations: UPN, uniform patient number; vs., versus; FC, fold-change.

Supplemental Figure 6

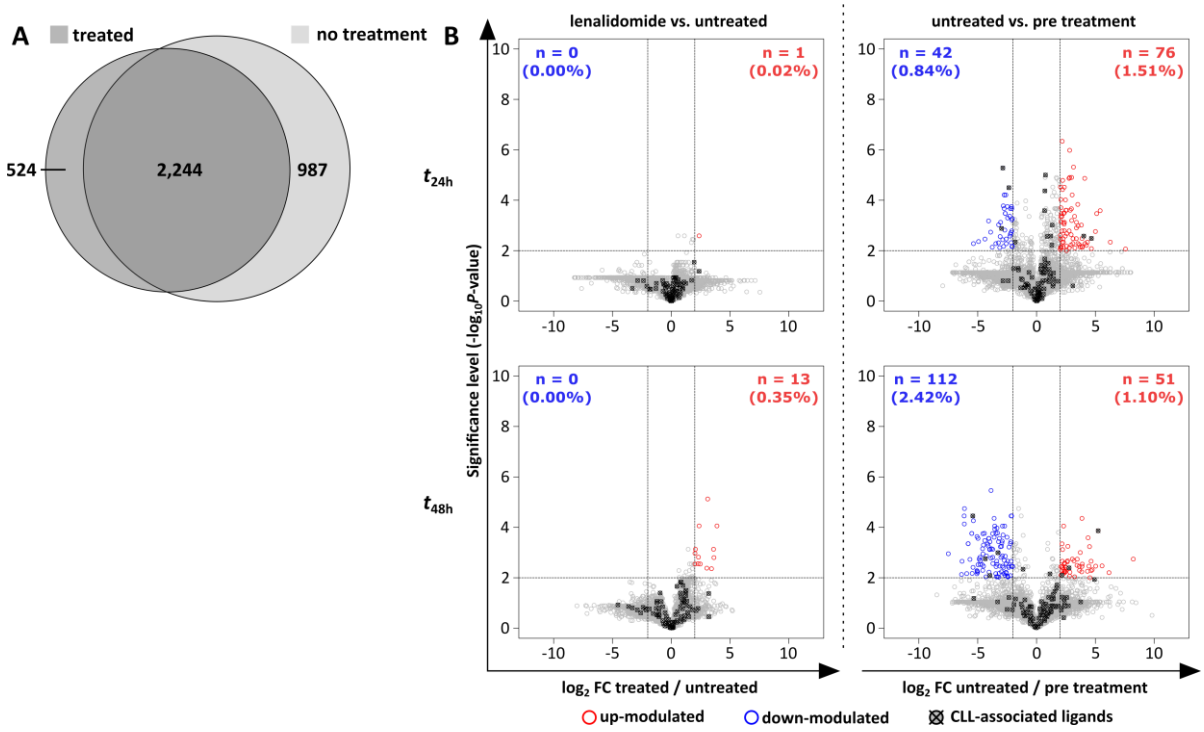

Figure S6: Mass spectrometric analysis of the HLA class II-presented peptidome of primary CLL cells (UPN3) under *in vitro* lenalidomide treatment. (A) Overlap analysis of UPN3 HLA class II ligands identified on lenalidomide-treated versus untreated (vehicle controls and pre treatment) cells. (B) Volcano plots of modulation in the relative abundances of HLA class II ligands on UPN3 cells in all biological replicates comparing the conditions indicated at t_{24h} and t_{48h}. Each dot represents a specific HLA ligand. Log_2 fold-changes of peptide abundance are indicated on the x-axis, the corresponding significance levels after Benjamini-Hochberg correction ($-log_{10}$ *P*-value) on the y-axis. HLA ligands showing significant up- or down-modulation (≥ log_2 2-fold-change in abundance with $P < 0.01$) are highlighted in red and blue, respectively. The absolute numbers and percentages of significantly modulated ligands are specified in the corresponding quadrants. Abbreviations: vs., versus; FC, fold-change.

Supplemental Figure 7

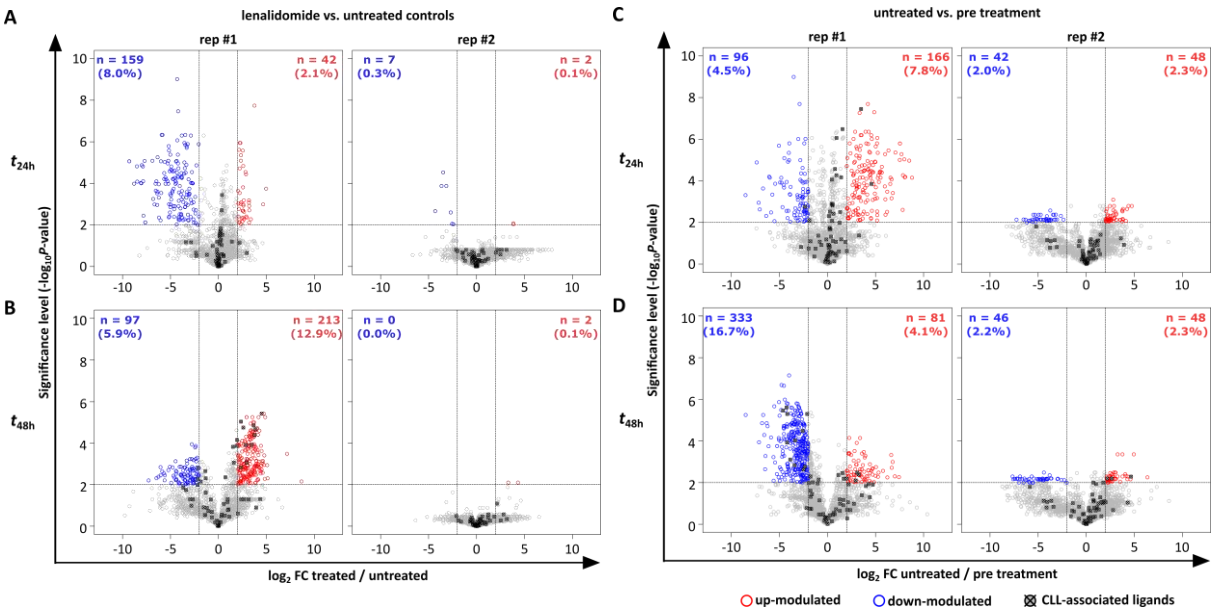

Figure S7: Mass spectrometric analysis of the HLA class II-presented peptidome of primary CLL cells (UPN3) under *in vitro* lenalidomide treatment in single biological replicate analysis. Volcano plots of modulation in the relative abundances of HLA class II ligands on UPN3 cells for each biological replicate separately comparing the conditions indicated at t_{24h} (A, C) and t_{48h} (B, D). Each dot represents a specific HLA ligand. Log_2 fold-changes of peptide abundance are indicated on the x-axis, the corresponding significance levels after Benjamini-Hochberg correction ($-log_{10}$ *P*-value) on the y-axis. HLA ligands showing significant up- or down-modulation (≥ log_2 2-fold-change in abundance with $P < 0.01$) are highlighted in red and blue, respectively. The absolute numbers and percentages of significantly modulated ligands are specified in the corresponding quadrants. Abbreviations: UPN, uniform patient number; vs., versus; FC, fold-change.

Supplemental Figure 8

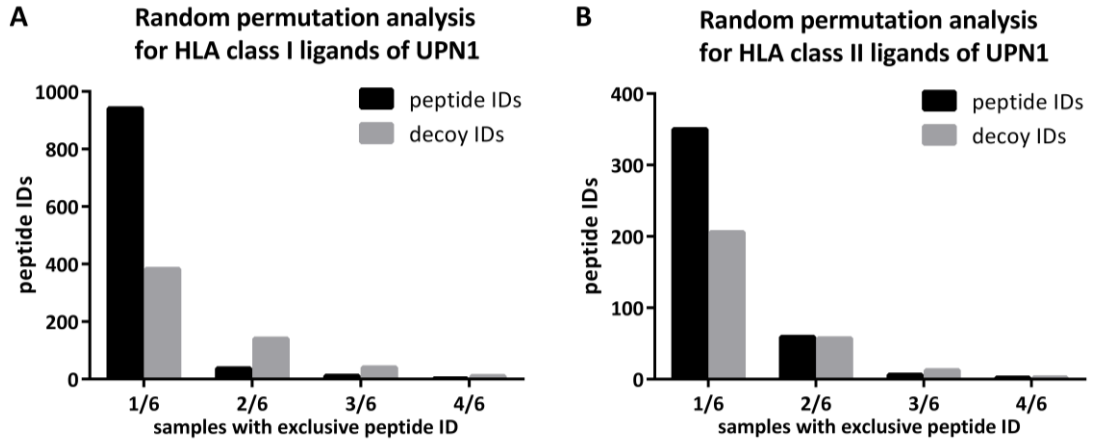

	1/6	2/6	3/6	4/6	1/6	2/6	3/6	4/6
peptide IDs	941	37	11	2	350	59	6	2
decoy IDs	383	140	41	10	206	57	13	2
FDR [%]	**38.8**	**79.5**	**80.3**	**86.3**	**40.0**	**52.0**	**65.8**	**58.6**

Figure S8: Definition of the significance thresholds for lenalidomide-associated HLA ligand presentation on UPN1. Based on permutation analysis, the FDRs of lenalidomide-associated HLA class I (A) and class II (B) peptide presentation were calculated for different presentation frequencies. The process of peptide randomization, cohort assembly and treatment-associated peptide identification was repeated 1,000 times and the mean value of resultant decoy identifications was calculated and plotted for the different threshold values together with the real peptide identifications. The corresponding FDRs for any chosen treatment-associated peptide threshold are listed below the x-axis.

11. SUPPLEMENT OF PART II

Supplemental Methods

Patients and blood samples

For HLA ligandome analysis, PBMCs from CML patients (Departments of Hematology and Oncology in Tübingen, Leipzig, and Aachen, Germany) at the time of diagnosis or in deep molecular remission (MR4.0, MR4.5, and MR5.0) as well as PBMCs, granulocytes, and BMNCs from HVs were isolated by density gradient centrifugation (Biocoll, Biochrom) and erythrocyte lysis (EL buffer, Qiagen). B cells and HPCs of HVs were enriched by $CD19^+$ and $CD34^+$ magnetic-activated cell sorting (Miltenyi), respectively. For T-cell-based assays PBMCs from HVs as well as CML patients at time of diagnosis or at different time points under therapy were isolated by density gradient centrifugation.

HLA surface molecule quantification

HLA surface expression on CML patient samples was determined using the QIFIKIT bead-based quantification flow cytometric assay (Dako) according to the manufacturer's instructions. Cells were stained with either pan-HLA class I-specific W6/32 mAb, HLA-DR-specific L243 mAb (produced in-house), or respective isotype control (BioLegend). Additional surface marker staining was carried out with directly labeled PE/Cy7 anti-human CD33, BV421 anti-human CD13, PE anti-human CD117 (BioLegend), and APC anti-human CD34 (BD) antibodies. Aqua fluorescent reactive dye (Invitrogen) was used as viability marker. Analysis was performed on a FACS Canto II cytometer (BD).

Isolation of HLA ligands

HLA class I and II molecules were isolated by standard immunoaffinity purification using the pan-HLA class I-specific W6/32, the pan-HLA class II-specific Tü-39, and the HLA-DR-specific L243 mAbs (produced in-house). For the immunoprecipitation of HLA class II-peptide complexes, we used a mixture of equal amounts of the L243 and Tü-39 mAbs. HLA-DR is known to be expressed at higher levels than the other class II allotypes. Therefore, the HLA-DR-specific L243 mAb was used at the given stoichiometry. Tü-39 mAb was utilized complementarily to pull-down the remaining class II complexes.

Spectrum validation

Spectrum validation of the experimentally eluted peptides was performed by computing the similarity of the spectra with corresponding synthetic peptides measured in a complex matrix (Figure S1, S2). Because the synthetic peptides were isotope-labeled, fragments which contain an isotope label have a mass shift compared to non-labeled fragments and therefore penalize spectral similarity score. In order to minimize such effects, the spectra of synthetic peptides were preprocessed by shifting isotope label containing single- or double-charged b- and y-ion peaks to the m/z position where their corresponding unlabeled fragment is supposed to be. The spectral correlation (Toprak *et al.* Mol Cell Proteomics 2014) was then calculated between eluted peptide spectra and preprocessed synthetic peptide spectra.

Amplification of peptide-specific T cells and IFNγ ELISPOT assay

PBMCs from CML patients and HVs were pulsed with 1 µg/mL (class I) or 5 µg/mL (class II) per peptide and cultured for 12 days adding 20 U/mL IL-2 (Novartis) on days 3, 5, and 7. Peptide-stimulated PBMCs were analyzed by ELISPOT assay on day 12. Spots were counted using an ImmunoSpot S5 analyzer (CTL) and T-cell responses were considered positive when >10 spots/well were counted and the mean spot count was at least three-fold higher than the mean spot count of the negative control according to the cancer immunoguiding program guidelines.

Cytokine and tetramer staining

The frequency and functionality of peptide-specific $CD8^+$ T cells was analyzed by tetramer and ICS, respectively. For ICS, cells were pulsed with 10 µg/mL of individual peptide and incubated with 10 µg/mL Brefeldin A (Sigma-Aldrich) and 10 µg/mL GolgiStop (BD) for 12 – 16 h. Staining was performed using Cytofix/Cytoperm (BD), PerCP anti-human CD8, Pacific Blue anti-human TNF, FITC anti-human CD107a (BioLegend), and PE anti-human IFNγ antibodies (BD). PMA and ionomycin (Sigma-Aldrich) served as positive control. Negative control peptides are listed in Table S3. The frequency of peptide-specific $CD8^+$ T cells after aAPC-based priming was determined by PerCP anti-human CD8 mAb and HLA:peptide tetramer-PE. For negative control tetramers of the same HLA allotype containing irrelevant control peptides were used. The priming was considered successful if the frequency of peptide-specific $CD8^+$ T cells was >0.1% of $CD8^+$ T cells within the viable single cell population and at least three-fold higher than the frequency of peptide-specific $CD8^+$ T cells in the negative control. The same evaluation criteria were applied for the ICS results. All samples were analyzed on a FACS Canto II cytometer (BD).

Supplemental Table S1: Patient characteristics

UPN	Phase of disease	Experiment	Age	CML-specific therapy	WBC (10^3/µl)	HLA class I typing	HLA class II typing	HLA class I		HLA class II	
								HLA ligand IDs	Protein IDs	Peptide IDs	Protein IDs
1	chronic phase	L	71	no	n.a.	A*23, A*25, B*18, B*57, C*06, C*12	DRB1*07, DRB1*15, DQB1*03, DQB1*06	1,572	1,491	1,162	394
2	chronic phase	L	55	no	n.a.	A*03, B*35, B*52, C*04	DRB1*04, DRB1*13, DQB1*03, DQB1*06	1,385	1,360	n.a.	n.a.
3	chronic phase	L	72	no	n.a.	A*01, B*08, C*07	DRB1*03, DRB1*15, DQB1*02, DQB1*06	535	457	n.a.	n.a.
4	chronic phase	L	66	no	n.a.	A*03, A*68, B*07, B*44, C*07	DRB1*11, DRB1*15, DQB1*03, DQB1*06	1,032	994	390	208
5	chronic phase	L	61	no	n.a.	A*24, A*68, B*27, B*57	DRB1*11, DRB1*14, DQB1*03, DQB1*05	539	628	507	162
6	chronic phase	L	56	no	n.a.	A*01, A*03, B*07, B*08, C*07	DRB1*03, DRB1*15, DQB1*02, DQB1*06	657	516	1,044	379
7	chronic phase	L	70	no	n.a.	A*02, A*03, B*13, B*15, C*03, C*06	DRB1*07, DRB1*13, DQB1*02, DQB1*06	1,270	1,180	641	209
8	chronic phase	L	57	no	n.a.	A*01, A*02, B*08, B*50, C*06, C*07	DRB1*03, DRB1*07, DQB1*02	747	832	381	137
9	chronic phase	L	68	no	n.a.	A*03, B*07, B*35, C*04, C*07	DRB1*01, DRB1*15, DQB1*05, DQB1*06	701	541	172	121
10	chronic phase	L	60	no	169	A*02, A*11, B*35, B*44, C*04	n.a.	1,676	1,529	900	405
11	chronic phase	L	41	no	190	A*03, B*35, C*04	n.a.	1,228	1,187	1,142	279
		E, T, L_{MR}	47	nilotinib 600 mg	5			523	456	108	65
12	chronic phase	L	n.a.	no	124	A*02, A*11, B*07, C*07, C*17	n.a.	639	659	533	209
13	blast crisis	L	37	no	131	A*02, B*18, B*57, C*06, C*07	DRB1*07, DRB1*11, DQB1*03	1,075	1,109	699	398
14	chronic phase	L	n.a.	n.a.	106	A*02, A*11, B*35, B*44, C*04	n.a.	907	926	398	182
15	chronic phase	L	44	no	310	A*01, A*02, B*35, B*41	n.a.	835	696	555	327
16	chronic phase	L	78	no	128	A*66, B*40, B*44, C*03, C*05	n.a.	866	701	500	234
17	chronic phase	L	27	no	80	A*03:01, A*23:01, B*07:02, B*18:01, C*07:01, C*07:02	DRB1*14:01, DRB1*16:01, DQB1*05:02, DQB1*05:03	2,107	1,543	668	285
18	accelerated phase	L	21	no	483	A*02:20, A*11:01, B*27:05, B*44:02, C*01:02, C*05:02	DRB1*01:01, DRB1*08:01, DQB1*04:02, DQB1*05:01	1,823	1,263	1,157	273
19	chronic phase	L, Q	39	no	156	A*02, A*11, B*07, B*51, C*07	n.a.	1,476	1,362	484	199
20	blast crisis	L	83	no	235	A*01, A*03, B*07, B*08, C*07	DRB1*03, DRB1*07, DQB1*02	791	846	721	385
21	chronic phase	L, Q	73	no	130	A*02, B*57, C*06	n.a.	820	898	359	205
		P	74	imatinib 400 mg	-			n.a.	n.a.	n.a.	n.a.
22	chronic phase	L	63	no	140	A*02, A*33, B*14, B*40	n.a.	n.a.	n.a.	411	178
23	chronic phase	Q	19	no	-	A*02:01, A*23:01, B*18:01, B*35:01, C*04:01, C*07:01	DRB1*01:01, DRB1*11:04, DQB1*03:01, DQB1*05:01	n.a.	n.a.	n.a.	n.a.
		P, T	23	dasatinib 100 mg	-			n.a.	n.a.	n.a.	n.a.
24	chronic phase	Q	26	no	-	A*23:01, A*68:01, B*07:02, B*50:01, C*06:02, C*07:10	DRB1*03:01, DRB1*13:01, DQB1*02:01, DQB1*06:03	n.a.	n.a.	n.a.	n.a.

Supplemental Table S1 continued

UPN	Phase of disease	Experiment	Age	CML-specific therapy	WBC (10^3/µl)	HLA class I typing	HLA class II typing	HLA class I		HLA class II	
								HLA ligand IDs	Protein IDs	Peptide IDs	Protein IDs
25	chronic phase	Q	49	no	-	A*24:02, A*26:01, B*51:01, B*55:01, C*03:03, C*15:02	DRB1*11:01, DRB1*16:01, DQB1*03:01, DQB1*05:02	n.a.	n.a.	n.a.	n.a.
		E	57	imatinib 400 mg	-			n.a.	n.a.	n.a.	n.a.
		L_{MR}	58	imatinib 400 mg	6			622	554	127	175
26	accelerated phase	Q	58	no	-	A*02:01, B*07:02, B*35:01, C*04:01, C*07:02	n.a.	n.a.	n.a.	n.a.	n.a.
27	chronic phase	Q	38	no	-	A*11, A*68, B*44, B*51, C*05, C*14	n.a.	n.a.	n.a.	n.a.	n.a.
		L_{MR}	41	no	7			904	975	232	153
28	chronic phase	P	54	no	-	A*02, A*03, B*18, B*44, C*12, C*16	n.a.	n.a.	n.a.	n.a.	n.a.
		L_{MR}	55	no	6			1,033	1,077	234	172
29	chronic phase	P, E	69	imatinib 400 mg	-	A*02, A*11, B*18, B*35, C*02, C*04	DRB1*01, DRB1*11, DQB1*03, DQB1*05	n.a.	n.a.	n.a.	n.a.
		L_{MR}	70	imatinib 400 mg	6			1,145	918	229	159
30	chronic phase	P, E	39	nilotinib 300 mg	-	A*02, A*03, B*18, B*73	n.a.	n.a.	n.a.	n.a.	n.a.
31	chronic phase	P, E	48	nilotinib 600 mg	-	A*03, A*24, B*07, B*49, C*07	n.a.	n.a.	n.a.	n.a.	n.a.
		L_{MR}	49	nilotinib 600 mg	6			417	498	193	257
32	chronic phase	E	55	imatinib 400 mg	-	A*11, A*32, B*27, B*47	n.a.	n.a.	n.a.	n.a.	n.a.
33	chronic phase	P, E, T	52	imatinib 400 mg	-	A*02:01, A*03:01, B*15:01, B*57:01, C*03:03, C*06:02	n.a.	n.a.	n.a.	n.a.	n.a.
34	chronic phase	E	80	nilotinib 600 mg	-	A*02, A*29, B*40, B*44, C*03, C*16	n.a.	n.a.	n.a.	n.a.	n.a.
		T, L_{MR}	81	nilotinib 800 mg	12			720	795	210	131
35	chronic phase	E	22	imatinib 400 mg	-	A*02, B*07, B*15	n.a.	n.a.	n.a.	n.a.	n.a.
36	chronic phase	P, E	58	nilotinib 800 mg	-	A*02:01, B*27:05, B*44:02, C*01:02, C*05:01	DRB1*04:08, DRB1*11:01, DQB1*03:01	n.a.	n.a.	n.a.	n.a.
37	chronic phase	E	57	dasatinib 100 mg	-	A*02:01, A*03:01, B*35:03, B*47:01, C*04:01, C*06:02	DRB1*04:05, DRB1*11:04, DQB1*03:01, DQB1*03:02	n.a.	n.a.	n.a.	n.a.
	accelerated phase	T	57	dasatinib 100 mg	-			n.a.	n.a.	n.a.	n.a.
38	chronic phase	E, T, L_{MR}	79	imatinib 400 mg	5	A*01, A*11, B*13, B*56, C*01, C*06	n.a.	311	289	122	129
39	chronic phase	E	46	imatinib 400 mg	-	A*01, A*32, B*15	n.a.	n.a.	n.a.	n.a.	n.a.
40	chronic phase	P, E	68	ponatinib 30 mg	-	A*03, A*24, B*18, B*58	n.a.	n.a.	n.a.	n.a.	n.a.
	accelerated phase	T	68	imatinib 400 mg, hydroxyurea 500 mg	-			n.a.	n.a.	n.a.	n.a.

Supplemental Table S1 continued

UPN	Phase of disease	Experiment	Age	CML-specific therapy	WBC (10^3/µl)	HLA class I typing	HLA class II typing	HLA class I		HLA class II	
								HLA ligand IDs	Protein IDs	Peptide IDs	Protein IDs
41	chronic phase	E	72	nilotinib 600 mg	-	A*01, B*08, B*44	n.a.	n.a.	n.a.	n.a.	n.a.
42	chronic phase	E	40	imatinib 400 mg	-	A*02, B*27, B*56	n.a.	n.a.	n.a.	n.a.	n.a.
43	chronic phase	E	63	imatinib 400 mg	-	A*01, B*08	n.a.	n.a.	n.a.	n.a.	n.a.
44	chronic phase	E, T	39	nilotinib 600 mg	-	A*02, B*13, B*18	n.a.	n.a.	n.a.	n.a.	n.a.
45	chronic phase	E, T	58	imatinib 400 mg	-	A*02:01, A*23:01, B*44:02, B*44:03, C*04:01, C*05:01	DRB1*04:01, DQB1*02:02, DQB1*03:02	n.a.	n.a.	n.a.	n.a.
46	chronic phase	P, E	62	imatinib 400 mg	-	A*02, A*24, B*18, B*58	n.a.	n.a.	n.a.	n.a.	n.a.
47	chronic phase	E	77	imatinib 400 mg	-	A*01, A*26, B*08, B*55	n.a.	n.a.	n.a.	n.a.	n.a.
48	chronic phase	T	43	bosutinib 500 mg	-	A*02, A*68, B*44, B*55	n.a.	n.a.	n.a.	n.a.	n.a.
		E	44	dasatinib 70 mg	-			n.a.	n.a.	n.a.	n.a.
49	chronic phase	P, E, T	68	imatinib 300 mg	-	A*02, A*25, B*08, B*13, C*06, C*07	n.a.	n.a.	n.a.	n.a.	n.a.
50	chronic phase	E	77	nilotinib 600 mg	-	A*01, A*03, B*08, B*49	n.a.	n.a.	n.a.	n.a.	n.a.
51	chronic phase	E, T	53	nilotinib 600 mg	-	A*02:01, A*30:01, B*13:02, B*58:01, C*06:02, C*07:01	DRB1*07:01, DRB1*13:02, DQB1*02:02, DQB1*06:04	n.a.	n.a.	n.a.	n.a.
52	chronic phase	E	72	interferon	-	A*02, A*03, B*07, B*08	n.a.	n.a.	n.a.	n.a.	n.a.
53	chronic phase	E	55	nilotinib 600 mg	-	A*02:01, A*03:01, B*18:01, B*53:01, C*04:01, C*12:03	DRB1*04:01, DRB1*15:03, DQB1*03:02, DQB1*06:02	n.a.	n.a.	n.a.	n.a.
		L_{MR}	56	interferon	7			416	355	281	215
54	chronic phase	E	59	imatinib 200 mg	-	A*01:01, B*08:01, C*07:01	DRB1*01:01, DRB1*03:01, DQB1*02:01, DQB1*05:01	n.a.	n.a.	n.a.	n.a.
55	accelerated phase	P, E	62	dasatinib 140 mg	-	A*02:01, B*07:02, B*35:01, C*04:01, C*07:02	DRB1*11:01, DRB1*16:01, DQB1*03:01, DQB1*05:02	n.a.	n.a.	n.a.	n.a.
56	chronic phase	E	61	nilotinib 600 mg	-	A*26, A*33, B*14, B*56, C*01, C*15	n.a.	n.a.	n.a.	n.a.	n.a.
		L_{MR}	61	nilotinib 600 mg, interferon	5			544	648	74	116
57	chronic phase	E	50	dasatinib 100 mg	-	A*01:01, A*25:01, B*08:01, B*18:01, C*07:01, C*12:03	DRB1*03:01, DRB1*15:01, DQB1*02:01, DQB1*06:02	n.a.	n.a.	n.a.	n.a.
58	chronic phase	E, T	74	imatinib 400 mg	-	A*02, A*03, B*07, B*44, C*07, C*16	DRB1*07:01, DRB1*13:01, DQB1*02:02, DQB1*06:03	n.a.	n.a.	n.a.	n.a.
59	chronic phase	T	37	imatinib 400 mg	-	A*02:01, A*29:02, B*44:02, B*58:01, C*05:01, C*07:01	DRB1*08:04, DRB1*13:01, DQB1*04:02, DQB1*06:03	n.a.	n.a.	n.a.	n.a.
		P	38	imatinib 800 mg	-			n.a.	n.a.	n.a.	n.a.
60	chronic phase	P, L_{MR}	67	imatinib 400 mg	4	A*02, B*18, B*52, C*02	n.a.	576	512	88	124
61	chronic phase	L_{MR}	68	imatinib 400 mg, interferon	6	A*02, B*27, B*44, C*01, C*05	DRB1*01:03, DRB1*11:01, DQB1*03:01, DQB1*05:01	646	741	136	72

Supplemental Table S1 continued

UPN	Phase of disease	Experi-ment	Age	CML-specific therapy	WBC (10^3/µl)	HLA class I typing	HLA class II typing	HLA class I		HLA class II	
								HLA ligand IDs	Protein IDs	Peptide IDs	Protein IDs
62	chronic phase	L_{MR}	57	interferon	7	A*24, A*31, B*18, B*40, C*03, C*07	n.a.	768	863	180	168
63	chronic phase	T	55	dasatinib 100 mg	-	A*02, B*18, B*44	n.a.	n.a.	n.a.	n.a.	n.a.
64	chronic phase	T	75	imatinib 400 mg	-	A*02, A*24, B*40, B*44	n.a.	n.a.	n.a.	n.a.	n.a.
65	chronic phase	T	36	nilotinib 600 mg	-	A*02:01, A*30:01, B*13:02, B*40:01, C*03:04, C*06:02	DRB1*04:04, DRB1*04:05, DQB1*03:02	n.a.	n.a.	n.a.	n.a.
66	chronic phase	T	46	imatinib 400 mg	-	A*02, B*39, B*55	n.a.	n.a.	n.a.	n.a.	n.a.
67	chronic phase	L_{MR}	37	imatinib 400 mg	5	A*01:01, A*02:01, B*14:01, B*57:01, C*06:02, C*08:02	n.a.	467	404	147	152
68	chronic phase	L_{MR}	75	imatinib 400 mg	5	A*26, A*33, B*14, B*56, C*01, C*08	n.a.	735	823	101	129

CML patients included in HLA ligandome analysis, quantification of HLA surface expression, *in vitro* T-cell priming experiments, and IFNγ ELISPOT assays. CML-specific treatment at the time of sample collection is given as dose per day. Lymphocyte count at the time of sample collection is indicated for patients included in HLA ligandome analysis. Abbreviations: UPN, uniform patient number; WBC, white blood cell count; IDs, identifications; L, HLA ligandome analysis for the identification of CML-associated target antigens; L_{MR}, HLA ligandome analysis of CML patients in deep molecular remission (MR4.0 or better) as additional comparative benign dataset; Q, HLA quantification; P, *in vitro* priming of naïve $CD8^+$ T cells; E, IFNγ ELISPOT assay; T, tetramer staining after 12-d stimulation; n.a., not available.

Supplemental Table S2: BCR-ABL- and ABL-BCR-derived peptides targeted by parallel reaction monitoring

Protein	Protein accession	Sequence	HLA restriction
BCR-ABL fusion protein			
p210, X9	A1Z199, A9UF02	IPLTINKEEAL	B*07
e3a11	Q8NF93	LPQAGAQIRGL	B*07
		TPAIFSPRL	B*07, B*35
e8a2	A9YD18	LELLTSEAL	B*18, B*40
e8a2	B0ZRR0	EEITPRRPL	B*18
		LPEALQRPV	B*07
		RPLSLPEAL	B*07, B*35
		SLPEALQRPV	A*02
		TPRRPLSL	B*08
e8a2	E7E8T7	TVKKGELLNRK	A*03
		VPSIPYLEAL	B*07, B*35
e13a3	A2RQD3	NKEGEKLRVLGY	A*01
e14a2	B0ZRR1	KQSSVPTSSK	A*03
		VPTSSKENLL	B*35
e14a3	A2RQD4, Q16189	SSEKLRVLGY	A*01
e18-int1b-a2	B0ZRQ9	FLRKRPQEAL	B*08
		RPQEALQRPV	B*07
X3	A9UEZ6	KLASQLGVYRV	A*02
X5	A9UEZ8	ILASEEITL	A*02
X6	A9UEZ9	LELQGKPSRW	B*44
X7	A9UF00	LEMRKWDPV	B*40
X7, Y4	A9UF00, A9UF06	DPVKMTPTF	B*35
		DPVKMTPTFSL	B*07
		ILWPVEITL	A*02
X8	A9UF01	AEEVFQKLL	B*40, B*44
		HPGAAEEVF	B*35
X9	A9UF02	EETYLSHLQM	B*18, B*44
Y2	A9UF04	RPPHLTELPV	B*07
Y3	A9UF05	EALGEDPSF	B*35
		FPASDGPRH	B*35
		GEGAFHGDAVL	B*40
		GVRRARLSL	B*07
		HQGVRRARL	B*08
		RARLSLEAL	B*07
		VPHQGVRRARL	B*07
Y4	A9UF06	LDPVKMTPTF	B*35
		SELDPVKMTPTF	B*44
Y5	A9UF07	QIKSDIQREK	A*03
		SPSSSPHRQL	B*35
		SPSSSPHRQLL	B*07
		SSSPHRQLLK	A*03
		ATGFKQSSK	A*03
		KQSSKALQR	A*03
n.s.	A0A127KQ99	RISQNFLSKK	A*03
n.s.	A6MF66	GEGAFHGDAAL	B*40
n.s.	A6MF66, A6MF67	ALRLLREPL	B*08
n.s.	A6MF66, A6MF67, A6MF68	RLLREPLQH	A*03
		HPGRVGSSSF	B*07, B*35
n.s.	A6MF67	IPLTINKEAL	B*07, B*35
n.s.	A6MF68	TLRLLREPL	B*08

Supplemental Table S2 continued

Protein	Protein accession	Sequence	HLA restriction
ABL-BCR fusion protein			
Iab3	n.s.	YLEDDESPGL	A*02
Iab3	n.s.	YLEDDESPGLY	A*01
Ibb3	n.s.	FVEHDDESPGLY	A*01

List of BCR-ABL- and ABL-BCR-derived peptide sequences with their corresponding HLA restriction targeted by parallel reaction monitoring. Abbreviation: n.s., not specified.

Supplemental Table S3: Positive and negative control peptides

Source protein	Peptide sequence	HLA restriction
Positive control peptides		
BRLF1_EBVB9	YVLDHLIVV	A*02
EBNA3_EBVB9	RLRAEAQVK	A*03
EBNA3_EBVB9	RPPIFIRRL	B*07
BZLF1_EBVB9	RAKFKQLL	B*08
EBNA6_EBVB9	AEGGVGWRHW	B*44
PP65_HCMVA	YQEFFWDANDIYRIF	class II
EBNA1_EBVB9	KTSLYNLRRGTALA	class II
PP65_HCMVA	HPTFTSQYRIQGKLEYR	class II
PP65_HCMVA	KPGKISHIMLDVAFTSH	class II
GP350_EBVB9	STNITAVVRAQGLDV	class II
GP350_EBVB9	PRPVSRFLGNNSILY	class II
Negative control peptides		
POL_HV1BR	GSEELRSLY	A*01
DDX5_HUMAN	YLLPAIVHI	A*02
GAG_HV1BR	RLRPGGKKK	A*03
UBC_HUMAN	QIFVKTLTGK	A*03
NEF_HV1BR	TPGPGVRYPL	B*07
ANM1_HUMAN	DEVRTLTY	B*18
FLNA_HUMAN	ETVITVDTKAAGKGK	class II

Positive and negative control peptides with their respective HLA restrictions used for IFNγ ELISPOT assays or aAPC-based *in vitro* priming experiments. Abbreviations: EBVB9, Epstein-Barr virus (strain B95-8); HCMVA, human cytomegalovirus (strain AD169); HV1BR, human immunodeficiency virus type 1 group M subtype B.

Supplemental Table S4: Identified CML-associated HLA class I antigens

Protein	Sequence	Peptide length	HLA restriction	Representation frequency in CML cohort	Representation frequency in HLA-matched CML samples
All HLA ligands					
PLSL	HLLEQVAPK	9	A*03	29%	75%
ARP2, ACTB	RLDIAGRDI	9	C*04, C*05, C*17	29%	n.a.
NDC80	SINKPTSER	9	A*03	29%	63%
*****	DMEKIWHHTFY	11	A*01, B*18, B*44	24%	n.a.
DHRS9	KIFWIPLSH	9	A*03	24%	63%
H12	AAKPKVVKPK	10	A*11	19%	80%
CSN6	ALHPLVILNI	10	A*02	19%	40%
BPI	AVNPGVVVR	9	A*11	19%	80%
RB27A	FRDAMGFLLL	10	C*04, C*05, C*07	19%	n.a.
PSB9	GTLGGMLTR	9	A*11, A*66	19%	n.a.
IQGA1	IFLLNKKFYGK	11	A*03	19%	50%
CEAM8	KLFIPNITTK	10	A*03	19%	50%

Supplement Table S4 continued

Protein	Sequence	Peptide length	HLA restriction	Representation frequency in CML cohort	Representation frequency in HLA-matched CML samples
BEX1, BEX2	KLREKQLSH	9	A*03	19%	50%
GELS	KQGFEPPSFV	10	A*02	19%	40%
**	KQVHPDTGISSK	12	A*03	19%	50%
S10A8	NTDGAVNFQEF	11	A*01, C*05	19%	n.a.
CD24	RAMVARLGL	9	B*07	19%	57%
UTP20	RIAKLEAAY	9	A*03	19%	50%
ANLN	RLLLIATGK	9	A*03	19%	50%
PCNA	RLVQGSILKK	10	A*03	19%	50%
PTN7	RTAGHPLTR	9	A*03	19%	50%
GFI1B, GFI1	TLSTHLLIH	9	A*03	19%	50%
XPO5	YRPEFLPQVF	10	C*07, B*07	19%	n.a.
HLA-A*02					
C3AR	KLIPSIIVL	9	A*02	24%	50%
CSN6	ALHPLVILNI	10	A*02	19%	40%
GELS	KQGFEPPSFV	10	A*02	19%	40%
BPI	LLFGADVVYK	10	A*02	48%	40%
HLA-A*03					
PLSL	HLLEQVAPK	9	A*03	29%	75%
DHRS9	KIFWIPLSH	9	A*03	24%	63%
BPI	LLFGADVVYK	10	A*03	48%	63%
NDC80	SINKPTSER	9	A*03	29%	63%
IQGA1	IFLLNKKFYGK	11	A*03	19%	50%
CEAM8	KLFIPNITTK	10	A*03	19%	50%
BEX1, BEX2	KLREKQLSH	9	A*03	19%	50%
**	KQVHPDTGISSK	12	A*03	19%	50%
GELS	KTASDFITK	9	A*03	29%	50%
UTP20	RIAKLEAAY	9	A*03	19%	50%
ANLN	RLLLIATGK	9	A*03	19%	50%
PCNA	RLVQGSILKK	10	A*03	19%	50%
PTN7	RTAGHPLTR	9	A*03	19%	50%
CKAP5	STLPKSLLK	9	A*03	24%	50%
GFI1B, GFI1	TLSTHLLIH	9	A*03	19%	50%
GPAA1	ALVFPPLTQR	10	A*03	14%	38%
CEAM8	GTFQQYTQK	9	A*03	29%	38%
PERM	GVSEPLKRK	9	A*03	24%	38%
LARP1	HSNTQTLGK	9	A*03	14%	38%
SSPN	IQFSMKLLY	9	A*03	14%	38%
PCNA	KIADMGHLKY	10	A*03	14%	38%
RIR1	KINGKVAER	9	A*03	14%	38%
BPI	KISGKWKAQK	10	A*03	14%	38%
GLE1	KLREAEQQRVK	11	A*03	14%	38%
DENR	KLTVENSPK	9	A*03	14%	38%
CQ085	KMISTPSPK	9	A*03	14%	38%
GTPB1	KMQSTKKGPLTK	12	A*03	14%	38%
PDIA1	KVHSFPTLK	9	A*03	14%	38%
KI67	RIQLPVVSK	9	A*03	33%	38%
HDGR2	RLKSRVLGPK	10	A*03	14%	38%
PDIP3	RLSDSPSMK	9	A*03	14%	38%

Supplement Table S4 continued

Protein	Sequence	Peptide length	HLA restriction	Representation frequency in CML cohort	Representation frequency in HLA-matched CML samples
RHG25	SAFQGANSSK	10	A*03	14%	38%
TCO1	SLVEKILSEK	10	A*03	14%	38%
LPPR3	SVISDTTKLLK	11	A*03	33%	38%
S10A8	VIKMGVAAHKK	11	A*03	14%	38%
HLA-A*11					
H12	AAKPKVVKPK	10	A*11	19%	80%
BPI	AVNPGVVVR	9	A*11	19%	80%
PCNA	KIADMGHLK	9	A*11	33%	80%
HLA-B*07					
CD24	RAMVARLGL	9	B*07	19%	57%
XPO5	YRPEFLPQVF	10	B*07, C*07	19%	57%
STT3B	APESKHKSSL	10	B*07	14%	43%
ATPA	APGIIPRISV	10	B*07	14%	43%
CEBPE	APGQPLRVL	9	B*07	14%	43%
BPI	NPTSGKPTI	9	B*07	14%	43%
HTR5A, HTR5B	SPGPPTRKL	9	B*07	14%	43%
ANLN	SPVKSTTSI	9	B*07	14%	43%

Panel of naturally presented, CML-associated, HLA class I-restricted peptide targets identified by HLA class I ligandome profiling of primary CML samples (n = 21) and a hematological benign dataset (n = 108). Peptides mapping in multiple proteins are marked with asterisks: *ACTBM, ACTB, ACTC, ACTG, ACTS, POTEE, POTEF, POTEI, POTEJ and **H2B1A, H2B1B, H2B1C, H2B1D, H2B1H, H2B1J, H2B1K, H2B1L, H2B1M, H2B1N, H2B1O, H2B2E, H2B2F, H2B3B, H2BFS. Abbreviation: n.a., not applicable.

Supplemental Table S5: Identified CML-associated HLA class II antigens

Protein	Sequence	Peptide length	Representation frequency	Peptide target	Protein target	Hotspot target
Peptide targets						
VAT1	**Synaptic vesicle membrane protein VAT-1 homolog**					
	VLFDFGNLQPGHSV	14	45%	x		x
TCPG	**T-complex protein 1 subunit gamma**					
	AMQVCRNVLLDPQLVPGG	18	25%	x		x
BPI	**Bactericidal permeability-increasing protein**					
	NEKLQKGFPLPTPARV	16	25%	x		x
KCY	**UMP-CMP kinase**					
	DEVVQIFDKEG	11	25%	x	x	x
MYO9B	**Unconventional myosin-IXb**					
	MEPAFIIQHF	10	25%	x		x
XRCC5	**X-ray repair cross-complementing protein 5**					
	EEASNQLINHIEQF	14	20%	x		x
Protein targets						
KCY	**UMP-CMP kinase**		25%			
	DEVVQIFDKEG	11	25%	x	x	x
TCPW	**T-complex protein 1 subunit zeta-2**		25%			
	ADALLIIPK	9	15%		x	x
	ADALLIIPKVL	11	10%		x	x
	ADALLIIPKVLA	12	5%		x	x

Supplemental Table S5 continued

Protein	Sequence	Peptide length	Representation frequency	Peptide target	Protein target	Hotspot target
MCM2	**DNA replication licensing factor MCM2**		20%			
	SENVDLTEPIISRF	14	5%		x	
	GPRLEIHHRF	10	5%		x	
	IESIENLEDLKGHSV	15	5%		x	
	ANGFPVFATVIL	12	5%		x	
PTBP2	**Polypyrimidine tract-binding protein 2**		20%			
	GLPFGKVTNIL	11	10%		x	
	FGVYGDVQRV	10	10%		x	
Hotspot targets						
RB27A	**Ras-related protein Rab-27A**		20%			
	FDLTNEQSFLNV	12	15%			x
	FDLTNEQSFL	10	5%			x
	DLTNEQSFLNV	11	5%			x

Panel of naturally presented, CML-associated HLA class II antigens identified by HLA class II ligandome profiling of primary CML samples (n = 20) and a hematological benign dataset (n = 88). Peptides are assigned to the respective group of target antigens (peptide targets, protein targets, and hotspot targets).

Supplemental Table S6: Numbers of identified HLA class I peptides derived from cancer/testis antigens

Protein		# of HLA peptides in CML patient ligandomes	# of HLA peptides in hematological benign ligandomes	Total # of unique HLA peptides
CML-exclusive				
CRIS2	Cysteine-rich secretory protein 2	1	0	1
MAGA6	Melanoma-associated antigen 6	1	0	1
SPG17	Sperm-associated antigen 17	1	0	1
TULP2	Tubby-related protein 2	1	0	1
CML-overrepresented				
DNJB8	DnaJ homolog subfamily B member 8	1	1	1
FA46D	Putative nucleotidyltransferase FAM46D	1	1	1
KDM5B	Lysine-specific demethylase 5B	10	15	20
KIF2C	Kinesin-like protein KIF2C	4	5	7
MAGA1	Melanoma-associated antigen 1	1	1	2
NUF2	Kinetochore protein Nuf2	4	11	13
ODFP2	Outer dense fiber protein 2	2	5	5
SO6A1	Solute carrier organic anion transporter family member 6A1	1	1	1
Benign-overrepresented				
HEMGN	Hemogen	3	10	11
POTEA	POTE ankyrin domain family member A	1	2	2
POTEE	POTE ankyrin domain family member E	30	70	74
Benign-exclusive				
ACRBP	Acrosin-binding protein	0	4	4
BRDT	Bromodomain testis-specific protein	0	2	2
CCNA1	Cyclin-A1	0	1	1
CE290	Centrosomal protein of 290 kDa	0	1	1

Supplemental Table S6 continued

Protein		# of HLA peptides in CML patient ligandomes	# of HLA peptides in hematological benign ligandomes	Total # of unique HLA peptides
CTCFL	Transcriptional repressor CTCFL	0	1	1
CTGE2	cTAGE family member 2	0	1	1
F133A	Protein FAM133A	0	1	1
GPAT2	Glycerol-3-phosphate acyltransferase 2, mitochondrial	0	1	1
LDHC	L-lactate dehydrogenase C chain	0	2	2
MAGAA	Melanoma-associated antigen 10	0	1	1
MAGC1	Melanoma-associated antigen C1	0	1	1
MORC1	MORC family CW-type zinc finger protein 1	0	3	3
MS18B	Protein Mis18-beta	0	1	1
PASD1	Circadian clock protein PASD1 (PAS domain containing 1)	0	1	1
PRS55	Serine protease 55	0	1	1
RGS22	Regulator of G-protein signaling 22	0	1	1
SSX1	Protein SSX1	0	1	1
SYCE1	Synaptonemal complex central element protein 1	0	1	1
TAF7L	Transcription initiation factor TFIID subunit 7-like	0	1	1
TSG10	Testis-specific gene 10 protein	0	1	1
XAGE2	X antigen family member 2	0	1	1
XAGE3	X antigen family member 3	0	1	1
XAGE5	X antigen family member 5	0	1	1
ZN165	Zinc finger protein 165	0	2	2

Numbers of naturally presented unique HLA class I peptides derived from predescribed cancer/testis antigens (Almeida *et al.* Nucleic Acids Res. 2009, GTEx Consortium Cancer Immunol Immunother. 2011) identified in CML patient (n = 21) and hematological benign (n = 108) ligandomes. Antigens are assigned to their degree of CML-association determined by their representation frequencies in both cohorts (CML-exclusive, CML-overrepresented, benign-overrepresented, benign-exclusive).

Supplemental Table S7: Numbers of identified HLA class II peptides derived from cancer/testis antigens

Protein		# of HLA peptides in CML patient ligandomes	# of HLA peptides in hematological benign ligandomes	Total # of unique HLA peptides
CML-overrepresented				
SPG17	Sperm-associated antigen 17	1	1	2
SO6A1	Solute carrier organic anion transporter family member 6A1	1	1	1
POTEE	POTE ankyrin domain family member E	173	300	333
Benign-exclusive				
ACRBP	Acrosin-binding protein	0	1	1
AKAP3	A-kinase anchor protein 3	0	1	1
CTGE2	cTAGE family member 2	0	4	4
HEMGN	Hemogen	0	19	19
HSP1	Sperm protamine P1	0	2	2
KDM5B	Lysine-specific demethylase 5B	0	1	1
LUZP4	Leucine zipper protein 4	0	3	3
MAGA1	Melanoma-associated antigen 1	0	3	3
MAGA4	Melanoma-associated antigen 4	0	1	3

Supplemental Table S7 continued

Protein		# of HLA peptides in CML patient ligandomes	# of HLA peptides in hematological benign ligandomes	Total # of unique HLA peptides
MAGC1	Melanoma-associated antigen C1	0	3	3
POTEA	POTE ankyrin domain family member A	0	1	1
SSX2	Protein SSX2	0	1	1
SYCP1	Synaptonemal complex protein 1	0	4	4
TAF7L	Transcription initiation factor TFIID subunit 7-like	0	1	1
TEX14	Inactive serine/threonine-protein kinase TEX14	0	2	2

Numbers of naturally presented unique HLA class II peptides derived from predescribed cancer/testis antigens (Almeida *et al.* Nucleic Acids Res 2009, GTEx Consortium Cancer Immunol Immunother 2011) identified in CML patient (n = 20) and hematological benign (n = 88) ligandomes. Antigens are assigned to their degree of CML-association determined by their representation frequencies in both cohorts (CML-overrepresented, benign-exclusive).

Supplemental Table S8: Numbers of identified HLA class I peptides derived from leukemia-associated antigens

Protein		# of HLA peptides in CML patient ligandomes	# of HLA peptides in hematological benign ligandomes	Total # of unique HLA peptides
CML-exclusive				
MAGA6	Melanoma-associated antigen 6	1	0	1
CML-overrepresented				
ABC3B	DNA dC->dU-editing enzyme APOBEC-3B	2	9	9
AURKA	Aurora kinase A	3	3	4
BMI1	Polycomb complex protein BMI-1	1	1	2
CATG	Cathepsin G	19	22	28
CLIC1	Chloride intracellular channel protein 1	7	14	14
CNTRL	Centriolin	3	12	13
COF1	Cofilin-1	21	29	33
CTDS1	Carboxy-terminal domain RNA polymerase II polypeptide A small phosphatase 1	1	5	5
DCTN3	Dynactin subunit 3	3	7	8
DDX6	Probable ATP-dependent RNA helicase DDX6	7	16	16
DEF1	Neutrophil defensin 1	14	18	26
DNLI3	DNA ligase 3	1	5	5
EF1A1	Elongation factor 1 alpha 1	28	37	48
EHD1	EH domain containing protein 1	6	25	26
ELNE	Neutrophil elastase	4	9	11
ENOA	Alpha-enolase	10	18	21
FES	Tyrosine-protein kinase Fes/Fps	2	11	12
GRK5	G protein-coupled receptor kinase 5	1	3	3
HBA	Hemoglobin subunit alpha	20	51	52
HBB	Hemoglobin subunit beta	20	39	41
HMMR	Hyaluronan mediated motility receptor	2	4	5
HNRPM	Heterogeneous nuclear ribonucleoprotein M	12	29	31
HSP7C	Heat shock cognate 71 kDa protein	15	46	46
IF1AY	Eukaryotic translation initiation factor 1A, Y-chromosomal	2	4	5

Supplemental Table S8 continued

Protein		# of HLA peptides in CML patient ligandomes	# of HLA peptides in hematological benign ligandomes	Total # of unique HLA peptides
INAR1	Interferon alpha/beta receptor 1	1	1	2
KAT3	Kynurenine--oxoglutarate transaminase 3	1	5	5
MAF	Transcription factor Maf	1	2	2
MYBA	Myb-related protein A	1	1	1
PCNA	Proliferating cell nuclear antigen	18	26	29
PLIN2	Perilipin-2	3	17	17
PPIA	Peptidyl-prolyl cis-trans isomerase A	2	5	5
PRTN3	Myeloblastin	13	15	19
R51A1	RAD51 associated protein 1	3	2	3
RAB38	Ras-related protein Rab-38	1	2	2
RAF1	RAF proto-oncogene serine/threonine-protein kinase	2	10	11
RBBP4	Histone-binding protein RBBP4	9	24	24
RIMS2	Regulating synaptic membrane exocytosis protein 2	1	1	2
RL18A	60S ribosomal protein L18a	4	7	7
S10A9	Protein S100-A9	13	12	16
STMN1	Stathmin	3	8	8
SUH	Recombining binding protein suppressor of hairless	2	3	3
TBB5	Tubulin beta chain	43	76	89
TKT	Transketolase	15	30	31
TRYB1	Tryptase alpha/beta-1	2	3	4
TSP1	Thrombospondin 1	8	18	23
TYB4Y	Thymosin beta-4, Y-chromosomal	1	5	5
VPS4B	Vacuolar protein sorting-associated protein 4B	3	5	6
Benign-overrepresented				
ADIP	Afadin- and alpha-actinin-binding protein	1	7	7
ALDOA	Fructose-bisphosphate aldolase A	7	23	23
BCR	Breakpoint cluster region protein	1	5	5
CBL	E3 ubiquitin-protein ligase CBL	1	12	12
CDN2D	Cyclin-dependent kinase 4 inhibitor D	2	7	7
CHD2	Chromodomain-helicase-DNA-binding protein 2	2	10	11
CKS1	Cyclin-dependent kinases regulatory subunit 1	1	3	4
CSK	Tyrosine-protein kinase CSK	1	14	14
CUL4B	Cullin-4B	2	19	19
DDX5	Probable ATP-dependent RNA helicase DDX5	11	34	36
DEMA	Dematin	3	10	11
DNJA1	DnaJ (Hsp40) homolog, subfamily A, member 1	3	12	12
DQB1	HLA class II histocompatibility antigen, DQ beta 1 chain	1	7	7
EM55	55 kDa erythrocyte membrane protein	5	22	22
FAK2	Protein tyrosine kinase 2 beta	10	22	24
G3P	Glyceraldehyde-3-phosphate dehydrogenase	5	28	29
GPKOW	G-patch domain and KOW motifs-containing protein	1	7	7
HS74L	Heat shock 70 kDa protein 4L	1	8	8

Supplemental Table S8 continued

Protein		# of HLA peptides in CML patient ligandomes	# of HLA peptides in hematological benign ligandomes	Total # of unique HLA peptides
ICE2	Little elongation complex subunit 2	1	6	6
IRAK3	Interleukin-1 receptor-associated kinase 3	2	9	10
ITB5	Integrin beta-5	1	14	14
M3K1	Mitogen-activated protein kinase kinase kinase 1	4	21	22
MGRN1	E3 ubiquitin-protein ligase MGRN1	1	8	8
NAB2	NGFI-A binding protein 2	1	2	2
NOLC1	Nucleolar and coiled-body phosphoprotein 1	2	10	10
NU155	Nuclear pore complex protein Nup155	2	17	18
NUDC1	NudC domain containing 1	1	7	7
PARP1	Poly (ADP-ribose) polymerase 1	4	32	32
PHRF1	PHD and RING finger domain-containing protein 1	1	5	5
PIM1	Serine/threonine-protein kinase pim-1	5	13	16
RBM25	RNA binding protein 25	2	7	8
RHG04	Rho GTPase activating protein 4	1	15	15
RSSA	40S ribosomal protein SA	3	9	10
SEPT4	Septin-4	2	8	8
SP110	SP110 nuclear body protein	1	8	8
SPB9	Serpin B9	1	7	7
TPM1	Tropomyosin alpha-1 chain	1	5	5
UBP32	Ubiquitin carboxyl-terminal hydrolase 32	2	5	6
VPS51	Vacuolar protein sorting-associated protein 51 homolog	3	11	11
WASC5	WASH complex subunit 5	2	13	14
WT1	Wilms tumor protein	1	2	2
Benign-exclusive				
AFAD	Afadin	0	2	2
AGAP3	ArfGAP with GTPase, ANK repeat and PH domain-containing protein 3	0	2	2
ANR50	Ankyrin repeat domain-containing protein 50	0	1	1
ARI5A	AT-rich interactive domain-containing protein 5A	0	3	3
AVR2B	Activin receptor type-2B	0	1	1
BCL2	Apoptosis regulator Bcl-2	0	5	5
BIRC5	Baculoviral IAP repeat-containing protein 5	0	2	2
BRAP	BRCA1 associated protein	0	3	3
CD3Z	T-cell surface glycoprotein CD3 zeta chain	0	3	3
CD44	CD44 antigen	0	1	1
CD5	T-cell surface glycoprotein CD5	0	1	1
CNN3	Calponin 3	0	6	6
COR2A	Coronin-2A	0	2	2
CREL2	Cysteine-rich with EGF-like domain protein 2	0	1	1
DNJC2	DnaJ (Hsp40) homolog, subfamily C, member 2	0	1	1
ELMO3	Engulfment and cell motility protein 3	0	2	2
EXOS5	Exosome complex component RRP46	0	3	3
EZH2	Histone-lysine N-methyltransferase EZH2	0	5	5

Supplemental Table S8 continued

Protein		# of HLA peptides in CML patient ligandomes	# of HLA peptides in hematological benign ligandomes	Total # of unique HLA peptides
FMO1	Dimethylaniline monooxygenase [N-oxide-forming] 1	0	1	1
GRAH	Granzyme H	0	2	2
IFT46	Intraflagellar transport protein 46 homolog	0	1	1
IFT88	Intraflagellar transport protein 88 homolog	0	5	5
JIP4	C-Jun-amino-terminal kinase-interacting protein 4	0	6	6
KS6C1	Ribosomal protein S6 kinase delta-1	0	4	4
MEMO1	Protein MEMO1	0	1	1
MVD1	Diphosphomevalonate decarboxylase	0	4	4
NDKB	Nucleoside diphosphate kinase B	0	4	4
OGFR	Opioid growth factor receptor	0	8	8
PASD1	Circadian clock protein PASD1	0	1	1
PEPD	Xaa-Pro dipeptidase	0	6	6
PTCD3	Pentatricopeptide repeat domain-containing protein 3, mitochondrial	0	1	1
RBBP5	Retinoblastoma binding protein 5	0	3	3
RET	Proto-oncogene tyrosine-protein kinase receptor Ret	0	4	4
RL12	60S ribosomal protein L12	0	6	6
RPC3	DNA-directed RNA polymerase III subunit RPC3	0	7	7
TBCE	Tubulin-specific chaperone E	0	2	2
TERT	Telomerase reverse transcriptase	0	2	2
TGFR2	TGF-beta receptor type-2	0	1	1
U119A	Protein unc-119 homolog A	0	5	5
UBR1	E3 ubiquitin-protein ligase UBR1	0	13	13
WDR4	tRNA (guanine-N(7)-)-methyltransferase non-catalytic subunit WDR4	0	4	4
ZN292	Zinc finger protein 292	0	14	14

Numbers of naturally presented unique HLA class I peptides derived from predescribed leukemia-associated antigens (Greiner *et al.* Eur J Haematol 2008, Smahel Cancer Immunol Immunother 2011) identified in CML patient (n = 21) and hematological benign (n = 108) ligandomes. Antigens are assigned to their degree of CML-association determined by their representation frequencies in both cohorts (CML-exclusive, CML-overrepresented, benign-overrepresented, benign-exclusive).

Supplemental Table S9: Numbers of identified HLA class II peptides derived from leukemia-associated antigens

Protein		# of HLA peptides in CML patient ligandomes	# of HLA peptides in hematological benign ligandomes	Total # of unique HLA peptides
CML-exclusive				
FAK2	Protein tyrosine kinase 2 beta	1	0	1
GPKOW	G-patch domain and KOW motifs-containing protein	1	0	1
OGFR	Opioid growth factor receptor	1	0	1
CML-overrepresented				
CATG	Cathepsin G	27	49	57
COF1	Cofilin 1	143	259	289
CSK	Tyrosine-protein kinase CSK	1	1	2

Supplemental Table S9 continued

Protein		# of HLA peptides in CML patient ligandomes	# of HLA peptides in hematological benign ligandomes	Total # of unique HLA peptides
DDX5	Probable ATP-dependent RNA helicase DDX5	2	6	7
DEF1	Neutrophil defensin 1	25	57	62
EF1A1	Elongation factor 1-alpha 1	103	152	205
EHD1	EH domain-containing protein 1	6	14	17
PARP1	Poly (ADP-ribose) polymerase 1	1	4	4
PCNA	Proliferating cell nuclear antigen	6	22	27
RL12	60S ribosomal protein L12	1	10	11
S10A9	Protein S100-A9	62	114	130
STMN1	Stathmin	6	35	40
TBB5	Tubulin beta chain	110	303	333
TSP1	Thrombospondin-1	20	47	59
TYB4Y	Thymosin beta-4, Y-chromosomal	1	2	3
Benign-overrepresented				
DEMA	Dematin	2	10	12
DNLI3	DNA ligase 3	1	4	4
ELNE	Neutrophil elastase	5	34	35
ENOA	Alpha-enolase	53	298	307
G3P	Glyceraldehyde-3-phosphate dehydrogenase	22	335	338
HBA	Hemoglobin subunit alpha	86	412	417
HBB	Hemoglobin subunit beta	159	432	444
HNRPM	Heterogeneous nuclear ribonucleoprotein M	2	16	18
HSP7C	Heat shock cognate 71 kDa protein	6	162	163
PPIA	Peptidyl-prolyl cis-trans isomerase A	11	78	81
PRTN3	Myeloblastin	12	36	42
TGFR2	TGF-beta receptor type-2	2	12	14
TKT	Transketolase	1	20	21
TPM1	Tropomyosin alpha-1 chain	5	13	13
VPS4B	Vacuolar protein sorting-associated protein 4B	1	10	10
Benign-exclusive				
AFAD	Afadin	0	1	1
ALDOA	Fructose-bisphosphate aldolase A	0	55	55
BCL2	Apoptosis regulator Bcl-2	0	1	1
BIRC5	Baculoviral IAP repeat-containing protein 5	0	7	7
BRAP	BRCA1 associated protein	0	1	1
CBL	E3 ubiquitin-protein ligase CBL	0	2	2
CD3Z	T-cell surface glycoprotein CD3 zeta chain	0	2	2
CD44	CD44 antigen	0	7	7
CHD2	Chromodomain helicase DNA binding protein 2	0	1	1
CLIC1	Chloride intracellular channel protein 1	0	10	10
CNN3	Calponin-3	0	1	1
CNTRL	Centriolin	0	2	2
CSF2R	Granulocyte-macrophage colony-stimulating factor receptor subunit alpha	0	1	1
CTDS1	CTD (carboxy-terminal domain, RNA polymerase II, polypeptide A) small phosphatase 1	0	3	3

Supplemental Table S9 continued

Protein		# of HLA peptides in CML patient ligandomes	# of HLA peptides in hematological benign ligandomes	Total # of unique HLA peptides
CUL4B	Cullin 4B	0	1	1
DDX6	Probable ATP-dependent RNA helicase DDX6	0	2	2
DNJA1	DnaJ (Hsp40) homolog, subfamily A, member 1	0	7	7
DQB1	Major histocompatibility complex, class II, DQ beta 1	0	19	19
EM55	55 kDa erythrocyte membrane protein	0	3	3
GRAH	Granzyme H	0	6	6
GRL1A	DNA-directed RNA polymerase II subunit GRINL1A	0	1	1
HMMR	Hyaluronan mediated motility receptor	0	1	1
IF1AY	Eukaryotic translation initiation factor 1A, Y-chromosomal	0	4	4
IFT88	Intraflagellar transport protein 88 homolog	0	1	1
IL1AP	Interleukin 1 receptor accessory protein	0	5	5
INAR1	Interferon alpha/beta receptor 1	0	8	8
ITB5	Integrin beta-5	0	2	2
JIP4	C-Jun-amino-terminal kinase-interacting protein 4	0	8	8
KAT3	Kynurenine--oxoglutarate transaminase 3	0	5	5
KS6C1	Ribosomal protein S6 kinase delta-1	0	1	1
NDKB	Nucleoside diphosphate kinase B	0	7	7
NU155	Nuclear pore complex protein Nup155	0	2	2
NUDC1	NudC domain-containing protein 1	0	1	1
KS6C1	Ribosomal protein S6 kinase delta-1	0	1	1
NDKB	Nucleoside diphosphate kinase B	0	7	7
NU155	Nuclear pore complex protein Nup155	0	2	2
NUDC1	NudC domain-containing protein 1	0	1	1
PEPD	Xaa-Pro dipeptidase	0	3	3
PLIN2	Perilipin 2	0	4	4
PNPT1	Polyribonucleotide nucleotidyltransferase 1, mitochondrial	0	1	1
RBBP4	Histone-binding protein RBBP4	0	1	1
RBM25	RNA binding protein 25	0	2	2
RET	Proto-oncogene tyrosine-protein kinase receptor Ret	0	1	1
RL18A	60S ribosomal protein L18a	0	40	40
RSSA	40S ribosomal protein SA	0	14	14
SPB9	Serpin B9	0	14	14
TRYB1	Tryptase alpha/beta-1	0	1	1
WT1	Wilms tumor protein	0	1	1

Numbers of naturally presented unique HLA class II peptides derived from predescribed leukemia-associated antigens (Greiner *et al.* Eur J Haematol 2008, Smahel Cancer Immunol Immunother 2011) identified in CML patient (n = 20) and hematological benign (n = 88) ligandomes. Antigens are assigned to their degree of CML-association determined by their representation frequencies in both cohorts (CML-exclusive, CML-overrepresented, benign-overrepresented, benign-exclusive).

Supplemental Figure 1

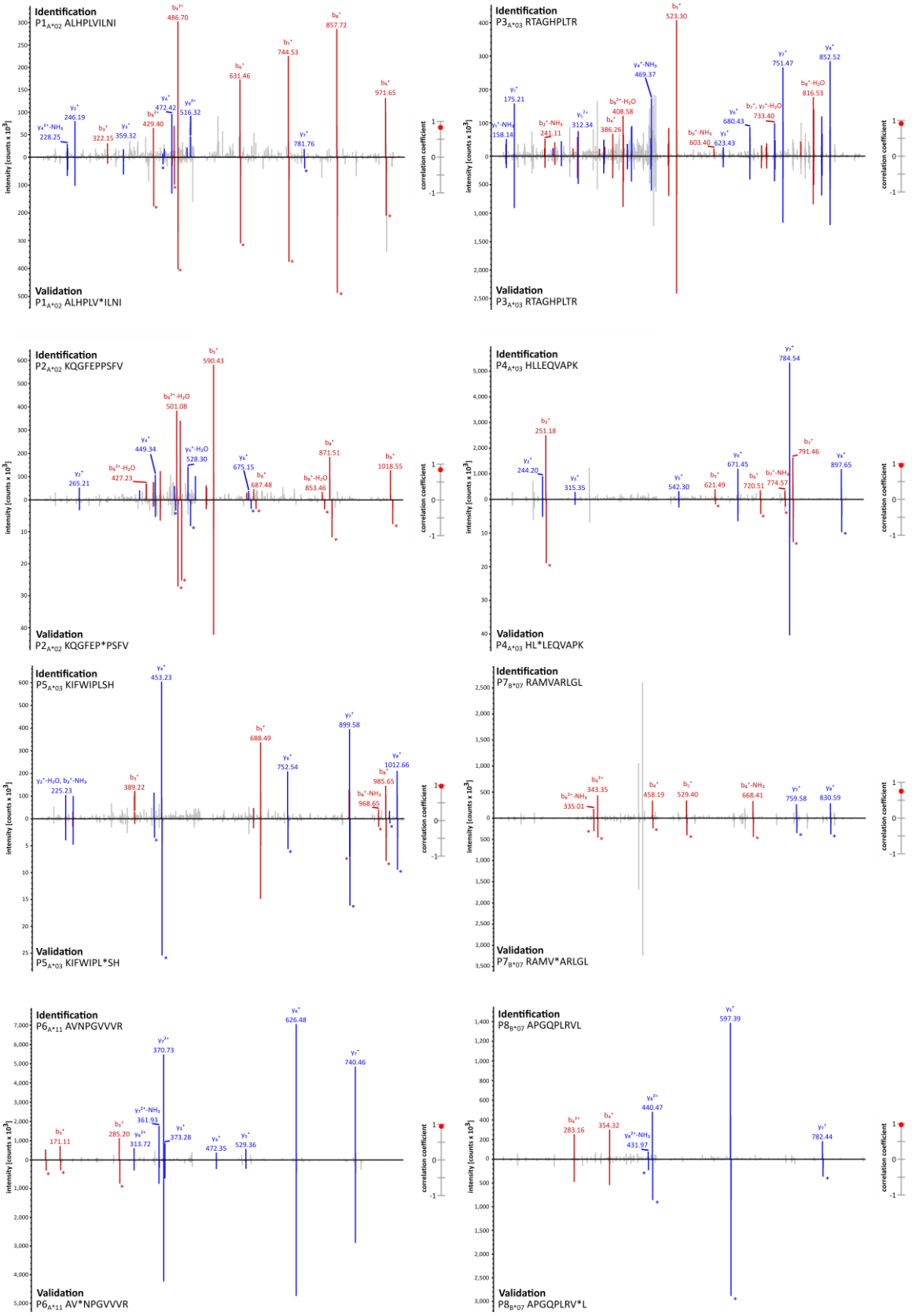

Figure S1: Validation of experimentally eluted HLA class I-restricted peptides by synthetic peptides. Comparison of fragment spectra (m/z on the x-axis) of HLA class I-restricted peptides eluted from primary CML patient samples (identification) to their corresponding synthetic peptides (validation). The spectra of the synthetic peptides are mirrored on the x-axis. Identified b- and y-ions are marked in red and blue, respectively. The calculated spectral correlation coefficients are depicted on the right graph, respectively. Ions containing isotopic labeled amino acids are marked with asterisks.

Supplemental Figure 2

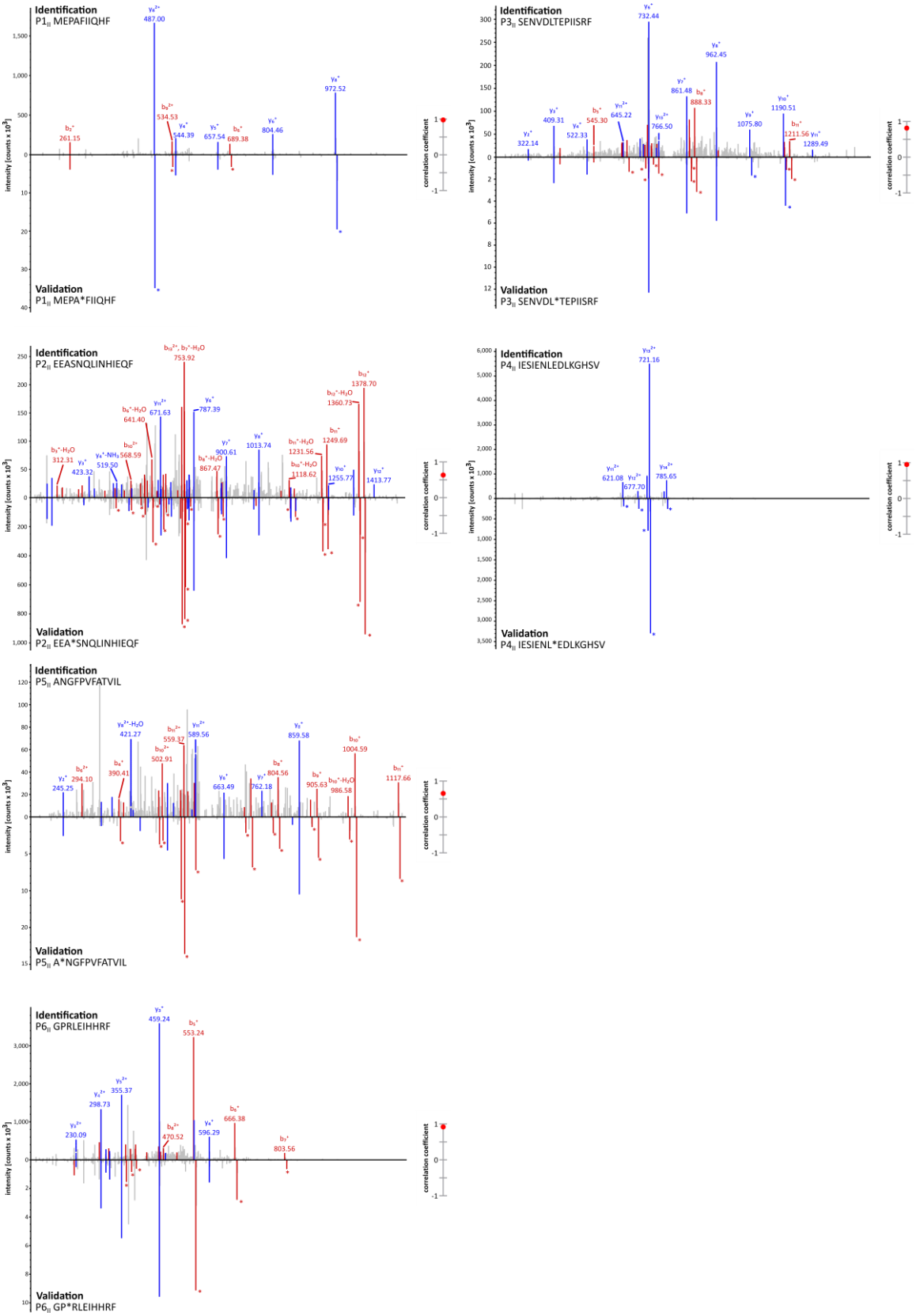

Figure S2: Validation of experimentally eluted HLA class II-restricted peptides by synthetic peptides. Comparison of fragment spectra (m/z on the x-axis) of HLA class II-restricted peptides eluted from primary CML patient samples (identification) to their corresponding synthetic peptides (validation). The spectra of the synthetic peptides are mirrored on the x-axis. Identified b- and y-ions are marked in red and blue, respectively. The calculated spectral correlation coefficients are depicted on the right graph, respectively. Ions containing isotopic labeled amino acids are marked with asterisks.

Supplemental Figure 3

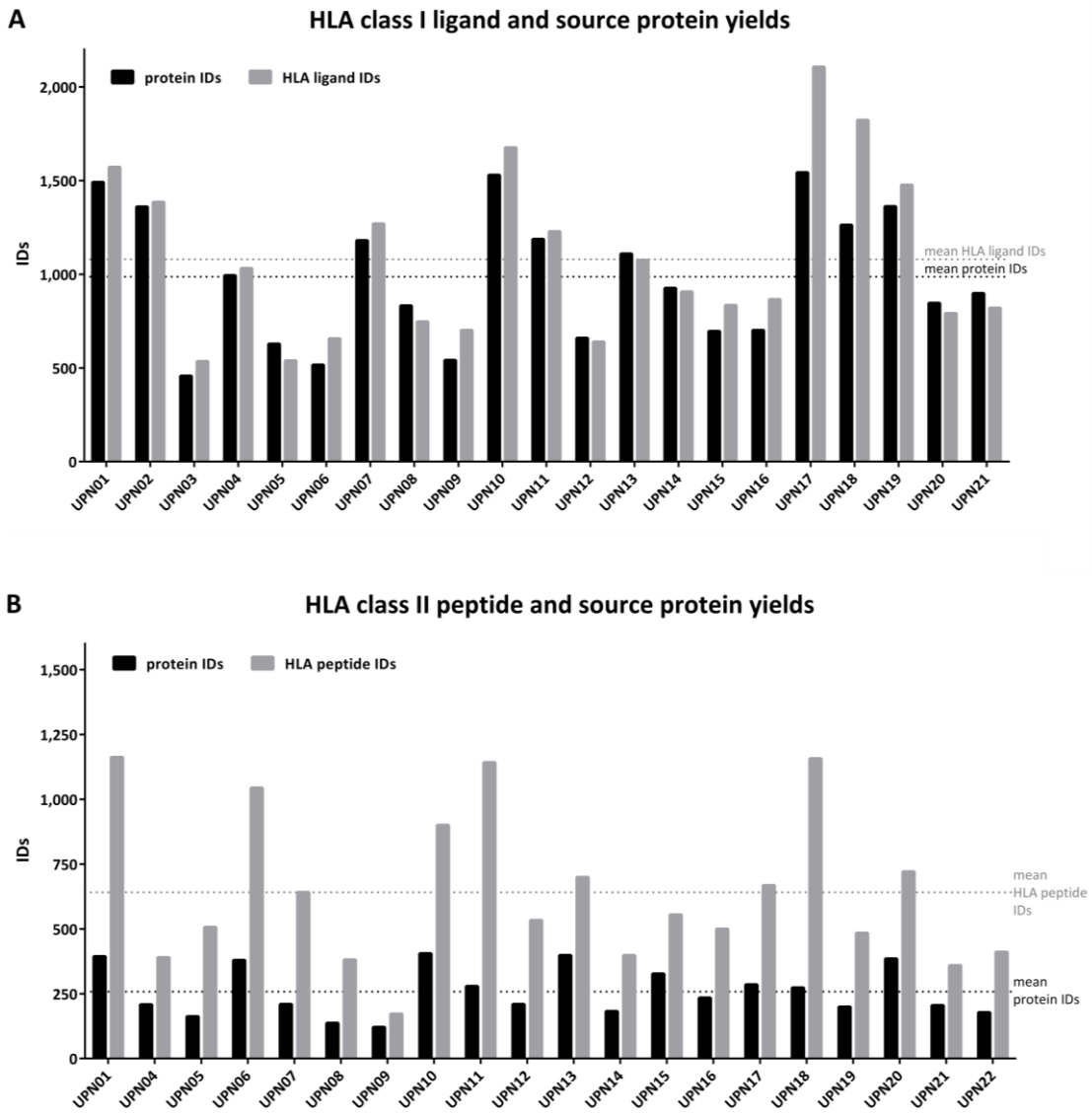

Figure S3: HLA class I and II peptide and source protein yields. (A) HLA class I ligand and respective source protein yields of primary CML samples (n = 21) as identified by mass spectrometry are indicated in grey and black bars, respectively. Mean HLA class I ligand and protein identifications are depicted by the grey and black dotted line, respectively. (B) Numbers of HLA class II peptides (grey bars) and source proteins (black bars) identified in primary CML samples (n = 20). Mean HLA class II peptide and protein identifications are illustrated by the grey and black dotted line, respectively. Abbreviations: IDs, identifications; UPN, uniform patient number.

Supplemental Figure 4

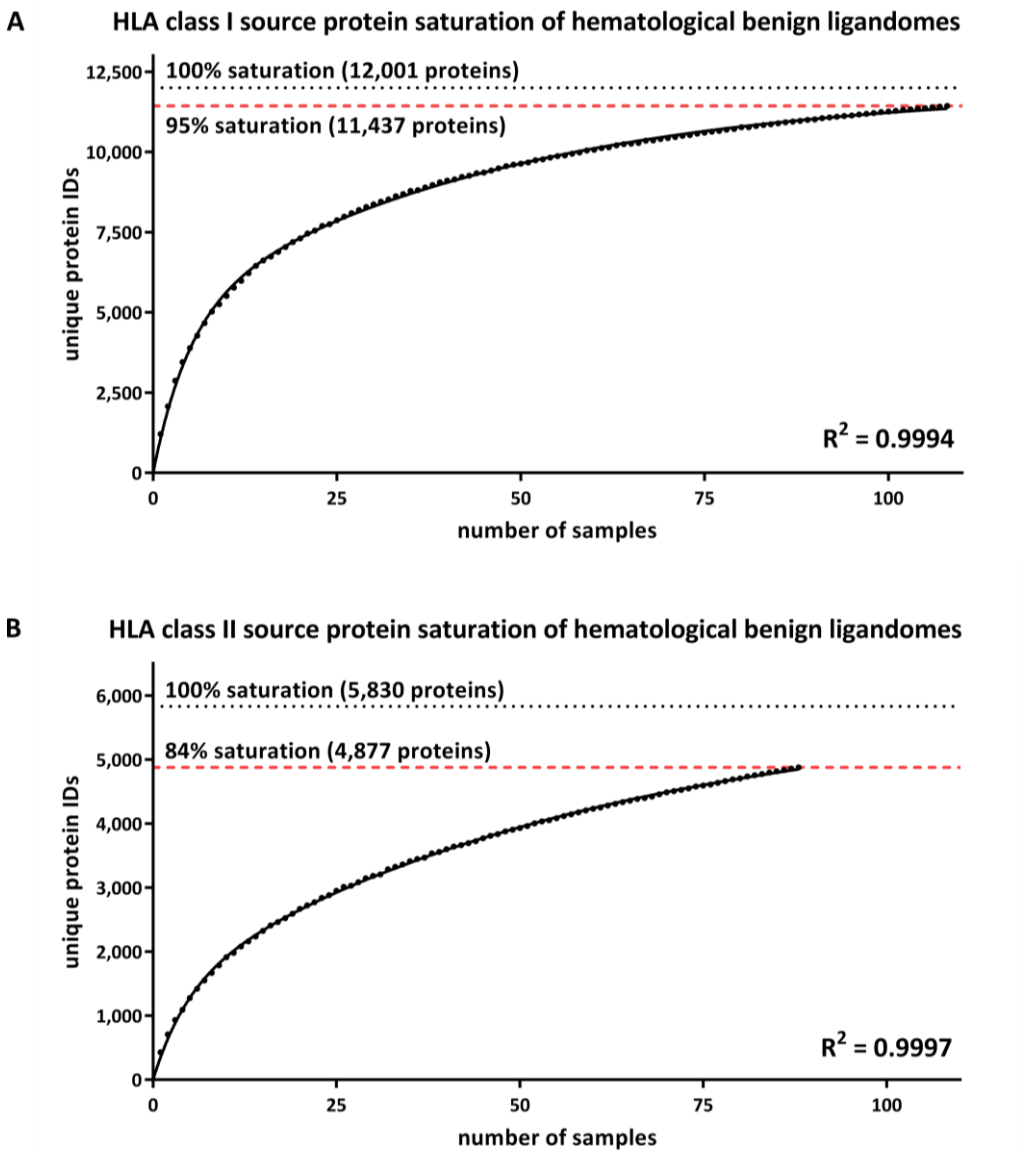

Figure S4: Saturation analysis of HLA peptide source proteins of hematological benign tissue. Saturation analysis of (A) HLA class I and (B) HLA class II peptide source proteins of the hematological benign tissue cohort. Number of unique HLA ligand source protein identifications shown as function of cumulative HLA ligandome analysis of hematological benign samples (n = 108 for HLA class I, n = 88 for HLA class II). Exponential regression allowed for the robust calculation (R^2=0.9994 for HLA class I, R^2=0.9997 for HLA class II) of the maximum attainable number of different source protein identifications (dotted line). The dashed red line depicts the source proteome coverage achieved in our hematological benign tissue cohort. Abbreviation: IDs, identifications.

Supplemental Figure 5

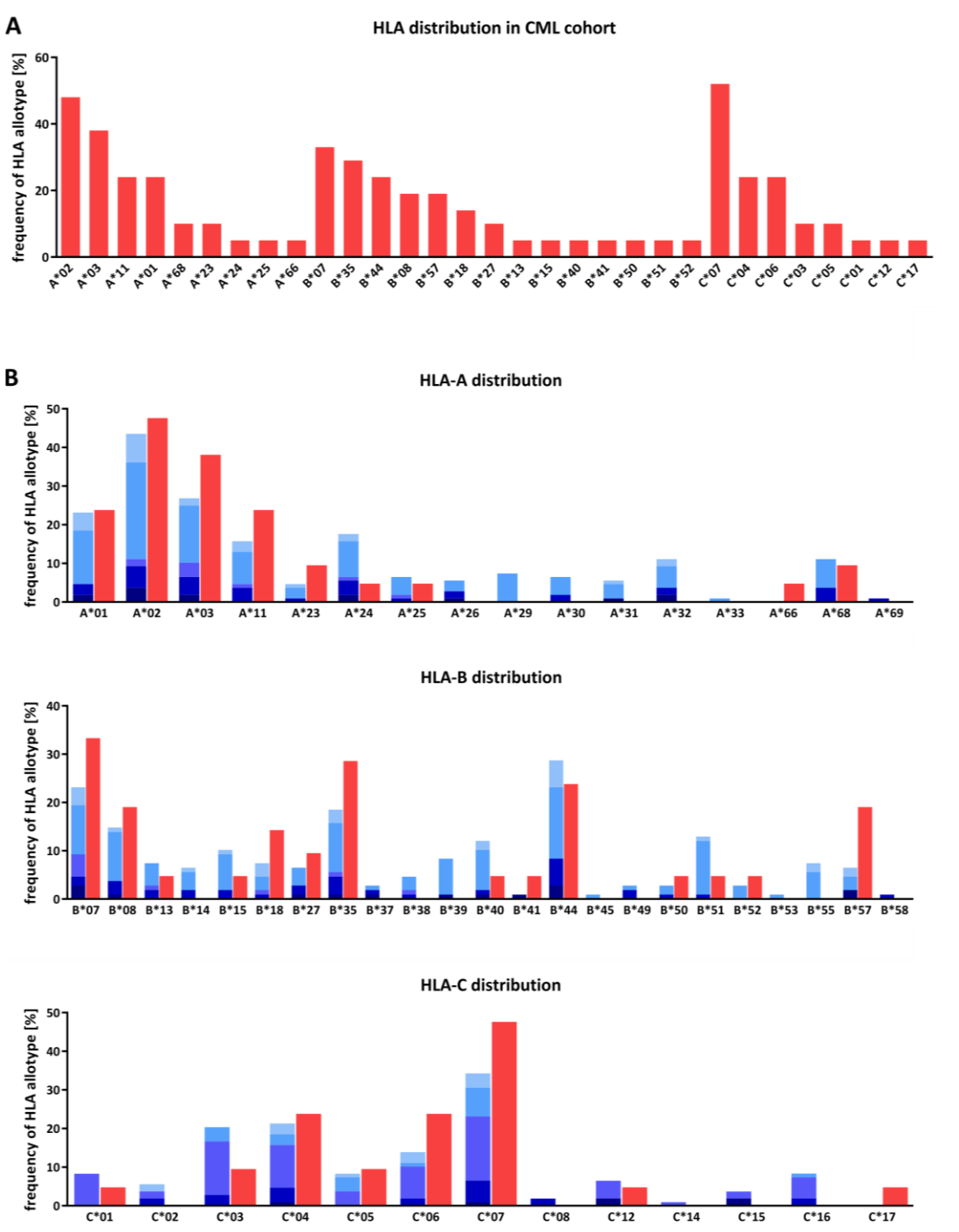

Figure S5: HLA allotype distribution in CML and hematological benign tissue cohorts. (A) HLA class I allotype frequencies in the CML patient cohort (n = 21) used for mass spectrometry-based analysis of naturally presented, CML-associated antigens. (B) HLA-A, -B, and -C allotype frequencies in CML patient (n = 21) and hematological benign tissue (n = 108) cohorts. Abbreviations: PBMCs, peripheral blood mononuclear cells; BM, bone marrow; HPCs, hematopoietic progenitor cells.

Supplemental Figure 6

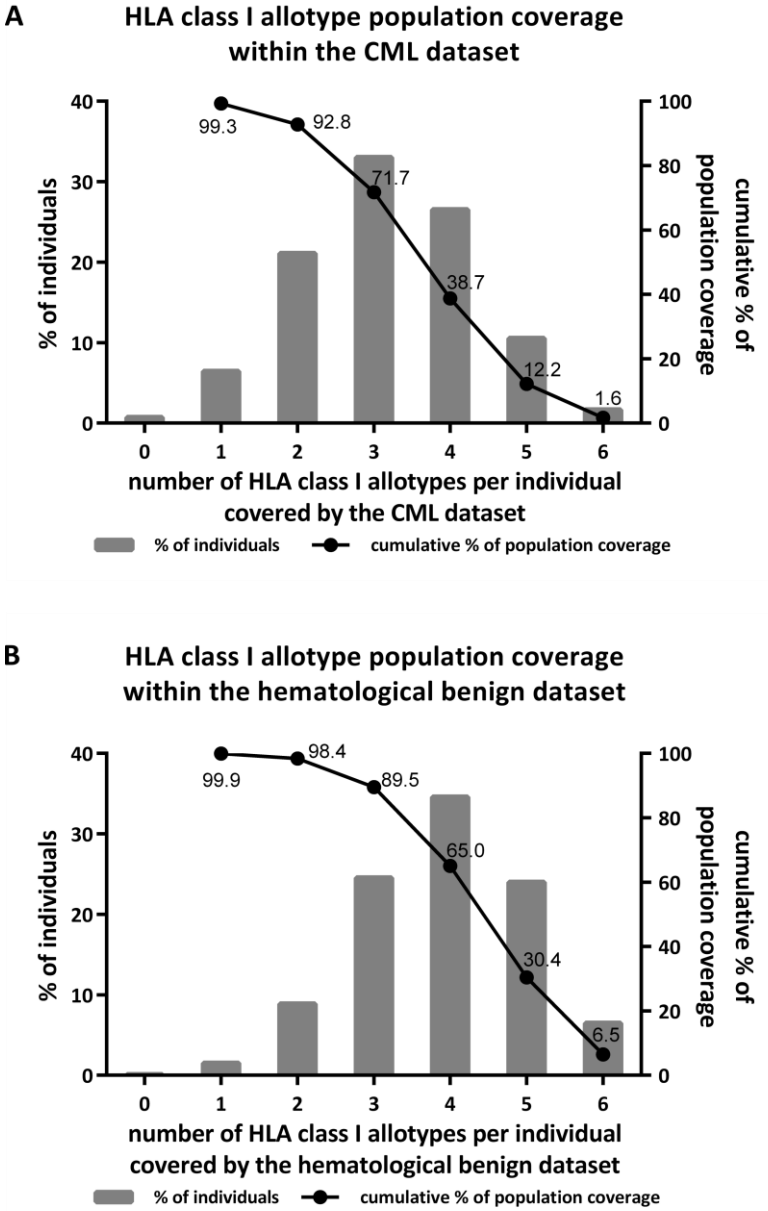

Figure S6: HLA class I allotype population coverage. HLA class I allotype population coverage within the (A) CML and (B) hematological benign tissue cohorts compared to the world population (calculated by the IEDB population coverage tool, www.iedb.org). The frequencies of individuals within the world population carrying up to six HLA allotypes (x-axis) of the respective CML or benign dataset are indicated as grey bars on the left y-axis. The cumulative percentage of population coverage is depicted as black dots on the right y-axis.

Supplemental Figure 7

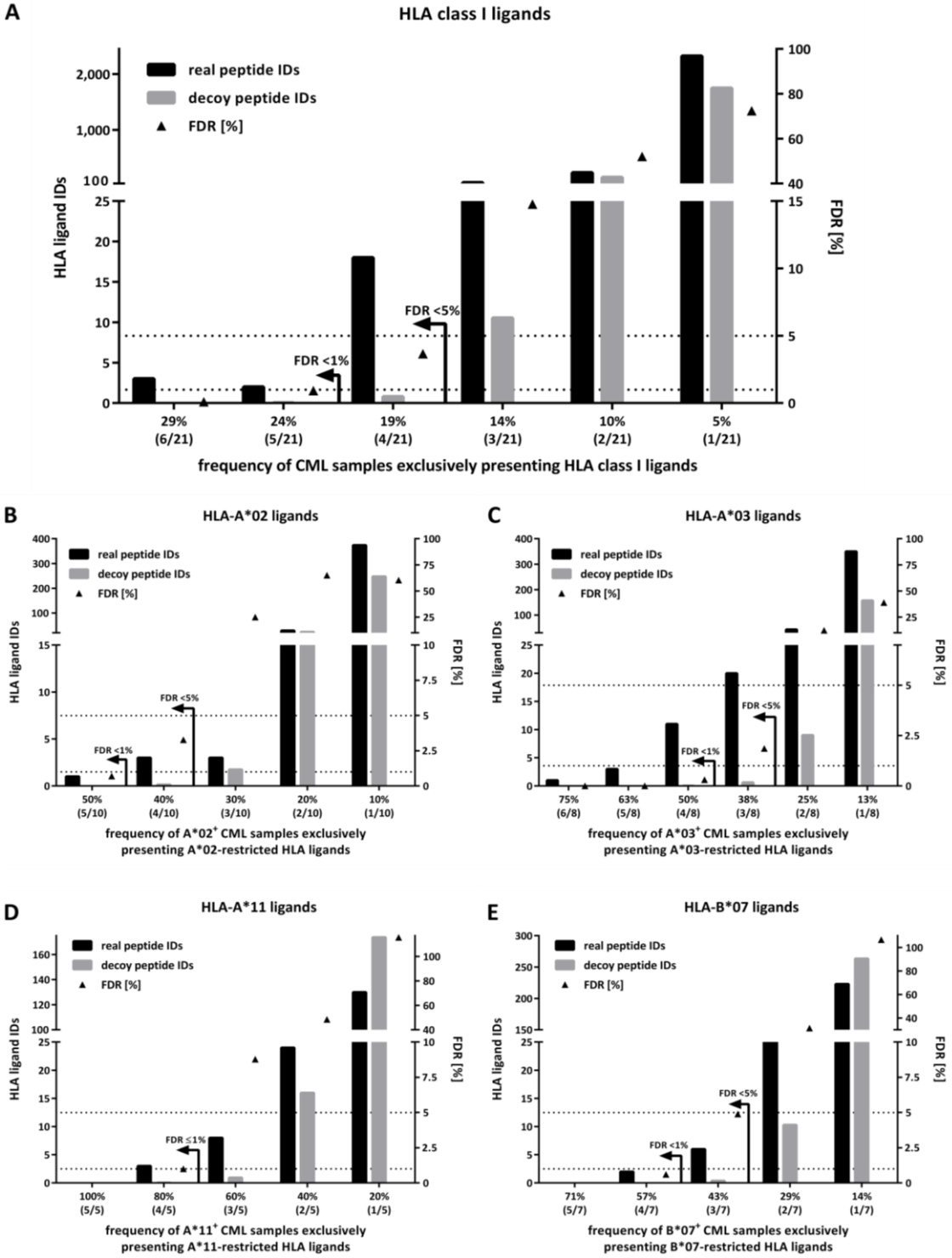

Figure S7: Statistical analysis of the proportion of false positive CML-associated HLA class I ligand identifications at different representation frequencies. The numbers of identified (A) HLA class I, (B) -A*02, (C) -A*03, (D) -A*11, and (E) -B*07 ligands based on the analysis of the CML and hematological benign tissue cohorts were compared with random virtual CML-associated HLA class I, -A*02, -A*03, -A*11, and -B*07 ligands (left y-axis), respectively. Virtual ligandomes of CML patient and hematological benign tissue samples were generated *in silico* based on random weighted sampling from the entirety of peptide identifications in both original cohorts. These randomized virtual ligandomes were used to define CML-associated antigens based on simulated cohorts of CML versus hematological benign tissue samples. The process of peptide randomization, cohort assembly, and CML-associated antigen identification was repeated 1,000 times and the mean value of resultant virtual CML-associated antigens was calculated and plotted for the different threshold values. The corresponding FDRs (right y-axis) for any chosen threshold (x-axis) were calculated and the 1% and 5% FDRs are indicated within the plot (dotted lines and arrows). Abbreviations: IDs, identifications; FDR, false discovery rate.

Supplemental Figure 8

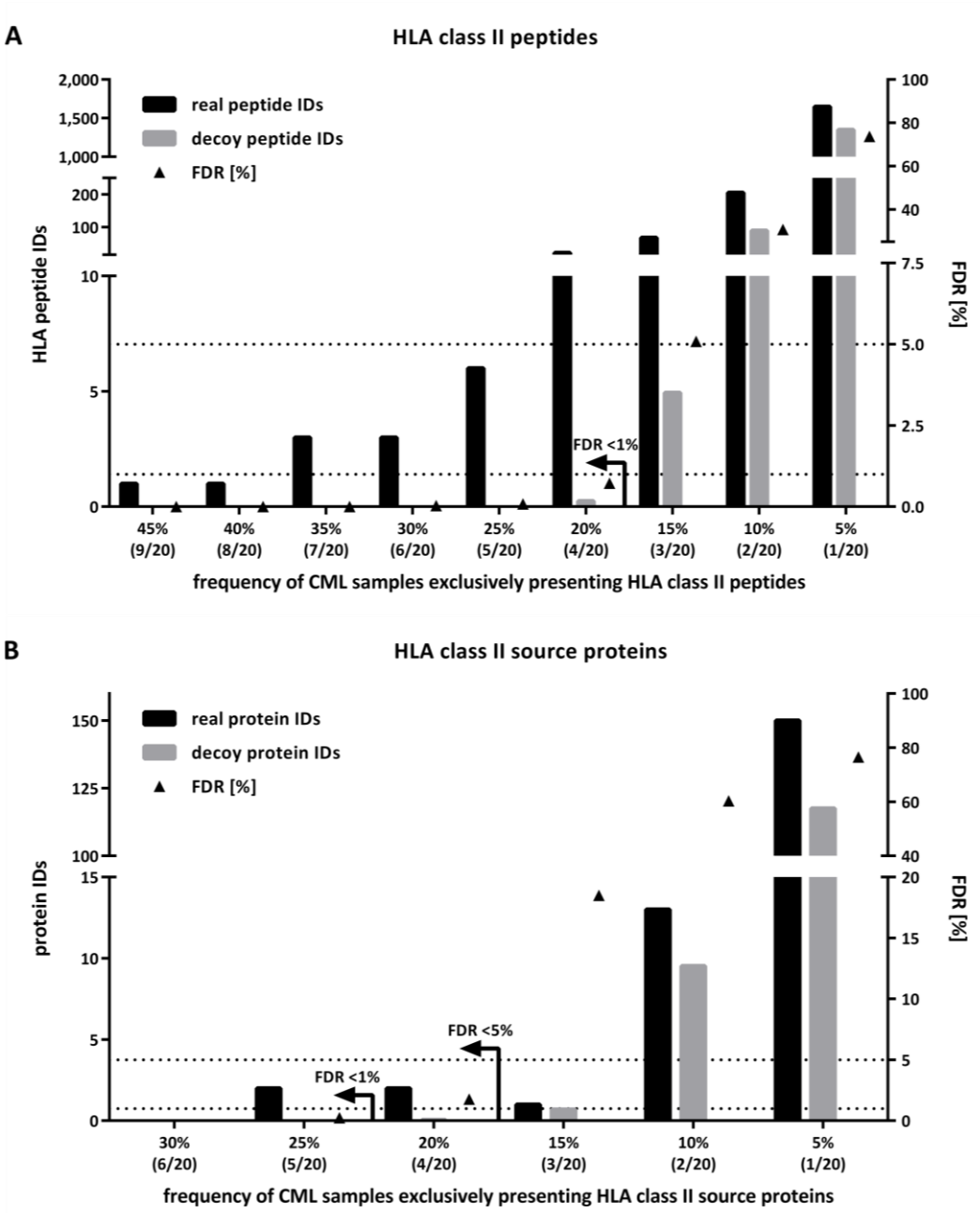

Figure S8: Statistical analysis of the proportion of false positive CML-associated HLA class II peptide and source protein identifications at different representation frequencies. The numbers of identified HLA class II (A) peptides and (B) source proteins based on the analysis of the CML and hematological benign tissue cohorts were compared with random virtual CML-associated HLA class II peptides and source proteins (left y-axis), respectively. Virtual ligandomes of CML patient and hematological benign tissue samples were generated *in silico* based on random weighted sampling from the entirety of peptide identifications in both original cohorts. These randomized virtual ligandomes were used to define CML-associated antigens based on simulated cohorts of CML versus hematological benign tissue samples. The process of peptide or source protein randomization, cohort assembly, and CML-associated antigen identification was repeated 1,000 times and the mean value of resultant virtual CML-associated antigens was calculated and plotted for the different threshold values. The corresponding FDRs (right y-axis) for any chosen threshold (x-axis) were calculated and the 1% and 5% FDRs are indicated within the plot (dotted lines and arrows). Abbreviations: IDs, identifications; FDR, false discovery rate.

Supplemental Figure 9

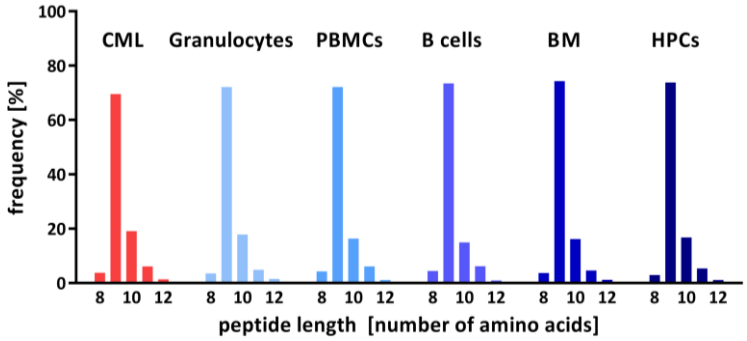

Figure S9: Peptide length distribution of HLA class I ligands. Tissue-specific HLA class I ligand length distribution (number of amino acids) of identified peptides on primary CML samples (n = 21), granulocytes (n = 14), PBMCs (n = 63), $CD19^+$ B cells (n = 5), bone marrow (n = 18), and $CD34^+$ HPCs (n = 8). Abbreviations: PBMCs, peripheral blood mononuclear cells; BM, bone marrow; HPCs, hematopoietic progenitor cells.

Supplemental Figure 10

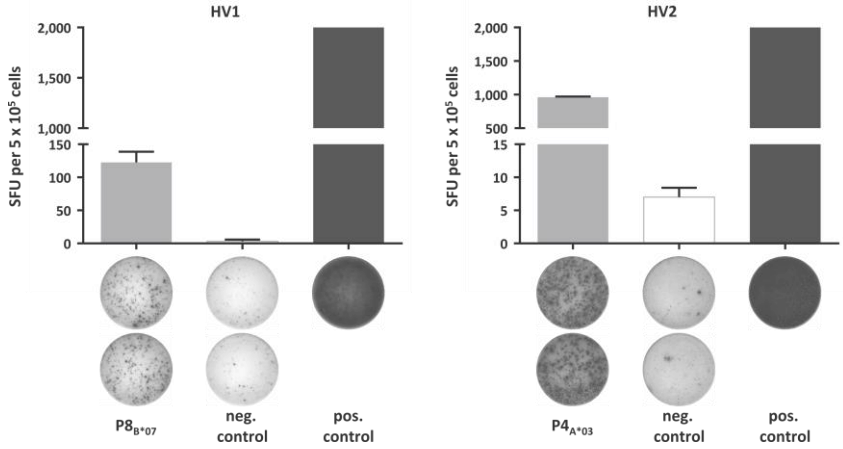

Figure S10: Preexisting T-cell responses of HLA class I-restricted, CML-associated antigens in healthy volunteers. Examples of CML-associated ligands evaluated in IFNγ ELISPOT assays after 12-d stimulation using PBMCs of healthy volunteers. Results are shown for immunoreactive peptides only. PHA was used as positive control. The HLA-B*07-restricted NEF_HV1BR$_{128-137}$ peptide TPGPGVRYPL as well as the HLA-A*03-restricted GAG_HV1BR$_{20-28}$ peptide RLRPGGKKK served as negative controls, respectively. Data are expressed as mean ± SD of two independent replicates. Abbreviations: HV, healthy volunteer; SFU, spot forming unit; neg., negative; pos., positive.

Supplemental Figure 11

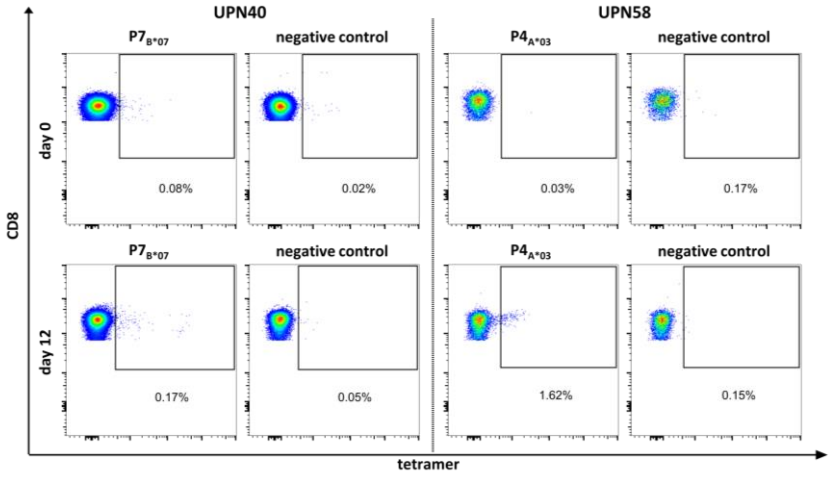

Figure S11: Examples of multimer stainings before and after 12-d stimulation. PBMCs of CML_{TKI} patients were stimulated *in vitro* for 12 days using CML-associated peptides. Graphs show single, viable cells stained for CD8 and PE-conjugated multimers of indicated specificity. HLA allotype-matched PE-conjugated multimers with irrelevant peptides served as negative controls, respectively. Stainings were performed *ex vivo* on day 0 with unstimulated cells as well as after 12-d stimulation. Abbreviation: UPN, uniform patient number.

Supplemental Figure 12

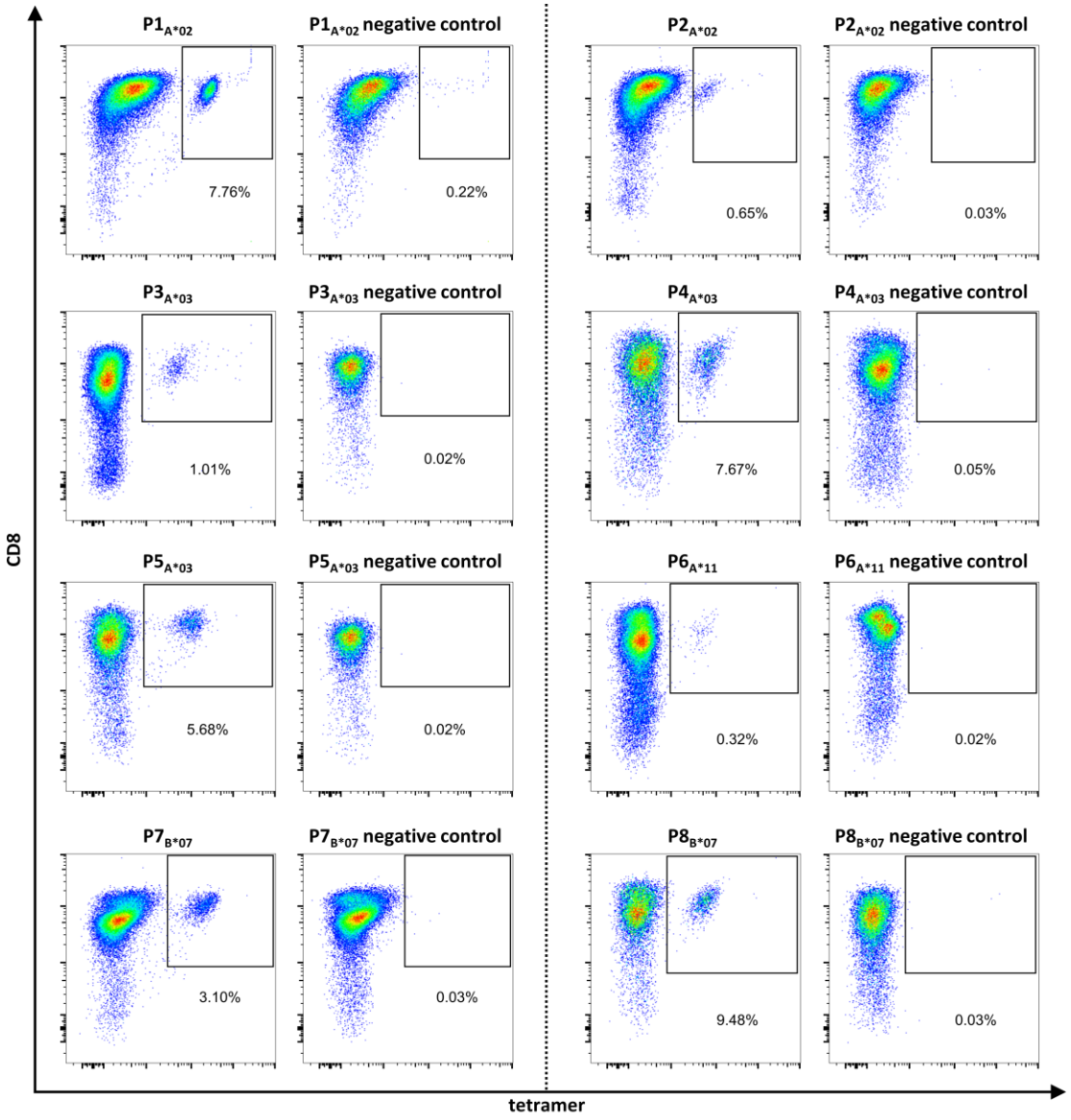

Figure S12: Representative examples of multimer stainings using HLA:peptide tetramers. Naïve $CD8^+$ T cells from healthy blood donors were primed *in vitro* using artificial APCs. Graphs show single, viable cells stained for CD8 and PE-conjugated multimers of indicated specificity. Tetramer staining was performed after four stimulation cycles with peptide-loaded aAPCs. Negative controls were performed using T cells from respective donors primed with irrelevant peptides and stained with the indicated tetramers.

Supplemental Figure 13

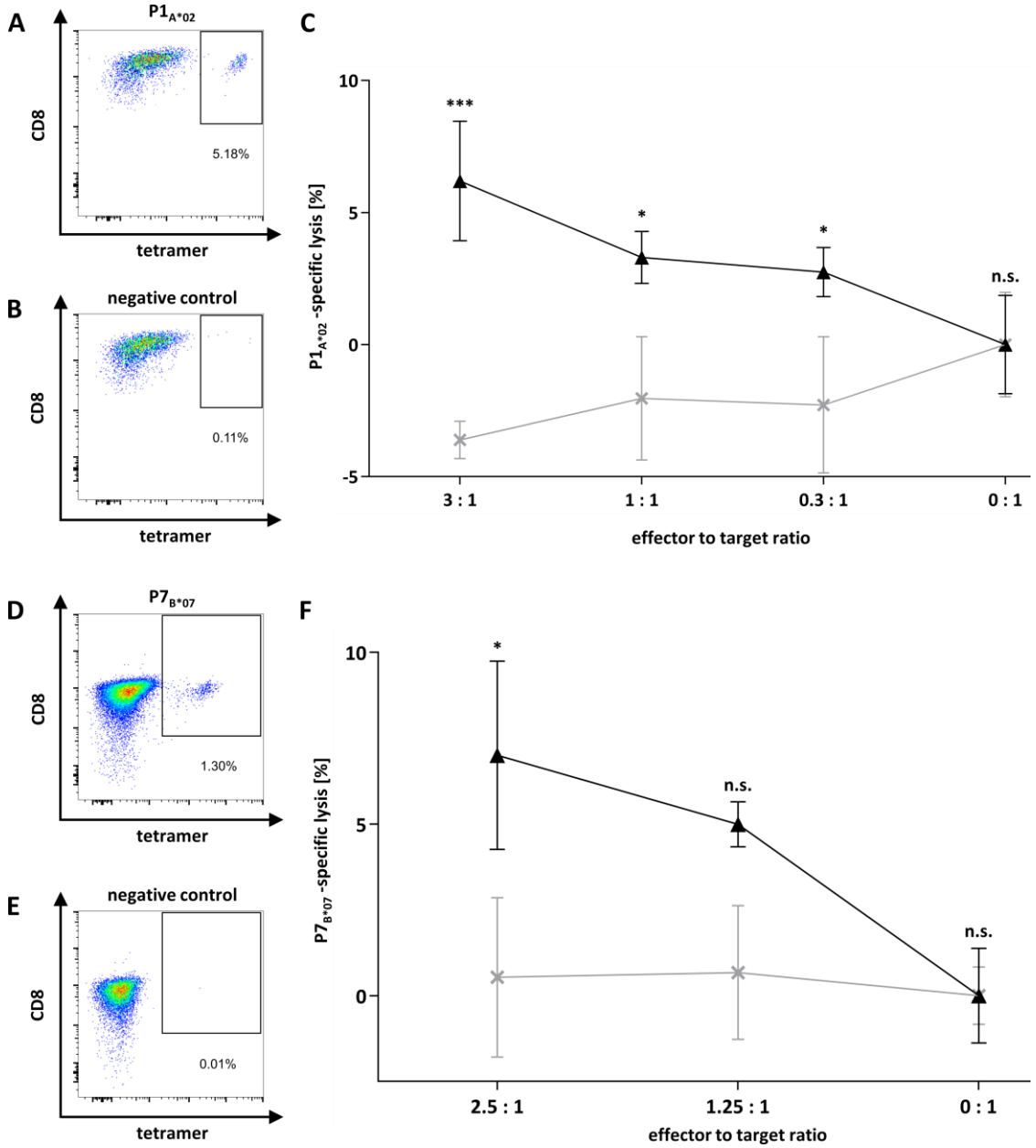

Figure S13: Cytotoxicity experiments using antigen-specific CD8$^+$ T cells. (A-C) Selective cytotoxicity of $P1_{A*02}$-specific effector T cells was analyzed in a VITAL cytotoxicity assay with *in vitro* primed CD8$^+$ effector cells of an HV. Tetramer staining of polyclonal effector cells before performance of the VITAL assay determined the amount of $P1_{A*02}$-specific effector cells in the (A) population of successfully $P1_{A*02}$-primed CD8$^+$ T cells and in the (B) population of control cells from the respective donor primed with an HLA-matched irrelevant peptide. (C) At an effector to target ratio of 3:1 $P1_{A*02}$-specific effectors (black) exerted 6.2% (±2.3%) $P1_{A*02}$-specific and significantly higher lysis of $P1_{A*02}$-loaded autologous target cells in comparison to control peptide-loaded target cells (HLA-A*02, YLLPAIVHI, DDX5_HUMAN$_{148-156}$). $P1_{A*02}$-unspecific effectors (grey) showed no unspecific lysis of the same targets. (D-F) Selective cytotoxicity of $P7_{B*07}$-specific effector T cells. Tetramer staining of polyclonal effector cells before performance of the VITAL assay determined the amount of $P7_{B*07}$-specific effector cells in the (D) population of successfully $P7_{B*07}$-primed CD8$^+$ T cells and in the (E) population of control cells from the respective donor primed with an HLA-matched irrelevant peptide. (F) At an effector to target ratio of 2.5:1 $P7_{B*07}$-specific effectors (black) exerted 7.0% (±2.7%) $P7_{B*07}$-specific and significantly higher lysis of $P7_{B*07}$-loaded autologous target cells in comparison to control peptide-loaded target cells (HLA-B*07, TPGPGVRYPL, NEF_HV1BR$_{128-137}$). $P7_{B*07}$-unspecific effectors (grey) only showed 0.5% (±2.3%) unspecific lysis of the same targets. Results are shown for three independent replicates. Error bars indicate ± SEM. Abbreviations: n.s., not significant; * p<0.05; *** p<0.001.

12. SUPPLEMENT OF PART III

Supplemental Methods

Peptide synthesis and spectrum validation

Peptides were produced by the peptide synthesizer Liberty Blue (CEM) using the 9-fluorenylmethyl-oxycarbonyl/tert-butyl strategy (Sturm *et al.* Nat Commun 2013). Spectrum validation of the experimentally eluted peptides was performed by isotope-labeled synthetic peptides measured in a complex matrix.

Validation of mutation-derived HLA ligands by targeted PRM

The validation of the NPM1 mutation-derived HLA-A*11-restricted peptide AVEEVSLRK ($P16_{A*11\_MUT}$) was performed using the more sensitive targeted PRM MS method (Peterson *et al.* Mol Cell Proteomics 2012). To generate the PRM assay library, the synthetic heavy isotope-labeled reference peptide was first spiked-in a complex biological matrix (HLA ligands isolated from JY cells) and analyzed on an LTQ Orbitrap Fusion Lumos mass spectrometer in PRM-triggered MS2 mode. For the validation of the mutation-derived HLA ligand the reference peptide were then spiked-in the respective samples and analyzed with a PRM MS method. The mass spectrometer was operated in PRM mode, triggering acquisition of a full mass spectrum at 120,000 resolution (AGC target 1.5×10^5, 50 ms maximum injection time) in the orbitrap followed by isolation of precursor ions in the quadrupole and MS2 scans in the orbitrap at 60,000 resolution (AGC target 7.0×10^4, 118 ms maximum injection time) as triggered by a scheduled inclusion list containing the masses of interest of the mutation-derived peptide with charge states 2+ and 3+ as well as the respective masses of the heavy isotope-labeled reference peptide. Ion activation was performed by CID at normalized collision energy of 35%. The software Skyline (version 3.7.0, MacLean *et al.* Bioinformatics 2010) was used to generate a spectral library from the msf files. The transition settings was set to precursor charges *2* and *3*, ion charges *1* and *2*, ion types *y, b, a,* and *p*, product ions from *ion 2* to *last ion -2*. The ion match tolerance for the library was set to *0.02 m/z* and *8* product ions are picked. The method match tolerance was set to *0.02 m/z* as well as the acquisition method for the MS/MS filtering to *targeted*.

Supplemental Table S1: Patient characteristics of AML *discovery cohort* for HLA ligandome analysis

UPN	Sex	Age	Cell source	WHO classification	FAB classification	AML-specific therapy	Molecular genetic	Karyotype	WBC (10^3/µl) (% blasts)	Cell count (10^6)	HLA class I typing	HLA class II typing	HLA class I		HLA class II	
													HLA ligand IDs	Protein IDs	Peptide IDs	Protein IDs
1	m	21	PB	recurrent genetic abnormalities	M4	no	CBFB/ MYH11	complex	138 (72)	13,760	A*11:01, B*07:02, B*44:03, C*07:02, C*16:01	DRB1*03:01, DRB1*07:01, DQB1*02:01, DQB1*02:02, DQA1*02:01, DQA1*05:01	11,240	5,769	8,491	1,833
2	m	63	PB	recurrent genetic abnormalities	M4	no	CBFB/ MYH11, FLT3-TKD	complex	100 (71)	3,740	A*01:01, B*07:02, B*08:01, C*07:01, C*07:02	DRB1*07:01, DRB1*15:01, DQB1*02:02, DQB1*06:02, DQA1*01:02, DQA1*02:01	6,941	4,527	10,733	2,107
3	n.a.	n.a.	PB	n.a.	n.a.	n.a.	n.a.	n.a.	n.a.	318	A*03:01, A*23:01, B*18:01, B*44:02, C*05:01, C*12:03	DRB1*13:01, DRB1*14:01, DQB1*05:03, DQB1*06:03, DQA1*01:01, DQA1*01:03	7,053	4,409	3,514	978
4	n.a.	n.a.	PB	n.a.	n.a.	n.a.	n.a.	n.a.	n.a.	600	A*02:01, A*31:01, B*40:01, B*44:02, C*03:04, C*05:01	DRB1*04:01, DRB1*09:01, DQB1*03:02, DQB1*03:03, DQA1*03:01	2,562	2,239	2,632	766
5	n.a.	n.a.	PB	n.a.	n.a.	n.a.	n.a.	n.a.	n.a.	210	A*01:01, A*29:02, B*08:01, B*44:03, C*07:01, C*16:01	DRB1*01:01, DRB1*07:01, DQB1*02:02, DQB1*05:01, DQA1*01:02, DQA1*02:01	6,073	3,959	3,184	973
6	n.a.	n.a.	PB	n.a.	n.a.	n.a.	n.a.	n.a.	n.a.	600	A*03:01, A*23:01, B*08:01, B*15:01, C*03:03, C*07:01	DRB1*11:01, DQB1*06:02, DQA1*01:01, DQA1*05:05	3,245	2,654	2,168	711
7	n.a.	n.a.	PB	n.a.	n.a.	n.a.	n.a.	n.a.	n.a.	280	A*02:01, A*24:10, B*14:02, B*35:30, C*04:01, C*08:02	DRB1*08:01, DRB1*12:04, DQB1*04:02, DQB1*05:02, DQA1*01:01, DQA1*04:01	3,581	2,727	2,950	968
8	n.a.	n.a.	PB	n.a.	n.a.	n.a.	n.a.	n.a.	n.a.	245	A*01:01, A*25:01, B*18:01, B*57:01, C*06:02, C*12:03	DRB1*07:01, DRB1*08:01, DQB1*03:03, DQB1*04:02, DQA1*02:01, DQA1*04:01	1,385	1,320	1,869	751
9	f	46	PB	AML, NOS	M5	no	FLT3-ITD	46, XX, t(1;3)(p36; q21)[22]	500 (70)	500	A*01:01, B*08:01, B*13:02, C*06:02, C*07:01	DRB1*03:01, DRB1*07:01, DQB1*02:01, DQB1*02:02, DQA1*02:01, DQA1*05:01	5,231	3,750	5,712	1,419
10	m	64	PB	recurrent genetic abnormalities	M4	no	NPM1_A, FLT3-ITD	46, XY	90 (90)	2,500	A*02:01, A*23:01, B*44:02, B*44:03, C*02:02, C*04:01	DRB1*07:01, DQB1*02:02, DQA1*02:02	6,221	4,011	5,070	1,539
11	n.a.	n.a.	PB	n.a.	n.a.	n.a.	n.a.	n.a.	n.a.	277	A*01:01, A*03:01, B*08:01, B*14:02, C*07:01, C*08:02	DRB1*03:01, DRB1*15:01, DQB1*02:01, DQB1*06:02, DQA1*01:01, DQA1*05:01	n.a.	n.a.	1,790	576
12	f	47	PB	recurrent genetic abnormalities	M5	no	NPM1_A	46, XX	100 (88)	2,500	A*02:01, A*02:05, B*51:01, B*58:01, C*03:02, C*14:02	DRB1*03:01, DRB1*16:01, DQB1*02:01, DQB1*05:02, DQA1*01:01, DQA1*05:01	5,962	3,958	2,149	764
		48	PB		relapse of M5	yes[2]			85 (88)	1,000			6,921	4,321	1,267	611
13	m	74	PB	recurrent genetic abnormalities	M4/M5	yes[1]	FLT3-ITD	n.a.	385 (100)	6,000	A*11:01, A*68:01, B*15:01, B*51:01, C*03:03, C*14:02	DRB1*13:01, DRB1*15:01, DQB1*06:02, DQB1*06:03, DQA1*01:02, DQA1*01:03	8,934	5,208	6,781	1,588
14	f	65	PB	AML, NOS	M1/M2	no	FLT3-ITD	46, XX	200 (94)	4,000	A*02:01, A*11:01, B*35:01, B*44:02, C*04:01, C*05:01	DRB1*03:01, DRB1*04:01, DQB1*03:02, DQB1*05:01, DQA1*01:01, DQA1*03:01	8,820	4,890	1,041	587
15	m	71	PB	recurrent genetic abnormalities	M5	no	NPM1_A	46, XY	73 (50)	4,000	A*02:01, A*11:01, B*08:01, B*57:01, C*07:01	DRB1*03:01, DRB1*07:01, DQB1*02:01, DQB1*03:03, DQA1*02:01, DQA1*05:01	7,911	4,590	2,811	875
16	f	58	BM	recurrent genetic abnormalities	M1	n.a.	NPM1_A	n.a.	60 (88)	200	A*03:01, A*26:01, B*07:02, B*35:01, C*04:01, C*07:02	DRB1*01:01, DRB1*04:04, DQB1*03:02, DQB1*05:01	4,242	3,268	608	314
			PB						60 (90)	200			4,538	3,343	907	381
17	f	56	PB	therapy-related	n.a.	yes[3]	NM	complex	33 (85)	1,200	A*03:01, A*66:01, B*14:01, B*41:02, C*08:02, C*17:01	DRB1*13:02, DRB1*13:03, DQB1*03:01, DQB1*06:09, DQA1*01:02, DQA1*05:05	5,188	3,747	4,523	1,217

Supplemental Table S1 continued

UPN	Sex	Age	Cell source	WHO classification	FAB classification	AML-specific therapy	Molecular genetic	Karyotype	WBC (10^3/µl) (% blasts)	Cell count (10^6)	HLA class I typing	HLA class II typing	HLA class I		HLA class II	
													HLA ligand IDs	Protein IDs	Peptide IDs	Protein IDs
18	m	51	PB	recurrent genetic abnormalities	M5	no	NPM1_A, FLT3-ITD	46, XY	100 (85)	800	A*02:01, A*24:02, B*07:02, B*51:01, C*07:02, C*14:02	DRB1*11:04, DRB1*13:01, DQB1*03:01, DQB1*05:01, DQA1*01:03, DQA1*05:05	4,984	3,487	4,206	1,165
19	m	70	PB	myelodysplasia-related changes	n.a.	no	CALR	47, XY, +21	49 (83)	560	A*02:01, A*31:01, B*07:02, C*07:02	DRB1*14:01, DRB1*15:01, DQB1*05:03, DQB1*06:02, DQA1*01:01, DQA1*01:02	4,913	3,472	3,319	1,018
20	f	50	PB	recurrent genetic abnormalities	M5	no	CEBPA	46, XX	66 (71)	1,000	A*02:05, A*24:02, B*07:02, B*55:01, C*01:02, C*07:02	DRB1*13:01, DRB1*14:01, DQB1*05:03, DQB1*06:03, DQA1*01:01, DQA1*01:03	4,656	3,376	1,708	643
21	m	57	PB	AML, NOS	n.a.	no	NM	47, XY, +8	190 (80)	1,000	A*02:01, A*25:01, B*44:02, B*57:01, C*05:01, C*06:02	DRB1*13:01, DRB1*13:03, DQB1*03:01, DQB1*06:03, DQA1*01:01, DQA1*05:03	4,508	3,239	4,290	1,097
22	f	82	PB	recurrent genetic abnormalities	M4/M5	no	NM	46, XX, t(9;11)	203 (87)	375	A*01:01, A*03:01, B*07:02, B*08:01, C*07:01, C*07:02	DRB1*03:01, DRB1*13:02, DQB1*02:01, DQB1*06:04, DQA1*01:02, DQA1*05:01	4,265	3,253	3,359	1,001
23	m	60	PB	AML, NOS	M1	no	NM	complex	53 (75)	800	A*02:02, A*11:01, B*35:02, B*44:05, C*02:02, C*04:01	DRB1*03:01, DRB1*16:01, DQB1*02:01, DQB1*05:02, DQA1*02:02, DQA1*05:01	3,952	2,977	2,936	823
24	f	70	PB	recurrent genetic abnormalities	M5	no	NPM1_D, FLT3-ITD	n.a.	270 (85)	5,000	A*03:01, A*24:02, B*07:02, B*51:01, C*07:02	DRB1*04:07, DRB1*15:01, DQB1*03:01, DQB1*06:02, DQA1*01:02, DQA1*02:01	3,929	3,005	4,330	1,179
25	f	71	PB	myelodysplasia-related changes	M2	yes[1]	NM	45, XX, -7	260 (80)	7,600	A*26:01, A*32:01, B*15:01, B*38:01, C*03:03, C*12:03	DRB1*04:04, DRB1*12:01, DQB1*03:01, DQB1*03:02, DQA1*03:01, DQA1*05:05	3,869	2,971	7,288	1,516
26	m	43	BM	n.a.	n.a.	n.a.	NM	n.a.	n.a. (76)	100	A*02:01, B*35:03, B*40:01, C*03:04, C*04:01	DRB1*13:01, DRB1*14:54, DQB1*05:03, DQB1*06:03	3,063	2,301	3,462	828
		43	PB						n.a. (86)	180			1,902	1,690	3,407	898
27	f	89	PB	recurrent genetic abnormalities	n.a.	yes[4]	NPM1_A, IDH2 R140Q	n.a.	75 (75)	200	A*02:01, A*33:01, B*13:02, B*14:02, C*06:02, C*08:02	DRB1*01:02, DRB1*07:01, DQB1*02:02, DQB1*05:01, DPB1*04:01	3,143	2,567	821	389
28	m	57	PB	recurrent genetic abnormalities	n.a.	no	NPM1_A	46, XY	80 (92)	300	A*30:01, A*33:03, B*13:02, B*44:02, C*06:02, C*07:04	DRB1*07:01, DRB1*11:01, DQB1*02:02, DQB1*03:01, DQA1*02:01, DQA1*05:05	2,841	2,366	2,731	774
29	f	66	PB	myelodysplasia-related changes	n.a.	no	NM	46, XX, del(12p)	45 (n.a.)	200	A*02:01, A*68:02, B*15:01, B*53:01, C*03:03, C*04:01	DRB1*11:04, DRB1*13:02, DQB1*03:01, DQB1*06:04, DPB1*03:01, DPB1*04:02	2,819	2,310	737	349
30	m	56	PB	recurrent genetic abnormalities	M1	yes[4]	NPM1_A, FLT3-ITD	46, XY, 11p15 abberation	137 (81)	200	A*24:02, A*25:01, B*07:02, B*52:01, C*07:02, C*12:02	DRB1*07:01, DRB1*15:02, DQB1*03:03, DQB1*06:01	2,102	1,960	1,148	494
		57	PB		relapse of M1	yes[1,3,4]			n.a.	200			1,418	1,422	1,469	625
31	f	67	PB	recurrent genetic abnormalities	M1	yes[1]	NPM1_A	46, XX, +21q	3 (31)	100	A*24:02, A*68:01, B*51:01, B*56:01, C*01:02, C*02:02	DRB1*04:01, DRB1*08:01, DQB1*03:01	1,870	1,751	1,169	554
32	m	47	PB	recurrent genetic abnormalities	M5	no	NPM1	46, XY	26 (n.a.)	200	A*01:01, A*24:02, B*35:01, B*57:01, C*04:01, C*06:02	DRB1*01:01, DRB1*07:01, DQB1*03:03, DQB1*05:01	1,720	1,583	845	417
33	m	66	BM	recurrent genetic abnormalities	M4	n.a.	KMT2A AF9	46, XY, t(9;11)(p22; q23)	n.a. (80)	200	A*02:01, A*26:01, B*07:10, B*40:01, C*03:04, C*07:02	DRB1*03:01, DRB1*13:02, DQB1*02:01, DQB1*06:04, DPB1*04:01	1,543	1,499	n.a.	n.a.
34	m	33	BM	recurrent genetic abnormalities	M4	no	CBFB/ MYH11	46, XY, inv(16)	105 (n.a.)	200	A*02:01, B*40:01, C*03:04	DRB1*08:01, DRB1*13:02, DQB1*04:02, DQB1*06:04, DPB1*03:01, DPB1*04:02	1,402	1,332	804	365
35	m	80	PB	AML, NOS	M5	no	NM	46, XY	73 (68)	1,000	A*01:01, A*31:01, B*08:01, B*55:01, C*03:03, C*07:01	DRB1*14:01, DRB1*14:06, DQB1*03:01, DQB1*05:03, DQA1*01:01, DQA1*05:03	1,390	1,400	4,925	1,268

Supplemental Table S1 continued

UPN	Sex	Age	Cell source	WHO classification	FAB classification	AML-specific therapy	Molecular genetic	Karyotype	WBC (10^3/µl) (% blasts)	Cell count (10^6)	HLA class I typing	HLA class II typing	HLA class I		HLA class II	
													HLA ligand IDs	Protein IDs	Peptide IDs	Protein IDs
36	f	75	BM	AML, NOS	M4	yes[3]	NPM1_A, FLT3-ITD, IDH1 R132C	46, XX	86 (31)	140	A*02:01, A*11:01, B*14:01, B*55:01, C*03:03, C*08:02	DRB1*14:54, DRB1*15:01, DQB1*05:03, DQB1*06:02, DPB1*04:02, DPB1*06:01	1,307	1,256	823	375
37	f	67	PB	myelodysplasia-related changes	n.a.	yes[3]	TET2	47, XX, +8	32 (n.a.)	200	A*01:01, A*02:01, B*08:01, B*15:01, C*03:04, C*07:01	DRB1*04:01, DQB1*03:02, DPB1*04:01	1,156	1,214	1,223	497
38	f	51	PB	recurrent genetic abnormalities	M1	yes[4]	NPM1_A, FLT3-ITD	46, XX	268 (93)	80	A*02:01, A*31:01, B*27:05, B*44:29, C*02:02, C*07:02	DRB1*13:01, DQB1*06:03, DQA1*01:03	1,075	1,190	908	452
39	m	69	PB	myelodysplasia-related changes	n.a.	no	NPM1_A, FLT3-ITD	46, XY	43 (80)	90	A*01:01, A*03:01, B*07:02, B*35:03, C*06:02, C*07:02	DRB1*13:05, DRB1*15:01, DQB1*03:01, DQB*06:02, DQA1*01:01, DQA1*05:05	970	1,016	n.a.	n.a.
40	f	58	PB	recurrent genetic abnormalities	M5	yes[2,4]	NPM1_A, FLT3-ITD	46, XX	87 (96)	80	A*02:01, A*23:01, B*44:02, B*49:01, C*05:01, C*07:01	DRB1*04:01, DRB1*15:01, DQB1*03:02, DQB1*06:02, DQA1*01:02, DQA1*03:01	888	938	n.a.	n.a.
41	f	29	PB	recurrent genetic abnormalities	M1	no	NM	45, XX, inv(3)(q21; q26), -7	16 (50)	90	A*11:01, A*24:02, B*49:01, B*52:01, C*07:01, C*12:02	DRB1*01:01, DRB1*11:04, DQB1*03:01, DQB1*05:01, DQA1*01:01, DQA1*05:05	874	934	852	306
42	m	49	PB	recurrent genetic abnormalities	M2	yes[1,3]	NPM1_A, n.a.	46, XY	5 (86)	110	A*01:01, A*24:02, B*07:02, B*08:01, C*07:01, C*07:02	n.a.	868	944	1,739	715
43	f	72	PB	recurrent genetic abnormalities	M2	no	NPM1_A, FLT3-ITD	46, XX	110 (98)	90	A*01:01, A*68:01, B*35:03, B*52:01, C*04:01, C*12:02	DRB1*11:03, DRB1*15:02, DQB1*03:01, DQB1*06:01	814	666	618	225
44	m	87	BM	recurrent genetic abnormalities	M0	no	n.a., NPM1 neg.	46, XY, -7q	43 (60)	200	A*01:01, A*02:01, B*08:01, B*38:01, C*07:01, C*12:03	DRB1*03:01, DRB1*13:01, DQB1*02:01, DQB1*06:03	709	792	n.a.	n.a.
45	f	59	PB	recurrent genetic abnormalities	n.a.	no	FLT3-ITD	46, XX, t(15;17)(q22; q12)	42 (96)	90	A*01:01, A*29:02, B*44:03, B*57:01, C*06:02, C*16:01	DRB1*07:01, DRB1*14:01, DQB1*02:02, DQB1*05:03	707	776	n.a.	n.a.
46	f	n.a.	PB	AML, NOS	M2	no	NM	46, XX	n.a.	200	A*02:01, A*31:01, B*15:01, B*18:01, C*03:04, C*07:01	DRB1*04:01, DRB1*13:01, DQB1*03:02, DQB1*06:03, DPB1*04:01	618	688	1,546	581
47	f	54	BM	myelodysplasia-related changes	M5	n.a.	NM	46, XX	n.a. (80)	200	A*01:01, A*02:01, B*08:01, B*44:02, C*05:01, C*07:01	DRB1*03:01, DRB1*14:54, DQB1*02:01, DQB1*05:03, DPB1*01:01, DPB1*09:01	555	656	2,559	884
48	f	60	PB	AML, NOS	n.a.	no	NM	46, XX, t(6;11)	4 (71)	100	A*24:02, A*68:01, B*15:17, B*40:01, C*03:04, C*07:01	DRB1*13:02, DQB1*06:04, DQA1*01:01, DQA1*01:03	542	647	1,120	372
49	m	87	BM	myelodysplasia-related changes	M2	no	n.a., NPM1 neg.	46, XY	20 (n.a.)	200	A*02:01, A*03:01, B*27:02, B*35:03, C*02:02, C*04:01	DRB1*01:01, DRB1*12:01, DQB1*03:01, DQB1*05:01, DPB1*04:01, DPB1*13:01	n.a.	n.a.	1,144	399
50	m	72	PB	recurrent genetic abnormalities	n.a.	yes[1]	NPM1_A, CEBPA	46, XY	190 (87)	80	A*03:01, A*30:01, B*35:01, B*44:03, C*04:01, C*16:01	DRB1*07:01, DRB1*11:01, DQB1*02:02, DQB1*03:01	n.a.	n.a.	615	311
51	f	79	PB	recurrent genetic abnormalities	n.a.	n.a.	NPM1_A	n.a.	n.a.	200	A*03:01, A*32:03, B*15:17, B*35:01, C*04:01, C*15:02	DRB1*01:01, DQB1*05:01	n.a.	n.a.	594	259
52	f	83	PB	AML, NOS	M1	no	NM	n.a.	121 (88)	80	A*01:01, A*02:06, B*27:05, B*35:01, C*03:03, C*04:01	DRB1*15:01, DQB1*06:02	n.a.	n.a.	590	322

AML patients included in HLA ligandome analysis for AML *discovery dataset*. AML-specific therapy: 1 cytarabine, 2 anthracycline-based chemotherapy, 3 demethylating agents, 4 hydroxyurea. Complex karyotype: ≥ 3 unrelated chromosomal abnormalities analogous to Swerdlow *et al.* (2008). Abbreviations: UPN, uniform patient number; WHO, World Health Organization; FAB, French-American-British; WBC, white blood cell count; IDs, identifications; n.a., not available; m, male; f, female; PB, peripheral blood; BM, bone marrow; NOS, not otherwise specified; NM, no mutation; ITD, internal tandem duplication; TKD, tyrosine kinase domain.

Supplemental Table S2: Patient characteristics of AML *validation cohort* for HLA ligandome analysis

UPN	Sex	Age	Cell source	WHO classification	FAB classification	AML-specific therapy	Molecular genetic	Karyotype	WBC (10^3/µl) (% blasts)	Cell count (10^6)	HLA class I typing	HLA class II typing	HLA class I		HLA class II	
													HLA ligand IDs	Protein IDs	Peptide IDs	Protein IDs
53	m	36	PB	recurrent genetic abnormalities	M2	no	FLT3-ITD	46, XY	187 (80)	8,400	A*02:01, A*66:01, B*15:01, B*40:01, C*01:02, C*03:04	DRB1*04:01, DRB1*13:02, DQB1*03:02, DQB1*06:04, DQA1*01:02, DQA1*03:01	2,578	2,166	583	334
54	m	63	PB	recurrent genetic abnormalities	M4	no	NPM1_B, FLT3-ITD	46, XY	55 (60)	1,500	A*02:01, A*24:02, B*15:01, C*07:02, C*07:04	DRB1*04:01, DRB1*07:01, DQB1*02:02, DQB1*03:02, DQA1*02:01, DQA1*03:01	1,546	1,464	200	262
55	f	22	PB	recurrent genetic abnormalities	M1	no	FLT3-ITD	46, XX	83 (90)	400	A*02:01, B*07:02, B*40:01, C*03:04, C*07:02	DRB1*11:01, DRB1*13:01, DQB1*03:01, DQB1*06:03, DQA1*01:03, DQA1*05:05	1,522	1,417	566	307
56	f	44	PB	recurrent genetic abnormalities	M5	no	NPM1_A, FLT3-ITD	46, XX	38 (84)	2,800	A*02:01, A*03:01, B*38:01, B*44:02, C*05:01, C*12:03	DRB1*04:01 , DRB1*13:01, DQB1*03:01, DQB1*06:03, DQA1*01:03, DQA1*03:01	1,392	1,343	173	177
57	m	68	PB	recurrent genetic abnormalities	n.a.	no	NPM1_A, FLT3-ITD	46, XY	148 (80)	5,000	A*01, A*02, B*08, B*13, C*06, C*07	DRB1*03:01, DRB1*07:01, DQB1*02:01, DQB1*02:02, DQA1*02:01, DQA1*05:01	1,332	1,356	719	442
58	m	79	PB	myelodysplasia-related changes	M0	no	NM	45, XY, -7, +13, -21	39 (84)	2,600	A*02:01, A*03:01, B*18:01, C*07:01	DRB1*07:01, DRB1*11:01, DQB1*02:02, DQB1*03:01, DQA1*02:01, DQA1*05:05	1,224	1,251	295	159
59	f	68	PB	n.a.	M4	no	n.a.	n.a.	214 (90)	1,000	A*01, A*03, B*07, B*08, C*07	n.a.	1,223	1,274	680	337
60	m	74	PB	recurrent genetic abnormalities	M5	no	FLT3-ITD	46, XY	250 (92)	1,900	A*02, A*24, B*44, B*50, C*05, C*06	n.a.	1,184	1,135	581	377
61	f	27	PB	recurrent genetic abnormalities	M5	no	NPM1_A	46, XX	50 (84)	1,600	A*02, A*03, B*44, B*52, C*02, C*12	DRB1*14:07, DRB1*16:01, DQB1*05:02, DQB1*05:03	1,174	1,165	n.a.	n.a.
62	f	78	PB	myelodysplasia-related changes	M1	no	NM	complex	223 (93)	3,500	A*29, A*32, B*40:02, B*44:03, C*16	n.a.	1,138	1,163	303	162
63	m	50	PB	myelodysplasia-related changes	M2	no	JAK2 V617F	complex	30 (83)	500	A*23:01, A*66:01, B*49:01, C*07:01	DRB1*11:01, DRB1*11:04, DQB1*03:01	1,076	1,097	448	319
64	m	83	PB	recurrent genetic abnormalities	M5	no	NPM1_A, FLT3-ITD	46, XY	46 (88)	700	A*11, A*25, B*07, B*51, C*07, C*14	n.a.	1,062	1,122	n.a.	n.a.
65	f	87	PB	n.a.	M2	no	n.a.	n.a.	256 (82)	650	A*03, A*29, B*07, B*35, C*06, C*07	n.a.	920	1,002	875	326
66	f	59	PB	myelodysplasia-related changes	M2	no	FLT3-ITD	46, XX	62 (92)	500	A*01:01, B*18:01, B*52:01, C*07:01, C*12:02	DRB1*04:03, DRB1*15:02, DQB1*03:02, DQB1*06:01, DQA1*02:01, DQA1*03:01	844	897	n.a.	n.a.
67	f	77	PB	myelodysplasia-related changes	M2	yes[3]	NM	46, XX	11 (80)	900	A*02, A*11, B*35, B*44, C*04, C*05	n.a.	829	888	496	326
68	m	30	PB	recurrent genetic abnormalities	M2	no	FLT3-ITD	46, XY	25 (51)	200	A*02:01, B*13:02, B*51:01, C*01:02, C*06:02	DRB1*04:02, DRB1*07:01, DQB1*02:02, DQB1*03:02, DQA1*02:01, DQA1*03:01	818	894	n.a.	n.a.
69	f	50	PB	recurrent genetic abnormalities	M2	no	NPM1_A, FLT3-ITD	46, XX	50 (27)	800	A*01:01, A*23:01, B*44:03, C*04:01, C*14:03	DRB1*07:01, DRB1*13:01, DQB1*02:02, DQB1*06:03, DQA1*01:03, DQA1*02:01	776	866	317	354
70	m	74	PB	AML, NOS	M5	no	FLT3-ITD	47, XY, +8	78 (80)	400	A*03:01, A*32:01, B*35:01, B*57:01, C*04:01, C*06:02	DRB1*07:01, DRB1*13:02, DQB1*03:03, DQB1*06:09, DQA1*01:02	764	832	426	300

Supplemental Table S2 continued

UPN	Sex	Age	Cell source	WHO classification	FAB classification	AML-specific therapy	Molecular genetic	Karyotype	WBC (10^3/µl) (% blasts)	Cell count (10^6)	HLA class I typing	HLA class II typing	HLA class I		HLA class II	
													HLA ligand IDs	Protein IDs	Peptide IDs	Protein IDs
71	m	41	PB	recurrent genetic abnormalities	M4/M5	no	NPM1_A, FLT3-TKD	46, XY	82 (75)	350	A*02:01, B*15:01, B*39:01, C*04:01, C*12:03	DRB1*01:01, DRB1*13:01, DQB1*05:01, DQB1*06:03, DQA1*01:01, DQA1*01:03	n.a.	n.a.	845	347
72	f	46	PB	recurrent genetic abnormalities	M1	no	NPM1_A, FLT3-ITD	46, XX	248 (80)	1,000	A*03:01, B*39:01, B*51:01, C*01:02, C*12:03	DRB1*01:01, DRB1*03:01, DQB1*02:01, DQB1*05:01, DQA1*01:01, DQA1*05:01	n.a.	n.a.	592	330
73	m	72	PB	myelodysplasia-related changes	M1	yes[3]	NM	complex	48 (90)	1,700	A*03:01, A*26:01, B*35:01, B*38:01, C*04:01, C*12:03	DRB1*04:08, DRB1*15:01, DQB1*03:04, DQB1*05:02, DQA1*01:02, DQA1*03:01	n.a.	n.a.	563	352
75	m	25	PB	recurrent genetic abnormalities	M4	no	CBFB/ MYH11	47, XY, inv(16)	27 (80)	400	A*02:01, B*39:01, B*51:01, C*04:01, C*07:02	DRB1*03:01, DRB1*04:01, DQB1*02:01, DQB1*03:02, DQA1*03:02, DQA1*05:01	n.a.	n.a.	312	280
74	f	77	PB	AML, NOS	M4	no	MLL-PTD	complex	142 (94)	100	A*02, A*31, B*27, B*44	n.a.	n.a.	n.a.	421	253
76	f	65	PB	recurrent genetic abnormalities	M2	no	NPM1_A, FLT3-ITD	46, XX	150 (96)	4,900	A*02, A*26:01, B*27:05, B*51, C*01:02	DRB1*01:01, DQB1*05:01, DQA1*01:01	n.a.	n.a.	150	91

AML patients included in HLA ligandome analysis for AML *validation dataset*. AML-specific therapy: 1 cytarabine, 2 anthracycline-based chemotherapy, 3 demethylating agents, 4 hydroxyurea. Complex karyotype: ≥ 3 unrelated chromosomal abnormalities analogous to Swerdlow *et al.* (2008). Abbreviations: UPN, uniform patient number; WHO, World Health Organization; FAB, French-American-British; WBC, white blood cell count; IDs, identifications; n.a., not available; m, male; f, female; PB, peripheral blood; NOS, not otherwise specified; NM, no mutation; ITD, internal tandem duplication; TKD, tyrosine kinase domain.

Supplemental Table S3: Patient characteristics of AML_{MR} patients for HLA ligandome analysis

UPN	Sex	Age	Cell source	WHO classification	FAB classification	AML-specific therapy	Molecular genetic	Karyotype	Remission status	WBC (10^3/µl) (% blasts)	Cell count (10^6)	HLA class I typing	HLA class II typing	HLA class I		HLA class II	
														HLA ligand IDs	Protein IDs	Peptide IDs	Protein IDs
20	f	51	PB	recurrent genetic abnormalities	M5	yes[2]	CEBPA	46, XX	MR	6.1 (0)	60	A*02:05, A*24:02, B*07:02, B*55:01, C*01:02, C*07:02	DRB1*13:01, DRB1*14:01, DQB1*05:03, DQB1*06:03, DQA1*01:01, DQA1*01:03	864	938	1,295	517
28	m	59	PB	recurrent genetic abnormalities	n.a.	yes[2]	NPM1_A	46, XY	MR	5.0 (0)	60	A*30:01, A*33:03, B*13:02, B*44:02, C*06:02, C*07:04	DRB1*07:01, DRB1*11:01, DQB1*02:02, DQB1*03:01, DQA1*02:01, DQA1*05:05	1,309	1,323	1,335	513
77	m	57	PB	recurrent genetic abnormalities	n.a.	yes[2]	RUNX1/ RUNX1T1	complex	MR	6.9 (0)	27	A*03:01, A*31:01, B*18:01, B*44:27, C*05:01, C*07:04	DRB1*03:01, DRB1*16:01, DQB1*02:01, DQB1*05:02	472	523	1,001	463
78	m	55	PB	recurrent genetic abnormalities	n.a.	yes[2]	CBFB/MYH11	complex	MR	5.9 (0)	63	A*11:01, B*55, B*57:01, C*03:03, C*06:02	DRB1*13:01, DRB1*15:01, DQB1*06:02, DQB1*06:03	1,467	1,379	1,352	499
79	f	64	PB	recurrent genetic abnormalities	n.a.	yes[2]	CBFB/MYH11	46, XX, inv16(p13.1q22)	MR	6.2 (0)	72	A*02:01, A*30:01, B*07:02, B*13:02, C*06:02, C*07:02	DRB1*07:01, DRB1*15:01, DQB1*02:02, DQB1*06:02	1,060	1,115	858	397
80	m	46	PB	recurrent genetic abnormalities	M5	yes[2]	CBFB/MYH11	46, XY, inv(16)(p13.1q22)	MR	3.6 (0)	36	A*02:01, A*03:01, B*27:05, B*51:01, C*02:02, C*07:02	DRB1*04:04, DRB1*15:01, DQB1*03:02, DQB1*06:02, DQA1*01:02, DAQ1*03:01	1,111	1,176	1,279	452
81	f	61	PB	recurrent genetic abnormalities	M5	yes[2]	NPM1_A, FLT3-ITD	n.a.	MR	8.5 (0)	90	A*02:01, A*03:01, B*35:01, B*35:03, C*04:01	DRB1*01:01, DRB1*16:01 DQB1*05:01, DQB1*05:02	2,270	2,012	1,770	637
82	f	53	PB	recurrent genetic abnormalities	M5 eo	yes[2]	CBFB/MYH11	46, XX, inv16(p13.1q22)	MR	4.0 (0)	47	A*11:01, B*52:01, C*12:02	DRB1*15:02, DQB*06:01	1,275	1,256	1,528	539

AML patients in molecular remission (AML_{MR}) included in HLA ligandome analysis for comparative benign AML_{MR} dataset. AML-specific therapy: 1 cytarabine, 2 anthracycline-based chemotherapy, 3 demethylating agents, 4 hydroxyurea. Complex karyotype: ≥3 unrelated chromosomal abnormalities analogous to Swerdlow *et al.* (2008). Abbreviations: UPN, uniform patient number; WHO, World Health Organization; FAB, French-American-British; WBC, white blood cell count; IDs, identifications; m, male; f, female; PB, peripheral blood; ITD, internal tandem duplication; MR, molecular remission.

Supplemental Table S4: Patient characteristics of AML patients for T-cell-based assays

UPN	Sex	Age	Experiment	WHO classification	FAB classification	AML-specific therapy	Molecular genetic	Karyotype	HSCT	time after HSCT	HLA class I typing	HLA class II typing
1	m	23	E, P	recurrent genetic abnormalities	M4	yes[2]	CBFB/MYH11	complex	yes	$t_{1\text{-}2y}$	A*11:01, B*07:02, B*44:03, C*07:02, C*16:01	DRB1*03:01, DRB1*07:01, DQB1*02:01, DQB1*02:02, DQA1*02:01, DQA1*05:01
10	m	68	E	recurrent genetic abnormalities	M4	yes[2,4]	NPM1_A, FLT3-ITD	46, XY	yes	$t_{2\text{-}5y}$	A*02:01, A*23:01, B*44:02, B*44:03, C*02:02, C*04:01	DRB1*07:01, DQB1*02:02, DQA1*02:02
12	f	48	E	recurrent genetic abnormalities	M5	yes[1,2]	NPM1_A	46, XX	no	t_{pre}	A*02:01, A*02:05, B*51:01, B*58:01, C*03:02, C*14:02	DRB1*03:01, DRB1*16:01, DQB1*02:01, DQB1*05:02, DQA1*01:01, DQA1*05:01
14	f	68	E, P	AML, NOS	M1/M2	yes[2]	FLT3-ITD	46, XX	yes	$t_{2\text{-}5y}$	A*02:01, A*11:01, B*35:01, B*44:02, C*04:01, C*05:01	DRB1*03:01, DRB1*04:01, DQB1*03:02, DQB1*05:01, DQA1*01:01, DQA1*03:01
15	m	71	E	recurrent genetic abnormalities	M5	yes[1]	NPM1_A	46, XY	no	t_{pre}	A*02:01, A*11:01, B*08:01, B*57:01, C*07:01	DRB1*03:01, DRB1*07:01, DQB1*02:01, DQB1*03:03, DQA1*02:01, DQA1*05:01
21	m	57	E	AML, NOS	n.a.	yes[2,4]	NM	46, XY, +8	no	t_{pre}	A*02:01, A*25:01, B*44:02, B*57:01, C*05:01, C*06:02	DRB1*13:01, DRB1*13:03, DQB1*03:01, DQB1*06:03, DQA1*01:01, DQA1*05:03
23	m	62	E, P	AML, NOS	M1	yes[2,4]	NM	complex	yes	$t_{1\text{-}2y}$	A*02:02, A*11:01, B*35:02, B*44:05, C*02:02, C*04:01	DRB1*03:01, DRB1*16:01, DQB1*02:01, DQB1*05:02, DQA1*02:02, DQA1*05:01
72	f	54	E	recurrent genetic abnormalities	M1	yes[1,2,4]	NPM1_A, FLT3-ITD	46, XX	yes	$t_{5\text{-}10y}$	A*03:01, B*39:01, B*51:01, C*01:02, C*12:03	DRB1*01:01, DRB1*03:01, DQB1*02:01, DQB1*05:01, DQA1*01:01, DQA1*05:01
76	f	69	E	recurrent genetic abnormalities	M2	yes[1,2]	NPM1_A, FLT3-ITD	46, XX	yes	$t_{2\text{-}5y}$	A*02, A*26:01, B*27:05, B*51, C*01:02	DRB1*01:01, DQB1*05:01, DQA1*01:01
86	m	72	E	myelodysplasia-related changes	n.a.	yes[2]	NM	n.a.	yes	$t_{5\text{-}10y}$	A*02:01, A*24:02, B*13:02, B*38:01, C*06:02, C*12:03	DRB1*07:01, DRB1*11:04, DQB1*02:02, DRB1*03:01
87	f	46	E	AML, NOS	M2	yes[2]	NM	46, XX, del(1)	yes	$t_{5\text{-}10y}$	A*02:01, A*32:01, B*15:01, B*51:01, C*03:03, C*14:02	DRB1*09:01, DRB1*11:01, DQB1*03:01, DQB1*03:03
88	m	69	E	AML, NOS	M4	yes[2]	NM	46, XY	yes	$t_{2\text{-}5y}$	A*02:01, B*57:01, C*06:02	DRB1*07:01, DRB1*13:03, DQB1*03:01, DQB1*03:03
89	f	73	E	myelodysplasia-related changes	n.a.	yes[1,2]	NM	47, XX, +8 [9]; 46, XX [14]	yes	$t_{2\text{-}5y}$	A*02:01, A*25:01, B*13:02, B*18:01, C*06:02, C*12:03	DRB1*07:01, DRB1*15:01, DQB1*02:02, DQB1*06:04
90	m	51	E	recurrent genetic abnormalities	M1	yes[2]	NPM1, FLT3-ITD	n.a.	yes	$t_{2\text{-}5y}$	A*02:01, A*30:02, B*18:01, B*51:01, C*05:01, C*15:02	DRB1*01:01, DRB1*16:01, DQB1*05:01, DQB1*05:02
91	m	64	E	myelodysplasia-related changes	n.a.	yes[2]	NM	46, XY	yes	$t_{1\text{-}2y}$	A*02:01, A*69:01, B*15:01, B*38:01, C*03:04, C*12:03	DRB1*04:02, DRB1*13:01, DQB1*03:02, DQB1*06:03
92	f	44	E	AML, NOS	M2	yes[2]	NM	46, XX, t(11;19)	yes	$t_{2\text{-}5y}$	A*11:01, A*24:02, B*27:05, B*51:01, C*02:02, C*15:02	DRB1*03:01, DRB1*04:04, DQB1*02:01, DQB1*03:02
94	m	57	E	myelodysplasia-related changes	M5	yes[2]	NM	46, XY	yes	$t_{5\text{-}10y}$	A*02:05, A*11:01, B*27:02, B*35:01, C*02:02, C*04:01	n.a.
95	f	74	E	myelodysplasia-related changes	n.a.	yes[1,2]	NM	46, XX	yes	$t_{5\text{-}10y}$	A*01:01, A*11:01, B*08:01, B*35:01, C*04:01, C*07:01	DRB1*03:01, DRB1*12:01, DQB1*02:01, DQB1*03:01
96	f	72	E	AML, NOS	M2	yes[2,3]	MLL amplification	complex	yes	$t_{<8m}$	A*01:01, A*02:01, B*37:01, B*44:02, C*05:01, C*06:02	DRB1*15:01, DQB1*06:02

Supplemental Table S4 continued

UPN	Sex	Age	Experiment	WHO classification	FAB classification	AML-specific therapy	Molecular genetic	Karyotype	HSCT	time after HSCT	HLA class I typing	HLA class II typing
97	m	50	E, P	recurrent genetic abnormalities	M4	yes[2]	NPM1, FLT3-ITD	46, XY, t(1;2)(q32;q21)	yes	$t_{2\text{-}5y}$	A*11:01, A*24:02, B*15:01, B*35:01, C*03:03, C*04:01	DRB1*07:01, DRB1*13:01, DQB1*03:03, DQB1*06:03
98	f	54	E, P	recurrent genetic abnormalities	M2	yes[1,2]	RUNX1-RUNX1T1	46, XX, t(8;21)(q22;q22)	yes	$t_{2\text{-}5y}$	A*02:01, A*11:01, B*08:01, B*40:01, C*03:04, C*07:01	DRB1*03:01, DRB1*08:01, DQB1*02:01, DQB1*04:02
99	f	68	E	recurrent genetic abnormalities	M5	yes[2]	MLLT3/MLL	46, XX, t(9;11)(p11:q23)	yes	$t_{2\text{-}5y}$	A*01:01, A*02:01, B*51:01, B*57:01, C*06:02, C*14:02	DRB1*07:01, DRB1*15:01, DQB1*03:03, DQB1*06:03
100	m	51	E	myelodysplasia-related changes	n.a.	yes[2]	CEPBA	46, XY	yes	$t_{2\text{-}5y}$	A*11:01, A*68:01, B*35:01, B*44:03, C*04:01, C*14:03	DRB1*04:05, DRB1*14:01, DQB1*03:02, DQB1*05:03
101	m	57	E, P	AML, NOS	M4	yes[2]	FLT3-ITD	46, XY	yes	$t_{10\text{-}20y}$	A*03, A*11, B*35, B*51, C*04, C*15	DRB1*04:04, DRB1*11:01, DQB1*03:01, DQB1*03:02
102	f	48	E	recurrent genetic abnormalities	M1	yes[1,2]	NPM1, FLT3-ITD	46, XX	yes	$t_{10\text{-}20y}$	A*11:01, A*24:02, B*27:02, B*35:01, C*02:02, C*04:01	DRB1*01:01, DRB1*16:01, DQB1*05:01, DQB1*05:02
103	m	70	E	myelodysplasia-related changes	M2	yes[2]	FLT3-ITD	46, XY	yes	$t_{5\text{-}10y}$	A*31, B*15, B*40	n.a.
104	f	70	E	myelodysplasia-related changes	n.a.	yes[3]	RUNX1	46, XX	yes	$t_{2\text{-}5y}$	A*23:01, A*29:01, B*44:03, C*04:01, C*16:01	DRB1*07:01, DRB1*15:01, DQB1*02:02, DQB1*06:02
105	f	53	E	recurrent genetic abnormalities	M4	yes[2]	NPM1	46, XX	yes	$t_{5\text{-}10y}$	A*26:01, A*32:01, B*27:05, B*38:01, C*05:01, C*12:03	DRB1*13:01, DRB1*15:01, DQB1*06:02, DQB1*06:03
106	m	54	E	AML, NOS	M4	yes[1]	FLT3-TKD	46, XY, t(2;3)(p21;q26)	yes	$t_{2\text{-}5y}$	A*03:01, A*25:01, B*35:01, B*40:01, C*03:04, C*12:03	DRB1*04:01, DRB1*15:02, DQB1*03:01, DQB1*06:01
107	f	55	E	recurrent genetic abnormalities	M5	yes[2]	NPM1, FLT3-ITD	46, XX	yes	$t_{1\text{-}2y}$	A*23:01, A*24:02, B*35:01, B*44:03, C*01:02, C*04:01	DRB1*01:01, DRB1*07:01, DQB1*02:02, DQB1*05:01
108	m	53	E	recurrent genetic abnormalities	M4	yes[2]	NPM1, FLT3-ITD	46, XY	yes	$t_{1\text{-}2y}$	A*03:01, A*24:02, B*15:01, B*44:02, C*03:03, C*05:01	DRB1*11:01, DRB1*13:01, DQB1*03:01, DQB1*06:03
109	f	45	E	recurrent genetic abnormalities	n.a.	yes[2]	RUNX1-RUNX1T1	45, X, -X, t(8;21)(q22;q22)	yes	$t_{2\text{-}5y}$	A*23:01, A*24:07, B*35:01, B*35:08, C*04:01, C*15:05	DRB1*04:03, DRB1*14:01, DQB1*03:02, DQB1*05:03
110	m	66	P	AML, NOS	M0	yes[2]	NM	48, XY, +4, +22	yes	$t_{2\text{-}5y}$	A*03:01, A*11:01, B*49:01, B*51:01, C*07:01, C*15:04	DRB1*11:01, DRB1*15:01, DQB1*03:01, DQB1*06:02
111	m	51	E	AML, NOS	M4	yes[2]	FLT3-ITD	46, XY	yes	$t_{10\text{-}20y}$	A*02:01, A*03:01, B*07:02, B*27:05, C*01:02, C*07:02	DRB1*01:01, DRB1*15:01, DQB1*05:01, DQB1*06:02
112	f	60	E	recurrent genetic abnormalities	n.a.	yes[2,4]	NPM1_A, FLT3-ITD	46, XX	yes	$t_{2\text{-}5y}$	A*03:01, A*24:02, B*07:02, B*35:03, C*04:01, C*07:02	DRB1*12:01, DRB1*15:01, DQB1*03:01, DQB1*06:02
113	m	65	E	AML, NOS	M1	yes[2]	NM	complex	yes	$t_{2\text{-}5y}$	A*03:01, A*24:02, B*07:02, B*35:01, C*04:01, C*07:02	DRB1*01:01, DRB1*04:03, DQB1*03:02, DQB1*05:01
114	m	61	E	AML, NOS	n.a.	yes[2]	FLT3	complex	yes	$t_{2\text{-}5y}$	A*03:01, A*24:02, B*07:02, B*40:01, C*03:04, C*07:02	DRB1*13:02, DRB1*15:01, DQB1*05:02, DQB1*06:04
115	m	68	E	recurrent genetic abnormalities	n.a.	yes[2]	NPM1_A, FLT3-TKD	46, XY	yes	$t_{1\text{-}2y}$	A*02:01, A*03:01, B*07:02, B*44:02, C*05:01, C*07:02	DRB1*11:01, DRB1*13:02, DQB1*03:01, DQB1*06:04

Supplemental Table S4 continued

UPN	Sex	Age	Experiment	WHO classification	FAB classification	AML-specific therapy	Molecular genetic	Karyotype	HSCT	time after HSCT	HLA class I typing	HLA class II typing
116	f	66	E	recurrent genetic abnormalities	M4	yes[2,4]	NPM1_A	46, XX	yes	$t_{1\text{-}2y}$	A*02:05, A*03:01, B*07:02, B*50:01, C*06:02, C*07:02	DRB1*07:01, DRB1*15:01, DQB1*02:02, DQB1*06:02
117	f	41	E	recurrent genetic abnormalities	n.a.	yes[2]	NPM1_A	46, XX	yes	$t_{2\text{-}5y}$	A*03:01, A*30:01, B*07:02, B*13:02, C*06:02, C*07:02	DRB1*14:54, DRB1*15:01, DQB1*05:03, DQB1*06:02

AML patients in remission used for *in vitro* T-cell-based assays. AML-specific therapy: 1 cytarabine, 2 anthracycline-based chemotherapy, 3 demethylating agents, 4 hydroxyurea. Complex karyotype: ≥3 unrelated chromosomal abnormalities analogous to Swerdlow *et al.* (2008). Abbreviations: UPN, uniform patient number; WHO, World Health Organization; FAB, French-American-British; HSCT, hematopoietic stem cell transplantation; m, male; f, female; E, IFNγ ELISPOT assay; P, *in vitro* artificial antigen-presenting cell-based priming experiment; NOS, not otherwise specified; ITD, internal tandem duplication; NM, no mutation; y, years; n.a., not available.

Supplemental Table S5: Sample characteristics for T-cell-based assays with PBMC samples of HVs

HV	Sex	Age	Experiment	HLA class I typing
1	m	46	E	A*02, A*33, B*07, B*08
2	m	61	E	A*02, A*03, B*07, B*15
3	m	39	E	A*02, B*07, B*40
4	m	54	E	A*02, A*26, B*07, B*38
5	m	47	E	A*02, B*07, B*44
6	m	62	E	A*02, A*03, B*07, B*15
7	m	58	E	A*02, A*24, B*07, B*39
8	f	63	E	A*02, A*24, B*07, B*57
9	m	65	E	A*02, B*07, B*08
10	m	55	E	A*02, A*03, B*07, B*27
11	m	56	E	A*01, A*03, B*08, B*38
12	m	57	E	A*01, A*02, B*08, B*50
13	f	40	E	A*01, B*08, B*37
14	m	30	E	A*01, A*02, B*08, B*57
15	m	55	E	A*01, B*08
16	m	42	E	A*01, A*24, B*08, B*57
17	m	65	E	A*01, B*08, B*44
18	m	30	E	A*01, A*02, B*08, B*57
19	m	38	E	A*01, A*31, B*08, B*27
20	m	55	E	A*01, A*03, B*08, B*15
21	m	34	E	n.a.
22	f	42	E	A*03, A*25, B*27, B*51
23	m	42	E	n.a.
24	m	26	E	A*02, A*26, B*27, B*40
25	m	47	E	A*02, A*24, B*07, B*35
26	m	50	E	A*02, A*23, B*44, B*51
27	m	40	E	A*02, A*29, B*27, B*44
28	m	28	E	A*01, A*03, B*07, B*18
29	m	21	E	A*02, B*44, B*51
30	m	48	E	A*03, A*25, B*18, B*51
31	m	35	E	A*02, A*11, B*15, B*39
32	f	54	E	A*03, A*11, B*15, B*35
33	m	57	E	A*01, A*02, B*40, B*44
33	m	67	E	A*03, A*29, B*07, B*44
34	m	66	E	A*03, A*68, B*07, B*38
35	f	41	E	A*03, B*07, B*35
36	m	61	E	A*03, A*31, B*38, B*51
37	m	58	E	A*01, A*03, B*35, B*40
38	m	52	E	A*01, A*03, B*08, B*35
39	m	51	E	A*03, A*68, B*41, B*56
40	f	50	E	A*03, A*31, B*44, B*49
41	m	64	E	A*11, A*24, B*07, B*57
42	m	45	E	A*01, A*11, B*07, B*14
43	m	33	E	A*01, A*11, B*07, B*08
44	m	65	E	A*11, A*24, B*07, B*57
45	m	51	E	A*01, A*11, B*08, B*35
46	m	29	E	A*11, A*33, B*15, B*57
47	m	61	E	A*03, B*07, B*35
100	m	42	P	A*11, A*24, B*51, B*55
101	m	48	P	A*11, A*30, B*13, B*40
102	m	46	P	A*01, A*11, B*18, B*55
103	f	48	P	A*02, A*32, B*14, B*27
104	m	36	P	A*02, A*32, B*07, B*44

Supplemental Table S6: Recurrent AML mutations for screening of mutation-derived HLA ligands

Gene	Protein	Mutations							
ABL1	ABL1	M244V	G250E	Q252H	Y253H	E255K	E255V	V299L	T315I
		F317L	M351T	E355G	F359V	H396R	E459K		
BCORL1	BCORL	G209S							
CBL	CBL	Y371H	L380P	R420Q					
CSF3R	CSF3R	T618I							
DNMT3A	DNM3A	G543C	S714C	R882C	R882H	R882P	R882S		
FLT3	FLT3	E573insE	S574insS	Q575insQ	L576insL	Q577insQ	M578insM	V579insV	Q580insQ
		V581insV	T582insT	G583insG	S584insS	S585insS	D586insD	N587insN	E588insE
		Y589insY	F590insF	Y591insY	V592insV	D593insD	F594insF	R595insR	R595insRE
		E596insE	E596insEY	Y597insY	E598insE	Y599insY	D600insD	L601insL	K602insK
		W603insW	E604insE	F605insF	P606insP	R607insR	E608insE	N609insN	L610insL
		E611insE	F612insF	G613insG	K614insK	N676K	F691L	D835V	D835G
		D835Y	D835F	D835A	D835E	D835H	D385N	D835S	I836LD
		I836del							
		S584insSSDNEYFYVDFR		E588insEYFYVDFR		F594insFREY		R595insREYEYD	
		S585insSDNEYFYVDFR		Y591insYVDFREYE		F594insFREYE		R595insREYEYDL	
		D586insDNEYFYVDF		V592insVDFREY		F594insFREYEYDL		Y597insYEYDLKW	
		D586insDNEYFYVDFR		V592insVDFREYE		F594insFREYEYD		E598insEYDLKWEF	
		E588insEYFYVDF		D593insDFREY		R595insREY		Y599insYDLKWEFP	
		V581insVTGSSDNEYFYVDFREYEYDLKWEFPRENL				S584insSSDNEYFYVDFREYEYDLKWEFP			
		G583insGSSDNEYFYVDFREY				S584insSSDNEYFYVDFREYEYDLKWEFPRE			
		G583insGSSDNEYFYVDFREYE				S584insSSDNEYFYVDFREYEYDLKWEFPRENL			
		G583insGSSDNEYFYVDFREYEYDLKWEFPRE				S585insSDNEYFYVDFREYEYDLKWEFP			
		G583insGSSDNEYFYVDFREYEYDLKWEFPRENL				S585insSDNEYFYVDFREYEYDLKWEFPRE			
		G583insGSSDNEYFYVDFREYEYDLKWEFPRENLE				N586insDNEYFYVDFREYEYDLKWEFP			
		S584insSSDNEYFYVDFRE				N587insNEYFYVDFREYEYDLKWE			
		S584insSSDNEYFYVDFREY				N587insNEYFYVDFREYEYDLKWEFP			
		S584insSSDNEYFYVDFREYEYD				E588insEYFYVDFREYEYDLKWEFP			
GDF5	GDF5	S276A							
IDH1	IDHC	R132C	R132G	R132H	R132L	R132S			
IDH2	IDHP	R140Q	R140W	R172K					
JAK2	JAK2	V617F	V617I						
KIT	KIT	D816H	D816V	D816Y	N822K				
KRAS	RASK	G12A	G12D	G12S	G12V	G13D	Q61H		
MPL	TPOR	S505N	W515K	W515L					
MYD88	MYD88	L252P							
NPM1	NMP1	type A	type B	type C	type D	type E			
NRAS	RASN	G12A	G12C	G12D	G12S	G12V	G13D	G13R	G13V
		Q61H	Q61K	Q61L	Q61R				
PTPN11	PTN11	G60V	D61V	D61Y	A72T	A72V	E76G	E76K	
SETBP1	SETBP	D868N	G870S	I871T					
SF3B1	SF3B1	E622D	H662Q	K666N	K666R	K666T	K700E		
SRSF2	SRSF2	P95H	P95L	P95R					
TET2	TET2	I1873T							
TP53	P53	R175H	V216M	Y220C	R248Q	R248W	R273C	R273H	C275Y
U2AF1	U2AF1	S34F	S34Y	R156H	Q157P	Q157R			

Recurrent AML-associated mutations including the TOP100 missense mutations specified in the COSMIC database, the most common NPM1 frame shift mutations, and FLT3-ITD and FLT3-TKD mutations.

Supplemental Table S7: Positive and negative control peptides

Positive control peptides		
Source protein	**Peptide sequence**	**HLA restriction**
RDRP_I34A1	VSDGGPNLY	A*01
NCAP_ I34A1	CTELKLSDY	A*01
CAPSH_ADE02	LTDLGQNLLY	A*01
PP65_HCMVA	YSEHPTFTSQY	A*01
M1_ I34A1	GILGFVFTL	A*02
LMP2_EBVB9	CLGGLLTMV	A*02
ICP27_EBVB9	GLCTLVAML	A*02
PP65_HCMVA	NLVPMVATV	A*02
RTA_EBVB9	YVLDHLIVV	A*02
LMP2_EBVB9	FLYALALLL	A*02
NCAP_ I34A1	RVLSFIKGTK	A*03
NCAP_ I34A1	ILRGSVAHK	A*03
RTA_EBVB9	RVRAYTYSK	A*03
EBNA3_EBVB9	RLRAEAQVK	A*03
M1_ I34A1	SIIPSGPLK	A*03
EBNA4_EBVB9	AVFDRKSDAK	A*03
RDRP_ I34A1	RVRDNMTKK	A*03
EBNA4_EBVB9	IVTDFSVIK	A*11
RTA_EBVB9	ATIGTAMYK	A*11
EBNA4_EBVB9	AVFDRKSDAK	A*11
EBNA3_EBVB9	RPPIFIRRL	B*07
PP65_HCMVA	TPRVTGGGAM	B*07
NCAP_ I34A1	ELRSRYWAI	B*08
BZLF1_EBVB9	RAKFKQLL	B*08
EBNA3_EBVB9	FLRGRAYGL	B*08
EBNA3_EBVB9	QAKWRLQTL	B*08
VIE1_HCMVA	ELRRKMMYM	B*08
PP65_HCMVA	YQEFFWDANDIYRIF	class II
GP350_EBVB9	PRPVSRFLGNNSILY	class II
EBNA1_EBVB9	IAEGLRALLARSHVERTTDE	class II
EBNA1_EBVB9	RRGTALAIPQCRLTPLSRLP	class II
EBNA2_EBVB9	RSPTVFYNIPPMPLPPSQL	class II
E3GL_ADE02	TLLYLKYKSRRSFID	class II
CAP3_ADE02	RQVMDRIMSLTARNP-NH2	class II
E1BS_ADE02	MHLWRAVVRHKNRLL	class II
E1BS_ADE02	KNRLLLLSSVRPAII	class II
LEAD_ADE02	TLVLAFVKTCAVLAA	class II
E3145_ADE02	RGIFCVVKQAKLTYE	class II
PKG1_ADE02	VSKFFHAFPSKLHDK	class II
CAPSH_ADE02	TFYLNHTFKKVAITF	class II
CAPSH_ADE02	PQKFFAIKNLLLLPG	class II

Supplemental Table S7 continued

Negative control peptides		
Source protein	**Peptide sequence**	**HLA restriction**
POL_HV1BR	GSEELRSLY	A*01
DDX5_HUMAN	YLLPAIVHI	A*02
GAG_HV1BR	RLRPGGKKK	A*03
MKX_HUMAN	ASEDYVAPPK	A*11
FLNA_HUMAN	ETVITVDTKAAGKGK	class II

Positive and negative control peptides with their respective HLA restrictions used for IFNγ ELISPOT assays and aAPC-based *in vitro* priming experiments. Abbreviations: I34A1, Influenza A virus (strain A/Puerto Rico/8/1934 H1N1); HCMVA, human cytomegalovirus (strain AD169); EBVB9, Epstein-Barr virus (strain B95-8); ADE, human adenovirus; HV1BR, human immunodeficiency virus type 1 group M subtype B.

Supplemental Table S8: HLA class I and II surface expression on primary AML samples

UPN	HLA class I expression on $CD34^+CD38^+$ blasts	HLA class I expression on $CD34^+CD38^-$ LPCs	HLA class II expression on $CD34^+CD38^+$ blasts	HLA class II expression on $CD34^+CD38^-$ LPCs
01	76,333	53,131	27,683	7,237
02	99,835	77,109	6,715	1,198
09	43,674	31,054	63,525	30,808
10	107,760	93,503	20,540	10,007
12	47,381	n.d.	3,949	n.d.
14	77,961	n.d.	6,262	n.d.
15	73,663	81,874	24,878	14,148
17	327,243	310,084	61,782	46,235
18	35,188	89,456	4,422	8,116
19	299,944	200,772	45,719	48,454
20	160,281	n.d.	30,276	n.d.
24	50,123	42,106	4,241	4,939
25	105,239	37,729	excld.	n.d.
48	65,682	69,117	17,491	25,498
64	159,011	103,186	18,131	7,322

HLA class I (HLA-A, -B, -C) and class II (HLA-DR) expression was determined by flow cytometry for $CD34^+CD38^+$ AML blasts and $CD34^+CD38^-$ LPCs from PBMC samples of $CD34^+$ AML patient samples (n = 15) at the time of diagnosis. Abbreviations: UPN, uniform patient number; LPCs, leukemic progenitor cells; n.d., not detectable indicating samples with less than 100 cells in the respective population.

Supplemental Table S9: LPC frequencies pre- and postenrichment

UPN	Enrichment method	WBC (10^3/µl) (% blasts)	LPC frequency presorting [%]	LPC frequency postsorting [%]	Cell count LPCs (10^6)	Cell count blasts (10^6)	Cell count $CD34^-$ (10^6)
01	MACS	138 (72)	10.32	92.10	560	4,900	8,300
02	MACS	100 (71)	3.24	90.41	18	1,284	2,825
03	FACS	n.a.	0.10	75.03	18	300	-
04	FACS	n.a.	2.40	98.40	300	300	-
05	FACS	n.a.	0.02	40.00	67	143	-
06	FACS	n.a.	40.60	99.70	200	400	-
07	FACS	n.a.	6.75	59.37	60	220	-
08	FACS	n.a.	17.57	97.16	45	200	-
09	MACS	500 (70)	1.16	90.31	7	290	1,980
10	MACS	90 (90)	5.27	92.26	2	5	500
11	FACS	n.a.	6.40	94.00	32	245	-
12	no	100 (88)	0.02	-	-	-	-
14	no	200 (94)	0.04	-	-	-	-
15	no	73 (50)	0.15	-	-	-	-
18	no	100 (85)	0.16	-	-	-	-
19	no	49 (83)	0.57	-	-	-	-
20	no	66 (71)	0.01	-	-	-	-
22	no	203 (87)	0.02	-	-	-	-
23	no	53 (75)	4.64	-	-	-	-
24	no	270 (85)	0.10	-	-	-	-
25	no	260 (80)	0.20	-	-	-	-
48	no	4 (71)	1.20	-	-	-	-
65	no	256 (82)	0.11	-	-	-	-
83	no	22 (82)	0.00	-	-	-	-
84	no	157 (88)	0.03	-	-	-	-
85	no	40 (73)	0.02	-	-	-	-

Abbreviations: UPN, uniform patient number; MACS, magnetic-activated cell sorting; FACS, fluorescence-activated cell sorting; WBC, white blood cell counts; LPCs, leukemic progenitor cells; n.a., not available.

Supplemental Table S10: AML-associated HLA class I targets

Protein	Sequence	Peptide length	HLA restriction	Allotype-specific representation frequency in AML cohort	Representation frequency in AML cohort	Representation frequency in LPC_{enr} cohort
All HLA ligands						
BC11A	RFPPTPPLF	9	A*23, A*24, A*32, C*04, C*07, C*08, C*14	-	21%	10%
HLA-A*01						
ARP2	DIDTRSEFY	9	A*01	57%	17%	20%
MYNN	FSEYFGAIY	9	A*01	50%	15%	10%
THMS2	LTDTFYYRL	9	A*01, C*04, C*07	50%	15%	0%
OSTF1	GLDKAGSTALY	11	A*01	43%	13%	10%
RTN4	ISEELVQKY	9	A*01	43%	13%	0%
CEBPA	YLDGRLEPLY	10	A*01	43%	13%	20%
EDC4	AADLNLVLY	9	A*01	36%	11%	0%
CSPG2	ETELKTTDY	9	A*01	36%	11%	10%
ANXA1	LADSDARALY	10	A*01	36%	11%	0%
RSSA	NLDFQMEQY	9	A*01	36%	11%	10%
ABCBA	VLDQGKITEY	10	A*01	36%	11%	10%
PSME3	YLDQISRYY	9	A*01	36%	11%	10%
H2B1A, H2B1L, H2B1B	ASEASRLAHY	10	A*01	29%	9%	10%
NISCH	DLDRVLMGY	9	A*01	29%	9%	0%
TBCEL	DSERFFIRY	9	A*01	29%	9%	20%
PPID	ELDPSNTKALY	11	A*01	29%	9%	0%
ZN653	ELDPTFGLY	9	A*01	29%	9%	10%
ZFP14	FLDPAQRDLY	10	A*01	29%	9%	10%
S352B	FSAPELQFY	9	A*01	29%	9%	10%
IDS	FSDIHAGELYF	11	A*01	29%	9%	10%
NSD3	HSDPMFSSY	9	A*01	29%	9%	10%
NUCL	IDGRSISLYY	10	A*01	29%	9%	0%
ZPR1	IMDDPAGNSY	10	A*01	29%	9%	0%
TCPG	ISDLAQHY	8	A*01	29%	9%	10%
KDM2A	ISDLSINSLY	10	A*01	29%	9%	10%
ACLY	ISEQTGKELLY	11	A*01	29%	9%	0%
IPP2, IPP2L	KIDEPSTPY	9	A*01	29%	9%	0%
ANXA2	LIDQDARDLY	10	A*01	29%	9%	0%
LA	LLILFKDDY	9	A*01	29%	9%	10%
FABP5	LVDSKGFDEY	10	A*01	29%	9%	10%
RN135	NLEEGKLAFY	10	A*01	29%	9%	0%
STXB5, STB5L	PTEIQRLTY	9	A*01	29%	9%	10%
TBB2A, TBB2B, TBB4, and others	QLERINVYY	9	A*01, B*15	29%	11%	10%
OAZ2	RDPSLSALIY	10	A*01	29%	9%	10%
RINI	RLEKLQLEY	9	A*01	29%	9%	10%
CASP3	SLDNSYKMDY	10	A*01	29%	9%	0%
SYQ	TIDKATGILLY	11	A*01	29%	9%	10%
DDX6L	TTDIIEKY	8	A*01	29%	9%	10%
CE192	VLDFGDLTY	9	A*01	29%	9%	0%
RN125	VLDRSLLEY	9	A*01	29%	9%	10%
KI18B	VLDSFLQGY	9	A*01	29%	9%	10%
PSB8	VSDLLHQY	8	A*01	29%	9%	10%
OTUD4	VSESHGQLSY	10	A*01	29%	9%	0%

Supplemental Table S10 continued

Protein	Sequence	Peptide length	HLA restriction	Allotype-specific representation frequency in AML cohort	Representation frequency in AML cohort	Representation frequency in LPC_{enr} cohort
UN13D	VTEASELLRY	10	A*01	29%	9%	10%
6PGD	WTAISALEY	9	A*01	29%	9%	10%
DHB4	YTELEAIMYA	10	A*01	29%	9%	0%
OSBL2	YTGTPDWLY	9	A*01	29%	9%	0%
HMCS1	YVDQAELEKY	10	A*01	29%	9%	0%
HLA-A*02						
U520	GLIEIISNA	9	A*02	30%	15%	0%
SPAST	RLSDFTESL	9	A*02	30%	15%	0%
CCNA1	SLLEADPFL	9	A*02	30%	15%	10%
ERGI3	AIIGGMFTV	9	A*02	26%	13%	0%
STT3A	FLAEEGFYKF	10	A*02	26%	13%	0%
DOCK8	IILDALPQL	9	A*02	26%	13%	10%
MTDC	ILADIVISA	9	A*02	26%	13%	0%
CP058	ILNDVAMFL	9	A*02	26%	13%	10%
TLR7	VLAELVAKL	9	A*02	26%	13%	0%
ATF6B	YLQGLEARL	9	A*02	26%	13%	0%
TM147	ALSTLALYV	9	A*02	22%	11%	0%
MED18	FLDHEMVFL	9	A*02	22%	11%	0%
PARVG	FLHLKEFYL	9	A*02	22%	11%	0%
IRAK3	FLSELEVLL	9	A*02	22%	11%	0%
DDX18	FQGASNLTL	9	A*02, B*15	22%	15%	0%
FLNB	GLAPLEVRV	9	A*02	22%	11%	0%
EMC1	GLDIYQTRV	9	A*02	22%	11%	0%
FRYL	GLDNETHFL	9	A*02	22%	11%	0%
TBCD5	GLVDYIFVA	9	A*02	22%	11%	0%
PCX3	GVLENIFGV	9	A*02	22%	11%	0%
BI1	ILMSALSLL	9	A*02	22%	11%	0%
AR6P6	ILNGIVAAL	9	A*02	22%	11%	0%
TM223	KLFDNTVGA	9	A*02	22%	11%	0%
MED24	KLGEILANL	9	A*02	22%	11%	0%
WDFY4	SLASHIQSL	9	A*02	22%	11%	0%
CLM6	VLLELPLLL	9	A*02	22%	11%	10%
TYOBP	VMGDLVLTV	9	A*02	22%	11%	0%
TOP1	YLDPRITVA	9	A*02	22%	11%	0%
HLA-B*07						
STT3B	APESKHKSSL	10	B*07	58%	15%	20%
IRF7	APGLHLEL	8	B*07	50%	13%	10%
OST48	APTIVGKSSL	10	B*07	50%	13%	10%
SNX19	GVASGRLHL	9	B*07, C*07	50%	13%	0%
AFF1	APAQPPSQTF	10	B*07	42%	11%	10%
HDAC6	APQPAKPRL	9	B*07	42%	11%	20%
PPM1G	APRLPLPYGF	10	B*07	42%	11%	0%
IST1	APRLQSEV	8	B*07	42%	11%	10%
CHCH2, CHCH9	APRQPGLMAQ	10	B*07	42%	11%	10%
TLE1, TLE2, TLE4	APTPRIKAEL	10	B*07, B*08	42%	17%	10%
DEFM	APVERAQL	8	B*07	42%	11%	10%
CAP7	FPRFVNVTV	9	B*07, B*51	42%	13%	10%
SHPS1	GPAPGRLGP	9	B*07	42%	11%	0%

Supplemental Table S10 continued

Protein	Sequence	Peptide length	HLA restriction	Allotype-specific representation frequency in AML cohort	Representation frequency in AML cohort	Representation frequency in LPC_{enr} cohort
ASC	IPRGALLSM	9	B*07	42%	11%	0%
ELF4	KPKIQHVGL	9	B*07	42%	11%	20%
SMC1A	KPTDEKLREL	10	B*07	42%	11%	10%
LPPR3	LPRASAPSL	9	B*07, B*51	42%	13%	0%
IF4G1	RPIDTSRLTKI	11	B*07	42%	11%	0%
LIMS1, LIMS2	RPIEGRVV	8	B*07	42%	11%	10%
CTU1	RPLSGQAL	8	B*07	42%	11%	10%
UBE4B	SPIGASGVAH	10	B*07	42%	11%	10%
IFFO1	SPIRPLGL	8	B*07	42%	11%	0%
NEP1	SPLNRAGL	8	B*07	42%	11%	10%
PRI2	SPSLSGLKL	9	B*07	42%	11%	0%
RPN2	TPHQTFVRL	9	B*07	42%	11%	10%
GWL	VPKPPSIEEF	10	B*07	42%	11%	10%
GDIR2	APGPITMDL	9	B*07	33%	9%	0%
ML12A, ML12B, MYL9	APIDKKGNF	9	B*07	33%	9%	10%
CDC7	APRAGTPGF	9	B*07	33%	9%	10%
PAF15	APRKVLGSSTSA	12	B*07	33%	9%	10%
CPXM1	APRNSVLGL	9	B*07	33%	9%	10%
KMT2B	APSSLRSAL	9	B*07	33%	9%	0%
ACTN4	APYKNVNVQNF	11	B*07	33%	9%	0%
DHX9	GPDHNRSFI	9	B*07	33%	9%	10%
SUSD1	GPISSYQVL	9	B*07	33%	9%	10%
RNZ2	GPLKGIEL	8	B*07	33%	9%	0%
CD34	GPRMPRGWTAL	11	B*07	33%	9%	10%
ITA5	GPRRRPPLLPL	11	B*07	33%	9%	10%
MO4L1, MO4L2	IPEELKPWL	9	B*07	33%	9%	10%
M18BP	IPIKNGSLL	9	B*07	33%	9%	10%
DEN1C	KPGAPLQAF	9	B*07	33%	9%	0%
SPB10	KPKAVGLQL	9	B*07	33%	9%	0%
CSPG2	KPRYEINSL	9	B*07	33%	9%	0%
TF2H3	LPDQDQRSQL	10	B*07	33%	9%	10%
PERM	QPVAATRTAV	10	B*07, B*35	33%	11%	10%
ZC3H3	RPAVGHSGL	9	B*07	33%	9%	10%
NSD2	RPKTSTTL	8	B*07	33%	9%	0%
M3K8	RPQESGILL	9	B*07	33%	9%	0%
TDT	RPRQTGALM	9	B*07	33%	9%	10%
DYR1A	RPVAANTL	8	B*07	33%	9%	0%
ITAX	RPVLWVGV	8	B*07	33%	9%	0%
WDR76	SPANPAHIL	9	B*07	33%	9%	10%
SNX17	SPDATRESM	9	B*07	33%	9%	10%
CDAN1	SPGAVRALL	9	B*07	33%	9%	0%
YS060	SPGGAHSNL	9	B*07	33%	9%	20%
HERC5	SPGRLAVL	8	B*07	33%	9%	0%
UBP22	SPHIPYKLL	9	B*07	33%	9%	10%
RRP12	SPQGPGALF	9	B*07	33%	9%	0%
NIPBL	SPSKDSTKLTL	11	B*07	33%	9%	10%
KCT2	SPSTAKDTL	9	B*07	33%	9%	10%
TMM71	TPVASSSRL	9	B*07	33%	9%	10%
IDD	VPKADSGAFL	10	B*07	33%	9%	10%
DOCK8	VPKSGAPTAL	10	B*07	33%	9%	0%

Supplemental Table S10 continued

Protein	Sequence	Peptide length	HLA restriction	Allotype-specific representation frequency in AML cohort	Representation frequency in AML cohort	Representation frequency in LPC_{enr} cohort
RAN	VPNWHRDL	8	B*07	33%	9%	0%
CCDB1	APAAAVPTL	9	B*07	25%	6%	0%
RL8	APAGRKVGLIA	11	B*07	25%	6%	0%
ECM29	APAIGRYIRTL	11	B*07	25%	6%	10%
ANR11	APARPLSTNL	10	B*07	25%	6%	0%
SKAP2	APDKRIYQF	9	B*07	25%	6%	10%
WASP	APGGGRGALL	10	B*07	25%	6%	0%
CQ062	APGIRSWSL	9	B*07	25%	6%	0%
TRM7	APGSWSQVL	9	B*07	25%	6%	10%
PA24D	APGVRLQL	8	B*07	25%	6%	0%
LMA2L	APLPPLSGL	9	B*07	25%	6%	0%
BFAR	APNTGRANQQM	11	B*07	25%	6%	10%
DDX51	APQYLRTYV	9	B*07	25%	6%	10%
CPNE1	APREALAQTV	10	B*07	25%	6%	10%
K1211	APREEQQRSL	10	B*07	25%	6%	10%
ZN185	APREHSYVL	9	B*07	25%	6%	10%
OAS1	APRWGNPRAL	10	B*07	25%	6%	10%
DOP2	APSFRAGAQL	10	B*07	25%	6%	0%
DOK1	APSSAAWVQTL	11	B*07	25%	6%	10%
TNR1B	APVAVWAAL	9	B*07	25%	6%	0%
ARRD1	APVSPRPGL	9	B*07	25%	6%	10%
VPS16	APYGGPIAL	9	B*07	25%	6%	10%
TM102	APYLLRTL	8	B*07	25%	6%	10%
CLC11	APYNWPVWL	9	B*07	25%	6%	10%
GEN	FPDSTKSSL	9	B*07	25%	6%	10%
H2AY	FPKQTAAQL	9	B*07	25%	6%	0%
AAAS	FPRFSPVL	8	B*07	25%	6%	10%
MADD	FPRPVVAF	8	B*07, B*35	25%	9%	20%
NOB1	GAFLRHAAL	9	B*07	25%	6%	0%
DPOD4	GPAGHSKGEL	10	B*07	25%	6%	0%
ANR63	GPGSGRLGL	9	B*07	25%	6%	20%
IRAK1	GPGSRPTAV	9	B*07	25%	6%	10%
FES	GPLSKLSLL	9	B*07	25%	6%	10%
RARA	GYPVPPYAFF	10	B*07, A*24	25%	9%	10%
GUAA	HPFPGPGL	8	B*07	25%	6%	0%
KLDC2	HPRGWNDHV	9	B*07	25%	6%	10%
S38AA	HPRPQAVL	8	B*07	25%	6%	0%
KYNU	HPTDERVAL	9	B*07	25%	6%	10%
UBP4	IPAERETRL	9	B*07	25%	6%	10%
PRP19	IPAILKAL	8	B*07	25%	6%	10%
HMDH	IPAYKLETL	9	B*07	25%	6%	0%
FA65B	IPEFHKKLSL	10	B*07	25%	6%	0%
AGAP3	IPIKQGILL	9	B*07	25%	6%	0%
DOCK2	IPLKASVL	8	B*07, B*08, B*35, B*51	25%	13%	0%
DNS2A	IPLLLAAL	8	B*07	25%	6%	0%
SYMPK	IPRRQEHDISL	11	B*07	25%	6%	0%
TET3	IPRSLGDTL	9	B*07	25%	6%	10%
KDM5B	IPVHLNSL	8	B*07	25%	6%	10%
CH059	KAKPVTTNL	9	B*07, B*57	25%	11%	10%
TYSY	KPGDFIHTL	9	B*07	25%	6%	0%

Supplemental Table S10 continued

Protein	Sequence	Peptide length	HLA restriction	Allotype-specific representation frequency in AML cohort	Representation frequency in AML cohort	Representation frequency in LPC_{enr} cohort
RL8	KPGDRGKL	8	B*07	25%	6%	10%
VP13B	KPIGGAAEL	9	B*07	25%	6%	0%
STXB3	KPKDKVSLI	9	B*07	25%	6%	0%
GBP4, GBP6	KPNHTLVLL	9	B*07	25%	6%	10%
SAC31	KPRPPPSQL	9	B*07	25%	6%	10%
KI18A	KPSSFTTSF	9	B*07	25%	6%	0%
RPC5	KPVAPSNVL	9	B*07	25%	6%	0%
OAS2	LPAPSWNVL	9	B*07, B*35	25%	9%	0%
MA2C1	LPKPGGAHSL	10	B*07	25%	6%	10%
RBP10	LPKQPPLML	9	B*07	25%	6%	0%
TGIF2	LPRGSSPSV	9	B*07, B*51	25%	9%	0%
OSCAR	LPRPSLVAL	9	B*07, B*08, B*35	25%	11%	0%
CSPG2	LPRSPASVFM	10	B*07	25%	6%	0%
SMHD1	LPSSHVARL	9	B*07	25%	6%	0%
MSLN	LPTARPLL	8	B*07	25%	6%	10%
TLR2	MPHTLWMVW	9	B*07	25%	6%	0%
PSF3	MPRLGAFFL	9	B*07	25%	6%	10%
IRF5	NPAGFRELL	9	B*07	25%	6%	0%
DJC13	NPQLPRLYL	9	B*07	25%	6%	0%
TROAP	QPRNPLEEL	9	B*07	25%	6%	0%
VILL	QPVDPKRHGQL	11	B*07	25%	6%	0%
UHRF1	RPASGSPFQLF	11	B*07	25%	6%	0%
MYD88	RPGASVGRLL	10	B*07	25%	6%	0%
S38AA	RPGQAQAL	8	B*07	25%	6%	0%
LYL1	RPIKMEQTAL	10	B*07	25%	6%	10%
PSA1	RPLPVSRLVSL	11	B*07	25%	6%	0%
PGAM5	RPNGRVAL	8	B*07	25%	6%	10%
CS024	RPPGASGSAL	10	B*07	25%	6%	10%
PER1	RPRLPATGTF	10	B*07	25%	6%	10%
SNX20	RPTPRGITL	9	B*07	25%	6%	0%
CREG1	SARALLAAL	9	B*07	25%	6%	0%
CTF18	SPAARNPVL	9	B*07	25%	6%	10%
IQGA2	SPAIGLNNL	9	B*07	25%	6%	0%
K1731	SPAIGRTSIL	10	B*07	25%	6%	10%
GEN	SPAIQRNTF	9	B*07	25%	6%	0%
SP2	SPASRAPHL	9	B*07	25%	6%	10%
WDR34	SPFHRNLFL	9	B*07	25%	6%	10%
TENS3	SPHSGSTISI	10	B*07	25%	6%	0%
FBX7	SPKGRFVML	9	B*07	25%	6%	0%
NMD3	SPKLAQSL	8	B*07	25%	6%	0%
CARD9	SPKQPFAAL	9	B*07	25%	6%	0%
UBR4	SPNPSLLHL	9	B*07	25%	6%	0%
NOXIN	SPNRSTNTL	9	B*07	25%	6%	10%
FANCA	SPPAGRSLEL	10	B*07	25%	6%	0%
FBRS	SPPDPWGRL	9	B*07	25%	6%	0%
CENPF	SPRLAAQKL	9	B*07	25%	6%	10%
CK5P3	SPRYVDRVTEF	11	B*07	25%	6%	0%
BMI1	SPSGNHQSSF	10	B*07	25%	6%	0%
HTR5B	SPSHIATKTRL	11	B*07	25%	6%	10%
BEST1	SPTNIHTTL	9	B*07	25%	6%	0%

Supplemental Table S10 continued

Protein	Sequence	Peptide length	HLA restriction	Allotype-specific representation frequency in AML cohort	Representation frequency in AML cohort	Representation frequency in LPC_{enr} cohort
TLE3	SPTPRIKAEL	10	B*07, B*08	25%	13%	0%
ADRM1	SPTQPIQL	8	B*07	25%	6%	0%
ANLN	SPVKSTTSI	9	B*07	25%	6%	10%
TF7L2	SPYLPNGSL	9	B*07	25%	6%	0%
SWAP1	TPGSGKTAL	9	B*07	25%	6%	0%
INCE	TPQGHRAPP	9	B*07	25%	6%	10%
PTN7	TPREVTLHFL	10	B*07	25%	6%	0%
ARGAL	TPRGHPDRLSL	11	B*07	25%	6%	0%
TLE4	TPSSKSKEL	9	B*07	25%	6%	10%
TLE4	TPSSKSKELSL	11	B*07	25%	6%	0%
U520	VPIPVKESI	9	B*07	25%	6%	0%
PPIA, PPID, PPIF	VPKTAENFRAL	11	B*07	25%	6%	0%
MED23	VPQESRFNL	9	B*07	25%	6%	0%
TMED3	VPRSASVLLLL	11	B*07	25%	6%	10%
PTN6	VPSEPGGVL	9	B*07	25%	6%	10%
KDM4C	VPSGERNSF	9	B*07	25%	6%	0%
CPSF2	VPSPKVVL	8	B*07, B*08	25%	13%	10%
BIRC1	WPRESAVGV	9	B*07, B*51	25%	9%	0%
GLE1	WPYGNRQEI	9	B*07, B*51	25%	13%	10%
MED14	YPAPGLKTFL	10	B*07	25%	6%	10%
ARI1	YPNSYFTGL	9	B*07	25%	6%	10%
CLCN7	YPRFPPIQSI	10	B*07, B*51	25%	11%	10%
HLA-B*08						
ABCF2	DLDTRVAL	8	B*08	55%	13%	10%
CFAD	HSWERLAVL	9	B*08, C*07	55%	13%	0%
PLRG1	AGKTRVTL	8	B*08	45%	11%	0%
TLE1, TLE2, TLE4	APTPRIKAEL	10	B*08, B*07	45%	17%	10%
SRP14	DGKKKISTV	9	B*08	45%	11%	10%
TEX2	DLGLKTSSL	9	B*08	45%	11%	0%
NCF2	DLKEALIQL	9	B*08	45%	11%	0%
GTF2I	DLRKQVEEL	9	B*08	45%	11%	0%
CEP85	DVIQKGSSL	9	B*08	45%	11%	0%
SF3A3	EGYGRYLDL	9	B*08, B*14	45%	15%	10%
ASAP1	EIFQKSSQL	9	B*08	45%	11%	0%
CNDG2	HGTIKNQL	8	B*08	45%	11%	10%
T3JAM	QSTQRSLAL	9	B*08	45%	11%	0%
ACSL1	SGIIRNNSL	9	B*08	45%	11%	10%
ALDOA	SIAKRLQSI	9	B*08	45%	11%	10%
TLE3	SPTPRIKAEL	10	B*08, B*07	45%	13%	0%
TTC7A	TLKSKQDEL	9	B*08	45%	11%	10%
CX021	TSIKEKSSL	9	B*08	45%	11%	0%
EVI2A	VLANKVSSL	9	B*08	45%	11%	0%
CPSF2	VPSPKVVL	8	B*08, B*07	45%	13%	10%
MTMRE	DGLIHTSL	8	B*08	36%	9%	0%
KNTC1	DGNIKTAL	8	B*08	36%	9%	10%
WDR3	DGSIRIFSL	9	B*08, B*14	36%	13%	0%
PTN6	DIENRVLEL	9	B*08	36%	9%	10%
STK3, STK4, TAOK1, TAOK3, SLK, STK39	DIKAGNIL	8	B*08	36%	9%	0%

Supplemental Table S10 continued

Protein	Sequence	Peptide length	HLA restriction	Allotype-specific representation frequency in AML cohort	Representation frequency in AML cohort	Representation frequency in LPC_{enr} cohort
RUFY1	DIKEVNQAL	9	B*08	36%	9%	10%
USF1	DLKNKNLLL	9	B*08	36%	9%	0%
PLSL	DPKISTSL	8	B*08	36%	9%	0%
PRP8	DPNMKYEL	8	B*08	36%	9%	10%
MYOF	DPYIKITL	8	B*08	36%	9%	10%
VRK3	DVSPKHVL	8	B*08	36%	9%	0%
SP16H	EGIVKQDSL	9	B*08	36%	9%	0%
SF3B1	EIQGKKAAL	9	B*08	36%	9%	0%
GRB2	EMKPHPWFF	9	B*08	36%	9%	0%
ADDA	EQKKRVSMI	9	B*08	36%	9%	0%
VP13C	FNLSRIVTL	9	B*08	36%	9%	0%
PSA5	LIILKQVM	8	B*08	36%	9%	0%
RCOR1	NIKQTNSAL	9	B*08	36%	9%	0%
KLH24	NIWIRVASL	9	B*08	36%	9%	0%
CY24B	NLKLKKIYF	9	B*08	36%	9%	0%
AT5G1, AT5G2, AT5G3	NPSLKQQL	8	B*08	36%	9%	10%
STAG1, STAG2	RFKDRIVSM	9	B*08	36%	9%	0%
AEBP2	SGKIKLLL	8	B*08	36%	9%	0%
NUCB2	TNKDRLVTL	9	B*08	36%	9%	20%
DMXL2	WVLLRSIDL	9	B*08	36%	9%	0%
PLEC	AALQRQLL	8	B*08	27%	6%	0%
NOL11	ALKKKDVQL	9	B*08	27%	6%	0%
STA5A, STA5B	ALQQKQVSL	9	B*08	27%	6%	0%
HMMR	ALREKTSL	8	B*08	27%	6%	10%
PIPSL, PSMD4	DALLKMTI	8	B*08	27%	6%	0%
RLP24	DAMKRVEEI	9	B*08	27%	6%	0%
PRP19	DATIRIWSV	9	B*08	27%	6%	0%
RAB44	DFRVKTLL	8	B*08	27%	6%	0%
M3K2, M3K3, M4K1, M4K3, M4K5, M4K2	DIKGANIL	8	B*08	27%	6%	10%
PTN2	DINIKQVL	8	B*08	27%	6%	10%
MAML1	DINIKTEF	8	B*08	27%	6%	0%
PR40A	DIRFTNML	8	B*08	27%	6%	0%
2AAA	DITTKHML	8	B*08	27%	6%	0%
ANKY2	DIYEKQQL	8	B*08	27%	6%	10%
H2AY	DKKLKSIAF	9	B*08	27%	6%	10%
ARH40	DLDVKQISL	9	B*08	27%	6%	20%
CNOT4	DLIEKELSV	9	B*08	27%	6%	0%
CSPG2	DLKETTVL	8	B*08	27%	6%	10%
PPID	DLKKAQGI	8	B*08	27%	6%	0%
NRBF2	DLKRHVEFL	9	B*08	27%	6%	0%
FBSL	DLLEKTRL	8	B*08	27%	6%	10%
CCD77	DLLKKLEL	8	B*08	27%	6%	10%
TBB1, TBB2A, TBB2B, TBB3, and others	DLRKLAVNM	9	B*08	27%	6%	0%
KMT2A	DLVSKSSSL	9	B*08	27%	6%	0%
CCD22	DMKTLGVSF	9	B*08	27%	6%	0%
GRN	DPALRQLL	8	B*08	27%	6%	0%
ABHD2	DPLVHESL	8	B*08	27%	6%	10%
DYHC1	DPQVHTVL	8	B*08	27%	6%	0%

Supplemental Table S10 continued

Protein	Sequence	Peptide length	HLA restriction	Allotype-specific representation frequency in AML cohort	Representation frequency in AML cohort	Representation frequency in LPC_{enr} cohort
CECR1	DSLLRNFTL	9	B*08, B*14	27%	9%	0%
TYDP1	DVIHKHDL	8	B*08	27%	6%	10%
HEAT6	DVNVRVSSL	9	B*08	27%	6%	10%
MCM2	EAHARIHL	8	B*08	27%	6%	0%
SMC1A	EASKRAATL	9	B*08	27%	6%	10%
1A01, 1A02, 1A03, 1A11, and others	EGLPKPLTL	9	B*08	27%	6%	0%
BAZ1B	EHKKRWASM	9	B*08	27%	6%	0%
MEFV	EIKQKIQLL	9	B*08	27%	6%	10%
DPOE1	EIKSKLASL	9	B*08	27%	6%	0%
NUCB2	ELKKKADEL	9	B*08	27%	6%	0%
TRI38	ELKSHILEL	9	B*08	27%	6%	10%
CENPF	ELNERVAAL	9	B*08	27%	6%	0%
MACOI	ELRSQISSL	9	B*08	27%	6%	0%
EMB	ETKLKITQL	9	B*08	27%	6%	0%
ZNT6	FGFERLEVL	9	B*08	27%	6%	0%
MIER1	FGKKKYNL	8	B*08	27%	6%	0%
TM189	FGLPRWVTL	9	B*08	27%	6%	0%
VPP3	FLAQHTML	8	B*08	27%	6%	0%
CPSF2	FNHKREIHL	9	B*08	27%	6%	0%
VATH	FNWIKTQL	8	B*08	27%	6%	0%
DOK1	FPKGSWTL	8	B*08	27%	6%	0%
TPR	FTRTKEEL	8	B*08	27%	6%	0%
MO4L1, MO4L2	FVRIGAML	8	B*08, B*07	27%	9%	0%
ZN609	GLKEREAAL	9	B*08	27%	6%	0%
RHG04	GPLRKSSL	8	B*08	27%	6%	10%
MAX	HIKDSFHSL	9	B*08	27%	6%	0%
SC31A	HLILKTTF	8	B*08	27%	6%	10%
GRP2	HLKDLVAL	8	B*08	27%	6%	0%
COMD9	HQNLKNLL	8	B*08	27%	6%	0%
TPR	IGRLKAEI	8	B*08	27%	6%	0%
O51G2	IIKTERSL	8	B*08	27%	6%	10%
ZN106	ILKTSREL	8	B*08	27%	6%	10%
TLR8	IPHVKYLDL	9	B*08, B*07	27%	9%	0%
VATE1	KIKVSNTL	8	B*08	27%	6%	0%
ARFG1	LFRDKVVAL	9	B*08	27%	6%	0%
PARP4	LGNVRPLL	8	B*08	27%	6%	10%
NEK6	LLDRKTVAL	9	B*08	27%	6%	0%
GCC1, NIN, WWC3	LLKEKEAL	8	B*08	27%	6%	0%
DYN2	LPALRSKL	8	B*08	27%	6%	0%
PCNA	MGHLKYYL	8	B*08	27%	6%	10%
IREB2	MGNKRWNSL	9	B*08	27%	6%	0%
AHNK	MPKIKMPKISM	11	B*08	27%	6%	0%
AHNK	MPKMKMPTF	9	B*08, B*35, C*12	27%	13%	0%
AHNK	MPKVKMPKFSM	11	B*08	27%	6%	0%
MNDA	MPSLKNLV	8	B*08	27%	6%	0%
KPCD	MVEKRVLTL	9	B*08	27%	6%	0%
NCOA2, NCOA3	NALLRYLL	8	B*08	27%	6%	0%
KDM4A, KDM4B, KDM4C	NIQKKAMTV	9	B*08	27%	6%	0%

Supplemental Table S10 continued

Protein	Sequence	Peptide length	HLA restriction	Allotype-specific representation frequency in AML cohort	Representation frequency in AML cohort	Representation frequency in LPC_{enr} cohort
RBM18	NLDPKITEY	9	B*08	27%	6%	0%
CHM1B	NLKFAAKEL	9	B*08	27%	6%	0%
HNRH3, HNRPF	NMQHRYIEL	9	B*08	27%	6%	0%
EMIL2	QGVQREVSM	9	B*08	27%	6%	0%
PIEZ1	QRMNFLVTL	9	B*08	27%	6%	0%
CEBPA	RLRKRVEQL	9	B*08	27%	6%	0%
FND3B	RPKHKEVHL	9	B*08	27%	6%	0%
PP4R1	SAALRASSL	9	B*08	27%	6%	0%
KDM3A	SGFLRNLL	8	B*08	27%	6%	0%
HXK1	SGKKRTVEM	9	B*08	27%	6%	0%
VPRBP	SPAIKKQL	8	B*08	27%	6%	10%
GAN	SPYIRTKL	8	B*08	27%	6%	0%
CCNH	SQKRHWTF	8	B*08	27%	6%	0%
TLE4	SSKSKELSL	9	B*08	27%	6%	0%
RSMB, RSMN	TGIARVPL	8	B*08	27%	6%	0%
2AAA	TIIPKVLAM	9	B*08	27%	6%	0%
TBA1B	TIKTKRSI	8	B*08	27%	6%	10%
NUDC1	VAKQQVASL	9	B*08	27%	6%	0%
OSB11	VGHSKLQSL	9	B*08	27%	6%	0%
THA11	VIRKKHGM	8	B*08	27%	6%	0%
KTN1	VLKEKENEL	9	B*08	27%	6%	0%
SNX1	VNHRKELAL	9	B*08	27%	6%	0%
MTMR6	VPNSHWQL	8	B*08	27%	6%	0%
KTN1	VPSKRQEAL	9	B*08	27%	6%	10%
TOP1	VPVEKRVF	8	B*08, B*35	27%	9%	0%
TBA1A, TBA1B, TBA1C, and others	VPYPRIHF	8	B*08	27%	6%	0%
BAZ2B	VSNVKPLSL	9	B*08	27%	6%	0%
EMP3	WLKAVQVL	8	B*08	27%	6%	0%
BASI	WLKGGVVL	8	B*08	27%	6%	0%
ZFAN5, ZFAN6	YGNPRTNGM	9	B*08	27%	6%	0%
SMCA2, SMCA4	YIIKDKHIL	9	B*08	27%	6%	0%
S30BP	YIIQRKKEF	9	B*08	27%	6%	0%
MYO1G, MYH6, MYH15, and others	YLLEKSRVI	9	B*08	27%	6%	10%
CHD1L	YMDYRGYSY	9	B*08, C*07	27%	9%	20%
UBQL1, UBQL2	YMRSMMQSL	9	B*08	27%	6%	0%
MNDA	YNRIKITDL	9	B*08	27%	6%	0%
DHX9	YPEVRIVL	8	B*08	27%	6%	0%
MET14	YPKLRELIRL	10	B*08	27%	6%	0%
UNG	YPPPHQVF	8	B*08, B*35	27%	9%	10%
PI4KA	YRLEYMRVL	9	B*08, C*07	27%	11%	10%
HLA-C*07						
RALY	IYSGYIFDY	9	C*07	27%	15%	10%
UBE3B, UBE3C	SRPPLLGF	8	C*07	27%	15%	20%
CSN3	AYHELAQVY	9	C*07, C*14	23%	15%	10%
SNX19	GVASGRLHL	9	C*07, B*07	23%	13%	0%
CFAD	HSWERLAVL	9	C*07, B*08	23%	13%	0%

Supplemental Table S10 continued

Protein	Sequence	Peptide length	HLA restriction	Allotype-specific representation frequency in AML cohort	Representation frequency in AML cohort	Representation frequency in LPC_{enr} cohort
RENT2	KRPPLQEY	8	C*07	23%	13%	10%
TMX2	KRVTWIVEF	9	C*07	23%	13%	10%
THMS2	LTDTFYYRL	9	C*07, C*04, A*01	23%	15%	0%
THOC2	NYPGFLTIL	9	C*07	23%	13%	10%
BC11A	RFPPTPPLF	9	C*07, A*23, A*24, A*32, C*08, C*14, C*04	23%	21%	10%
POMT1	VYYGQYISF	9	C*07, C*14	23%	15%	10%

Panel of naturally presented, AML-associated, HLA class I-restricted peptide targets identified by HLA class I ligandome profiling of primary AML samples of the AML *discovery dataset* (n = 47) with a benign dataset comprising hematological (n = 130) and non-hematological benign tissue and cell samples (n = 202).

Supplemental Table S11: HLA class I and class II peptide and protein identifications of LPC_{enr} and LPC-depleted blast samples

UPN	HLA class I				HLA class II			
	LPCs		Blasts		LPCs		Blasts	
	HLA ligand IDs	Protein IDs	HLA ligand IDs	Protein IDs	HLA peptide IDs	Protein IDs	HLA peptide IDs	Protein IDs
01	7,603	4,307	10,489	5,161	1,458	501	468	189
02	2,437	2,053	6,350	4,000	450	404	4,969	1,496
03	2,407	1,962	6,598	3,809	655	377	5,592	1,372
04	2,191	1,901	1,491	1,455	1,319	638	818	413
05	2,128	1,852	5,948	3,502	1,931	750	2,070	713
06	1,731	1,631	3,090	2,458	1,243	529	1,893	633
07	1,074	1,020	3,096	2,351	512	333	3,136	951
08	930	867	1,151	1,109	1,623	524	2,029	670
09	137	165	5,228	3,245	3,132	830	2,238	725
10	127	233	6,199	3,861	3,656	1,111	10,217	2,008
11	n.a.	n.a.	n.a.	n.a.	6,218	1,500	4,940	1,238

Abbreviations: UPN, uniform patient number; LPCs, leukemic progenitor cells; IDs, identifications; n.a., not available.

Supplemental Table S12: AML-associated HLA class II peptide, protein, and hotspot targets

Protein	Sequence	Peptide length	Frequency on AML	Frequency on LPCs	Peptide target	Protein target	Hotspot target
Peptide targets							
GALT7	**N-acetylgalactosaminyltransferase 7**						
	GNQLFRINEANQLMQ	15	21%	18%	x		x
IL1AP	**Interleukin-1 receptor accessory protein**						
	NGRTFHLTRTLTVK	14	15%	27%	x		x
APOB	**Apolipoprotein B-100**						
	LGQEVALNANTKNQKIR	17	15%	18%	x		x
CLC11	**C-type lectin domain family 11 member A**						
	DRQQMEALTRYLRAAL	16	15%	9%	x		x
RBMX	**RNA-binding motif protein, X chromosome**						
	SSRDYPSSRDTRDYAPPPRDYTY	23	15%	0%	x		x

Supplemental Table S12 continued

Protein	Sequence	Peptide length	Frequency on AML	Frequency on LPCs	Peptide target	Protein target	Hotspot target
Protein targets							
CCL23	**C-C motif chemokine 23**		17%	9%			
	SKPGVIFLTKKGRRF	15	13%	9%		x	
	KPGVIFLTKKGRRF	14	11%	9%		x	
	TEFMMSKLPLENPVL	15	6%	0%		x	
	RVTKDAETEFMMSKLPLENP	20	4%	0%		x	
	TEFMMSKLPLENP	13	4%	0%		x	
	TEFMMSKLPLENPV	14	4%	0%		x	
	DAETEFMMSKLPLENPVLLD	20	2%	0%		x	
RRS1	**Ribosome biogenesis regulatory protein homolog**		15%	0%			
	KKTNLVWDEVSGQWRRRWGYQR	22	11%	0%		x	x
	KKTNLVWDEVSGQWRRRWGYQ	21	9%	0%		x	x
Hotspot targets							
FLT3	**Receptor-type tyrosine-protein kinase FLT3**		19%	0%			
	SPGPFPFIQDNISFYA	16	13%	0%			x
	SPGPFPFIQDNISFY	15	9%	0%			x
	SPGPFPFIQDNISFYAT	17	9%	0%			x
	SPGPFPFIQD	10	6%	0%			x
	SPGPFPFIQDNISF	14	4%	0%			x
IL1AP	**Interleukin-1 receptor accessory protein**		15%	18%			
	LDTMRQIQVFEDEPAR	16	9%	18%			x
	LDTMRQIQVFEDEPA	15	9%	9%			x
	RQIQVFEDEPARIK	14	6%	0%			x
	DTMRQIQVFEDEPAR	15	2%	9%			x
HPRT	**Hypoxanthine-guanine phosphoribosyltransferase**		15%	9%			
	VVGYALDYNEYFR	13	11%	9%			x
	VVGYALDYNEYFRDL	15	9%	9%			x
KIT	**Mast/stem cell growth factor receptor Kit**		15%	9%			
	IGSYIERDVTPAIM	14	13%	9%			x
	IGSYIERDVTPAIME	15	9%	9%			x
	IGSYIERDVTPAIMED	16	6%	9%			x
	IGSYIERDVTPAI	13	4%	0%			x
	IGSYIERDVTPAIMEDD	17	4%	9%			x
	RRSVRIGSYIERDVTPA	17	2%	0%			x
	IERDVTPAIMEDDE	14	2%	9%			x
AP2B1	**AP-2 complex subunit beta**		15%	0%			
	IHTPLMPNQSIDVSLPL	17	11%	0%			x
	TPLMPNQSIDVSLPL	15	9%	0%			x

Panel of naturally presented, AML-associated HLA class II antigens identified by HLA class II ligandome profiling of primary AML samples (n = 47) with a hematological benign (n = 89) and a non-hematological benign (n = 223) dataset. The representation frequencies within the AML *discovery cohort* (n = 47) and the LPC cohort (n = 11) are indicated. Peptides are assigned to the respective group of target antigens (peptide targets, protein targets, and hotspot targets). Abbreviation: LPCs, leukemic progenitor cells.

Supplemental Table S13: LPC-exclusive and -associated HLA class II antigens

Protein	Sequence	Peptide length	Frequency on LPCs	Frequency on AML
LPC-exclusive targets				
Peptide targets				
LTV1	**Protein LTV1 homolog**			
	PHRKKKPFIEKKKAVSFHLVHR	22	27%	0%
LPC-associated targets				
Peptide targets				
IL1AP	**Interleukin-1 receptor accessory protein**			
	NGRTFHLTRTLTVK	14	27%	11%
CTSA	**Lysosomal protective protein**			
	KHLHYWFVESQKDPEN	16	27%	9%
ITGAL	**Integrin alpha-L**			
	ETLHKFASKPASEFVK	16	27%	9%
G6PC3	**Glucose-6-phosphatase 3**			
	ERPEWIHVDSRPF	13	27%	4%
Protein targets				
TACT	**T-cell surface protein tactile**		27%	9%
	DRVKLGTDYRLHLSPV	16	9%	4%
	ITWFIDGSFLHDEK	14	0%	2%
	LHDEKEGIYITNEERK	16	9%	2%
	LHDEKEGIYITNEERKG	17	0%	2%
	HDEKEGIYITNEERK	15	0%	2%
	DEKEGIYITNEERKGKDG	18	9%	2%
G6PC3	**Glucose-6-phosphatase 3**		27%	4%
	ERPEWIHVDSRPF	13	27%	4%
LTV1	**Protein LTV1 homolog**		27%	4%
	PHRKKKPFIEKKKAVSFHLVHR	22	27%	0%
	PHRKKKPFIEKKKAVSF	17	0%	4%

Panel of naturally presented, LPC-exclusive and -associated HLA class II antigens identified by HLA class II ligandome profiling of enriched LPC samples (n = 11) and primary AML samples (n = 47) with a hematological benign (n = 89) and a non-hematological benign (n = 223) dataset. The representation frequencies within the LPC and the AML *discovery cohort* are indicated. Abbreviation: LPCs, leukemic progenitor cells.

Supplemental Figure 1

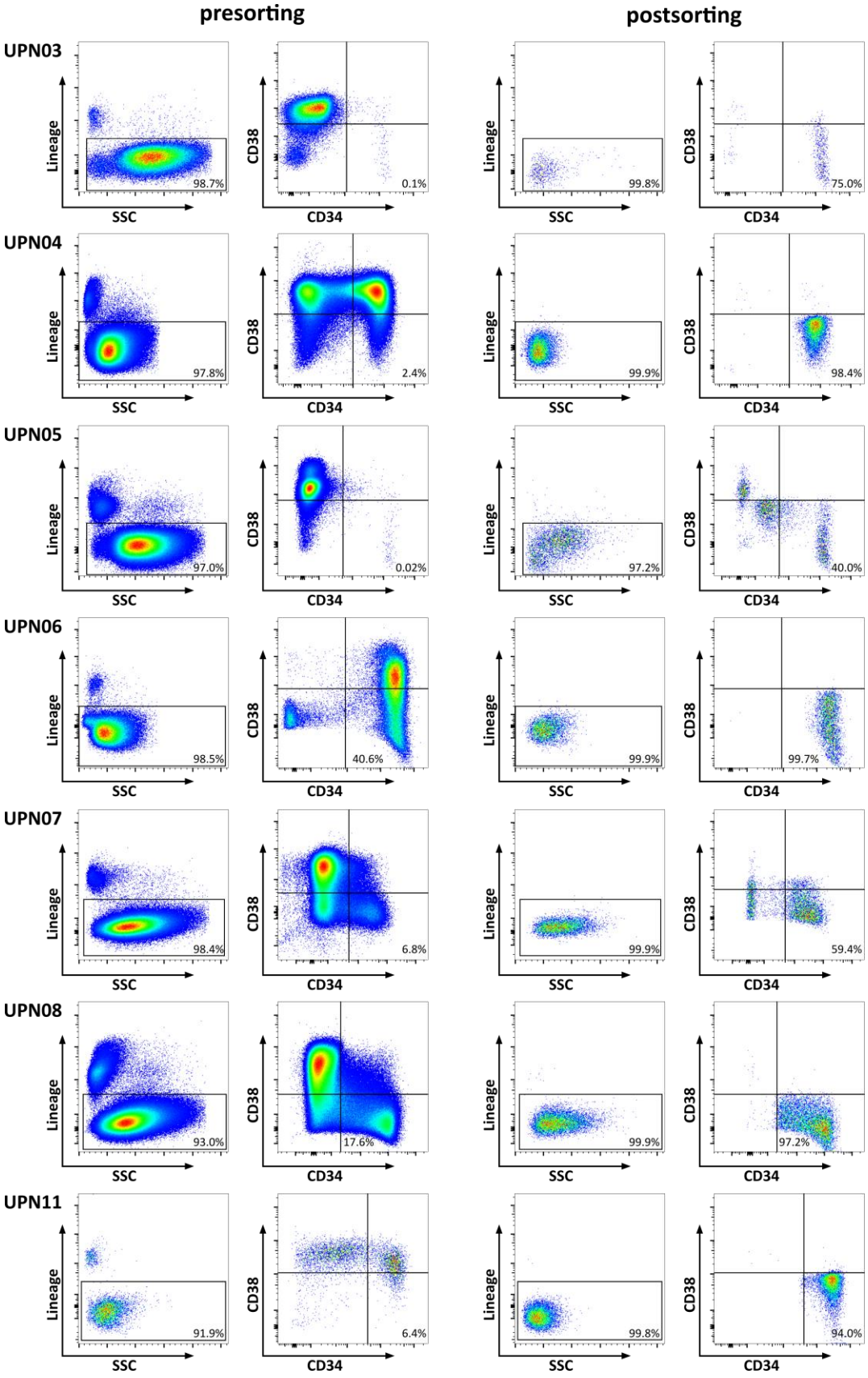

Supplemental Figure S1: FACS enrichment of Lin$^-$CD34$^+$CD38$^-$ LPCs from PBMC samples of AML patients. Flow cytometry analyses of pre- and postenriched LPC frequencies of FACS-sorted samples. Graphs show single, viable cells stained for the lineage markers CD3, CD19, CD20, and CD56 as well as the LPC markers CD34 and CD38. Percentages indicate frequencies within viable cells, respectively. Abbreviations: UPN, uniform patient number; SSC, side scatter.

Supplemental Figure 2

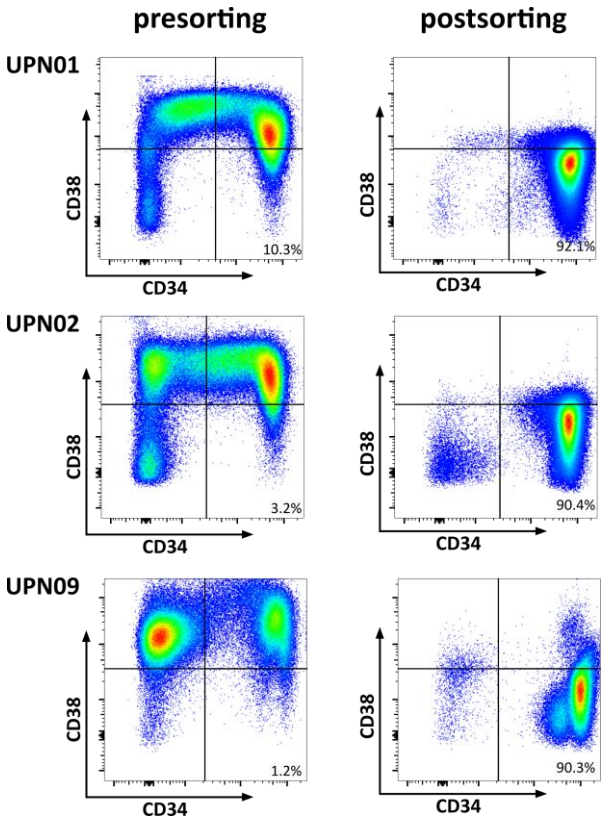

Supplemental Figure S2: MACS enrichment of CD34$^+$CD38$^-$ LPCs from PBMC samples of AML patients. Flow cytometry analyses of pre- and postenriched LPC frequencies of MACS-sorted samples. Graphs show single, viable cells stained for the LPC markers CD34 and CD38. Percentages indicate frequencies within viable cells. Abbreviations: UPN, uniform patient number.

Supplemental Figure 3

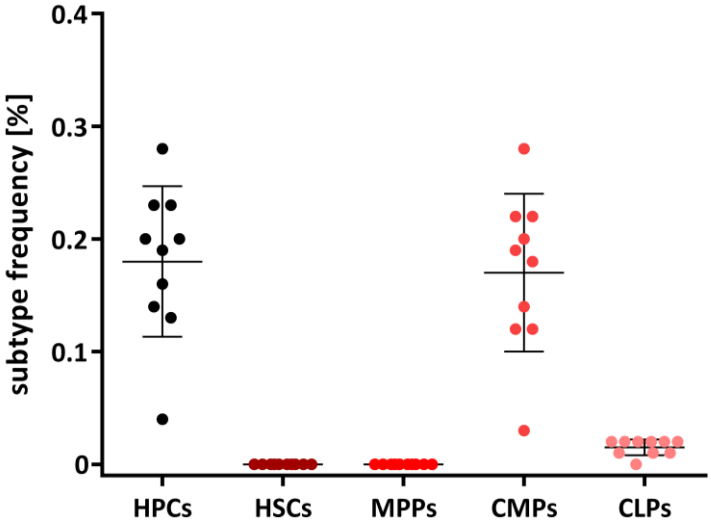

Supplemental Figure S3: Frequencies of CD34$^+$ HPCs and their subtypes in PBMC samples of HVs. Flow cytometry analyses of the frequencies of Lin$^-$CD34$^+$ HPCs and their subtypes (HSCs, MPPs, CMPs, and CLPs) in PBMC samples of HVs (n = 10). Data points represent individual donors. Horizontal lines indicate mean values ± SD. Abbreviations: HPC, CD34$^+$ hematopoietic progenitor; HSCs, CD34$^+$CD38$^-$CD90$^+$ hematopoietic stem cells; MPPs, CD34$^+$CD38$^-$CD90$^-$ multipotent progenitors; CMPs, CD34$^+$CD38$^+$CD117$^+$ common myeloid progenitors; CLPs, CD34$^+$CD38$^+$CD117^{low} common lymphoid progenitors.

Supplemental Figure 4

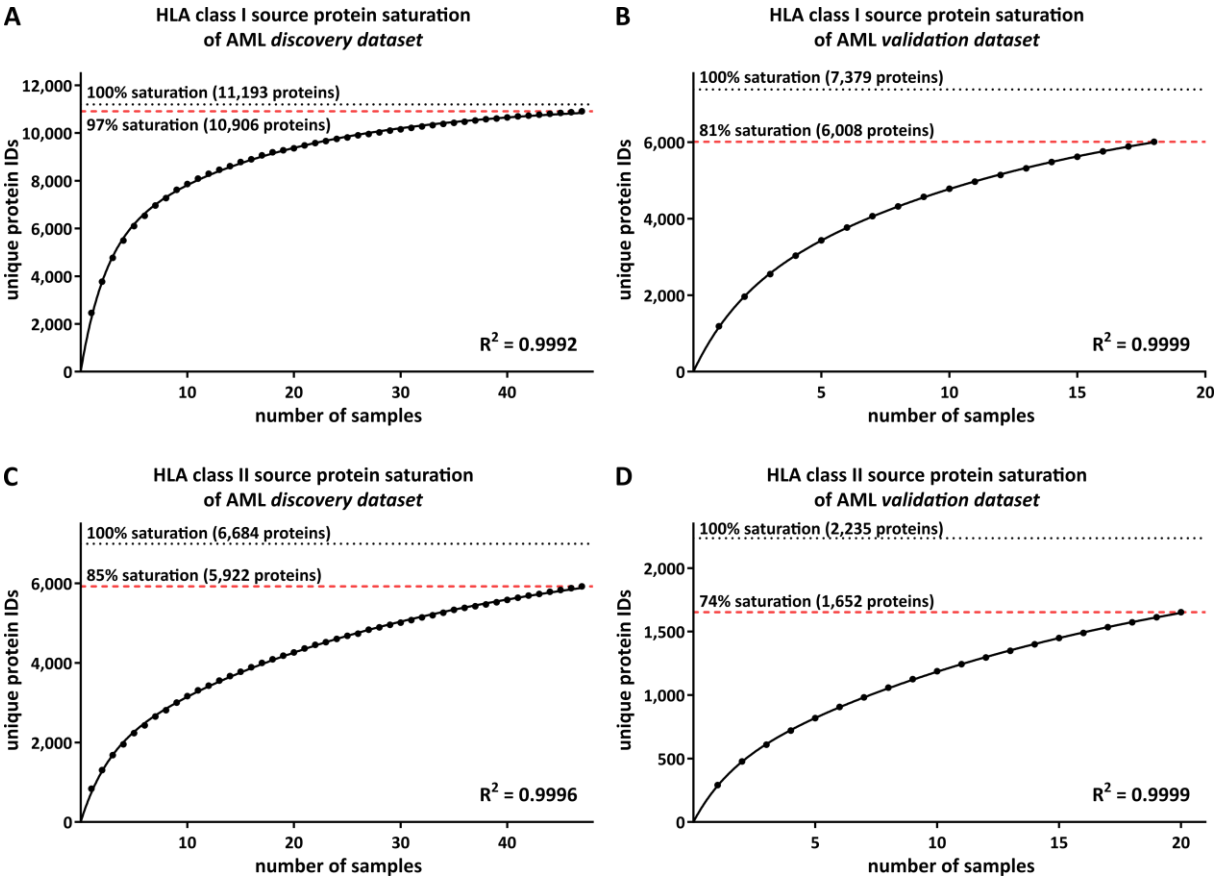

Figure S4: Saturation analysis of HLA peptide source proteins of AML *discovery* and *validation datasets*. Saturation analysis of (A,B) HLA class I and (C,D) HLA class II peptide source proteins of the (A,C) AML *discovery* and the (B,D) AML *validation datasets*. Number of unique HLA ligand source protein identifications shown as function of cumulative HLA ligandome analysis of AML samples (n = 47 for HLA class I *discovery*, n = 18 for HLA class I *validation*, n = 47 for HLA class II *discovery*, n = 20 for HLA class II *validation*). Exponential regression allowed for the robust calculation (R^2 = 0.9992 to R^2 = 0.9999) of the maximum attainable number of different source protein identifications (dotted line). The dashed red lines depict the source proteome coverage achieved in the different cohorts. Abbreviation: IDs, identifications.

Supplemental Figure 5

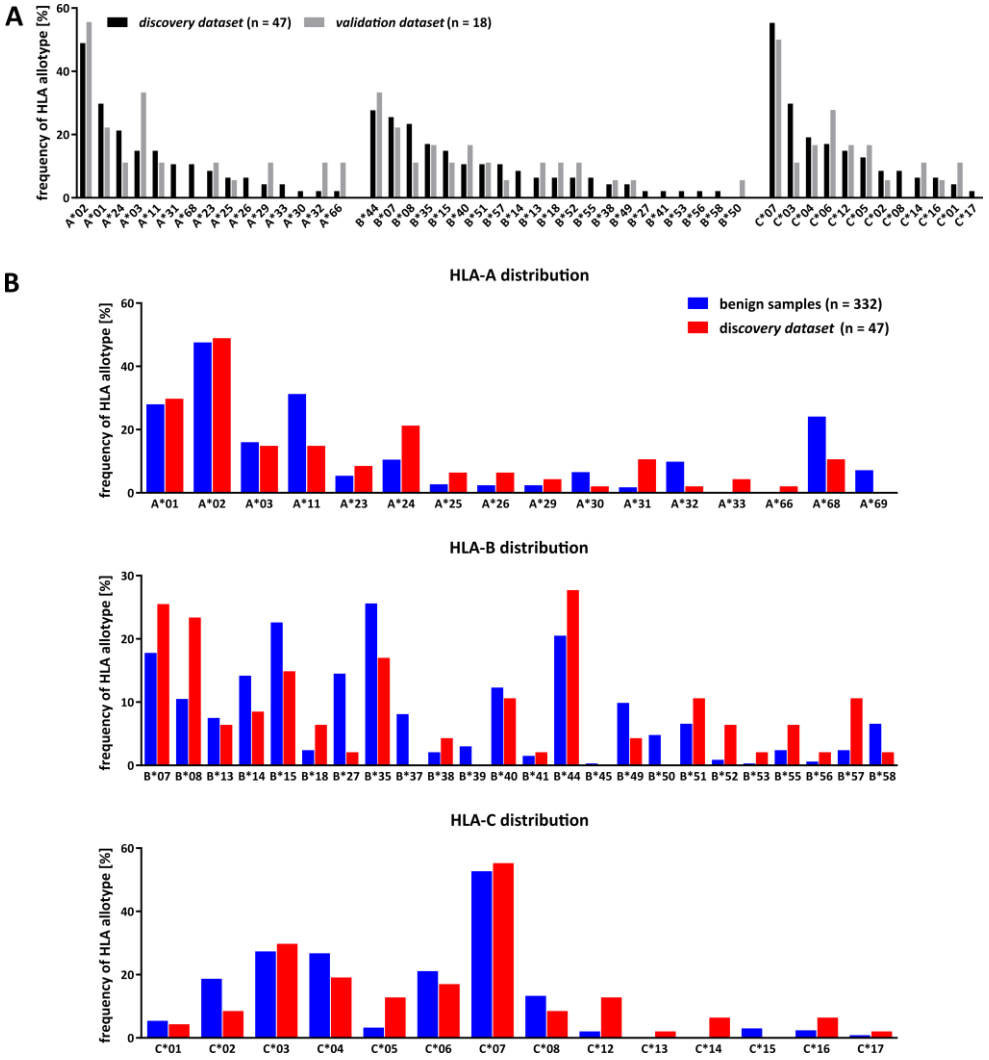

Figure S5: HLA allotype distribution in the AML and benign tissue cohorts. (A) HLA class I allotype frequencies in the AML *discovery* (n = 47) and *validation* (n = 18) *cohorts*. (B) HLA-A, -B, and -C allotype frequencies in the AML *discovery cohort* (n = 47) and the benign tissue cohort (n = 332) used for mass spectrometry-based definition of naturally presented, AML-associated antigens.

Supplemental Figure 6

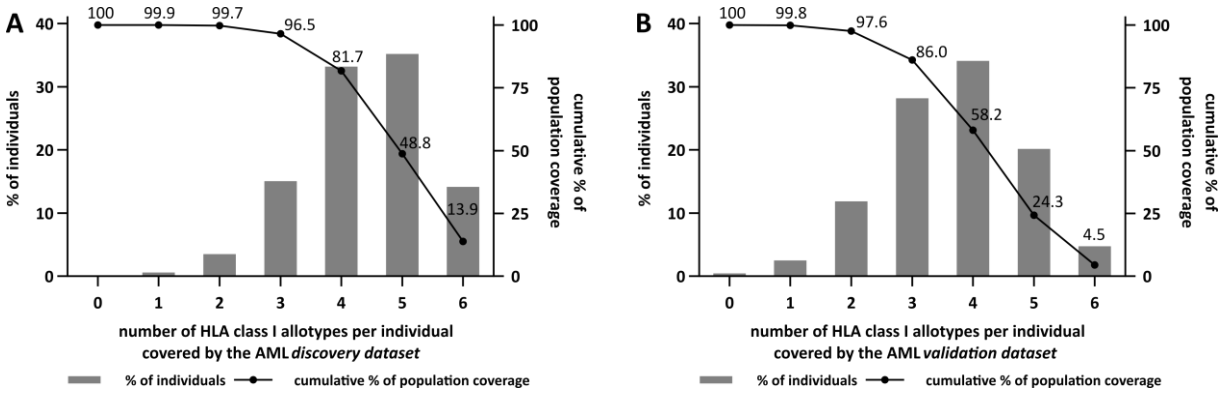

Figure S6: HLA class I allotype population coverage. HLA class I allotype population coverage within the (A) AML *discovery* and (B) AML *validation cohorts* compared to the world population (calculated by the IEDB population coverage tool, www.iedb.org). The frequencies of individuals within the world population carrying up to six HLA allotypes (x-axis) of the respective AML dataset are indicated as grey bars on the left y-axis. The cumulative percentage of population coverage is depicted as black dots on the right y-axis.

Supplemental Figure 7

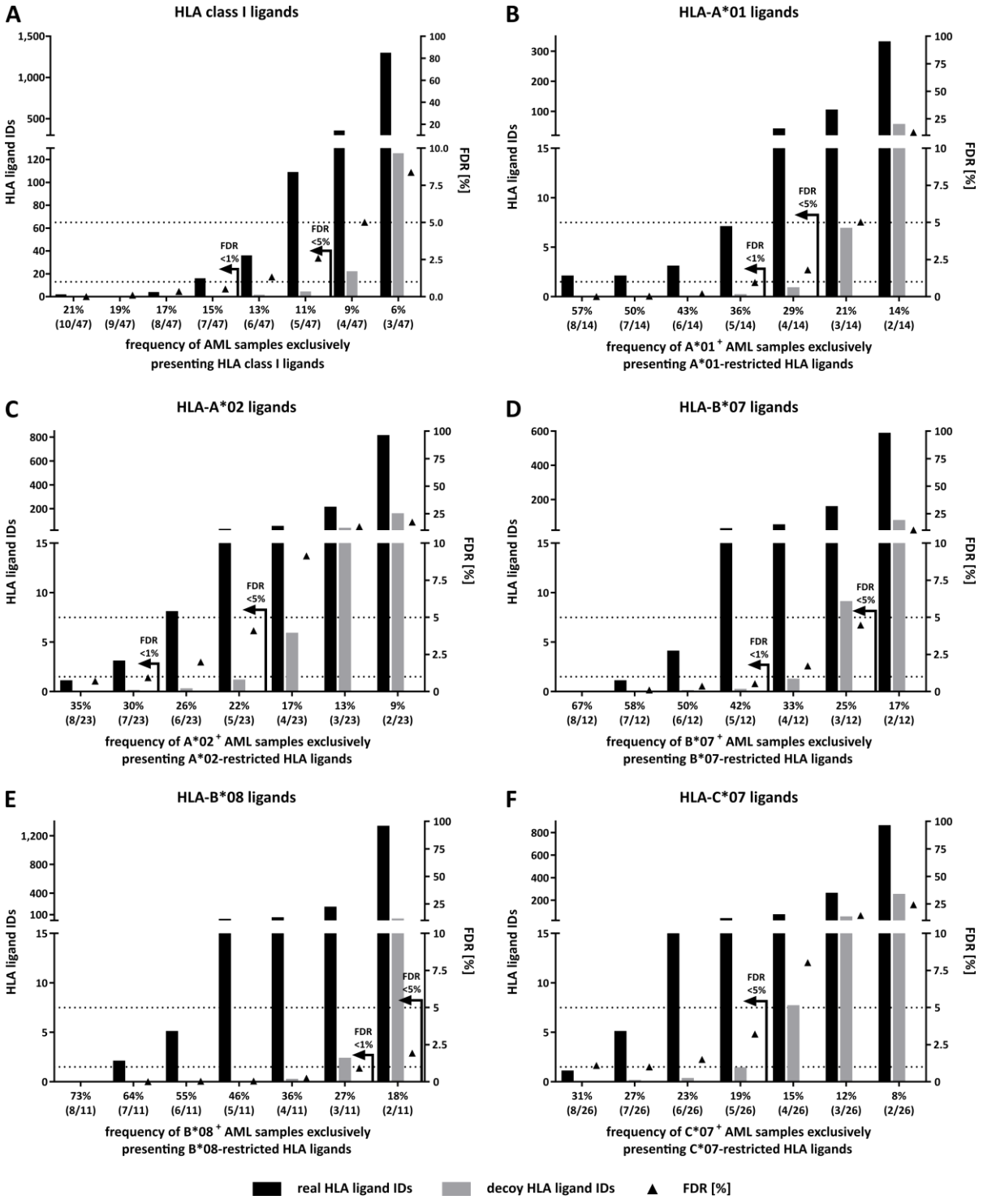

Figure S7: Statistical analysis of the proportion of false positive AML-associated HLA class I ligand identifications at different representation frequencies. The numbers of identified (A) HLA class I, (B) -A*01, (C) -A*02, (D) -B*07, (E) -B*08, and (F) -C*07 ligands based on the analysis of the AML *discovery* and benign tissue cohorts were compared with random virtual AML-associated HLA class I, -A*01, -A*02, -B*07, -B*08, and -C*07 ligands (left y-axis), respectively. Virtual ligandomes of AML patient and benign tissue samples were generated *in silico* based on random weighted sampling from the entirety of peptide identifications in both original cohorts. These randomized virtual ligandomes were used to define AML-associated antigens based on simulated cohorts of AML versus benign tissue samples. The process of peptide randomization, cohort assembly, and AML-associated antigen identification was repeated 1,000 times and the mean value of resultant virtual AML-associated antigens was calculated and plotted for the different threshold values. The corresponding FDRs (right y-axis) for any chosen threshold (x-axis) were calculated and the 1% and 5% FDRs are indicated within the plot (dotted lines and arrows). Abbreviations: IDs, identifications; FDR, false discovery rate.

Supplemental Figure 8

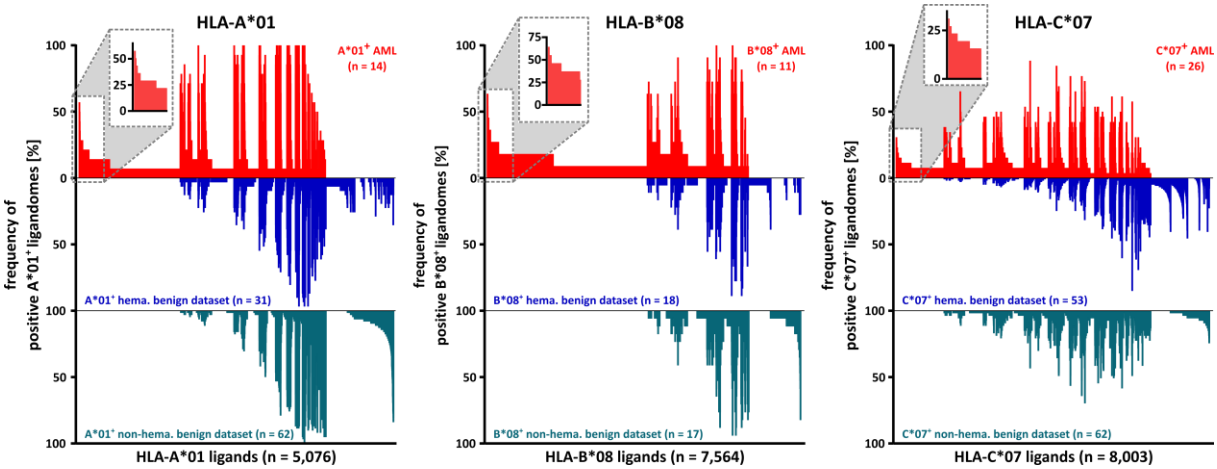

Figure S8: Comparative HLA allotype-specific ligandome profiling and identification of AML-associated antigens. Comparative profiling of HLA-A*01, -B*08, and -C*07 ligands based on the frequency of HLA-restricted presentation in HLA-matched AML and HLA-matched benign ligandomes. Frequencies of positive immunopeptidomes for the respective HLA ligands (x-axis) are indicated on the y-axis. To allow for better readability, HLA ligands identified on < 5% of the samples within the respective cohort were not depicted in this plot. The boxes on the left of each graph and their magnifications highlight the subset of AML-associated antigens showing AML-exclusive, highly frequent presentation. Abbreviation: hema., hematological.

Supplemental Figure 9

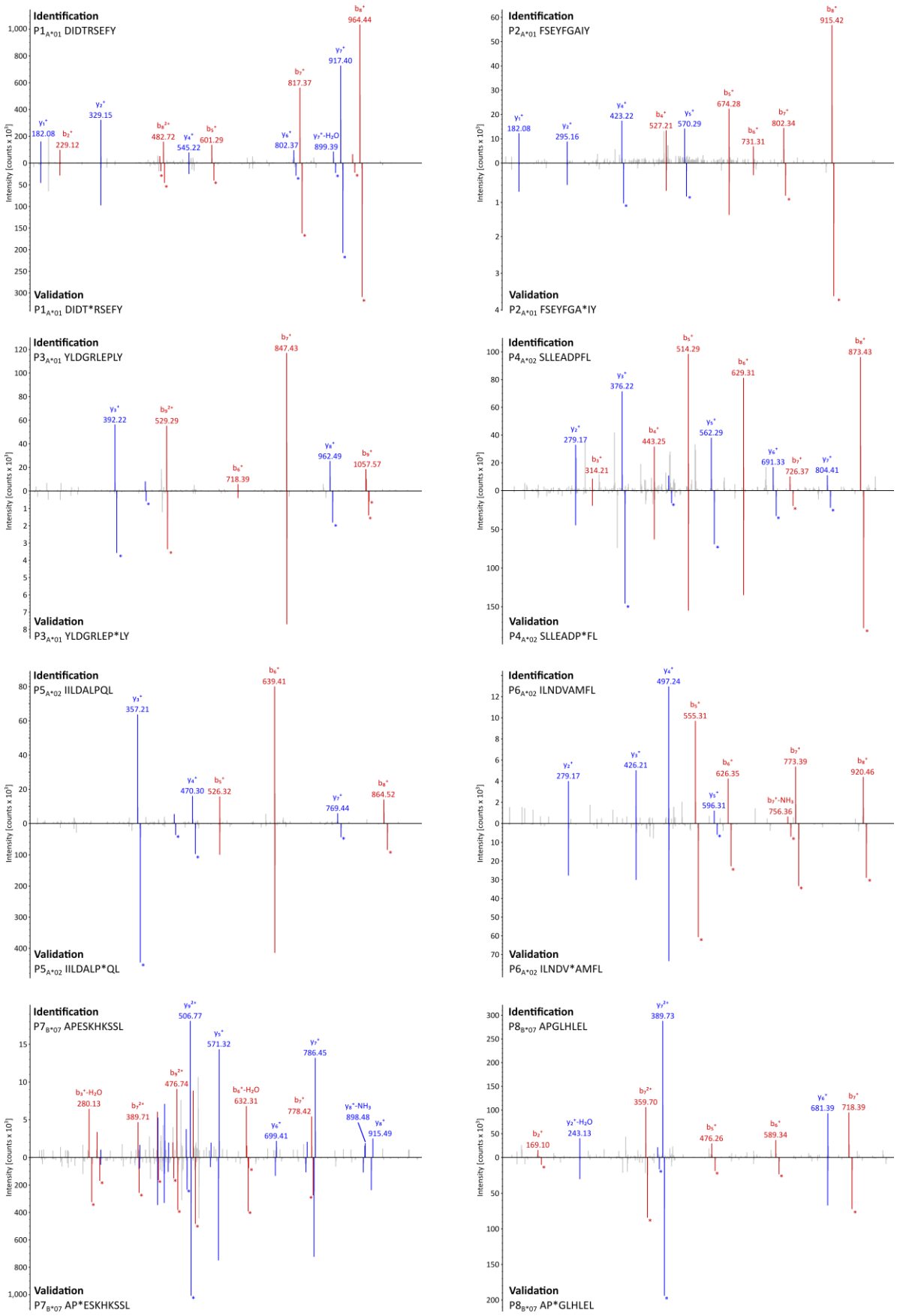

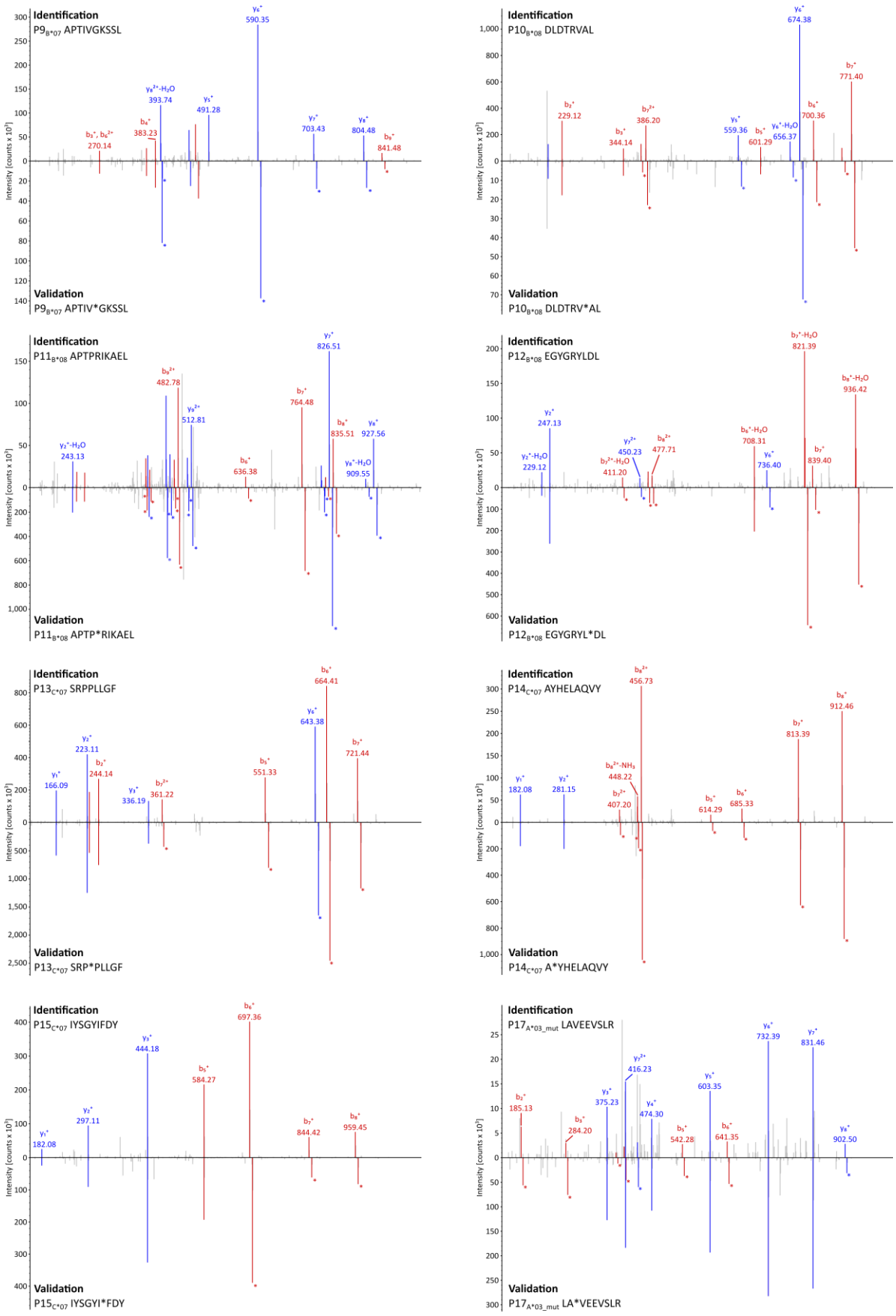

Figure S9: Validation of experimentally eluted HLA class I-presented peptides by isotope-labeled synthetic peptides. Comparison of fragment spectra (m/z on the x-axis) of HLA class I peptides eluted from primary AML patient samples (identification) to their corresponding synthetic peptides (validation). The spectra of the synthetic peptides are mirrored on the x-axis. Identified b- and y-ions are marked in red and blue, respectively. Ions containing isotopic labeled amino acids are marked with asterisks.

Supplemental Figure 10

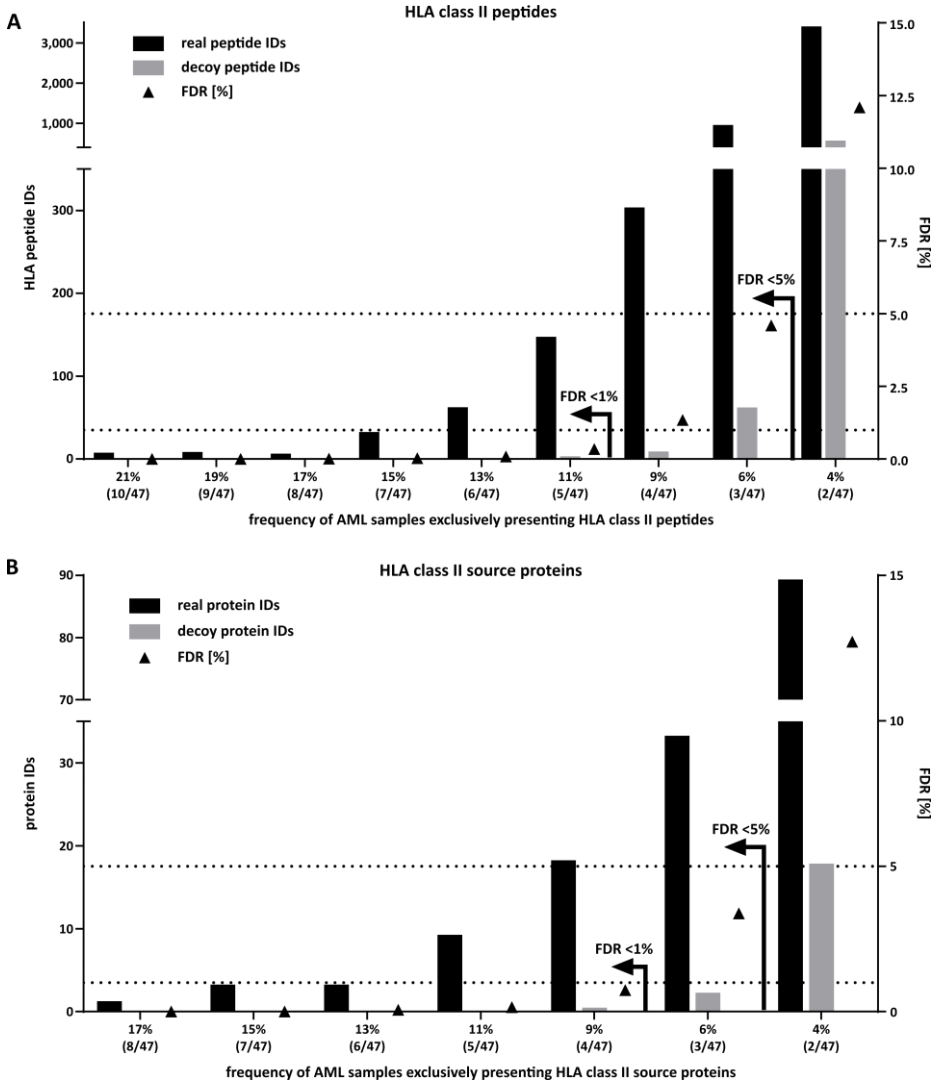

Figure S10: Statistical analysis of the proportion of false positive AML-associated HLA class II peptide and source protein identifications at different representation frequencies. The numbers of identified (A) HLA class II peptides and (B) source proteins based on the analysis of the AML *discovery* and benign tissue cohorts were compared with random virtual AML-associated HLA class II peptides and source proteins (left y-axis), respectively. Virtual ligandomes of AML patient and benign tissue samples were generated *in silico* based on random weighted sampling from the entirety of peptide or source protein identifications in both original cohorts. These randomized virtual ligandomes were used to define AML-associated antigens based on simulated cohorts of AML versus benign tissue samples. The process of randomization, cohort assembly, and AML-associated antigen identification was repeated 1,000 times and the mean value of resultant virtual AML-associated antigens was calculated and plotted for the different threshold values. The corresponding FDRs (right y-axis) for any chosen threshold (x-axis) were calculated and the 1% and 5% FDRs are indicated within the plot (dotted lines and arrows). Abbreviations: IDs, identifications; FDR, false discovery rate.

Supplemental Figure 11

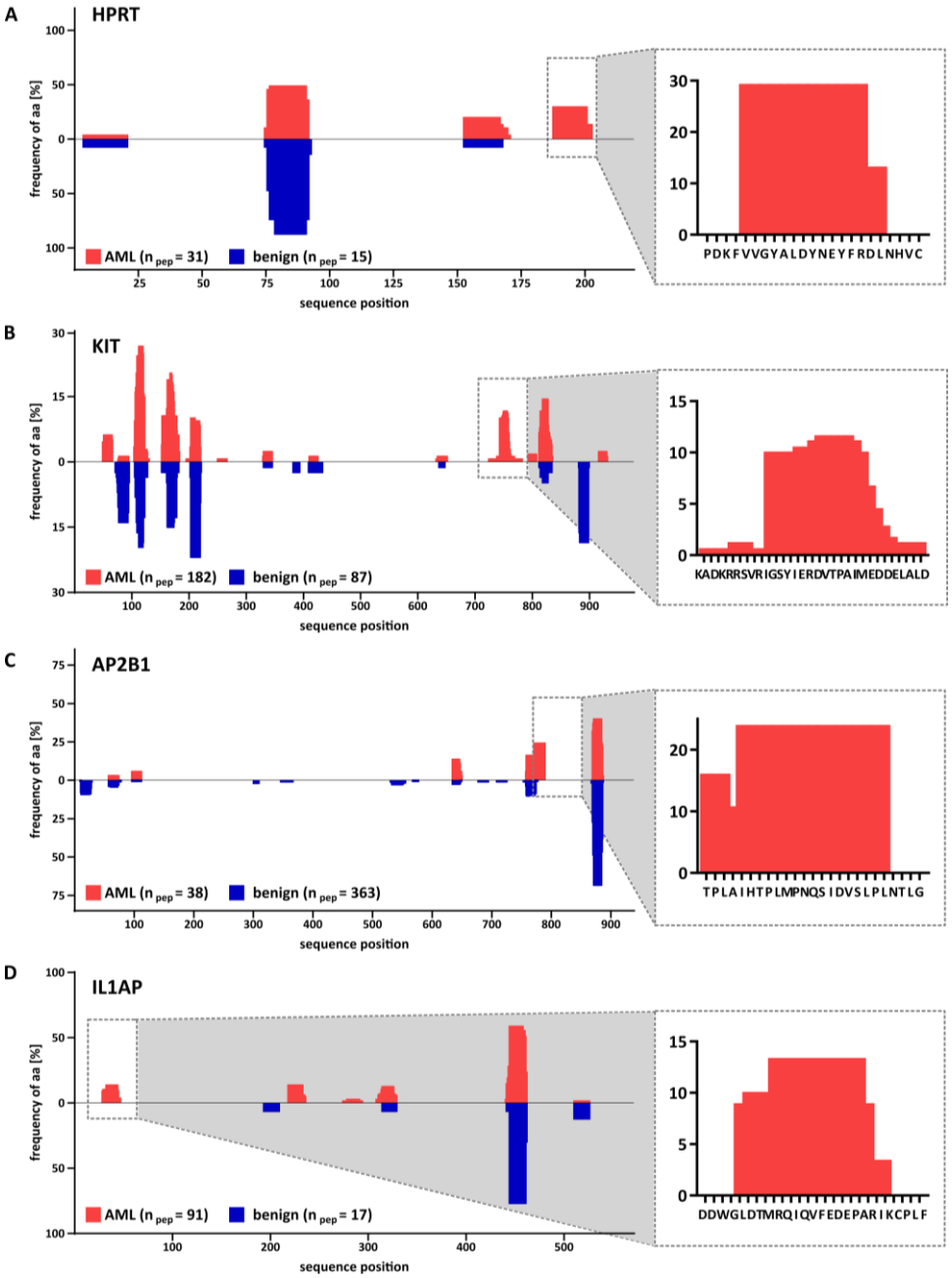

Figure S11: Hotspot analysis of HLA class II peptides. Hotspot analysis of AML-associated hotspots of the proteins (A) HPRT, (B) KIT, (C) AP2B1, and (D) IL1AP by peptide clustering. Identified peptides were mapped to their amino acid positions within the source protein. Representation frequencies of amino acid counts within each cohort for the respective amino acid position (x-axis) were calculated and are indicated on the y-axis. The boxes and their magnifications highlight the identified hotspots with the respective amino acids on the x-axis. Abbreviations: aa, amino acid; n_{pep}, number of peptides.

Supplemental Figure 12

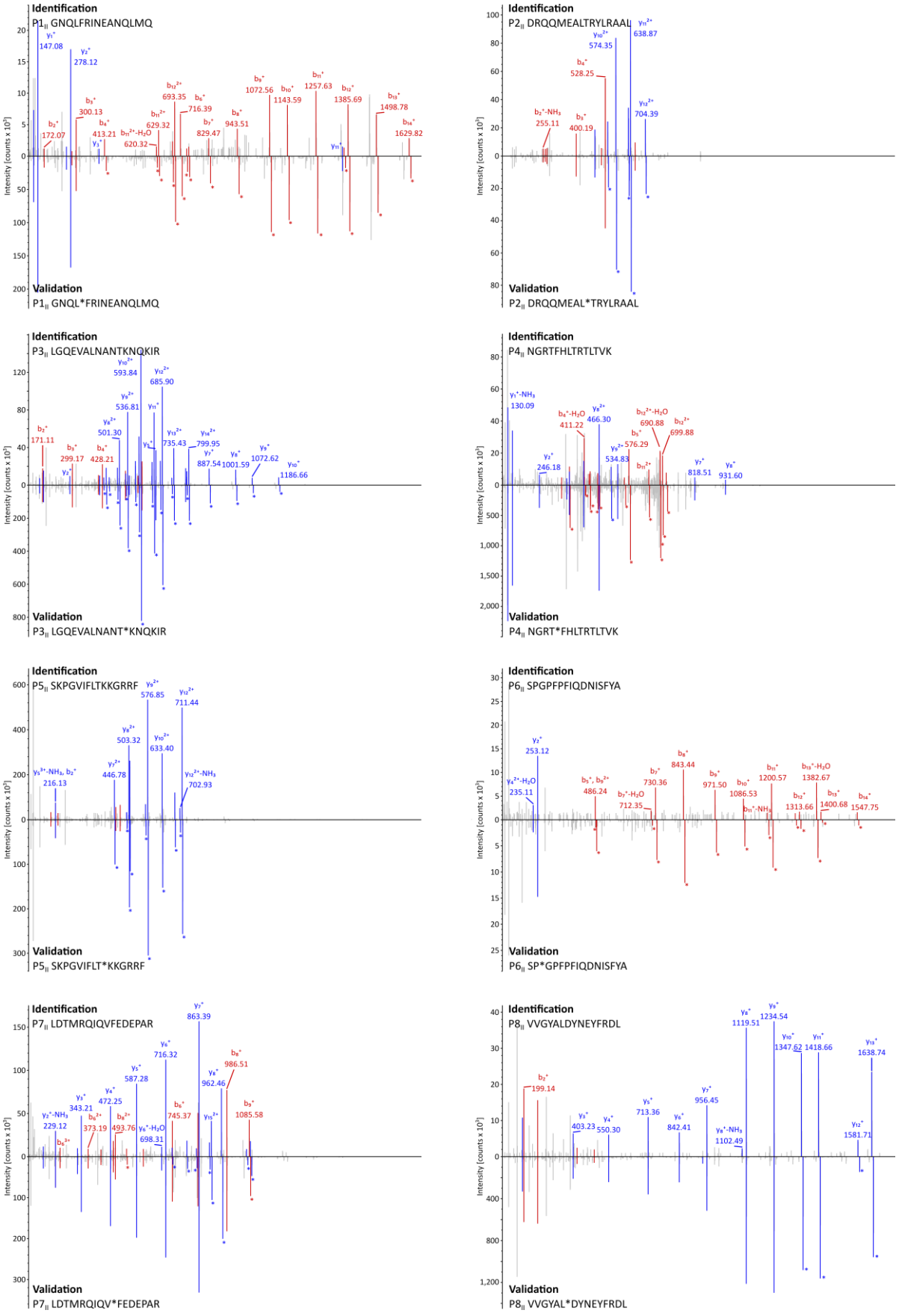

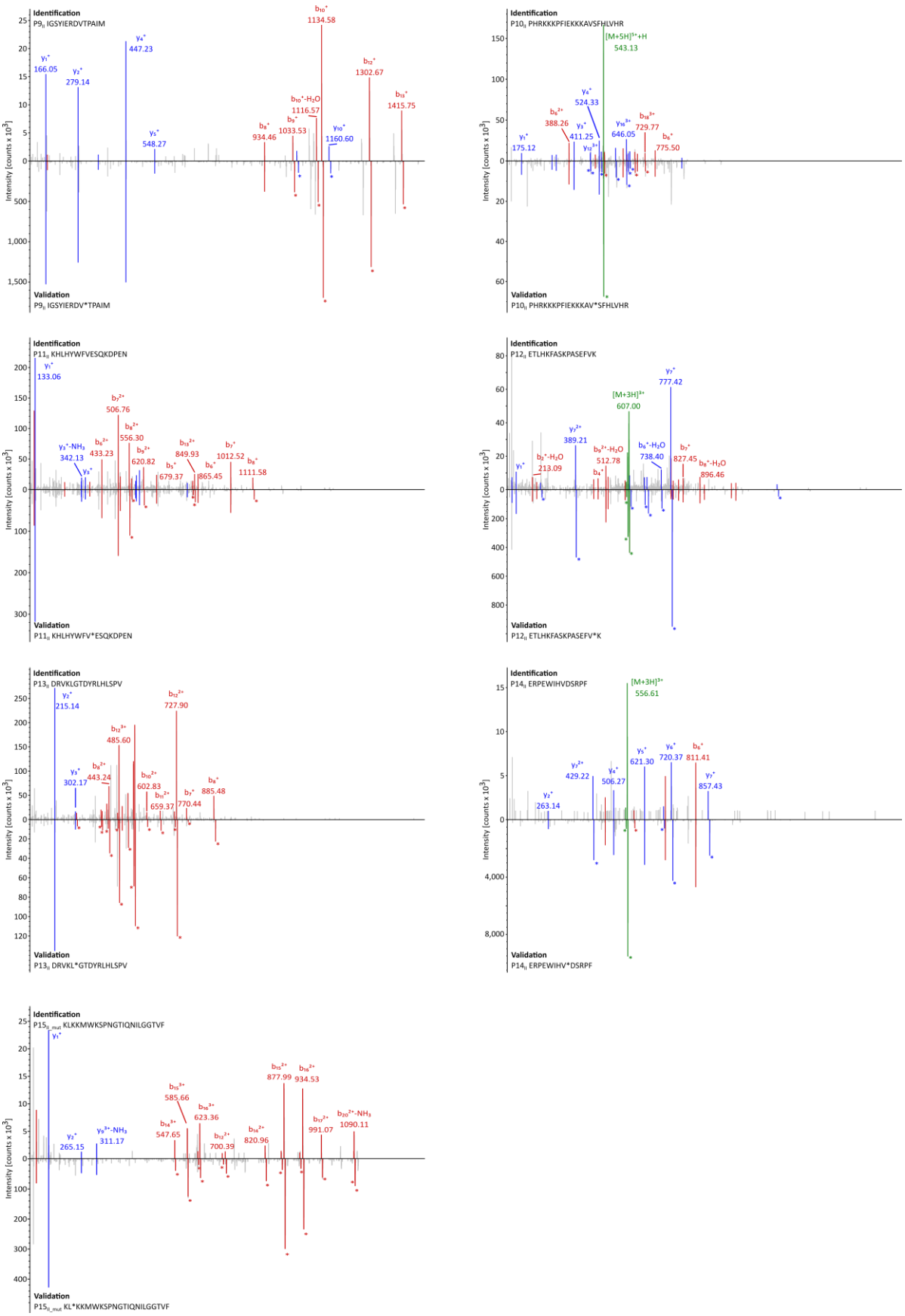

Figure S12: Validation of experimentally eluted HLA class II-presented peptides by isotope-labeled synthetic peptides. Comparison of fragment spectra (m/z on the x-axis) of HLA class II peptides eluted from primary AML patient samples (identification) to their corresponding synthetic peptides (validation). The spectra of the synthetic peptides are mirrored on the x-axis. Identified b- and y-ions are marked in red and blue, respectively. Ions containing isotope-labeled amino acids are marked with asterisks.

Supplemental Figure 13

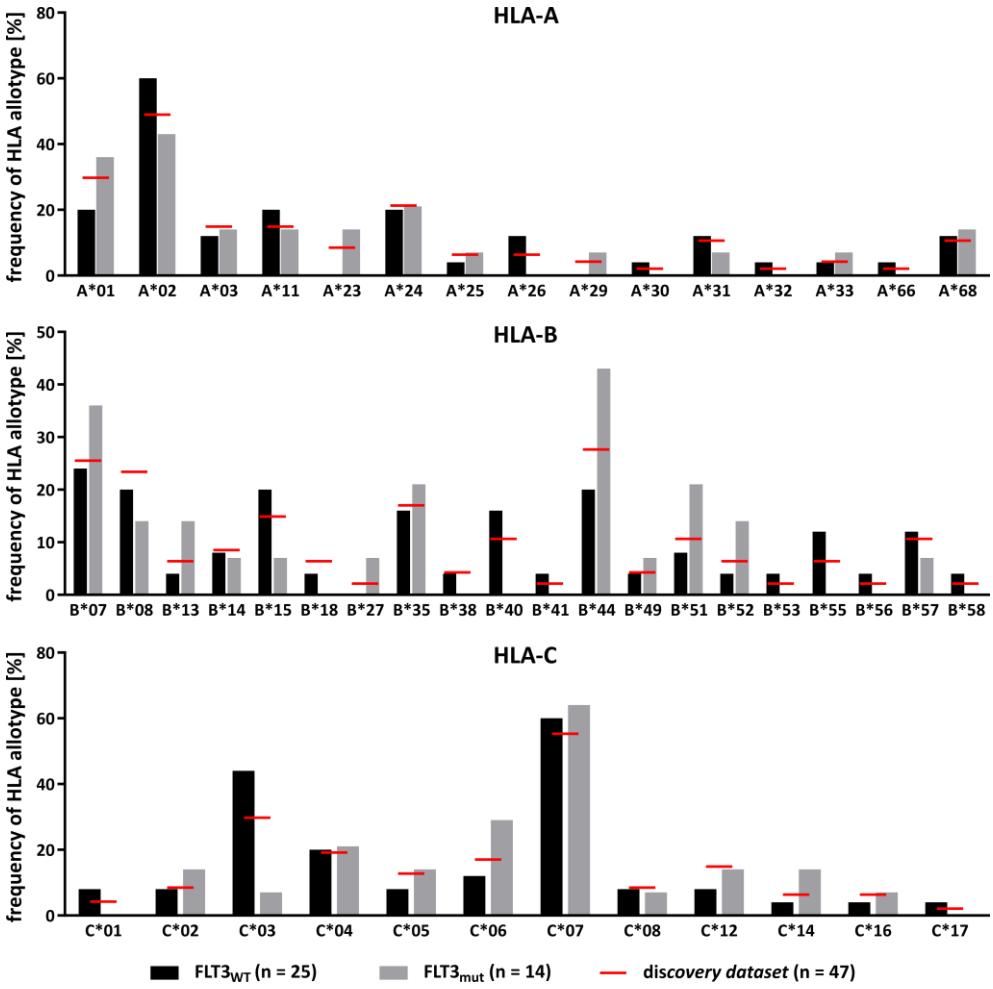

Figure S13: HLA allotype distribution in $FLT3_{WT}$ and $FLT3_{mut}$ AML samples in comparison to the AML *discovery dataset*. HLA-A, -B, and -C allotype frequencies in $FLT3_{WT}$ (n = 25) and $FLT3_{mut}$ (n = 14) AML samples.